Faculté d'Ingénierie Biologique,
Agronomique et Environnementale
Earth and Life Institute,
Environmental Sciences
Université catholique de Louvain

The impact of the 1991 Plinian eruption of Mt. Pinatubo, Philippines on soil development, phytolith accumulation, phosphorus status, and crop productivity

Michelle Castillo Quimbo

These présentée en vue de l'obtention du grade de Docteur en Sciences Agronomiques et Ingénierie Biologique

Louvain-la-Neuve, Belgium
March 2020

Membres du jury:

Présidént	Prof. Marnik Vanclooster (UCLouvain, Belgium)
Promoteurs	Prof. Pierre Delmelle (UCLouvain, Belgium)
	Prof. Pearl Sanchez (University of the Philippines Los Baños, Philippines)
Lecteurs	Prof. Sophie Opfergelt (UCLouvain, Belgium)
	Prof. Alain Bernard (Universite libre de Bruxelles, Belgium)

This PhD thesis was funded by the **Académie De Recherche et D'Enseignement Supérieur (ARES)** in the framework of the **Commission Universitaire pour Le Developpement (CUD)**
in collaboration with the
University of the Philippines Los Baños (UPLB),
Université Libre de Bruxelles (ULB), and
Philippine Institute of Volcanology and Seismology (PHILVOCS)









Acknowledgment

"If you always do what is easy and choose the path of least resistance, you never step outside your comfort zone. Great things don't come from comfort zones."

- *Roy T. Bennett, The Light in the Heart*

First and foremost, praises and thanks to God, the Almighty, for being the source of my strength, wisdom, protection, blessings, and hope to accomplish the research successfully.

I would like to express my deepest gratitude to all my supervisors and advisory/jury members both in Belgium and the Philippines, for without their guidance and support this dissertation would not have materialized. To my research supervisor, Prof. Pierre Delmelle (UCLouvain), thank you for challenging and pushing me to be a better researcher. Your dynamism, motivation, and immense knowledge have inspired me. You taught me a different approach on how to carry out the research work, write, and present the results as concise and clear as possible. It was a great privilege and honor to study under your supervision. Merci beaucoup for your patience and sense of humor which lighten up our cumbersome discussions. To my advisory chair, Prof. Pearl Sanchez (UPLB), warmest thanks for giving me this rare opportunity to conduct a joint research program with UPLB and UCLouvain, and for providing invaluable assistance and advice throughout the conduct of this study. To Prof. Alain Bernard (ULB), for drafting the whole research project which granted the three of us, Ph.D. scholars together with Mariton and Raymond, the chance to study in premier universities of Belgium, UCLouvain and ULB, and be of help to our local farmers and community with the outputs of our research. You and Prof. Delmelle have been very supportive and secured me with the privileges of the scholarship throughout the duration of the project and even after it has ended. To Prof. Sophie Opfergelt (UCLouvain) and Prof. Rodrigo Badayos (UPLB), for sharing your expertise and for

the fruitful discussions to improve my data chapters. To Prof. Marnik Vanclooster (UCLouvain), Prof. Erlinda Paterno (UPLB), and Prof. Pompe Sta. Cruz (UPLB), I truly appreciate the insightful comments, recommendations, and encouragement to improve the quality of my manuscript.

I am truly indebted to the funding agencies from whom I received financial assistance. To the Academy of Research and Higher Education – Scholarships Program for Developing Countries (ARES), Commission Universitaire Pour Le Développement (CUD) in Belgium and the Philippine Rice Research Institute, without your generosity, the conduct of this research and sustenance of my daily living will not be possible.

I am very fortunate and grateful to be a part of the SOLS-ELIE Laboratory, UCLouvain, my second home, where I spent about 2 years of my Ph.D. stint doing laboratory work and writing. To the amazing laboratory technicians, Anne Iserentant and Claudine Givron, thank you for all the help in the lab and for giving me lectures from time to time so I can understand fully the outcome of my analysis. To Françoise Hauwen, our ever-caring secretary, thanks for the assistance that you have extended to me in the lab and for securing that I have everything that I need to work well. To the best labmates in the world, Zimin, Marlon, Clairia, Gaby, Mathilde, Carlos, Noa, Catherine, Elisabeth, Arthur, Aubry, François, Inga, Rawaa, Yolly, Charles, Benoît, Brieuc, Marie Liesse, and Fidèle, for being very accommodating, for always showing your support, and for the friendship. Special thanks to Elena for assisting me in the lab and in the university center during my first time in Belgium back in 2016. You are such a sweet and kind friend. I also would like to acknowledge the UCLouvain International students' coordinators, Danisa Zapparata and especially to Gabriela Greising, for being very efficient in facilitating my scholarship grant, for the concern, and for being very good friends.

I would also like to extend my appreciation to the Soils Laboratory and Department office of ASI-UPLB, Tita Lucy, Tita Lita, Tita Rose, Ate Wana, Kuya Allan, Kuya Dante, Tita Eli, Tita Ydang, Tita Mona, who provided assistance when I was doing some analysis and also for facilitating the documents needed during the conduct of my study. Special thanks to UPLB-FI personnel, Sir Doy, Ate Jopin, Ate Lie, and Tita Perl for the management of the project's funding.

My gratitude also goes to PhilRice LB, headed by our branch manager Remilyn Relado, for allowing me to use the facilities of the Soils and Hybrid laboratories and for the assistance they provided during the conduct of my thesis. My sincere appreciation to the field technicians who assisted me in the sample preparation, Kuya Dads, Ate Jenny, Kuya Teddy, Kuya Cris, Kuya Benjie and especially to Kuya Badong and Kuya Menes for helping me in my fieldwork. Thank you also to the administrative personnel of PhilRice who facilitated my scholarship grant, Tita Tess and Kuya Kris.

Throughout the journey of my Ph.D. life, I am blessed to come across people who treated me like a family, to whom I shared laughter and distresses that I will cherish all my life, boosted my self-esteem, and offered their prayers for my success. Thank you to the Pinays of Wallonian: Tita's Luz, Sara, Edith, Normita, Ken, Irene especially Tita Estelita for welcoming me in your group and for the good memories we shared; my bible study group in Belgium: Pastora Edith, Ate Cora, Eléonore for strengthening my faith; Marie-Madeleine and Michel for giving me a home and treating me like a family member; Babes of Belgium: Angelo, Allen, Howell, RJ, Kuya Raymond, Kuya Lito, Phoebe, Pia and especially to Donna, Mariton, Alellie, and Monica for being the best buddies for keeps; PhilRice colleagues: Glyza, Ate Nene, Diana, Ate Jeanette, Ate Loids, Gina, Rem, Tita Marilyn, Lorraine, Tita Belen, Wacky, Tin-tin, Ate Mel for your constant prayers and for sharing my ups and downs; my favorite godparents and former supervisor Ninong Cez and Ninang Nits for your neverending support; to my sisses: Aicee, Khat, Kharla, Angel, Bes Kaye, Ana, Ena, Noli,

Janet, Ela for the encouragement. To my former housemates, Christelle, Cladisse, Yolande, Luke, Francois and to all the people that I met and became friends in Belgium, I truly am thankful for knowing you.

Last but not the least, I want to acknowledge the fervent support, prayers, sacrifices and great love of my family to whom I dedicate my achievements. I am very thankful to my husband, Glenn, for your full support of my decision to pursue this graduate study even though it means that I will not be there to take care of our daughter, Chloe, for some time. Your unconditional love, encouragement, faithfulness, and dedication to providing for our family needs in spite of our difficult times have inspired me to push forward in finishing my Ph.D. I am also very grateful for having wonderful family members and relatives whose love, understanding, prayers and moral support have strengthened my will to complete this research work. To my parents in law, Mommy Ana, and Dad Jim, I cannot thank you enough for all the support you provided for us especially when I am in Belgium. To my parents, nanay Margie and tatay †Noel, who raised and loved me well, and sacrificed a lot to provide the best education for me, I dedicate my accomplishments to both of you. To my siblings Monina and Michael, for your love and support to all my endeavors and for taking care of our parents always. Thank you also to the moral support of my sisters-in-law Ces and Trisha and to all my relatives and cousins from the Castillo and Quimbo family. I would also like to acknowledge Tita Mining, Remi and especially Jen for taking good care of Chloe especially when I'm in Belgium.

Abstract

The catastrophic 1991 eruption of Mt. Pinatubo in the Philippines inflicted severe damages to agriculture. It blanketed the landscape with a thick layer of unconsolidated silica-rich tephra. The remobilization of this material by rain produced debris flows (or lahars) that flooded and buried the lowland soils. Nearly three decades after this catastrophic event, agriculture has not yet fully recovered and adapted, making the livelihoods of farmers more vulnerable to a future shock. The objectives of this Ph.D. research were to assess the impacts of the eruption on soil properties and development. We investigated (i) the weathering of the pyroclastic (tephra and lahar) deposits from which a new soil is being formed; (ii) the accumulation of biogenic silicon (phytolith) and (iii) the status of phosphorus, a typically limiting nutrient, in the newly formed soils under different vegetation covers. These analyses were compared to the properties of the ~500 years old soils buried by the 1991 volcanic products. Finally, we interviewed the small-scale farmers in order to identify the main problems that they face while reestablishing agriculture in the tephra- and lahar-impacted area. We show that very limited weathering has taken place in the recent tephra and lahar deposits. However, in most cases, the ~500 years buried soil exhibits roughly similar properties, suggesting slow weathering reactions despite a tropical climate. The early weathering of the fresh pyroclasts seems to promote biogenic silicon accumulation in the newly formed soil. Phosphorus is not limiting plant growth as the tephra and, to a lesser extent, the lahar materials contain ample bioavailable phosphorus. The farmers complain about the highly heterogeneous nature of the substrate on which they now have to cultivate. This exhibits peculiar hydrological properties that are probably responsible for poor or excessive drainage conditions (depending on the location), high acidity and reduced nutrient retention. Our results provide new insights into the protracted and largely overlooked effects of tephra and lahar deposits on agricultural soils. It paves the way for future studies aimed at favouring recovery and adaptation in tropical regions devastated by volcanic eruptions.

Table of Contents

Abstract i
Table of Contents iii
List of Tables viii
List of Figures x
List of Appendix Tables xvii
List of Appendix Figures xix
List of Symbols and Abbreviations xxi
Chapter 1 Introduction and Objectives 1
1.1 General Context 1
1.2 Thesis background 3
1.3 Research objectives and thesis outline 7
1.4 References 10
Chapter 2 State of the Art 15
2.1 Geography, geology, and mineralogy of Mt. Pinatubo 15
2.2 Ash tephra and lahar pyroclastic materials 16
2.3 Volcanic soils 17
2.4 Pedogenic processes occurring in volcanic soils 19
2.4.1 Factors affecting soil formation 19
2.4.2 Primary mineral weathering and formation of secondary minerals 21
2.4.3 Chemical weathering of volcanic materials 24
2.4.4 Weathering indices to assess the degree of volcanic soil formation 26
2.5 Impact of soil burial by volcanic materials 28
2.6 Silicon and phytoliths in plants and soils 28
2.7 Phosphorus in plants and soils 32
2.7.1 Impact of tephra deposition and weathering on P availability 34

Table of Contents

2.8 Local research studies conducted on Mt. Pinatubo pyroclast deposits 35
2.8.1 Chemical properties of Pinatubo ash deposit 35
2.8.2 Physical properties of Pinatubo ash deposit 36
2.8.3 Chemical properties of the Pinatubo lahar deposit 36
2.8.4 Constraints identified and recommended adaptation practices based on local research studies 37
2.8.5 Farmers adaptation practices 38
2.9 References 40
Chapter 3 Early-stage of weathering and soil formation processes in the pyroclast deposits from the 1991 Plinian eruption of Mt. Pinatubo, Philippines 53
3.1 Introduction 53
3.2 Materials and Methods 55
3.2.1 Site characterization and soil sampling 55
3.2.2 Soil physical and chemical analysis 61
3.2.3 Soil mineralogical analysis 67
3.2.4 Weathering Indices 69
3.3 Results 71
3.3.1 Morphology 71
3.3.2 Particle size analyses 73
3.3.3 Mineralogy 75
3.3.4 General soil chemical properties 86
3.3.5 Selective dissolutions of Si, Al, and Fe 97
3.3.6. Weathering indices 109
3.4 Discussion 116
3.4.1 Horizonation of the soil profiles 116
3.4.2 Early-stage of soil formation in pyroclast deposits 117
3.4.3 Development stage of the buried soil across different land-use types 131
3.4.4 Soil classification 139

Table of Contents

3.5 Conclusion 140
3.6 References 142
Chapter 4 Phytolith accumulation in a 26-year dacitic ash deposit grown to lowland rice, Tarlac, Philippines 153
4.1 Introduction 153
4.2 Materials and Methods 156
4.2.1 Site characterization and soil sampling 156
4.2.2 Soil physicochemical and mineralogical analyses 160
4.2.3 Overview of the BSi cycle in the soil-rice plant system after the 1991 Pinatubo eruption 162
4.2.4 Extraction of phytoliths in the silt-size fraction of soil horizons, ash, and pumice layers 164
4.2.5 Microscopic observation of BSi and GSi components 166
4.2.6 Plant sample collection and analysis 168
4.2.7 Extraction of phytoliths in rice sheath and leaves 169
4.2.8 Total Si and Ca analysis of soil phytoliths and rice sheath phytoliths 169
4.2.9 Biomass yield scenarios 170
4.3 Results 172
4.3.1 General description of the soil profiles 172
4.3.2 Mineralogical Analysis 172
4.3.3 Physicochemical properties of the soil horizons and ash layers 173
4.3.4 Elemental composition of soil horizons and ash layer 175
4.3.5 Phytolith and Si contents, and morphologies of the rice plant 177
4.3.7 Morphologies and contents of phytoliths and silicate glass contents extracted from the silt-size fraction of soil horizons 179
4.4 Discussion 186
4.4.1 Estimated phytolith and silicon fluxes from rice biomass production to the modern soil 186

Table of Contents

4.4.2 Weathering state of the ash in the modern and buried soils 189
4.4.3 Proportion of total Si from measured rice phytoliths to the total silicon concentrations of bulk MS and BS 191
4.4.4 Predicted and measured stocks and fluxes of extracted rice phytoliths in soil horizons 194
4.5 Conclusion 203
4.6 References 205
Chapter 5 Phosphorus status in soils forming in the pyroclast deposits from the 1991 Plinian eruption of Mt. Pinatubo, Philippines 213
5.1 Introduction 213
5.2 Materials and Methods 215
5.2.1 Site characterization and soil sampling 215
5.2.2 Soil physical and chemical analysis 216
5.3 Results 219
5.3.1 Phosphorus contents of the modern soil and pyroclast deposit 219
5.3.2 Phosphorus contents of the buried soils 221
5.4 Discussion 224
5.4.1 Total phosphorus content 224
5.4.2 Available phosphorus content 229
5.4.3 Phosphorus retention 232
5.5 Conclusion 237
5.6 References 239
Chapter 6 Rebuilding agriculture after the 1991 Plinian eruption of Mt. Pinatubo, Philippines: soil constraints and adaptation strategies 245
6.1 Introduction 245
6.2 Materials and Methods 249
6.2.1 Reconnaissance survey and farmers' interview 249
6.2.2 Structure of interview process and organization of data from the farmers' responses 251

Table of Contents

6.3 Results.....255
6.3.1 General description of the land utilization types.....255
6.3.2 Land quality constraints on crop production as perceived by the farmers/agricultural technicians.....265
6.3.3 Adaptation of farming practices.....269
6.4.4 Positive effects of pyroclast materials on crop production as perceived by the farmers.....274
6.4 Discussion.....276
6.4.1 Land/soil quality constraints in relation to the type of pyroclastic deposit.....276
6.4.2 Adaptation and rehabilitation strategies.....282
6.4.3 Crop productivity in relation to soil constraints and farmers adaptation practices.....284
6.5 Conclusion.....296
6.6 References.....299
Chapter 7 Conclusions and Perspectives.....305
7.1 General Concusions.....305
7.2 Limitations and Perspectives.....307
7.3 References.....313
Chapter 8 Appendices.....315
8.1 Appendices for Chapter 3.....315
8.2 Appendices for Chapter 4.....330
8.3 Appendices for Chapter 5.....336
8.4 Appendices for Chapter 6.....337
Publications.....359

List of Tables

Table 3.1. X-ray diffraction parameters of common soil minerals. 68
Table 3.2. Weathering indices and expected trend with increasing degree of chemical weathering. 70
Table 3.3. Mineralogy of the bulk (< 2 mm) and clay (< 2 μm) samples in the Fo-Ash (P1-a, Tarlac province), IR-Ash (P2-a, Tarlac province), Gr-LA-Ash (P3-a, Pampanga province), Gr-HA-Ash (P4-a, Pampanga province) and IR-Lahar (P5-a, Zambales province) soil profiles.....76

Table 4.1. Estimated abundance and weight percent equivalent of rice sheath phytoliths (BSi_{rs}) based on the microscopic evaluation of the extracted soil phytolith [BSi_t + GSi] assemblage.....168
Table 4.2. Particle-size distribution of the soil horizons, ash and pumice layers from Bamban, Tarlac province.....174
Table 4.3. Soil chemical properties of the soil horizons, ash, and pumice layers from three soil profiles at Bamban, Tarlac Province. 176
Table 4.4. Mean abundances of BSi_t and GSi from the [BSi_t + GSi] extracted from the silt-size fraction of soil horizons and ash layer at Bamban, Tarlac province. 181
Table 4.5. Concentrations and stocks of rice sheath phytoliths, grass phytoliths and silicate glass in the silt-size fraction of the soil horizons and ash layer at Bamban, Tarlac province. 185
Table 4.6. Predicted Si fluxes from annual rice leaf and sheath biomass incorporation to the modern soil of the paddy lowland rice soil profile at Bamban, Tarlac province. 187
Table 4.7. Measured and predicted silicon stocks, estimated fluxes and dissolution rates from BSi_{rs} in the modern and buried soils of three soil profiles at Bamban, Tarlac province. 196

Table 6.1. General description of the land utilization types (LUT) associated with different types of pyroclastic deposits in Tarlac, Pampanga, and Zambales provinces. 256

Table of Contents

Table 6.1 (cont'd). General description of the land utilization types (LUT) associated with different types of pyroclastic deposits in Tarlac, Pampanga, and Zambales provinces.....257
Table 6.1 (cont'd). General description of the land utilization types (LUT) associated with different types of pyroclastic deposits in Tarlac, Pampanga, and Zambales provinces.....258
Table 6.2. Comparison of the current and pre-1991 management of land utilization types, thickness of pyroclast deposits, fertilization rate, type of variety used, farmers crop yields and comparative regional crop yield averages at present (2017) and during pre-1991 production (1990).....286
Table 6.2 (cont'd). Comparison of the current and pre-1991 management of land utilization types, thickness of pyroclast deposits, fertilization rate, type of variety used, farmers crop yields and comparative regional crop yield averages at present (2017) and during pre-1991 production (1990). 287
Table 6.3. Comparison of the current and pre-1991 management of land utilization types, cultivation method, major constraints, adaptation practices, and present condition as perceived by the farmers.....289
Table 6.4. Primary and secondary constraints on land/soil qualities imposed by pyroclast deposition, the impacts on crop and soil productivity, and the recommended adaptation strategies based on farmers' practices and from published sources. 298

Table of Contents

List of Figures

Figure 1.1. Schematic view of the structure of the Ph.D. dissertation showing the titles and links among the data chapters. 8

Figure 2.1. Hazards associated with a volcanic eruption.. 17
Figure 2.2. Summary of the factors that influence rock weathering. ..20
Figure 2.3. Stability series for the common primary minerals and volcanic glass. 22
Figure 2.4. Simplified model illustrating the impact of silicon and aluminum leaching conditions on the formation of secondary minerals during weathering of volcanic tephra, and the likely occurrence or not of Andisols as a result.....26
Figure 2.5. Silicon cycle in the soil-plant system affected by volcanic ash deposition.....30
Figure 2.6. Soil phosphorus cycle affected by pyroclastic deposition. 33

Figure 3.1. Location map of the study sites in Central Luzon, Philippines showing its proximity to Mt. Pinatubo volcano.. ...56
Figure 3.2. Photograph of representative soil profiles from non-cultivated (forest, grassland) ash-affected soils and cultivated (paddy rice) ash and lahar-affected soils from Tarlac, Pampanga and Zambales, Philippines.. 58
Figure 3.3. Distribution of *(a)* 0.014 km^3 tephra-fall deposited on June 12, 1991, consisting of andesitic scoria, ash, and accidental lithic fragments southwest of the volcano (phase IV), *(b)* 0.2 km^3, laminated, mostly fine-grained ash-fall deposit from late June 12 and early afternoon of June 15, 1991 (later part of phase IV to phase V), *(c)* ~4.4 km^3 dacitic pumice-fall deposit from June 15 (phase VI), *(d)* 0.2 km^3 fine-grained laminated tephra-fall that immediately followed the climactic eruption and continued for about 6 weeks (phase VII).. 60

Table of Contents

Figure 3.4. Step-by-step process in the mineral identification of the soil (bulk and clay) and pyroclast samples. 68
Figure 3.5. Variation with depth of sand-, silt- and clay-sized fractions in the Fo-Ash (P1-a, Tarlac province), IR-Ash (P2-a, Tarlac province), Gr-LA-Ash (P3-a, Pampanga province), Gr-HA-Ash (P4-a, Pampanga province) and IR-Lahar (P5-a, Zambales province) soil profiles.....74
Figure 3.6. XRD pattern of the bulk (< 2 mm) and clay (< 2 μm) fractions of the Fo-Ash profile samples (P1-a, Tarlac Province): *(a)* bulk MS, *(b)* clay MS, *(c)* bulk ash, *(d)* clay ash, *(e)* bulk pumice, *(f)* bulk BS, *(g)* clay BS. 78
Figure 3.7. XRD pattern of the K and Mg-treated clays along the soil profile depth of Fo-Ash (P1-a, Tarlac Province), *(a)* MS horizon, *(b)* ash layer, *(c)* pumice layer, *(d)* BS horizon. 81
Figure 3.8. Variation with depth of pH_{H2O} and pH_{KCl} in the Fo-Ash (P1-a, P1-b; Tarlac province), IR-Ash (P2-a, P2-b; Tarlac province), Gr-LA-Ash (P3-a, P3-b; Pampanga province), Gr-HA-Ash (P4-a, P4-b; Pampanga province) and IR-Lahar (P5-a, P5-b; Zambales province) soil profiles. 87
Figure 3.9a. Oxalate-extracted Si, Al, and Fe contents in the Fo-Ash (P1-a, P1-b; Tarlac province), IR-Ash (P2-a, P2-b; Tarlac province), Gr-LA-Ash (P3-a, P3-b; Pampanga province), Gr-HA-Ash (P4-a, P4-b; Pampanga province) and IR-Lahar (P5-a, P5-b; Zambales province) soil profiles. 98
Figure 3.9b. DCB-extracted Fe content in the Fo-Ash (P1-a, P1-b; Tarlac province), IR-Ash (P2-a, P2-b; Tarlac province), Gr-LA-Ash (P3-a, P3-b; Pampanga province), Gr-HA-Ash (P4-a, P4-b; Pampanga province) and IR-Lahar (P5-a, P5-b; Zambales province) soil profiles.....102
Figure 3.9c. Pyrophosphate-extracted Fe and Al contents in the Fo-Ash (P1-a, P1-b; Tarlac province), IR-Ash (P2-a, P2-b; Tarlac province), Gr-LA-Ash (P3-a, P3-b; Pampanga province), Gr-HA-Ash (P4-a, P4-b; Pampanga province) and IR-Lahar (P5-a, P5-b; Zambales province) soil profiles. 104

Figure 3.9d. Allophane and ferrihydrite contents in the Fo-Ash (P1-a, P1-b; Tarlac province), IR-Ash (P2-a, P2-b; Tarlac province), Gr-LA-Ash (P3-a, P3-b; Pampanga province), Gr-HA-Ash (P4-a, P4-b; Pampanga province) and IR-Lahar (P5-a, P5-b; Zambales province) soil profiles.....107
Figure 3.10a. TRB content in the Fo-Ash (P1-a, P1-b; Tarlac province), IR-Ash (P2-a, P2-b; Tarlac province), Gr-LA-Ash (P3-a, P3-b; Pampanga province), Gr-HA-Ash (P4-a, P4-b; Pampanga province) and IR-Lahar (P5-a, P5-b; Zambales province) soil profiles.....110
Figure 3.10b. Fe_d/Fe_t content in the Fo-Ash (P1-a, P1-b; Tarlac province), IR-Ash (P2-a, P2-b; Tarlac province), Gr-LA-Ash (P3-a, P3-b; Pampanga province), Gr-HA-Ash (P4-a, P4-b; Pampanga province) and IR-Lahar (P5-a, P5-b; Zambales province) soil profiles.....112
Figure 3.10c. Ratio of Al and Si in the Fo-Ash (P1-a, P1-b; Tarlac province), IR-Ash (P2-a, P2-b; Tarlac province), Gr-LA-Ash (P3-a, P3-b; Pampanga province), Gr-HA-Ash (P4-a, P4-b; Pampanga province) and IR-Lahar (P5-a, P5-b; Zambales province) soil profiles.....115
Figure 3.11. Soil profile horizonation of the non-cultivated and cultivated sampling sites affected by pyroclastic materials from the 1991 Mt. Pinatubo eruption. 116
Figure 3.12. Plot graph of organic C vs. Al_o in the modern soil and C1 horizon of Fo-Ash (P1-a, P1-b; Tarlac province), IR-Ash (P2-a, P2-b; Tarlac province), Gr-LA-Ash (P3-a, P3-b; Pampanga province), Gr-HA-Ash (P4-a, P4-b; Pampanga province) and IR-Lahar (P5-a, P5-b; Zambales province) soil profiles.. 123
Figure 3.13. Plot graph of TRB versus $Si_o + Al_o$ in the modern and buried soils of Fo-Ash (P1-a, P1-b; Tarlac province), IR-Ash (P2-a, P2-b; Tarlac province), Gr-LA-Ash (P3-a, P3-b; Pampanga province), Gr-HA-Ash (P4-a, P4-b; Pampanga province) and IR-Lahar (P5-a, P5-b; Zambales province) soil profiles.....133

Figure 3.14. Plot graph of TRB versus CEC in the modern and buried soils of Fo-Ash (P1-a, P1-b; Tarlac province), IR-Ash (P2-a, P2-b; Tarlac province), Gr-LA-Ash (P3-a, P3-b; Pampanga province), Gr-HA-Ash (P4-a, P4-b; Pampanga province) and IR-Lahar (P5-a, P5-b; Zambales province) soil profiles. 135
Figure 3.15. Plot graph of organic C versus CEC in the modern and buried soils of Fo-Ash (P1-a, P1-b; Tarlac province), IR-Ash (P2-a, P2-b; Tarlac province), Gr-LA-Ash (P3-a, P3-b; Pampanga province), Gr-HA-Ash (P4-a, P4-b; Pampanga province) and IR-Lahar (P5-a, P5-b; Zambales province) soil profiles.....137
Figure 3.16. Plot graph of TRB versus Fe_d/Fe_t and in the modern and buried soils of Fo-Ash (P1-a, P1-b; Tarlac province), IR-Ash (P2-a, P2-b; Tarlac province), Gr-LA-Ash (P3-a, P3-b; Pampanga province), Gr-HA-Ash (P4-a, P4-b; Pampanga province) and IR-Lahar (P5-a, P5-b; Zambales province) soil profiles.....138

Figure 4.1. Simplified geological map of the Mt. Pinatubo region showing the main rock formation. 157
Figure 4.2. Location map of the study site in Bamban, Tarlac province showing the *(a)* ground distance (in kilometers) of the soil pits from the Mt. Pinatubo crater, and *(b)* distance (in meters) between the three (P1, P2, and P3) soil profile pits. 158
Figure 4.3. Photographs of the three soil profiles P1, P2, and P3 sampled in a lowland rice-cultivated paddy soil in Bamban, Tarlac Province. 159
Figure 4.4. BSi cycle in the soil-rice plant system as envisaged 26 years after the 1991 Pinatubo eruption.....163
Figure 4.5. Diagram showing the different steps used for extracting BSi from the silt-sized fraction of bulk soil and ash.....164
Figure 4.6. Chart for estimating percentage abundance of BSi_{rs}, 0.1% (a), 0.5% (b), 2% (c), 5% (d) 167

Table of Contents

Figure 4.7. Comparison of phytolith and equivalent total Si mean contents (n=2) in rice sheath (rs) and leaves (rl).....177
Figure 4.8. Phytolith assemblage of *(a)* PSi_{rs} and *(b)* PSi_{rl}. 178
Figure 4.9. Proportions of bulliform and bilobate phytoliths in the PSi_{rs} and PSi_{rl} of rice plant (see section 4.2.5 for calculation of estimated abundance and weight equivalent). 179
Figure 4.10. Mean abundances (% wt. equivalent) of BSi_{rs}, $BSi_{g,}$ and GSi from the total [BSi_t + GSi] in the silt-size fraction of the MS *(a)* and BS *(b)* horizons, and ash layer *(c)* at Bamban, Tarlac province. 182
Figure 4.11. Microscopic assemblage of phytoliths [BSi_t + GSi] from the representative silt-sized fraction of *(a)* modern soil, *(b)* ash layer, and (c) buried soil.. 183
Figure 4.12. Proportion of silicon concentration of BSi_{rs} from the total Si concentration of the MS and BS silt-sized fraction at Bamban, Tarlac province. 193
Figure 4.13. Phytolith (Si) stocks and estimated fluxes in a soil-paddy rice plant system affected by 1991 Pinatubo ash deposit at Bamban, Tarlac province.....204

Figure 5.1. Variations with depth of the total P (Ptotal) and plant-available P (Pavail) contents in the Fo-Ash (P1-a, P1-b; Tarlac province), IR-Ash (P2-a, P2-b; Tarlac province), Gr-LA-Ash (P3-a, P3-b; Pampanga province), Gr-HA-Ash (P4-a, P4-b; Pampanga province) and IR-Lahar (P5-a, P5-b; Zambales province) soil profiles.....222
Figure 5.2. Variations with depth of the P retention in the Fo-Ash (P1-a, P1-b; Tarlac province), IR-Ash (P2-a, P2-b; Tarlac province), Gr-LA-Ash (P3-a, P3-b; Pampanga province), Gr-HA-Ash (P4-a, P4-b; Pampanga province) and IR-Lahar (P5-a, P5-b; Zambales province) soil profiles.....223
Figure 5.3. Total P content ratio of the modern soils to its tephra parent material; the C horizon [MS/C]; modern soil to the fresh tephra [MS/$tephra_{(1991)}$]; and C horizon to the fresh 1991 tephra

[C/tephra$_{(1991)}$] of Fo-Ash (P1-a, P1-b; Tarlac province), IR-Ash (P2-a, P2-b; Tarlac province), Gr-LA-Ash (P3-a, P3-b; Pampanga province), Gr-HA-Ash (P4-a, P4-b; Pampanga province) and IR-Lahar (P5-a, P5-b; Zambales province) soil profiles..... 227

Figure 5.4. Variations with depth of the plant-available P to total P ratio (P_{avail}/P_{total}) in the Fo-Ash (P1-a, P1-b; Tarlac province), IR-Ash (P2-a, P2-b; Tarlac province), Gr-LA-Ash (P3-a, P3-b; Pampanga province), Gr-HA-Ash (P4-a, P4-b; Pampanga province) and IR-Lahar (P5-a, P5-b; Zambales province) soil profiles..... 231

Figure 5.5. Plot graph of P retention vs. $Al_o + ½ Fe_o$ in the soil horizons and pyroclast layers of Fo-Ash (P1-a, P1-b; Tarlac province), IR-Ash (P2-a, P2-b; Tarlac province), Gr-LA-Ash (P3-a, P3-b; Pampanga province), Gr-HA-Ash (P4-a, P4-b; Pampanga province) and IR-Lahar (P5-a, P5-b; Zambales province) soil profiles..... 234

Figure 5.6. Plot graphs of P retention vs. *(a)* TRB and *(b)* Fe_d/Fe_t in the soil horizons and pyroclast layers of Fo-Ash (P1-a, P1-b; Tarlac province), IR-Ash (P2-a, P2-b; Tarlac province), Gr-LA-Ash (P3-a, P3-b; Pampanga province), Gr-HA-Ash (P4-a, P4-b; Pampanga province) and IR-Lahar (P5-a, P5-b; Zambales province) soil profiles..... 235

Figure 5.7. Plot graph of P retention vs. $[Al_p + Fe_p]$ in the soil horizons and pyroclast layers of Fo-Ash (P1-a, P1-b; Tarlac province), IR-Ash (P2-a, P2-b; Tarlac province), Gr-LA-Ash (P3-a, P3-b; Pampanga province), Gr-HA-Ash (P4-a, P4-b; Pampanga province) and IR-Lahar (P5-a, P5-b; Zambales province) soil profiles..... 237

Figure 6.1. Geographical location and elevation maps of the surveyed sites in Tarlac, Pampanga, and Zambales provinces in relation to the distribution of 1991 lahar and pyroclastic flows, and thickness of tephra-fall deposits..... 250

Figure 6.2. Flow diagram showing the structure of the questionnaire and the key topics that were discussed with the farmers and/or agricultural technicians.....252
Figure 6.3. Land cover map of the pyroclast-affected sites in Tarlac, Pampanga, and Zambales provinces. 260
Figure 6.4. Young rice plants grown in lahar soil at San Marcelino, Zambales showing stunted growth and chlorosis. 266
Figure 6.5. Waterlogging during the rainy season in a lahar soil (LUT L9) cultivated with taro at Capas, Tarlac. 267
Figure 6.6. Lahar-affected soils in San Narciso, Zambales left barren during the dry season due to lack of irrigation but is flooded during the wet season *(a)*, rice plants grown in a portion of the land during the dry season but has wilted due to severe moisture stress *(b)*.....269
Figure 6.7. Some types of irrigation systems installed/constructed by farmers in pyroclast-affected farms, *(a)* deepwell, *(b)* small farm reservoirs, *(c)* engine-powered water pump, *(d)* diversion of free-flowing water.....270
Figure 6.8. Mulching of rice straw residues to conserve moisture in a vegetable farm affected by ash at San Narciso, Zambales (LUT A3).....271
Figure 6.9. Sugarcane farm affected by ash in Capas, Tarlac (LUT A10) *(a)*, soil profile showing the hardpan below the 20 cm surface ash layer (b). 275
Figure 6.10. Spring onion *(a)* and camote tops *(b)* grown in an ash-affected soil (LUT A8) in Porac, Pampanga 275
Figure 6.11. Sugarcane grown in a lahar soil (LUT L8) at Concepcion, Tarlac.....275
Figure 6.12. Primary and secondary constraints on land/soil qualities imposed by pyroclast deposition, the impacts on crop and soil productivity, and the recommended adaptation strategies based on farmers' practices and from published sources. 298

List of Appendix Tables

Table A3.1. Detailed morphological description of the soil profiles collected from selected sites in Tarlac, Pampanga, and Zambales.....315
Table A3.2. Particle-size distribution in the Fo-Ash (P1-a and P1-b, Tarlac province), IR-Ash (P2-a and P2-b, Tarlac province), Gr-LA-Ash (P3-a and P3-b, Pampanga province), Gr-HA-Ash (P4-a and P4-b, Pampanga province) and IR-Lahar (P5-a and P5-b, Zambales province) soil profiles.....320
Table A3.3. Major soil chemical properties in the Fo-Ash (P1-a and P1-b, Tarlac province), IR-Ash (P2-a and P2-b, Tarlac province), Gr-LA-Ash (P3-a and P3-b, Pampanga province), Gr-HA-Ash (P4-a and P4-b, Pampanga province) and IR-Lahar (P5-a and P5-b, Zambales province) soil profiles. 321
Table A3.4. Oxalate-extractable Si, Al, and Fe, DCB-extractable Fe, and pyrophosphate extractable Al and Fe in the Fo-Ash (P1-a and P1-b, Tarlac province), IR-Ash (P2-a and P2-b, Tarlac province), Gr-LA-Ash (P3-a and P3-b, Pampanga province), Gr-HA-Ash (P4-a and P4-b, Pampanga province) and IR-Lahar (P5-a and P5-b, Zambales province) soil profiles. 323
Table A3.5. Indices to assess the degree of weathering of the Fo-Ash (P1-a and P1-b, Tarlac province), IR-Ash (P2-a and P2-b, Tarlac province), Gr-LA-Ash (P3-a and P3-b, Pampanga province), Gr-HA-Ash (P4-a and P4-b, Pampanga province) and IR-Lahar (P5-a and P5-b, Zambales province) soil profiles. 325
Table A3.6. Mean contents of total and exchangeable bases in the Fo-Ash (P1-a and P1-b, Tarlac province), IR-Ash (P2-a and P2-b, Tarlac province), Gr-LA-Ash (P3-a and P3-b, Pampanga province), Gr-HA-Ash (P4-a and P4-b, Pampanga province) and IR-Lahar (P5-a and P5-b, Zambales province) soil profiles....326
Table A3.7. Major and trace element composition in the Fo-Ash (P1-a and P1-b, Tarlac province), IR-Ash (P2-a and P2-b, Tarlac province), Gr-LA-Ash (P3-a and P3-b, Pampanga province), Gr-

Table of Contents

HA-Ash (P4-a and P4-b, Pampanga province) and IR-Lahar (P5-a and P5-b, Zambales province) soil profiles. 327

Table A4.1. Morphological characteristics of the lowland rice soil profiles from Bamban, Tarlac province. 330
Table A4.2. Total element concentration (< 2 µm) in the soil horizons, ash, and pumice layers from lowland rice soil profiles at Bamban, Tarlac province.....332
Table A4.3. Photomicrographs of individual BSi (BSi_{rs}, BSi_{g}), and non-BSi (GSi) observed from the lowland rice soil profile horizons (MS, BS, and ash layer) at Bamban, Tarlac province. 333

Table A5.1. Phosphorus contents along soil profile depth of the different land-use types in selected sites of Tarlac, Pampanga, and Zambales provinces. 336

Table A6.1. Guide questionnaire used in the characterization of pyroclast-affected sites and assessment of farmers adaptation practices on land quality constraints. 337
Table A6.2. Description of the land utilization types affected by pyroclast deposits based on farmer/agricultural technician interview in Tarlac, Pampanga, and Zambales provinces based on key attributes. 340
Table A6.3. Perception of the farmers/agricultural technicians on the constraints related to pyroclastic deposition and also by other factors (classified as pyroclast or non-pyroclast impact) on land qualities and associated land characteristics indicating the specific land utilization types where it is observed, and the specific adaptation practices employed to cope with the specified constraints. 346
Table A6.4. Perception of the farmers/agricultural technicians on the positive effects on land qualities and associated land characteristics of pyroclastic deposits indicating the specific land utilization types where it is observed.....355

List of Appendix Figures

Figure A6.1. Slope map of the pyroclast-affected sites in Tarlac, Pampanga, and Zambales provinces. Relatively flat (0-4 %), gently undulating (5-9 %), slightly undulating (10-18 %), strongly undulating (19-30 %), rolling (> 30 %).. 357

Table of Contents

List of Symbols and Abbreviations (unit)

Al_o	Oxalate-extracted aluminum (wt.%)
Al_p	Pyrophosphate-extracted aluminum (wt.%)
Al:Si	Total aluminum to total silicon ratio
$ash_{(1991)}$	Element composition of 1991 Pinatubo ash adapted from Castillo and Punongbayan (1996) (wt.%)
BD	Bulk density (g cm^{-3})
BS	Buried soil
% BS	Base saturation (%)
BSi	Phytoliths of plant extracted from the soil
BSi_{rl}	Phytoliths of rice leaf extracted from the soil
BSi_{rs}	Phytoliths of rice sheath extracted from the soil
BSi_t	Phytoliths of rice sheath and other grasses extracted from the soil
BSi_t + GSi	Phytoliths of rice sheath and other grasses extracted from the soil plus silicate glasses
BSi_g	Phytoliths of other grasses extracted from the soil
Ca/Si	Total calcium to total silicon ratio
$\frac{Ca}{Si}_{BSi_t+GSi}$	$\frac{Ca}{Si}$ ratio of [BSi_t + GSi] extracted from soil horizon or ash layer
$\frac{Ca}{Si}_{GSi}$	$\frac{Ca}{Si}$ ratio of silicate glasses extracted from soil horizon or ash layer
$\frac{Ca}{Si}_{PSi_{rs}}$	$\frac{Ca}{Si}$ ratio of phytoliths extracted from rice sheath
CEC	Cation exchange capacity ($cmol_c$ kg^{-1})
CIA	Communal irrigation association
DCB	Dithionite-citrate bicarbonate
$dBSi_{rs(MS)}$	Total dissolution of BSi_{rs} per unit surface area of BSi_{rs} during 13 years in the modern soil (mg m^{-2})
$dBSi_{rs(BS)}$	Total dissolution of BSi_{rs} per unit surface area of BSi_{rs} during 39 years in the buried soil
$fBSi_{rs(MS)}$	Measured BSi_{rs} flux in the MS (g Si m^{-2} y^{-1})

Abbreviations

fBSi$_{rs\ (BS)}$	Measured BSi$_{rs}$ flux in the BS (g Si m^{-2} y^{-1})
fPSi	PSi flux to the soil (g Si m^{-2} y^{-1})
fPSi$_{rs}$	PSi$_{rs}$ flux to the soil (g Si m^{-2} y^{-1})
fPSi$_{rl}$	PSi$_{rl}$ flux to the soil (g Si m^{-2} y^{-1})
fPBSi$_{rs(MS)}$	Predicted BSi$_{rs}$ flux in the MS (g Si m^{-2} y^{-1})
fPBSi$_{rs(BS)}$	Predicted BSi$_{rs}$ flux in the BS (g Si m^{-2} y^{-1})
Fe$_d$	DCB-extracted iron (wt.%)
Fe$_d$/Fe$_t$	DCB-extracted iron to total iron ratio
Fe$_o$	Oxalate-extracted iron (wt.%)
Fe$_p$	Pyrophosphate extracted iron (wt.%)
Fe$_t$	Total iron (wt.%)
DSi	Dissolved silicon
GSi	Silicate glass
ICP-AES	Inductively Coupled Plasma-Atomic Emission Spectroscopy
LUT	Land utilization type
MS	Modern soil
NIS	National irrigation system
PBSi$_{rs(MS)}$	Predicted BSi$_{rs}$ stock in the MS (kg Si m^{-2})
PBSi$_{rs(BS)}$	Predicted BSi$_{rs}$ stock in the BS (kg Si m^{-2})
P$_{total}$	Total phosphorus (mg kg^{-1})
P$_{avail}$	Plant-available phosphorus (mg kg^{-1})
P$_{ret}$	Phosphate retention (%)
PSi	Phytoliths extracted from rice plant
PSi$_{rl}$	Phytoliths extracted from rice leaf
PSi$_{rs}$	Phytoliths extracted from rice sheath
pumice$_{(1991)}$	Element composition of 1991 Pinatubo pumice adapted from Castillo & Punongbayan (1996) (wt.%)
rB	Dissolution rate of bamboo BSi at a pH 5.5 (mol BSi m^{-2} BSi y^{-1})
rBSi$_{rs(MS)}$	Mean dissolution rates of BSi$_{rs}$ stock in the modern soil (mg BSi$_{rs}$ m^{-2} soil y^{-1})
rBSi$_{rs(BS)}$	Mean dissolution rates of BSi$_{rs}$ stock in the buried soil (mg BSi$_{rs}$ m^{-2} soil y^{-1})

Abbreviations

SA_b	Specific surface area of bamboo BSi per unit weight (m^2 BSi g^{-1} BSi)
$SA_{BSirs(MS)}$	Total specific surface areas of BSi_{rs} stock in the modern soil per unit surface area (m^2 BSi_{rs} m^{-2} BSi_{rs})
$SA_{BSirs(BS)}$	Total specific surface areas of BSi_{rs} stock in the buried soil per unit surface area (m^2 BSi_{rs} m^{-2} BSi_{rs})
Si_o	Oxalate-extracted silicon (wt.%)
SFR	Small-farm reservoir
SOM	Soil organic matter (wt.%)
SRO	Short-range-order minerals
STW	Shallow tube well
$tephra_{(1991)}$	P contents of 1991 Pinatubo ash adapted from Nanzyo (1997) (mg kg^{-1})
TRB	Total reserve in bases ($cmol_c$ kg^{-1})
$TSi_{(MS)}$	Mean total Si content of modern soil (g Si kg^{-1})
$TSi_{(BS)}$	Mean total Si content of buried soil (g Si kg^{-1})
$TSi_{BSirs(MS)}$	Mean total Si content of BSi_{rs} in the MS (g Si kg^{-1})
$TSi_{BSirs(BS)}$	Mean total Si content of BSi_{rs} in the BS (g Si kg^{-1})
$TSiO_{2(MS)}$	Mean total SiO2 content in the modern soil (wt.%)
$TSiO_{2(BS)}$	Mean total SiO2 content in the buried soil (wt.%)
x_{GSi}	Proportion in abundance of silicate glasses in the soil horizon or ash layer (wt.%)
XRD	X-ray diffractogram
y_{BSit}	Proportion in abundance of B_{Sit} in the soil horizon or ash layer (wt.%)
Y_{MS}	Rice biomass yield assumptions ('high' and 'low') incorporated in the modern soil (g m^{-2} y^{-1})
Y_{BS}	Rice biomass yield assumptions ('high' and 'low') incorporated in the buried soil (g m^{-2} y^{-1})
Y_{rl}	Rice leaf biomass stock incorporated in soil (g m^{-2} y^{-1})
Y_{rs}	Rice sheath biomass stock incorporated in soil (g m^{-2} y^{-1})

Chapter 1 Introduction and Objectives

1.1 General Context

Volcanic eruptions and associated hazards are cataclysmic leading to impairment of the community, livelihood and agricultural resources. An estimated 800 million people in 86 countries live within 100 km of active volcanoes that have the potential to erupt, 226 million live within 30 km, and 29 million live within 10 km (Loughlin et al., 2015). About 90 % of the threatened people settle along the subduction zones of the Pacific Ring of Fire, where 75 % of Earth's 850 active volcanoes are found. Most of the active volcanoes are on the west side of the Ring of Fire, from the Kamchatka Peninsula in Russia, through the islands of Japan and Southeast Asia and to New Zealand (USGS, 2012). In Southeast Asia alone, there are ~750 active and potentially active volcanoes recorded. Ash generated by eruptions of VEI ≤ 3 (Volcanic Explosivity Index) causes mostly local hazards, whereas eruptions of VEI ≥ 4 could disrupt travel, trade, and daily life at the regional or even continental scale (Whelly et al., 2015).

Volcanic hazards include ashfall, tephra, bombs, gases, lava, pyroclastic flows/base surges, landslide or debris avalanche, and mudflows (Newhall et al., 2008). The hazards of utmost concern are pyroclastic density currents, tephra fall (ashfall), and rainfall-induced mudflows (lahar) due to pervasive socio-economic impacts such as loss of lives, infrastructures, and means of living (Calder et al., 2015). Huge eruptions recorded from 1902 (Mt. Pelee, Martinique) to 1991 (Mt. Pinatubo, Philippines) suggest that among the hazards, ashfall and mudflows or “lahar”, are the major cause of deaths with a total of 45,672 and 41,210 human fatalities, respectively (Blong, 1984). Pyroclastic density currents are the dominant fatal cause within 5 to 15 km distance from the volcano while lahars, tsunami, and tephra dominate after about 15 km based on a volcanic fatality database from 1500 AD to 2017 (Brown et al., 2015). Losses on agriculture due to

volcanic eruptions can be severe, for instance, $ 39 M was the cost of damages incurred from the 1980 eruption of Mount St. Helens, Washington, $ 181,312 from the 1955 lava flows of Mt. Kilauea, Hawaii (Murton & Shimabukuro, 1972), and approximately $ 25 M from 1991 eruption of Mt. Pinatubo (Global Volcanism Program, 2011).

In the active volcanic regions particularly in Southeast Asia, the risk and frequency of pyroclastic material deposition are high. Ashfall can have proximal-to-regional and in extreme cases, global effects. Lahars and pyroclastic density currents are more localized but mobile types capable of reaching distal drainages over 100 km from the volcano (Calder et al. 2015). The degree of impact depends on the particle-size distribution and thickness of pyroclastic material (Ayris & Delmelle, 2012). When the pyroclastic materials are thick enough, the complete burial of the surface soil may occur, and new soil will eventually form upon weathering and organic matter accumulation in the fresh ash. Pyroclastic materials such as tephra (ashfall, bombs, lapilli), pyroclastic flows, base surge, and lahars are parent materials with a variable physicochemical and mineralogical composition that highly influence soil development (Shoji et al., 1993).

Volcanic ash soils have excellent fertility that is capable to support agriculture and sustain high population densities in many parts of the world (Shoji et al., 1993; Delmelle et al., 2015). It is widely used for cash crop production such as rice and other crops including sugarcane, and vegetables in Southeast Asian regions (OECD/FAO, 2017). The complexity in the productivity of volcanic ash soils arises from the variability of its parent material composition, duration of weathering, the thickness of deposit, the post-deposition environmental conditions, and anthropogenic management. For instance, the capacity of newly developing soils from ash and lahar to support plant growth have been documented but contrasting claims arise from previous reports. Shoji et al., (1993) claimed that tephra deposits serve as excellent media for plant growth soon after deposition. However, Dahlgren et al. (1999) and

Cook et al. (1981) cited that tephra deposits are not very fertile especially when it is freshly deposited due to low cation exchange capacity (CEC) and negligible amounts of organic carbon (C) and nitrogen (N). Bliss (1980) claimed that lahar deposits tend to be more fertile than tephra, pumice or decomposed lava because new deposits come from older, reworked volcanic materials, plus a bit of topsoil, plant and animal remains.

1.2 Thesis background

The volcanic threat in the economy and population of a small island nation with an active volcano is higher in magnitude than in larger countries even if they have many volcanoes (Brown et al., 2015). The Philippines with 355 volcanoes, 24 considered active (PHILVOCS, 2008; 2013), and 30 million exposed population places 2nd to Indonesia having the highest overall volcanic threat to life. It was rated as the 13th most populated country in the world, between Mexico and Ethiopia, with over 108 M people at 1.72% growth rate from 2010-2015 (World Population Review, 2019). Japan ranks 3rd for the overall threat to life with 9 million exposed population while Italy, New Zealand, and Chile rank 8th, 18th and 19th, respectively, due to lower exposed population (Brown et al., 2015). Hence, reducing the impact of volcanic hazards is more difficult for many small and developing countries rimming the Pacific Ocean due to unabated population growth.

The Plinian eruption of Mt. Pinatubo in 1991(VEI 6) is the second-largest eruption of the 20th century that affected a heavily populated area after ~500 years of quiescence (Newhall & Punongbayan, 1996). The eruption period lasted for almost three months and was followed in 1992 and 1993 by two eruptive episodes of much lower explosivity (VEI 1). The estimated pyroclastic-flow and tephra-fall deposits represent 3.7 to 5.3 km^3 of erupted magma based on dense rock equivalent or DRE (Scott et al. 1996; Newhall & Punongbayan, 1996).

About 1 M people and 20,000 indigenous “Aetas” that lived and subsisted at the flanks of the volcano were affected (Newhall et al., 1998).

Mt. Pinatubo ash deposit of ~ 5 cm severely affected ~ 385,500 ha of agricultural land including forestry and aquaculture (Rantucci, 1994) while the most affected agricultural soils within 30 km of the volcano were buried up with to ~ 40 cm ash fall (Reyes & Neue, 1991). Voluminous rain-induced volcanic mudflows (lahars) buried many towns up to 40 km away by 5-10 m of sand and gravel two months after the eruption (Newhall et al., 1998). Major direct effects on agriculture were destruction of irrigation facilities, alteration of soil structure, and burial of prime agricultural lands and riverbeds with thick sand (Mendoza & Cabangbang, 1992). Cereals (rice and corn), sugarcane, mango, root crops (i.e. cassava), coconut, legumes (i.e. peanut) and vegetables (sweet pepper, eggplant, pole sitao, lady’s finger) were adversely affected by ashfall (Herrera, 1992). Hundreds of square kilometers of formerly arable land remain unproductive due to pyroclastic deposits and lahar (Global Volcanism Program, 2011). Significant deposits of lahar and volcanic materials fill the middle slopes of Mt. Pinatubo and eight rivers drain lahar to Pampanga, Zambales and Tarlac areas during rainy seasons even after 24 years (Orejas, 2015).

Pyroclastic deposition marks time zero in soil genesis that evolves with the changing of the elemental and mineralogical compositions of the fresh deposit as well as the buried soils underneath (Shoji et al., 1993, Dahlgren et al., 2004). A complete burial of soil with pyroclastic deposits such as lahar or tephra is predicted to have an immediate negative impact on soil fertility. However, as the pyroclastic materials start to weather after deposition through dissolution and leaching processes, nutrient elements are released and made available for the plants. In an experiment conducted on Mt. St. Helens tephra weathering, the application of tephra to unaffected soils was able to release high amounts of dissolved sulfate (SO_4), magnesium (Mg),

calcium (Ca), sodium (Na) and potassium (K) concentrations within the first 4 months of leaching reflecting the removal of soluble salts from tephra surfaces (Dahlgren et al., 1999). Silicon and phosphorus are important nutrient elements for plant growth and development which are increasingly abundant in fresh volcanic materials. The sudden emplacement of a substantial amount of volcanic materials in the soil is predicted to influence significantly the availability and pathways of these elements within the newly developing modern soil and the underlying buried soil. For instance, silicon (Si) in the form of plant-precipitated phytoliths (BSi) serves as an important long-term Si reserve in the soil but its stock in the buried soil may be affected by the early weathering stages of the fresh ash deposit.

Delmelle et al., (2015) remarked that very few studies address the direct and indirect effects of newly emplaced pyroclast deposits on the physical, chemical, and biological properties of the buried soil where soil formation processes may be abruptly terminated. Most of the research conducted emphasized on the characterization and weathering of the fresh pyroclast deposits, i.e. characterization of fresh pyroclastic deposits from volcanic products of 2008 Kasatochi Island volcano in Alaska (Wang et al., 2019), 2001 Etna volcano in Italy (Scollo et al., 2007), and 2006 eruption of Mt. Merapi, Indonesia (Fiantis et al., 2009). Extensive studies have been undertaken to understand the early weathering processes and chemistry of the 1980 Mt. St. Helen's surface tephra deposits through the analysis of the physicochemical and mineralogical properties of the weathered tephra, and leaching experiments (Dahlgren et al., 1997; Dethier et. al., 1981; White et al., 1986). Local studies observed the properties of the 1991 Mt Pinatubo's volcanic deposits (i.e. ash, lahar) (Reyes & Neue, 1991; Grifal, 1992) and assessed its immediate impact on the crop production and soil properties after the pyroclasts have been mixed with the soil (Mendoza & Cabangbang, 1992; Samonte et al., 1993).

Chapter 1 : Introduction and Objectives

The consequences of volcanic material deposition may cause slight to severe impacts on crop production. Earlier post-eruption surveys have been conducted to determine the coping strategies of the farmers in addressing the immediate volcanic constraints on their crop production in the aftermath of the 1991 eruption (Nelson, 2013; Mendoza & Cabangbang, 1992). Research studies and on-farm trials were also done with the aim of improving crop production and developing new technologies to cope with the ash and lahar depositions (Samonte et al., 1993; Samonte et al., 1992; Mateo, 1992; Aganon & Undan, 1992; Rasco & Lopez, 1992; Suyat et al., 1992; Grifal, 1992; Marinas et al., 1992).

Gaps between farmers and scientific knowledge often prevent the formulation of appropriate mitigation strategies (Mitsui, 1993; Barrios et al., 2006). Investigation of the young volcanic soils from the 1991 Mt. Pinatubo deposits provides an excellent opportunity to recognize the immediate and potential long term impacts of the two most widespread and dangerous volcanic hazards, ashfall and lahar, during its deposition and early soil development which can exert a strong influence on the agricultural recovery. First-hand experiences and coping practices of farmers that reflect their indigenous knowledge and technical skills can be linked with the current observation of the weathering status of the pyroclast affected soils and also from published sources. With this, possible mitigation strategies can be recommended to the farmers to address the tenacious soil constraints following the eruption of Mt. Pinatubo.

1.3 Research objectives and thesis outline

The general objective of this Ph.D. thesis is to understand the impacts of the early weathering processes of the pyroclastic deposits, specifically ash and lahar ejected by Mt. Pinatubo in 1991, on soil development and crop productivity after 26 years.

The research questions aimed to address the main objective of the study are the following:

Research Questions:

(1) What are the chemical and mineralogical changes that occur in the tephra and lahar materials during the initial 26 years of weathering and how did it affect the pedogenesis of the underlying buried soil? (**Chapter 3)**

(2) What are the impacts of ash deposition and its 26-yr weathering on the abundance, concentration, and stocks of phytoliths in the newly developing modern soil from ash and in the older buried volcanic soil? (**Chapter 4)**

(3) What are the total P, plant-available P, and P retention in soils developed from the 26-yr pyroclast deposits (i.e. ash, pumice, lahar) compared to that of the former soils buried by this deposit as influenced by pedogenesis and varying land uses? (**Chapter 5**)

(4) What is the impact of the pyroclast emplacement after 26 years of soil development in terms of soil quality constraints, benefits, and crop productivity, and how did the farmers adapt to cope with the identified constraints? (**Chapter 6**)

A schematical diagram showing the different chapters to address the main objective of the thesis is illustrated in Figure 1.1.

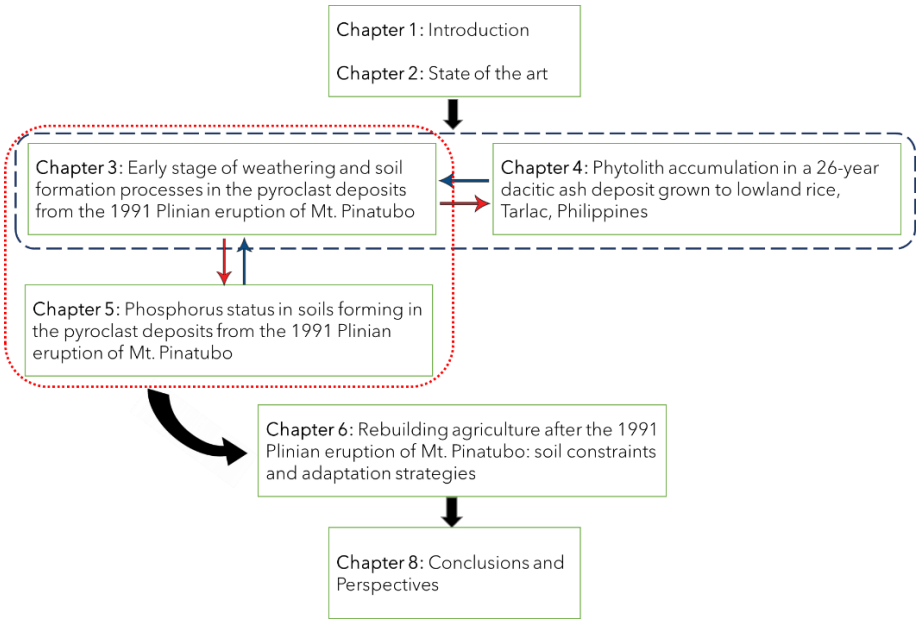

Figure 1.1. Schematic view of the structure of the Ph.D. dissertation showing the titles and links among the data chapters.

This Ph.D. thesis constitutes (Fig. 1.1):

Chapter 1 provides the general introduction, background, objectives, and outline of the dissertation.

Chapter 2 presents the overview and state-of-the-art to give a better understanding of the concepts and compile the outputs of other studies related to the objectives of this research.

Chapter 3 determines the initial stages of weathering of the 1991 pyroclast deposits by assessing the chemical and mineralogical properties of the new soils that have been forming on tephra fall (i.e.

ash, pumice) and lahar materials since 1991 and comparing them with the original, ~500-yr old soil buried under these deposits.

Chapter 4 aims to understand the biogeochemical cycling of Si derived from phytoliths in a paddy soil-plant system impacted by ~15 cm of the Mt. Pinatubo ash by *(a)* quantifying the abundance, concentration, and stocks of phytoliths from the rice plant biomass, *(b)* comparing the abundance, concentrations, stocks, fluxes, and dissolution rates of phytoliths in the newly developing modern soil from pyroclast and in the older buried soil, and *(c)* assessing the influence of weathering degree and processes on the accumulation phytoliths in the modern and buried soils.

Chapter 5 focuses on the *(a)* assessment of total P and plant-available P contents in soils developed from the 26-yr Mt. Pinatubo pyroclast deposits and in the former soils buried by this deposit, and *(b)* evaluate the influence of pedogenesis and varying land uses on P contents and retention.

Chapter 6 aims to *(a)* determine the major constraints associated with the cultivation of the Mt. Pinatubo's pyroclast deposits, 26 years after the eruption, *(b)* identify the adaptation practices of farmers to cope with the land quality constraints, and *(c)* assess the current crop productivity and to compare it with previous figures.

Chapter 7 summarizes the main findings obtained in Chapters 3 to 6 and provides some perspectives for future studies.

Finally, ***Appendices*** are presented for Chapters 3 to 6.

1.4 References

Aganon, C. P., & Undan, R. C. (1992). CLSU's research and development activities in Mt. Pinatubo-affected areas. In *Proceedings of symposium on sustainable agricultural development of Mt. Pinatubo-affected areas.* November 5-6, 1992. Farming Systems and Soil Resources Institute, College of Agriculture, University of the Philippines, Los Banos, College, Laguna.

Ayris, P. M., & Delmelle, P. (2012). The immediate environmental effects of tephra emission. *Bulletin of Volcanology*, *74*, 1905–1936. https://doi.org/10.1007/s00445-012-0654-5.

Barrios, E., Delve, R. J., Bekunda, M., Mowo, J., Agunda, J., Ramisch, J., … Thomas, R. J. (2006). Indicators of soil quality: A South-South development of a methodological guide for linking local and technical knowledge. *Geoderma*, *135*, 248–259. https://doi.org/10.1016/j.geoderma.2005.12.007.

Bliss, L. C. (1980). Lahar Deposits, Chapter 3. pp. 27–42. faculty.washington.edu/moral/pdf/Folio 05.pdf. Accessed on November 21, 2019 at 10:09 A.M.

Blong, R. J. (1984). Volcanic Hazards. *A Sourcebook on the Effects of Eruptions*, Australia, Academic Press.

Brown, S. K., Auker, M. R., & Sparks, R. S. J. (2015). Populations around Holocene volcanoes and development of a population exposure index. In *Loughlin, S. C., Sparks, S., Brown, S. K., Jenkins, S. F., V.-B., C. (Eds.). Global Volcanic Hazards and Risk*. Cambridge University Press. https://doi.org/10.1017/CBO9781107415324.004.

Calder, E., Wagner, K., & Ogburn, S.E. (2015). Volcanic hazard maps. In *Loughlin, S. C., Sparks, S., Brown, S. K., Jenkins, S. F., V.-B., C. (Eds.). Global Volcanic Hazards and Risk*. Cambridge University Press. https://doi.org/10.1017/CBO9781107415324.004.

Cook R. J., Barron, J. C., Papendick, R. I., Williams, G. J. (1981). Impact of Agriculture of the Mount St. Helens Eruptions. *Science 211*:16–22.

Dahlgren, R.A., Dragoo, J.P., & Ugolini, F.C. (1997). Weathering of Mt. St. Helens tephra under a cryic-udic climatic regime. Division S-9 Soil Mineralogy. Published in *Soil Sci. Am. J. 61*:1519-1525.

Dahlgren, R. A., Ugolini, F. C., & Casey, W. H. (1999). Field weathering rates of Mt. St. Helens tephra. *Geochimica et Cosmochimica Acta, 63*(5), 587–598. https://doi.org/10.1016/S0016-7037(99)00067-8.

Dahlgren, R. A., Saigusa, M., & Ugolini, F. C. (2004). The nature, properties, and management of volcanic soils. *Advances in Agronomy, 82*, 113–182. https://doi.org/10.1016/S0065-2113(03)82003-5.

Dethier, D. P, Pevear, D. R., Frank, D. (1981). Alteration of new volcanic deposits. In Lipman P. W., Mullineaux, D. R. (Eds.). *The 1980 eruptions of Mount St. Helens, Washington. US Geol Surv Prof Pap 1250*, Washington, pp 649–665.

Delmelle, P., Opfergelt, S., Cornelis, J.-T., & Ping, C.-L. (2015). Volcanic Soils. In Sigurdsson, H., Houghton, B., Rymer, H., Stix, J., McNutt, S. (Eds.), *The Encyclopedia of Volcanoes* (pp. 1253–1264). Elsevier Inc.

Fiantis, D., Nelson, M., Van Ranst, E., Shamshuddin, J., & Qafoku, N. P. (2009). Chemical weathering of new pyroclastic deposits from Mt. Merapi (Java), Indonesia. *Journal of Mountain Science, 6*, 240–254. https://doi.org/10.1007/s11629-009-1041-3.

Global Volcanism Program. (2011). Report on Pinatubo (Philippines). In *Wunderman, R (Ed.), Bulletin of the Global Volcanism Network, 36:*11. Smithsonian Institution. Accessed June 21, 2016.

Grifal, R. (1992). Physico-chemical, mineralogical, and hydrological characterization of volcanic ash and lahar and their utilization and management for agricultural crops. In *Proceedings of the symposium on sustainable agricultural development of Mt. Pinatubo-affected areas. November 5-6, 1992.* Biotech Seminar Room, UPLB, College, Laguna. Farming Systems and Soil Resources Institute, College of Agriculture. University of the Philippines at Los Baños, College, Laguna

Herrera, I. O. (1992). Mt. Pinatubo R & D program of the department of agriculture-Region III. In *Proceedings of the symposium on sustainable agricultural development of Mt. Pinatubo-affected areas.* November 5-6, 1992. Farming Systems and Soil Resources Institute, College of Agriculture, University of the Philippines, Los Banos, College, Laguna.

Loughlin, S. C., Sparks, S., Brown, S. K., Jenkins, S. F., V.-B., C. (2015). Global volcanic hazards and risk. Cambridge University Press. https://doi.org/10.1017/CBO9781107415324.004.

Marinas, M. E., Lim, R. S., & dela Rosa, E. A. (1992). Performance trial and cultural management studies of sweet potato and cassava under volcanic soil. In *Proceedings on the symposium on sustainable agricultural development of Mt. Pinatubo-affected areas. November 5-6, 1992.* Biotech Seminar Room, UPLB, College, Laguna. Farming Systems and Soil Resources Institute, College of Agriculture. University of the Philippines at Los Baños, College, Laguna.

Mateo, L. (1992). Characterization and amelioration of lowland rice soils affected by volcanic ejecta from Mt. Pinatubo. Doctor of Philosophy. Dissertation manuscript. 127 p. Philippines.

Mendoza, T. C., & Cabangbang, R. P. (1992). Effects of Mt. Pinatubo eruption in crop production systems. *The Philippine Agriculturist*, *75*(1 & 2), 1–8.

Nelson, G. L. (2013). Land rehabilitation techniques of rice farmers in Pampanga (Philippines) after the Mt. Pinatubo Eruption. *Asia Life Sciences*, *22*(1), 155–181.

Newhall, C., & Punongbayan R (Eds.). (1996). Fire and Mud. Eruptions and lahars of Mount Pinatubo, Philippines, *University of Washington Press*, Seattle, pp. 1063- 1070.

Newhall, C., Hendley II, J. W. & Stauffer, P. H. (1998). The Cataclysmic 1991 Eruption of Mount Pinatubo, Philippines. *U.S. Geological Survey Fact Sheet: 113-97.*

OECD/FAO. (2017). Southeast Asia: Prospects and challenges. Chapter 2. *OECD-FAO Agricultural Outlook 2017-2016*.

Orejas, T. (2015). Philvocs: Pinatubo lahar threats not over. *Inquirer Central Luzon, Philippine Daily Inquirer.* June 16, 2015. Accessed June 24, 2017, 7:05 AM.

PHILVOCS. (2008). List of active volcanoes. 30 July 2008. Philippine Institute of Volcanology and Seismology.

PHIVOLCS. (2013). List of inactive volcanoes. Philippine Institute of Volcanology and Seismology.

Rantucci, G. (1994). Geological disaster in the Philippines: The July 1990 earthquake and the June 1991 eruption of Mount Pinatubo – Description, effects, and lessons learned. Italian Ministry of Foreign Affairs, Directorate General for Development Cooperation.

Rasco Jr., E. T., & Lopez, P. J. S. (1992). Rehabilitating the sweet potato areas in Central Luzon after the Mt. Pinatubo eruption. Integrated pest management for the control of sweet potato weevil. In *Proceedings of*

symposium on sustainable agricultural development of Mt. Pinatubo-affected areas. November 5-6, 1992. Farming Systems and Soil Resources Institute, College of Agriculture, University of the Philippines, Los Banos, College, Laguna.

Reyes, R. Y., & Neue, H. U. (1991). Characterization of the volcanic ejecta from Mount Pinatubo and its impact on rice production. *Philippine Journal of Crop Science, 16*(2), 69–73.

Samonte, H. P., Badayos, R. B., Ocampo, A. M., Capunpon, E. G., delos Santos, E. G., & Willauer III, J. L. (1992). Improving the fertility status and productivity of areas affected by volcanic ash deposits of Mt. Pinatubo. In *Proceedings of the symposium on sustainable agricultural development of Mt. Pinatubo-affected areas. November 5-6, 1992.* Biotech Seminar Room, UPLB, College, Laguna. Farming Systems and Soil Resources Institute, College of Agriculture. University of the Philippines at Los Baños, College, Laguna.

Samonte, H. P., Nanzyo, M., Ocampo, A. M., Kimura, K., Kanno, H., Ito, T., … Chino, M. (1993). Improving the production of corn and rice with controlled availability fertilizers (CAF) in Pinatubo Lahar. *NRCP Research Journal, 3*(2).

Scollo, S., Carlo, P. D., Coltelli, M. (2007). Tephra Fallout of 2001 Etna Flank Eruption: Analysis of the Deposit and Plume Dispersion. *Journal of Volcanology and Geothermal Research 160*:147-164.

Scott, K. M., Janda, R. J., de la Cruz, E., Gabinete, E., Eto, I., Isada, M., Sexon, M., and Hadley, K. C. (1996). Channel and sedimentation responses to large volumes of 1991 volcanic deposits on the east flank of Mount Pinatubo. In *Newhall, C. G. & Punongbayan, R. S. (Eds.) Fire and mud: Eruptions and Lahar of Mount Pinatubo, Philippines.* Philippine Institute of Volcanology and Seismology, Quezon City. University of Washington Press, Seattle, and London. Printed in Hongkong.

Shoji, S., Nanzyo, M., & Dahlgren, R. A. (1993). Volcanic Ash Soils - Genesis, Properties and Utilization. *Elsevier*, Amsterdam, the Netherlands. 288 p.

Suyat, M. N., Lacson, R. T., & Bayot, A. J. (1992). Adaptability test of different field crops under lahar-laden soils. In *Proceedings of the symposium on sustainable agricultural development of Mt. Pinatubo-affected areas. November 5-6, 1992.* Biotech Seminar Room, UPLB, College, Laguna. Farming Systems and Soil Resources Institute,

College of Agriculture. University of the Philippines at Los Baños, College, Laguna.

USGS. (2012). Ring of fire. *Earthquake hazards program.* United States Geological Survey. Science for a changing world. Accessed on October 11, 2018, at 8:53 PM.

Wang, B., Michaelson, G., Ping, C.-L., Plumlee, G., & Hageman, P. (2010). Characterization of pyroclastic deposits and pre-eruptive soils following the 2008 eruption of Kasatochi Island Volcano, Alaska. *Arctic, Antarctic, and Alpine Research*, *42*(3), 276–284. https://doi.org/10.1657/1938-4246-42.3.276.

White, A. F., Benson, L. V., Yee, A. (1986). Chemical weathering of the May 18, 1980, Mount St. Helens ash fall and the effect on the iron creek watershed, Washington. In *Rates of chemical weathering of rocks and minerals* (pp. 351–374). Academic Press, Inc., Harcourt Brace Jovanovich, Publishers.

World Population Review. (2019). Philippines Population. (2019-06-10). Retrieved 2019-11-21, from http://worldpopulationreview.com/countries/philippines.

Chapter 2 State of the Art

2.1 Geography, geology, and mineralogy of Mt. Pinatubo

Mt. Pinatubo (15°08.2' N., 120°21.1' E) is an active stratovolcano that lies 100 km northwest of Manila bounded by three Central Luzon provinces; Zambales on the west, Tarlac on the northeast and Pampanga on the southeast. The volcano initially had the highest peak at 1,745 m.a.s.l but the summit collapsed to 1,485 m.a.s.l and created a 2.5 km width caldera after the June 12-15, 1991 eruption (Rantucci, 1994). This volcano was noted to have at least six episodic major eruptive periods during the past 35,000 years in which the last eruption was reported to occur during the Buag period ~500 years B.P (Newhall & Punongbayan, 1996). The Mt. Pinatubo consisting of eruptive products from >35 ka to present is identified as a dacite-andesite dome complex surrounded by widespread pyroclastic-flow and lahar deposits from huge explosive dacitic eruptions.

The composition of the June l99l Mount Pinatubo's erupted magma was reported to be a dacite with an overall constant composition (~64.5 wt. % SiO_2) but having variable amounts of phenocrysts (Bernard et al., 1996). Dacite is an intermediate extrusive igneous rock that has higher silica levels than basalt (~63 vs. ~53 %), respectively. The ~5 km^3 (DRE) dacite produced by Mt. Pinatubo comprised of hydrous, sulfur-rich, anhydrite-bearing magmas that erupt from subduction-zone volcanoes. The mineral assemblage is plagioclase, hornblende, titanomagnetite, ilmenite, cummingtonite, biotite, quartz, apatite, anhydrite, sulfides, rare zircon, and xenocrystic olivine plus chromite, augite, and orthopyroxene (Luhr & Melson, 1996; Bernard et al., 1996).

2.2 Ash tephra and lahar pyroclastic materials

Volcanic hazards associated with volcanic eruption include tephra, volcanic gases, lava flows, and domes pyroclastic flows, volcano landslides, and lahars as shown in Figure 2.1. In the context of this Ph.D. thesis, we focused on two major hazards that are concomitant with the explosive eruption of Mt. Pinatubo in 1991, the ashfall and lahar. Tephras are airborne pyroclastic materials classified based on size: dust (< 63 μm), ash (63 μm-2 mm), lapilli (2-64 mm), and blocks and bombs (> 64 mm). Scoria and pumice are glassy, vesicular fragments in the lapilli and bomb-size range (Orton, 1996).

Ash tephra ('ash' as referred in the main text) is composed of the fragmented materials (< 2 mm) ejected during an eruption comprised of tiny pieces of rocks, minerals, and a large quantity of sand- and silt-sized silicate glasses. It also consists of very small ash particles, < 1 μm across, that rise high into the air forming large eruption columns and spreading over wide areas as an ashfall (Myers et al., 2008; Kenedi et al., 2000; Shoji et al., 1993). Ash deposits nearest the volcano are the densest materials while the fine ashfall follows the prevailing wind patterns outward from the mountain (Myers et al., 2008; Dale et al., 2005). The ash deposits near the volcano may partially or completely bury the vegetation while those deposited further away lodges in the surfaces of plant leaves which may cause alteration in photosynthesis and plant growth (Myers et al., 2008; Dale et al., 2005; Cochran et al., 1983; Bilderback & Carlson, 1987).

Mudflows ('lahar' as referred to in the main text) are composed mainly of volcanic materials on the flanks of a volcano that were moved loosely during or after an eruption due to intense rain (Bliss, 1980). It is a rapidly flowing mixture of volcanic rock debris and water which normally contain 40 to 90 percent sediment by weight, hence having a consistency ranging from muddy water to a dense slurry (Janda et al., 1996). Lahar flows down in valleys and stream channels at 20 to 40

miles per hour and can move up to > 50 miles (80 km). The area covered by mudflow is dependent on the slope and the amount of material that was moved similar to that of alluvial fan deposits (Newhall et al., 1998; Dale et al., 2005).

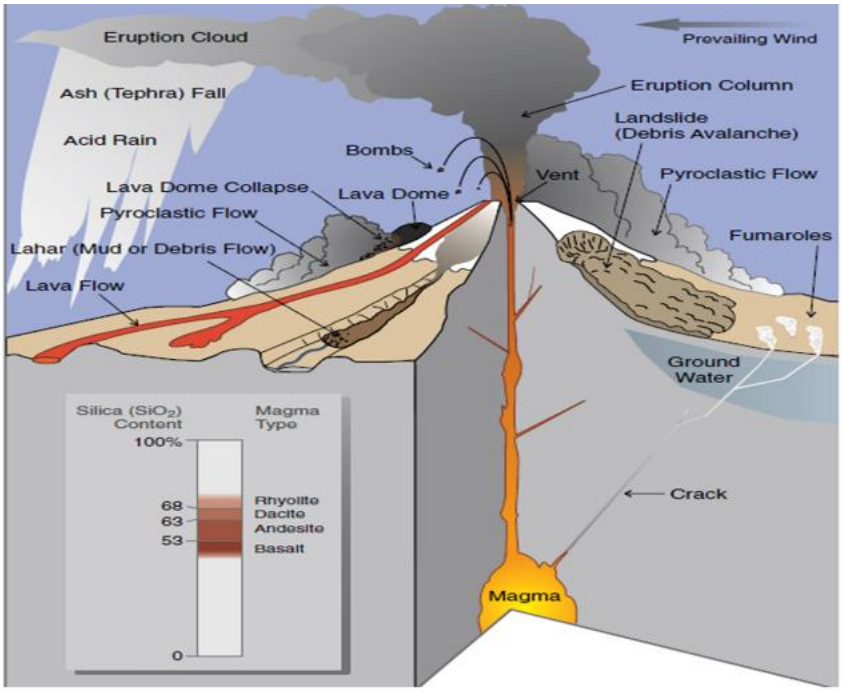

Figure 2.1. Hazards associated with a volcanic eruption. *Adapted from Myers et al. (2008).*

2.3 Volcanic soils

Volcanic soils generally referred to as Andosols (IUSS Working Group WRB, 2006) or Andisols (Soil Survey Staff, 2010), the 11th order in soil taxonomy, are products of volcanic material weathering. It can be found in both temperate and tropical environments with sufficient moisture and exhibits andic soil properties (Dahlgren et al., 2004). An andic horizon should have soil materials that contain less than 25 % organic C. It should also meet the following requirements in the fine-

earth fraction: *(i)* the Al_o (oxalate-extracted Al) + ½ Fe_o (iron-extracted Fe) is greater than or equal to 2.0, *(ii)* bulk density at 33 kPa water retention greater than or equal to 0.9 g cm^{-3}, *(iii)* P retention greater than or equal to 85 %, and *(iv)* at least 30 cm thickness of andic horizon. It was estimated that about 200 to 300 years may be sufficient to form an Andisol/andic character from fresh tephra under a humid weathering regime. In temperate regions, Andisols can reach maturity in 2000 to 3000 years. Typical Andisols in Japan are 4000 to 7000 years old (Shoji et al., 1993).

Andisols are largely dominated by silicate glass and the colloidal fraction consists of short-range order (SRO) mineral components (i.e. allophane/imogolite, ferrihydrite) and Al/Fe-humus complexes (Tan, 1984; Shoji et al., 1993). These secondary minerals are amorphous in nature and have pH-dependent variable charges (Leamy, 1984). Allophane/imogolite aluminosilicates and ferrihydrite, an Fe (hydr)oxide, are formed due to the rapid weathering of silicate glasses from volcanic materials (Ugolini & Dahglren, 2002; Lowe, 1986). Andisols generally form rapidly in humid climates and modify to other soil orders as soil age and degree of weathering increase (Ugolini & Dahlgren, 2002).

Andisols possess favorable characteristics due to the presence of SRO minerals and high humus accumulation. The SRO minerals and humus are responsible for the high water holding capacity, high phosphate retention, low bulk density, high friability, and formation of stable aggregates in Andisols (Ugolini & Dahlgren, 2002; Shoji et al., 1993). Organic carbon (OC) is stabilized and prevented from microbial decomposition due to complexation of humus with Al and Fe, and adsorption to SRO minerals (i.e. allophane/imogolite, ferrihydrite) (Dahlgren et al., 2004; Delmelle et al., 2015).

While tephra deposited on soil may release agronomically significant amounts of nutrient cations along with sulfur and phosphorus during the early stage of weathering (Ayris & Delmelle, 2012), a range of

elemental deficiencies is reported in Andisols, especially in those formed from silica-rich parent materials such as dacite, as they have low-nutrient contents (Delmelle et al., 2015). Reports on macro- and micro-nutrient deficiencies (i.e. N, S, Cu, Zn, B, Mn) and toxicity (i.e. Al) were also observed even in mature Andisols (Nanzyo, 2002, Shoji et al., 1993; Besoain et al. 1995).

2.4 Pedogenic processes occurring in volcanic soils

2.4.1 Factors affecting soil formation

A vital step in the formation of soil from rock involves weathering of the rock into small-sized and/or chemically altered parts (Yatsu, 1988). Weathering is the physical and chemical alteration of rocks and minerals at or near the Earth's surface as they adjust toward an equilibrium state in the surface environment, mediated by biological, chemical and physical agents or their combination (Pope et al., 2002).

The primary minerals in rocks are unstable within soils and weather to secondary minerals, commonly clay minerals (Schaetzl & Anderson, 2005). Figure 2.2 shows how different soil-forming factors influence the weathering rate of rocks which leads to the formation of clay minerals. The major factors that influence soil formation and weathering rates are parent material (solubility of minerals, sizes of grains, and patterns of fragmentation, such as joints and cleavage, in the bedrock), climate (temperatures, precipitation levels, and their seasonal patterns of variation), topography (slope steepness and the direction the slope faces, i.e. gentler slopes that face toward the sun promote better soil development), vegetation (crop type, land use, and management, organic matter accumulation), organisms (the diversity and abundance of organisms living in the soil), and time (the amount of time that a soil has to form) (Grotzinger & Jordan, 2014; Schaetzl & Anderson, 2005; van Breemen & Buurman, 1998).

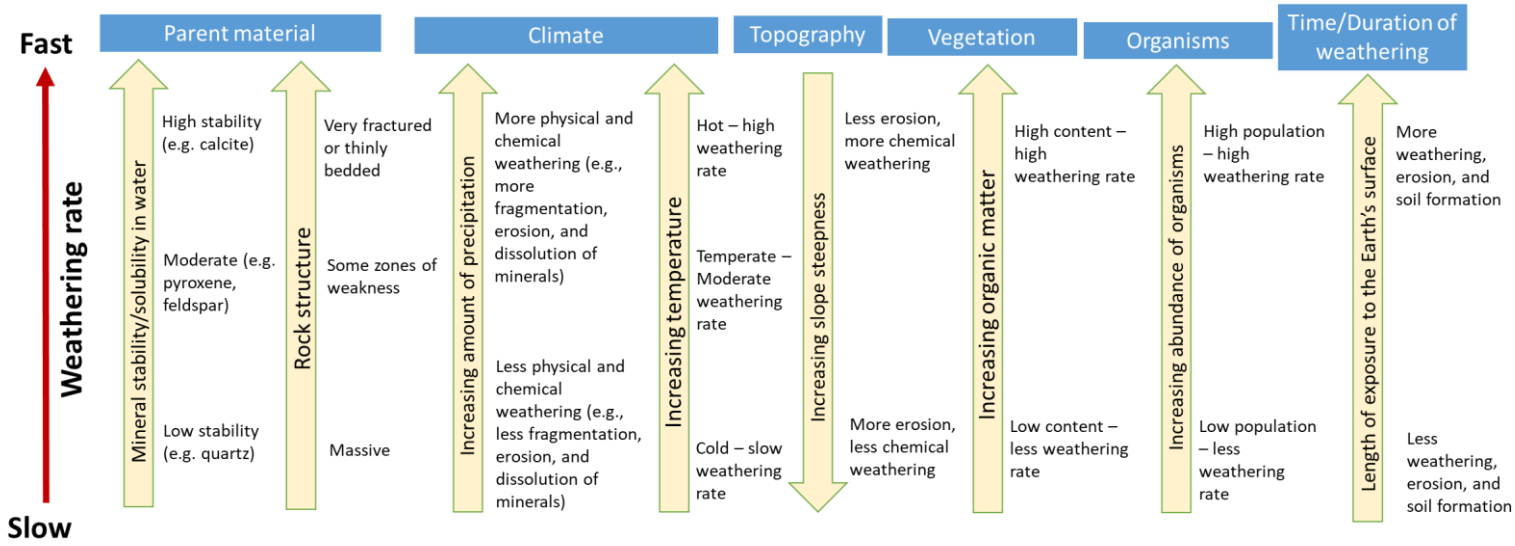

Figure 2.2. Summary of the factors that influence rock weathering. *Modified after Grotzinger & Jordan (2014).*

2.4.2 Primary mineral weathering and formation of secondary minerals

Weathering involves the (1) dissolution of minerals, (2) oxidation of some mineral compounds, the (3) leaching of dissolution products, and the (4) recombination or neoformation of weathering products to secondary minerals that are stable at the earth's surface. Clay minerals and iron compounds are by far the most important secondary minerals (van Breemen & Buurman, 2003). Figure 2.3 shows the stability of common primary minerals and volcanic glass to weathering. Minerals that weather slowly is termed as ‘‘resistant” minerals whereas those that weather more quickly is referred to as ‘‘weatherable” or ‘‘weak” minerals.

The vulnerability of various minerals to weathering is described in Bowen’s series, which illustrates that minerals that crystallize first from a molten state, i.e. the minerals which crystallized from magma at a higher temperature, are most susceptible to breakdown due to its instability in the surface temperature of the Earth (White & Brantley, 1995). The basalt, glasses, and olivines are normally the first phases altered by weathering (Wolff-Boenisch et al., 2004). Aside from crystallinity and chemical composition, the grain size and vesicularity which affects the surface area available for reactions also influences the rate of weathering (Delmelle et al., 2015).

Hydrolysis of the primary minerals and silicate glass requires the presence of water (Churchman & Lowe, 2012). This results in the removal of the more soluble components in the original or primary mineral (i.e. base cations and silica) followed by the precipitation or synthesis of a solid alteration product from the solution products referred to as “neogenesis”. In the process, new clays and other secondary materials are formed. An example of the hydrolysis wherein K-feldspar is transformed into kaolinite is given below:

$$2KAlSi_3O_8 + 9H_2O + 2H^+ \rightarrow Al_2Si_2O_5(OH)_4 + 4H_4SiO_4 + 2K^+$$

K-feldspar — Kaolinite — Silicic acid

Eq. 2.1

The hydrolysis of silicates such as potassium (K)-feldspar in water releases an acid (silicic acid) and a base (hydroxyl-Al-Si, *kaolinite*). The weathering that proceeds in aqueous solutions are acidic because water (H_2O) is charged with dissolved CO_2, hence there is a continuous supply of carbonic acid and H^+ ions. Hydrogen ions are important weathering agents (Carroll, 1970; Chamley, 1989).

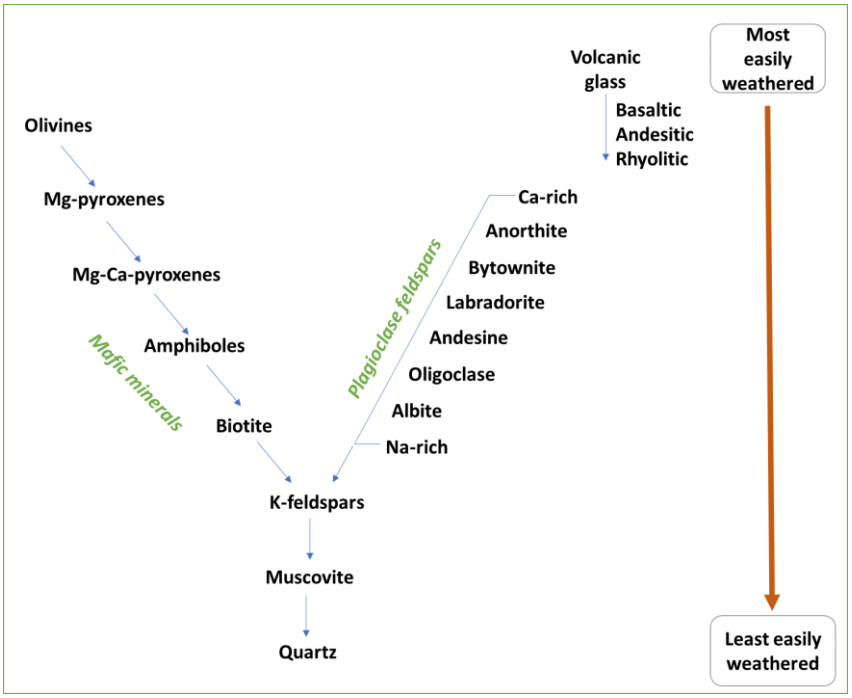

Figure 2.3. Stability series for the common primary minerals and volcanic glass. *Modified after Goldich (1938) and Wolff-Boenisch et al. (2004*).

Primary minerals tend to dominate in coarser size fractions, whereas secondary minerals are most abundant in the clay and fine silt fractions. The ferromagnesian minerals pyroxenes and amphiboles, although slightly more stable than olivines, tend to break down in a similar fashion to the olivines in the field. Weathering of these minerals involves an initial loss of their divalent cations, typically Mg, Ca and Fe (II) which may result in the formation of smectite (Loughnan, 1969; Eggleton & Boland, 1982; Huang, 1989). Amphibole weathering led to the formation of dioctahedral (montmorillonite) and a trioctahedral (saponite) smectite, and also kaolinite-smectite simultaneously at the early stages of alteration based on the fine-scale examination of the mineral grain (Proust et al., 2006). Furthermore, the pyroxenes and amphiboles could give rise to kaolinite and Fe (III) oxides which have simpler structures (Wilson, 2004). Alteration of pyroxenes can also result in the formation of amorphous or non-crystalline intermediates (Churchman & Lowe, 2012). Feldspars have been considered as the source minerals for micas (Carroll, 1970; Millot, 1970) and very often also for kaolinites and halloysites (Eswaran & Wong, 1978; Calvert et al., 1980; Anand et al., 1985).

Secondary minerals could also derive elemental constituents from the breakdown of more than one primary mineral. Olivines, for instance, could give rise to smectite, kaolinite, halloysite, and also various (hydr)oxides of Fe (Huang, 1989). Smectites tend to form and persist in soils rich in silica, Mg^{2+}, and Ca^{2+}. These mobile elements can be found in both poorly drained environments and in those with intense long dry seasons. It can also form either by partial weathering of other 2:1 clays such as mica, vermiculite, and chlorite or neoformed by the dissolution of other minerals with subsequent precipitation/recrystallization of dissolved ions (Folkoff & Meentemeyer, 1985).

2.4.3 Chemical weathering of volcanic materials

In explosive eruptions, magma is fragmented by the rapid exsolution of dissolved volatile components to produce pyroclastic materials (Nakagawa & Ohba, 2002). Pyroclastic materials contain a large quantity of volcanic glass that has the least resistance to weathering resulting in the formation of SRO minerals (Shoji et al., 1993; Duchaufour, 1984). In volcanic materials, the major soil-forming processes that take place are the accumulation of organic matter and formation of SRO minerals (i.e. allophane, imogolite, ferrihydrite, opaline silica) acted upon by active Si, Al, and Fe compounds which is collectively known as the andosolization process (Ugolini & Dahlgren, 2002; Shoji et al., 1993).

The chemical weathering of easily weatherable minerals and volcanic glass produces relatively high concentrations of Ca, Mg, Al, Fe, and silica in solution. With this, solutions are super-saturated with respect to minerals of low solubility, and insufficient time is available for proper arrangement into crystalline structures. This results in the precipitation of amorphous Al, Fe, and Si components such as allophane, imogolite, opal, and ferrihydrite which do not have a regular three-dimensional structural framework, therefore exhibiting low resistance to chemical weathering (Dahlgren et al., 2004; Shoji & Ono, 1978; Shoji et al., 1985; Shoji et al., 1993; Dahlgren et al., 1993). The dissolved basic cations (Ca, Mg, K, Na) and part of the silica (H_4SiO_4, *silicic acid*) which are byproducts of the weathering process are removed with the drainage water (Van Breemen & Buurman, 1998).

Allophane aluminosilicate is purely amorphous and does not have a repeat of structural units in contrast to imogolite which is paracrystalline (Dahlgren et al., 1993). It is a weathering product of volcanic glass and feldspars or neoformed from weathering solutions which sometimes has a composition similar to kaolinite but in general exhibits a molar ratio of Al:Si = 2 (Wada, 1989). Ferrihydrite formation has been shown to occur preferentially when Fe^{2+}-containing waters are

oxidized very quickly or in the presence of constituents which impede crystal nucleation and growth (Schwertmann & Taylor, 1989). Ferrihydrite can be sorbed to silicates and organic matter, thereby inhibiting the crystallization of goethite and other Fe oxides such as lepidocrocite (Churchman, 2000; Bigham et al., 2002). Wada & Harward (1974) reported that nearly all varieties of volcanic ash (i.e. basalt, andesite, dacite, or rhyolite) produce allophane and allophane-like constituents, though some variation may occur in terms of nature, stability, and amount.

Dahlgren et al. (1993) cautioned that the composition of the minerals in the colloidal fraction of volcanic soils varies broadly depending on the (1) chemical, mineralogical, and physical properties of the parent material for the synthesis of secondary materials, (2) post-depositional weathering environment determined by interactions of soil temperature, rainfall, leaching, organic matter accumulations, addition of ash deposits, pH of weathering environment, and (3) stage of soil formation that considers the length of time that weathering has proceeded in a given deposit.

The fine particle size, glassy nature of the particles, high porosity and permeability of tephra deposits enhance chemical weathering rates (Dahlgren et al., 1997; Lowe, 1986; Ugolini & Dahlgren, 2002). Figure 2.4 shows a model relating to the effect of soil drainage and leaching conditions on allophane/imogolite versus halloysite formation. Increasing rainfall and leaching will result in the depletion in solution Si and preferential formation of Al-organic matter complexes instead of allophane/imogolite also termed as “anti-allophanic effect”. It is also triggered by the presence of crystalline 2:1 layer silicate clays such as smectite and vermiculite since these mineral phases also bind Al in solution. Thus, volcanic ash soils can be divided into two major groups based on their mineralogical composition: *(1)* “allophanic” are dominated by allophane and imogolite; and (2) “non-allophanic” dominated by Al-humus complexes and 2:1 layer silicates especially for those in humid weathering environments (Dahlgren et al., 2004;

Shoji & Ono, 1978; Shoji, 1985). Under low rainfall and leaching conditions, Si tends to accumulate, thereby promoting the accumulation of halloysite and silica-rich allophane. However, the andic properties should be met by these soils to be classified as Andisols.

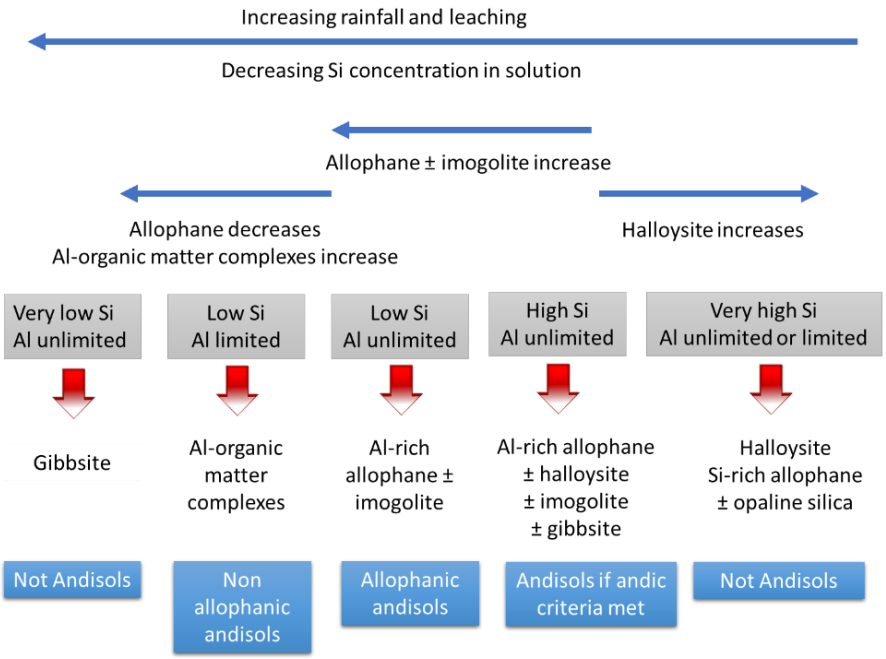

Figure 2.4. Simplified model illustrating the impact of silicon and aluminum leaching conditions on the formation of secondary minerals during weathering of volcanic tephra, and the likely occurrence or not of Andisols as a result. ± indicates the mineral may also be present. *Adapted from Delmelle et al. (2015), Churchman & David (2011), and McDaniel et al. (2011).*

2.4.4 Weathering indices to assess the degree of volcanic soil formation

Various geochemical weathering indices have been introduced to determine the degree of volcanic soil formation. The formation of secondary minerals (i.e. crystalline and SRO clays), depletion of silica

from volcanic glass components, and changes in the total elemental analysis of the bulk soil samples from the fresh tephra are used to estimate the degree of weathering (Dahlgren et al., 1993; Nanzyo et al., 1993). Aluminum is one of the major elements in tephras and in the secondary SRO aluminosilicates, hence, used to estimate the rate of chemical weathering in Andisols when soil age is known (Shoji et al., 1993).

The total reserve in bases (TRB) which gives the sum of total base cations, calcium (Ca), magnesium (Mg), potassium (K) and sodium (Na) to estimate the weatherable minerals in soils (Herbillon, 1989) is widely accepted and used as a weathering index given that the age of volcanic deposits are known. The TRB includes the bases occluded in primary minerals, adsorbed on exchange sites, and perhaps in the secondary clay minerals (Delvaux et al., 1989). The ratio of secondary Fe oxides, measured by dithionite-citrate-bicarbonate, to the total Fe present in the soil (Fe_d/Fe_t), increases as weathering proceeds (Mehra & Jackson, 1960), hence it is commonly used as a weathering index (Ameijeiras-Mariño, 2017; Vermiere, 2016). The changes in the elemental composition of tephras under leaching conditions can be demonstrated as a function of the secondary clay content to estimate the degree of weathering (Nanzyo et al., 1993; Dahlgren et al., 1997; White et al., 1986; Dethier et al., 1981).

Several weathering indices derived from the chemical and mineralogical data of pyroclastic deposits have been proposed by various researchers. These indices were used as basis by Fiantis et al. (2009; 2017) to assess the weathering degree of the young volcanic soils in Mt. Merapi as well as the paddy soils in the vicinity of other volcanoes in West Sumatra, Indonesia (i.e. Mt. Sago, Mt. Singgalang, Mt. Tandikek, and Caldera Maninjau). Among the weathering indices are the Ruxton ratio [R] (Ruxton, 1968), weathering index of Parker [WIP] (Parker, 1970), Vogt's residual index [V] (Vogt, 1927), chemical index of alteration [CIA] (Nesbitt & Young, 1982), chemical index of weathering [CIW] (Harnois & Moore, 1988), plagioclase index of

alteration [PIA] (Fedo et al., 1995), desilication index [DI] (Singh et al., 1998; Stockmann et al., 2016), Ba/Sr leaching (Nesbitt et al., 1980); loss of bases (Kronberg & Nesbitt, 1981); elemental ratio of elements resistant to weathering (Stockmann et al., 2016), and calcium to titanium ratio [CTR] (Bétard, 2012).

2.5 Impact of soil burial by volcanic materials

Shoji et al. (1993) suggested the clay formation in the buried soil proceeds similarly to that of the non-humus horizon in a manner that Al/Fe-humus complexes and pedogenic opal formation are halted due to prevention of OM addition but allophane/imogolite formation are favored in the process. However, the review paper of Delmelle et al. (2015) provided some evidence that burying the soil with new tephra deposits potentially stop soil formation as tephra isolates the buried soil from the pedogenic processes. Organic matter is also preserved especially when surface soil horizons are buried due to intermittent ash deposition (Dahlgren et al., 2004; Tan, 1984). The organic matter becomes isolated from soil macro- and mesofauna via encapsulation within small pores and abundant soil aggregates after tephra addition. The ability of microorganisms to degrade organic materials is prevented due to reduced soil aeration (Delmelle et al., 2015; Dahlgren et al., 2004). The rate of tephra accumulation and burial may have a significant effect on on-site conditions which can affect the weathering conditions, for instance, change in topography influences lateral drainage (Taylor, 1933; Gibbs, 1968).

2.6 Silicon and phytoliths in plants and soils

Silicon (Si) is one of the most abundant element of the earth's crust with nearly 29 % mean content (Rao et al., 2018). Although Si is a non-essential nutrient element, it is generally known to improve resistance

to lodging, pest, and diseases; erectness; water-use efficiency; photosynthetic rate; metal toxicity alleviation; NPK fertilizer efficiency; and improve grain yields (Klotzbücher et al., 2015; Guntzer et al. 2012; Sauer et al., 2006; Ma & Takahashi, 1990).

Most of the Si in the soil is stored in primary minerals, precipitated in crystalline and amorphous clay minerals, or adsorbed in sesquioxide complexes. These minerals release Si to the soil solution through chemical weathering where rates are affected by the type and particle size of the minerals (Drever, 1994; Jackson et al., 1948). Amorphous silica originates from volcanic glass (geogenic), opal (pedogenic), plant phytoliths and microorganism remnants (biogenic) (Cornelis et al., 2014). It is more soluble than primary and secondary crystalline silicate minerals (Clymans et al., 2013; Puppe et al., 2017; Barão et al., 2014; Oehler, 1979; Fraysse et al., 2006).

In a soil-plant system, the processes that govern the Si cycle are closely related to the weathering of silicates and in the same manner, the terrestrial plant contributes significantly to soil formation (Keller, 2012). The readily-soluble Si components that are present in young volcanic ash soils such as pedogenic, geogenic, biogenic and those adsorbed Si on Fe oxides (i.e. ferrihydrite) and SRO minerals (i.e. allophane and imogolite) contribute in the Si balance (Cornelis et al., 2014).

Figure 2.5 illustrates the pools and fluxes of Si in the soil-plant system from Cornelis & Delvaux (2016) slightly modified based on the context of this study. The deposition of ash affects the soil Si cycle through the addition of Si-rich volcanic glass in the pool of primary minerals (LSi) which can be readily dissolved as DSi. The DSi may be absorbed by plants and precipitate as BSi. It returns to the soil as BSi upon biomass restitution and decomposition. The DSi can also be absorbed by soil heterotrophs (ZSi), leached out to groundwater and rivers, reprecipitate as secondary clay minerals (SCi), or gets adsorbed on Fe and Al oxide surfaces. The BSi and SCi may dissolve and contribute to the DSi pool,

depending on the activity of DSi in the soil solution. The BSi and SCi may also be carried down in suspension to the groundwater. Potential BSi addition to the soil from the plant biomass may also be disrupted due to biomass export.

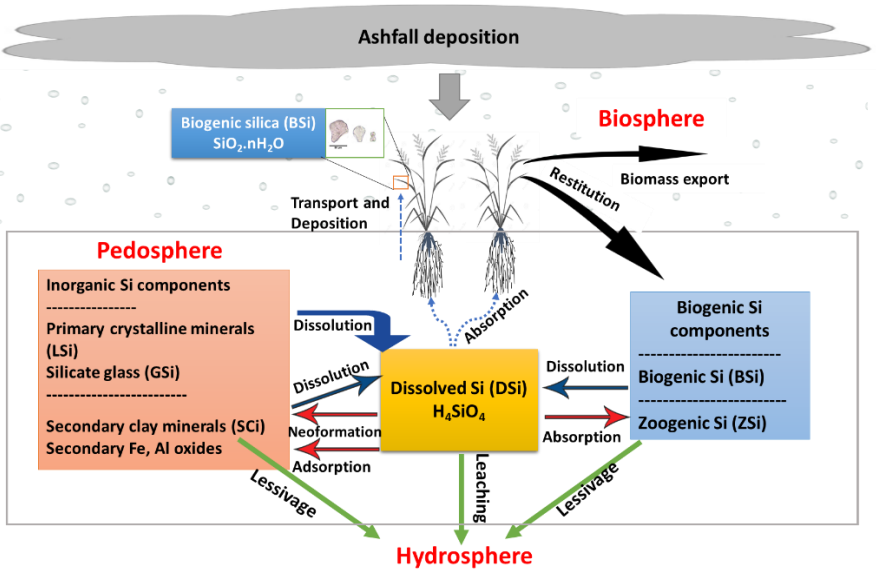

Figure 2.5. Silicon cycle in the soil-plant system affected by volcanic ash deposition. *Modified from Cornelis & Delvaux (2016).*

Phytoliths also referred to as biogenic silica (BSi), phytogenic silica, plant opal, amorphous opal-A, biogenic opal in various papers (herein excluding the BSi that is derived from microorganism remnants or 'zoogenic silica' or ZSi) are microscopic, a non-crystalline form of hydrated silica ($SiO_2 \cdot nH_2O$).

It is precipitated in the intracellular and/or intercellular spaces of plant tissues which form various shapes within species (Piperno, 1988; Cornelis et al., 2014; Gallego & Distel, 2004; Rovner, 1983; Clarke, 2003). It consists of 95 % non-crystalline dioxide (SiO_2) while the remaining includes 5 % includes water and other elements such as C,

Fe, Al, Ca (Puppe et al., 2017; Song et al., 2012; Buján, 2013). It may be colorless, light brown, or opaque while most are transparent and has a refractive index ranging from 1.41-1.47 and a specific density of 1.5-2.3 g cm^{-3} (Piperno, 2006).

The BSi are mostly deposited in the aerial parts of the plant (i.e leaves, stems, fruits, and even inflorescences). Within the plant, a higher proportion of BSi is accumulated in the leaves (aerial parts' transpiration termini) particularly in the cell wall and leaf epidermis (Puppe et al., 2017). In rice (*Oryza sativa)*, accumulation of BSi is maximum in the leaf sheath (12 %, dry matter), followed by leaf blade (7 %), stem (4 %), and the least is found in grains (2 %) (Li et al., 2014).

The majority of high Si-accumulators are monocotyledons, in particular *Graminae* (e.g. rice, sugarcane, and wheat) and *Cyperaceae* (e.g. sedges) (Henriet, 2008; Ma & Takahashi, 2002). Rice is a high-Si accumulating plant where BSi accounts for up to 10 % of the shoot dry weight (Deshmukh et al., 2017). *Oryza* species such as rice form three distinctive BSi shapes: (a) bilobate-shape or sheet element dumbbells (dumbbell with scooped ends paralleled arrangement) found in stems and leaves, (b) rice cuneiform or bulliform (fan-shaped) in rice leaves, and (c) double-peaked glume-shaped in the epidermis of rice husk (Zuo et al., 2016; Ball et al., 2015; Lu et al., 1997). The bulliform-shaped BSi which is abundant and unique to the rice leaf is highly resistant to decomposition (Zuo et al., 2017) while the bilobate-shaped BSi is typical of the *Oryzoideae* subfamily (Lu et al., 1997). Wet conditions may decrease the formation of bilobate BSi (Zuo et al., 2016).

A study of the biogeochemical cycle of silica in the Congo rain forest shows that BSi controls the dynamics of silica in soil solution (Alexandre et al., 1997). During soil formation, the dissolved Si released to the soil solution from lithogenic and biogenic silicates contributes to the neoformation of secondary phyllosilicates (Sommer et al., 2006). Silicon cycling by plants are shown to impact clay mineral stability or neoformation in upper soil horizons through "nutrient

uplift", in the process of BSi formation, which can counteract Si leaching (Cornelis et al., 2014; Lucas et al., 1993).

Recent researches show that plant BSi accumulation is influenced by type, age, and weathering stage of parent material because the latter factors affect the availability of plant-available Si, the monosilicic acid or dissolved silica (H_4SiO_4), from primary and secondary mineral weathering (Henriet, 2008; Cornelis et al., 2014; Opfergelt et al., 2008). Land use, climate, and soil conditions such as poor soil drainage and seasonal to permanent waterlogging in monsoonal tropics, tropical islands, and grasslands are said to promote BSi formation (Conley et al., 2006).

2.7 Phosphorus in plants and soils

Phosphorus (P) is essential for plant growth due to its functional role in cell division, root lengthening, seed and fruit development, and early ripening. It is a part of several plant compounds including oils and amino acids. It is highly involved in photosynthesis and other physiological and biochemical processes in plants (Pansu & Gautheyrou, 2006; Blaskó, 2011). The P compounds adenosine diphosphate (ADP) and adenosine triphosphate (ATP) serve as energy carriers within the plants (Roy et al., 2006). Sufficient P contents encourage vigorous root and shoot growth, promote early maturity, increase water use efficiency and grain yield of crops (USDA- NRCS, 1994). It is also beneficial for disease resistance and tolerance against bacterial or fungal crop diseases (e.g. phytophthora of potatoes) in plants (Roy et al. 2006).

Phosphorus is quantitatively ranked as the 9th most abundant element found at the earth's crust. In soil, it is common in the orthophosphate state ($-PO_4$) bound to calcium (apatites) with average contents estimated at approximately 0.1 % (Pansu & Gautheyrou, 2006). Unlike N, soil P is relatively stable in soil and is not as mobile. Soils with pH

values between 6.0 and 7.5 are ideal for P bioavailability, while pH values below 5.5 limit the availability of P due to fixation by Al and Fe, and at pH 7.5 to 8.5, P is fixed by Ca (USDA-NRCS, 1994). These complexed P constituents are not easily dissolved and become slowly available to crops over several years depending on the type of soil and P compound type (USDA-NRCS, 1994; Smith et al. 2015; Blaskó, 2011). Plants can only assimilate P directly in the form of hydrogen phosphates [HPO_4^{2-} (pH > 7.2), $H_2PO_4^-$ (pH < 7.2)] in the soil solution depending on soil pH (Pansu & Gautheyrou, 2006; Roy et al., 2006).

Phosphate occurs in the soil in both organic and inorganic forms that differ greatly in terms of their solubility and mobility. Figure 2.6 illustrates the P cycle in the soil-plant system affected by pyroclastic deposition (modified from Pierzynski et al., 2000). The P cycle of a soil buried by pyroclast is altered due to the addition and release of plant-available P upon weathering of the fresh deposit.

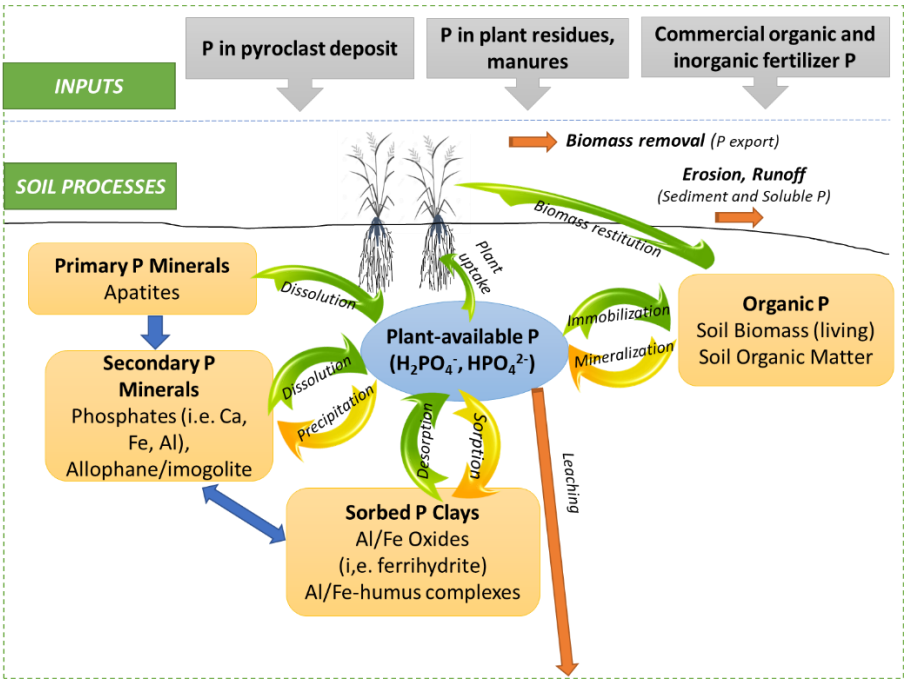

Figure 2.6. Soil phosphorus cycle affected by pyroclastic deposition. *Modified from Pierzynski et al. (2000).*

The P released also interacts with the products of chemical weathering including secondary crystalline clays (i.e. Al, Fe, and Ca phosphates) and SRO minerals (i.e. allophane/imogolite, ferrihydrite, Al/Fe-oxides, and Al/Fe-humus complexes). Organic P sources are added through the restitution of plant residues and manures in forested, grassland, and pasture lands. It can also be supplied from outside sources such as the application of dried manure and commercial organic fertilizers in croplands. Inorganic P comes from easily soluble P fertilizers applied in a cropland ecosystem. Phosphorus in the soil is absorbed by plants in its available form, orthophosphates ($H_2PO_4^-$, HPO_4^{2-}), through the dissolution of primary and secondary P minerals, desorption from Al/Fe-oxides and humus complexes, and mineralization from organic matter. Phosphorus is retained in the soil in less soluble forms when the plant-available P is precipitated with secondary P minerals, adsorbed to sesquioxides and humus complexes, and immobilized by microorganisms in organic form. Plant-available P is taken up by the plant and is returned back in the soil upon biomass restitution or lost in the soil when the biomass is exported from the field. Other losses of P are due to soil erosion, runoff, and leaching.

2.7.1 Impact of tephra deposition and weathering on P availability

Fresh tephra can release P upon its addition due to the rapid weathering of P-bearing minerals (Nanzyo et al., 1997). It is suggested that apatite [$Ca_5(PO_4)_3$(F,Cl,OH], the primary P-bearing mineral in fresh tephras which is fairly soluble in acid solutions, has significantly contributed to the rapid revegetation of tephra-affected areas in the early stage of weathering of young volcanic soils (Nanzyo et al., 1997; Nakamaru et al., 2000; Shoji & Takahashi, 2002; Nanzyo, 2002).

The propensity to retain P in volcanic soils is very high, due to the high content of Al and Fe compounds (Ugolini & Zasocki 1979). This makes them highly suitable for agricultural activities as it reduces the need for added fertilization leading to better yields and potentially lower costs of production. The strong fixation, however, can lead to problems that

can be resolved by applying corrective measures such as P fertilizer application (Brady & Weil 2004; Lebon, 2009).

2.8 Local research studies conducted on Mt. Pinatubo pyroclast deposits

2.8.1 Chemical properties of Pinatubo ash deposit

Grifal (1992) in his study attested that all plant nutrients decreased with increasing thickness of volcanic ash plowed into the soil, except for sulfate (SO_4) which tended to increase. Sulfate increased with increasing thickness of volcanic ash mixed into the soil from less than 100 ppm at 0 cm ash to near 2000 ppm at 20 cm thick. However, SO_4 concentration gradually decreased with time. The average soil pH decreased with time but did not show any significant change with increasing ash plowed into the soil. Furthermore, pH did not change with distance from the crater (near pH 7). Samonte et al. (1992) showed that the cation exchange capacity (CEC) decreased with increasing thickness of ash mixed into the soil. Ash deposits had much lower CEC (2.4 $cmol_c\ kg^{-1}$) and organic matter (0.21 wt.%) as compared with the soils' CEC of 10.6 $cmol_c\ kg^{-1}$ and 1.9 wt.% OM. The upper ash layers had a pH of 6.0 while the finer texture lowest layer had a pH of 4.48. Phosphorus (P) and K increased with increasing distance from crater. The calcium (Ca), SO_4, sodium (Na), silica (SiO_2), zinc (Zn), and manganese (Mn) were highest within 20 to 40 km radius. Ash layers contained lower exchangeable Ca, magnesium (Mg) and K than the soil but only Mg and K may be considered to show some deficiencies.

Reyes & Neue (1991) revealed that the volcanic materials are almost devoid of carbon (C) and nitrogen (N). In addition, P availability is also low even if it has an adequate amount of total P. The pH is near neutral to alkaline, although the more recent volcanic ejecta are acidic while lahars are likewise even more acidic. The soluble cations are moderately high, but the capacity to hold and exchange cations is very

low favoring leaching of these nutrients. The electrical conductivity measurements range from 4-9 dS/m.

2.8.2 Physical properties of Pinatubo ash deposit

The hydraulic conductivity increased and water holding capacity decreased with increasing ash mixed into the soil. The silt and clay decreased while the sand particles increased with increasing thickness of volcanic ash plowed into the soil (Grifal, 1992). It was observed however that the lowest layer of ash deposit was finer containing more silt and clay than the upper ash layers (Samonte et al., 1992). The texture of the ash shows varied contents of sand and silt but the clay content of all samples analyzed is less than 5 %. The texture of the ash is progressively finer as the distance from the volcano increases. The ash is 90-95 % sand, mainly medium to coarse sand, and also pumice rocks ranging in size from 0.5 cm to 3 cm within 30 km of the volcano (Reyes & Neue, 1991). Aganon & Undan (1992) observed that the soil temperature tended to increase to as high as 45 ^{o}C during noontime. The lahar hardens after application of irrigation water or after the occurrence of rain.

2.8.3 Chemical properties of the Pinatubo lahar deposit

The physicochemical properties of the initial lahar deposits in 1991 are as follows: acidic pH from 4.2 to 5.1 which is much lower than the ash, moderately high soluble bases, electrical conductivity of 2 to 4 dS/m, organic carbon and total nitrogen almost nil, marginal available P, sulfate-S is within normal range (Reyes & Neue, 1991). The availability of nutrient elements with time is variable as shown by Grifal (1992), i.e. P and copper (Cu) content increased by ~30 wt.% and 56 wt.%, respectively within 20 days; K decreased by as much as 66%, available sodium (Na) decreased by 67%, magnesium (Mg) decreased by almost 99%, zinc (Zn) decreased by ~55%, and manganese (Mn) decreased by

72% within 20 days; and iron (Fe) increased variably from 4% to 900% within 20 days; SO_4 was very variable but it tended to decrease with time.

2.8.4 Constraints identified and recommended adaptation practices based on local research studies

The major impacts of the Mt. Pinatubo eruption on rice production according to Mendoza & Cabangbang (1992) was the destruction of irrigation infrastructures and the change in soil texture which lead to the increased cost of rice production for rice. Furthermore, the effect of sand deposition under irrigated rice culture was *(1)* decreased water holding capacity of the soil, hence an increase in the duration and frequency of irrigation, *(2)* quick hardening of the soil when it dries up posing difficulty in cultivation and plant growing.

Various experiments have been undertaken to assess the agricultural productivity and rehabilitate the ash and lahar-affected farming areas in Central Luzon (Aganon, et. al., 1996; Icamina, 1992; Samonte et al. 1992; Mateo, 1993). Cowpea, corn, mungbean, and peanut are found to be responsive to fertilization on soils affected by volcanic ash. The most suitable crops for lahar are sweet potato, cassava, mungbean, peanut, red cowpea, pigeon pea, corn, sorghum, sesame, and leguminous cover crops (Samonte et al., 1992). Suyat (1992) demonstrated that lahar can support the growth and development of selected farm crops and gave reasonable yields when provided with an adequate amount of water and fertilizer. The application of 6 to 12 t ha^{-1} of chicken manure improved the properties of the mixed ash and buried soil, respectively compared to the pure ash, respectively, i.e. 0.20 vs. 0.04 wt.% OM, 47 vs. 5 ppm P, 0.29 vs. 0.05 $cmol_c\ kg^{-1}$ K, and 2.4 vs. 0.04 $cmol_c\ kg^{-1}$ CEC (Samonte et al., 1992).

According to Herrera (1992), lowland rice responded significantly to 90-30-30 and 120-30-30 N-P-K levels of fertilizers attaining grain yields of 4.9 to 5.3 t ha^{-1}. Other management recommendations for rice

include *(1)* planting of early maturing varieties, *(2)* deep plowing and thorough mixing of the ash/sand with the original soil, *(3)* incorporation of organic matter to attain at least 2 % OM in the new ash/soil mixture. Soils in submerged conditions should be allowed 2 to 4 weeks before transplanting/seeding in order to reduce the potential for hydrogen sulfide (H_2S) toxicity in the young plant where S/SO_4 concentration is high, *(4)* dry or wet seeding is recommended to shorten land preparation and crop establishment, *(5)* increase the application of NPK fertilizer to about 30 % higher than the recommended prior to eruption (for 50:50 mix) which can be reduced proportionately depending on the thickness of the ash, (*6)* if strong smell of H_2S is observed (similar to odor of rotten egg) and where roots are predominantly black, drain the field and irrigate after 3 to 5 days.

The compaction of sand-soil mixture rendered difficulty in rice transplanting. The wet and dry method of rice seeding was observed to be more suitable than transplanting in terms of plant recovery and grain production on soil covered with 5 to 15 cm sand. In < 5 cm of sand deposits, transplanting of rice seedlings was done without much difficulty (Herrera, 1992). According to Nelson (2013), the critical requirement for rehabilitation is the presence of irrigation water because the lack of it will entail difficulty in plowing the land properly for the suitable growth of rice.

2.8.5 Farmers adaptation practices

Nelson (2013) documented the land rehabilitation techniques employed by rice farmers in Pampanga to cope with the damage caused by volcanic ashfall and other debris. To cope with the constraints brought by the deposition of volcanic materials on their soil, the farmers scrape the sand and put in more fertilizers and water. Quarrying, removal of stones, and bulldozers were used to flatten the land are the adaptation practices of farmers with severely damaged farms.

In rice monocropping farms, the farmers have diverted their production system to high-value upland crops (vegetables, green corn, peanut, cucurbits, etc.) during the dry season. Farmers used organic fertilizer and recycled crop/animal residues. They also learned some adaptive cultural practices like hill method of planting crops, multiple cropping and more frequent application of fertilizer in small doses than one or two split applications. Some farmers shift to direct seeding of rice (DSR) even though the farmers are aware that they spend more in DSR in terms of added seeds (125-150 kg ha^{-1} seed) (Mendoza & Cabangbang, 1992).

2.9 References

Aganon, C. P., & Undan, R. C. (1992). CLSU's research and development activities in Mt. Pinatubo-affected areas. In *Proceedings of the symposium on sustainable agricultural development of Mt. Pinatubo-affected areas. November 5-6, 1992*. Farming Systems and Soil Resources Institute, College of Agriculture, University of the Philippines, Los Banos, College, Laguna.

Aganon, C. P., De La Cruz, N., Patricio, M. G. & Galindez, J. L. (1996). Fertilizer management for promising crops in ash and lahar laden areas in Central Luzon, Philippines; A Research and Development Effort. *Philippine Journal of Crop Science, May. Volume no. 21* Supplement no. 1. page 18.

Alexandre, A., Meunier, J.-D., Colin, F., & Koud, J.-M. (1997). Plant impact on the biogeochemical cycle of silicon and related weathering processes. Geochim. Cosmochim. *Acta 61*, 677–682.

Ameijeiras-Mariño, Y. (2017). Impact of forest conversion to cropland on soil weathering: a geochemical study at the pedon, slope and catchment scale. *Ph.D thesis.* Agronomique et Environnementale Earth and Life Institute, Environmental Sciences Université Catholique de Louvain.

Anand, R. R., Gilkes, R. J., Armitage, T. M., & Hillyer, J. W. (1985). Feldspar weathering in lateritic saprolite. *Clays Clay Miner. 33*:31–43.

Ayris, P. M., & Delmelle, P. (2012). The immediate environmental effects of tephra emission. *Bulletin of Volcanology*, *74*, 1905–1936. https://doi.org/10.1007/s00445-012-0654-5.

Ball, T., Chandler-Ezell, K., Dickau, R., Duncan, N., Hart, T. C., Iriarte, J., … Zhang, J. (2015). Phytoliths as a tool for investigations of agricultural origins and dispersals around the world. *Journal of Archaeological Science*, 1–14. https://doi.org/10.1016/j.jas.2015.08.010.

Barão, L., Clymans, W., Vandevenne, F., Meire, P., Conley, D. J., & Struyf, E. (2014). Pedogenic and biogenic alkaline-extracted silicon distributions along a temperate land-use gradient, *Eur. J. Soil Sci., 65*, 693–705, 2014.

Bernard, A., Knittel, U., Weber, B., Weis, D., Albrecht, A., Hattori, K., … Oles, D. (1996). Petrology and Geochemistry of the 1991 Eruption Products of Mount Pinatubo. In *C.. Newhall & R. S. Punongbayan*

(Eds.), Fire and mud, eruptions and lahars of Mount Pinatubo, Philippines (pp. 767–797). Univ. Washington Press, Seattle.

Besoain, R. & Hepp. (1995). The Hudson eruption and its effects on agriculture in the XI region [in Spanish], *Agricultura Técnica (Chile), 55*: 1-2, pp. 204-219.

Bétard, F. (2012). Spatial variation of soil weathering processes in a tropical mountain environment: the Baturité massif and its pediment (Ceará, NE Brazil). *Catena 93*, 18–28.

Bigham, J. M., Fitzpatrick, R. W., & Schulze, D. G. (2002). Iron oxides. In *J.B. Dixon and D.G. Schulze (Eds.) Soil mineralogy with environmental applications.* p. 323–366. SSSA Book Series 7. SSSA, Madison, WI.

Bilderback, D. E., & Carlson, C. E. 1987. Effects of persistent volcanic ash on Douglas-fir in Northern Idaho. *US Department of Agriculture Forest Service Intermountain Research Station Research Paper, 380*, 1-3.

Blaskó, L. (2011). Soil science. Debreceni Egyetem. Agrár- és Gazdálkodástudományok Centruma.

Bliss, L. C. (1980). Lahar Deposits, 27–42.

Brady, N., & Weil, R. (2004). "Elements of the nature and properties of soils", Pearson Education, New Jersey, 606 p.

Buján, E. (2013). Elemental composition of phytoliths in modern plants (Ericaceae), Quatern. Int., 287, 114–120, 2013.

Calvert, C. S., Buol, S. W., & Weed, S. B. (1980). Mineralogical transformations of a vertical rock–saprolite–soil sequence in the North Carolina Piedmont. *Soil Sci. Soc. Am. J. 44*:1096–1112.

Carroll, D. (1970). Rock Weathering. *Monographs in Geoscience.* Plenum Press, New York.

Chamley, H. (1989). Clay sedimentology. *Springer-Verlag*, Berlin, Germany.

Chrurchman, G. J. (2000). The alteration and formation of soil minerals by weathering. In *Sumner, M. E. (Ed.). Handbook of soil science.* CRC Press. Boca Raton London New York Washington, D.C. pp. F.3-F.76.

Churchman, G.J., David, J.L., 2011. Alteration, formation, and occurrence of minerals in soils. In: *Huang, P.M., Li, Y., Summer, M.E. (Eds.), Handbook of Soil Sciences. CRC Press*, pp. 1e72.

Churchman, G., & Lowe, D. (2012). Alteration, formation, and occurrence of minerals in soils. *CRC Press*, *1*, 20–72. https://doi.org/doi:10.1201/b11267-24.

Cochran, V. L., Bezdicek, D. F., Elliott, L. F. (1983). The effect of Mount St. Helen's volcanic ash on plant growth and mineral uptake. *Journal of Environmental Quality, 12,* 415-418.

Conley, D. J., Sommer, M., Meunier, J. D., Kaczorek, D., Saccone, L. (2006). Silicon in the terrestrial biogeosphere. In Ittekot V, Unger D, Humborg C, Tac An N (Eds.), *The Silicon Cycle.* Human perturbations and impacts on aquatic systems. SCOPE, 66, pp 13-28.

Cornelis, J.-T., & Delvaux, B. (2016). Soil processes drive the biological silicon feedback loop. Funct. Ecol. 30, 1298–1310.

Cornelis, J. T., Dumon, M., Tolossa, A. R., Delvaux, B., Deckers, J., & Van Ranst, E. (2014). The effect of pedological conditions on the sources and sinks of silicon in the Vertic Planosols in South-western Ethiopia. *Catena*, *112*, 131–138. https://doi.org/10.1016/j.catena.2013.02.014.

Clarke, J. (2003). The occurrence and significance of biogenic opal in the regolith, *In Earth-Science Reviews, Volume 60,* Issues 3–4, 2003, Pages 175-194.

Clymans, W., Verbeeck, T., Tielens, S., Struyf, E., Vandevenne, F., & Govers, G. (2013). Amorphous silica preservation in an anthropogenic soil: An explorative study of "plaggen" soils. *ACS Symposium Series*, *1154*, 3–14. https://doi.org/10.1021/bk-2013-1154.ch001.

Dahlgren, R. A., Dragoo, J. P., & Ugolini, F. C. (1997). Weathering of Mt. St. Helens tephra under a cryic-udic climatic regime. *Division S-9 Soil Mineralogy. Published in Soil Sci. Am. J. 61*:1519-1525.

Dahlgren, R., Shoji, S., & Nanzyo, M. (1993). Mineralogical characteristics of volcanic ash soils. In *Shoji, S., Nanzyo, M. & Dahlgren, R (Eds.). Volcanic ash soils: Genesis, properties, & utilization. Developments in Soil Science 21,* Elsevier, Amsterdam: 101-143.

Dahlgren, R. A., Saigusa, M., & Ugolini, F. C. (2004). The nature, properties, and management of volcanic soils. *Advances in Agronomy, 82,* 113–182. https://doi.org/10.1016/S0065-2113(03)82003-5.

Dale, V. H, Delgado-Acevedo, J., & MacMahon, J. (2005). Effects of modern volcanic eruptions on vegetation. In G. G. J. Martí, J, Ernst (Ed.), *Volcanoes and the Environment* (pp. 227–248). Cambridge University Press.

Delmelle, P., Opfergelt, S., Cornelis, J.-T., & Ping, C.-L. (2015). Volcanic Soils. In Sigurdsson, H., Houghton, B., Rymer, H., Stix, J., McNutt, S. (Eds.), *The Encyclopedia of Volcanoes* (pp. 1253–1264). Elsevier Inc.

Delvaux, B., Herbillon, A. J., & Vielvoye, L. (1989). Characterization of a weathering sequence of soils derived from volcanic ash in Cameroon. Taxonomic, mineralogical and agronomic implications. *Geoderma, 45*, 375–388. https://doi.org/10.1016/0016-7061(89)90017-7.

Deshmukh, R. K., Ma, J. F., & Bélanger, R. R. (2017). Role of Silicon in Plants. *Frontiers in Plant Science*. https://doi.org/10.3389/978-2-88945-352-8. 187 p.

Dethier, D. P, Pevear, D. R., Frank, D. (1981). Alteration of new volcanic deposits. In *Lipman P. W., Mullineaux, D. R. (Eds.). The 1980 eruptions of Mount St. Helens, Washington. US Geol Surv Prof Pap 1250*, Washington, pp 649–665.

Drever, J. I. (1994). The effect of land plants on weathering rates of silicates minerals. *Geochim Cosmochim Acta 58:* 2325– 2332.

Duchaufour, P. (1984). Edafología, Parte 1, Edafogénesis y clasificación: Barcelona, Masson, 433 p.

Eggleton, R. A., & Boland, J. N. (1982). Weathering of enstatite to talc through a sequence of transitional phases. *Clays Clay Miner. 30*:11–20.

Eswaran, H., & Wong, C. B. (1978). A study of a deep weathering profile on granite in Peninsular Malaysia. Parts I, II, and III. *Soil Sci. Soc. Am. J. 42*:144–158.

Fedo, C. M., Nesbitt, H. W., & Young, G. M. (1995). Unraveling the effects of potassium metasomatism in sedimentary rocks and paleosols, with implications for paleoweathering conditions and provenance. *Geology 23*, 921–924.

Fiantis, D., Nelson, M., Van Ranst, E., Shamshuddin, J., & Qafoku, N. P. (2009). Chemical weathering of new pyroclastic deposits from Mt. Merapi (Java), Indonesia. *Journal of Mountain Science, 6*, 240–254. https://doi.org/10.1007/s11629-009-1041-3.

Fiantis, D., Gusnidar, Malone, B., Pallasser, R., Van Ranst, E., & Minasny, B. (2017). Geochemical fingerprinting of volcanic soils used for wetland rice in West Sumatra, Indonesia. *Geoderma Regional*, *10*(April), 48–63. https://doi.org/10.1016/j.geodrs.2017.04.004.

Folkoff, M. E. & Meentemeyer, V. (1985). Climatic control of the assemblages of secondary clay minerals in the A-horizon of United States soils. *Earth Surf. Proc. Landforms 10*: 621–633. 1987. Climatic control on the geography of clay minerals genesis. Ann. Assoc. Am. Geog. 77: 635–650.

Fraysse, F., Pokrovsky, O. S., Schott J., & Meunier, J. D. (2006). Surface properties, solubility, and dissolution kinetics of bamboo phytoliths. *Geochim. Cosmochim. Acta 70*, 1939–1951.

Gallego, L., & Distel, R. A. (2004). Phytolith assemblages in grasses native to central Argentina. *Annals of Botany, 94*, 865–874. https://doi.org/10.1093/aob/mch214.

Gibbs, H. S. (1968). Volcanic-ash soils in New Zealand. *Information Series No. 65*. Wellington, New Zealand: New Zealand Department of Scientific and Industrial Research.

Goldich, S. S. (1938). A study in rock weathering. *J. Geol. 46*:17–58.

Grifal, R. (1992). Physico-chemical, mineralogical, and hydrological characterization of volcanic ash and lahar and their utilization and management for agricultural crops. In *Proceedings of the symposium on sustainable agricultural development of Mt. Pinatubo-affected areas. November 5-6, 1992.* Biotech Seminar Room, UPLB, College, Laguna. Farming Systems and Soil Resources Institute, College of Agriculture. University of the Philippines at Los Baños, College, Laguna

Grotzinger, J. P., & Jordan, T. H. (2014). Understanding earth. Seventh Edition. Printed in the United States of America.

Guntzer, F., Keller, C., Poulton, P. R., Mcgrath, S. P., & Meunier, J. (2012). Long-term removal of wheat straw decreases soil amorphous silica at Broadbalk, Rothamsted. *Plant Soil (2012), 352*, 173–184. https://doi.org/10.1007/s11104-011-0987-4.

Henriet, C. (2008). Silicon in banana (Musa spp.): A soil-plant system approach. PhD thesis. Université catholique de Louvain. UCL - AGRO - Sciences agronomiques et ingénierie biologique.

Herbillon, A. J, (1989). Chemical estimation of weatherable minerals present in the diagnostic horizons of low activity clay soils. *8th. Int. Soil Classif. Workshop 1986 (Brazil)*, pp. 39-48.

Herrera, I. O. (1992). Mt. Pinatubo R & D program of the department of agriculture-Region III. In *Proceedings of the symposium on sustainable agricultural development of Mt. Pinatubo- affected areas.* November 5-6, 1992. Farming Systems and Soil Resources Institute, College of Agriculture, University of the Philippines, Los Banos, College, Laguna.

Huang, P. M. (1989). Feldspars, olivines, pyroxenes, and amphiboles, p. 975–1050. In *Dixon, J. B., & Weed, S. B. (Eds.) Minerals in soil environments. 2nd edn*. SSSA, Madison, WI.

Icamina, P. (1992). Life after Pinatubo: Conjuring crops from fire, mud, and ash. Press Foundation of Asia, Phil. The FAO review (FAO) 24:2 pp.23-28.

IUSS Working Group WRB. (2006). World reference base for soil resources 2006. *World soil resources report no. 103*. Rome: FAO.

Jackson, M. L., Tyler, S. A., Willis, A. L., Bourbeau, G. A., & Pennington, R. P. (1948). Weathering sequence of clay-size minerals in soils and sediments. I. Fundamental generalizations. *Journal of Physical and Colloid Chemistry 52*:1237-1260.

Janda, R. J., Daag, A. S., Delos Reyes, P. J., Newhall, C. G., Pierson, T. C., Punongbayan, R. S., Rodolfo, K. S., Solidum, R. U., Umbal, J. V. (1996). Assessment and response to lahar hazard around Mount Pinatubo, 1991 to 1993. In *Newhall CG, Punongbayan RS (eds) Fire and Mud: Eruptions and Lahars of Mount Pinatubo, Philippines*. Philippine Institute of Volcanology and Seismology, Quezon City, and University of Washington Press, Seattle, pp 107–139.

Kenedi, C. A., Brantley, S. R., Hendley II, J. W., & Stauffer, P. H. (2000). Volcanic Ash Fall—A "Hard Rain" of Abrasive Particles. *USGS Fact Sheet 027-00. U.S. Geological Survey-Reducing the Risk from Volcano Hazards.*

Keller, C., Guntzer, F., Barboni, D., & Meunier, J. (2012). Comptes Rendus Geoscience Impact of agriculture on the Si biogeochemical cycle: Input from phytolith studies ´ ochimique du silicium : *apport des e les phytolithes*, *344*, 739–746. https://doi.org/10.1016/j.crte.2012.10.004.

Klotzbücher, T., Marxen, A., Vetterlein, D., Schneiker, J., Türke, M., van Sinh, N., … Jahn, R. (2015a). Plant-available silicon in paddy soils as a key factor for sustainable rice production in Southeast Asia. *Basic and Applied Ecology*, *16*, 665–673. https://doi.org/10.1016/j.baae.2014.08.002.

Kronberg, G. I., & Nesbitt, H. W. (1981). Quantification of weathering of soil chemistry and soil fertility. *J. Soil Sci. 32*, 453–459.

Leamy, M. L. (1984). International committee on the classification of Andisols (ICOMAND) *Circular letter No. 6*, New Zealand Soil Bureau. DSIR, Lower Hutt.

Lebon, S. L. G. (2009). *Volcanic activity and environment: Impacts on agriculture and use of geological data to improve recovery processes*. Master in Environmental Sciences and Natural Resources Management. University of Iceland.

Li, Z., Song, Z., & Cornelis, J. (2014). Impact of rice cultivar and organ on elemental composition of phytoliths and the release of bio-available silicon. *Frontiers in Plant Science, 5*(October), 1–8. https://doi.org/10.3389/fpls.2014.00529.

Loughnan, F. C. (1969). Chemical weathering of the silicate minerals. *Elsevier*, New York.

Lowe, D. J. (1986). Controls on the rates of weathering and clay mineral genesis in airfall tephras: a review and New Zealand case study. In Colman, S. M. & Dethier, D. P. (*Eds.*). Rates of chemical weathering of rocks and minerals. pp. 265-330. Academic Press, Orlando.

Lu, H. Y., Wu, N. Q., & Lu, B. Z. (1997). Recognition of rice phytoliths. In *Pinilla, A., Juan- Tresserras, J., Machado, M.J. (Eds.), Estado actual de los estudios defitolitos en suelosy plantas: The State-of-the-art Phytoliths in Soils and Plants.* Centro de Ciencas Medioambientales, Madrid, pp. 159-174.

Lucas, Y., Luizão, F. J., Chauvel, A., Rouiller, J., & Nahon, D. (1993). The relation between biological activity of the rainforest and mineralogical composition of soils, *Science, 260*(5107), 521–523, doi:10.1126/science.260.5107.521.

Luhr, J. F., & Melson, W. G. (1996). Mineral and glass compositions in June 15, 1991, pumices: Evidence for dynamic disequilibrium in the dacite of Mount Pinatubo. In *Newhall, C.G. and Punongbayan, R.S. (Eds.). Fire and mud. Eruptions and Lahar of Mount Pinatubo, Philippines. Philippine Institute of Volcanology and Seismology, Quezon City*. University of Washington Press, Seattle, and London. Printed in Hongkong.

Ma, J. F. & Takahashi, E. (1990). Effect of silicon on the growth and phosphorus uptake of rice. *Plant and Soil, 126*, 115–119.

Ma, J. F., &, Takahashi, E. (2002). Soil, Fertilizer, and Plant Silicon Research in Japan. Amsterdam, the Netherland: Elsevier.

Mateo, L. (1992). Characterization and amelioration of lowland rice soils affected by volcanic ejecta from Mt. Pinatubo. *Doctor of Philosophy. Dissertation manuscript*. 127 p. Philippines.

McDaniel, P.A., Lowe, D.J., Arnalds, O., Ping, C.-L., 2011. Andisols. In *Huang, P.M., Li, Y., Summer, M.E. (Eds.), Handbook of Soil Sciences. CRC Press,* pp. 29-45.

Mehra, O. P., & Jackson, M. L. (1960). Iron oxides removal from soils and clays by dithionite-citrate system buffered with sodium bicarbonate.

In: Proceeding of 7th National Conference Clay Minerals, Washington, pp 317-327.

Mendoza, T. C., & Cabangbang, R. P. (1992). Effects of Mt. Pinatubo eruption in crop production systems. *The Philippine Agriculturist, 75*(1 & 2), 1–8.

Millot, G. (1970). Geology of clays. *Springer-Verlag*, New York

Myers, B., Brantley, S. R., Stauffer, P., & Hendley II, J. W. (2008). What are Volcano Hazards? *U.S. Geological Survey Fact Sheet 002-97.*

Nakagawa, M., & Ohba, T. (2002). Minerals in volcanic ash 1: primary minerals and volcanic glass. *Resource Geology, 52*(2), 41–51.

Nakamaru, Y., Nanzyo, M., & Yamasaki, S. (2000). Utilization of apatite in fresh volcanic ash by pigeon pea and chickpea. *Soil Sci. Plant Nutri., 46*:591-600.

Nanzyo, M., Dahlgren, R., & Shoji, S. (1993). Chemical characteristics of volcanic ash soils. In Shoji, S., Nanzyo, M., & Dahlgren, R., *Volcanic ash soils - genesis, properties, and utilization. Developments in Soil Science 21*, Elsevier, Amsterdam: 145-188.

Nanzyo, M., Takahashi, T., Sato, A., Shoji, S., & Yamada, I. (1997). Dilute acid-soluble phosphorus in fresh air-borne tephras and fixation with an increase in active aluminum and iron. *Soil Science and Plant Nutrition, 43*(4), 839–848. https://doi.org/10.1080/00380768.1997.10414650.

Nanzyo, M. (2002). Unique properties of volcanic ash soils. *Glob. Environ. Res. 6.*

Nelson, G. L. (2013). Land rehabilitation techniques of rice farmers in Pampanga (Philippines) after the Mt. Pinatubo Eruption. *Asia Life Sciences, 22*(1), 155–181.

Nesbitt, H. W., Markovics, G., & Price, R. (1980). Chemical processes affecting alkalis and alkaline earths during continental weathering. *Geochim. Cosmochim. Acta 44*, 1659–1666.

Nesbitt, H. W., & Young, G. M. (1982). Early proterozoic climates and plate motions inferred from major element chemistry of lutites. *Nature 299*: 715-717.

Newhall, C. G., & Punongbayan, R. S. (1996). Fire and mud. Eruptions and Lahar of Mount Pinatubo, Philippines. *Philippine Institute of Volcanology and Seismology*, Quezon City. University of Washington Press, Seattle, and London. Printed in Hongkong.

Newhall, C., Hendley II, J. W. & Stauffer, P. H. (1998). The Cataclysmic 1991 Eruption of Mount Pinatubo, Philippines. *U.S. Geological Survey Fact Sheet: 113-97.*

Oehler, J. H. (1979). Deposition and diagnesis of biogenic silica. *In Biogeochemical cycling of mineral-forming elements (Trudinger, P.A., and Swaine, D.J., eds.),* Elsevier, Amsterdam, pp. 467-483.

Opfergelt S., Delvaux B., AndrÉ, L., & Cardinal, D. (2008). Plant silicon isotopic signature might reflect soil weathering degree. *Biogeochemistry 91*, 163–175.

Orton, G. J. (1996). Volcanic environments. In Reading, H. G. (Ed.) *Sedimentary environments processes, facies and stratigraphy*. Cambridge, MA, Blackwell Science, pp. 485–567.

Pansu, M., & Gautheyrou, J. (2006). Handbook of Soil Analysis: Mineralogical, Organic and Inorganic Methods. Springer. 993 p.

Parker, A. (1970). An index of weathering for silicate rocks. *Geological Magazine 107*: 501-504.

Pierzynski, M., Sims, J. T., Vance, G. F. (2000). Soil phosphorus and environmental quality. In: *Soils and Environmental Quality*, CRC Press, Boca Raton, USA,155-207.

Piperno, D. R. (1988). Phytolith Analysis: An Archaeological and Geological Perspective. Academic Press, London, 280 pp.

Piperno, D. R. (2006). Phytoliths: A Comprehensive Guide for Archaeologists and Paleoecologists. Oxford: Altamira Press.

Pope, G. A., Meierding, T. C., & Paradise, T. R. (2002). Geomorphology's role in the study of weathering of cultural stone. *Geomorphology 47*: 211–225.

Proust, D., Caillaud, J., & Fontaine, C. (2006). Clay minerals in early amphibole weathering: Tri- to dioctahedral sequence as a function of crystallization sites in the amphibole. *Clays Clay Miner. 54*:351–362.

Puppe, D., Höhn, A., Kaczorek, D., Wanner, M., Wehrhan, M., & Sommer, M. (2017). How big is the influence of biogenic silicon pools on short-term changes in water-soluble silicon in soils? Implications from a study of a 10-year-old soil-plant system. *Biogeosciences, 14*, 5239–5252. https://doi.org/10.5194/bg-14-5239-2017.

Rantucci, G. (1994). Geological Disaster's in the Philippines: The July 1990 earthquake and the June 1991 eruption of Mount Pinatubo - Description. *Effects and Lessons Learned. Report in cooperation with PHILVOLCS,* Rome: Italian Ministry of Foreign Affairs, Directorate-

General for Development Cooperation.

Rao, G. B., Pi, P. Y., & Syriac, E. K. (2018). Effect of various silicon sources on nutrient uptake by rice and available nutrient status in soil. *Journal of Pharmacognosy and Phytochemistry*, *7*(2), 1449–1452.

Reyes, R. Y., & Neue, H. U. (1991). Characterization of the volcanic ejecta from Mount Pinatubo and its impact on rice production. *Philippine Journal of Crop Science, 16*(2), 69–73.

Rovner, I. (1983). Plant opal phytolith analysis: major advances in archaeobotanical research. In: Schiffer M (Ed.), *Advances in archaeological method and theory*. New York: Academic Press, 225–260.

Roy, R. N., Finck, A., Blair, G., & Tandon, H. (2006). Plant nutrition for food security: A guide for integrated nutrient management. *FAO Fertilizer and Plant Nutrition Bulletin, (16)*, 21.

Ruxton, B. P. (1968). Measures of the degree of chemical weathering of rocks. *Journal of Geology 76*: 518-527.

Samonte, H. P., Badayos, R. B., Ocampo, A. M., Capunpon, E. G., delos Santos, E. G., & Willauer III, J. L. (1992). Improving the fertility status and productivity of areas affected by volcanic ash deposits of Mt. Pinatubo. In *Proceedings of the symposium on sustainable agricultural development of Mt. Pinatubo-affected areas. November 5-6, 1992*. Biotech Seminar Room, UPLB, College, Laguna. Farming Systems and Soil Resources Institute, College of Agriculture. University of the Philippines at Los Baños, College, Laguna.

Sauer, D., Saccone, L., Conley, D. J., Herrmann, L., & Sommer, M. (2006). Review of methodologies for extracting plant-available and amorphous Si from soils and aquatic sediments. *Biogeochemistry, 80(1*), 89–108. https://doi.org/10.1007/s10533-005-5879-3.

Savant, N.K., Snyder, G.H., & Datnoff, L.E. (1997). Silicon management and sustainable rice production. *Adv. Agron. 58,* 151-199.

Schaetzl, R., Anderson, S. (2005). Soils: Genesis and Geomorphology. Cambridge University Press. Cambridge university press Cambridge, New York, Melbourne, Madrid, Cape Town, Singapore, São Paulo Cambridge. https://doi.org/10.2136/vzj2007.0030br.

Schwertmann, U., & Taylor, R. M. (1989). Iron oxides. In *Dixon, J. B. & Weed, S. B. (Eds.) Minerals in soil environments. 2nd edn.* p. 379–438. SSSA, Madison, WI.

Shoji, S. (1985). Genesis and properties of non-allophanic Andisols in Japan. *Applied Clay Sci. I*, 83-88.

Shoji, S., & Ono, T. (1978). Physical and chemical properties and clay mineralogy of Andosols from Kitakami, Japan. *Soil Sci., 125*:297-312.

Shoji, S., Nanzyo, M., & Dahlgren, R. A. (1993). Genesis of volcanic ash soils. In Volcanic Ash Soils: Genesis, properties and utilization. *Developments in Soil Science 21*, Elsevier, Amsterdam-London-New York-Tokyo.

Shoji, S., & Takahashi, T. (2002). Environmental and agricultural significance of volcanic ash soils. Global Environmental Research-English Edition, 6(2), 113–135.

Singh, L. P., Parkash, B., & Singhvi, A. K. (1998). Evolution of the lower gangetic plain landforms and soils in West Bengal, India. *Catena 33*, 75–104.

Smith, P., Cotrufo, M. F., Rumpel, C., Paustian, K., Kuikman, P. J., Elliott, J. A., … Scholes, M. C. (2015). Biogeochemical cycles and biodiversity as key drivers of ecosystem services provided by soils. *Soil, 1*(2), 665–685. https://doi.org/10.5194/soil-1-665-2015.

Soil Survey Staff. (2010) Keys to soil taxonomy, *11th edn*. USDA-Natural Resources Conservation Service, Washington, DC.

Song, Z. L., Wang, H. L., Strong, P. J., Li, Z. M., & Jiang, P. K. (2012). Plant impact on the coupled terrestrial biogeochemical cycles of silicon and carbon: Implications for biogeochemical carbon sequestration. *Earth-Sci. Rev. 155*, 319–331. doi: 10.1016/j.earscirev.2012.09.006.

Sommer, M., Kaczorek, D., Kuzyakov, Y., & Breuer, J. (2006). Silicon pools and fluxes in soils and landscapes-a review. *Journal of Plant Nutrition and Soil Science, 169,* 310–329.

Stockmann, U., Cattle, S. R., Minasny, B., & McBratney, A. B. (2016). Utilizing portable X-ray fluorescence spectrometry for in-field investigation of pedogenesis. *Catena 139*, 220–231.

Suyat, M. N., Lacson, R. T., & Bayot, A. J. (1992). Adaptability test of different field crops under lahar-laden soils. In *Proceedings of the symposium on sustainable agricultural development of Mt. Pinatubo-affected areas. November 5-6, 1992*. Biotech Seminar Room, UPLB, College, Laguna. Farming Systems and Soil Resources Institute, College of Agriculture. University of the Philippines at Los Baños, College, Laguna.

Tan, K. H. (1984). Andosols. *Van Nostrand Reinhold Company Inc. Benchmark Papers in Soil Sciences, Volume 4*.

Taylor, N. H. (1933). Soil processes in volcanic ash beds, Part I. *New Zealand Journ. Sci. and Tech., Vol. 14,* p. 193-202, Wellington, New Zealand.

Ugolini, F. C., & Zasoski, R. J. (1979). Soils Derived from Tephra. In *Volcanic Activity and Human Ecology*. https://doi.org/10.1016/b978-0-12-639120-6.50009-1.

Ugolini, F. C., & Dahlgren, R. A. (2002). Soil Development in Volcanic Ash, 69–81.

USDA-NRCS. (1994). Soil Phosphorus: Soil Quality Kit- Guides for Educators. *United States Department of Agriculture: Natural Resources Conservation Service*, 1–6. Retrieved from http://www.nrcs.usda.gov/Internet/FSE_DOCUMENTS/nrcs142p2_053254.pdf.

van Breemen, N., & Buurman, P. (1998). Soil formation. Dordrecht, The Netherlands. *Kluwer Academic Publishers.*

van Breemen, N., & Buurman, P. (2003). Soil formation Second edition. *Kluwer Academic Publishers*, New York, Boston, Dordrecht, London, Moscow.

Vermiere, M., Cornu, S., Fekiacova, Z., Detienne, M., Delvaux, B., & Cornelis, J. (2016). Rare earth elements dynamics along pedogenesis in a chronosequence of podzolic soils, *Chemical Geology* (2016).

Wada, K. (1989). Allophane and imogolite. In *Dixon, J. B., & Weed, S.B. (Eds.), Minerals in soil environments, 2nd edn. Soil Sci. Soc. Am.*, Madison, WI. pp, 1051-1087.

Wada, K., & Harward, M. E. (1974). Amorphous clay constituents of soils. *Advances in Agronomy 26*:211-260.

White, A. F., & Brantley, S. L. (Eds.). (1995). Chemical weathering rates of silicate minerals. *Rev. Mineral. 31*: 1–583.

White, A. F., Benson, L. V., & Yee, A. (1986). Chemical weathering of the May 18, 1980, Mount St. Helens ash fall and the effect on the iron creek watershed, Washington. In *Rates of chemical weathering of rocks and minerals (pp. 351–374).* Academic Press, Inc., Harcourt Brace Jovanovich, Publishers.

Wilson, M. J. (2004). Weathering of the primary rock-forming minerals: Processes, products and rates. *Clay Miner. 39*:233–266.

Wolff-Boenisch, D., Gislason, S. R., Oelkers, E. H., & Putnis, C. V. (2004). The dissolution rates of natural glasses as a function of their

composition at pH 4 and 10.6, and temperatures from 25 to 74 °C. *Geochimica et Cosmochimica Acta 68*: 4843-4858.

Zuo, X., Lu, H., Li, Z., Song, B., Xu, D., Zou, Y., … He, K. (2016). Phytolith and diatom evidence for rice exploitation and environmental changes during the early mid-Holocene in the Yangtze Delta. *Quaternary Research, 86,* 304–315. https://doi.org/10.1016/j.yqres.2016.08.001.

Zuo, X., Lu, H., Jiang, L., Zhang, J., Yang, X., Huan, X., … Wu, N. (2017). Dating rice remains through phytolith carbon-14 study reveals domestication at the beginning of the Holocene. *Proceedings of the National Academy of Sciences, 114*(25), 6486–6491. https://doi.org/10.1073/pnas.1704304114.

Chapter 3 Early-stage of weathering and soil formation processes in the pyroclast deposits from the 1991 Plinian eruption of Mt. Pinatubo, Philippines

3.1 Introduction

Volcanic soils are typically associated with continental volcanic regions. They include all soils derived from the weathering of eruption products such as tephra (< 2-64 mm grain size), pyroclastic density currents, debris or mudflows (lahar) deposits, and lava flows (Shoji et al., 1993). They cover about 1 % of the world's land surface (~110 to 124 million ha). The large majority of volcanic soils are classified as Andisols, i.e. soils with Andic properties (Shoji et al., 1993). These soils, which occur in both temperate and tropical environments with sufficient moisture, typically contain glass and short-range-order colloidal weathering products such as allophanes, imogolite, and ferrihydrite (minerals). They are also rich in organic matter. A such composition confers to Andisols a set of unique characteristics, including a high water retention capacity, good drainage, good structure, adequate cation exchange capacity, high phosphate retention, and excellent tilth (Dahlgren et al., 2004; Shoji et al., 1993; Nanzyo, 2002; Besoain et al., 1995). Accordingly, they usually exhibit high fertility and are intensively used in agriculture. Despite their limited extension, they sustain approximately 10 % of the world's population (Kimble et al., 2000).

Most volcanic soils derive from volcanic ejecta (pyroclasts). These include tephra fall, pyroclastic density current, and debris flow deposits. The Andic character is the result of moderate weathering. If not rejuvenated with fresh volcanic materials, Andisols evolve over time to other, more weathered soil types. Rejuvenation occurs more or less

frequently depending on volcanic activity. If the deposit is not too thick, the fresh material is incorporated by bioturbation/cryoturbation in the surface horizon and pedogenesis is continued. However, if the deposit exceeds 10-20 cm, soil development may be halted, i.e. the pre-eruption soil is buried and isolated from the atmosphere by the volcanic ejecta or debris (NRCS, 2013; Chaopricha & Marín-Spiotta, 2014). A new cycle of soil formation will then begin, driven by weathering of the freshly-emplaced deposit and eventually leading to the formation of young surface soil with Andic characteristics.

Rapid weathering of the glassy component of fresh fragmentary volcanic materials is fundamental to pedogenesis in volcanic deposits. It is responsible for the formation of several poorly ordered and metastable solid phases (Dahlgren & Ugolini, 1989; Shoji et al., 1993) that impart the distinctive properties of Andisols. In general, weathering in the soil environment is strongly affected by soil temperature, leaching intensity, the flux of protons, pH, and complexing ligand concentrations of the percolating soil solution (Lowe, 1986; Shoji et al., 1993). Time and climate are regarded as the key factors governing mineralogical transformations in tephra deposits (e.g., Lowe, 1986; Wada, 1989; Shoji et al., 1993; Ugolini & Dahlgren, 2002),

Long-term weathering patterns have been studied by examining the mineralogical characteristics of tephra deposits spanning hundreds to thousands of years (Lowe, 1986; Ruxton, 1988; Smith et al., 1999). These analyses suggest half-lives for volcanic glass ranging from 1650 to 7000 yr (Wada, 1987; Ruxton, 1988; Shoji et al., 1993) and a generalized mineralogical transformation pathway consisting of opaline silica, Al-organic matter complexes, allophane, and imogolite as early weathering products with halloysite and gibbsite forming during later stages of weathering. In contrast, investigations on chemical weathering and mineralogical transformations occurring over decades of time are scarce. Dahlgren et al. (1989) focused on the initial stage of weathering in tephra from the 1980 eruption of Mt. St. Helens, USA. Ten years of weathering under a cryic-udic (2300 mm annual rainfall, 5.5 °C air

temperature) climatic regime led to the accumulation of Al and Fe as alteration products, but there was no evidence of opaline, allophanes, or imogolite formation. In Hokkaido, Japan, soils developed on Mt. Usu's volcanic ash show Entisolic properties after 25 years of weathering in a udic soil moisture regime (Shoji, 1993), but allophanes/imogolite had not yet accumulated. To the best of our knowledge, there is no equivalent study documenting the early stage of weathering and soil formation processes in newly emplaced volcanic deposits in a tropical climate.

In this chapter, we seek to answer several key questions concerning the initial stages of weathering of the pyroclast deposit and soil formation from the 1991 eruption of Mt. Pinatubo, Philippines. We examine the properties of the new soils that have been forming on tephra fall and lahar materials since 1991, and we compare them with those measured for the original, ~500-yr old soil buried under these deposits. We seek to address the following questions (i) what chemical and mineralogical changes occur in the tephra and lahar materials during the initial 26 years of weathering?, and (ii) what is the fate of the Si, Al, and Fe released by weathering?

3.2 Materials and Methods

3.2.1 Site characterization and soil sampling

Location and climate of the study area

The study took place in the provinces of Pampanga (Porac and Floridablanca municipalities) on the east and southeast, respectively, Tarlac (Bamban municipality) on the northeast, and Zambales (San Marcelino municipality) on the southwest of Mt. Pinatubo in Central Luzon, Philippines (Figure 3.1). The selected sites in Pampanga and Tarlac are affected by ashfall whereas the site in Zambales is buried by

lahar deposit during the 1991 Mt. Pinatubo eruption due to their close proximity to the volcano (Bautista, 1996).

The provinces of Tarlac, Pampanga, and Zambales have a tropical monsoon climate. The annual mean rainfall of Zambales (western side of Mt. Pinatubo) is higher, i.e. 3502 mm (1990-2018; Iba, Zambales weather station) than in Pampanga and Tarlac provinces (east of Mt. Pinatubo) with 2002 mm (1998-2018; Clark, Pampanga weather station). The annual mean temperature of all the study sites is 27 °C (PAGASA, 2019).

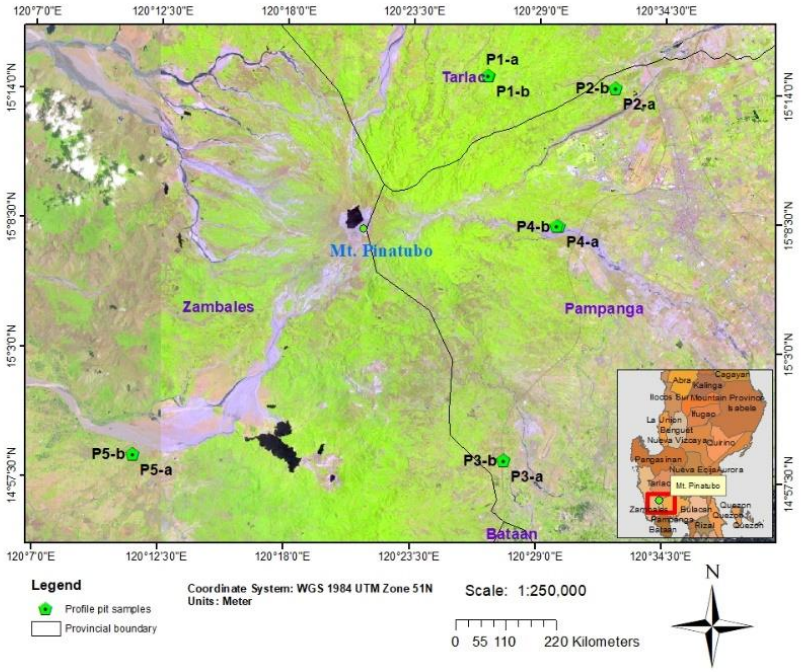

Figure 3.1. Location map of the study sites in Central Luzon, Philippines showing its proximity to Mt. Pinatubo volcano. *Two soil profile pits were collected each from the five study sites with varying land uses (green dotted pentagons). P1-a and P1-b are ash affected-forest soil profiles (Fo-Ash; Bamban, Tarlac), P2-a and P2-b are ash affected-paddy (irrigated) rice soil profiles (IR-Ash; Bamban, Tarlac),*

P3-a and P3-b are ash-affected grassland soil profiles located in low altitude (Gr-LA-Ash; Floridablanca, Pampanga), P4-a and P4-b are ash affected-grassland soil profiles located in high altitude (Gr-HA-Ash; Porac, Pampanga), P5-a and P5-b are paddy rice-lahar affected soils (IR-Lahar; San Marcelino, Zambales).

General characteristics of the study sites and field soil sampling

The general site description (i.e. location, altitude, slope, distance from the crater) and the photograph of a representative soil profile are shown in Figure 3.2. The complete site description of all the ten soil profiles (i.e. two soil profiles per sampling site) is shown in Table A.3.1.

The five sampling sites vary according to land use, altitude, slope, type and thickness of the pyroclastic deposit. Uncultivated soils affected by ash are collected from [P1] forest (Fo-Ash; Bamban, Tarlac), [P4] grassland located in high altitude (Gr-HA-Ash; Porac, Pampanga), and [P3] grassland located in low altitude (Gr-LA-Ash; Floridablanca, Pampanga). Two soils are collected in agricultural (cultivated) soils grown to paddy rice, one affected with ash [P2] (IR-Ash; Bamban, Tarlac) and another with lahar [P5] (IR-Lahar; San Marcelino, Zambales). The soil profiles selected showed a clear stratification of the newly developing modern soil (MS horizon) from the 1991 Mt. Pinatubo pyroclastic deposit, and the buried soil (BS horizon) developed from the previous volcanic deposit emplaced ~500 years ago (Newhall & Punongbayan, 1996).

Two adjacent soil profiles, 20 to 50 meters apart, were collected for each of the five study sites to serve as pseudo-replicates. The depth of the soil profiles range from ~40 to 90 cm. The soil profiles from P1 and P5 sites were collected on April 13, 2018, and those from P2, P3, and P4 on September 19-21, 2017.

Non-cultivated soils

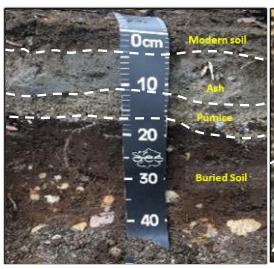

Land Use: Forest (P1-a; Fo-Ash)
Pyroclast depth: 17 cm
Alt: 503 m.a.s.l
Slope: 5-9 %
Dist. from Mt. Pinatubo crater: 15 km NE
Location: Bamban, Tarlac

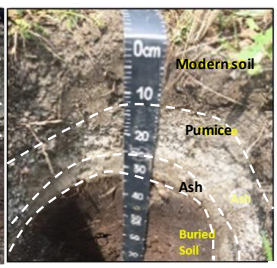

Land Use: Grassland in high altitude (P4-b; Gr-HA-Ash)
Pyroclast depth: 33 cm
Alt: 286 m.a.s.l
Slope: 5-9 %
Dist. from Mt. Pinatubo crater: : 16 km E
Location: Porac, Pampanga

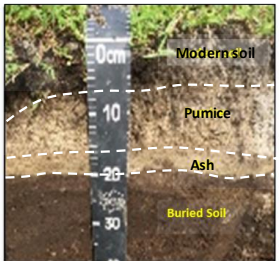

Land Use: Grassland in low altitude (P3-a; Gr-LA-Ash)
Pyroclast depth: 18 cm
Alt: 46 m.a.s.l
Slope: 0-4 %
Dist. from Mt. Pinatubo crater: 22 km SE
Location: Floridablanca, Pampanga

Cultivated soils



Land Use: Irrigated Rice (P2-b; IR-Ash)
Pyroclast depth: 31 cm
Alt: 105 m.a.s.l
Slope: 0-4 %
Dist. from Mt. Pinatubo crater: 23 km NE
Location: Bamban, Tarlac

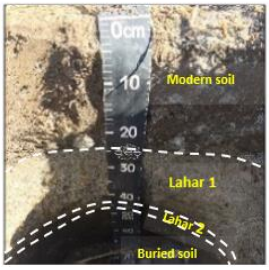

Land Use: Irrigated Rice (P5-b; IR-Lahar)
Pyroclast depth: 37 cm
Alt: 45 m.a.s.l
Slope: 0-4 %
Dist. from Mt. Pinatubo crater: 25 km SW
Location: San Marcelino, Zambales

Figure 3.2. Photograph of representative soil profiles from non-cultivated (forest, grassland) ash-affected soils and cultivated (paddy rice) ash and lahar-affected soils from Tarlac, Pampanga and Zambales, Philippines. *Alt: altitude, Dist: distance, E: east, SE: southeast; NE: northeast, SW: southwest*.

The Fo-Ash (P1-a, P1-b) soil profiles blanketed with 17 to 25 cm thick of ash (including pumice) are located ~15 km northeast of the Pinatubo crater at Brgy. Sto Niño, Bamban, Tarlac. It lies at an altitude of 503 to 512 m.a.s.l, with a gently undulating slope of 5 to 9 %. The Gr-HA-Ash (P4-a, P4-b) soil profiles collected at Brgy. Sapang-uwak, Porac, Pampanga have 27 to 33 cm thick ash deposit located 16 km east of Mt. Pinatubo crater, at an altitude of 283 to 286 m.a.s.l. and slope of 5 to 9 %. The Gr-LA-Ash (P3-a, P3-b) soil profiles at Brgy. Pabanlag, Floridablanca, Pampanga have thinner ash deposit (18-20 cm) than Fo-Ash and Gr-HA-Ash and is located farther from Mt. Pinatubo crater (22 km southeast). It is located at a lower altitude (40-46 m.a.s.l) with a relatively flat slope of 0 to 4 % compared to Gr-HA-Ash. The IR-ash (P2-a, P2-b) soil profiles at Brgy. San Vicente, Bamban, Tarlac have 31 to 39 cm thick ash deposit, located 23 km northeast of Pinatubo crater at 87 to 105 m.a.s.l and 0 to 4 % slope. The IR-lahar (P5-a, P5-b) soil profiles with 37 to 45 cm thick lahar deposit are located at San Marcelino, Zambales, 25 km southwest of Mt. Pinatubo crater. It is situated in a relatively flat area (0-4 % slope) at low altitude levels (45-48 m.as.l.).

The stratigraphy of the soil profiles consisting of fine ash and coarser pumice layers is influenced by the grain size nature of the tephra from various phases of the June 1991 Mt. Pinatubo eruption. Melosantos et al. (1996) illustrated in isopach maps the extent, distribution, and thickness of the tephra fall of the major eruption phases. Figure 3.3[a-d] shows the impact of the different eruption phases on the heterogeneity in grain sizes of the studied soil profiles.

The Fo-Ash, Gr-HA-Ash, and Gr-LA-Ash sites are not cultivated for agricultural crops prior to and after the eruption. In Fo-Ash, some trees and woods are utilized for house construction while some edible plants that grow inadvertently are consumed by some community residents at present. The IR-Ash and IR-Lahar are grown to irrigated paddy rice even before the 1991 eruption. The IR-Ash is re-established and grown to paddy rice since 2005. At present, rice is grown in this soil for two-

three seasons per year with a mean rice yield of 3.6 t ha^{-1} $season^{-1}$. Nutrient inputs are ~64 kg N ha^{-1}, ~7 kg P_2O_5 ha^{-1}, and ~7 kg K_2O ha^{-1}. In IR-lahar, irrigated rice is cultivated one-two times a year depending on the availability of water since its re-establishment in 2006. The farmer harvests about 3.9 t ha^{-1} $season^{-1}$ with nutrient input of ~92 kg N ha^{-1} (as per interview of farm owners).

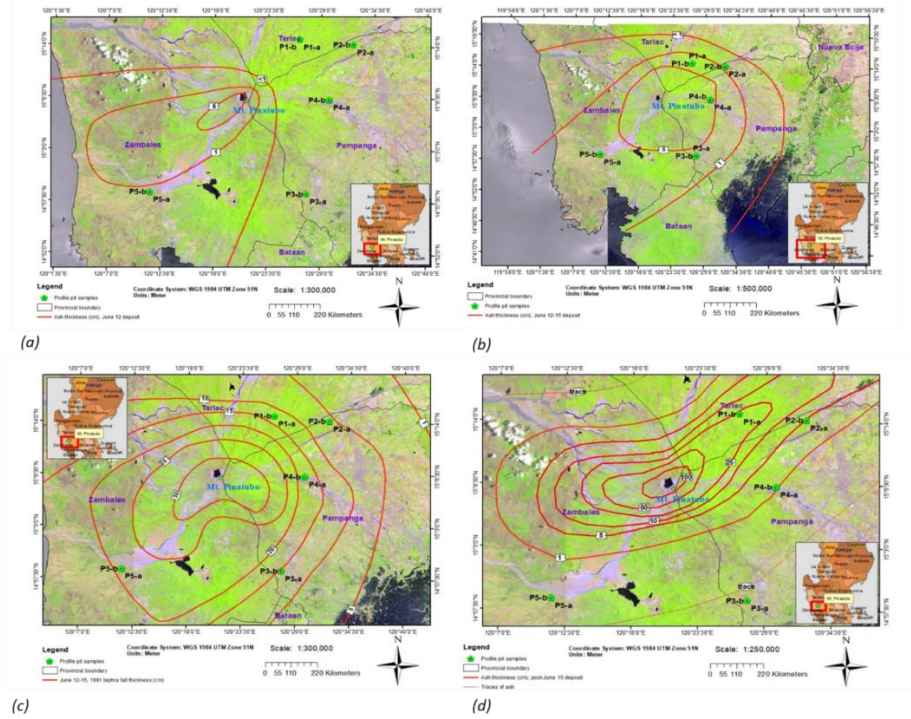

Figure 3.3. Distribution of *(a)* 0.014 km^3 tephra-fall deposited on June 12, 1991, consisting of andesitic scoria, ash, and accidental lithic fragments southwest of the volcano (phase IV), *(b)* 0.2 km^3, laminated, mostly fine-grained ash-fall deposit from late June 12 and early afternoon of June 15, 1991 (later part of phase IV to phase V), *(c)* ~4.4 km^3 dacitic pumice-fall deposit from June 15 (phase VI), *(d)* 0.2 km^3 fine-grained laminated tephra-fall that immediately followed the climactic eruption and continued for about 6 weeks (phase VII). *Isopachs are in centimeters. P1-a,b (Fo-Ash), P2-a,b (IR-Ash), P3-a,b (Gr-LA-Ash), P4-a,b (Gr-HA-Ash), P5-a,b (IR-Lahar). Maps used with the permission of the Philippine Institute of Volcanology and Seismology (PHILVOCS). Sampling sites are the green hexagon dotted points on the map.*

3.2.2 Soil physical and chemical analysis

A composite sample of 250 g was collected from each soil horizon and pyroclast layer. The samples were air-dried, crushed and passed through a 2 mm sieve. All the chemical analyses were conducted on the fine-earth fraction ≤ 2 mm (bulk). The chemical analyses were done in duplicates for some samples randomly selected for each analysis.

Soil profile description

Soil color was determined by taking a small amount of sample and breaking it to expose a fresh face. When dry, the sample is moistened. The color was determined for both dry and moist samples using the Munsell notation of hue value/chroma (Oyama, 1991). Other parameters including soil texture, structure, root abundance, stickiness, plasticity, and presence of mottles were described using standard terminologies according to Hodgson (1976) and Buol et al. (1997).

Particle-size distribution

Particle size distribution was determined through the quantitative recovery of clay (< 2 µm), silt (2 – 50 µm) and sand (50 µm – 2 mm) fractions after sonication and dispersion with Na^+-saturated resins for complete clay dispersion, followed by decanting and pipetting (Rouiller et al., 1972). There is no prior oxidation of organic matter using hydrogen peroxide (H_2O_2). The particle size distribution of sand, silt, and clay were expressed in weight percent (wt.%) of the bulk soil. Only one soil profile was analyzed for each of the Fo-ash, Gr-LA-Ash, Gr-HA-Ash, and IR-Lahar while two soil profiles were analyzed for IR-Ash.

pH measurements using water (H_2O) and potassium chloride (KCl)

The pH of soil and ash samples were measured potentiometrically in a benchtop digital pH meter using H_2O and 1N KCl at a 5:25 ratio (Page et al., 1982). The pH determined by the 1 N KCl method is an index of soil acidity (Soil Survey Staff, 2014).

Bulk density (BD)

Two samples were collected from the MS horizon of each soil profile using a stainless core sampler (20 cm^3) to extract the soil and pyroclast. Bulk density is the ratio of the solid mass to the bulk volume expressed as g cm^{-3} dry weight (Soil Survey Staff, 2014).

$$BD = \frac{M_s}{V_t} \qquad \textbf{\textit{Eq. 3.1}}$$

where BD is the bulk density (g cm^{-3}), M_s is the oven-dry mass (g), and V_t is the total volume (cm^3) of the sample.

Cation exchange capacity (CEC) and base saturation (BS)

The CEC was determined by saturating the exchange sites with ammonium (NH_4^+); washing the soil and pyroclast samples to remove excess saturated salt; displacing the NH_4^+ adsorbed by the samples; and finally measuring the amount of the NH_4^+ from the extract (Soil Survey Staff, 2014; Sobecki, 1990).

Specifically, crushed soil and ash samples (~500 mg) were leached with 1 N ammonium acetate (NH_4OAc) at pH 7. The extract was analyzed for base cations (Ca^{2+}, Mg^{2+}, K^+, and Na^+) using the ICAP 6000 Series, Inductively Coupled Plasma—Atomic Emission Spectrometer (ICP-AES). The NH_4^+ saturated sample was rinsed with methanol to remove the NH_4^+ that was not adsorbed. The residue was then distilled using

the Kjeldahl method after saturation with 50 % sodium hydroxide (NaOH) to displace all the NH_4^+ in a 2 % boric (H_3BO_3) acid. Afterward, the boric acid solution was titrated with 0.01 M sulfuric acid (H_2SO_4) to determine the NH_4^+ adsorbed on the soil exchange complex. The CEC is reported as $cmol_c\ kg^{-1}$ of the bulk soil.

Base saturation (% BS) is the sum of the NH_4OAc extractable bases divided by CEC and given by the following equation:

$$BS = \frac{A}{B} \times 100 \qquad \textbf{\textit{Eq. 3.2}}$$

where A is the sum of NH_4OAc extractable bases (Ca^{2+}, Mg^{2+}, K^+, Na^+) in $cmol_c\ kg^{-1}$ and B is the CEC concentration in $cmol_c\ kg^{-1}$.

The proportion of an exchangeable base cation in the exchange complex expressed in % is derived from the sum of NH_4OAc extractable bases:

$$\text{Exchangeable cation} = \frac{A}{B} \times 100 \qquad \textbf{\textit{Eq. 3.3}}$$

where A is any base cation (i.e. Ca^{2+}, Mg^{2+}, K^+, Na^+), and B is the sum of NH_4OAc extractable bases (Ca^{2+}, Mg^{2+}, K^+, Na^+).

Total carbon (C), total nitrogen (N), and organic matter (OM)

A 70-80 mg crushed sample (< 2 mm) was subjected to dry combustion (temp. > 900 °C). Total C (mainly organic C) and total N is measured using the Elementar Vario El Cube series elemental analyzer (Pansu et al., 2001) and expressed in wt.% of the dry matter. Soil organic matter (SOM) content was estimated from the organic C with the assumption that OM contains 58 % C (100/58 = 1.724 van Bemmelen factor) (Pansu & Gautheyrou, 2006).

$$SOM = \frac{\text{Organic C}}{1.724} \times 100 \qquad \textit{Eq. 3.4}$$

Where total C content is mainly organic, hence can be used interchangeably with organic C; and 1.724 is the van Bemmelen factor.

Total element analysis

Elemental analysis was carried out through loss on ignition at 1000 °C followed by borate fusion and dissolution of fusion crystals in 10 % nitric acid (HNO_3) (Chao & Sanzolone, 1992). In detail, a crushed sample (80-100 mg) was mixed with 0.4 g Li-tetraborate and 1.6 g Li-metaborate in a graphite crucible then heated at 1000 °C for 5 minutes until it melts and forms into a crystal bead. The crystal bead is then dissolved in 100 ml of 2 M nitric acid (HNO_3) while magnetically agitated at 100 °C. The concentration of Si, Al, Fe, Ca, Mg, Na, K, Mg, P, and Ti were measured using ICP–AES and expressed as wt.% oxide.

The total cations (Ca, Mg, Na, K) were summed up as the total reserve in bases (TRB) expressed in $cmol_c\ kg^{-1}$ soil. The TRB is used as an index of weathering. It includes the total Ca, Mg, Na, and K in primary minerals, on soil colloids' exchange sites and possibly also within secondary clay minerals (Herbillon, 1989; Delvaux et al., 1989).

Selective dissolution extractions using dithionite–citrate–bicarbonate, ammonium oxalate, and sodium-pyrophosphate

The dithionite-citrate-bicarbonate [DCB] Fe and Al (Fe_d, Al_d), ammonium oxalate extracted-Fe, Al, Si (Fe_o, Al_o, Si_o), and Na-pyrophosphate extracted-Fe, Al (Fe_p, Al_p) were selectively extracted from crushed bulk samples. The amount of samples used was ~700 mg for DCB and ~400 mg for both oxalate and Na-pyrophosphate extractions following the methods of Mehra & Jackson (1960), Bascomb (1968), and Blakemore et al. (1987), respectively. The extracted elements were expressed in wt.%.

The DCB is a selective dissolution extractant for organically complexed Fe and Al, short-range-order 'SRO' hydr(oxides) of Fe (i.e. ferrihydrite), and Al from SRO aluminosilicates (i.e. allophane/imogolite). It also extracts "free" (amorphous and crystalline) forms of Fe and Al that are not tied up in the lattice of primary minerals, has been weathered and released to the soil solution. It does not extract opal, Si, or other constituents of silicate minerals (Wada, 1989).

The Na-pyrophosphate (1M $Na_4P_2O_7$) selectively extracts organically bound forms of Al and Fe (Al_p, Fe_p) gauging the abundance of organo-metallic complexes (Wada, 1989). It does not extract opal, crystalline silicates, layer silicates, and crystalline hydrous oxides of Fe and Al (Yuan et al., 1993).

The Fe, Al, and Si extracted by ammonium oxalate comprises principally of (i) Al and Fe in organic complexes, (ii) Fe in SRO (hydr)oxides (i.e. ferrihydrite), and (iii) Al and Si in SRO aluminosilicates (i.e. allophane/imogolite) (Dahlgren et al., 1997; Dahlgren and Ugolini, 1989). It does not dissolve opaline ($SiO_2 \cdot nH_2O$) and crystalline silica (SiO_2) (Wada, 1982).

The analysis of oxalate extractable Si (Si_o) is a relatively sensitive method that can detect allophane and imogolite concentrations (Dahlgren et al., 1997; Dahlgren & Ugolini, 1989). Estimated allophane/imogolite content is given by the formula of Parfitt & Henmi (1982).

$$\text{Allophane/imogolite content} = Si_o \times 7.1 \qquad \textbf{\textit{Eq. 3.5}}$$

Where Si_o is the oxalate-extractable Si expressed in wt.%; 7.1 is the factor to convert Si_o to allophane/imogolite.

Ferrihydrite contents are estimated based on the oxalate-extracted Fe using the following equation of Childs et al. (1991),

$$\text{Ferrihydrite content} = Fe_o \times 1.7 \qquad \textbf{\textit{Eq. 3.6}}$$

where Fe_o is the oxalate-extractable Fe expressed in wt.%; 1.7 is the conversion factor of Fe_o to ferrihydrite.

Phosphate retention (P-retention)

Phosphate retention is also called P adsorption, sorption, or fixation. It refers to the percent P retained by the soil after equilibration with 100 mg kg^{-1} P solution containing soluble P for 24 hours. A 2 g bulk sample was shaken in a 10 ml P-retention solution for 24 h. The P-retention solution was prepared by mixing 4.40 g potassium dihydrogen phosphate (KH_2PO_4), 16.4 g anhydrous sodium acetate (CH_3COONa), and 11.5 ml glacial acetic acid in 1 L distilled water. The mixture (soil + P retention solution) was centrifuged at 2000 rpm for 15 minutes. An aliquot of the supernatant was analyzed using the ICP-AES. The P retention of soil material is a measure for andic soil properties (Soil Survey Staff, 2014; Blakemore et al., 1987).

$$\text{P retention} = \text{Initial P concentration} - \text{P remaining in sample solution} \qquad \textbf{\textit{Eq. 3.7}}$$

Where 'P retention' is the P retained in the sample after equilibration (24-hr shaking) with the initial P concentration of 100 mg kg^{-1} P solution expressed in percentage.

3.2.3 Soil mineralogical analysis

Mineralogy of the bulk soil and clay-sized fraction

Soil mineralogy was done on the bulk sample (< 2 mm, crushed to a fine powder), and clay-sized fractions (< 2 μm) using X-ray diffraction (XRD). Figure 3.4 shows a step-by-step process of the mineral identification for both the bulk and clay-sized fractions of the soil and pyroclast samples. The samples were analyzed using a Bruker D8 Advance X-ray diffractometer operated at 40 kV and 30 mA with a step width of 0.02° and a counting time of 2.0 sec/step, using Kα radiation sourced from a Cu target anode. Randomly oriented mounts of the crushed materials were used (Fejdi & Holocsy, 2001). X-ray diffraction methods allow for the distinction among various clays based on the expansion or contraction of the interlayer space, i.e. the region between adjacent 2:1 or 1:1 layers, in the presence of different cations and solvents (Brown & Brindley, 1980, Whittig & Allardice, 1986).

The clay-sized particles were subjected to K^+ and Mg^{2+} saturation, ethylene glycol solvation and thermal treatments at 105, 300 and 550 °C before XRD analysis. These pre-treatments steps will remove the aggregating agents (i.e. oxides, organic matter, carbonates) and isolate the clay fraction for thorough identification of the phyllosilicate minerals (Kunze & Dixon, 1986; Moore & Reynolds, 1989). All diffractograms were processed using the X-Ray peak matching software EVA© where the database of mineral patterns is programmed. The changes in XRD peak intensity, position and shape are diagnostic features for identifying the different minerals (Pansu & Gautheyrou, 2006). Table 3.1 shows a reference of the x-ray diffraction parameters (*d-spacings*) of common soil minerals after the pre-treatments which was used in the proper identification of phyllosilicate minerals.

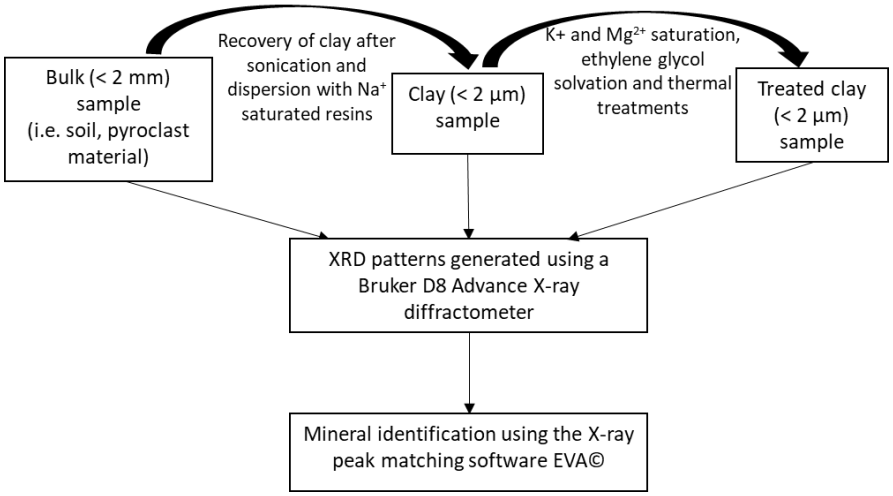

Figure 3.4. Step-by-step process in the mineral identification of the soil (bulk and clay) and pyroclast samples.

Table 3.1. X-ray diffraction parameters of common soil minerals.

MINERAL	TREATMENT				
	Mg^{2+} 20 °C	**Mg^{2+} Gly**	**K^{+} 20 °C**	**K^{+} 300 °C**	**K^{+} 550 °C**
	(diffraction spacing in angstroms, Å)				
Kaolinite	7	7	7	7	LD[1]
Halloysite	7B[2]	7B	7B	7B	LD
[3]Halloysite	4.48	4.48	4.48	4.48	LD
Vermicullite	14	14	10	10	10
Smectite	14	18	12.5	10	10
Mica (Illite)	10	10	10	10	10
Gibbsite	4.85	4.85	4.85	LD	LD
Goethite	4.18	4.18	4.18	LD	LD
Quartz	3.34 and 4.27 for all treatments				

Adapted from Wilson, 1994; [1]LD - lattice destroyed, [2]B – broad peak is common, [3]secondary peak of halloysite (Wyatt et al., 2010). *'Gly' ethylene glycol*

3.2.4 Weathering Indices

Total Reserve in Bases (TRB). The sum of base cations (Ca^{2+}, Mg^{2+}, Na^{+}, and K^{+}) from primary and secondary minerals and exchangeable sites measured as TRB is a recognized weathering index to predict the stage of weathering (Herbillon, 1989; Delvaux et al., 1989) if the TRB of the parent material is known. We used this index to determine the relative weathering degree of our samples in comparison to the pristine 1991 Mt. Pinatubo tephra. The decrease in the TRB of the soil and pyroclast from that of the pristine 1991 tephra (i.e. ash, pumice) is an indication of soil chemical weathering. The TRB is given by the formula,

$$TRB = Ca + Na + Mg + K \qquad \textit{Eq. 3.8}$$

where Ca, Na, Mg, and K expressed in $cmol_c\ kg^{-1}$ soil are the total contents.

Fe_d/Fe_t. It is the proportion of the DCB-extracted Fe as "free" Fe oxides to the total Fe concentration. The "free" forms of Fe originate from the oxidation of amorphous (silicate glass) and crystalline (ferromagnesian minerals) compounds forming amorphous hydrous oxides (i.e. ferrihydrite) and Fe-humus complexes (Mehra & Jackson, 1960). Therefore, an increase in Fe_d/Fe_t ratio indicates an advancement of soil chemical weathering. The relative content of free Fe oxides is estimated using the expression:

$$\frac{Fe_d}{Fe_t}\,(\text{unitless}) \qquad \textit{Eq. 3.9}$$

where Fe_d is the DCB-extractable Fe and Fe_t is the total Fe content of the sample.

Al:Si. Aluminum is one of the major elements in tephras as well as in amorphous materials (i.e. silicate glass), hence, used to estimate the rate of chemical weathering in Andisols when soil age is known (Shoji et al., 1993). Weathered soils are highly aluminous since Al is relatively immobile than Si (Nanzyo et al., 1993). Therefore, increasing Al:Si of the soil or pyroclast with respect to that of the 1991 Mt. Pinatubo tephra indicates an advance of soil chemical weathering. The total Al:Si ratio is given by the formula:

$$\frac{\text{Al}}{\text{Si}} \text{ (unitless)} \qquad \textit{Eq. 3.10}$$

Where Al:Si is the molar ratio of total Al to total Si.

The summary of the weathering indices used in this study and the expected trend that expresses the advance in weathering degree are shown in Table 3.2.

Table 3.2. Weathering indices and expected trend with increasing degree of chemical weathering.

WEATHERING INDEX	*EXPECTED TREND WITH INCREASING DEGREE OF WEATHERING
TRB	↓
Fe_d/Fe_t	↑
Al:Si	↑

*Weathering increases as the total reserve in bases 'TRB' decreases, DCB-extracted Fe to the total Fe ratio 'Fe_d/Fe_t' increases, and total aluminum to silicon 'Al:Si ratio' increases in comparison to that of pristine pyroclast deposit; ↑ Increase, ↓ Decrease

3.3 Results

3.3.1 Morphology

The detailed morphology of the two soil profiles for each of the sampling sites (i.e. Fo-Ash, Gr-HA-Ash, Gr-LA-Ash, IR-Ash, IR-Lahar) is described in Table A3.1. Only the main characteristics of the profiles are outlined.

Fo-Ash (P1-a, P1-b). The MS horizon of the two soil profiles (P1-a and P1-b) is 3-4 cm thick. It has a sandy clay loam texture, granular structure, and it contains many medium and fine roots. The bulk density of the MS horizon varies between 0.75 and 0.85 g cm^{-3}, respectively. The ash layer beneath the MS horizon is 8 and 9 cm thick, respectively, with a sandy loam texture. Medium and coarse roots are common. The pumice layer, 6 and 12 cm thick, respectively has a sandy texture with fine particles. The BS horizons of P1-a and P1-b are 15 and 23 cm thick, respectively, with clay loam texture and subangular blocky structure. Distinct red mottles are present.

IR-ash (P2-a, P2-b). The MS horizon of the two soil profiles, 14-15 cm thick, is plowed. It has a bulk density of 0.79 and 0.81 g cm^{-3} in P2-a and P2-b, respectively. The texture is silt loam and the structure is subangular blocky with many fine and coarse roots. It also has many distinct yellow mottles present. The remobilized ash layer, 5 and 11 cm thick, respectively, has silt loam texture and granular to subangular blocky structure with very few fine roots. The ash layer, 5 cm (P2-a) and 7 cm (P2-b) thick, has a sandy loam texture and subangular blocky to a granular structure. Fine roots are very few to none. The pumice layer, 6 cm thick in both soil profiles, are sandy and structureless and contains small rock fragments. Another thin ash layer (1 cm thick) beneath the pumice layer of the P2-a profile has a loamy texture and granular structure. The BS horizon, 24 cm (P2-a) and 51 cm (P2-b)

thick is loamy and has a subangular blocky structure. Many distinct red mottles are observed.

Gr-LA-Ash (P3-a, P3-b). The MS horizon of the P3-a and P3-b profiles, 6 and 7 cm, respectively, has a loamy sand texture, granular structure, and respectively bulk densities of 0.98 g cm^{-3} and 1.02 g cm^{-3}. The pumice layer, 8-9 cm thick, is sandy, structureless and contains very few small rock fragments. The succeeding ash layer, 4 cm thick in both soil profiles, has a sandy clay texture and granular structure. Fine to medium roots are common. The BS horizon, 17 cm thick in both soil profiles, has a sandy loam texture and subangular blocky structure. Few very fine roots are observed.

Gr-HA-Ash (P4-a, P4-b). The MS horizon with a thickness of 12 and 13 cm (P4-a and P4-b, respectively) has a sandy clay loam texture, granular structure, and with many coarse and fine roots. The bulk density varies from 0.79 and 0.93 g cm^{-3}, respectively. The pumice layer with thickness varying from 9 and 14 cm, respectively, is sandy and structureless. The ash layer, 5 and 7 cm thick, respectively, has a clay texture and subangular blocky to a granular structure. The thickness of the BS horizon is 23 and 40 cm, respectively, and both have sandy loam texture and subangular blocky structure. Many distinct red mottles are present.

IR-Lahar (P5-a, P5-b). The thickness of the plowed MS horizon is 18 and 24 cm thick (P5-a and P5-b profiles, respectively). The bulk density is 0.79 and 0.91 g cm^{-3}, respectively. It has a loamy sand texture and is structureless with many big and small rock fragments. Many fine and medium roots are also present. The lahar 1 layer, 16 cm, and 18 cm thick, respectively, is sandy, structureless, with big and medium rock fragments, and few fine roots. The lahar 2 layer, three cm thick in both soil profiles, is sandy, structureless, with small rock fragments. Common, fine, and distinct reddish to yellowish mottles are also present. The BS horizon, 13 and 20 cm thick, respectively, has a sandy clay loam texture, subangular blocky structure, and common fine roots.

3.3.2 Particle size analyses

The sand, silt, and clay contents along the soil profile depth are shown in Figure 3.5. The values are also shown in Table A.3.2.

Fo-Ash (P1-a). The MS horizon of P1-a contains 58.5 wt.% sand, 8.0 wt.% silt, and 30.1 wt.% clay. The ash and pumice layers have a higher sand content, i.e. respectively, 80.2 and 69.7 wt.%. The ash layer has lower silt and clay contents than the pumice layer (2.4 vs. 3.7 wt.% silt and 15.3 vs. 24.9 wt.% clay), respectively. Silt- (32.2 wt.%) and clay- (36.4 wt.%) sized particles dominate in the BS and contents are higher than in the MS horizon.

IR-Ash (P2-a, P2-b). The MS horizons of the two soil profiles (P2-a and P2-b, respectively) have higher contents of silt (53.8 and 67.3 wt.%, respectively) compared to sand (12.4 and 26.5 wt.%, respectively) and clay (16.5 and 17.7 wt.%, respectively). Similarly, the remobilized ash layer of P2-a and P2-b profiles consist mainly of silt (74.2 and 79.9 wt.%, respectively) and lower contents of clay (14.4 and 16.3 wt.%, respectively) and sand (3.3 and 7.3 wt.%, respectively). The underlying ash layer of both P2-a and P2-b have higher sand contents (52.8 and 56.3 wt.%, respectively), lower silt (36.5 and 39.8 wt.%, respectively) and clay (4.1 and 4.4 wt.%, respectively) contents compared to the remobilized ash layer. Sand (94.3 wt.%) dominates in the pumice layer of the P2-a profile. The thin ash layer underneath the pumice layer in the P2-a soil profile consists of 47.6 wt.% sand, 43.6 wt.% silt, and 6.3 wt.% clay. The clay content of the BS horizon in P2-a and P2-b (17.0 and 18.1 wt.%, respectively) are comparable to that of the MS horizon. However, this horizon has ~five times more sand (44.1 and 47.6 wt.%, respectively for P2-a and P2-b) and ~two times less silt (30.9 and 36.5 wt.%, respectively) than in the MS horizon.

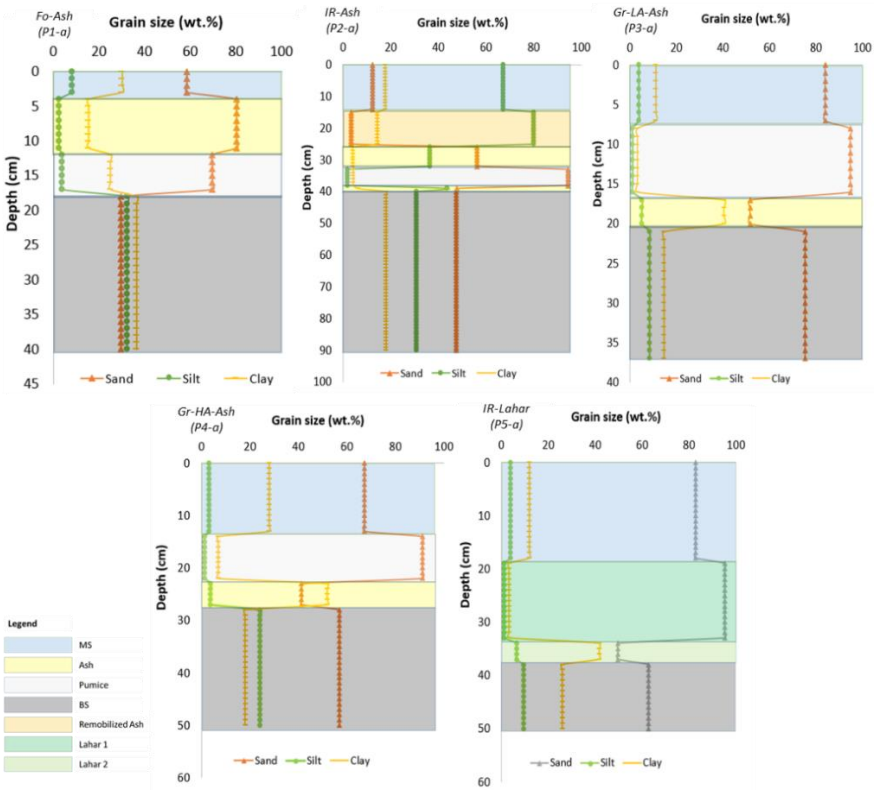

Figure 3.5. Variation with depth of sand-, silt- and clay-sized fractions in the Fo-Ash (P1-a, Tarlac province), IR-Ash (P2-a, Tarlac province), Gr-LA-Ash (P3-a, Pampanga province), Gr-HA-Ash (P4-a, Pampanga province), and IR-Lahar (P5-a, Zambales province) soil profiles.

Gr-LA-Ash (P3-a). The MS horizon of P3-a contains 83.9 wt.% sand, 3.9 wt.% silt, and 11.1 wt.% clay. The underlying pumice layer is dominated by sand (94.8 wt.%) while that of the ash layer is 51.7 wt.%. The ash layer is dominated by clay-sized particles (40.4 wt.%). The BS horizon has a comparable sand content (75.3 wt.%), but slightly higher contents of silt (8.5 wt.%) and clay (14.6 wt.%) compared to that of MS horizon.

Gr-HA-Ash (P4-a). The sand, silt and clay contents of the MS horizon (P4-a profile) are 67.3 wt.%, 3.1 wt.% and 27.9 wt.%, respectively. The pumice layer is constituted mainly by sand (94.8 wt.%). The ash layer is dominated by the clay- and sand-sized fractions, amounting to 51.8 and 41.3 wt.%, respectively. The BS horizon has 56.9 wt.% sand and 24.2 wt.% silt. Its clay content (18.0 wt.%) is ~two times lower than that of the MS horizon.

IR-Lahar (P5-a). The MS horizon (P5-a) is comprised mainly of sand (82.7 wt.%), and low contents of silt (3.8 wt.%) and clay (11.9 wt.%). The lahar 1 layer is dominated by sand (95.2 wt.%) whereas the lahar 2 layer has an almost equal proportion of sand (49.7 wt.%) and clay (41.7 wt.%). The BS horizon has lower sand (62.8 wt.%) and about two times higher silt (9.3 wt.%) and clay (25.9 wt.%) contents than that in the MS horizon.

3.3.3 Mineralogy

The mineralogical composition of the bulk and clay samples for each of the soil and pyroclast samples are shown in Table 3.3. The XRD patterns of representative bulk and clay samples from the Fo-Ash site are shown in Figures 3.6[a-g]. Figures 3.7[a-e] illustrates the XRD patterns of K^+ and Mg^{2+}-saturated clay samples from the representative soil profiles of the five sampling sites.

The bulk samples from the MS and BS horizons and pyroclast layers in the two soil profiles per sampling site are generally composed of plagioclase feldspars, quartz, amphiboles, pyroxene, mica, and Fe-oxide. The presence of phyllosilicate clays (i.e. kaolinite, halloysite, smectite, vermiculite) is also observed in the bulk fraction. In the same manner, amorphous materials (i.e. silicate glass) are also apparent in all the samples as evidenced by the broad background/curved x-ray patterns.

Table 3.3. Mineralogy of the bulk (< 2 mm) and clay (< 2 µm) samples in the Fo-Ash (P1-a, Tarlac province), IR-Ash (P2-a, Tarlac province), Gr-LA-Ash (P3-a, Pampanga province), Gr-HA-Ash (P4-a, Pampanga province) and IR-Lahar (P5-a, Zambales province) soil profiles.

PROFILE CODE	DEPTH (cm)		HORIZON/ LAYER	BULK SAMPLE (< 2 mm)		CLAY FRACTION (< 2 µm)	
	a[1]	b[2]		Primary minerals	Presence of clay minerals	Primary minerals	Clay minerals
Fo-Ash (P1)	0-3	0-4	Modern soil	PF, Q, Am, Mi, Py, Fe-ox	Yes	PF, Q, Am, Mi, Py, Fe-ox	Ka, Ha, Ve
	3-11	4-13	Ash	PF, Q, Am, Mi, Py, Fe-ox	Yes	PF, Q, Am, Mi, Py, Fe-ox	Ve
	11-17	13-25	Pumice	PF, Q, Am, Mi, Py, Fe-ox	Yes	PF, Q, Am, Mi, Py, Fe-ox	Ve
	17-40	25-40	Buried soil	PF, Q, Am, Mi, Py, Fe-ox	Yes	PF, Q, Am, Mi, Py, Fe-ox	Ka, Ha, Ve
IR-Ash (P2)	0-14	0-15	Modern soil	PF, Q, Am, Mi, Py, Fe-ox	Yes	PF, Q, Am, Mi, Py, Fe-ox	Ka, Ha, Sm, Ve
	14-25	15-20	Remobilized Ash	PF, Q, Am, Mi, Py, Fe-ox	Yes	PF, Q, Am, Mi, Py, Fe-ox	Ka, Ve, Sm
	25-32	20-25	Ash	PF, Q, Am, Mi, Py, Fe-ox	Yes	PF, Q, Am, Mi, Py, Fe-ox	Ve, Sm
	32-38	25-31	Pumice	PF, Q, Am, Mi, Py, Fe-ox	Yes	PF, Q, Am, Mi, Py, Fe-ox	Ve
	38-39	-	Ash	n.a.	n.a.	n.a.	n.a.
	39-90	31-55	Buried soil	PF, Q, Am, Mi, Py, Fe-ox	Yes	PF, Q, Am, Mi, Py, Fe-ox	Ka, Ha, Ve
Gr-LA-Ash (P3)	0-7	0-6	Modern soil	PF, Q, Am, Mi, Py, Fe-ox	Yes	PF, Q, Am, Mi, Py, Fe-ox	Sm, Ve
	7-16	6-14	Pumice	PF, Q, Am, Mi, Py, Fe-ox	Yes	PF, Q, Am, Mi, Py, Fe-ox	Ka, Ve, Sm
	16-20	14-18	Ash	PF, Q, Am, Mi, Py, Fe-ox	Yes	PF, Q, Am, Mi, Py, Fe-ox	Ve
	20-37	18-35	Buried soil	PF, Q, Am, Mi, Py, Fe-ox	Yes	PF, Q, Am, Mi, Py, Fe-ox	Ka, Ve, Sm
Gr-HA-Ash (P4)	0-13	0-12	Modern soil	PF, Q, Am, Mi, Py, Fe-ox	Yes	PF, Q, Am, Mi, Py, Fe-ox	Ve
	13-22	12-26	Pumice	PF, Q, Am, Mi, Py, Fe-ox	Yes	PF, Q, Am, Mi, Py, Fe-ox	Ve, Sm
	22-27	26-33	Ash	PF, Q, Am, Mi, Py, Fe-ox	Yes	PF, Q, Am, Mi, Py, Fe-ox	Ve
	27-50	33-73	Buried soil	PF, Q, Am, Mi, Py, Fe-ox	Yes	PF, Q, Am, Mi, Py, Fe-ox	Ka, Ha, Ve
IR-Lahar (P5)	0-18	0-24	Modern soil	PF, Q, Am, Mi, Py, Fe-ox	Yes	PF, Q, Am, Mi, Py, Fe-ox	Ka
	18-34	24-42	Lahar 1	PF, Q, Am, Mi, Py, Fe-ox	Yes	PF, Q, Am, Mi, Py, Fe-ox	Ka, Ve
	34-37	42-45	Lahar 2	PF, Q, Am, Mi, Py, Fe-ox	Yes	PF, Q, Am, Mi, Py, Fe-ox	Ve
	37-50	45-65	Buried soil	PF, Q, Am, Mi, Py, Fe-ox	Yes	PF, Q, Am, Mi, Py, Fe-ox	Ka, Ve

[1,2] Pseudoreplicate profiles; 'PF' plagioclase feldspar, 'Q' quartz, 'Am' amphibole, 'Mi' mica, 'Py' pyroxene, 'Fe-ox' iron-oxide, 'Ka' kaolinite, 'Ha' halloysite, 'Ve' vermiculite, 'Sm' smectite. 'n.a' not analyzed.

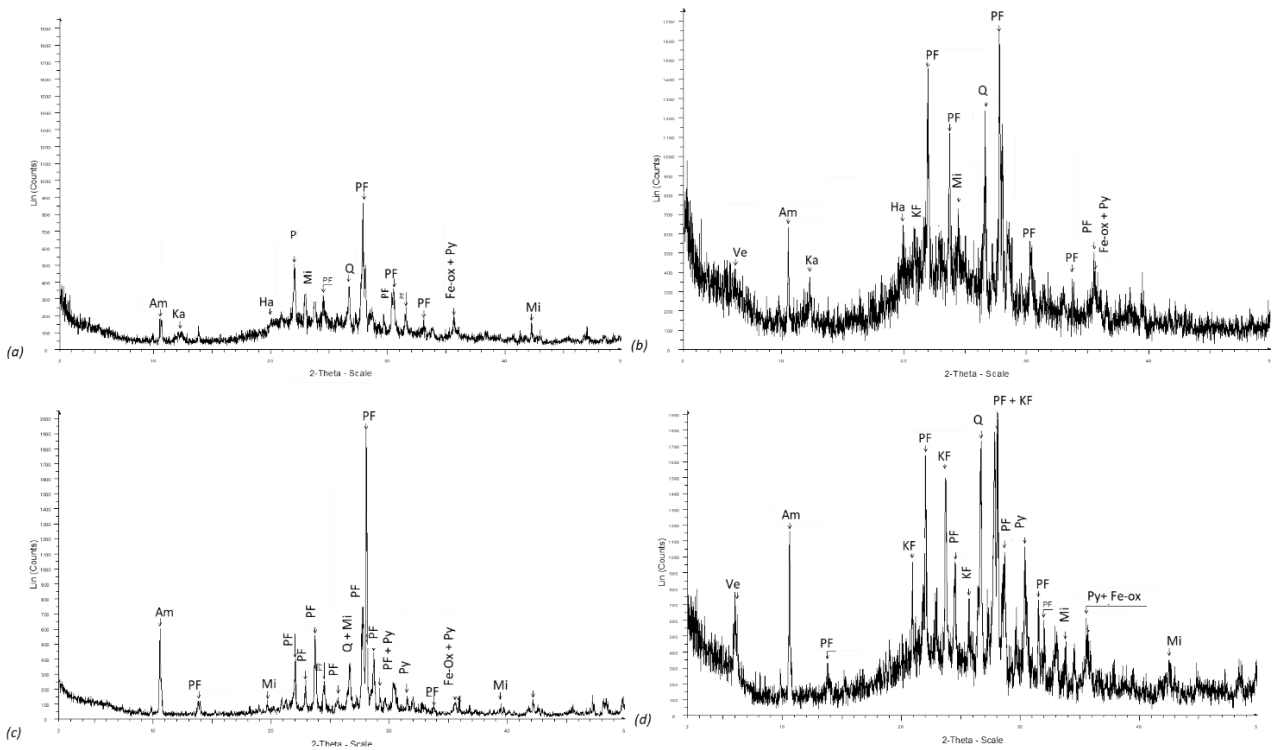
(a)
Lin (Counts)
2-Theta - Scale
Am
Ka
Ha
Mi
PF
Q
Fe-ox + Py
(b)
Lin (Counts)
2-Theta - Scale
Ve
Am
Ka
Ha
KF
PF
Mi
Q
Fe-ox + Py
(c)
Lin (Counts)
2-Theta - Scale
Am
PF
Mi
Q + Mi
PF + Py
Py
Fe-Ox + Py
(d)
Lin (Counts)
2-Theta - Scale
PF + KF
Ve
Am
KF
PF
Q
Py
Py+ Fe-ox
Mi

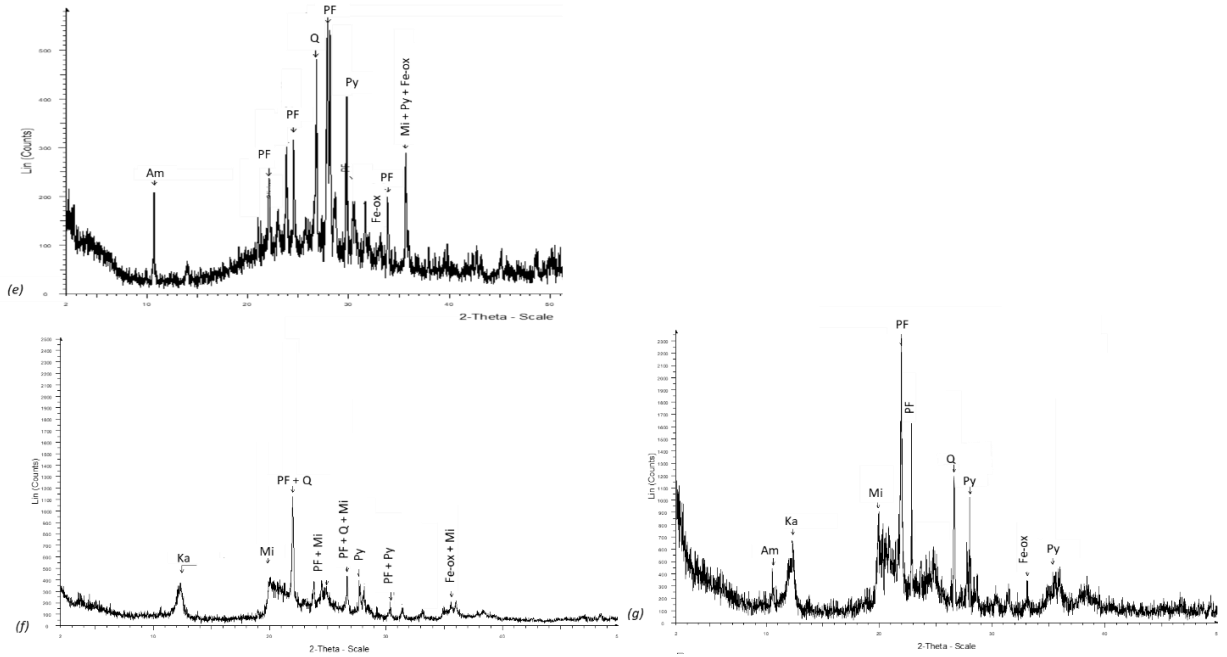

Figure 3.6. XRD pattern of the bulk (< 2 mm) and clay (< 2 µm) fractions of the Fo-Ash profile samples (P1-a, Tarlac Province): *(a)* bulk MS, *(b)* clay MS, *(c)* bulk ash, *(d)* clay ash, *(e)* bulk pumice, *(f)* bulk BS, *(g)* clay BS. *'PF' plagioclase feldspar, 'Q' quartz, 'Am' amphibole, 'Mi' mica, 'Py' pyroxene, 'Fe-ox' iron-oxide, 'Ka' kaolinite, 'Ha' halloysite, 'Ve' vermiculite.*

In general, the clay-sized fraction of MS and BS horizons and pyroclast layers from the five sampling sites are comprised of both primary and secondary minerals. All the primary minerals identified from the bulk fraction of each sample are also present in its clay fraction. The presence of amorphous materials is inferred to be present in all the samples of the different soil profiles due to the appearance of distinct broad, curved peaks in the XRD patterns as shown in the representative bulk and clay samples of Fo-Ash in Figures 3.6a-g. The treated clay fraction of the soil profile horizons and pyroclast layers consist of one or a combination of 1:1 and 2:1 type of layer silicates (phyllosilicates) which varied among the sampling sites as described below.

Fo-Ash (P1-a). The clay fraction of the MS horizon (P1-a profile) shows the presence of kaolinite, halloysite, and vermiculite at low-intensity peaks. The ash and pumice layers both contain vermiculite but pumice has a relatively higher intensity of peaks at 14.0 and 10.0 Å. The BS horizon has a lower peak of vermiculite but the kaolinite and halloysite peaks are broader compared to that of the MS horizon.

IR-Ash (P2-a). The presence of 1:1 (kaolinite, halloysite) and 2:1 (smectite, vermiculite) phyllosilicates are observed in the clay fraction MS horizon of the P2-a profile. Kaolinite (7.2 Å) and vermiculite (14.2 Å) have broad and well-defined peaks while halloysite (4.4 Å) is present at lower peak intensity. The presence of smectite was confirmed from its well-defined peaks in the ethylene glycol saturation and heated treatments. The remobilized ash layer contains all the phyllosilicates mentioned previously in the MS horizon except for the halloysite. Furthermore, there is a lower peak of kaolinite compared to that of the MS horizon. The succeeding ash layer has high-intensity peaks for smectite (16.5 Å) and vermiculite. The pumice layer has a well-defined peak for vermiculite. The BS horizon consists of vermiculite at lower peak intensity compared to the upper soil horizon and ash layers. The peak of kaolinite is broad and well-defined comparable to that of the MS horizon. Halloysite is also present at low peak intensity similar to the MS horizon.

Gr-LA-Ash (P3-a). Vermiculite and smectite are present at very low peak intensities. The pumice layer has a sharp peak for vermiculite and it also contains smectite and kaolinite at very low peaks. The ash layer only contains vermiculite but the peak at 14 Å is sharper compared to the MS horizon. The BS horizon has low-intensity peaks for kaolinite and smectite and has a moderately well-defined peak for vermiculite.

Gr-HA-Ash (P4-a). Both the MS horizon and ash layer have similar peak intensities at 14.1 Å indicating the presence of vermiculite. The pumice layer contains well-defined peaks of both vermiculite and smectite. The BS horizon has a low-intensity peak for vermiculite and halloysite but has a broader well-defined peak for kaolinite (7.2 Å).

IR-Lahar (P5-a). The MS horizon and lahar 1 layer have very low-intensity peaks at 7.1 Å suggesting the presence of kaolinite. Lahar 1 layer also contained vermiculite in addition to kaolinite. Lahar 2 layer consists of vermiculite alone that is well-defined at 14.2 Å peak. The BS horizon has well-defined peaks of vermiculite and kaolinite.

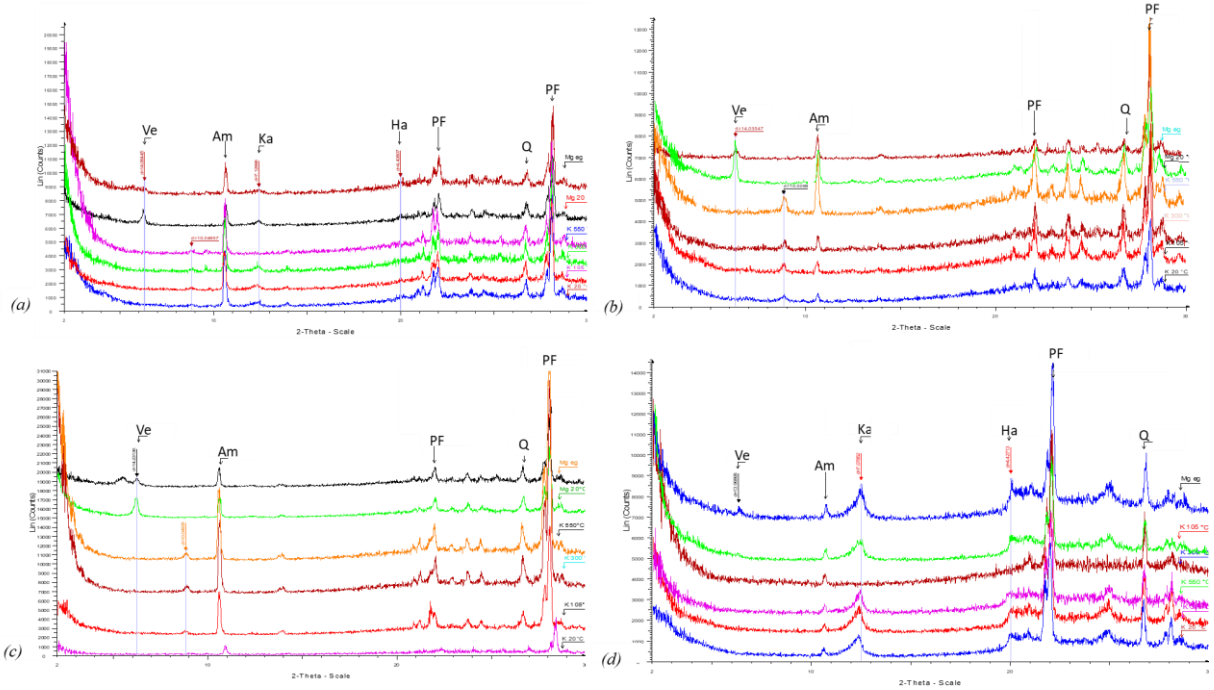

Figure 3.7a. XRD pattern of the K and Mg-treated clays along with the soil profile depth of Fo-Ash (P1-a, Tarlac Province), *(a)* MS horizon, *(b)* ash layer, *(c)* pumice layer, *(d)* BS horizon. *'Ve' vermiculite, 'Ka' kaolinite, 'Ha' halloysite, 'Am' amphibole, 'PF' plagioclase feldspar, 'Q' quartz.*

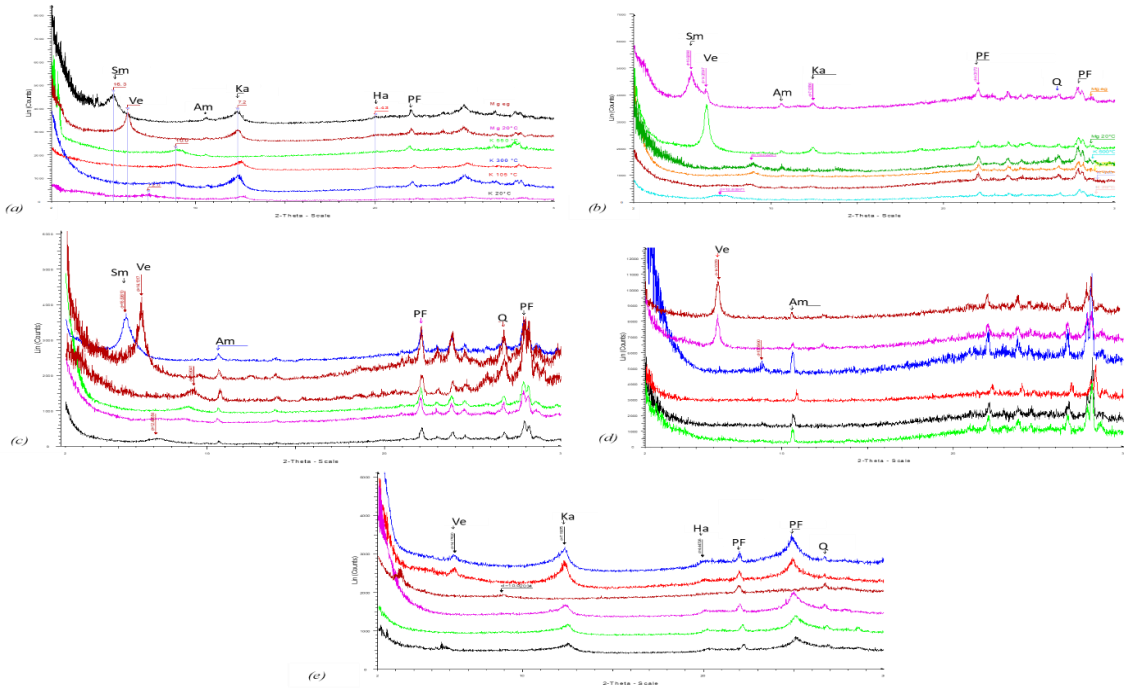

Figure 3.7b. XRD pattern of the K and Mg-saturated clays along with the soil profile depth of IR-Ash (P2-a, Tarlac Province), *(a)* MS horizon, *(b)* remobilized ash layer, *(c)* ash layer, *(d)* pumice layer, *(e)* BS horizon. *'Ve' vermiculite, 'Sm' smectite, 'Ka' kaolinite, 'Ha' halloysite, 'Am' amphibole, 'PF' plagioclase feldspar, 'Q' quartz.*

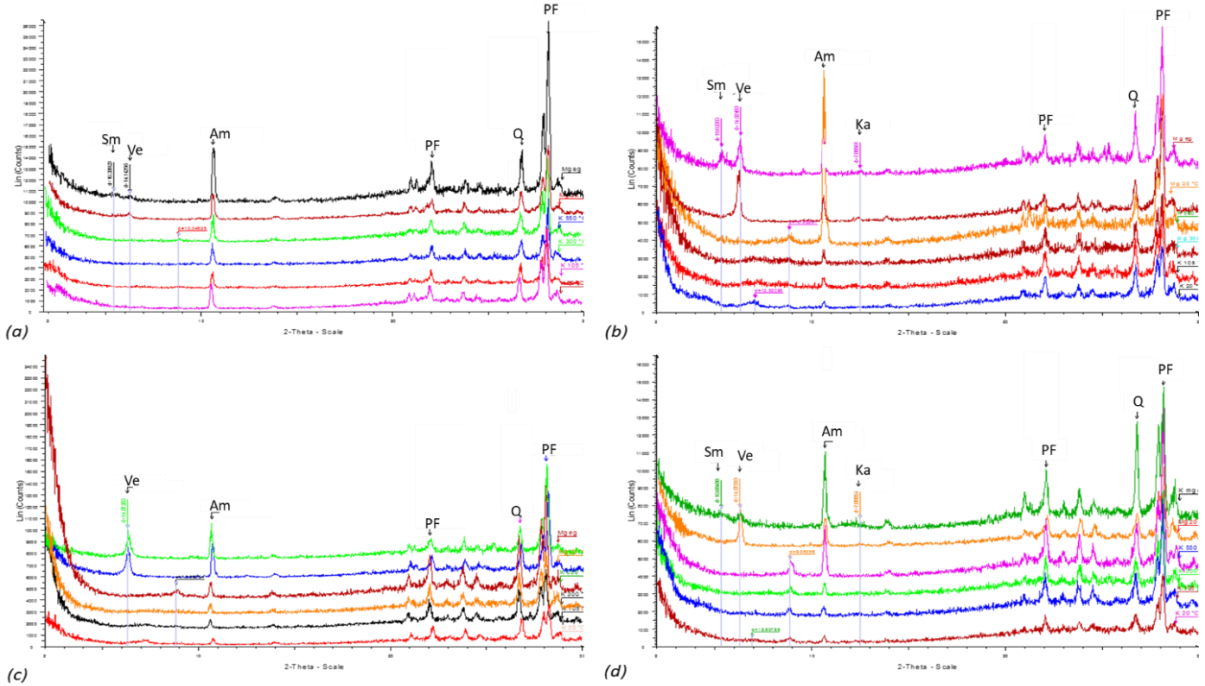

Figure 3.7c. XRD pattern of the K and Mg-saturated clays along with the soil profile depth of Gr-LA-Ash (P3-a, Pampanga Province), *(a)* MS horizon, *(b)* pumice layer, *(c)* ash layer, *(d)* BS horizon. *'Ve' vermiculite, 'Sm' smectite, 'Ka' kaolinite, 'Ha' halloysite, 'Am' amphibole, 'PF' plagioclase feldspar, 'Q' quartz.*

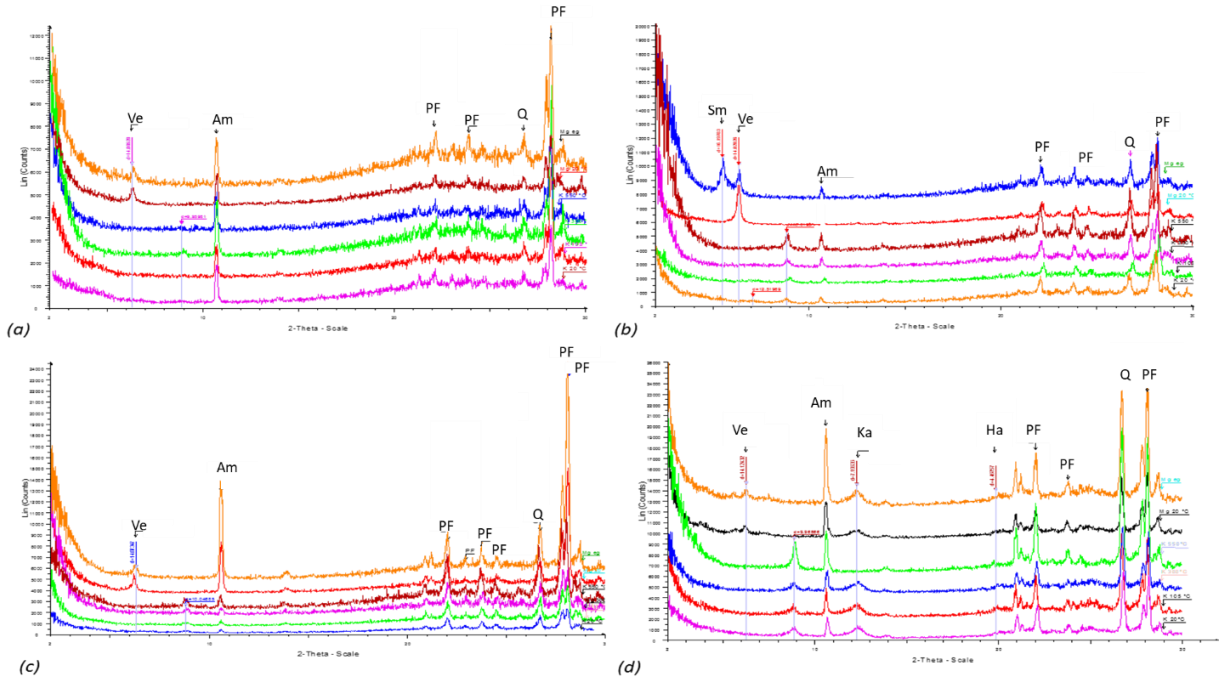

Figure 3.7d. XRD pattern of the K and Mg-saturated clays along with the soil profile depth of Gr-HA-Ash (P4-a, Pampanga Province), *(a)* MS horizon, *(b)* pumice layer, *(c)* ash layer, *(d)* BS horizon. *'Ve' vermiculite, 'Sm' smectite, 'Ka' kaolinite, 'Ha' halloysite, 'Am' amphibole, 'PF' plagioclase feldspar, 'Q' quartz.*

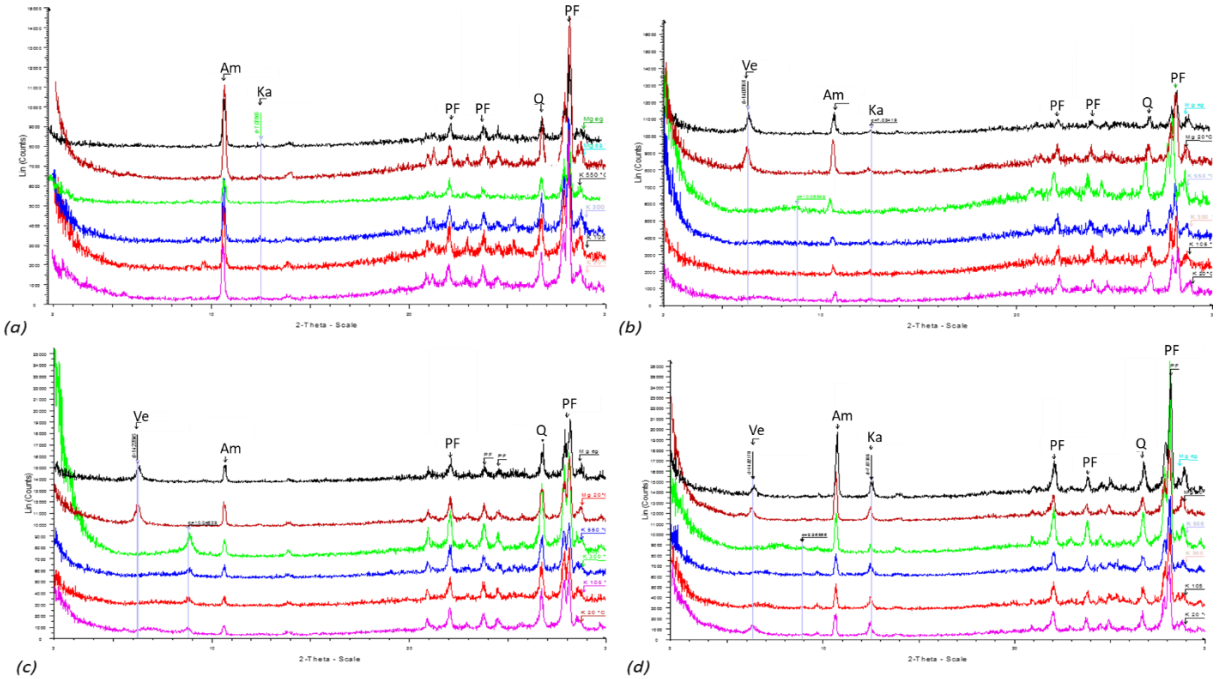

Figure 3.7e. XRD pattern of the K and Mg-saturated clays along with the soil depth of IR-Lahar (P5-a, Zambales Province), *(a)* MS horizon, *(b)* lahar 1 layer, *(c)* lahar 2 layer, *(d)* BS horizon. *'Ve' vermiculite, 'Ka' kaolinite, 'Am' amphibole, 'PF' plagioclase feldspar, 'Q' quartz.*

3.3.4 General soil chemical properties

The soil chemical properties, including pH (H_2O and KCl), CEC, % BS, the proportion of base cations, total (organic) C content, P retention of the two soil profiles per sampling site, are shown in Figures 3.8[a-e], respectively. The measured values are also shown in Table A.3.3. The graph of P retention is shown in Figure 5.2. The P retention described in this chapter is used as an index of andosolization. A full chapter about P availability and retention is discussed in detail in Chapter 5.

pH_{H2O} and pH_{KCl}

Fo-Ash (P1-a, P1-b). The pH_{H2O} of the MS horizon in the two soil profiles (P1-a and P1-b) is 6.68 and 7.60 pH_{H2O} and, 5.97 and 7.16 pH_{KCl}, respectively. The pH_{H2O} of the ash and pumice layers vary from 5.93 to 6.27 (P1-a) and 7.07 to 7.24 (P1-b). In the previously mentioned layers, lower pH_{KCl} values are measured: 5.26 (P1-a) and 6.46 (P1-b). The BS horizon has a pH_{H2O} value of 5.63 (P1-a) and 6.85 (P1-a) which is one magnitude lower than in the MS horizon. It also displays much lower pH_{KCl} values, i.e. 4.16 (P1-a) and 5.45 (P1-b).

IR-Ash (P2-a, P2-b). The pH_{H2O} of the MS horizon in P2-a and P2-b soil profiles are 4.62 and 4.91, respectively, while the pH_{KCl} is 4.13 and 4.19, respectively. The pH_{H2O} of the remobilized ash layer, 5.85 (P2-a) and 5.99 (P2-b), are one magnitude higher than in the MS horizon. Consequently, the pH_{KCl} of the remobilized ash layer, 4.76 (P2-a) and 4.99 (P2-b), is also higher than that of the MS horizon. The pH_{H2O} of the ash and pumice layers vary from 5.45 to 5.78 (P2-a) and 6.03 to 6.10 (P2-b) which are also higher than that of the MS horizon. The pH_{KCl} in these layers is likewise higher varying from 4.86 to 5.28 (P2-a) and 5.02 to 5.23 (P2-b). The pH_{H2O} of BS horizon, 4.76 (P2-a) and 5.81 (P2-b), as well as its pH_{KCl}, 4.18 (P2-a) and 5.03 (P2-b) are slightly higher than that of the MS horizon.

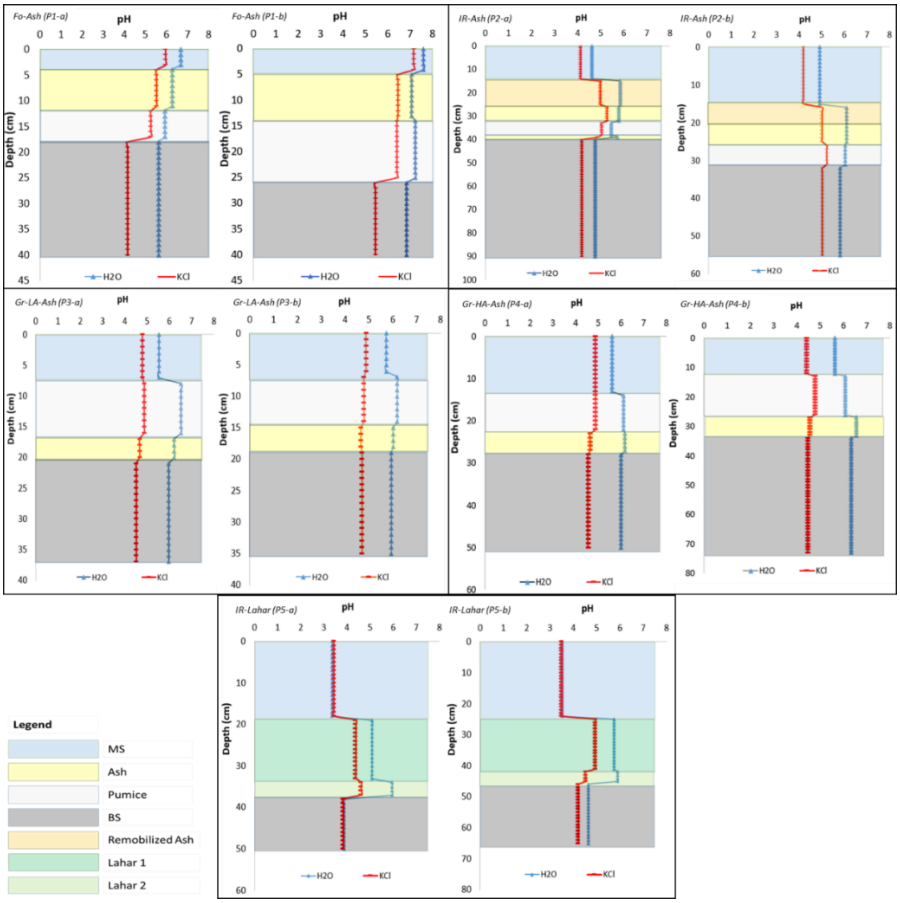

Figure 3.8a. Variation with depth of pH_{H2O} and pH_{KCl} in the Fo-Ash (P1-a, P1-b; Tarlac province), IR-Ash (P2-a, P2-b; Tarlac province), Gr-LA-Ash (P3-a, P3-b; Pampanga province), Gr-HA-Ash (P4-a, P4-b; Pampanga province) and IR-Lahar (P5-a, P5-b; Zambales province) soil profiles.

Gr-LA-Ash (P3-a, P3-b). The pH_{H2O} of the MS horizon which is 5.53 and 5.72 in P3-a and P3-b profiles, respectively, is lower than that of the succeeding layers of pumice and ash (6.02-6.52). It is also slightly lower compared to the BS horizon (5.97, P3-a and 5.94, P3-b). The pH_{KCl} is consistently lower in all soil horizon and ash (including pumice) layers varying from 4.52 to 4.87 (P3-a) and 4.66 to 4.88 (P3-b), respectively.

Gr-HA-Ash (P4-a, P4-b). The pH_{H2O} of the MS horizon is lower (5.60 and 5.62, P4-a and P4-b profiles, respectively) compared to that of BS horizon, ash, and pumice layers which vary from 6.01 to 6.18 (P4-a) and 6.09 to 6.56 (P4-b). The pH_{KCl} in the soil horizons and pyroclast layers are in the range of 4.40 to 4.88 for the two profiles.

IR-Lahar (P5-a, P5-b). The pH_{H2O} of the MS horizon, 3.35 (P5-a) and 3.53 (P5-b), and BS horizon, 3.88 (P5-a) and 4.64 (P5-b) are very low. The pH_{KCl} of the MS horizon exhibits comparable values with its $pH_{H2O,}$ 3.44 (P5-a) and 3.49 (P5-b). The BS horizon has slightly lower pH_{KCl}, 3.84 (P5-a) and 4.22 (P5-b) when compared to its pH_{H2O} values. The lahar 1 and lahar 2 layers, respectively, have relatively higher pH_{H2O} values (5.09-5.95, P5-a and 5.75-5.89, P5-b) compared to the soil horizons. The pH_{KCl} of the lahar layers (4.38-4.61, P5-a and 4.53-4.94, P5-b) is also higher than of the soil horizons.

CEC

Fo-Ash (P1-a, P1-b). The CEC of the MS horizon in P1-a and P1-b profiles, respectively, are 3.85 and 4.17 $cmol_c\ kg^{-1}$. These values are roughly threefold higher than those measured for the underlying layers of ash (0.97 and 1.23 $cmol_c\ kg^{-1}$, respectively) and pumice (1.44 and 1.64 $cmol_c\ kg^{-1}$, respectively). The BS horizon displays a CEC of 7.11 (P1-a) and 9.66 (P1-b) $cmol_c\ kg^{-1}$, i.e. two to three times higher than the CEC of the MS horizon.

IR-Ash (P2-a, P2-b). The MS and BS horizons in the two soil profiles (P2-a and P2-b, respectively) have comparable CEC, i.e. MS horizon has 8.73 and 6.77 $cmol_c\ kg^{-1}$, respectively; BS horizon has 7.80 and 7.59 $cmol_c\ kg^{-1}$, respectively. The CEC of the remobilized ash layer is ~two times lower than the soil horizons, i.e. 3.58 (P2-a) and 4.39 (P2-b) $cmol_c\ kg^{-1}$. The CEC of the succeeding ash layers and pumice layers are lower compared to those found in the soil horizons (1.17-3.56 $cmol_c\ kg^{-1}$ in the two profiles).

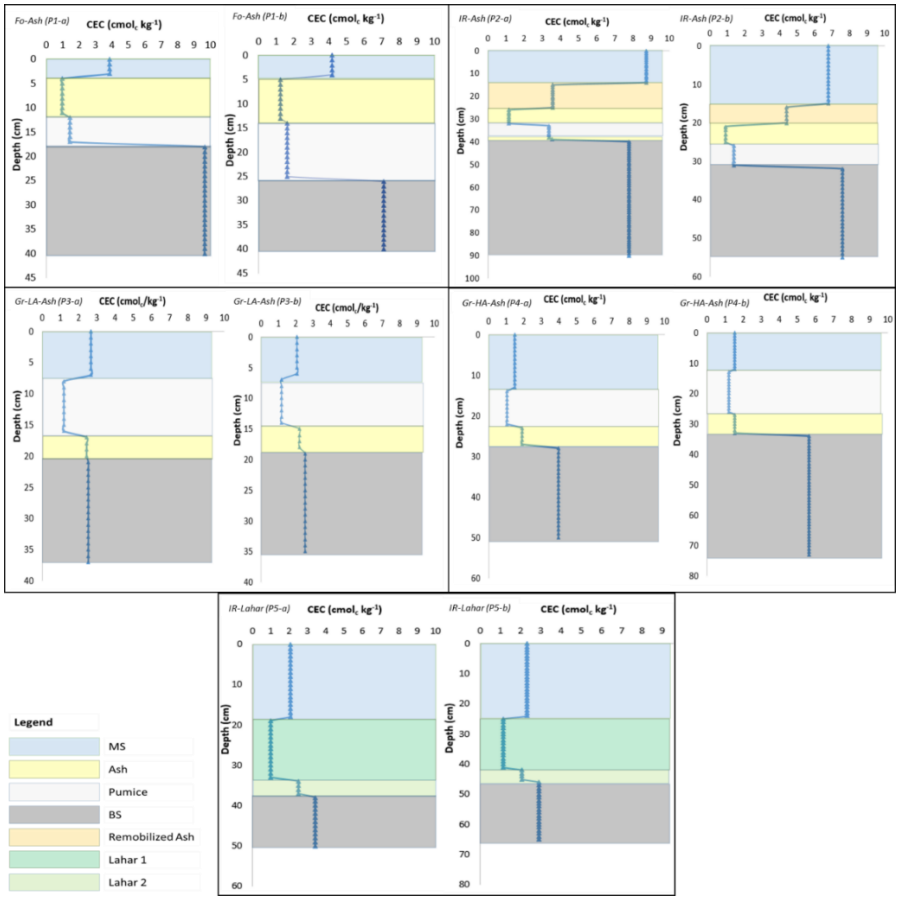

Figure 3.8b. Variation with depth of CEC content in the Fo-Ash (P1-a, P1-b; Tarlac province), IR-Ash (P2-a, P2-b; Tarlac province), Gr-LA-Ash (P3-a, P3-b; Pampanga province), Gr-HA-Ash (P4-a, P4-b; Pampanga province) and IR-Lahar (P5-a, P5-b; Zambales province) soil profiles.

Gr-LA-Ash (P3-a, P3-b). The CEC of the soil horizons and ash layers vary from 2.43 to 2.67 $cmol_c\ kg^{-1}$ (P3-a) and 2.08 to 2.54 (P3-b). The CEC of the pumice layer is lower by one magnitude (1.18-1.19 $cmol_c\ kg^{-1}$).

Gr-HA-Ash (P4-a, P4-b). The CEC of the MS horizon and ash layer are comparable in both P4-a and P4-b soil profiles, i.e. MS horizon has 1.47 and 1.53 $cmol_c\ kg^{-1}$ CEC, respectively; ash layer has 1.90 and 1.54

$cmol_c\ kg^{-1}$, respectively. The pumice layer underneath the MS horizon has slightly lower values, 1.06 $cmol_c\ kg^{-1}$ (P4-a) and 1.21 $cmol_c\ kg^{-1}$ (P4-b), compared to the MS horizon and ash layer. The BS horizon has CEC values, 3.96 $cmol_c\ kg^{-1}$ (P4-a) and 5.63 $cmol_c\ kg^{-1}$ (P4-b), that are ~three times higher than that of the MS horizon, ash, and pumice layers.

IR-Lahar (P5-a, P5-b). The CEC of the MS horizon and lahar 2 layer in the two soil profiles are comparable, i.e. MS horizon has 2.08 $cmol_c\ kg^{-1}$ (P5-a) and 2.33 $cmol_c\ kg^{-1}$ (P5-b), lahar 2 layer has 2.53 $cmol_c\ kg^{-1}$ (P5-a) and 2.07 $cmol_c\ kg^{-1}$ (P5-b). The CEC of the lahar 1 layer, 0.99 $cmol_c\ kg^{-1}$ (P5-a) and 1.14 $cmol_c\ kg^{-1}$ (P5-b), is ~two times lower compared to the overlying MS horizon. The BS horizon has CEC values, 3.44 $cmol_c\ kg^{-1}$ (P5-a) and 2.90 $cmol_c\ kg^{-1}$ (P5-b), which are 20 to 40 % higher than that contained in the MS horizon.

Percent BS and proportion of exchangeable bases

Fo-Ash (P1-a, P1-b). The MS horizon has a relatively higher % BS compared to the ash layer, although both exceeded 100 % (i.e. 162 vs. 139 %, respectively, in P1-a and 192 vs. 162 %, respectively, in P1-b). Lower % BS is shown in the pumice layer and BS horizon (i.e. 78 and 56, respectively, in P1-a and 135 and 136 %, respectively, in P1-b) (Fig. 3.8c). The exchange complex is generally occupied by Ca (48-88 %) followed by Mg (5-26 %) in all the samples. The proportion of exchangeable K is lower ranging from 3 to 10 %. The proportion of exchangeable Na is also generally low ranging from 4 to 15 % except in the ash layer of P1-a profile wherein the proportion of Na is 32 % (Fig. 3.8d).

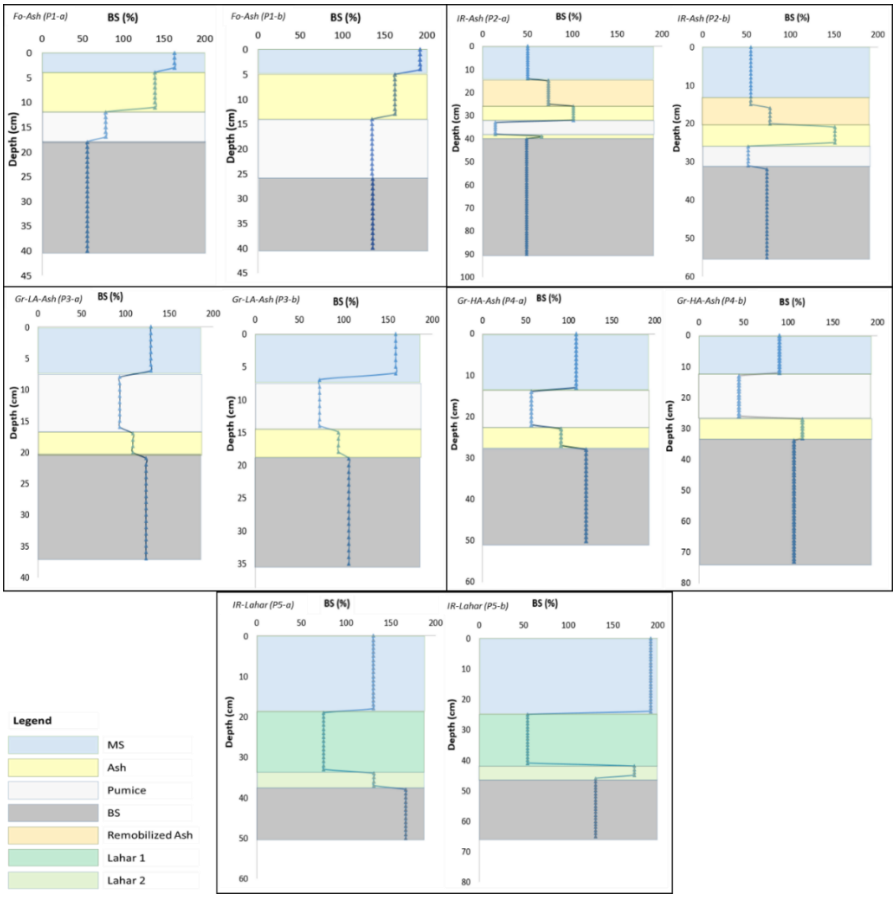

Figure 3.8c. Variation with depth of percent base saturation in the Fo-Ash (P1-a, P1-b; Tarlac province), IR-Ash (P2-a, P2-b; Tarlac province), Gr-LA-Ash (P3-a, P3-b; Pampanga province), Gr-HA-Ash (P4-a, P4- b; Pampanga province) and IR-Lahar (P5-a, P5-b; Zambales province) soil profiles.

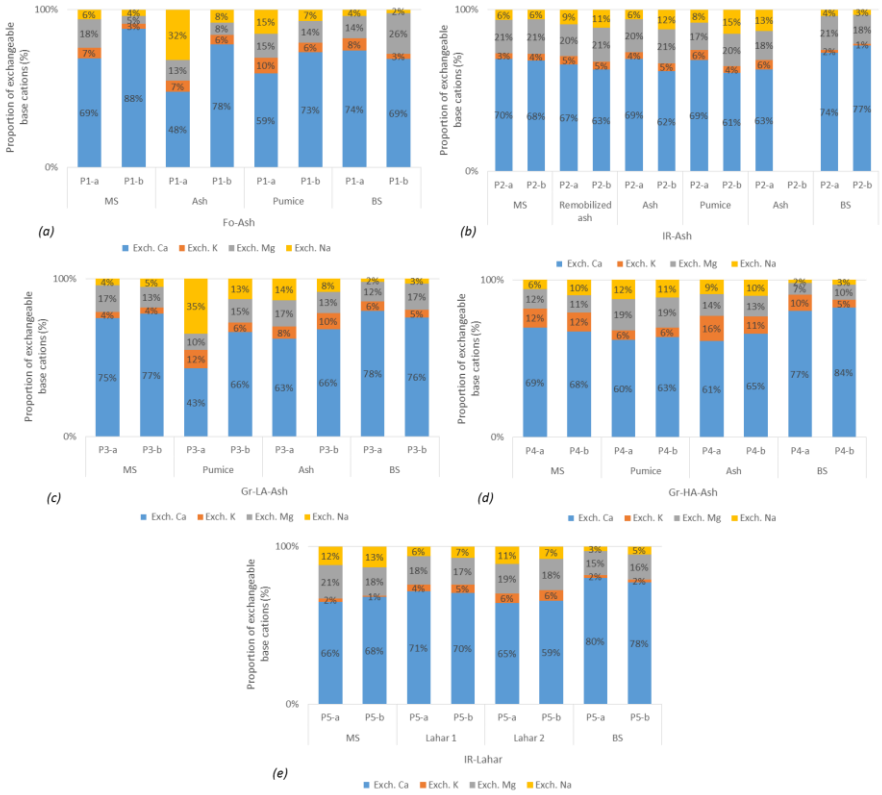

Figure 3.8d. Proportion of exchangeable Ca, K, Mg, and Na in the exchange complex of *(a)* Fo-Ash (P1-a, P1-b; Tarlac province), *(b)* IR-Ash (P2-a, P2-b; Tarlac province), *(c)* Gr-LA-Ash (P3-a, P3-b; Pampanga province), *(d)* Gr-HA-Ash (P4-a, P4-b; Pampanga province), and *(e)* IR-Lahar (P5-a, P5-b; Zambales province) soil profiles.

IR-Ash (P2-a, P2-b). The % BS in the MS horizon (50 %, P2-a and 55 %, P2-b) is lower than that found in the remobilized ash layer (74 %, P2-a and 77 %, P2-b). The ash layer has a high % BS both in P2-a (101 %) and P2-b (151 %) soil profiles while the pumice layer has low % (14 and 52 %, respectively in P2-a and P2-b). The BS horizon has 49 (P1-a) and 73 (P1-b) % BS which is close to that of the MS horizon. The proportion of bases in the exchange complex of the soil horizons, ash and pumice layers of the P2-a and P2-b soil profiles are increasing in

the following order: Na (3-15 %) ≈ K (4-6 %) < Mg (17-21 %) < Ca (61-77 %).

Gr-LA-Ash (P3-a, P3-b). The % BS of the MS horizon is exceedingly higher than the underlying pumice layer in P3-a and P3-b soil profiles, respectively (129 vs. 93 % and 159 vs. 73). The ash layer also has a high % BS (i.e. 108 % in P1-a and 94 % in P1-b). The BS horizon also contained a very high % BS similar to the MS horizon (123 %, P3-a and 106 %, P3-b). The soil horizons, ash and pumice layers of the two soil profiles (P3-a and P3-b) are occupied by exchangeable bases in the following proportion: K (4-12 %) < Na (2-35 %) ≈ Mg (12-17 %) < Ca (43-78 %). The large range in the proportion of exchangeable Na is due to the exceptionally high value obtained from the P3-a pumice layer (i.e. 35 %).

Gr-HA-Ash (P4-a, P4-b). The % BS of the MS horizon is twofold higher than the pumice layer (109 vs. 57 %, respectively, in P4-a and 90 vs. 45 %, respectively, in P4-b). The ash layer has a high % BS in P4-a (91 %) and P4-b (116 %) soil profiles. The BS horizon consistently has a higher % BS than in the MS horizon (i.e. 120 vs. 109 %, respectively, in P4-a and 106 vs. 90 %, respectively, in P4-b). The proportion of exchangeable Ca in the soil horizons, ash and pumice layers varies from 60 to 84 % in the two soil profiles. The remaining fraction is occupied by exchangeable Mg (7-19 %), exchangeable K (5-16 %), and exchangeable Na (2-12 %).

IR-Lahar (P5-a, P5-b). The MS horizon has ~two to four times higher % BS compared to the lahar 1 layer (130 vs. 75 %, respectively, in P5-a and 192 vs. 54 %, respectively, in P5-b). Similarly, the lahar 2 layer and BS horizon have high % BS in P5-a (131 and 167, respectively) and P5-b (174 and 130 %, respectively) which are comparable to the MS horizon. The dominance of bases in the exchangeable complex of the soil horizons and lahar layers in the two soil profiles (P5-a and P5-b) follows the increasing order of sequence: K (1-6 %) < Na (3-13 %) < Mg (15-21 %) < Ca (59-80 %).

Organic C

Fo-Ash (P1-a, P1-b). The organic C content of the BS horizon is slightly higher than in the MS horizon in P1-a and P1-b soil profiles, respectively (1.83 vs. 1.28 wt.%, respectively and 1.34 vs. 1.23 wt.%, respectively). Ash and pumice layers have ~five times lower organic C content than that of the soil horizons (0.24-0.34 wt.%) in the two soil profiles.

IR-Ash (P2-a, P2-b). The MS horizon of the two soil profiles contains 2.03 wt.% (P2-a) and 1.45 wt.% (P2-b) organic C, i.e. it is ~seven times higher than that of the remobilized ash layer (0.19 wt.%, P2-a and 0.30 wt.%, P2-b) and ~two times higher compared to the BS horizon (0.96 wt.%, P2-a and 0.61 wt.%, P2-b). The ash and pumice layers have even lower organic C contents varying from 0.07 to 0.17 in the two soil profiles.

Gr-LA-Ash (P3-a, P3-b). The organic C content of the MS horizon in the two soil profiles, P3-a and P3-b are 1.34 and 1.81 wt.%, respectively, which are ~threefold higher compared to that contained in the BS horizon, 0.43 and 0.46 wt.%, respectively. Furthermore, the organic C contents of the MS horizons are ~eight times higher than that of the pumice and ash layers which vary from 0.16 to 0.30 wt.% in the two profiles.

Gr-HA-Ash (P4-a, P4-b). The MS horizon contains 0.61 and 1.01 wt.% organic C in P4-a and P4-b profiles, respectively, which is ~ten times higher compared to its underlying pumice and ash layers (0.08-0.11 wt.% in the two profiles). The organic C content in the BS horizon, 0.38 wt.% (P4-a) and 0.94 wt.% (P4-b), is slightly lower than in the MS horizon.

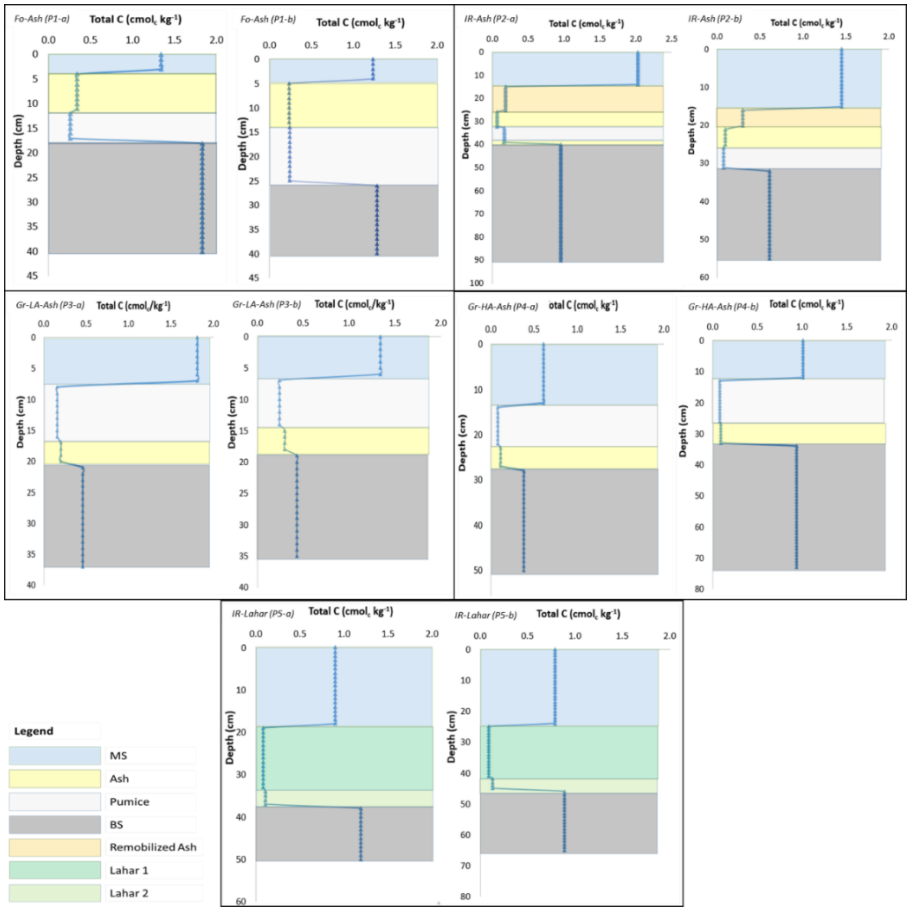

Figure 3.8e. Variation with depth of total organic carbon content in the Fo-Ash (P1-a, P1-b; Tarlac province), IR-Ash (P2-a, P2-b; Tarlac province), Gr-LA-Ash (P3-a, P3-b; Pampanga province), Gr-HA-Ash (P4-a, P4-b; Pampanga province) and IR-Lahar (P5-a, P5-b; Zambales province) soil profiles.

IR-Lahar (P5-a, P5-b). The organic C content of the MS horizon in P5-a and P5-b profiles, respectively, are 0.90 and 0.79 wt.%, which are up to ten times higher than that of the lahar layers (0.08-0.13 wt.% in the two profiles). However, the MS horizon has slightly lower organic C content than that of the BS horizon, respectively (0.90 vs. 1.19 wt.%, in P5-a and 0.79 vs. 0.89 wt.% in P5-b).

P retention

Fo-Ash (P1-a, P1-b). The P retention of the BS horizon in both soil profiles (P1-a and P1-b, respectively) are two to six times higher than that of the MS horizon (26.06 and 21.55 %, respectively vs. 4.23 and 8.62 %, respectively). The ash and pumice layers did not retain P in both P1-a and P1-b profiles (Table 5.2).

IR-Ash (P2-a, P2-b). The MS horizon retains 11.79 and 15.79 % in P2-a and P2-b soil profiles, respectively. Its P retention is ~two times higher than in the remobilized ash layer, 7.26 % (P2-a) and 5.56 % (P2-b). The MS horizon also has relatively higher P retention than that in the BS horizon (11.79 vs. 12.21 %, respectively, in P2-a and 15.79 vs. 3.26 %, respectively, in P2-b). The ash and pumice layers have lower P retention values varying from 0.73 to 4.89 % (P2-a) and 0 to 1.88 % (P2-b).

Gr-LA-Ash (P3-a, P3-b). The MS horizons and pumice layers did not retain P in both P3-a and P3-b profiles. However, the ash layer and BS horizon have retained P (1.88-4.31 % in the two profiles).

Gr-HA-Ash (P4-a, P4-b). The P retained in the BS horizon is three to ten times higher than that of the MS horizon (0 vs. 10.10 %, respectively, in P4-a and 4.51 vs. 13.59 %, respectively, in P4-b). The pumice and ash layers did not retain P in both soil profiles.

IR-Lahar (P5-a, P5-b). The P retained in the MS horizon of P5-a and P5-b soil profiles, respectively, 7.23 and 10.21 %, are slightly lower than that retained in the BS horizon, 10.95 and 16.22 %, respectively. The lahar 1 and lahar 2 layers have lower P retention varying from 0 to 2.53 % for the two profiles.

3.3.5 Selective dissolutions of Si, Al, and Fe

The results of selective dissolution extractions of Fe using DCB; Si, Al, and Fe extracted by ammonium oxalate; and, Fe and Al using Na-pyrophosphate from the two soil profiles of the five sampling sites are shown in Figures 3.9[a-c]. The allophane/imogolite and ferrihydrite contents are also reported in Figure 3.9d. Table A.3.4 reports the measured values for the selective dissolution extractions of Si, Al, and Fe, allophane/imogolite, and ferrihydrite contents.

Si_o, Al_o, and Fe_o contents

Fo-Ash (P1-a, P1-b). The Si_o content of the MS horizon, ash, and pumice layers vary in the range 0.016–0.034 wt.% (P1-a and P1-b soil profiles). The BS horizon has higher Si_o content than that of the MS horizon (0.041 vs. 0.034, respectively, in P1-a and 0.050 vs. 0.033, respectively, in P1-b). The MS horizon has ~two times higher Al_o content in P1-a and P1-b soil profiles (0.11 wt.% and 0.10 wt.%, respectively) than that of the ash and pumice layers (0.04-0.07 wt.% in the two soil profiles). In the BS horizon, the Al_o content is ~three times higher than in the MS horizon (0.32 vs. 0.11 wt.%, respectively, in P1-a and 0.30 vs 0.10 wt.%, respectively, in P1-b). The Fe_o content of the MS horizon and ash layer in the two soil profiles (P1-a and P1-b) are comparable ranging from 0.34 to 0.43 wt.%. The pumice layer has more variable Fe_o content between the P1-a and P1-b soil profiles (0.56 and 0.26 wt.%, respectively). The BS horizon has slightly higher Fe_o content than that of the MS horizon (0.51 vs. 0.43 wt.%, respectively, in P1-a and 0.44 vs. 0.36 wt.%, respectively, in P1-b).

IR-Ash (P2-a, P2-b). The Si_o content of the MS horizon is ~20 % lower than in the remobilized ash layer in P2-a and P2-b soil profiles, respectively (0.040 vs. 0.034 wt.%, respectively and 0.045 vs. 0.040 wt.%, respectively). The ash and pumice layers underlying the remobilized ash layer has 0.016 to 0.043 wt.% Si_o contents in the two soil profiles. The BS horizon has comparable Si_o content with that of

the MS horizon (i.e. 0.032 vs. 0.040 wt.%, P2-a and 0.030 vs. 0.034 wt.%, P2-b), respectively.

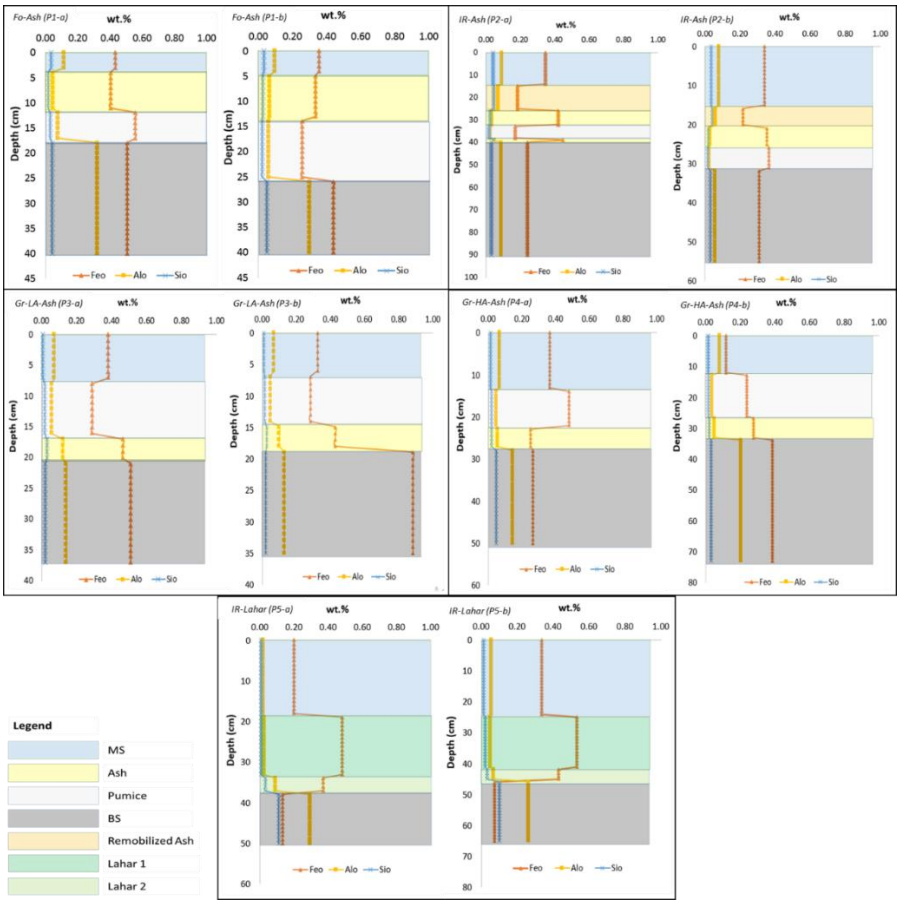

Figure 3.9a. Oxalate-extracted Si, Al, and Fe contents in the Fo-Ash (P1-a, P1-b; Tarlac province), IR-Ash (P2-a, P2-b; Tarlac province), Gr-LA-Ash (P3-a, P3-b; Pampanga province), Gr-HA-Ash (P4-a, P4-b; Pampanga province) and IR-Lahar (P5-a, P5-b; Zambales province) soil profiles.

The Al_o content of the MS horizon is slightly higher compared to that of the remobilized ash layer (0.09 vs. 0.07 wt.%, P2-a and 0.08 vs. 0.06

wt.%, P2-b), respectively. The ash and pumice layers have much smaller values varying between 0.02 to 0.05 wt.% in P2-a and 0.02 to 0.03 wt.% Alo in P2-b, respectively. The BS horizon has 0.09 and 0.06 wt.% Al_o in P2-a and P2-b soil profiles, respectively, which is comparable to that of the MS horizon.

The MS horizon has increased its Fe_o content from that of the remobilized ash layer in P2-a and P2-b soil profiles, respectively (0.35 vs. 0.18 wt.%, respectively and 0.34 vs. 0.22 wt. %, respectively). The Fe_o content of the MS horizon is also slightly higher than that of the BS horizon (0.35 vs. 0.24 wt.%, respectively in P2-a and 0.34 vs. 0.31 wt. %, respectively in P2-b). The rest of the ash and pumice layers have Fe_o contents varying from 0.17 to 0.45 wt.% in the two profiles.

Gr-LA-Ash (P3-a, P3-b). The Si_o content of the MS horizon is 0.009 wt.% (both P3-a and P3-b profiles) while that of the pumice layer has 0.019 wt.% (P3-a) and 0.014 wt.% (P3-b). The ash layer has three times more Si_o content than in the MS horizon (0.030 and 0.026 wt.% in both P3-a and P3-b profiles). The Si_o content in the BS horizon (0.022 and 0.020 wt.% in P3-a and P3-b, respectively) is ~two times higher than that in the MS horizon.

The Al_o content of the MS horizon (0.07 wt.%, P3-a and P3-b) has increased by ~20 % compared to the pumice layer (0.06 wt.%, P3-a and 0.05 wt.%, P3-b) but is ~two times lower than that of the ash layer (0.14 wt.%, P3-a and 0.13 wt.%, P3-b). The BS horizon also has ~two times higher Al_o content than that of the MS horizon, respectively (0.14 vs. 0.07 wt.%, in P3-a and 0.13 vs. 0.07 wt.%, in P3-b).

The Fe_o content of the MS horizon is slightly higher compared to the pumice layers in P3-a and P3-b soil profiles, respectively (0.38 vs. 0.29 wt.%, respectively and 0.32 vs. 0.28 wt.%, respectively). The ash layer has slightly higher Fe_o content than that of the MS in the two soil profiles, respectively, i.e. 0.46 vs. 0.38 wt.% (P3-a) and 0.43 vs. 0.32 wt.% (P3-b). Similarly, the BS horizon contains roughly two times

higher Fe_o content than that of the MS horizon in the two soil profiles, respectively, i.e. 0.51 vs 0.38 wt.% (P3-a), 0.88 vs 0.32 wt.% (P3-b).

Gr-HA-Ash (P4-a, P4-b). The BS horizon has a Si_o content of 0.047 wt.% (P4-a) and 0.031 wt.% (P4-b) that are approximately two times higher than that of MS horizon, pumice and ash layers varying from 0.014 to 0.020 wt.% in the two soil profiles.

The Al_o content of the MS horizon is up to 50 % higher than that of pumice layer but ~two times lower compared to the BS horizon (0.07 vs. 0.05 vs. 0.14 wt.%, respectively, in P4-a and 0.08 vs. 0.04 vs. 0.13 wt.%, respectively, in P4-b). The Al_o content of the MS horizon is also lower than that of the ash layer in the P4-a and P4-b soil profiles, respectively (0.07 vs. 0.06 wt.%, respectively and 0.08 vs. 0.05 wt.%, respectively).

The Fe_o content of the MS horizon is lower compared to the pumice layer in P4-a and P4-b soil profiles, respectively (0.36 vs. 0.48 wt.%, respectively and 0.12 vs. 0.24 wt.%, respectively). There is large variability in the Fe_o content of MS horizon (0.36 wt.%, P4-a and 0.12 wt.%, P4-b), i.e. it is somewhat comparable to that of the BS horizon (0.27 wt.%, P4-a and 0.38 wt.%, P4-b) and ash layer (0.25 wt.%, P4-a and 0.28 wt.%, P4-b).

IR-Lahar (P5-a, P5-b). The Si_o content of the lahar 1 layer (0.007 and 0.023 wt.% in P5-a and P5-b, respectively) is slightly higher than that of the MS horizon with 0.005 wt.% (P5-a) and 0.014 wt.% (P5-b). The lahar 2 layer has three times more Si_o content (0.031 vs. 0.032 wt.%, respectively in P5-a and P5-b profiles) than in the MS horizon. The BS horizon contains up to 20 times more Si_o compared to the MS horizon, i.e. 0.110 vs. 0.005 wt.% in P5-a, respectively and 0.101 vs. 0.014 wt.% in P5-b, respectively.

The Al_o content of the MS horizon and lahar 1 layer is comparable (0.02 wt.% in the two profiles), however, that of the lahar 2 layer is higher than the MS horizon (i.e. 0.09 vs. 0.02 wt.% in P5-a, respectively, and

0.07 vs. 0.06 wt.% in P5-b, respectively). The Al_o content of the BS horizon (0.26 and 0.30 wt.%) is up to 13 times higher compared to the MS horizon (0.26 vs. 0.02 in P5-a, respectively and 0.30 vs. 0.06 wt.% in P5-b, respectively).

The Fe_o content of the MS horizon (P5-a and P5-b, respectively) are lower (i.e. 0.20 and 0.34 wt.%) than that of underlying lahar 1 and lahar 2 layers (0.37-0.53 wt.%). The BS horizon contains 0.07 wt.% (P5-a) and 0.13 wt.% (P5-b) Fe_o; it is ~three times lower compared to that of the MS horizon containing 0.20 wt.% (P5-a) and 0.34 wt.% (P5-b).

Fe_d content

Fo-Ash (P1-a, P1-b). The Fe_d content in the MS horizon of the P1-a and P1-b soil profiles (0.30 and 0.46 wt.%, respectively) are two to three times higher than that of the ash (0.15 and 0.14 wt.%, respectively) and pumice (0.17 and 0.17 wt.%, respectively) layers. The BS horizon has ~five times higher Fe_d content (1.52 and 1.84 wt.%, respectively) than that of the MS horizon.

IR-Ash (P2-a, P2-b). The MS horizon has slightly higher Fe_d content compared to the remobilized ash layer in the two soil horizons (i.e. 0.43 vs. 0.32 wt.%, respectively, in P2-a and 0.38 vs. 0.36 wt.%, respectively, in P2-b). Lower Fe_d contents are measured in the subsequent ash in P2-a and P2-b profiles (0.19 and 0.20 wt.%, respectively) and pumice (0.12 and 0.09 wt.%, respectively) layers. The BS horizon of P2-a soil profile has lower Fe_d content than the MS horizon (0.33 vs. 0.43 wt.%), however, in the P2-b soil profile, the Fe_d content of the MS and BS horizons are both 0.38 wt.%.

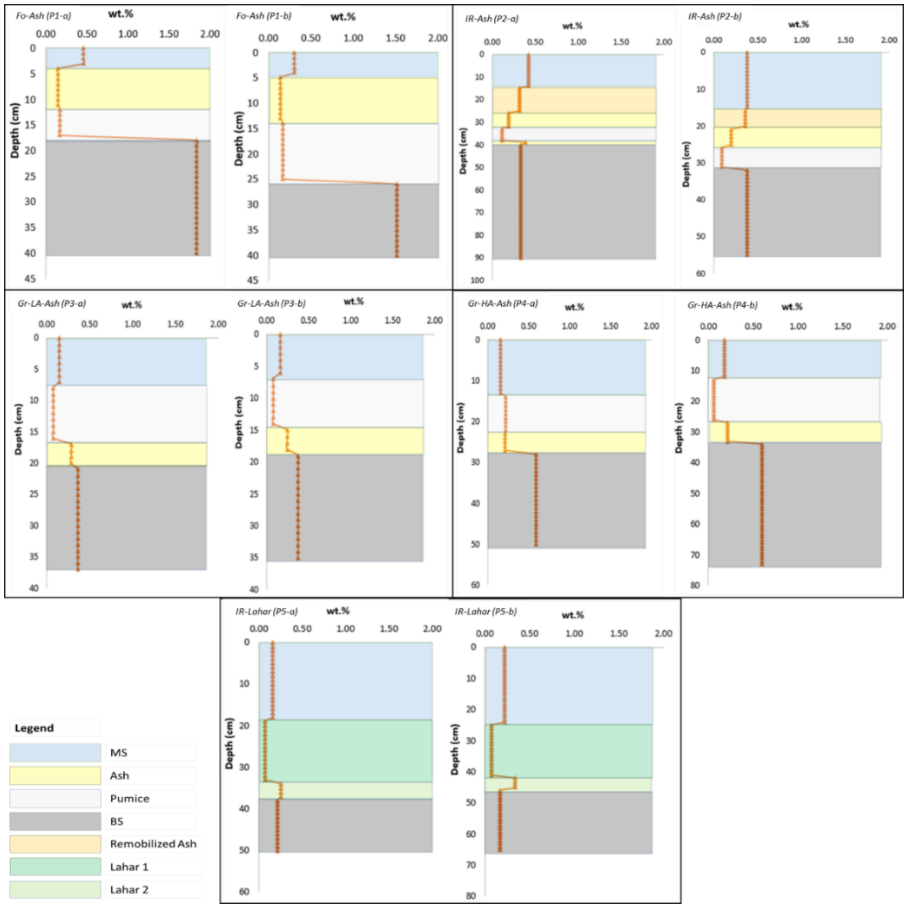

Figure 3.9b. DCB-extracted Fe content in the Fo-Ash (P1-a, P1-b; Tarlac province), IR-Ash (P2-a, P2-b; Tarlac province), Gr-LA-Ash (P3-a, P3-b; Pampanga province), Gr-HA-Ash (P4-a, P4-b; Pampanga province) and IR-Lahar (P5-a, P5-b; Zambales province) soil profiles.

Gr-LA-Ash (P3-a, P3-b). The MS horizon of the two soil profiles (P3-a and P3-b) has 0.14 and 0.16 wt.% Fe_d, respectively, which are two times higher than in the pumice layer (0.08 wt.% in both soil profiles). The Fe_d content of the ash layer (0.28 wt.%, P3-a and 0.25 wt.%, P3-b) and BS horizon (0.36 wt.%, P3-a and 0.38 wt.%, P3-b) are ~two times higher than in the MS horizon.

Gr-HA-Ash (P4-a, P4-b). The MS horizon has 0.16 and 0.18 wt.% Fe_d in the P4-a and P4-b profiles, respectively; it is lower than in the ash layer (0.22 and 0.21 wt.%, respectively). The Fe_d content of the pumice layer varies largely between 0.22 wt.% (P4-a) and 0.06 wt.% (P4-b). The BS horizon has ~three times more Fe_d content compared to the MS horizon (0.59 vs. 0.16 wt.%, respectively, in P4-a and 0.60 vs. 0.18 wt.%, respectively, in P4-b).

IR-Lahar (P5-a, P5-b). The soil horizons (MS and BS) of the two soil profiles have comparable Fe_d contents (i.e. 0.16-0.22 wt.%). The Fe_d content of the lahar 1 layer is ~two times lower than that of the MS horizon in the P5-a and P5-b soil profiles, respectively (0.07 vs. 0.16 wt.%, respectively and 0.07 vs. 0.22 wt.%, respectively) while that of lahar 2 layer is slightly higher compared to the MS horizon (0.26 vs. 0.16 wt.%, respectively and 0.34 vs. 0.22 wt.%, respectively).

Al_p and Fe_p contents

Fo-Ash (P1-a, P1-b). The Al_p content in the MS horizon is 0.04 wt.% in both P1-a and P1-b soil profiles; it is ~five times lower than in the BS horizon (0.24 and 0.19 wt.%, respectively). The ash and pumice layers have much lower Al_p contents (0.02-0.03 wt.%, P1-a, and P1-b) than in the soil horizons. The Fe_p content of the MS horizon (0.03 wt.%, P1-a and 0.04 wt.%, P1-b) is also significantly lower than that of the BS horizon (0.22 wt.%, P1-a and 0.18 wt.% wt.%, P1-b). The ash and pumice layers contain less Fe_p (0.01-0.02 wt.%, P1-a and P1-b) than the soil horizons.

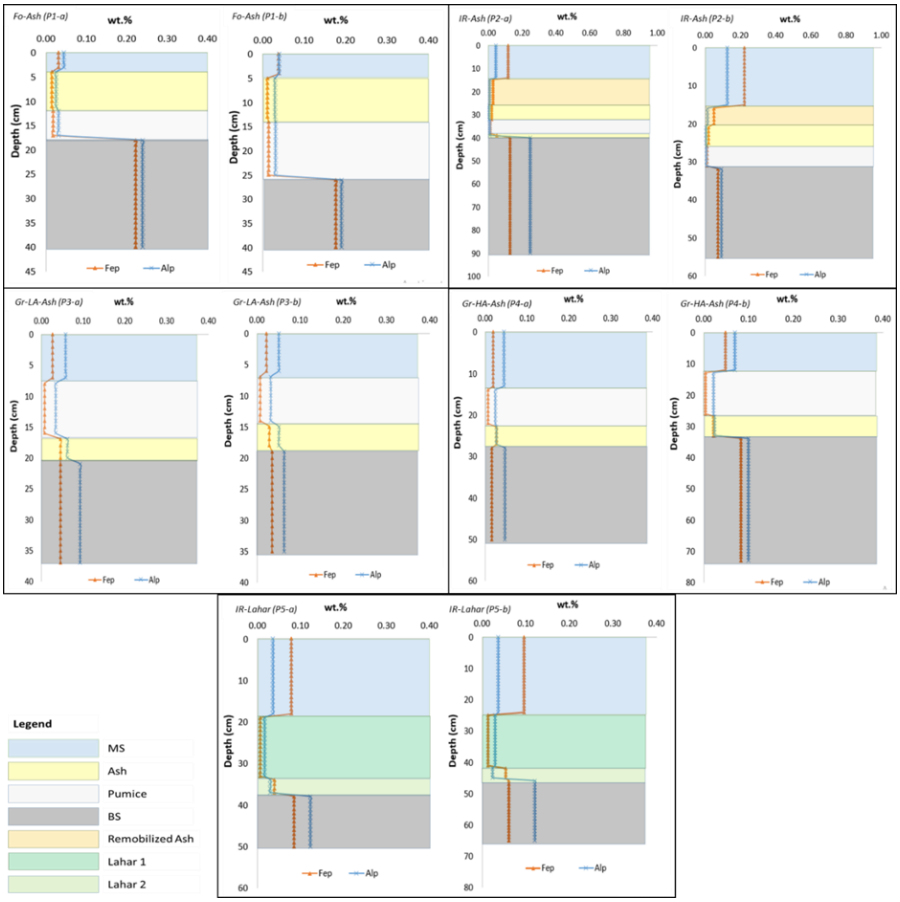

Figure 3.9c. Pyrophosphate-extracted Fe and Al in the Fo-Ash (P1-a, P1-b; Tarlac province), IR-Ash (P2-a, P2-b; Tarlac province), Gr-LA-Ash (P3-a, P3-b; Pampanga province), Gr-HA-Ash (P4-a, P4-b; Pampanga province) and IR-Lahar (P5-a, P5-b; Zambales province) soil profiles.

IR-Ash (P2-a, P2-b). The MS horizon has 0.04 and 0.12 wt.% Al_p in P2-a and P2-b soil profiles, respectively; The Al_p content in P2-a MS horizon is ~sixfold lower than that contained in the BS horizon (0.04 vs. 0.25 wt.%, respectively) while in the P2-b MS horizon, the Al_p content is slightly higher (0.12 vs. 0.09 wt.%, respectively). The remobilized ash, ash, and pumice layers have negligible Alp contents (0-0.01 wt.%, P2-a, and P2-b). The Fe_p content of the MS horizon (0.12

wt.%, P2-a and 0.22 wt.%, P2-b) is higher than in the BS horizon (0.13 wt.%, P2-a and 0.07 wt.%, P2-b). The remobilized ash, ash and pumice layers have low Fe_p contents varying from 0.01 to 0.05 wt.% in the two soil profiles.

Gr-LA-Ash (P3-a, P3-b). The Al_p contents of the MS horizon and ash layers are 0.06 and 0.05 wt.%, respectively, in P3-a and P3-b soil profiles; they are twofold higher than that in the pumice layer (0.03 wt.% in both soil profiles). The BS horizon has slightly higher Al_p contents than in the MS horizon (0.09 vs. 0.06 wt.%, respectively in P3-a and 0.06 vs. 0.05 wt.% respectively, in P3-b). The Fe_p content of the MS horizon (0.03 and 0.02 wt.%) in P3-a and P3-b, respectively, are two to three times higher than that of the pumice layer (0.01 wt.%, in both profiles). The BS horizon and ash layer contain higher Fe_p (i.e. 0.05 and 0.03 wt.%, respectively, in both profiles) than in the MS horizon.

Gr-HA-Ash (P4-a, P4-b). The MS horizon has two to three times more Al_p content in the P4-a and P4-b profiles (0.04 and 0.07 wt.%, respectively) than in the pumice and ash layers (0.02-0.03 wt.%, P4-a, and P4-b). The BS horizon contains slightly higher Al_p content compared to the MS horizon in P4-a (0.05 vs. 0.04 wt.%, respectively) and P4-b (0.10 vs. 0.07 wt.%, respectively) profiles. The Fe_p content of the MS horizon is up to five times higher than that of the pumice layer, i.e. 0.02 vs. 0.01 wt.%, respectively, in P4-a and 0.05 vs. 0.00 wt.%, respectively, in P4-b profile. The ash layer has 0.03 wt.% (P4-a) and 0.02 wt.% (P4-b) Fe_p content. The BS horizon of P4-a has similar Fe_p content with the MS horizon (0.02 wt.%) while that of the P4-b soil profile, the BS horizon has a comparative advantage (0.08 vs. 0.05 wt.%, respectively).

IR-Lahar (P5-a, P5-b). The Al_p content of the MS horizon (0.04 wt.% in both P5-a and P5-b soil profiles) is a little higher than in the lahar layers (0.02-0.03 wt.%). The BS horizon has ~three times higher Al_p content than the MS horizon (0.12 vs. 0.04 wt.% in both profiles). On the other hand, the Fe_p content of the MS horizon P5-a and P5-b profiles

(0.08 and 0.10 wt.%, respectively) are ~ten times higher than that of the lahar 1 layer (0.01 wt.% in both profiles). The lahar 2 layer also has low Fe_p (0.04-0.05 wt.%; P5-a and P5-b). The BS horizon has the same Fe_p content with the P5-a MS horizon (0.08 wt.%) but has smaller Fe_p content than in P5-b MS horizon (0.06 vs. 0.10 wt.%, respectively).

Allophane/imogolite and ferrihydrite contents

Fo-Ash (P1-a, P2-b). The allophane/imogolite content, as estimated using Eq. 3.5, of the MS horizon in P1-a and P1-b soil profiles are both 0.24 wt.%; it is roughly two times higher than that derived for the ash layer (0.12 wt.%, P1-a and 0.18 wt.%, P1-b) and also slightly higher than the pumice layer (0.20 wt.%, P1-a and 0.16 wt.%, P1-b). The BS horizon has a slightly higher content of allophane/imogolite compared to that in the MS horizon (0.29 vs. 0.24 wt.%, respectively, in P1-a and 0.35 vs. 0.24 wt.%, respectively, in P1-b). The estimated ferrihydrite content inferred by applying Eq. 3.6 shows that the content in the MS horizon is comparable to the underlying ash layer in P1-a (0.74 vs. 0.69 wt.%, respectively) and P1-b (0.61 vs. 0.57 wt.%, respectively). The pumice layer has a larger variation in ferrihydrite content between the two soil profiles (i.e. 0.95 wt.% in P1-a and 0.43 wt.% in P1-b), nevertheless, these values are higher compared to that derived in the MS horizon. The BS horizon has a slightly higher content of ferrihydrite than the MS horizon in both the P1-a (0.86 vs. 0.74 wt.%, respectively) and P1-b (0.75 vs. 0.61 wt.%), respectively.

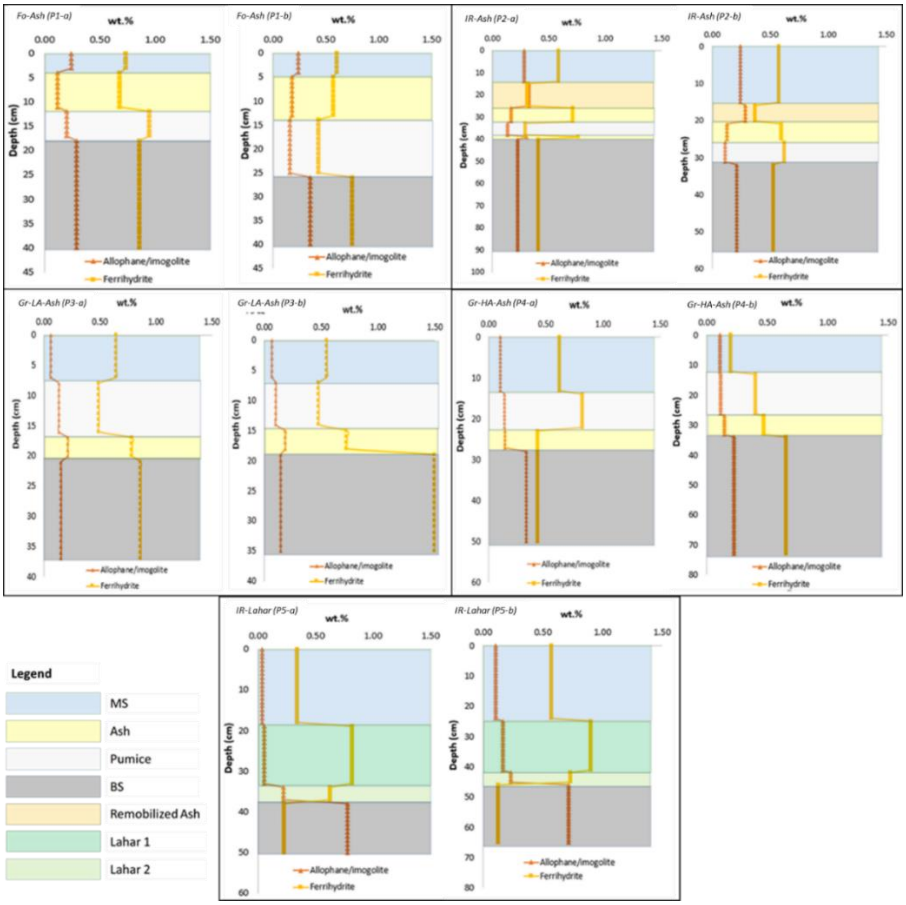

Figure 3.9d. Allophane and ferrihydrite contents in the Fo-Ash (P1-a, P1-b; Tarlac province), IR-Ash (P2-a, P2-b; Tarlac province), Gr-LA-Ash (P3-a, P3-b; Pampanga province), Gr-HA-Ash (P4-a, P4-b; Pampanga province) and IR-Lahar (P5-a, P5-b; Zambales province) soil profiles.

IR-Ash (P2-a, P2-b). The allophane/imogolite content of the MS horizon is slightly lower compared to the remobilized ash layer in the P2-a (0.28 vs. 0.32 wt.%, respectively) and P2-b (0.24 vs. 0.29 wt.%, respectively) soil profiles. The succeeding layers of ash and pumice have lower contents of allophane and imogolite varying from 0.11 to 0.17 in both soil profiles except for the 1 cm thick ash layer in the P2-a profile which has 0.30 wt.% allophane/imogolite content. The BS horizon has slightly lower allophane/imogolite content than that of the

MS horizon (0.22 vs. 0.28 wt.%, respectively, in P2-a and 0.21 vs. 0.24 wt.%, respectively, in P2-b). On the other hand, it appears that ferrihydrite content of the MS horizon is ~twofold higher than in the remobilized ash layer in the P2-a and P2-b profiles, respectively (0.59 vs. 0.31 wt.%, respectively, and 0.58 vs. 0.37 wt.%, respectively). The content of ferrihydrite varies from 0.29 to 0.76 (P2-a and P2-b) in the ash and pumice layers. Ferrihydrite content in the BS horizon is slightly lower compared to the MS horizon (0.41 vs. 0.59 wt.%, respectively, in P2-a and 0.53 vs. 0.58, respectively, in P2-b).

Gr-LA-Ash (P3-a, P3-b). The allophane/imogolite content of the MS horizon in P3-a (0.06 wt.%) and P3-b (0.07 wt.%) soil profiles are significantly lower compared to that of the pumice layer (0.13 and 0.10, respectively), ash layer (0.21 and 0.18 wt.%, respectively), and BS horizon (0.15 and 0.14, respectively). The ferrihydrite content of the MS horizon in the two soil profiles (P3-a and P3-b) is 0.65 and 0.55 wt.%, respectively; it is slightly higher than that of the pumice layer (0.49 and 0.48 wt.%, respectively) but lower compared to the ash layer (0.79 and 0.73 wt.%, respectively). The BS horizon has considerably higher ferrihydrite content than in the MS horizon (0.87 vs. 0.65 wt.%, respectively, in P2-a and 1.50 vs. 0.55 wt.%, respectively, in P2-b).

Gr-HA-Ash (P4-a, P4-b). The allophane/imogolite content of the MS horizon (0.10 and 0.11 wt.%, respectively in P4-a and P4-b soil profiles) are a little lower than that what is derived from the pumice (0.12 and 0.14 wt.%, respectively) and ash layers (0.14 wt.% in both soil profiles). The BS horizon accumulated two to three times more allophane/imogolite compared to the MS horizon (0.33 vs. 0.10 wt.%, respectively, in P4-a and 0.22 vs. 0.11 wt.%, respectively, in P4-b). The ferrihydrite content of the MS horizon is appreciably lower than in the pumice layer in P4-a (0.62 vs. 0.81 wt.%, respectively) and P4-b (0.20 vs. 0.40 wt.%) profiles. The ash layer has 0.43 and 0.47 wt.% ferrihydrite content in P4-a and P4-b soil profiles, respectively. The BS horizon has lower ferrihydrite content compared to the MS horizon in P4-a (0.45 vs. 0.62 wt.%, respectively) but vice versa in the P4-b soil profile (0.65 vs. 0.20 wt.%, respectively).

IR-Lahar (P5-a, P5-b). The allophane/imogolite content gradually increase with depth within the two soil profiles, P5-a and P5-b, respectively, i.e. MS horizon (04 and 0.10 wt.%, respectively), lahar 1 layer (0.05 and 0.16 wt.%, respectively), lahar 2 layer (0.22 and 0.23 wt.%, respectively), and BS horizon (0.72 and 0.78 wt.%, respectively). The ferrihydrite content of the MS horizon (0.34 wt.%, P5-a and 0.57 wt.%, P5-b) are ~twofold lower compared to the lahar layers varying from 0.63 to 0.90 wt.% (P5a and P5-b). The BS horizon has considerably lower ferrihydrite content than the MS horizon in P5-a (0.23 and 0.34 wt.%, respectively) and P5-b (0.13 vs. 0.57 wt.%, respectively) soil profiles.

3.3.6. Weathering indices

The TRB, Fe_d/Fe_t, and Al:Si ratio measured values along soil profile depth are shown in Figures 3.10[a-c]. The detailed measurements are presented in Table A3.5.

TRB

Fo-Ash (P1-a, P1-b). The TRB (Eq. 3.8) of the MS horizon is lower than that of the underlying ash layer in the P1-a (378 vs. 505 $cmol_c\ kg^{-1}$, respectively) and P1-b (423 vs. 463 $cmol_c\ kg^{-1}$, respectively) soil profiles. The pumice layer has 423 and 414 $cmol_c\ kg^{-1}$ in P1-a and P1-b, respectively, which is comparable to the MS horizon. The BS horizon shows the lowest TRB values (118 $cmol_c\ kg^{-1}$, P1-a and 128 $cmol_c\ kg^{-1}$, P1-b).

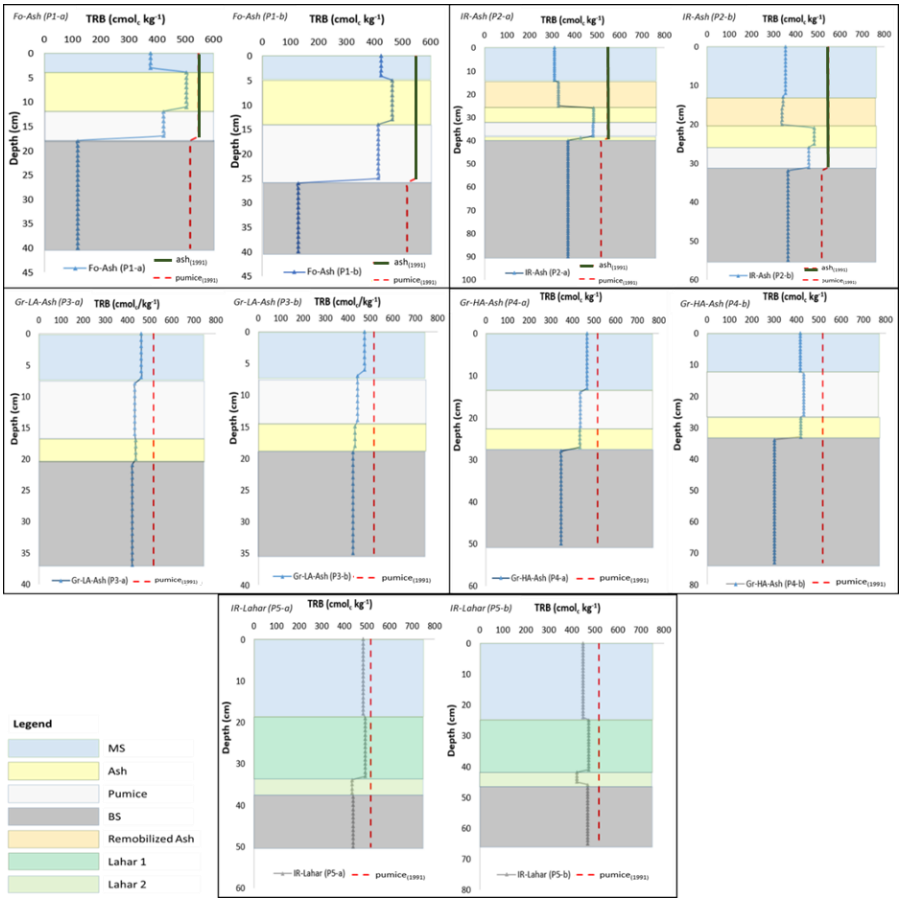

Figure 3.10a. TRB content in the Fo-Ash (P1-a, P1-b; Tarlac province), IR-Ash (P2-a, P2-b; Tarlac province), Gr-LA-Ash (P3-a, P3-b; Pampanga province), Gr-HA-Ash (P4-a, P4-b; Pampanga province) and IR-Lahar (P5-a, P5-b; Zambales province) soil profiles. **1991 fresh ash (used in Fo-Ash and IR-Ash soil profiles where the MS has developed from the underlying ash layer) and 1991 fresh pumice (used in Gr-LA-Ash, Gr-HA-Ash, and IR-Lahar where the MS has developed from pumice; also used in the BS of all the soil profiles) TRB data adapted from Castillo and Punongbayan (1996).*

IR-Ash (P2-a, P2-b). In the two soil profiles, P2-a and P2-b, the TRB obtained in the MS horizon (311 and 349 cmol$_c$ kg^{-1}, respectively) and remobilized ash layer (330 and 338 cmol$_c$ kg^{-1}, respectively) are comparable. The ash and pumice layers in P2-a and P2-b profiles have

higher TRB values varying from 428 to 486 $cmol_c\ kg^{-1}$. The BS horizon has comparatively higher TRB values than that of MS horizon in P2-a (370 vs. 311 $cmol_c\ kg^{-1}$) and P2-b (365 vs. 349 $cmol_c\ kg^{-1}$) soil profiles, respectively.

Gr-LA-Ash (P3-a, P3-b). The MS horizon has slightly higher TRB in the two soil profiles, P3-a and P3-b, respectively (463 and 475 $cmol_c\ kg^{-1}$) compared to the pumice (434 and 444 $cmol_c\ kg^{-1}$) and ash (437 and 431 $cmol_c\ kg^{-1}$) layers. The BS horizon has the lowest TRB values (422 $cmol_c\ kg^{-1}$ in both soil profiles).

Gr-HA-Ash (P4-a, P4-b). In general, the TRB values are gradually decreasing within the soil profile from the surface to the bottom, i.e. TRB values in P4-a and P4-b soil profiles are 467 and 418 $cmol_c\ kg^{-1}$, respectively (MS horizon), 437 and 432 $cmol_c\ kg^{-1}$, respectively (pumice layer), 434 and 419 $cmol_c\ kg^{-1}$, respectively (ash layer), and 348 and 301 $cmol_c\ kg^{-1}$, respectively (BS horizon).

IR-Lahar (P5-a, P5-b). The TRB of the MS horizon is slightly lower compared to that of the lahar 1 layer in P5-a and P5-b soil profiles, respectively (483 vs. 493 $cmol_c\ kg^{-1}$ and 449 vs. 473 $cmol_c\ kg^{-1}$). The lahar 2 layer has much lower values (434 $cmol_c\ kg^{-1}$, P5-a and 422 $cmol_c\ kg^{-1}$, P5-b). The BS horizon has comparable TRB value with that of the MS horizon varying from 440 and 469 $cmol_c\ kg^{-1}$ in P2-a and P2-b profiles, respectively.

Fe_d/Fe_t ratio

Fo-Ash (P1-a, P1-b). The Fe_d/Fe_t ratio (Eq. 3.9) of the MS horizon of the P1-a and P1-b soil profiles (0.10 and 0.14, respectively) is approximately two times higher than that of the ash and pumice layers varying from 0.04 to 0.06 in both soil profiles. The BS horizon has 0.30 and 0.31 Fe_d/Fe_t ratio (P1-a and P1-b, respectively) which is ~three times higher than that of the MS horizon.

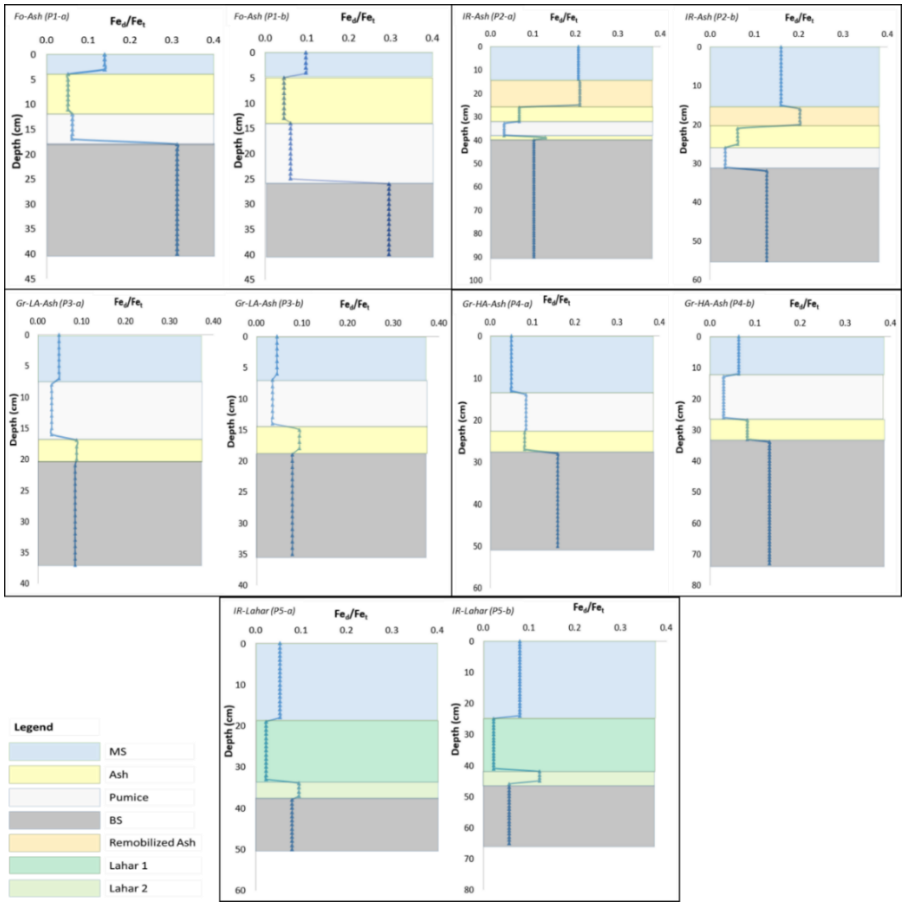

Figure 3.10b. Fe_d/Fe_t ratio in the Fo-Ash (P1-a, P1-b; Tarlac province), IR-Ash (P2-a, P2-b; Tarlac province), Gr-LA-Ash (P3-a, P3-b; Pampanga province), Gr-HA-Ash (P4-a, P4-b; Pampanga province) and IR-Lahar (P5-a, P5-b; Zambales province) soil profiles.

IR-Ash (P2-a, P2-b). The MS horizon and remobilized ash layers have the same Fe_d/Fe_t ratio in the P2-a soil profile (0.21), however, in the P2-b soil profile, the MS horizon has a slightly lower Fe_d/Fe_t ratio than the remobilized ash layer (0.16 vs. 0.20, respectively). The succeeding ash and pumice layers have lower Fe_d/Fe_t ratios varying from 0.03 to 0.13 in both soil profiles. The BS horizon has a Fe_d/Fe_t ratio that is up to two times lower than the MS horizon (0.10 vs. 0.21, respectively, in P2-a and 0.13 vs. 0.16, respectively, in P2-b).

Gr-LA-Ash (P3-a. P3-b). The Fe_d/Fe_t ratio of the MS horizon and pumice layer in P3-a and P3-b soil profiles are comparable varying from 0.03 to 0.05. The ash layer and BS horizon in P1-a and P2-b soil profiles, respectively, have higher Fe_d/Fe_t ratios (0.08-0.09) compared to that in the MS horizon (0.04 and 0.05, respectively).

Gr-HA-Ash (P4-a, P4-b). The P4-a MS horizon has a lower Fe_d/Fe_t ratio than that of the pumice layer (0.05 vs. 0.08, respectively), however, vice versa is observed in the P4-b MS horizon (0.06 vs. 0.03, respectively). The Fe_d/Fe_t ratio of the ash layer is 0.08 in both soil profiles, while that of the BS horizon is threefold higher compared to that in the MS horizon (0.16 vs. 0.05, respectively in P4-a and 0.13 vs. 0.06, respectively in P4-b).

IR-Lahar (P5-a, P5-b). The Fe_d/Fe_t ratio of the MS horizon (0.05, P5-a and 0.08, P5-b) is up to four times higher than that of the lahar 1 layer (0.02, in both soil profiles). The lahar 2 layer has the highest Fe_d/Fe_t ratio (0.09 and 0.12 in P5-a and P5-b profiles, respectively) among the samples. The Fe_d/Fe_t ratio of the MS and BS horizons is comparable varying from 0.05 to 0.08 in the two soil profiles.

Al:Si ratio

Fo-Ash. The Al:Si ratio of the MS horizon, ash, and pumice layers are comparable varying from 0.25 to 0.29 (P1-a and P1-b soil profiles). The BS horizon has nearly double Al:Si ratio compared to that of the MS horizon (0.46 vs. 0.28, respectively, in P1-a and 0.45 vs. 0.26, respectively, in P1-b).

IR-Ash (P2-a, P2-b). The MS horizon has a slightly higher Al:Si ratio compared to that of the remobilized ash layer in P2-a and P2-b soil profiles, respectively (0.22 vs. 0.19 and 0.24 vs. 0.20). The succeeding ash and pumice layers have a higher Al:Si ratio ranging from 0.24 to 0.31 in the two soil profiles. The Al:Si ratio of the BS horizon is slightly higher than that of the MS horizon (0.28 vs. 0.22, respectively, in P2-a and 0.25 vs. 0.24, respectively, in P2-b).

Gr-LA-Ash (P3-a, P3-b). The Al:Si ratio of the MS horizon is slightly higher compared to the pumice layer in both P3-a and P3-b soil profiles, respectively (0.30 vs. 0.24 and 0.31 vs. 0.30). The ash layer has generally lower Al:Si ratio (0.25-0.26) in the two soil profiles. The Al:Si ratio of the BS horizon is similar to that of the MS horizon which varies from 0.30 to 0.33 (P3-a and P3-b).

Gr-HA-Ash (P4-a, P4-b). The ratio of Al:Si in the MS horizon specifically in the P4-b soil profile is slightly lower compared to its underlying pumice layer (0.23 vs. 0.27, respectively); in the P4-a profile the difference is not significant (0.28 vs. 0.27, respectively). The BS horizon has noticeably higher Al:Si ratio than that of MS horizon in P4-a and P4-b soil profiles, respectively (0.35 vs. 0.28 and 0.32 vs. 0.23).

IR-Lahar (P5-a, P5-b). Lower Al:Si ratio is observed in the MS horizon in comparison with that of the lahar 1 layer, i.e. 0.26 vs. 0.30, respectively, in P4-a and 0.24 vs. 0.28, respectively, in P5-b. The ash layer has 0.25 and 0.24 Al:Si ratio, in P5-a and P5-b, respectively which is comparable to that of the MS horizon. The BS horizon has a small

increment in the Al:Si ratio as compared to that of the MS horizon (0.27 vs. 0.26, respectively, in P5-a and 0.27 vs. 0.24, respectively, in P5-b).

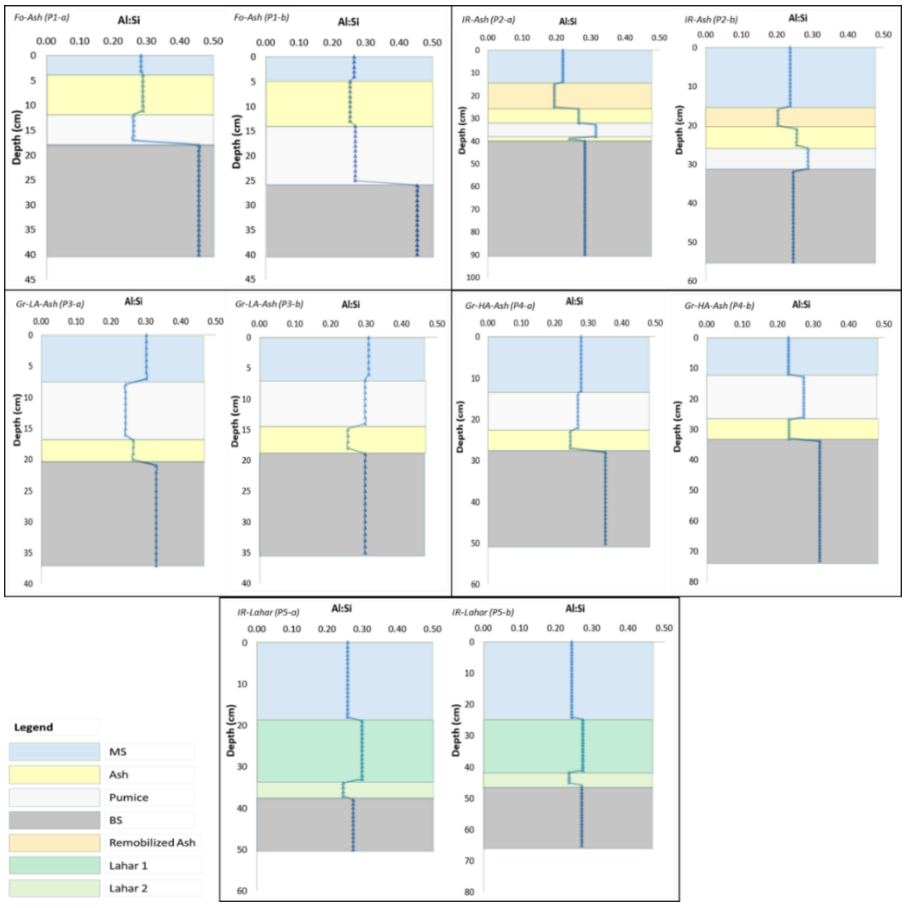

Figure 3.10c. Ratio of Al:Si in the Fo-Ash (P1-a, P1-b; Tarlac province), IR-Ash (P2-a, P2-b; Tarlac province), Gr-LA-Ash (P3-a, P3-b; Pampanga province), Gr-HA-Ash (P4-a, P4-b; Pampanga province) and IR-Lahar (P5-a, P5-b; Zambales province) soil profiles.

3.4 Discussion

3.4.1 Horizonation of the soil profiles

A graphical illustration of the horizonation of the five soil profiles with different land-use is presented in Figure 3.11. Each profile consists of an MS (A horizon). The MS has developed from its parent material (C1 horizon), the underlying 26-yr dacitic pyroclast deposit (i.e. ash, pumice, lahar). The C horizon is comprised of two to four horizons with number designations because of its heterogeneity in terms of grain size. It features layers of ash and pumice, both emplaced by the same eruption, but with changing dynamics (Scott et al., 1996). The isopach maps presented by Melosantos et al. (1996) revealed that the soil profiles received varying thickness, type, and grain size of tephra produced during phases IV to VII of the Mt. Pinatubo eruption (Figures 3.3[a-d]), respectively.

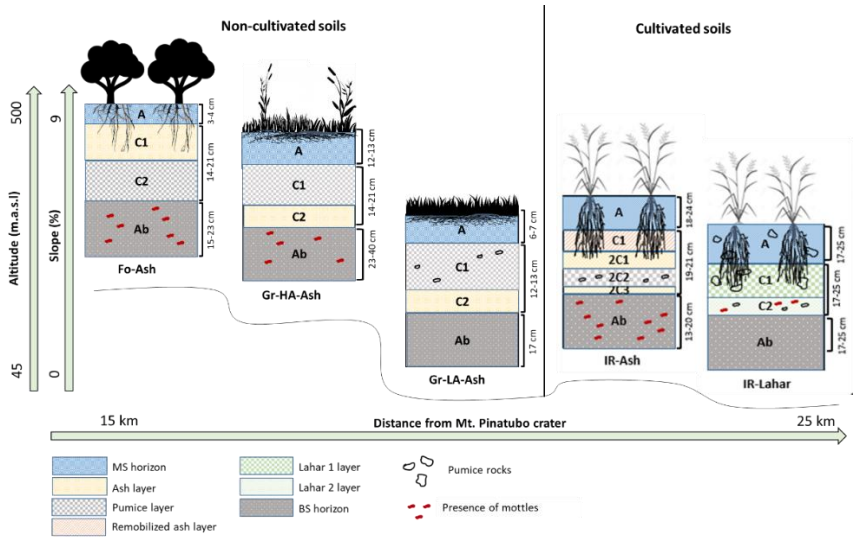

Figure 3.11. Soil profile horizonation of the non-cultivated and cultivated sampling sites affected by pyroclastic materials from the 1991 Mt. Pinatubo eruption. *Fo-Ash (forest soil affected by ash), Gr-HA-Ash (grassland soil in higher altitude affected by ash), Gr-LA-Ash*

(grassland soil in lower altitude affected by ash), IR-Ash (paddy rice soil affected by ash), IR-Lahar (paddy rice soil affected by lahar).

In IR-Ash and IR-Lahar soils, the C1 horizon is derived from remobilized volcanic materials (remobilized ash and lahar, respectively) induced by flooding. Thus, it consists of fresh and old lithic materials, pumices, and possibly soil sediments. Finally, the BS is the buried soil (Ab horizon) that has developed from the ~500 yr old volcanic materials ejected by a previous Plinian activity of Mt. Pinatubo (Newhall & Punongbayan, 1996).

3.4.2 Early-stage of soil formation in pyroclast deposits

Granulometry and Mineralogy

The grain size distribution of the MS is characterized by a lower sand content compared to its C1 parent material (i.e. 56.9-83.9 vs. 80.2-95.2 wt.%), except for IR-Ash which contains a larger fraction of silt (61 wt.%) than sand (19 wt.%). The clay content of the soil profiles varies from 11.1 to 30.1 wt.% in the MS which has increased by 52 to 72 % from their respective C1 horizons (3.1 to 14.4 wt.%) (Fig. 3.5; Table A3.2). The change in the grain sizes from coarse to fine is due to the effect of mechanical (i.e. rock fragmentation from rainfall) and chemical weathering (i.e. dissolution of coarse sand-sized primary minerals and silicate glass).

The mineralogy of the MS and pyroclast layers consisting of primary minerals (i.e. plagioclase feldspars, quartz, amphiboles, pyroxene, mica, Fe(Ti) oxide) in both their bulk and clay fractions are consistent with the bulk mineralogy of the June 15 tephra fall deposits (Bernard et al., 1996; Melosantos et al., 1996).

The presence of clay minerals together with primary minerals in the < 2 µm fraction of the MS and pyroclast layers (Table 3.3; Fig. 3.7[a-e]) is an evidence of chemical weathering. Since the clay fraction also

consisted of primary minerals, the measured value is an overestimate of the actual amount of pedogenic clay minerals (Table A3.2). Furthermore, amorphous materials, are also present in the < 2 μm samples as suggested from the broad background XRD patterns (e.g. Fig 3.6b). Luhr & Melson (1996) indicate that the silicate glass component of the fresh Pinatubo pumice was ~47 wt.%. In Chapter 4 of this thesis, silicate glasses are found to predominate the MS and pyroclast phytolith samples (63 and 85 wt.% abundance) which are extracted from the silt-sized fraction of IR-Ash soil profile (Table 4.4; Fig. 4.10-4.11).

The presence of 1:1 (kaolinite, halloysite) and/or 2:1 (vermiculite, smectite) phyllosilicates in the MS and pyroclast layers further verifies the alteration and/or dissolution of primary silicate minerals into more stable crystalline silicates in response to chemical weathering. The MS clay fraction (except for grassland soils), including some of the ash (i.e. IR-Ash), pumice (i.e. Gr-LA-Ash), and lahar (i.e. IR-Lahar) layers, contain kaolinite ($Al_2Si_2O_5(OH)_4$). Halloysite [$Al_2Si_2O_5(OH)_4$] has also been observed in the MS clay samples of Fo-Ash and IR-Ash. These secondary clays can form during the weathering of primary mineral constituents such as feldspars (Calvert et al., 1980; Anand et al., 1985), pyroxene, and amphibole (Huang, 1989; Wilson, 2004) (e.g. Eq. 2.1). The neogenesis/neoformation of 1:1 clay minerals may also be the result of glass weathering (Churchman & Lowe, 2012).

Clay mineral neoformation during weathering of the 1991 pyroclast material may be favored by the udic-hyperthermic climatic regime that prevails in the Mt. Pinatubo area. These conditions are characterized by sufficient moisture, distinct dry and wet seasons, adequate leaching, and warm conditions. The high amount of rainfall occurring during the wet season (June to November) followed by a cooler dry season (December to February) and hot dry summer months (March to May) (PAGASA, 2015) may also allow for resilication and neogenesis of secondary clays. The dacitic composition of Mt. Pinatubo's ejecta may allow the development of a silica-rich environment during weathering, in turn favoring the direct crystallization of halloysite from the soil solution

(Dahlgren, et al., 2004; Parfitt & Wilson, 1985). Its formation is also promoted in soils with impeded or poor drainage such as in paddy conditions (e.g. IR-Ash) because these situations give rise to a buildup of Si (Saigusa, et al., 1978; Parfitt et al., 1983).

Trioctahedral vermiculite ($22MgO{\cdot}5Al_2O_3{\cdot}Fe_2O_3{\cdot}22SiO_2{\cdot}4OH_2O$) is the most common phyllosilicate found in the MS and pyroclast layers (except for the MS of IR-Lahar). Vermiculite may be a weathering product of primary mica (i.e. biotite), here the interlayer K^+ is replaced with hydrated Mg^{2+} (Wilson, 2017; Lowe, 1986). It may also form from the transformation of other ferromagnesian minerals, including amphiboles and pyroxenes present in the pyroclasts (e.g. Tokashiki & Wada, 1975; Mizota, 1976). In the volcanic soils developed from ash materials of Mt. Rototuna in the Waikato region, New Zealand, the occurrence of vermiculite was linked to high and low concentrations of Si and Al, respectively, alternate wetting and drying, periodic oxidizing conditions, and impeded drainage (Lowe, 1986).

Smectite [$(Na,Ca)0,3(Al,Mg)_2Si_4O_{10}(OH)_2{\bullet}n(H_2O)$] is detected occasionally in the MS and pumice layer (i.e. IR-Ash and Gr-LA-Ash), and in the ash layer (i.e. IR-Ash). Ugolini et al. (1991) and Dahlgren et al. (1997) found 2:1 clays (vermiculite and smectite) after seven to ten years of weathering of the 1980 Mt. St. Helens tephra. However, lithic fragments occurred in the tephra and the clay minerals were concluded to have a detrital origin. In the case of 1991 Mt. Pinatubo ash, we believe that the 1:1 and 2:1 phyllosilicates have been transformed from the primary minerals by pedogenesis. The eruption of Mt. Pinatubo occurred in seven eruption phases and released a voluminous amount of pyroclastic materials (~5 km^3 DRE; Melosantos et al., 1996). The detrital smectite and vermiculite, if any, must have been deposited together with the tephra fall during the first few phases of the eruption but were most likely depleted during the last and major eruption phase from where the Pinatubo parent material of the modern soils is derived. Previous studies report minor amounts of pedogenic vermiculite in tephra deposits (e.g. Sudo & Shimoda, 1978; Wada, 1980; Lowe & Nelson, 1983). Folkoff & Meentemeyer (1985) confirmed that

smectites tend to form and persist in soils rich in silica, Mg and Ca, which are found in poorly drained and low-leaching environments. The presence of smectite in some of our samples may attest to a similar weathering environment.

The formation of vermiculite and/or smectite in the pumice layer (i.e. Fo-Ash, Gr-LA-Ash, Gr-HA-Ash) may highlight the development of local physicochemical conditions favoring chemical weathering within the porosity of the vesicular pumices. Using high-resolution transmission electron microscopy, Banfield & Barker (1994) concluded that partial depolymerization of amphibole to smectite can occur. Further, this transformation can occur without bulk water but only sustaining from the hydration water of the smectite product.

All the soil profiles have accumulated small but non-negligible amounts, i.e. < 1 wt.%, for each of the DCB-extracted Fe (Fe_d), oxalate-extracted Si, Al and Fe (Si_o, Al_o, Fe_o) and pyrophosphate-extracted Al and Fe (Al_p and Fe_p) (Fig. 3.9[a-c]; Table A3.4). The DCB gives a measure of the "free" Fe (amorphous and crystalline forms) that is released from silicate weathering, and those extracted from hydr(oxides) (i.e. ferrihydrite), and Fe-organic matter complexes (Wada, 1989). The Na-pyrophosphate principally extracts the Al and Fe that are bound to organic matter (Wada, 1989). The oxalate extraction determines the amount of Si, Al, Fe that are bound to organic matter and in SRO minerals (i.e. allophane/imogolite, ferrihydrite) (Dahlgren et al., 1997; Dahlgren & Ugolini, 1989).

The very low contents of Si_o (0.01-0.04 wt.%), Al_o (0.02-0.11 wt.%), and Fe_o (0.12-0.43 wt.%), and consequently low estimated allophane/imogolite (0.04-0.28 wt.%) and ferrihydrite (0.20-0.74 wt.%) in the modern soils suggest three possibilities, (1) the dissolution of silicate glasses are minimal, (2) dissolution products are neoformed to more stable crystalline materials, (3) dissolution products form complexes with organic matter. We have confirmed in the earlier discussion that the phyllosilicate minerals found in the modern soils are formed pedogenetically due to the chemical weathering of primary

minerals. Even though we did not measure the quantity of silicate glasses for each soil profile, it is known that these materials are less resistant to weathering than the primary minerals due to its amorphous nature (Fig. 2.3; Wolff-Boenisch et al., 2004). Therefore, it is expected that the weathering of silicate glasses will prevail and would be followed by the formation of SRO minerals particularly allophane/imogolite. Metastable allophane/imogolite [$(Al_2O_3.SiO_2 \cdot nH_2O$] and ferrihydrite [$5Fe_2O_3 \cdot 9H_2O$] should be the first secondary solid phases that normally form due to the rapid oversaturation of elements in the soil solution in response to glass weathering (Shoji et al., 1993; Dahlgren et al., 1993).

We infer that the limited formation of SRO minerals in our soils is due to the high rainfall (2000-3500 mm) but with seasonal dry and wet soil conditions, and warm temperature of the study sites. Dahlgren et al. (2004) pointed out that periods of wetting and drying promotes the formation of crystalline minerals rather than the poorly crystalline SRO minerals. Leaching is also limited under warm/dry conditions leading to high base saturation conducive for the formation of phyllosilicates (Ugolini & Dahlgren, 1991). Several authors projected that the type and abundance of clay minerals increases or decreases according to the degree of Si leaching which is a function of rainfall (Fig. 2.4; Parfitt et al., 1983; Churchmann & David, 2011; McDaniel et al., 2011; Delmelle et al. 2015). Based on their proposed weathering sequence, the Si-rich allophane (Al:Si = 2:1) and halloysite are noted to form favorably under conditions of low rainfall (< 1,800 mm) due to the lower rate of Si leaching. While this is true for matured Andisols, it may not be the case for young ash soils derived from dacite, which are essentially Si-rich. It is probable that the occurrence of rainy months from June to November facilitates the dissolution of silicate materials (i.e. primary minerals, silicate glass) followed by reprecipitation of dissolved elements (i.e. silica, Al, base cations) during dry summer months, from December to May. Hence, significant leaching of Si and base cations are minimized resulting in the neoformation of phyllosilicates.

Few weathering studies conducted on soils developing from recently deposited volcanic materials also showed the low accumulation rate of SRO minerals after few years of tephra deposition. For example, the 10-yr of weathering in Mt. St. Helens tephra (5 and 15 cm thick deposit) formed an estimated amount of 0.07 wt.% allophane/imogolite and 0.48 wt.% ferrihydrite based on the extracted 0.01 wt.% Si_o and 0.28 wt.% Fe_o contents, respectively (Dahlgren et al., 1997). These values are within the range of our measurements. Dahlgren et al. (1997) considered the very low value of allophane/imogolite as negligible. The ferrihydrite content of the 10-yr old Mt. St. Helens tephra was also low (0.48 wt.%). It is comparable to that measured in the MS of our studied soil profiles (i.e. 0.41 to 0.67 wt.%; Fig. 3.9d; Table A3.4). In the Altiplano, Chile, the 16-yr weathered Mt. Irruputuncu tephra and lahar deposited in areas with varying slope (2-30 %) and land use type (barren, forest, grassland) had ferrihydrite contents ranging from 0.51 to 0.78 wt.% estimated based on the measured 0.30 to 0.46 wt.% Fe_o contents (Norambuena et al., 2011). These values are also comparable to our measurements.

The Al_p content of the modern soils is two to eight times higher than the values measured for the C1 horizon (0.04-0.12 vs. 0.01-0.03 wt.%), suggesting the formation of Al-organic matter complexes. Since ammonium oxalate preferentially extracts Al bound to or dissolved from allophane/imogolite and also that in organo-metallic complexes (Wada, 1977; Dahlgren et al. 2004), the Al_p/Al_o ratio is useful to determine the relative proportion of active Al that are bound to soil organic matter or humus. The Al_p/Al_o ratios of the modern soils range from 0.39 to 1.78 (Table A3.4). This implies that a significant amount of oxalate-extracted Al tends to form complexes with organic matter even though the content of the latter is relatively small in the modern soils. The organic matter provides organic molecules that can complex the Al released during glass dissolution. As a result, there is no enough Al to combine with Si to form allophane/imogolite. This assumption is supported by the positive relationship of organic carbon with Al_p in the MS and C1 horizons ($r = 0.63$, $p<0.05$; Fig. 3.12), respectively. The plot reveals that as the organic C increases with weathering of the modern

soils and pyroclast, the Al associated with it also increases. This reaction is similar to what has been observed by Dahlgren et al. (1997) and Nanzyo et al. (1993) which led to the conclusion that allophane/imogolite formation is hindered by the preferential complexation of Al with organic matter, thereby becoming unavailable for allophane/imogolite precipitation.

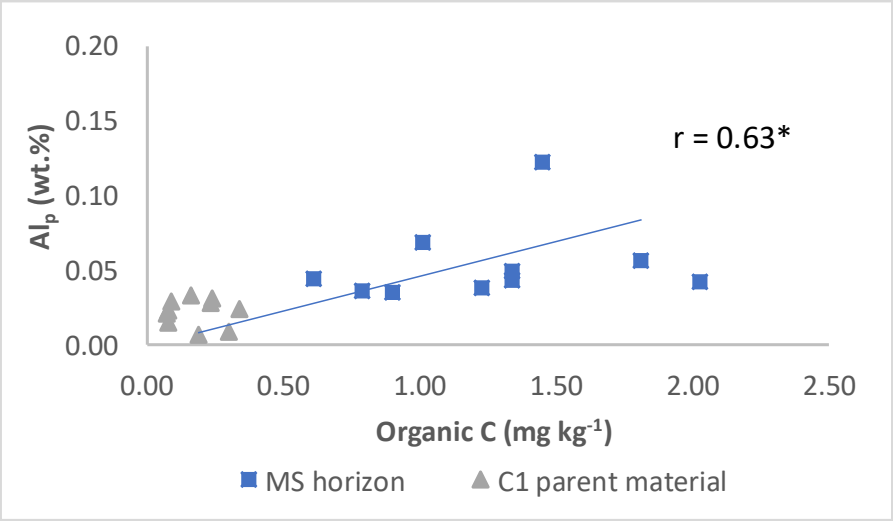

Figure 3.12. Plot graph of organic C vs. Al_p in the modern soil and C1 horizon of Fo-Ash (P1-a, P1-b; Tarlac province), IR-Ash (P2-a, P2-b; Tarlac province), Gr-LA-Ash (P3-a, P3-b; Pampanga province), Gr-HA-Ash (P4-a, P4-b; Pampanga province) and IR-Lahar (P5-a, P5-b; Zambales province) soil profiles. *'Al_p' pyrophosphate-extracted Al.*

According to Shoji et al. (1993) and Dahlgren et al. (1997), the presence of 2:1 phyllosilicates (i.e. vermiculite, smectite) may also hinder the formation of allophane/imogolite due to preferential incorporation of Al into the hydroxyl-Al interlayers of the 2:1 phyllosilicates that serves as a sink for Al released by weathering. Therefore, the low contents of SRO minerals (allophane/imogolite, ferrihydrite) are most probably influenced by the presence of soil organic matter even in low quantities and 2:1 phyllosilicates due to competition for Al.

The ratio Fe_o/Fe_d gives the proportion of ferrihydrite and Fe-organic matter components and indirectly estimates the proportion of crystallized Fe oxides. The results showed that the modern soils consist mainly of ferrihydrite and organically complexed Fe given the Fe_o/Fe_d ratio of 0.66 to 1.98. This is confirmed by our mineralogical data wherein we did not observe the presence of crystalline Fe oxides (i.e. goethite). The Fe_p content in the modern soils is two to nine times higher than that of their respective C1 horizon (0.02-0.22 vs. 0-0.05 wt.%; Fig. 3.9c; Table A3.4). Furthermore, the Fe_p/Fe_o ratio of the MS across the land use types are 2 to 23 times higher compared to their C1 horizon (0.05-0.41 vs. 0.01-0.22 wt.%; Table A3.4). This indicates that the organic matter present in the MS have formed complexes with the oxidized Fe during the weathering process. However, the Fe_p/Fe_o ratio also indicates that > 50 % of oxalate extracted Fe in the modern soils may be in the form of ferrihydrite.

Physico-chemical properties

The pH_{H2O} of the modern soils differs depending on the kind of land use and type of pyroclast deposit. The neutral to slightly basic pH_{H2O} of the Fo-Ash MS (6.68-7.60) compared to that of Gr-LA-Ash and Gr-HA-Ash (5.53-5.72) are higher than what we expect for a forest soil (Fig. 3.8a; Table A3.3). Forest soils are generally more acidic than grasslands due to the continuous production of organic acids and CO_2 from decomposing litters (Osman, 2013). Reyes & Neue (1991) noted high pH_{H2O} values ranging from 7.1 to 8.0 for the volcanic materials ejected during the June 12-15, 1991 eruption. The currently high pH_{H2O} of Fo-Ash especially in the MS may be due to the presence of easily weatherable minerals such as glass which consumes proton during weathering, thereby buffering the pH of the soil solution.

In general, low CEC values are measured in the MS (1.47 to 8.73 $cmol_c$ kg^{-1}; Fig. 3.8b; Table A3.3). This is expected as the soils are still young, dominated by coarse-sized particles, and with low SOM and secondary

mineral contents. Hence, the negative charge exchange sites/surfaces are low in quantity. For instance, Dahlgren (2004) cited that the primary mineral feldspar in the tephra occurs as coarse particles with low specific surface area, thus having low CEC values. Young developing volcanic ash soils such as the 10-yr Mt. St. Helens weathered tephra grown to the subalpine forest had lower CEC values than in the MS of our studies soil profiles, i.e. 1.18 and 1.11 $cmol_c\ kg^{-1}$ for the 5- and 15-cm tephra thickness, respectively (Dahlgren et al., 1997). Similarly, the 16-yr tephra deposit of Mt. Irruputuncu, Antiplano of the Iquique Province, Chile has CEC values between 6 to 10 $cmol_c\ kg^{-1}$ (Norambuena, 2011) which is comparable to our measurement in IR-Ash MS. Low CEC values (i.e. 1.75 to 2.00 $cmol_c\ kg^{-1}$) were also obtained for the 3-yr moist and leached basaltic-andesitic pyroclastic deposits from Mt. Merapi in Java Island, Indonesia (Fiantis et al., 2009). It is comparable to the values obtained in Gr-LA-Ash/b, Gr-HA-Ash, and IR-Lahar modern soils.

The CEC values are comparatively higher in the MS of IR-Ash (6.77-8.73 $cmol_c\ kg^{-1}$) due to the presence of both variable and permanent-charge clays (i.e. 1:1 and 2:1 phyllosilicates) and relatively higher quantity of soil organic matter (1.45-2.03 wt.%) compared to the other soils. Soil organic matter makes a very significant contribution to cation exchange due to its high CEC range, i.e. 200 to 400 $cmol_c\ kg^{-1}$, owing to its large number of charged functional groups. On the other hand, vermiculite and smectite contribute 100 to 150 and 60 to 100 $cmol_c\ kg^{-1}$ CEC, respectively. Kaolinite contributes the lowest with 2 to 16 $cmol_c\ kg^{-1}$ CEC (NSSL Staff, 1975).

The acidic pH_{H2O} and pH_{KCl} in the MS (3.35-3.53 and 3.44-3.49), respectively of IR-Lahar; i.e. ~1-2 units lower than its C1 horizon (5.09-5.75 and 4.38-4.94), respectively and ~one magnitude lower than that of IR-Ash MS (i.e. 4.62-4.91 and 4.13-4.19), respectively is not anticipated (Fig. 3.8a; Table A3.3). The findings of Ponnamperuma (1972) showed that flooding normally shifts the soil pH towards neutral as observed in paddy soils.

Lahar has inherently low pH_{H2O} (4.2-5.1) compared to ash as confirmed from the analysis of lahar samples in Bacolor, Pampanga (eastern side of Mt. Pinatubo) (Reyes & Neue, 1991). The acidity of IR-Lahar soil is probably worsened by the thick deposition of lahar which may contain pyrite minerals (FeS_2) from remobilized sediments. The altering of reducing (waterlogged)-oxidizing (drained) conditions may favor the oxidative dissolution of pyrite resulting in the production of H_2SO_4. The H_2SO_4 is a strong acid and should promote weathering and low pH values.

The % BS of the modern soils exceeded 100 % (109-192 %) except for IR-Ash (50-55 %) and Gr-HA-Ash/b (90 %) (Fig. 3.8c; Table A3.3). The % BS exceeding 100 indicates that some bases are probably derived from the silicate glass component. With this, the % BS data may not truly reflect the proportion of the exchangeable base cations (Ca^{2+}, Mg^{2+}, Na^{+}, K^{+}) that occupy the CEC sites of the modern soils and pyroclast layers as it contains significant amounts of silicate glasses during the early stage of pedogenesis. Nonetheless, the exchange complex of the soil profile is dominated by exchangeable bases with amounts decreasing in the following sequence, $Ca^{2+} > Mg^{2+} > Na^{+} \approx K^{+}$. Exchangeable Ca^{2+} and Mg^{2+} are the dominant cations since the Pinatubo pyroclast is constituted mainly by Ca-rich feldspars (i.e. anorthite, bytownite, labradorite) and ferromagnesian minerals (mica, amphiboles, pyroxene). The weathering of these minerals will release a high concentration of exchangeable Ca^{2+} and Mg^{2+} in solution especially during the initial stages of weathering (Nanzyo et al., 1993; Shoji et al., 1993). Na-rich (i.e. albite) feldspar is also present in the bulk and clay soil fractions. It is more stable and less easily weathered (Churchmann & Lowe, 2012). The K^{+} and Mg^{2+} can be held in the interlayer positions of the 2:1 phyllosilicate (i.e. smectite, vermiculite) and prevent them from being leached out of the soil system (Nanzyo et al., 1993; Delmelle et al., 2015; Dahlgren et al., 2004). Hence, even though total K content is two to five times lower compared to total Na (Table A3.6) due to the limitation of orthoclase feldspars, exchangeable K^{+} content in the exchange complex is comparable to that of exchangeable Na^{+}.

Organic C content

The organic C content in the modern soils are generally very low (i.e. 0.61-2.03 wt.%), corresponding to SOM contents roughly in the range 1.5-3.5 wt.% (Fig. 3.8e; Table A3.3). The organic C content in the corresponding parent material (C1 horizon) is four to ten times lower, suggesting the build-up of organic C from biomass restitution. The organic C content of IR-Ash MS is ~two times higher than IR-Lahar (1.45-2.03 vs. 0.79-0.90 wt.%). This could reflect the higher intensity of biomass production in the former, i.e. IR-Ash soil recycles the biomass from two to three cropping seasons yr^{-1} while IR-Lahar soil receives biomass from only one or two croppings yr^{-1}. The accumulation rate of organic C in non-cultivated soils (i.e. Fo-Ash, Gr-LA-Ash, and Gr-HA-Ash) range from 0.02 to 0.07 wt.% per year.

Studies conducted on young soils developing from tephra also showed low content and accumulation rate of organic C. Ugolini et al. (1991) showed that the 4-6 yr old Mt. St. Helens pyroclastic flow deposit accumulated a negligible amount of organic C (0.09 wt.% or 0.02 wt.% y^{-1}). Low accumulation rate (< 0.004 wt.% y^{-1}) was also observed in the 5-yr basaltic pyroclast deposits of Mt. Kasotchi, Alaska as it started to be re-colonized by plants and microbes. This reflects the importance of vegetation on the accumulation of organic C (Zeglin et al., 2016). The 5- and 15-cm tephra thick dacitic tephra deposit of Mt. St. Helens accumulated 0.33 and 0.45 wt.% organic C (0.03-0.05 wt.% y^{-1}), respectively, after 10 years of deposition in a subalpine forest ecosystem (cryic-udic moisture regime) (Dahlgren et al., 1997). Twenty-five years later, the Mt. St. Helens tephra-derived volcanic soil showed a lower accumulation rate of 0.02 wt.% y^{-1} (Halvorson & Smith, 2009). This value is similar to the lower range of organic C accumulation in our non-cultivated forest and grassland study areas. Norambuena (2011) reported a low organic C accumulation of 0.17 to 1.32 wt.% (0.01-0.08 wt.% y^{-1}) from the 16-yr rhyolitic tephra deposit of Mt. Irruputuncu, Antiplano of the Iquique Province, Chile under ustic-frigid moisture regime (~80 mm annual precipitation; 5-8 °C soil

temperature) subjected to varying land uses (i.e. grassland, barren, cropland). The 91-yr volcanic soil from andesitic tephra deposits of Mt. Bandai in Japan, which has a cool temperate and humid climate, accumulated 0.06 wt.% organic C y^{-1} (Morisada et al., 2002). The contents and accumulation rate of the latter soils cited, even though varying in parent rock material and climatic environment, are on par with the organic C values that we measured in our studied 26-yr old soil profiles.

Degree of weathering of the newly formed soil

Three indices of weathering including TRB (Eq. 3.8), Fe_d/Fe_t (Eq. 3.9), and total Al:Si molar ratio (Eq. 3.10) are used to assess the degree of chemical weathering of the modern soils. The decrease in base cation contents (particularly Ca, Mg, K, Na) assessed by TRB, the increase in amorphous and crystallized forms of Fe from the total Fe given by the Fe_d/Fe_t ratio, and the increase in total Al contents relative to total Si (Al:Si ratio) compared to the fresh Mt. Pinatubo tephra are indicators that weathering has advanced.

Since we do not have the samples of the fresh tephra, we utilized the previous report of Castillo & Punongbayan (1996) which presented the chemical composition of the June 1991 ash '$ash_{(1991)}$' and pumice '$pumice_{(1991)}$' deposits. Where appropriate, we used the $ash_{(1991)}$ TRB and Al:Si ratio data for soil profiles wherein the MS has developed from an ash C1 horizon (i.e. Fo-Ash, IR-Ash) while we used the $pumice_{(1991)}$ data for those with pumice and lahar C1 horizon (i.e. Gr-LA-Ash, Gr-HA-Ash, IR-Lahar). On the other hand, since there is no available data on the DCB-extracted Fe of the fresh tephra deposit, we just opt to compare the Fe_d/Fe_t ratio of the modern soils from its respective C1 horizon for the different land uses based on the assumption that the C1 horizon is more pristine compared to the modern soil.

In general, the TRB values of the MS (311-483 $cmol_c\ kg^{-1}$), C1 horizon (330-505 $cmol_c\ kg^{-1}$), and the subsequent stratified C layers (414-486 $cmol_c\ kg^{-1}$) across the land use types were lower compared to the

$ash_{(1991)}$ (547 $cmol_c\ kg^{-1}$) and $pumice_{(1991)}$ (517 $cmol_c\ kg^{-1}$) values (Fig. 3.10a; Table A3.5). In modern soils, the rate of decrease in TRB ranges from 7 to 43 %. We attribute this loss in TRB due to the chemical weathering of silicate minerals (including silicate glasses) wherein the dissolved base cations (Ca^{2+}, Mg^{2+}, Na^{+}, K^{+}) are released and subsequently leached out from the soil surface down to the drainage water (Van Breemen & Buurman, 1998). However, the comparative difference between the TRB of the modern soils and its subsequent C1 horizon is not significant, indicative of limited weathering.

The loss in TRB of the MS and pyroclast layers after 26 years from the $ash_{(1991)}$ is higher compared to that of the Mt. St. Helens tephra deposition simulated experiment in a subalpine forest ecosystem in Washington conducted by Dahlgren et al. (1997). After 10 years of weathering of the 5 and 15 cm thick Mt. St. Helens dacitic tephra, the TRB values are only reduced by ~1 % from the unweathered tephra. This rate of decrease is generally lower than what we obtained in our five study sites. Assuming a similar yearly reduction in TRB, the Mt. St Helens tephra will only lose ~3 % of its original TRB after 26 yrs which is 2 to 14 times lower compared to the reduction in TRB of the modern soils in our study sites.

TRB values may vary between different types of magma. While both Mt. St. Helens and Mt. Pinatubo pyroclastic deposits are derived from the same parent rock material, dacite, the difference in weathering pattern may be attributed to other soil-forming factors such as climate. Again we highlight the impact of the favorable climatic condition (udic-hyperthermic moisture regime characterized by seasonal wet and dry season, warm temperature, adequate leaching, and moisture conditions) in Mt. Pinatubo area compared to that of Mt. St. Helens tephra experimental site (cryic-udic moisture regime) in the enhancement of chemical weathering processes. Scheffer & Schachtschabel (1998) cited that tropical regions under forest vegetation cause intensive weathering (i.e. high dissolution of minerals, high release & leaching of bases, eluviation of clay, and decomposition of organic matter) due to excessive rainfall and high temperatures.

Except for IR-Ash and Gr-HA-Ash soils, the Fe_d/Fe_t of the MS increased by two to four times compared to its C1 horizon (0.05-0.14 vs. 0.02-0.05; Fig. 3.10b; Table A3.5) suggesting that Fe from ferromagnesian minerals (i.e. amphibole, pyroxene, mica) and silicate glasses has been released and oxidized leading to the formation of Fe oxyhydroxides (i.e. ferrihydrite). The more crystalline phases of Fe oxides such as goethite did not form. The comparable Al:Si ratio of the MS (0.22-0.28) and C1 (0.19-0.30) horizon to the $ash_{(1991)}$ and $pumice_{(1991)}$ samples (0.27-0.28; Fig. 3.10c; Table A3.5) in all the land use types suggest that the advance of weathering is not significant enough to change the bulk ratio of Al to Si.

The IR-Ash MS exhibited comparatively lower TRB, higher Fe_d/Fe_t values, and consequently, more phyllosilicate mineral formation compared to the other soil profiles. These suggest that the ash weathering conditions of the MS and parent C1 material are favored. The opposite is observed in IR-Lahar where higher TRB value and lower Fe_d/Fe_t ratio is measured, and less phyllosilicate clay has formed even though both IR-Ash and IR-Lahar has the same type of vegetation and both are subjected to waterlogging for paddy rice cultivation. As shown in Figure 3.11, The C1 parent material of these two soil profiles where the MS has developed are both remobilized volcanic materials, however, the grain size composition greatly varied. The IR-Ash C1 consists of finer remobilized ash material while that of IR-Lahar has coarser composition due to the heterogeneous nature of lahar materials (section 3.4.1; Fig. 3.11). The sand-size composition of the IR-Lahar in its C1 and MS horizon (i.e. 95.2 and 82.7 wt.%), respectively are 17 and 4 times higher than the sand content of the IR-Ash C1 and MS horizon (i.e. 5.3 and 19.4 wt.%), respectively (Table A3.2). Ash is known to weather rapidly due to its relatively high surface area exposed to weathering, high porosity, and permeability, thereby enhancing the leaching of bases and silica. With this, we may attribute the difference in weathering between IR-Ash and IR-Lahar soils to the difference in their textures which lead to the higher rate of weathering in the former soil profile compared to the latter.

3.4.3 Development stage of the buried soil across different land-use types

Granulometry and mineralogy

The primary minerals identified in the bulk and clay fractions of the MS are also found in the BS suggesting that the latter still contains weatherable silicate minerals after ~500 years of weathering (Table 3.3). All the five soil profiles feature kaolinite and vermiculite in the BS. Halloysite is also present in some of the soils (i.e. Fo-Ash, IR-Ash, Gr-HA-Ash). Smectite was found in the Gr-LA-Ash. Differences in the types of clays formed in the respective MS and BS are observed in some profiles. In IR-Ash for instance, smectite is observed in its MS but not in its BS. On the other hand, more types of phyllosilicate minerals are found in the BS of Gr-LA-Ash, Gr-HA-Ash, and IR-Lahar compared to their respective MS. Similarly, the Fo-Ash soil produced more distinct peaks of the phyllosilicates (i.e. kaolinite, halloysite, vermiculite) in the BS implying that their abundance tended to increase in this horizon compared to the MS (Fig. 3.7a; Table 3.3). These observations suggest a more advanced stage of weathering in the BS compared to the MS.
In the BS of IR-Ash, although kaolinite and halloysite are more dominant compared to the MS, the vermiculite peak is weak and smectite is absent (Fig. 3.7b; Table 3.3). Previous research projected that halloysite is a product of resilication under buried soil conditions. The weathering solutions of the overlying pyroclast layers are accumulated in the buried soil, thereby promoting halloysite formation through resilication (Lowe, 1986; Parfitt & Wilson, 1985; Parfitt et al., 1983; Saigusa, et al., 1978). In the Towada Andisols of northeastern Japan, it was reported that halloysite formed via resilication in the deeply buried soils (Ugolini & Zasoski, 1979; Violante & Wilson, 1983).

Other studies also verified that halloysite forms favorably in volcanic ash derived soils under paddy condition, in areas with distinct dry

season climates, and in buried soil layers with poor drainage due to the accumulation of silica (Takahashi et al., 2001; Lowe, 1986). The formation of halloysite instead of allophane is also seen to occur in areas where there is a thick overburden of volcanic deposits (Meija et al., 1968; Aomine & Mizota, 1973).

In general, the buried soils generated very low and almost negligible quantities of SRO minerals (allophane/imogolite, ferrihydrite) and Al/Fe-organo complexes as estimated from the low (< 1 wt.%) accumulated Si_o, Al_o, Fe_o, Fe_p, Al_p. Nevertheless, the quantities of active Si, Al, and Fe in the BS are higher compared to the MS in most of the land-use types. Except for IR-Ash soil, the BS compared to the MS tended to increase significantly the Si_o (0.02-0.11 vs. 0.01-0.03 wt.%) and Al_o (0.14-0.32 vs. 0.02-0.11 wt.%) contents. This may indicate a higher accumulation of allophane/imogolite minerals in the former soil. To confirm this, we plotted the relationship between TRB and $Al_o + Si_o$ of the modern and buried soils from the five soil profiles. The significant negative relationship between TRB and $Al_o + Si_o$ ($r = -0.52$, $p<0.05$; Fig. 3.13) reveals that the allophane/imogolite constituents tend to increase with decreasing TRB values. As earlier mentioned, the decrease in TRB value suggests an advancement of weathering. The Fe_o contents of the BS are ~two times higher compared to the MS (0.27-0.88 vs. 0.12-0.46 wt.%) (except for IR-Ash, IR-Lahar, Gr-HA-Ash/a) (Table A3.4), suggesting that ferrihydrite has accumulated only in some of the soil profiles (i.e. Fo-Ash, Gr-LA-Ash, Gr-HA-Ash/b) with time. Ferrihydrite must have been dissolved during waterlogged conditions in paddy soils and the generation of a reducing environment (i.e. IR-Ash, IR-Lahar). The small size, high surface area, and poor crystallinity of ferrihydrite make it very reactive and susceptible to dissolution (Schaetzl & Anderson, 2005).

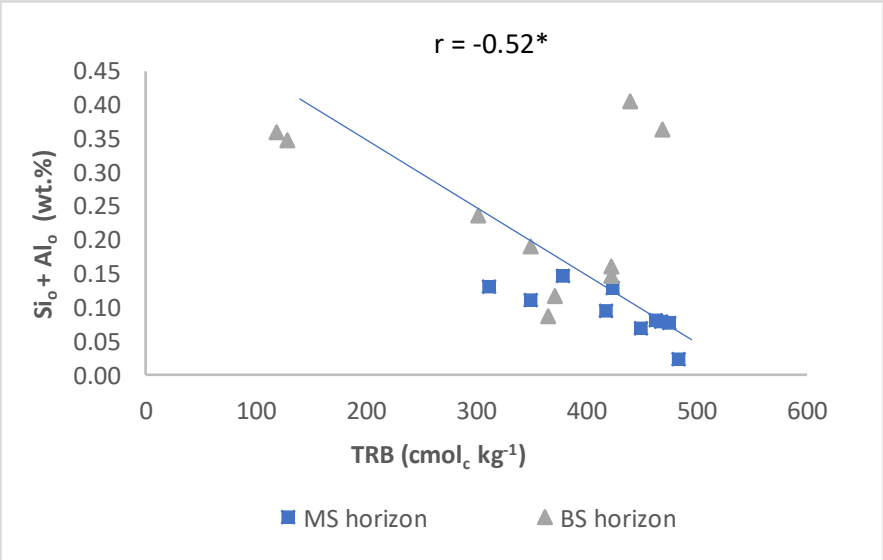

Figure 3.13. Plot graph of TRB versus Si_o + Al_o in the modern and buried soils of Fo-Ash (P1-a, P1-b; Tarlac province), IR-Ash (P2-a, P2-b; Tarlac province), Gr-LA-Ash (P3-a, P3-b; Pampanga province), Gr-HA-Ash (P4-a, P4-b; Pampanga province) and IR-Lahar (P5-a, P5-b; Zambales province) soil profiles.

The generally low contents of Al_p (0.07-0.21 wt.%) and Fe_p (0.04-0.20 wt.%) in the buried soils are attributed to the low contents of soil organic matter (< 3 wt.%) available for complexation in the BS. A higher Al_p content in the BS of Fo-Ash, IR-Ash, and IR-Lahar compared to their respective MS suggests that the low accumulation of SRO minerals (allophane/imogolite, ferrihydrite) in the BS horizon with time may be due to the preferential formation of more stable crystalline minerals. The relatively high ratio of Al_p/Al_o (0.41-2.71) also shows that active Al can be strongly associated with organic matter (Table A3.4). Allophane and imogolite are believed to form primarily by precipitation from weathering solutions (Wada, 1989), but under conditions of low complexing organic compounds and absence of 2:1 phyllosilicates. Since there was an increase of more stable crystalline minerals, the Al tended to precipitate preferably with Si forming the latter minerals. Dahlgren et al. (1993) stated that humic substances

strongly compete with orthosilicic acid for the coordination sites of Al and it also hinders the hydrolysis and polymerization of Al, thus affecting the allophane/imogolite synthesis. Hence, the presence of SOM, although in minute amounts, and 2:1 phyllosilicate (i.e. vermiculite) must have depleted the available Al^{3+} ions needed for the formation allophane/imogolite.

Physico-chemical properties

The pH_{H2O} of BS varies with land use type and the values (~3.9-6.9) compare reasonably well with those measured for the MS (3.4-7.6; Fig. 3.8a; Table A3.3), except in the cases of the Fo-Ash and IR-Lahar profiles for which significantly more acidic values (one pH unit) occurred in the deep soil.

The CEC values are also very low ranging (2-10 $cmol_c\ kg^{-1}$; Fig. 3.8b; Table A3.3) but are consistently higher compared to the MS (except for IR-Ash). The CEC of the BS in the IR-Ash does not differ from that of its MS, perhaps due to a lesser content of 2:1 phyllosilicate minerals. Nevertheless, this implies that the formation of secondary minerals with the advance of weathering, though in small quantities, may increase significantly the negative surface charges for some soils. The negative relationship between TRB and CEC ($r = -0.79$, $p<0.001$; Fig. 3.14) further confirms that as weathering degree increases (i.e. decreasing TRB values), the CEC content also increases in response to increasing abundance of phyllosilicates, SRO minerals, and organic matter.

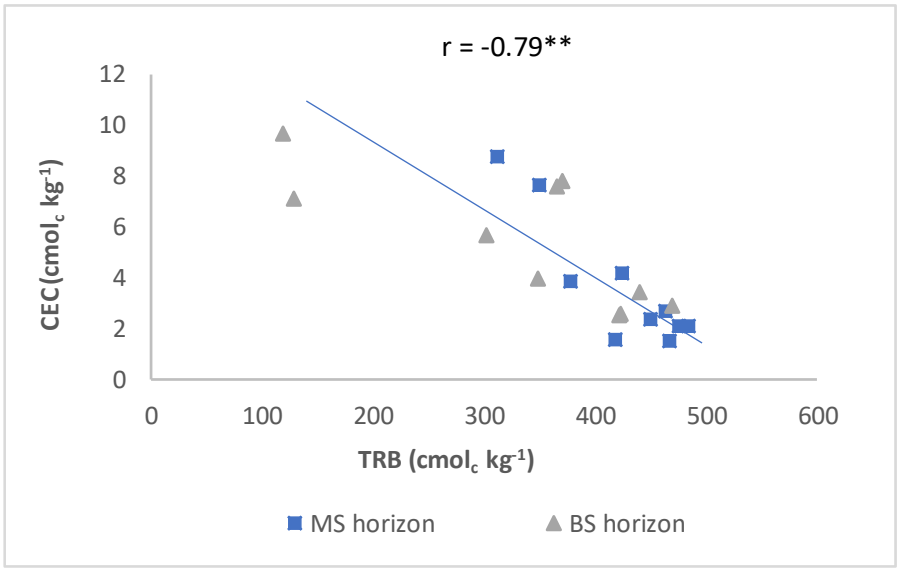

Figure 3.14. Plot graph of TRB versus CEC in the modern and buried soils of Fo-Ash (P1-a, P1-b; Tarlac province), IR-Ash (P2-a, P2-b; Tarlac province), Gr-LA-Ash (P3-a, P3-b; Pampanga province), Gr-HA-Ash (P4-a, P4-b; Pampanga province) and IR-Lahar (P5-a, P5-b; Zambales province) soil profiles.

The high base saturation exceeding 100 % except for IR-Ash (49-73 %) and Fo-Ash/a (56 %) implies that silicate glasses are still present in the BS and leaching of bases due to weathering processes is not substantial (Fig. 3.8c; Table A3.3). The lower BS of IR-Ash and Fo-Ash/a may be attributed to higher weathering of silicate minerals including glasses and eventual leaching from the soil. The abundance of silicate glasses is measured from the phytoliths extracted in the MS and BS-silt fraction of IR-Ash using the Ca/Si ratio (Chapter 4). Silicate glass may also partition during the phytolith extraction due to their comparable density ($\leq$ 2.3 g cm^{-3}). The estimated silicate glass abundance of the phytoliths in IR-Ash' BS is only 4 wt.% compared to the 63 wt.% in that of the MS (Table 4.4). Thus, we infer that the low base saturation in the buried of IR-Ash is in part due to the dissolution and leaching of bases from silicate glass dissolution.

Organic C content

The organic C content of the BS horizon is generally low (< 2 wt.%; Fig. 3.8e; Table A3.3) and is comparable to the MS except for IR-Ash and Gr-LA-Ash/a where a twofold decrease was observed. Burial of the soil with pyroclast may have impacted the organic C content as it hampered the accumulation of organic C from biomass restitution. Furthermore, the stored organic matter in the BS horizon is decomposed by microorganisms with time resulting in carbon loss as CO_2 and/or leaching in the groundwater (Ontl & Schulte, 2012). Thus, the more labile C will disappear, leaving only the more stable fraction which can be stabilized due to complexation with Al and Fe, or due to interaction with the partially weathered surfaces of the glass (allophane-like surfaces). According to Ruxton (1968) and Gibbs (1971), deep burial alters pedogenesis especially on the organic cycle due to the reduction of organic input. The dissolved organic C content decreased in artificially covered 15 cm Mt. St. Helens tephra attributed to the reduction of organic matter decomposition (Dahlgren & Ugolini, 1989).

Nonetheless, even if the organic C values were small, its contribution to increasing the CEC content is still valuable. This is shown by the positive relationship between organic C and CEC ($r = 0.47$, $p<0.05$; Fig. 3.15) where increasing organic C content tends to increase CEC in the modern and buried soils.

Degree of weathering of the buried soil

The BS which developed from the pre-1991 Mt. Pinatubo volcanic deposits ~500 years ago is believed to have a similar composition from the magmas released over the past > 35,000 yr (Pallister et al., 1993; Newhall et al., 1996). Since the $pumice_{(1991)}$ consisting of 64 wt.% SiO_2 (Castillo & Punongbayan, 1996) is comparable to that of the ~500 yr pumice deposit (65 wt.% SiO_2, Newhall et al., 1996), we assumed that the TRB of both dacitic parent material (pumiceous) are also comparable. Hence we also used the $pumice_{(1991)}$ data on TRB (517

$cmol_c\ kg^{-1}$) and Al:Si (0.27) by Castillo & Punongbayan (1996) for comparison with the measurements of the buried soils. Due to a lack of information on the Fe_d/Fe_t ratio of the 1991 pumice, the Fe_d/Fe_t ratio of the BS is just compared to that of MS for each soil profile.

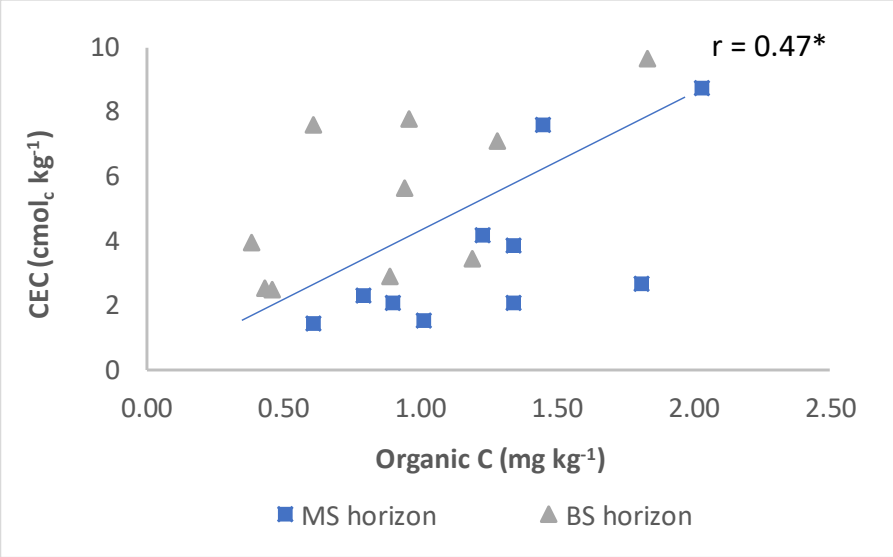

Figure 3.15. Plot graph of organic C versus CEC in the modern and buried soils of Fo-Ash (P1-a, P1-b; Tarlac province), IR-Ash (P2-a, P2-b; Tarlac province), Gr-LA-Ash (P3-a, P3-b; Pampanga province), Gr-HA-Ash (P4-a, P4-b; Pampanga province) and IR-Lahar (P5-a, P5-b; Zambales province) soil profiles.

The TRB of the BS across the land use types is lower compared to that of the $pumice_{(1991)}$ (118-469 vs. 517 $cmol_c\ kg^{-1}$) and the MS (118-469 vs. 311-483 $cmol_c\ kg^{-1}$) suggesting the loss of bases from silicate mineral weathering but the degree of loss differ with the type of land-use (Fig. 3.10a, Table A3.5). On a similar note, the increase in the Fe_d/Fe_t of the BS compared to the MS suggests an advance in weathering due to the increase in "free" Fe from the oxidation of minerals and glass components. However, this was observed only in the Fo-Ash and Gr-HA-Ash profiles (0.13-0.31 vs. 0.05-0.14; Fig. 3.10b,

Table A3.5). The Fe_d/Fe_t values in the BS of the IR-Ash, IR-Lahar, and Gr-LA-Ash profiles are comparable to their values in the corresponding MS (0.06-0.13 vs. 0.05-0.21; Fig. 3.10b, Table A3.5). However, the strong negative relationship between TRB and Fe_d/Fe_t ($r = 0.97$, $p<0.001$; Fig. 3.16) in the modern and buried soils supports the idea that increasing weathering (i.e. decreasing TRB values) increase the amount of active 'free' Fe in solution in response to the oxidation of ferromagnesian minerals and glass.

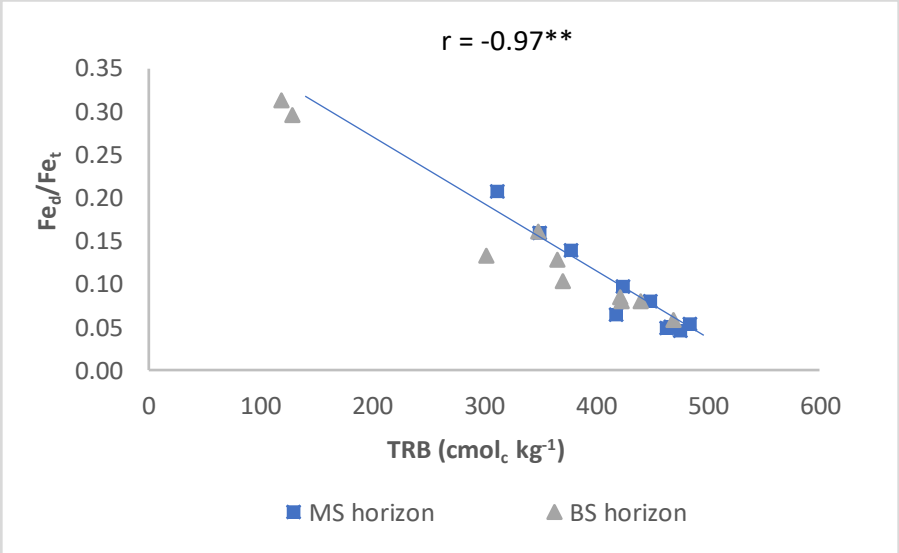

Figure 3.16. Plot graph of TRB versus Fe_d/Fe_t and in the modern and buried soils of Fo-Ash (P1-a, P1-b; Tarlac province), IR-Ash (P2-a, P2-b; Tarlac province), Gr-LA-Ash (P3-a, P3-b; Pampanga province), Gr-HA-Ash (P4-a, P4-b; Pampanga province) and IR-Lahar (P5-a, P5-b; Zambales province) soil profiles.

The Fo-Ash' BS appeared to have been weathered significantly among all the soil profiles as the TRB went down by as much as 80 % (118-128 vs. 517 $cmol_c\ kg^{-1}$). Notably, the BS of Fo-Ash is also lower by three to four times compared to its MS horizon suggesting a higher rate of chemical weathering and leaching of bases. The loss of silica is also evident in Fo-Ash as the total Al:Si ratio of its BS horizon is ~two times higher in magnitude compared to the $pumice_{(1991)}$ (0.46 vs. 0.27; Fig.

3.10c; Table A3.5) suggesting that dissolved silica is being leached along the with the bases. Similarly, the ~threefold increase in Fe_d/Fe_t ratio of the BS compared to the MS in Fo-Ash (0.30 vs. 0.12; Fig. 3.10b; Table A3.5) denotes a higher content of "free" forms of Fe from the oxidation of Fe-bearing minerals.

Similarly, the Gr-HA-Ash' BS has ~two times and ~30 % lower TRB value compared to the pumice$_{(1991)}$ and MS, respectively. Moreover, the Fe_d/Fe_t ratios are comparatively higher (~2x) than its MS and to the BS of other soil profiles (i.e. Gr-LA-Ash, IR-Lahar, IR-Ash/a). These suggest that bases are substantially lost subsequent to weathering and secondary mineral formation. This trend in Gr-HA-Ash has not been observed in Gr-LA-Ash despite the same vegetation type suggesting that the latter is weakly weathered compared to the former. The lower TRB values of IR-Ash' BS compared to that of IR Lahar (365-370 vs. 440-469 $cmol_c\ kg^{-1}$), respectively suggest that the former has undergone a higher degree of weathering.

3.4.4 Soil classification

The MS of all the soil profiles exemplified very weak andic properties. The organic C accumulation (i.e. 0.31-2.03 wt.%) is way below the 25 wt.% organic C requirement. The Al_o + ½ Fe_o content reflecting the abundance of SRO minerals, particularly allophane/imogolite and ferrihydrite is also lower by ~6 to 17 times than the 2 % minimum requirement (i.e. ~0.12-0.33 to wt.%, Table A3.4). The minimum depth of soil (30 cm) exhibiting andic property is also not met as the modern soils that have developed are between 0 to 18 cm. Phosphate retention of the MS horizon ranging from 0 to 10.2 % (Fig. 5.2; Table A3.3) is also lower than the 85 % andic criteria. Therefore, the limited weathering of the 26-yr ash and lahar soils characterized by an AC horizonation is classified as an Entisol.

The buried soils in general, despite its long time of deposition than the modern soils (~500 vs. 26 yrs), except for Fo-Ash soil are considered

as an Entisol due to its limited pedogenesis. The measurements for andic properties such as organic C (0.38-1.83 wt.%, Fig. 3.8e; Table A3.3), P retention (2-26 %; Fig. 5.2; Table A3.3), and Al_o + ½ Fe_o (i.e. 0.28-0.57 wt.%; Table A3.4) contents in the BS are below the minimum requirement. The Fo-Ash' BS has demonstrated some vitric properties. The Al_o + ½ Fe_o of 0.52 to 0.57 wt.% and phosphate retention of 22-26 % qualifies for a vitric horizon which requires ≥ 0.4 % Al_o + ½ Fe_o and > 25 % P retention. Vitric horizons are displayed in weakly weathered Andisols and distinguished from andic horizons by their lesser degree of weathering and have the lowest amounts of weathering products among Andisols (Soil Survey Staff, 1975).

3.5 Conclusion

Under generally similar climatic condition (udic-hyperthermic) and mineralogical composition of the fresh 1991 Mt. Pinatubo pyroclastic deposits, the degree of chemical weathering and secondary mineral formation may still be influenced by various factors such as type and grain size distribution (i.e. ash, pumice, lahar), deposit thickness, moisture conditions, vegetation type, and land use management (volume of crop cover, biomass restitution, biomass removal).

It is evident that the 26-yr pyroclast deposits in the tested forest, grassland, and paddy rice soils have undergone pedogenesis resulting in the development of modern soil overlying the parent pyroclastic material. The properties of the modern soils show a relatively higher organic carbon and CEC, and formation of secondary minerals including phyllosilicates and SRO minerals (in minute quantities) in its colloidal fraction compared to its parent material. The modern soils have formed 1:1 (kaolinite, halloysite) and/or 2:1 (vermiculite, smectite) phyllosilicates as early weathering products which differ in combination depending on the type of land use and pyroclast deposit. We infer that the low accumulation of allophane/imogolite in the modern soils are influenced by *(1)* climate, i.e. seasonal wet and dry

conditions and warm temperatures enhancing primary mineral (including silicate glasses) dissolution and resilication favoring the formation of phyllosilicates instead of allophane/imogolite, and *(2)* the presence of organic matter and phyllosilicates (i.e. vermiculite) which effectively competes with Al and Fe substrates for allophane/imogolite and ferrihydrite formation.

The buried soils showed a generally higher degree of soil development compared to the modern soils as shown by an increased abundance of phyllosilicate and SRO minerals, and comparatively higher CEC values. The downside of burying the soil with pyroclast material is the diminution of labile organic carbon due to impedance of biomass restitution and possible continuous mineralization of stored organic matter leaving only the more stable forms of carbon. Resilication and neogenesis may occur in the buried soils as evidenced by the formation of halloysite. This is imparted by the high silica concentration from in-situ weathering and possible accumulation from silica leaching of overlying pyroclast deposits.

In general, both the modern and buried soils of weathering soil profiles from the forest, grassland, and paddy soils did not meet the level required for an andic character except for the buried soil of forest which showed some vitric properties of Andisol. Therefore, the soils are generally classified as Entisols.

The presence of significant quantities of weatherable primary minerals in the bulk fraction of the modern soils and the improvement in physiochemical and mineralogical properties in such a short span of time (26 yrs) shows the high capacity of volcanic soils to support crop production.

3.6 References

Anand, R. R., Gilkes, R. J., Armitage, T. M., & Hillyer, J. W. (1985). Feldspar weathering in lateritic saprolite. *Clays Clay Miner. 33*:31–43.

Aomine, S., & Mizota, C. (1973). Distribution and genesis of imogolite in volcanic ash soils of northern Kanto, Japan. pp. 207-213. In *Serratosa, J. M. (Ed). Proc. Int. Clay Conf.* (Madrid, Spain) 1972.

Ayris, P. M., & Delmelle, P. (2012). *The immediate environmental effects of tephra emission. Bulletin of Volcanology, 74,* 1905–1936. https://doi.org/10.1007/s00445-012-0654-5.

Banfield, J. F. & Barker, W. W. (1994). Direct observation of reactant-product interface formed in natural weathering of exsolved, defective amphibole to smectite: Evidence of episodic, isovolumetric reactions involving structural inheritance. *Geochimica et Cosmochimica Acta 58*: 1419-1429.

Bascomb, C. L. (1968). Distribution of pyrophosphate-extractable iron and organic carbon in soils of various groups. *Journal of Soil Science, 19*, 251-268.

Bautista, C. B. (1996). The Mount Pinatubo disaster and the people of Central Luzon. In *C. G., Newhall & R. S., Punongbayan (Eds). Fire and Mud: Eruptions and Lahars of Mount Pinatubo, Philippines.* Philippine Institute of Volcanology and Seismology, Quezon City. University of Washington Press, Seattle, and London. Printed in Hongkong.

Bernard, A., Knittel, U., Weber, B., Weis, D., Albrecht, A., Hattori, K., … Oles, D. (1996). Petrology and Geochemistry of the 1991 Eruption Products of Mount Pinatubo. In *Newhall, C. & Punongbayan, R. S. (Eds.), Fire and mud, eruptions and lahars of Mount Pinatubo, Philippines* (pp. 767–797). Univ. Washington Press, Seattle.

Besoain, R. & Hepp. (1995). The Hudson eruption and its effects on agriculture in the XI region [in Spanish], *Agricultura Técnica (Chile), 55*: 1-2, pp. 204-219.

Blakemore, L. C., Searle, P. L. & Daly, B. K. (1987). Methods for chemical analysis of soils. *Bur. Sci. Rep. 80*, N. Z. Soil Bur. Lower Hutt, New Zealand. 43 p.

Brown, G. & Brindley, G. W. (1980). X-ray diffraction procedures for clay mineral identification. In *Brindley, G. W. & Brown, G. (Eds.) Crystal Structures of Clay Minerals and their X-Ray Identification, Monograph no. 5.* London, Mineralogical Society, pp. 305–359.

Buol, S. W., Hole, F. D., McCracken, R. J. & Southard, R. J. (1997). Soil genesis and classification, Fourth Edition. *Iowa State University Press*.

Calvert, C. S., Buol, S. W., & Weed, S. B. (1980). Mineralogical transformations of a vertical rock–saprolite–soil sequence in the North Carolina Piedmont. *Soil Sci. Soc. Am. J. 44*:1096– 1112.

Castillo, P. R., Punongbayan, R. S. (1996). Petrology and Sr, Nd, and Pb Isotopic Geochemistry. In *R. S. Newhall, Christopher G., Punongbayan (Ed.), Fire and Mud* (pp. 799–805). Philippine Institute of Volcanology and Seismology, Quezon City; University of Washington Press, Seattle, and London.

Chao, T. T. & Sanzolone, R. F. (1992). Decomposition techniques. *Journal of Geochemical Exploration, 44*, 65-106.

Chaopricha, N. & Marín-Spiotta, E. (2014). Soil burial contributes to deep soil organic carbon storage. *Soil Biology and Biochemistry, 69*, 251-264.

Childs, C.W., Matsue, N., & Yoshinaga, N. (1991). Ferrihydrite in volcanic ash soils of Japan. *Soil Science and Plant Nutrition 37*, 299–311.

Churchman, G. J., & David, J. L. (2011). Alteration, formation, and occurrence of minerals in soils. In *Huang, P. M., Li, Y., Summer, M. E. (Eds.), Handbook of Soil Sciences*. CRC Press, pp. 1-72.

Churchman, G., & Lowe, D. (2012). Alteration, formation, and occurrence of minerals in soils. *CRC Press, 1*, 20–72. https://doi.org/doi:10.1201/b11267-24.

Cochran, V. L., Bezdicek, D. F., Elliott, L. F. (1983). The effect of Mount St. Helen's volcanic ash on plant growth and mineral uptake. *Journal of Environmental Quality, 12*, 415-418.

Dahlgren, R. A., & Ugolini, F. C. (1989). Effect of tephra addition on soil processes in Spodosols in the Cascade Range, Washington, U.S.A. Geoderma, 45, 331-335.

Dahlgren, R.A, Shoji, S., & Nanzyo, M. (1993). Mineralogical characteristics of volcanic ash soils. In *Shoji, S., Nanzyo, M., Dahlgren, R. Volcanic ash soils. Genesis, properties and utilization. Developments in Soil Science 21*. Elsevier. Amsterdam-London-New York-Tokyo.

Dahlgren, R. A., Dragoo, J. P., & Ugolini, F. C. (1997). Weathering of Mt. St. Helens tephra under a cryic-udic climatic regime. Division S-9 Soil Mineralogy. *Soil Sci. Am. J. 61*:1519-1525 (1997).

Dahlgren, R. A., Ugolini, F. C., & Casey, W. H. (1999). Field weathering rates of Mt. St. Helens tephra. *Geochimica et Cosmochimica Acta, 63*(5), 587–598. https://doi.org/10.1016/S0016-7037(99)00067- 8.

Dahlgren, R. A., Saigusa, M., & Ugolini, F. C. (2004). The nature, properties, and management of volcanic soils. *Advances in Agronomy. Volume 82*. Academic Press.

Dale, V. H., Swanson, F. J., & Crisafulli, C. M. (Eds.). (2005). Ecology responses to the 1980 eruption of Mount St. Helens. New York, Springer-Verlag.

Delmelle, P., Opfergelt, S., Cornelis, J-T., Ping, C-L. (2015). Volcanic soils. In *Sigurdsson, H., Houghton, B., Rymer, H., Stix, J., McNutt, S. (Eds.). The Encyclopedia of Volcanoes*, pp. 1253-1264. ISBN: 9780123859389. Elsevier Inc. All rights reserved. Academic Press.

Delvaux, B., Herbillon, A. J., & Vielvoye, L. (1989). Characterization of a weathering sequence of soils derived from volcanic ash in Cameroon - Taxonomic, Mineralogical and Agronomic Implications. In *Geoderma, Vol. 45*, no. 3-4, p. 375-388.

Dethier, D. P, Pevear, D. R., & Frank, D. (1981). Alteration of new volcanic deposits. In *Lipman P. W., Mullineaux, D. R. (Eds.). The 1980 eruptions of Mount St. Helens, Washington. US Geol Surv Prof Pap 1250*, Washington, pp 649–665.

Fejdi, P., & Holocsy, A. (2001). Relationship between crystal morphology and preferred orientation in polycrystalline specimens for diffraction experiments. *Materials Structure, 8*, 22-24.

Fiantis, D., Nelson, M., Ranst, E. V., Shamshuddin, J., & Qafoku, N. P. (2009). Chemical weathering of new pyroclastic deposits from Mt. Merapi (Java), Indonesia. J. *Mt. Sci (2009) 6*: 240-254.

Folkoff, M. E. & Meentemeyer, V. (1985). Climatic control of the assemblages of secondary clay minerals in the A-horizon of United States soils. *Earth Surf. Proc. Landforms 10*: 621–633. 1987.

Gibbs, H. S. (1968). Volcanic-ash soils in New Zealand. *Information Series No. 65.* Wellington, New Zealand: New Zealand Department of Scientific and Industrial Research.

Grotzinger, J. P., & Jordan, T. H. (2014). Understanding earth. *Seventh Edition.* Printed in the United States of America.

Halvorson, J. J., & Smith, J. L. (2009). Carbon and nitrogen accumulation and microbial activity in Mount St. Helens pyroclastic substrates after 25 years. *Plant Soil 2009, 315*, 211–228.

Herbillon, A. J. (1989). Chemical estimation of weatherable minerals present in the diagnostic horizons of low activity clay soils. *8th. Int. Soil Classif*. Workshop 1986 (Brazil), pp. 39-48.

Hodgson, J. M. (1976). Soil survey field handbook: describing and sampling soil profiles. *Soil Survey of England*, Harpenden.

Huang, P. M. (1989). Feldspars, olivines, pyroxenes, and amphiboles, p. 975–1050. In *Dixon, J. B., & Weed, S. B. (Eds.) Minerals in soil environments. 2nd edn*. SSSA, Madison, WI.

Kenedi, C. A., Brantley, S. R., Hendley II, J. W., & Stauffer, P. H. (2000). Volcanic Ash Fall—A "Hard Rain" of Abrasive Particles. *USGS Fact Sheet 027-00. U.S. Geological Survey- Reducing the Risk from Volcano Hazards.*

Kimble, J. M., Ping, C. L., Sumner, M. E., & Wilding, L. P. (2000). Andisols. In *Sumner, E. D. (Ed.). Handbook of Soil Science.* pp. E209-224, CRC Press, Boca Raton, FL.

Kunze, G. W. & Dixon, J. B. (1986). Pretreatment for mineralogical analysis. In *Klute, A. (Ed), Methods of Soil Analysis, Part 1, Physical and Mineralogical Methods, Agronomy Monograph no. 9, 2nd edn.* Madison, WI, American Soil Association and Soil Science Society of America, pp. 91–100

Loughlin, S. C., Sparks, S., Brown, S. K., Jenkins, S. F., V.-B., C. (2015). Global volcanic hazards and risk. *Cambridge University Press*. https://doi.org/10.1017/CBO9781107415324.004.

Lowe, D. J., & Nelson, C. S. 1983. Guide to the nature and methods of analysis of the clay fraction of tephras from the South Auckland region, New Zealand. *Earth Sciences University of Waikato occasional report 11.*

Lowe, D. J. (1986). Controls on the rates of weathering and clay mineral genesis in airfall tephras: a review and New Zealand case study. In *Colman, S. M. & Dethier, D. P. (Eds.). Rates of chemical weathering of rocks and minerals.* pp. 265-330. Academic Press, Orlando.

Luhr, J. F., & Melson, W. G. (1996). Mineral and glass compositions in June 15, 1991, pumices: Evidence for dynamic disequilibrium in the dacite of Mount Pinatubo. In *Newhall, C. G. & Punongbayan, R. S. (Eds.). Fire and mud. Eruptions and Lahar of Mount Pinatubo, Philippines.* Philippine Institute of Volcanology and Seismology, Quezon City. University of Washington Press, Seattle and London. Printed in Hongkong.

McDaniel, P. A., Lowe, D. J., Arnalds, O. & Ping, C. L. (2011). Andisols. In *Huang, P.M., Li, Y., Summer, M.E. (Eds.), Handbook of Soil Sciences*. CRC Press, pp. 29-45.

Mehra, O. P., & Jackson, M. L. (1960). Iron oxides removal from soils and clays by dithionite- citrate system buffered with sodium bicarbonate. In

Proceeding of 7th National Conference Clay Minerals, Washington, pp 317-327.

Mejia, G., Kohnke, H., & White, J. L. (1968). Clay mineralogy of certain soils of Columbia. *Soil Science Society of America Proceedings 32*: 665-670.

Melosantos, M. O. P, Solidum, R. U., Scott, W. E., Quiambao, R. B., Umbal, J. V., Rodolfo, K. S., Tubianosa, B. S., Delos Reyes, P. J., Alonso, R. A., & Ruelo, H. (1996). Tephra falls of the 1991 eruptions of Mount Pinatubo. In *Newhall, C.G. & Punongbayan, R. S. (Eds). Fire and mud.* Eruptions and Lahar of Mount Pinatubo, Philippines. Philippine Institute of Volcanology and Seismology, Quezon City. University of Washington Press, Seattle and London. Printed in Hongkong.

Mendoza, T. C., & Cabangbang, R. P. (1992). Effects of Mt. Pinatubo eruption in crop production systems. *The Philippine Agriculturist*, *75*(1 & 2), 1–8.

Mizota, C. (1976). Relationships between the primary mineral and the clay mineral compositions of some recent andosols: *Soil Sci. Plant Nutr. (Tokyo) 22*, 257-268.

Moore, D. M., & Reynolds, R. C. Jr. (1989). X-Ray diffraction and the identification and analysis of clay minerals. Oxford, UK, *Oxford University Press*.

Morisada, K., Imaya, A., & Ono, K. (2002). Temporal changes in organic carbon of soils developed on volcanic andesitic deposits in Japan. *Forest Ecol. Manag. 2002, 171,* 113–120.

Myers, B., Brantley, S. R., Stauffer, P., & Hendley II, J. W. (2008). What are Volcano Hazards*? U.S. Geological Survey Fact Sheet 002*-97.

Nanzyo, M. (2002). Unique properties of volcanic ash soils. *Glob. Environ. Res. 6.*

Nanzyo, M., Dahlgren, R., & Shoji, S. (1993). Chemical characteristics of volcanic ash soils. In *Shoji, S., Nanzyo, M., & Dahlgren, R. Volcanic ash soils. Genesis, properties and utilization. Developments in Soil Science 21.* Elsevier. Amsterdam-London-New York-Tokyo.

National Soil Survey Laboratory Staff. (1975). Proposed tables for soil survey reports. *RSSIU, USDA–SCS*, Lincoln, NE.

Nelson, G. L. (2013). Land rehabilitation techniques of rice farmers in Pampanga (Philippines) after the Mt. Pinatubo Eruption. *Asia Life Sciences, 22*(1), 155–181.

Newhall, C. G., & Punongbayan, R. S. (1996). Fire and mud. Eruptions and Lahar of Mount Pinatubo, Philippines. *Philippine Institute of*

Volcanology and Seismology, Quezon City. University of Washington Press, Seattle, and London. Printed in Hongkong.

Newhall, C., Stauffer, P. H. & Hendley II, J. W. (1997). Reducing the risk from volcanic hazards: Lahars of Mount Pinatubo, Philippines. *U.S. Geological Survey Fact Sheet 114*-97.

Norambuena, P. V., Luzio, W. L., Zepeda, O., Stern, J., & Reinoso, F. (2011). Preliminary survey of some soils from Chilean Antiplano near Iquique. *J. Soil Sci. Plant Nutr. 11 (2)*:62-71 (2011).

NRCS. (2013). Buried Soils and Their Effect on Taxonomic Classification.

Ontl, T. A. & Schulte, L. A. (2012). Soil Carbon Storage. *Nature Education Knowledge 3*(10):35.

Osman, K. T. (2013). Forest soils: Properties and Management. *Springer International Publishing Switzerland* 2013.

Oyama, M. (1991). Revised standard soil color charts. Published by Utrecht Van Boekhoven- Bosch. United States Department of Agriculture, Soil Conservation Service (1971). Compiled and edited by Rebecca Burt. Soil survey field and laboratory methods manual. 2014. *Soil survey investigations Report No. 51*. Version 2.

PAGASA. (2019). Monthly rainfall data from 1990 to 2018. Climatology and Agrometeorology Division (CAD), Philippine Atmospheric, Geophysical, and Astronomical Services Administration.

PAGASA. (2015). Climate of the Philippines. *Philippine Atmospheric, Geophysical, and Astronomical Services Administration.*

Page J. R., Miller, R. H., Keeney, D. H., Baker, D. E., Roscoe, J. R. & J.D., R. (Eds.) (1982). Methods of soil analysis: part 2, chemical and microbiological properties, *2nd edn*, Madison, WI.

Pallister, J. S., Hoblitt, R. P., Meeker, G. P., Knight, R. J., & Siems, D. F. (1996). Magma mixing at Mount Pinatubo: Petrographic and chemical evidence from the 1991 deposits. *In Newhall, C. G. & Punongbayan, R. S (Eds.). Fire and mud. Eruptions and Lahar of Mount Pinatubo, Philippines. (Eds:.)* Philippine Institute of Volcanology and Seismology, Quezon City. University of Washington Press, Seattle, and London. Printed in Hongkong.

Pansu, M., & Gautheyrou, J. (2006). Handbook of Soil Analysis: Mineralogical, Organic and Inorganic Methods. *Springer*. 993 p.

Pansu, M., Gautheyrou, J. & Loyer, J. Y. (2001). Soil analysis – sampling, instrumentation and quality control., *Balkema, Lisse, Abington, Exton, Tokyo*, 489 pp.

Parfitt, R.L. & Henmi, T. (1982). Comparison of an oxalate-extraction method and an infrared spectroscopic method for determining allophane in soil clays. *Soil Sci. Plant Nutr., 28*, 183-190

Parfitt, R. L., & Childs, W. (1988). Estimation of Forms of Fe and Al: A Review, and Analysis of Contrasting Soils by Dissolution and Moessbauer Methods. *Soil Chemistry and Mineralogy, Aust. J. Soil Res., 1*(26), 121–144.

Parfitt, R. L. & Wilson, A. D. (1985). Estimation of allophane and halloysite in three sequences of volcanic soils, New Zealand. In *Caldas, E. F., & Yaalon, D. H. (Eds.). Volcanic soils. Catena Suppl. 7,* pp. 1-8.

Parfitt, R. L., Russell, M., & Orbell, G. E. (1983). Weathering sequence of soils from volcanic ash involving allophane and halloysite, New Zealand. *Geoderma 29*:41–57.

PHILVOCS. (1992). Daily Volcano Bulletins, Pinatubo Volcano, April 7, 1991-December 1992: Quezon City. Philippine Institute of Volcanology and Seismology.

Ponnamperuma, F. N. (1972). The chemistry of submerged soils. *Adv. Agron. 24*:29–96.

Reyes, R. Y., & Neue, H. U. (1991). Characterization of the volcanic ejecta from Mount Pinatubo and its impact on rice production. *Philippine Journal of Crop Science, 16*(2), 69–73.

Rouiller, J., Burtin, G., & Souchier, B. (1972). La dispersion des sols dans l'analyse granulométrique. Méthode utilisant les résines échangeuses d'ions. *ENSAIA Nancy 14* : 194-205.Scaillet and Evans, 1997.

Ruxton, B. P. (1968). Measures of the degree of chemical weathering of rocks. *Journal of Geology 76*: 518-527.

Ruxton B. P. (1988). Towards a weathering model of mount lamington ash, Papua New Guinea. *Earth-Science Reviews 25*(5):387-397

Saigusa, M., Shoji, S., & Kato, T. (1978). Origin and nature of halloysite in Ando soils from Towada tephra, Japan. Geoderma, 20:115-129.

Samonte, H. P., Badayos, R. B., Ocampo, A. M., Capunpon, E. G., delos Santos, E. G., & Willauer III, J. L. (1992). Improving the fertility status and productivity of areas affected by volcanic ash deposits of Mt. Pinatubo. In *Proceedings of the symposium on sustainable agricultural development of Mt. Pinatubo-affected areas. November 5-6, 1992.* Biotech Seminar Room, UPLB, College, Laguna. Farming Systems and Soil Resources Institute, College of Agriculture. University of the Philippines at Los Baños, College, Laguna.

Sasaki, R., Yoshida, M., Ohtsu, Y., Miyahira, M., Ohta, H., Watanabe, M., & Suzuki, S. (2003). Soil formation of new lahar materials derived from Mt. Pinatubo. I. Physical and chemical properties of new lahar materials and soils formed by old lahar materials. *Soil Science and Plant Nutrition, 49*(4), 575–582.

Schaetzl, R., & Anderson, S. (2005). Soils: Genesis and Geomorphology. *Cambridge University Press*. Cambridge university press Cambridge, New York, Melbourne, Madrid, Cape Town, Singapore, São Paulo Cambridge. https://doi.org/10.2136/vzj2007.0030br.

Scheffer, F., & Schachtschabel P. (1998). Lehrbuch der Bodenkunde. Enke, Stuttgart.

Scott, K. M., Janda, R. J., de la Cruz, E., Gabinete, E., Eto, I., Isada, M., Sexon, M., & Hadley, K. C. (1996). Channel and sedimentation responses to large volumes of 1991 volcanic deposits on the east flank of Mount Pinatubo. In *Newhall, C. G. & Punongbayan, R. S. (Eds.) Fire and Mud: Eruptions and Lahar of Mount Pinatubo, Philippines*. Philippine Institute of Volcanology and Seismology, Quezon City. University of Washington Press, Seattle, and London. Printed in Hongkong.

Shoji, S. (1993) Studies on early weathering of volcanic ash and rehabilitation of soil environment. Report No.04453126 for the Grant-in-Aid of Scientific Research from the Ministry of Education.

Shoji, S., Dahlgren, R., & Nanzyo, M. (1993). Genesis of volcanic ash soils. In *Shoji, S., Nanzyo, M., Dahlgren, R. Volcanic ash soils. Genesis, properties and utilization. Developments in Soil Science 21*. Elsevier. Amsterdam-London-New York-Tokyo.

Smith, C. A. S., Ping, C. L., Fox, C. A., Kodama, H. (1999). Weathering characteristics of some soils formed in White River Tephra, Yukon Territory, Canada. *Canadian Journal of Soil Science 79*(4):603-613

Sobecki, T. M. (1990). Field procedure for base saturation and cation-exchange capacity (CEC) by ammonium acetate, pH 7, Version 1.0. *USDA–SCS, National Soil Survey Center,* Lincoln, NE.

Soil Survey Staff. (1975). Soil Taxonomy. *Agric. Handbook 436.* Soil Conservation Service, USDA Washington, DC, 754 pp.

Soil Survey Staff. (2014). Soil survey field and laboratory methods manual. *Burt, R. & Soil Survey Staff (Ed.). Soil Survey Investigations Report No. 51, Version 2.0*. U.S. Department of Agriculture, Natural Resources Conservation Service.

Sudo, T., & Shimoda, S. (1978). Clays and minerals of Japan. Developments in sedimentology. First. Edition. Volume 26. Elsevier Science.

Takahashi, T., Dahlgren, R. A., Theng, B .K. G., Whitton, J. S., & Soma, M. (2001). Potassium- selective, halloysite-rich soils formed in volcanic materials from northern California. Soil Sci. Soc. Am. J. 65: 516-526.

Tokashiki, Y., & Wada, K. (1975). Weathering implications of the mineralogy of clay fractions of two Ando Soils, Kyushu. *Geoderma 14*:47-62.

Ugolini, F. C., & Zasoski, R. J. (1979). Soils Derived from Tephra. In *Volcanic Activity and Human Ecology*. https://doi.org/10.1016/b978-0-12-639120-6.50009-1.

Ugolini, F. C. & Dahlgren, R. A. (1991). Weathering environments and occurrence of imogolite/allophane in selected Andisols and Spodosols. *Soil Science Society of America Journal, 55*:1166-1171.

Ugolini, F. C., & Dahlgren, R. A. (2002). Soil Development in Volcanic Ash, 69–81 pp.

Ugolini, F. C., Dahlgren, R., LaManna, J., Nuhn, W., & Zachara, J. (1991). Mineralogy and weathering processes in Recent and Holocene tephra deposits of the Pacific Northwest. *Geoderma, 51*:277-299.

Van Breemen, N., & Castro, R. U. (1980). Variation in zinc deficiency in rice along a toposequence of soils in Tiaong, Quezon Province, Philippines. III Cropping experiment. *Plant and Soil, 57*: 215-221.

Violante, P., & Wilson, M. J. Mineralogy of some Italian Andosols with special reference to the origin of the clay fraction. (1983). *Geoderma, Vol. 29*, No. 2, 1983, pp. 157- 174. doi:10.1016/0016-7061(83)90039-3

Wada, K. (1977). Active aluminum in Kuroboku soils and non- and para-crystalline clay minerals. *Nendo Kagaku, 17*:143-151. (In Japanese).

Wada, K. (1980). Mineralogical characteristics of Andisols. In *Theng, B. K. G. (Ed.), Soils with variable charge. NZ Soc. Soil Sci*. DSIR, New Zealand. Pp. 87-107.

Wada, K. (1982). Allophane and imogolite. In Dixon, J. B. & Weed, S. B. (Eds). Minerals in soil environments. *Soil Sci. Soc. Am.*, Madison, USA, pp. 603–638.

Wada, K. (1987). Minerals formed and mineral formation from volcanic ash by weathering. *Chemical Geology 60*(1):17-28

Wada, K. (1989). Allophane and imogolite. In *Dixon, J. B., & Weed, S.B. (Eds.), Minerals in soil environments, 2nd edn. Soil Sci. Soc. Am.*, Madison, WI. pp, 1051-1087.

Wang, B., Michaelson, G., Ping, C.-L., Plumlee, G., & Hageman, P. (2010). Characterization of pyroclastic deposits and pre-eruptive soils

following the 2008 eruption of Kasatochi Island Volcano, Alaska. *Arctic, Antarctic, and Alpine Research, 42(3)*, 276–284. https://doi.org/10.1657/1938-4246-42.3.276.

White, A. F., Benson, L. V., & Yee, A. (1986). Chemical weathering of the May 18, 1980, Mount St. Helens ash fall and the effect on the iron creek watershed, Washington. In *Rates of chemical weathering of rocks and minerals (pp. 351–374)*. Academic Press, Inc., Harcourt Brace Jovanovich, Publishers.

Whittig, L. D., & W. R. Allardice. (1986). X-ray diffraction techniques. In *Klute, A. (Ed.). Methods of Soil Analysis, Part 1. Physical and Mineralogical Methods, Agronomy Monograph no. 9, 2nd edn. American Soil Association and Soil Science Society of America*, Madison, WI, pp. 331–362.

Wiesner, M. G., Wetzel, A., Catane, S. G., Listanco, E. L., & Mirabueno, H. T. (2004). Grain size, areal thickness distribution, and controls on sedimentation of the 1991 Mount Pinatubo tephra layer in the South China Sea. *Bull Volcanol, 66*, 226–242. https://doi.org/10.1007/s00445-003-0306-x.

Wilson, M. A., Anderson, S. P., Arroues, K. D., Southard, S. B., D'Agostino, R. L., & Baird, S. L. (1994). November 15, 1994. No. 6, Publication of laboratory data in soil surveys. *National Soil Survey Center Soil Technical Note Handbook 430*–VI Amendment 5.

Wilson, M. J. (2004). Weathering of the primary rock-forming minerals: Processes, products, and rates. *Clay Miner. 39*:233–266.

Wilson, S. G., Lambert, J., Nanzyo, M., & Dahlgren, R. A. (2017). Geoderma Soil genesis and mineralogy across a volcanic lithosequence. *Geoderma, 285*, 301–312.

Wolfe, E. W. (1992). The 1991 eruptions of Mount Pinatubo, Philippines: *Earthquakes and Volcanoes, v. 23*, no. 1, p. 5-37.

Wolff-Boenisch, D., Gislason, S. R., Oelkers, E. H., & Putnis, C. V. (2004). The dissolution rates of natural glasses as a function of their composition at pH 4 and 10.6, and temperatures from 25 to 74 °C. *Geochimica et Cosmochimica Acta 68*: 4843-4858.

Wyatt, J., Lowe, D., Moon, V., Jock, G. J. C. (2010). Discovery of halloysite books in a ~270,000-year-old buried tephra deposit in northern New Zealand. *21st Australian Clay Minerals Conference.* https://doi.org/10.1016/0042-207X(87)90343-5.

Yuan, G., Lavkulich, L. M., & Wang, C. (1993). A method for estimating organic-bound iron and aluminum contents in soils. *Commun. Soil Sci. Plant Anal. 24*(11&12):1333–1343.

Zeglin, L. H., Wang, B., Waythomas, C., Rainey, F., & Talbot, S. L. (2016). Organic matter quantity and source affects microbial community structure and function following volcanic eruption on Kasatochi Island, Alaska. *Environ. Microbiol. 2016, 18*, 146–158.

Chapter 4 Phytolith accumulation in a 26-year dacitic ash deposit grown to lowland rice, Tarlac, Philippines

4.1 Introduction

Although silicon (Si) is not an essential nutrient, its uptake by plants improves resistance to biotic and abiotic stresses (Klotzbücher et al., 2015; Guntzer et al. 2012; Sauer et al., 2006). It is also beneficial for the normal growth and better yields of crops, especially those that require relatively high amounts of Si such as rice and sugarcane (Sauer et al., 2006; Lanning, 1963; Ma & Takahashi, 1990).

Silicon accumulates in plants due to precipitation of non-crystalline (amorphous) form of hydrated silica ($SiO_2 \cdot nH_2O$), called phytolith (PSi), in plant tissues (Oehler, 1979; Puppe et al., 2017; Song et al., 2012; Buján, 2013). Phytoliths from the plant tissues are then returned back to the soil (BSi) with leaf litter deposition (Gérard et al., 2008; White et al., 2012), and contributes a large pool of BSi to the global biogeochemical Si cycle (Conley, 2002). The solubility product of BSi, although still not well constrained, is slightly lower than that of amorphous silica but ~10 times higher than that of quartz (Fraysse et al. 2006). Therefore, BSi can act as a long-term reserve of Si in the soil for plant use (Luo et al., 2016; Opfergelt et al. 2008; Piperno, 2006; Gallego and Distel, 2004).

Volcanic ash has 40 to 70 wt.% SiO_2 consisting of silicate glasses (GSi), which is a fast weathering source of Si, Al (and other elements) for secondary mineral neogenesis (Shoji et al., 1993; Churchman & Lowe, 2012; Grotzinger & Jordan, 2014). The weathering conditions of volcanic ash, especially the high rate of weathering and high level of dissolved Si in the soil solution, contribute to the precipitation of short-range-order (SRO) aluminosilicates (i.e. allophane, imogolite), or to Si

adsorption onto the surfaces of poorly crystalline Fe-oxyhydroxide (i.e. ferrihydrite) (Shoji et al., 1993; Dahlgren et al. 1993). Therefore, volcanic ash emplacement plays an important role in dictating the soil Si stock and availability for plant uptake and hence, BSi formation.

Plant Si uptake may also vary with the stock of weatherable minerals, type, and age of parent material, degree of soil weathering (Wilding & Drees, 1971; Henriet, 2008), climate, and presence of volcanic materials (Clarke, 2003; Hart, 1992). Meunier et al. (1999) reported a 15-cm-thick BSi-rich (97-138 kg m^{-2} yr^{-1} SiO_2) horizon from trachytic ash soils grown with bamboos in Reunion Island (Indian Ocean) which accumulated through the biogeochemical recycling of SiO_2 from parent material weathering. Higher content of primary minerals undergoing weathering is believed to provide more Si to plants for greater BSi accumulation (Henriet, 2008; Opfergelt et al., 2008; Tavakkoli et al., 2011; Cornelis et al., 2010, 2014).

Rice is one of the most cultivated crops (Guntzer et al., 2012) and a major food crop worldwide especially in Asia where nearly 90 % of the world's rice is produced and consumed (FAO, 1998). It is known to accumulate phytoliths for up to 10 % of its shoot dry weight (Deshmukh et al., 2017; Ma et al., 2006). Rice plant absorbs much more Si compared with other Graminae crops such as wheat, barley, and grasses (Yoshida et al., 1959). The forms and fluxes of plant-available Si in paddy systems have been studied in detail showing the high ability of rice to accumulate Si (e.g. Klotzbücher et al. 2015; Ma et al. 2001; Desplanques et al. 2006). Hence, the BSi stock of rice soils are relatively higher than in other land uses (Li et al., 2013; Desplanques et al., 2006; Makabe et al., 2009).

Rice is typically encountered in volcanic regions, where the soils have developed on volcanic products such as lava and pyroclastic deposits. These so-called volcanic soils are largely represented by the Andisols order (Shoji et al., 1993; Dahlgren et al., 2004). Andisols are renowned for their excellent physical and chemical fertility (Shoji et al., 1993).

However, the contribution of phytoliths as Si source particularly in young volcanic ash soils grown to rice are still scarce. Previous studies (Henriet, 2008; Opfergelt et al., 2008; Opfergelt et al., 2010; Meunier, 1999) dealing with Si in the soil-plant system refer to well-developed Andisols. Some studies on Si and phytolith accumulation were conducted on the soil-rice system of non-volcanic origin (Desplanques et al., 2006; Li et al. 2013, 2014; Makabe et al., 2009). However, in many active volcanic regions, which are found dominantly in developing countries, cultivated Andisols are repeatedly exposed to volcanic ashfall. Ash particles correspond to tephra < 2 mm in diameter. It is a material generated by the explosive fragmentation of magmas and which is typically comprised of amorphous glass and crystalline silicates, along with minor Fe and Ti oxides (Tan, 1984; Shoji et al., 1993; Dale et al., 2005). The impact of ash deposition, sometimes leading to complete soil burial, on the biogeochemical cycle of Si in the soil-plant system is not known.

This study aims to understand the biogeochemical cycling of Si derived from phytoliths in a paddy soil-plant system impacted by ~15 cm Mt. Pinatubo ash deposit after 26 years of weathering period. The objectives of this study are to *(1)* quantify the abundance, concentration, and stocks of phytoliths from the rice plant biomass *(2)* compare the abundance, concentrations, stocks, fluxes, and dissolution rates of phytoliths in the newly developing modern soil from pyroclast and in the older buried soil, and *(3)* assess the influence of weathering degree and processes on the accumulation of phytoliths in the modern and buried soils.

4.2 Materials and Methods

4.2.1 Site characterization and soil sampling

The study took place in a lowland rice-cultivated paddy soil affected by ash from the 12-15 June 1991 Plinian eruption of Mt. Pinatubo at Bamban, Tarlac Province, Central Luzon, Philippines (Fig. 4.1). The soil profile used in this study is the same as the IR-Ash (irrigated rice soil affected by ash) soil profile in Chapter 3 section of this Ph.D. thesis which focused on the study of weathering.

The area is underlain by volcanic products from the modern Mt. Pinatubo emplaced during Holocene and late Pleistocene, 40 ka to present (Fig. 4.1). These consist mainly of dacitic pyroclastic-flow and lahar deposits. The climate in Tarlac Province is tropical with 2,002 mm mean annual rainfall (1998-2018; Clark, Pampanga weather station) and 27 °C mean annual temperature (PAGASA, 2019). Tarlac can be classified under the udic moisture regime (i.e. common in humid climates that have well-distributed precipitation) as the soil is not dry in any part for as long as 90 cumulative days (three months) in normal years (Kottek et al., 2006; Carating et al. 2014).

Tarlac province was affected by the 1991 eruption of Mt. Pinatubo. This explosive event was the second-largest eruption of the 20th century (Volcanic Explosivity Index 6; Wiesner et al., 2004). It was powered by a dacitic magma (i.e. 62.66 wt.% SiO_2; Castillo & Punongbayan, 1996). The total volume of magma disgorged as pyroclastic materials, including ash falls and pyroclastic density currents were ~5 km^3 dense rock equivalent (Luhr & Melson, 1996; Bernard et al., 1996). The total surface area covered by more than 1 cm of tephra was about 2000 km^2 (Melosantos et al., 1996). According to the tephra fall isopach map (Fig. 3.3c), the thickness of the tephra deposit varied between ~1 cm 35 km away from the volcano up to ~33 cm at proximal sites.

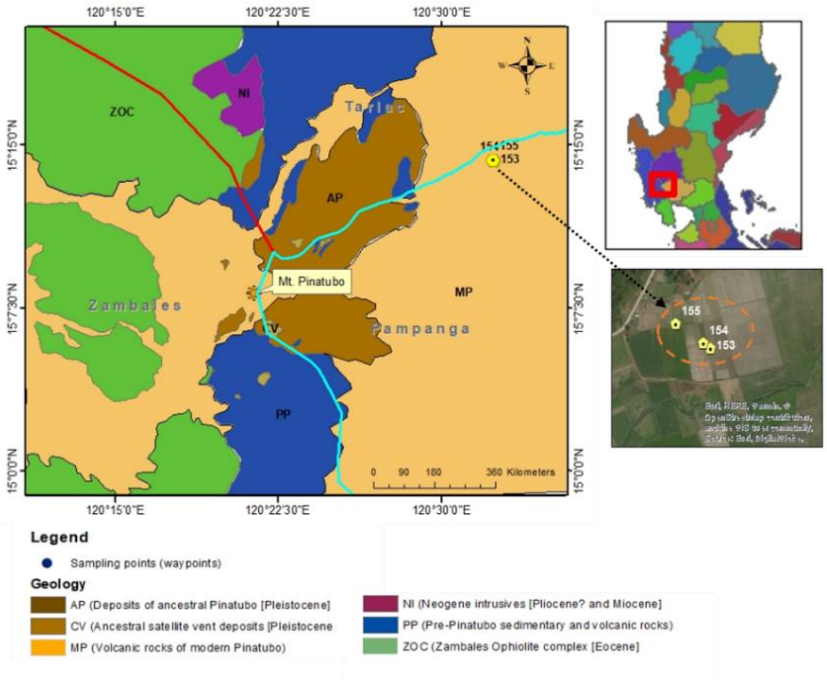

Figure 4.1. Simplified geological map of the Mt. Pinatubo region showing the main rock formation. The dotted yellow circle indicates the paddy fields where the study took place (see map inset showing the distribution of three soil profiles in Bamban, Tarlac province). *Adapted from the geologic map (altitude in meters) of Mount Pinatubo and environs (after the Philippine Bureau of Mines, 1963 and Delfin, 1983; 1984) cited in Newhall & Punongbayan, 1996.*

Three soil profile pits (55-90 cm depth) were excavated from the rice paddy area on 21 September 2017. Samples of the surface (modern) soil (MS), 1991 ash deposit (ash layer), and the ash-buried soil (BS) were collected from each of the soil profiles. The soil profile pits (P1, P2 and P3) were located 22 km (ground distance) northeast of Mt. Pinatubo (~15°14'14.4" N, ~120°32'21.5" E) (Fig. 4.2). The mean altitude of the studied site is 97 m a.s.l. Photographs of the soil pits are shown in Figure 4.3.

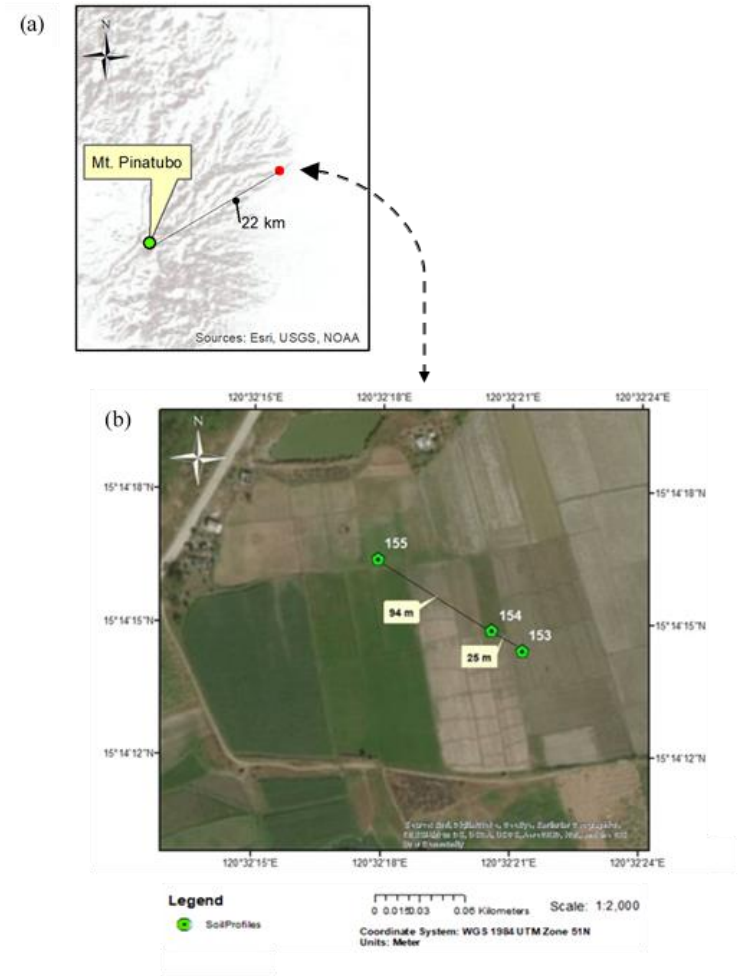

Figure 4.2. Location map of the study site in Bamban, Tarlac province showing the *(a)* ground distance (in kilometers) of the soil pits from the Mt. Pinatubo crater, and *(b)* distance (in meters) between the three (P1, P2, and P3) soil profile pits. *Waypoints 153, 155, and 154 correspond to profile soil pits P1, P2, and P3, respectively.*

The P1, P2, and P3 soil profiles are stratified into soil horizons, ash, and pumice layers (Fig. 4.3). The MS horizons at the surface of the three soil profiles range from 14 to 15 cm thick. The P1 and P3 soil profiles have only one MS and BS horizons. The P2 soil profile has one BS

horizon and two successive MS horizons distinguished based on differences in morphology (i.e. color). The 1991 ash deposit underneath the MS, 17 to 30 cm thick, are stratified into four to five layers of ash delineated based on field morphological differences (i.e. color; texture). Ash layers which have coarser (pumiceous) sand-size particles (> 90 %) are classified as "pumice" (i.e. P1-4, P2-5, P3-4; Fig. 4.3) while the other ash layers that are less coarse are classified as "ash". Each of the three soil horizons has two to three layers of ash and one layer of pumice. The BS horizons of the three soil profiles are 25 to 52 cm thick. A thorough characterization of the ash layers consisting of varying composition and grain sizes is presented in Chapter 3 weathering section of this Ph.D. thesis (Table A3.1).

According to the local farmers, the surface (modern) soil has been cultivated with rice since 2005, i.e. 13 years at the time of sampling. The ash-buried soil was cultivated with rice during 39 pre-eruption years (1953-1991). At present, fertilizer inputs to rice are urea (46-0-0), complete (14-14-14), and ammonium sulfate (21-0-0). These are supplied in low rates, ~54 kg N ha^{-1}, ~14 kg P_2O_5 ha^{-1}, and ~14 kg K_2O ha^{-1} obtaining rice yield of ~3.6 t ha^{-1} $season^{-1}$. The farmers have never used silicate materials as fertilizers.

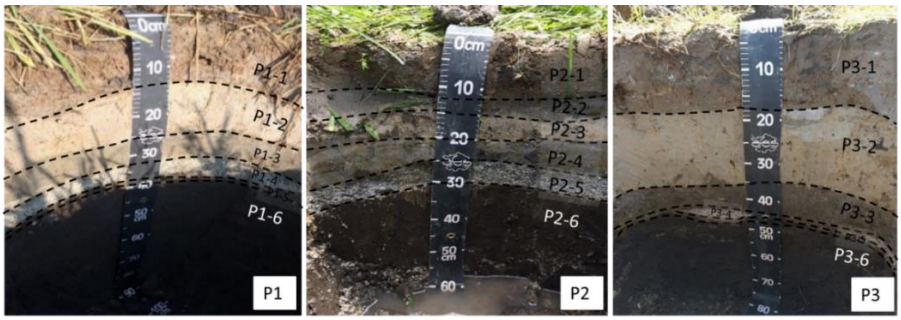

Figure 4.3. Photographs of the three soil profiles P1, P2, and P3 sampled in a lowland rice-cultivated paddy soil in Bamban, Tarlac Province. '*MS horizon' (P1-1, P2-1, P3-1); stratified 1991 'ash layer' in P1 (P1-2, P1-3, P1-5), P2 (P2-2, P2-3, P2-4), and P3 (P3-2, P3-3, P3-5); pumice layer (P1-4, P2-5, P3-4), 'BS horizon' (P1-6, P2-6, P3-6).*

4.2.2 Soil physicochemical and mineralogical analyses

Composite samples were collected from each soil horizon, ash, and pumice layers of the three soil profiles. The samples were mixed thoroughly to obtain a homogenous aggregate sample of 250 g to represent each of the soil horizons (MS and BS), and individual ash layers. The samples were air-dried, crushed and passed through a 2 mm sieve. All the chemical analyses were conducted on the fine-earth fraction < 2 mm (bulk). The protocols used to carry out the soil and ash physicochemical analyses, including morphological characterization in the field, soil physical, chemical, and mineralogical properties are presented in chapter 3 (method section 3.2.2).

Analytical data on soil properties of the MS horizon, BS horizon, and ash layers (including pumice) in each of the three soil profiles (P1, P2, and P3; Fig. 4.3) are collated and presented either in range or mean in the main text. The two MS horizons of P2 profile are averaged and the value obtained is used to represent the MS of P2 except for phytolith stocks wherein the values from these two horizons were added. Since the three to four ash layers (including pumiceous layer) from each of the soil profiles have shown comparable results in most of the chemical properties, the values were presented either in range, sum (i.e. phytolith stocks) or mean values in the interpretation and comparison of aggregated “ash layer” data with the soil horizons. Therefore, when ash layer is mentioned in the main text, it pertains to the data range of the stratified ash including the pumice layer that were analyzed in all the three soil profiles, unless a specific ash layer (s) of the soil profile(s) is/are referred to which is mentioned in the main text or annotated below the result table (i.e. Tables 4.4 and 4.5).

The general field description of the soil horizons, ash, and pumice layers in terms of soil color, texture, structure, root abundance, stickiness, plasticity, and presence of mottles were described according to Oyama (1991), Hodgson (1976) and Buol et al. (1997). The particle-size distribution was determined through ultrasonic and Na-saturated

resin dispersion to quantify the wt.% of grain-size fractions (sand, silt, and clay) (Rouiller et al., 1972). This was also conducted to separate the silt particles that were utilized for the extraction of BSi. The pH (H_2O and KCl) and bulk density were analyzed based on Page et al. (1982) and Soil Survey Staff (2014), respectively. The cation exchange capacity (CEC, $cmol_c\ kg^{-1}$) and percentage base saturation (% BS) were determined after ammonium extraction to quantify the base cations (Ca^{2+}, Mg^{2+}, $K^{+,}$ and Na^{+}) content and distillation using Kjehldahl method to determine the NH_4^+ adsorbed on the soil exchange complex (Sobecki, 1990; Soil Survey Staff, 2014; Chapman, 1965). The analysis of total organic C (wt.%) and N (wt.%) were done following the method of Pansu & Gautheyrou (2006). The soil organic matter (SOM) content was estimated from the total organic C using the van Bemmelen factor 1.724 (Pansu & Gautheyrou, 2006). The total element analysis (Si, Al, Fe, Ca, Mg, Na, K, and Ti) expressed in wt.% was determined using the method of Chao and Sanzolone (1992).

Subsequently, the TRB was calculated for both the soil horizons and the ash layer in comparison with the pristine 1991 ash deposit to estimate the degree of weathering (Herbillon, 1989; Delvaux et al., 1989). The oxalate-extracted Si, Al, and Fe (Si_o, Al_o, Fe_o) contents were measured according to the method of Blakemore et al. (1987) to determine the (i) Al and Fe in organic complexes, (ii) Fe in SRO (hydr)oxides (i.e. ferrihydrite), (iii) Al and Si in SRO aluminosilicates (i.e. allophane/imogolite) (Dahlgren et al., 1997; Dahlgren & Ugolini, 1989). The dithionite citrate bicarbonate (DCB)-extractable ($_d$) and Na-pyrophosphate ($_p$) extractable Fe and Al (Fe_d, Fe_p, Al_p), respectively were extracted according to Mehra and Jackson (1960) and Bascomb (1968), respectively. The DCB is a selective dissolution extractant for organically complexed, non-crystalline hydrous oxides, amorphous aluminosilicates, and “free” (amorphous and crystalline) forms of Fe that is not tied up in the lattice of primary minerals and which has been weathered and released to the soil solution. The Na-pyrophosphate selectively extracts organically bound forms of Fe and Al providing a good indicator of the abundance of organo-metallic complexes (Wada,

1989). Allophane/imogolite contents are derived from Si_o (Eq. 3.5; Parfitt & Henmi, 1982). The ferrihydrite content is estimated from Fe_o (Eq. 3.6; Dahlgren et al., 2004). All the elements were measured by Inductively Coupled Plasma—Atomic Emission Spectrometer (ICP-AES), ICAP 6000 Series. The chemical analyses were done in duplicates or triplicates (i.e. pH) for some samples randomly selected for every analysis.

The mineralogical analysis for the identification of primary and secondary minerals in the bulk and clay-sized (fine-earth < 2 µm) fractions using X-ray diffraction (XRD) and EVA© software are described in chapter 3 method section 3.2.3.

4.2.3 Overview of the BSi cycle in the soil-rice plant system after the 1991 Pinatubo eruption

The transfer of phytolith components in the studied volcanic soil-rice plant system is sketched in Figure 4.4. The dissolved silica (DSi, monosilicic acid, [H_2SiO_4]) is the plant-available form of Si. It is absorbed by the plant roots and precipitated in rice tissues as PSi. We refer to the PSi in rice sheath as PSi_{rs} and that from the rice leaves as PSi_{rl}. The rice leaves, ~30 wt. % of the harvested biomass is removed from the field after harvesting (Castillo et al., 2012), hence most of the PSi_l are lost from the system. During plowing, the rice sheath biomass is deposited back into the soil and PSi_{rs} is released upon decomposition; we denote the PSi_{rs} deposited in the soil as BSi_{rs}.

Phytoliths from other grasses that are deposited in the soil are referred to as BSi_g. The BSi_{rs} and BSi_g comprise the total BSi (BSi_t). An important source of DSi in this system is the tephra, and more specifically its glass component (GSi). Volcanic ash soils are developed from tephra. The dissolution of BSi_t and GSi release DSi back to the system where it can be leached or re-absorbed by the plant. Other pathways of the DSi (not shown in the diagram) are *(i)* incorporation in

less soluble secondary (crystalline) mineral phases (i.e. kaolinite, halloysite), *(ii)* precipitation as amorphous silica (i.e. opal), *(iii)* incorporation in SRO aluminosilicates (i.e. allophane, imogolite), and *(iv)* adsorption to poorly crystalline Fe-oxides (i.e. ferrihydrite). Upon weathering of these minerals, DSi is released back in soil solution and the cycle continues (Cornelis et al., 2014).

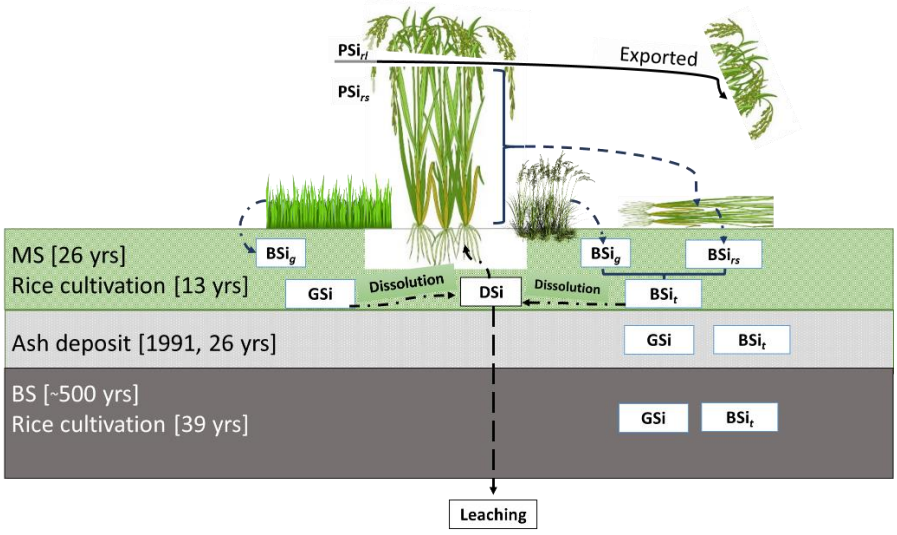

Figure 4.4. BSi cycle in the soil-rice plant system as envisaged 26 years after the 1991 Pinatubo eruption. *'PSi$_{rl}$' (phytoliths extracted from rice leaf); 'PSi$_{rs}$' (phytoliths extracted from rice sheath); 'BSi' plant phytoliths extracted from the soil; 'BSi$_{rs}$' (phytoliths of rice sheath extracted from the soil); 'BSi$_g$' (phytoliths of other grasses extracted from the soil); 'BSi$_t$' (total phytoliths from rice sheath plus other grasses extracted from the soil by heavy liquid extraction; section 4.2.4); 'GSi' (silicate glasses); 'DSi' (dissolved Si).*

4.2.4 Extraction of phytoliths in the silt-size fraction of soil horizons, ash, and pumice layers

Briefly, BSi with a density of ≤ 2.3 g cm^{-3} were extracted from the silt-sized fraction (2–50 μm) chemically followed by heavy liquid separation. The method is adapted from Madella et al. (1998). The sequential process of soil BSi extraction is shown in Figure 4.5.

The soil and ash samples were air-dried at room temperature during 24 h then sieved to collect the bulk sample (2 mm). Particle size analysis was done to obtain the silt-size particles. Most BSi fall in the 5 to 200 μm size range, but are more abundant in the 5 to 50 μm fraction (Zhao & Pearsall, 1998; Jones & Beavers, 1964). Thus, we assumed that the BSi from the sand fraction (50 μm to 2 mm) was negligible, hence the pumice layers of the soil profiles (Fig. 4.3) were not considered.

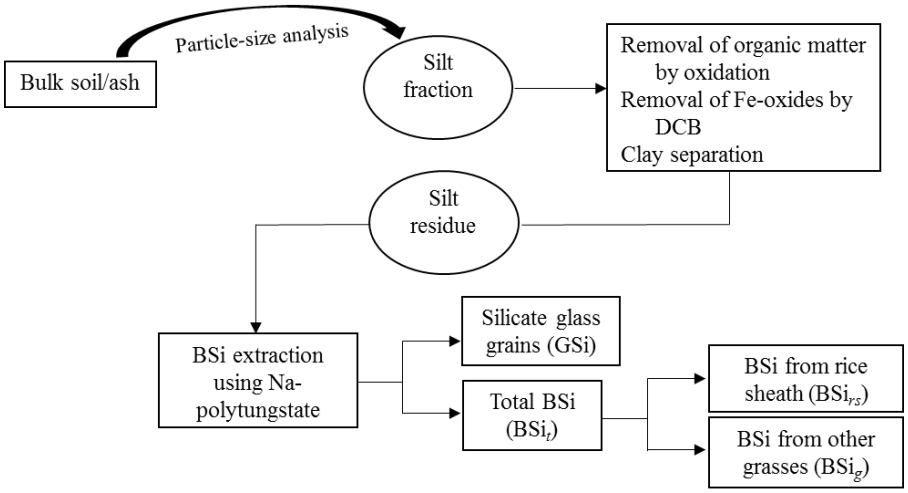

Figure 4.5. Diagram showing the different steps used for extracting BSi from the silt-sized fraction of bulk soil and ash.

Silt particles were treated with 6 vol.% H_2O_2 until the organic matter is fully oxidized (color of the sample changed to grayish-white and became homogenous), and afterward by DCB to extract and eventually

discard the crystallized and amorphous Fe oxides (Mehra & Jackson, 1960). These steps were done to break down soil aggregates and release the BSi that are bound within the organic matter and Fe oxides. The silt sample was dispersed with Na^+ resin followed by decanting and pipetting to remove the remaining clay-sized particles (Rouiller et al., 1972).

In order to extract the BSi components, the silt residue was treated with a heavy liquid, Na-polytungstate [$Na_6(H_2W_{12}O_{40})H_2O$], a non-toxic, high density (1.0-3.1 g cm^{-3}) separating compound which generates an almost neutral solution (pH 6) of relatively low viscosity (Munsterman & Kerstholt, 1996). Since the density of the ash's glass component is similar to that of BSi ($\leq$ 2.3 g cm^{-3}), silicate glass grains (GSi) may also partition together with BSi. Furthermore, the BSi extract consists of BSi from rice mostly from rice sheath [BSi_{rs}] since the upper portion of rice plants mainly the leaves are exported from the field after harvesting, and also BSi from other grasses (i.e. from weeds that grow with rice [BSi_g]. We refer to this cluster of BSi as total [BSi_t]. Hence, the final phytolith extract represents the sum of BSi_t and GSi, i.e. [BSi_t + GSi].

Each silt residue was mixed thoroughly with 20 ml of Na-polytungstate and centrifuged at 4000 t min^{-1} for 10 min (Fig 4.5). The supernatant containing the floating [BSi_t + GSi] particles were carefully pipetted and filtered in a Teflon (PTFE, < 0.002 mm) filter. Another cycle of Na-polytungstate saturation was done but this time, only adding 5 ml of the heavy liquid to extract the remaining [BSi_t + GSi]. The collected [BSi_t + GSi] was rinsed with 1M HCl followed by distilled water. The extract was dried at 105 °C until constant weight for gravimetric quantification (modified from Kelly, 1990 and Madella et al., 1998).

The concentration of [BSi_t + GSi] was calculated based on the ratio of extracted [BSi_t + GSi] over the initial dry weight (DW) of the bulk soil (< 2 mm) expressed as mg g^{-1} given by the following equation:

$$[BSi_t + GSi] = \frac{A}{B} \times 1000 \qquad \textit{Eq. 4.1}$$

where A and B are the gravimetric weight of [BSi_t + GSi] and bulk soil (< 2 mm) at 105 °C, respectively.

The stocks of [BSi_t + GSi] expressed in kg m^{-2} was also calculated taking into account the thickness and bulk density of each soil horizon and ash layer using the following equation:

$$[BS_t + GSi] = \frac{(BD \times HT) \times [BS_t + GSi]}{100} \qquad \textit{Eq. 4.2}$$

where BD is the bulk density of soil/ash (g cm^{-3}), HT is the soil horizon or ash layer thickness (cm), [BSi_t + GSi] (mg g^{-1}) is the phytolith extract consisting of BSi_{rs}, BSi_g, and GSi, and 100 is the conversion factor from mg cm^{-2} to kg m^{-2}.

4.2.5 Microscopic observation of BSi and GSi components

Identification of BSi was done through observation of [BSi_t + GSi] assemblage using a light microscope and matching the morphologies of BSi from those isolated in grasses (i.e. rice, weeds) by Zuo et al. (2016), Luo et al. (2016), Ball et al. (2015), and Twiss et al. (1969). The BSi usually have more regular and symmetrical morphologies (Madella et al., 2005) compared to GSi which are found in masses with curved, irregular surfaces (Grotzinger & Jordan, 2014).

Estimation of the abundance in percent of phytoliths (i.e. PSi; BSi_{rs} and BSi_g from [BSi_t + GSi]) was estimated quantitatively after observation with an Ortholux optical microscope under 250x magnification. Minute amounts of [BSi_t + GSi] samples were mounted on a clear glass slide and photomicrographs were taken. Each sample was replicated five times and the standard deviation of the mean was determined. The percentage abundance of BSi_{rs} was based on abundance per surface unit adapted from Hodgson (1976) as shown in Figure 4.6. The BSi_{rs} was expressed in wt.% based on the abundance value (Table 4.1).

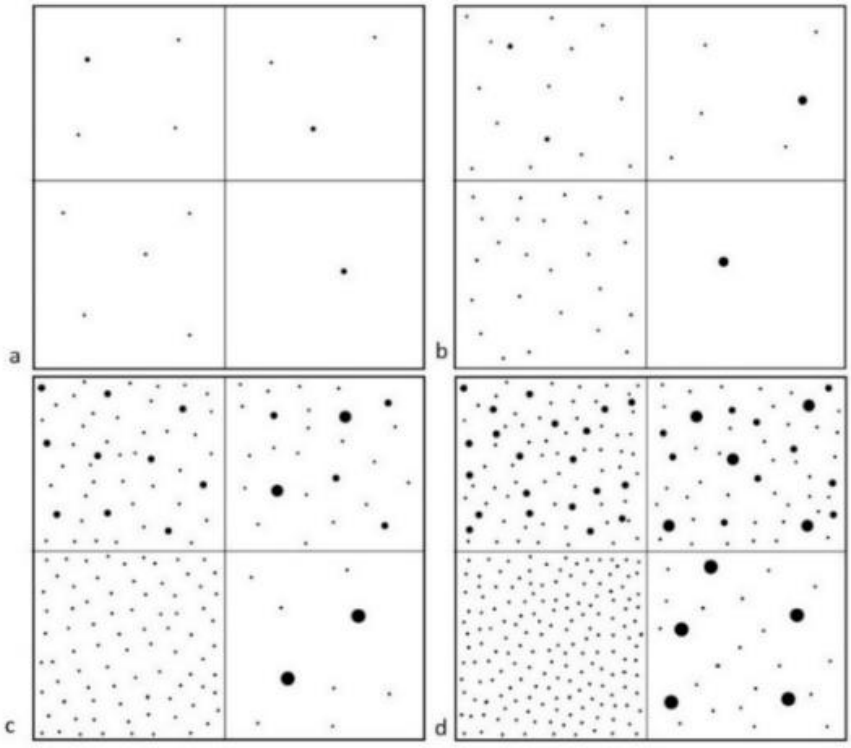

Figure 4.6. Chart for estimating percentage abundance of phytoliths, 0.1% (a), 0.5% (b), 2% (c), 5% (d). *Adapted from Hodgson (1976).*

Table 4.1. Estimated abundance and weight percent equivalent of rice sheath phytoliths (BSi_{rs}) based on the microscopic evaluation of the extracted soil phytolith [BSi_t + GSi] assemblage.

*MICROSCOPIC ABUNDANCE	ABUNDANCE WEIGHT EQUIVALENT
%	*wt.%*
0.00 – 0.45	0 – 9
0.50 – 2.05	10 – 41
2.10 – 3.05	42 – 61
3.10 – 4.05	62 – 81
4.10– 5.00	82 - 100

*Also used to estimate the abundance of PSi and BSi_g

4.2.6 Plant sample collection and analysis

Plant sampling

Plant samples of NSIC Rc160 variety (96 cm average height, 5.6 t ha^{-1} average yield; PhilRice, 2019) were collected 2 weeks after harvesting last September 2017. Prior to the eruption, harvesting of rice was manually done using a sickle. At present, harvesting is done mechanically using a combine harvester. In both cases, threshed straw composed mainly of leaves is exported from the field and fed to animals while the remaining biomass mostly rice sheath/stem are incorporated back into the soil during plowing. Samples of rice sheath were collected from five sampling points (1 m^2 per sampling point, ~10 rice hills). Composite sampling was done in each sampling point to finally obtain five replicate samples (~100 g/sample) from the sampling site. Some of the rice leaves left from the five sampling points were collected and composite samples were also obtained for analysis.

Total Si analysis of rice plant

Total Si of both rice sheath and leaves were determined after ignition at 1000 °C followed by borate fusion (Chao and Sanzolone, 1992). Briefly, plant samples were rinsed with water followed by 10 % HCl to remove aeolian dust and subsequently dried at 60 °C. Dried samples were cut into fine pieces. Approximately 500 mg of dried plant sample was mixed with 0.4 g Li-tetraborate and 1.6 g Li-metaborate in a graphite crucible then heated at 1000 °C for 5 minutes. The cooled crystal bead was dissolved in 100 ml of 2 M HNO_3 while magnetically agitated at 100 °C. Total Si was measured with ICP–AES and expressed as SiO_2 wt.%.

4.2.7 Extraction of phytoliths in rice sheath and leaves

In order to measure the PSi_{rs} and PSi_l concentrations, rice sheath and leaves were successively washed with deionized water, 1 M HCl, 70% ethanol, and deionized water again to remove the aeolian dust (Kelly 1990). About 5 g of dry matter, cut into small pieces, was digested at 120°C in a 70:30 vol. the ratio of concentrated nitric acid to hydrogen peroxide, HNO_3/H_2O_2, mixture until the reaction ceased (~10 days). The extract was filtered in a pre-weighed 0.4 µm filter paper then rinsed with deionized water and dried at 105 °C. The concentrations of PSi_{rs} and PSi_l were determined gravimetrically and expressed as wt.% (Kelly 1990; Carnelli et al. 2001).

4.2.8 Total Si and Ca analysis of soil phytoliths and rice sheath phytoliths

Measurements of the total Si and Ca were carried out to estimate the proportion of GSi components from [BSi_t + GSi] extracted in soil and ash using Ca/Si ratios. The total Si and Ca contents of PSi_{rs} was also determined to obtain its Ca/Si ratio. The analysis was performed following the alkaline fusion method by Chao and Sanzolone (1992)

described in Chapter 3 (section 3.2.2). About 40-70 mg of each sample was used in the analysis. The contents of Si and Ca were measured using ICP–AES and expressed as mg kg^{-1}.

Some of the ash layers from the soil profiles P1, P2, and P3 have not been analyzed due to insufficient samples. For P1, only P1-2 and P1-5 were analyzed. In P2 and P3, the ash layers analyzed were P2-3 and P3-2, respectively.

4.2.9 Biomass yield scenarios

The estimated rice biomass accumulation in both the modern and buried soils which are necessary to evaluate the phytolith stocks is based on farm owners' response, field measurements, and local information from the scientific literature. Low and high yield scenarios (Scenario 'A' and 'B', respectively) incorporated in the modern soil are based on information collected through. In the buried soil, low and high yield scenarios (Scenario 'C' and 'D', respectively) were based on the historical rice yields in the study area in the 1970s and 1980s (PhilRice, 2018).

In the modern soil, the 'low' biomass yield assumption is 378 g m^{-2} y^{-1}, dry weight basis (DW) (Scenario 'A'). It is derived from a grain yield of 300 g m^{-2} $season^{-1}$, 2 cropping seasons y^{-1}, and a harvest index [HI] of 50 (Yoshida, 1981). The HI suggests a 50:50 ratio of grain to biomass, for instance, a 300 g m^{-2} grain yield is equivalent to 300 g m^{-2} biomass. A moisture content [MC] of 37 wt.% was deducted from the biomass yield assumption. This is an actual value determined through oven-drying and gravimetric measurement of the collected fresh biomass from the field. A 200 g sample (3 replications) of rice biomass was oven-dried until a constant weight is achieved. The 'high' biomass yield assumption is 945 g m^{-2} y^{-1}, DW (Scenario 'B'). This is derived from a 500 g m^{-2} rice yield, 3 cropping seasons y^{-1}; 37 % MC, 50:50 grain to biomass ratio, and 37 wt.% MC.

In the buried soil, the ‘low’ (Scenario ‘C’) and ‘high’ (Scenario ‘D’) yield assumptions are 126 g m^{-2} y^{-1} (i.e. 200 g m^{-2} rice yield; 1 season $year^{-1}$; 50:50 HI; 37 % MC) and 756 g m^{-2} y^{-1}. (i.e. 400 g m^{-2} rice yield; 3 seasons $year^{-1}$; 50:50 HI; 37 % MC). The 37 % MC is also adapted for the biomass yield assumptions in the buried soil to convert the historical biomass yield data into dry weight.

In the Philippines, the common practice for rice straw management after harvesting is to remove the threshed straws/rice leaves (rl) and feed to ruminant animals (i.e. cattle). Therefore, the biomass incorporated in the soil is the standing stubbles left after harvesting consisting mainly of rice sheath (rs). The study of Castillo et al. (2012) showed that about 70 wt.% of a rice plant comprised of rice sheath is left while the remaining ~30 %, mainly rice leaves, are exported from the field after harvesting in Laguna, Philippines. We used these proportions to fractionate the amount of biomass that is incorporated back into the soil.

4.3 Results

4.3.1 General description of the soil profiles

The morphological characteristics of the soil (MS and BS) horizons and ash layer of P1, P2, and P3 soil profiles are shown in Table A4.1. The MS is plowed having granular to subangular blocky structure and with many fine and coarse roots. The textural class is silt loam, not sticky but very plastic, brownish color when moist with distinct yellow mottles. Ash and pumice layers are light grays to grayish-yellow when moist. The ash layer has granular to subangular blocky structure, is moderately sticky and moderately plastic, while pumice is structureless, not sticky and not plastic. The BS is brownish-black with many distinct red mottles, a subangular blocky structure, moderately sticky and very plastic.

4.3.2 Mineralogical Analysis

The major primary minerals and secondary clay minerals in the bulk and saturated clay-sized fractions of soil horizons, ash, and pumiceous layers are shown in Table 3.3 and Figure 3.7b (P2-a soil profile). The major primary minerals observed in the bulk fraction of soil horizons and ash layer are plagioclase feldspars, quartz, amphibole, pyroxene, mica, and iron oxides. The clay-sized fraction of the soil horizons and ash layer show that they are not merely composed of secondary clay minerals but also primary minerals. The secondary clay minerals found in the MS horizon consist of 1:1 (kaolinite, halloysite) and 2:1 (vermiculite, smectite) phyllosilicates. In the BS horizon, kaolinite, halloysite, and vermiculite are observed.

4.3.3 Physicochemical properties of the soil horizons and ash layers

Particle-size distribution

The particle-size distribution of the soil horizons, ash and pumice layers are shown in Table 4.2. The content of clay-sized particles in the MS of the three profiles which range from 16.1 to 17.7 wt.% is similar to the BS (15.6-18.1 wt.%). The ash layers of the three soil profiles (P1-2, P2-3, P3-2) underlying the MS also have comparable clay contents (14.4-18.6 wt.%). The silt fraction dominates in the MS horizon, ash, and pumice layers which ranged from 74.2 to 80.4 wt.%. In contrast, sand is the most abundant size fraction in the BS (43.3-47.6 wt.%); it is only 12.4 to 26.8 wt.% in the MS and 0.5 to 7.3 wt.% in the ash layers underneath MS (P1-2, P2-3, P3-2). The pumice layer (P1-4) and ash layers (P1-3, P1-5, P2-4, P3-3, P3-5) on top of the BS horizon consist mainly of sand with 94.3 wt. % (pumice layer) and 47.6 to 62.5 wt.% (ash layers).

General soil chemical properties

Table 4.3 shows the measurements of chemical properties including BD, pH (H_2O and KCl), CEC, % BS, exchangeable bases (Ca^{2+}, Mg^{2+}, Na^{+}, K^{+}), total C, total N, SOM, and C:N ratio. The pH_{H2O} is generally acidic in the MS and BS horizons ranging from 4.82 to 5.87. The pH_{H2O} of the soil horizons are slightly lower than that of the ash layer which ranged from 5.21 6.13. The pH_{KCl} is systematically lower than the pH_{H2O}, i.e. 4.15 to 4.51 (MS), 4.16 to 5.03 (BS) and 4.20 to 5.24 (ash). The bulk density is lower in the MS (0.77-0.85 g cm^{-3}) than the BS (1.20 g cm^{-3}).

The MS has 2.46 to 3.31 $cmol_c$ Ca^{2+} kg^{-1}, 0.80 to 0.93 $cmol_c$ Mg^{2+} kg^{-1}, 0.05 to 0.15 $cmol_c$ K^{+} kg^{-1}, and 0.22 to 0.39 $cmol_c$ Na^{+} kg^{-1}. The BS has 2.86 to 3.86 $cmol_c$ Ca^{2+} kg^{-1}, 0.80 to 1.46 $cmol_c$ Mg^{2+} kg^{-1}, 0.05 to 0.09

$cmol_c\ K^+\ kg^{-1}$ and 0.10 to 0.19 $cmol_c\ Na^+\ kg^{-1}$. The % BS in the MS and BS horizons are comparable ranging from 49 to 81 %.

Table 4.2. Particle-size distribution of the soil horizons, ash and pumice layers from Bamban, Tarlac province.

PROFILE	DEPTH	HORIZON	PARTICLE-SIZE DISTRIBUTION		
			SAND (50 µm – 2 mm)	SILT (2–50 µm)	CLAY (< 2 µm)
#	cm		---------- wt.% ----------		
P1 - 1	0-14	Modern soil	12.4	67.3	17.7
P1 - 2	14-25	Remobilized Ash	3.3	79.9	14.4
P1 - 3	25-32	Ash	56.3	36.5	4.1
P1 - 4	32-38	Pumice	94.3	1.9	4.3
P1 - 5	38-39	Ash	47.6	43.6	6.2
P1 - 6	39-90	Buried soil	47.6	30.9	18.1
P2 - 1	0-12	Modern soil	26.8	53.5	16.1
P2 - 2	12-15	Modern soil	26.1	54.0	16.9
P2 - 3	15-20	Remobilized Ash	7.3	74.2	16.2
P2 - 4	20-25	Ash	52.8	39.8	4.4
P2 - 5	25-31	Pumice	n.a.	n.a.	4.3
P2 - 6	31-55	Buried soil	44.1	36.5	17.0
P3 - 1	0-15	Modern soil	20.8	60.7	15.8
P3 - 2	15-34	Remobilized Ash	0.5	80.4	18.6
P3 - 3	34-41	Ash	62.5	30.4	4.5
P3 - 4	41-44	Pumice	n.a.	n.a.	4.3
P3 - 5	44-45	Ash	57.1	35.2	5.0
P3 - 6	45-73	Buried soil	43.3	38.2	15.6

P1, P2, P3 - pseudoreplicate soil profiles

Total C, total N and SOM contents of the soil horizons and ash layer are generally low. Between the soil horizons, the contents in MS are approximately 40 % higher compared to BS in the abovementioned properties. The MS has 0.78 to 2.03 wt.% total C, 0.19 to 0.30 wt.% total N, and 1.33 to 3.49 wt.% SOM while BS has 0.61 to 1.07 wt.% total C, 0.11 to 0.17 wt.% N, and 1.05 to 1.85 wt.% SOM. The ash has very low total C (0.07-0.30 wt.%), total N (0.06-0.10 wt.%) and SOM (0.12-0.52 %). The C:N ratio for BS (5.7-6.1) and MS (4.0-6.7) are higher than ash (1.0-3.2) (Table 4.3).

4.3.4 Elemental composition of soil horizons and ash layer

The total element composition in the soil horizons and the ash layer is shown in Table A4.2. The elemental oxides of BS are higher than MS horizons except for K_2O. The K_2O in the MS horizon is four-fold higher in magnitude compared to BS. The total SiO_2 contents of the MS and BS are similar (62.2-66.7 wt.%). These soil horizons also exhibit comparable total SiO_2 composition with that of the 1991 fresh ash deposit (62.7 wt.%; Castillo & Punongbayan, 1996).

Differences in total base concentrations (Ca, Mg, Na, K) between soil horizons are not large. The total Ca and Mg concentrations are higher in BS compared to MS and vice versa with total Na and K. Total Ca in MS and BS ranges from 93 to 120 $cmol_c\ kg^{-1}$ and 131 to 152 $cmol_c\ kg^{-1}$, respectively. The total Mg ranges from 67 to 82 $cmol_c\ kg^{-1}$ in MS and 88 to 98 $cmol_c\ kg^{-1}$ in BS. The differences in concentration of total Na and K in the MS and BS are as follows: total Na (110-122 *vs.* 95 to 112 $cmol_c\ kg^{-1}$, respectively), and total K (33-40 *vs.* 10 $cmol_c\ kg^{-1}$, respectively).

The TRB values of soil horizons varied to some extent with BS (324-370 $cmol_c\ kg^{-1}$) having slightly higher TRB than MS (311-354 $cmol_c\ kg^{-1}$). When compared to the TRB of 1991 ash deposit, the TRB of MS is lower by ~38 % and ~35 % for the BS. The TRB range of the ash layer (324-486 $cmol_c\ kg^{-1}$) is higher compared to the soil horizons (Table 4.3).

Table 4.3. Soil chemical properties of the soil horizons, ash, and pumice layers from three soil profiles at Bamban, Tarlac Province.

PROFILE	DEPTH	HORIZON/ LAYER	BD	pH		EXCHANGEABLE BASES					CEC	BS	C	N	OM	C:N	TRB
				H_2O	KCl	Ca^{2+}	K^+	Mg^{2+}	Na^+	Sum of Bases							
#	*cm*		*g cm* $^{-3}$			---------- *cmol* $_c$ *kg* $^{-1}$ ----------						*%*	---------- *wt.%* ----------				cmol$_c$ kg^{-1}
P1 - 1	0-14	Modern soil	0.83 ± 0.02	4.82 ± 0.3	4.15 ± 0.03	3.06	0.15	0.90	0.28	4.40	8.73	50	2.03	0.30	3.49	6.7	311
P1 - 2	14-25	Remobilized Ash	n.a.	5.96 ± 0.2	4.94 ± 0.07	1.78	0.12	0.52	0.21	2.63	3.58	74	0.19	0.10	0.33	1.8	330
P1 - 3	25-32	Ash	n.a.	5.93 ± 0.2	5.24 ± 0.05	0.82	0.05	0.24	0.08	1.18	1.17	101	0.07	0.06	0.12	1.0	486
P1 - 4	32-38	Pumice	n.a.	5.66 ± 0.3	5.03 ± 0.01	0.33	0.03	0.08	0.04	0.49	3.38	14	0.17	0.09	0.29	2.2	483
P1 - 5	38-39	Ash	n.a.	5.84 ± 0.2	4.86 ± 0.01	1.48	0.14	0.43	0.31	2.35	3.56	66	0.16	0.10	0.28	1.6	428
P1 - 6	39-90	Buried soil	n.a.	4.82 ± 0.1	4.16 ± 0.02	2.86	0.09	0.80	0.10	3.84	7.80	49	0.96	0.17	1.65	5.7	370
P2 - 1	0-12	Modern soil	0.77 ± 0.02	5.05 ± 0.3	4.18 ± 0.01	2.55	0.14	0.80	0.22	3.71	7.61	49	1.63	0.25	2.80	6.5	354
P2 - 2	12-15	Modern soil	0.90 ± 0.00	5.11 ± 0.2	4.20 ± 0.00	2.46	0.14	0.78	0.25	3.63	5.93	61	1.27	0.21	2.18	6.1	344
P2 - 3	15-20	Remolized ash	1.02 ± 0.02	6.02 ± 0.1	4.74 ± 0.03	2.12	0.16	0.75	0.35	3.37	4.39	77	0.30	0.09	0.52	3.2	338
P2 - 4	20-25	Ash	1.16 ± 0.01	6.13 ± 0.1	4.97 ± 0.08	0.85	0.06	0.28	0.17	1.36	0.90	151	0.10	0.07	0.17	1.4	484
P2 - 5	25-31	Pumice	0.85 ± 0.01	6.07 ± 0.1	5.23 ± 0.01	0.43	0.03	0.14	0.11	0.70	1.35	52	0.08	0.08	0.14	1.0	460
P2 - 6	31-55	Buried soil	1.20 ± 0.05	5.87 ± 0.1	5.03 ± 0.02	3.86	0.05	1.46	0.19	5.56	7.59	73	0.61	0.11	1.05	5.8	365
P3 - 1	0-15	Modern soil	0.85 ± 0.00	5.12 ± 0.2	4.51 ± 0.03	3.31	0.05	0.93	0.39	4.67	8.49	55	0.78	0.19	1.33	4.0	349
P3 - 2	15-34	Remobilized ash	n.a.	5.64 ± 0.2	4.72 ± 0.08	1.86	0.17	0.62	0.43	3.08	3.32	93	0.17	0.10	0.29	1.7	324
P3 - 3	34-41	Ash	n.a.	5.35 ± 0.2	4.64 ± 0.09	1.07	0.05	0.35	0.17	1.63	3.05	54	0.11	0.08	0.19	1.4	468
P3 - 4	41-44	Pumice	n.a.	5.30 ± 0.1	4.67 ± 0.05	0.44	0.02	0.15	0.11	0.72	1.36	53	0.10	0.06	0.18	1.7	467
P3 - 5	44-45	Ash	n.a.	5.21 ± 0.1	4.42 ± 0.09	2.24	0.13	0.44	0.33	3.14	2.68	117	0.18	0.09	0.30	2.0	443
P3 - 6	45-73	Buried soil	n.a.	5.29 ± 0.2	4.89 ± 0.07	2.93	0.07	0.93	0.13	4.07	5.04	81	1.07	0.17	1.85	6.1	324

P1, P2, P3 – pseudoreplicate soil profiles; 'n.a' - not measured

4.3.5 Phytolith and Si contents, and morphologies of the rice plant

Phytolith and Si contents of the rice plant

The total Si content of rice leaves (n = 5) ranges from 7.0 to 7.9 wt.% (14.9-16.9 wt.% SiO_2) (Fig. 4.7). It is slightly higher than the Si content in rice sheaths which ranges from 5.7 to 6.9 wt.% (12.2-14.8 wt.% SiO_2). These values are above the 5 wt.% critical level for Si deficiency in plants (Dobermann & Fairhurst, 2000).

The PSi content of the rice leaves (16.3-18.0 wt.%) is slightly higher than the PSi content of the rice sheath (15.9-16.9 wt.%) as shown in Figure 4.7. In terms of composition, the PSi_{rl} and PSi_{rs} are mainly composed of SiO_2, with PSi_{rl} having slightly higher SiO_2 than PSi_{rs} (96.9-97.9 wt.% vs. 94.4-95.7 wt.%; not shown). The remaining 3 wt.% and 5 wt.% of the PSi_{rl} and PSi_{rs} composition, respectively, are water and trace amounts of elements (i.e. Al, K [< 0.001 wt.%]; Fe, Ca, K, Mg, Na [< 0.0001 wt.%].

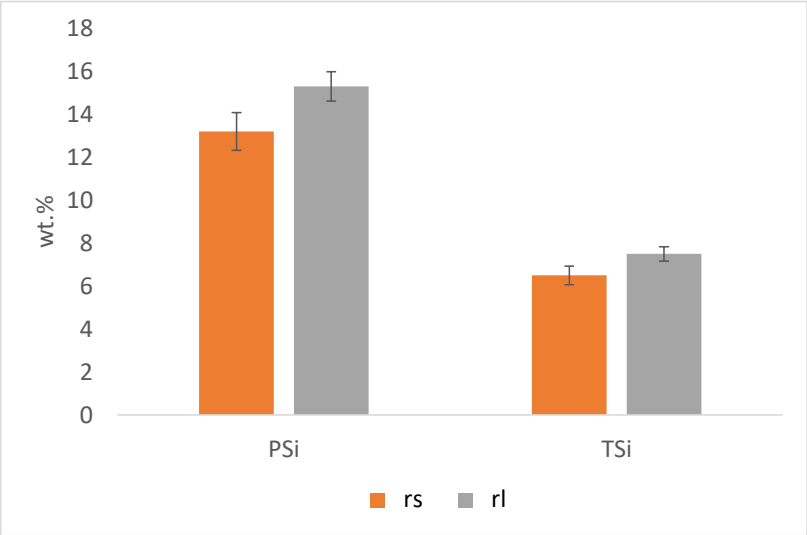

Figure 4.7. Comparison of phytolith and equivalent total Si mean contents (n=2) in rice sheath (rs) and leaves (rl). *'PSi' ($SiO_2.nH_2O$) extracted phytoliths from the rice plant parts), 'TSi' (total Si content in the rice plant parts).*

Microscopic assemblages of rice plant phytoliths

Major rice plant phytoliths (PSi) morphologies observed were bilobate (dumbbell-shaped with scooped ends; ~ 10 µm in size), and bulliform (fan-shaped; ~ 50 µm in size) as named by Zuo et al. (2016); Luo et al. (2016) and Ball et al. (2015). Microphotographs of the PSi assemblage show the presence of bilobate and bulliform phytoliths in rice sheath (PSi_{rs}) and rice leaf (PSi_{rl}), but in various proportions (Fig. 4.8).

The bilobate PSi abundance is ~28 wt.% in both PSi_{rs} and PSi_{rl}. However, PSi_{rl} has a higher abundance of bulliform phytolith (32 wt.%) compared to PSi_{rs} (8 wt.%) (Fig. 4.9; refer to method section Fig. 4.6 and Table 4.1 for estimation of abundance).

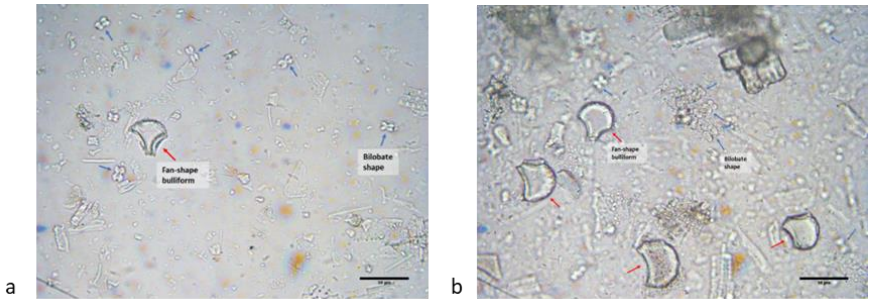

Figure 4.8. Phytolith assemblage of (a) rice sheath and (b) rice leaf. Scale bar = 50 µm. *Red arrows point to fan-shaped bulliform phytolith. Blue arrows point to bilobate-shaped phytolith.*

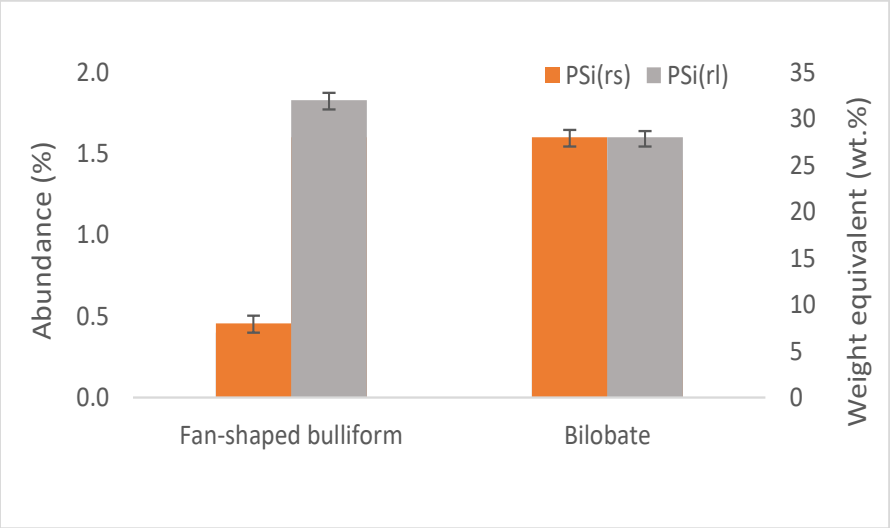

Figure 4.9. Proportions of bulliform and bilobate phytoliths in the PSi_{rs} and PSi_{rl} of the rice plant. *Refer to section 4.2.5 for the calculation of estimated abundance and weight equivalent.*

4.3.7 Morphologies and contents of phytoliths and silicate glass contents extracted from the silt-size fraction of soil horizons

Phytoliths and silicate glass fractions extracted from soil horizons

The content of total Si and Ca, Ca/Si ratio, and weight percent abundance of GSi, BSi_t, BSi_{rs}, and BSi_g components in the extracted [BSi_t + GSi] of the soil horizons and ash layer are presented in Table 4.4. Also shown in this table is the total Si and Ca, and Ca/Si ratio of the extracted PSi*rs* in the rice sheath and GSi in the Pinatubo glass matrix (Scaillet & Evans, 1997).

The total Si content of the [BSi_t + GSi] in the soil horizons and ash layer varies in the range of 353 to 439 mg kg^{-1}. The total Si of the PSi_{rs} in rice sheath and GSi in Pinatubo glass are 445 and 363 mg kg^{-1}, respectively. The total Ca content of the [BSi_t + GSi] in the MS and ash layer as well as in the GSi of the Pinatubo glass are comparable ranging

from 6.0 to 9.0 mg kg^{-1}. On the other hand, the total Ca content of the [BSi_t + GSi] in the BS is comparable with that of the PSi_{rs} of the rice sheath (0.9 vs. 0.3 mg kg^{-1}, respectively). The [BSi_t + GSi] in the MS and ash layer has comparable Ca/Si ratios (0.016-0.022). The Ca/Si of the [BSi_t + GSi] in the BS (i.e. 0.006) are lower by ~three times than that of the MS and ash layer. The Ca/Si ratio of the PSi_{rs} in the rice sheath is very low while that of the GSi in the Pinatubo glass matrix is 25 times higher (0.001 vs. 0.025, respectively).

The proportion of GSi and BSi_t from the measured [BSi_t + GSi] are determined using the Ca/Si ratios of PSi_{rs}, [BSi_t + GSi], and GSi. The BSi_t and GSi expressed in wt.% abundance (i.e. y_{BSi_t} and x_{GSi}, respectively) are calculated using equations Eqs. 4.3, 4.4 and 4.5, below. Since the Ca concentration of PSi_{rs} is almost negligible (0.001 mg kg^{-1}; Table 4.4), the difference in the Ca/Si ratio of the [BSi_t + GSi] with PSi_{rs} will approximate the fraction of GSi (Eq. 4.3 and 4.5). The y_{BSit} term in Eq. 4.3 can be derived from Eq. 4.4. In the calculation, we assume that the Ca/Si ratio of the BSi_g is similar to that of PSi_{rs}. Previous studies have shown that phytoliths generally consist of approximately 95 % SiO_2 and 5 % of other elements such as C, Fe, Al or Ca (Puppe et al., 2017; Song et al., 2012; Buján, 2013). Hence, the Ca/Si ratio of BSi_g will not have a large difference with that of PSi_{rs}.

$$x_{Gsi} + y_{BSi_t} = 1 \qquad \textit{Eq. 4.3}$$

$$y_{BSi_t} = (1 - x_{GSi}) \times 100 \qquad \textit{Eq. 4.4}$$

$$\left(\frac{Ca}{Si}\right)_{[BSi_t+GSi]} = x_{GSi}\left[\left(\frac{Ca}{Si}\right)_{GSi}\right] + (1-x_{GSi})\left[\left(\frac{Ca}{Si}\right)_{PSi_{rs}}\right] \qquad \textit{Eq. 4. 5}$$

where $\mathbf{x_{Gsi}}$ is wt.% GSi; $\mathbf{y_{BSi_t}}$ is wt.% BSi_t; $\left(\frac{Ca}{Si}\right)_{[BSi_t+GSi]}$ is the $\frac{Ca}{Si}$ ratio of [BSi_t + GSi] extracted from each soil horizon and ash layer; $\left(\frac{Ca}{Si}\right)_{GSi}$ is the $\frac{Ca}{Si}$ ratio of GSi (0.025; Scaillet & Evans, 1997), and $\left(\frac{Ca}{Si}\right)_{PSi_{rs}}$ is the $\frac{Ca}{Si}$ ratio of PSi_{rs}.

Table 4.4. Mean abundances of BSi_t and GSi from the [BSi_t + GSi] extracted in the silt-size fraction of soil horizons and ash layer at Bamban, Tarlac province.

Parameter	Total Si	Total Ca	Ca/Si ratio	[4]GSi	[4]BSi_t (BSi_{rs} + BSi_g)	[5]BSi_{rs}	[5]BSi_g	[6] *n*
	----- *mg kg^{-1}* ------			---------- *wt.%* ----------				
[1][BSi_t + GSi] in MS horizon	378 ± 3	6.0 ± 0.2	0.016 ± 0.001	62.5 ± 2.9	37.5 ± 2.9	14	23	*4*
[1][BSi_t + GSi] in BS horizon	439 ± 3	0.9 ± 0.1	0.006 ± 0.000	4.2 ± 0.0	95.8 ± 0.0	59	37	*3*
[1][BSi_t + GSi] in ash layer	353 ± 1	7.6 ± 0.3	0.022 ± 0.001	85.4 ± 2.1	14.6 ± 2.1	0	15	*4*
[2]PSi_{rs} in rice sheath	445 ± 3	0.3 ± 0.0	0.001 ± 0.001	-	-			*2*
[3]GSi in glass matrix	363	9.0	0.025	-	-			*13*

[1]Phytoliths and silicate glasses extracted from the MS and BS horizons and ash layer; [2]phytoliths extracted from rice sheath; [3]Mt. Pinatubo ash matrix glass, Scaillet & Evans (1997); [4]proportion based on Ca/Si ratio (Eqs. 4.3-4.5); [5]based on microscopic abundance (refer to method section 4.2.5), [6]number of samples analyzed.

The estimated GSi fraction in the measured [BSi_t + GSi] in the MS (58.3-66.7 wt.%) is ~15-fold higher compared to that estimated for BS (4.2 wt.%). The [BSi_t + GSi] of the ash is mostly made up of silicate glass grains with a fraction of 83.3 to 87.5 wt.% GSi (Table 4.4). On the other hand, the fraction of BSi_t (consisting of BSi_{rs} and BSi_g) in the BS is the highest (95.8 wt.%) followed by that found in the MS (34.6-40.4 wt.%) and lastly, in the ash (12.5-16.7 wt.%).

The proportions (wt.% abundance) of BSi_{rs} and BSi_g from the BSi_t (estimated based on [BSi_t + GSi] microscopic assemblage) from the silt-fraction of soil horizons and ash layer are displayed in Figure 4.10 and Table 4.4. The BSi_{rs} abundances in the MS and BS horizons range from 5 to 22 and 46 to 68 wt.%, respectively. The ash layer has no BSi_{rs}. On the other hand, the mean BSi_g abundances in the silt-size fraction of the MS and BS horizons and ash layer range are 20 to 28, 28-50 and 13-17 wt.%, respectively.

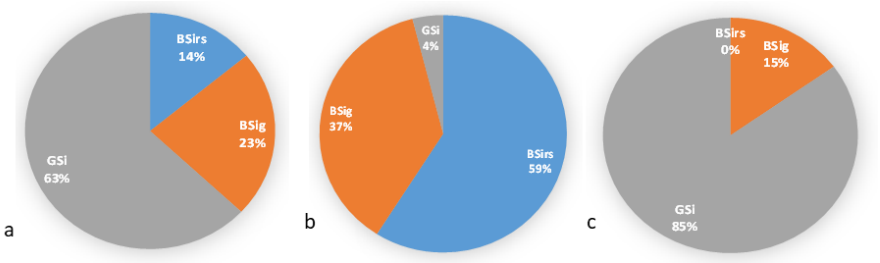

Figure 4.10. Mean abundances (% wt. equivalent) of BSi_{rs}, BSi_{g}, and GSi from the total [BSi_t + GSi] in the silt-size fraction of the MS *(a)* and BS *(b)* horizons, and ash layer *(c)* at Bamban, Tarlac province. *BSi_{rs} and BSi_g proportions are based on abundance estimated from the extracted [BSi_t + GSi] microscopic assemblage (see method section 4.2.5).*

Microscopic assemblages of phytoliths extracted from soil horizons and ash layer

Microphotographs of the [BSi_t + GSi] assemblages show the presence of BSi_{rs}, BSi_g and GSi in the soil horizons and ash layer except that BSi_{rs} is not observed in the latter (Fig. 4.11). The ash layer is dominated by GSi and contains a few BSi_g. More GSi is found in the MS compared to the BS. In turn, the abundance of BSi_{rs} in the BS horizon is about four times higher than the MS (Fig. 4.11a-b).

Some of the BSi_{rs} have slight to moderate pitting of bulliforms. The bilobate BSi_{rs} were seldom identified unambiguously due to their smaller size compared to bulliform BSi_{rs}. Furthermore, fragmented and unrecognizable BSi materials are not counted. Individual types and morphologies of BSi_{rs}, BSi_g, and GSi observed in the [BSi_t + GSi] assemblages are described in Table A4.3.

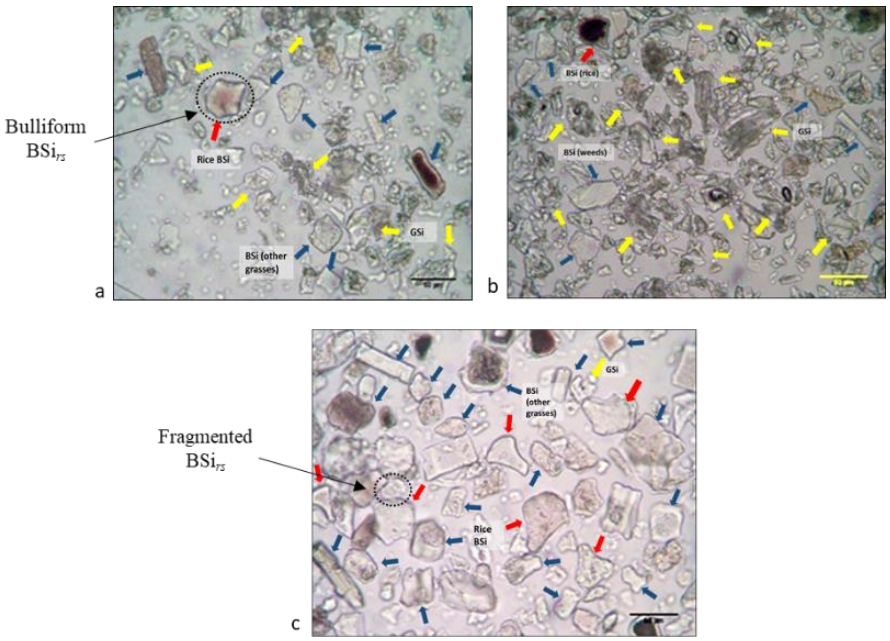

Figure 4.11. Microscopic assemblage of phytoliths [BSi$_t$ + GSi] from the representative silt-sized fraction of *(a)* modern soil, *(b)* ash layer, and *(c)* buried soil. *Red arrows point to BSi$_{rs}$, blue arrows point to BSi$_g$ and yellow arrows point to GSi. Scale bar = 50 µm.*

Rice phytoliths, grass phytoliths, and silicate glass concentrations from soil phytoliths extracted in the silt-size fractions of soil horizons and ash layer

The concentrations of BSi$_{rs}$, BSi$_g$, and GSi from measured [BSi$_t$ + GSi] are presented in Table 4.5. The BS horizon has the highest concentration of [BSi$_t$ + GSi] ranging from 55 to 78 mg g^{-1} which mainly consists of 36 to 48 mg BSi$_{rs}$ g^{-1}, 15 to 39 mg BSi$_g$ g^{-1} and a small quantity of GSi (2-3 mg g^{-1}). The MS horizon contains 38 to 58 mg [BSi$_t$ + GSi] g^{-1}, comprised of 2 to 8 mg BSi$_{rs}$ g^{-1}, 10 to 14 mg BSi$_g$ g^{-1} and a higher content of GSi ranging from 25 to 36 mg g^{-1} than that found in the BS. The ash layer has the lowest concentration of [BSi$_t$ + GSi] (10-36 mg g^{-1}), consisting mainly of GSi (9-27 mg g^{-1}) and low BSi$_g$ (1-9 mg g^{-1}). BSi$_{rs}$ is not present in ash.

Rice phytoliths, grass phytoliths, and silicate glass stocks from soil phytoliths extracted in the silt-size fractions of soil horizons and ash layer

The stocks of BSi_{rs}, BSi_g, and GSi from measured [BSi_t + GSi] are presented in Table 4.5. The total [BSi_t + GSi] stock in the BS is 15.9 to 47.4 kg m^{-2}. It is about five times higher than that of the MS (4.9-6.7 kg m^{-2}). The ash layer has much smaller [BSi_t + GSi] stock, which ranges from 0.4 to 2.1 kg m^{-2}. The BSi_{rs} (10.8-21.8 kg m^{-2}) stock in BS horizon is ~25 times higher than that in the MS horizon (0.2-0.9 kg m^{-2}). Moreover, the stock of BSi_g (4.4-23.6 kg m^{-2}) in BS is also about nine and 69 times higher than that estimated for MS (1.0-1.7 kg m^{-2}) and the ash layer (0.1-0.3 kg m^{-2}), respectively. The GSi stock is highest in the MS ranging from 3.2 to 4.2 kg m^{-2}, i.e. it is two to three times higher than that in BS (0.7-2.0 kg m^{-2}). The ash layer (0.6-2.1 kg m^{-2}) has lower GSi stock compared to that in MS and BS horizons.

Table 4.5. Concentrations and stocks of rice sheath phytoliths, grass phytoliths, and silicate glass in the silt-size fraction of the soil horizons and ash layer at Bamban, Tarlac province.

Profile Code	Depth	Horizon	[1][BSi_t + GSi]	[2]GSi	[2]BSi_t		[BSi_t + GSi]	GSi	BSi_t	
					[3]BSi_g	[3]BSi_{rs}			BSi_g	BSi_{rs}
#	*cm*		----------	*mg g^{-1}*	----------		----------		*kg m^{-2}*	----------
P1 - 1	0-14	Modern soil	58	36	14	8	6.7	4.2	1.7	0.9
P1 - 2	14-25	Ash	19	17	2	0	2.1	1.8	0.3	0.0
P1 - 3	25-32	Ash	12	n.a	n.a	n.a	1.0	n.a	n.a	n.a
P1 - 4	32-38	Pumice	-	-	-	-	-	-	-	-
P1 - 5	38-39	Ash	32	27	5	0	0	0.3	0.1	0.0
P1 - 6	39-90	Buried soil	78	3	39	36	47.4	2.0	23.6	21.8
P2 - 1	0-12	Modern soil	44	27	10	6	4.1	2.5	1.0	0.6
P2 - 2	12-15	Modern soil	45	26	9	10	1.2	0.7	0.2	0.3
P2 - 3	15-20	Ash	13	11	2	0	0.7	0.6	0.1	0.0
P2 - 4	20-25	Ash	13	n.a	n.a	n.a	0.8	n.a	n.a	n.a
P2 - 5	25-31	Pumice	-	-	-	-	-	-	-	-
P2 - 6	31-55	Buried soil	55	2	15	38	15.9	0.7	4.4	10.8
P3 - 1	0-15	Modern soil	38	25	11	2	4.9	3.3	1.4	0.2
P3 - 2	15-34	Ash	10	9	1	0	2.0	1.8	0.3	0.0
P3 - 3	34-41	Ash	24	n.a	n.a	n.a	1.9	n.a	n.a	n.a
P3 - 4	41-44	Pumice	-	-	-	-	-	-	-	-
P3 - 5	44-45	Ash	36	n.a	n.a	n.a	0.4	n.a	n.a	n.a
P3 - 6	45-73	Buried soil	74	3	24	48	24.9	1.0	7.9	16.0
	n	*Modern soil*	*4*	*4*	*4*	*4*	*4*	*4*	*4*	*4*
		Ash	*8*	*4*	*4*	*4*	*8*	*4*	*4*	*4*
		Buried soil	*3*	*3*	*3*	*3*	*3*	*3*	*3*	*3*
	SD	*Modern soil*	*7*	*4*	*2*	*3*	*2.0*	*1.3*	*0.5*	*0.3*
		Ash	*9*	*7*	*2*	*0*	*0.7*	*0.7*	*0.1*	*0.0*
		Buried soil	*10*	*0*	*10*	*5*	*13.3*	*0.6*	*8.3*	*4.5*

[1]Measured values from heavy liquid extraction (section 4.2.4); [2]BSi_t and GSi estimates based on the Ca/Si ratio (Fig. 4.10); [3]Based on wt.% abundance from [BSi_t + GSi] microscope assemblage (Fig. 4.10); '-' (no data) pumice layers not considered in analysis; In P2, the stocks (e.g. BSi_{rs}, GSi) from the two MS horizons (i.e. P2-1, P2-2) are added; 'n.a.' (not analyzed) due to insufficient amount of samples; the values obtained from the stratified ash layers were averaged to represent the concentration value (e.g. BSi_{rs} concentration) or added to represent the stock value (e.g. BSi_{rs} stock). 'BSi_{rs}'(rice phytoliths); BSi_g (grass phytoliths); 'BSi_t' (sum of BSi_{rs} and BSi_g); 'GSi' (silicate glass); n (number of samples analyzed); 'SD' (standard deviation).

4.4 Discussion

4.4.1 Estimated phytolith and silicon fluxes from rice biomass production to the modern soil

In order to gain insight into the potential Si accumulation, derived from phytoliths, to the MS horizon from rice production with partial exportation of biomass (mainly from rice leaves), we estimated the total PSi, $PSi_{rs,}$ and PSi_{rl} fluxes and their equivalent Si fluxes based on low and high biomass yield assumptions (Scenario A and B, respectively; section 4.2.9). We considered the PSi contents that were measured previously from rice plant parts (i.e. sheath and leaf; Fig. 4.7). The PSi and corresponding Si flux from rice biomass plant parts (i.e. leaf, sheath) to the MS horizon as estimated from Eqs. [4.6a-e] are compiled in Table 4.6.

The total PSi flux, including the PSi_{rs} and PSi_{rl} fluxes from the rice biomass to the MS, are calculated using the equations below:

$$f\text{PSi} = f\text{PSi}_{rs} + f\text{PSi}_{rl} \qquad \textbf{\textit{Eq. 4.6a}}$$

$$f\text{PSi}_{rs} = Y_{rs} \text{ x } \left(\frac{\overline{\text{PSi}_{rs}}}{100}\right) \qquad \textbf{\textit{Eq. 4.6b}}$$

$$f\text{PSi}_{rl} = Y_{rl} \text{ x } \left(\frac{\overline{\text{PSi}_{rl}}}{100}\right) \qquad \textbf{\textit{Eq. 4.6c}}$$

$$Y_{rs} = A \text{ x } \left(\frac{B_{rs}}{100}\right) \qquad \textbf{\textit{Eq. 4.6d}}$$

$$Y_{rl} = A \text{ x } \left(\frac{B_{rl}}{100}\right) \qquad \textbf{\textit{Eq. 4.6e}}$$

where fPSi, $f\text{PSi}_{rs}$, and $f\text{PSi}_{rl}$ are the total PSi, PSi_{rs} and PSi_{rl} fluxes to the MS, respectively, expressed in dry matter weights (g m^{-2} y^{-1}). Y_{rs} is the sheath biomass stock incorporated in the modern soil (g m^{-2} y^{-1}, DW) and $\overline{\text{PSi}_{rs}}$ is the mean PSi_{rs} content (i.e. 16.4 wt.%, Fig. 4.7). Y_{rl} is the leaf biomass stock incorporated in soil (g m^{-2} y^{-1}, DW) and $\overline{\text{PSi}_{rl}}$ is the mean PSi_{rl} content (i.e. 17.1 wt.%, Fig. 4.7). A is the total rice

biomass stock (g m^{-2} y^{-1}, DW); B_{rs} and B_{rl} are the estimated fractions of the sheath (~70 wt.%) and leaf (~30 wt.%) biomass from A (Castillo et al., 2012). The Y_{rl} and Y_{rs} assume low (Scenario 'A') and high (Scenario 'B') biomass yield assumptions. The yield scenarios are described in detail in method section 4.2.9.

Table 4.6. Predicted Si fluxes from annual rice leaf and sheath biomass incorporation to the modern soil of the paddy lowland rice soil profile at Bamban, Tarlac province.

	Si FLUXES	
	LOW BIOMASS YIELD (Scenario A)	**HIGH BIOMASS YIELD (Scenario B)**
	g m^{-2} y^{-1}	
*f*PSi	28	70
*f*PSi$_{rl}$	9	22
*f*PSi$_{rs}$	19	48

'PSi' (phytoliths [SiO_2] from rice leaf and sheath biomass; 95 wt.% of PSi is SiO_2); 'Si' (equivalent Si flux from PSi flux computed by dividing the PSi value by the factor, 2.1393, to convert PSi [SiO_2] to Si); '*f*PSi' (total PSi flux from rice leaf and sheath biomass to the MS); '*f*PSi$_{rl}$' (PSi flux from rice leaf biomass to the MS); '*f*PSi$_{rs}$' (PSi flux from rice sheath biomass to the MS).

The estimated 'low' and 'high' *f*PSi from rice biomass production to the MS horizon are 28 and 70 g m^{-2} y^{-1} (dry matter wt.), respectively (Table 4.6). The *f*PSi$_{rs}$ to the MS horizon is 19 and 48 g Si m^{-2} y^{-1} for the 'low' and 'high' yields, respectively. The *f*PSi$_{rl}$ for the 'low' and 'high' yield assumptions are 9 and 22 g Si m^{-2} y^{-1}, respectively.

Li et al. (2013) showed that *f*PSi$_{rs}$ (23 g Si m^{-2} yr^{-1}) and *f*PSi$_{rl}$ (9 g Si m^{-2} yr^{-1}) of local rice cultivars (e.g. Jiahua11, Ning81) grown in 50-yr cultivated rice soil (Gleysol) at Jiaxing experimental station, Zhejiang Province, southeast China is 16 % higher than our 'low' *f*PSi$_{rs}$ estimate (i.e. 19 g Si m^{-2} yr^{-1}; Table 4.6) and similar to estimated 'low' *f*PSi$_{rl}$ (i.e. 9 Si g m^{-2} yr^{-1}; Table 4.6), respectively. IRRI (2018) reported that the

yield average of rice biomass in China is 650 g m^{-2} fresh weight (FW) which is 30 % higher than our low biomass yield assumption (i.e. 518 g m^{-2}, FW). As such, assuming that other variables are held equal using Equations [4.6b-c], $fPSi_{rs}$ and $fPSi_{rl}$ obtained by Li et al. (2013) should be 30 % higher than that of our measurements.

In another paper of Li et al. (2014), they showed that the PSi_{rs} and PSi_{rl} extracted from the same cultivars and grown in the same location as in Li et al. (2013) range from 10.3 to 14.4 wt.% PSi_{rs} and 6.5 to 7.9 wt.% PSi_{rl}, respectively. The PSi_{rs} and PSi_{rl} values they obtained are lower by ~25 % and ~42 % than our measurements for PSi_{rs} (15.9-16.9 wt.%) and PSi_{rl} (16.3-18.0 wt.% (Fig. 4.7). Furthermore, the SiO_2 composition of PSi_{rl} (83.2 to 93.5 wt.%) and PSi_{rs} (80.2-87.4 wt.%) from the rice biomass reported by Li et al. (2014) are also lower by ~9 and ~12 %, respectively, than the values we obtained, 94.4-95.7 wt.% in PSi_{rl} and 96.9-97.9 wt.% in PSi_{rs}. The higher PSi_{rs} and PSi_{rl} contents of our rice plant sample (NSIC Rc160 variety) resulted in comparatively higher estimated PSi_{rs} and PSi_{rl} fluxes to the MS. The higher PSi contents of NSIC Rc160 biomass are likely promoted by a higher available DSi in soil solution released from ash silicate weathering that the plants were able to absorb. Klotzbücher et al. (2015) confirmed that the Luzon region in the Philippines has large plant-available Si (141–322 mg Si kg^{-1}) in topsoils of paddy fields due to the mineral weathering of volcanic materials. The rate of chemical weathering significantly increases with higher moisture and warmer climate (Shoji et al., 1993; Buol, 1997; Dahlgren et al., 2004). The higher precipitation (2,004 mm yr^{-1} vs. 1,200 mm) and temperature (26.9 °C vs. 16.0 °C) in our study site compared to Zhejiang, southeast China would induce a higher rate of silicate weathering increasing available Si concentration for plant uptake and subsequent phytolith precipitation in plant tissues.

Due to partial exportation of the biomass as practiced by farmers in the study site, (~30 % rice biomass, mostly leaves, are exported after panicle harvesting as cited by Castillo et al. [2012]), it reduces PSi addition to the MS, and thus potentially its accumulation. The PSi_{rl}

contains a minimum of '9' g Si m^{-2} yr^{-1} and a maximum of '22' g Si m^{-2} yr^{-1} assuming 'low' and 'high' yield assumptions, respectively (Table 4.6). Some studies have shown that plant biomass export affects soil Si pool due to the removal of PSi. Desplanques et al. (2006) showed that Si loss due to the exportation of PSi is equivalent to 27 g Si m^{-2} yr^{-1} in a 21-yr rice cultivated farm at Camargue, France. It is more than the estimated 'high' $fPSi_{rl}$ (i.e. 22 g Si m^{-2} yr^{-1}; Table 4.6) in the MS horizon. Keller et al. (2012) noted that 12 years of wheat straw removal from a long-term field trial at Boigneville, France resulted in a reduction in phytolith soil Si from 1.5 to 2.9 mg Si kg^{-1} y^{-1} in the surface soil (20 cm) when straw was removed.

4.4.2 Weathering state of the ash in the modern and buried soils

The BSi_{rs} concentration in BS is 6 times higher compared to that in the MS (i.e. 2-10 mg g^{-1} vs. 36-48 mg g^{-1}). Similarly, BS has ~23 times more BSi_{rs} stock than the MS (i.e. 10.8-21.8 kg m^{-2} vs. 0.2-0.9 kg m^{-2} (Table 4.5).

We compared the degree of soil development between the two soil horizons in order to evaluate whether silicate glass and primary mineral weathering influence their BSi_{rs} concentration and stocks. The current state of soil development in both the MS and BS were assessed by *(1)* estimating the GSi contents (i.e. extracted together with BSi from the soils' silt-sized fraction during heavy liquid extraction), and by *(2)* using weathering indices (i.e. TRB and secondary clay contents). Even though we did not measure DSi in soil solution, it is known that when silicate-containing primary minerals and glasses undergo weathering, it releases DSi in soil solution (Grotzinger & Jordan, 2014; Schaetzl & Anderson, 2005). The increased DSi in soil solution will enhance higher Si uptake and BSi_{rs} formation in plant shoots (Dove, 1995; Dove et al., 2008). The Si concentration in plants primarily depends on the concentration of DSi in the soil solution (Ding et al., 2005; Henriet, 2008; Jones & Handreck, 1967).

Difference in silicate glass concentrations of modern and buried soil horizons

The GSi is highly weatherable and becomes depleted as weathering proceeds (Dahlgren et al., 2004; Dahlgren et al., 1993; Wolff-Boenisch et al., 2004). It has a higher rate of dissolution compared to crystalline minerals (Fraysse et al., 2006). The dissolved Si [H_4SiO_4] is released from the amorphous glass upon weathering similar to crystalline silicate minerals in natural ecosystems. The DSi from glass can be leached due to its high relative mobility compared to Al and Fe, incorporated into crystalline and short-range order clay minerals, adsorbed in (hydr)oxide surfaces, (Dahlgren et al., 2004; Savant et al., 1997; Saigusa, 2000), or absorbed by the plant and precipitated as BSi in its tissues (Piperno, 1988; Cornelis et al., 2014; Gallego & Distel, 2004; Rovner, 1983; Clarke, 2003) (Fig. 2.5 in Chapter 2). Therefore, if the concentration of GSi in the soil is low, it is indicative that the availability of DSi for plant absorption is possibly high at some point before it is leached or transformed to other forms of secondary silica. This may lead to higher BSi_{rs} accumulation.

The GSi concentration in the MS is ~11 times higher than that in the BS (25-36 mg g^{-1} vs. 2-3 mg g^{-1}, respectively). Furthermore, the GSi stock in the MS is ~two times higher than that in the BS (2.5-4.2 kg m^{-2} vs. 0.7-2.0 kg m^{-2}, respectively) (Table 4.5). The lower GSi concentration and stock in the BS are due to the fact that it was developed from an older pyroclast deposit (~500 yrs B.P.) compared to the MS which developed from a very recent ash deposit in 1991 (26-yrs), and therefore has undergone longer duration of glass weathering. It is probable that the higher BSi_{rs} concentration in the BS is due to higher accumulation of Si (released from glass weathering) by the rice plants grown prior to 1991 ash deposition which is then stored as BSi_{rs} in the soil after plant restitution and decay.

TRB and mineralogy differences between the modern and buried soil horizons

The TRB of the MS and BS are compared to the TRB of the 1991 Pinatubo fresh ash deposit to assess the degree of silicate mineral weathering between the two horizons. The results showed that MS and BS have comparable TRB contents (i.e. 311-354 vs. 324-370 $cmol_c\ kg^{-1}$; Table 4.3), respectively. The MS has developed from the 26-yr old 1991 fresh ash deposit and cultivated with rice for 13 years. The BS developed from an ash deposit emplaced ~500 yrs ago by a previous eruption of Mt. Pinatubo. It was cultivated with rice for 39 years prior to 1991 eruption of the volcano. Thus, we expected lower TRB values in the older BS compared to the MS. The high TRB values in both soil horizons are due to significant quantities of primary minerals in their bulk and clay-sized fractions (Table 3.3). Mineralogy of the bulk MS and BS revealed the existence of primary minerals (i.e. feldspar, quartz, amphibole, mica, pyroxene) which are rich sources of weatherable elements (i.e. Ca, Mg, Na, K).

4.4.3 Proportion of total Si from measured rice phytoliths to the total silicon concentrations of bulk MS and BS

To assess the contribution of BSi_{rs} to the total Si concentration of the MS and BS horizons, we calculated the total Si concentration of the soil horizons and those BSi_{rs} extracted from the soils' silt-sized fraction. The total Si concentrations of the soil horizons and BSi_{rs} are computed using Equations 4.7[a-d] and illustrated in Figure 4.12.

$$TSi_{(MS)} = \frac{\overline{TSiO_{2(MS)}} \times 10}{2.1393} \qquad \textit{Eq. 4.7a}$$

$$TSi_{(BS)} = \frac{\overline{TSiO_{2(BS)}} \times 10}{2.1393} \qquad \textit{Eq. 4.7b}$$

$$TSi_{BSi_{rs(MS)}} = \frac{\overline{BSi_{rs(MS)}} \times \left[\frac{\overline{PSi_{rs(SiO2)}}}{100}\right]}{2.1393} \qquad \textit{Eq. 4.7c}$$

$$TSi_{BSi_{rs(BS)}} = \frac{\overline{BSi_{rs(BS)}} \times \left[\frac{\overline{PSi_{rs(SiO2)}}}{100}\right]}{2.1393} \qquad \textit{Eq. 4.7d}$$

Where $TSi_{(MS)}$ and $TSi_{(BS)}$ are the mean total Si contents of the MS and BS, respectively, expressed in g kg^{-1} (Eqs. 4.7a-b). $TSi_{BSi_{rs(MS)}}$ and $TSi_{BSi_{rs(BS)}}$ are the mean total Si contents of BSi_{rs} in the MS and BS, respectively, expressed in g kg^{-1} (Eqs. 4.7c-d). $\overline{TSiO_{2(MS)}}$ and $\overline{TSiO_{2(BS)}}$ are the mean total SiO_2 concentrations of the MS and BS (i.e. 65.8 wt.% [MS], 64.6 wt.% [BS]; Table A.4.2). '10' is the factor used to convert % to g kg^{-1}. $\overline{BSi_{rs(MS)}}$ and $\overline{BSi_{rsBS)}}$ are the mean concentrations of BSi_{rs} in the MS and BS (i.e. 6.4 mg g^{-1} [MS], 40.4 mg g^{-1} [BS]; Table 4.5). $\overline{PSi_{rs(SiO_2)}}$ is the mean content of SiO_2 in PSi_{rs} (95 wt.%). '2.1393' is the constant factor to convert SiO_2 to Si.

The TSi contents in the MS and BS horizons are comparable ranging from 302 to 311 and 291 to 312 g Si kg^{-1}, respectively (Fig. 4.12). About 1 % of the TSi in the MS comes from BSi_{rs}, which ranges from 1 to 4 g Si kg^{-1}. In the BS, the total Si of BSi_{rs} ranging from 17 to 22 g Si kg^{-1} accounts for 6 % of the TSi. Phytoliths are a minor constituent of most soils ranging from 0.7 to 3% (Bartoli, 1981). Our measurements showed that the total Si of MS consisting of primary minerals and glasses is 123 times higher while that of BS is 15 times higher than its BSi pool. However, this suggests that even if the BSi_{rs} is low, it is a non-negligible pool of Si in the soil.

Comparing our results with previous studies, it appears that rice grown in an ash parent material under tropical climate contains generally higher contents of BSi than the cereals (i.e. rice, wheat) grown in non-volcanic soils of temperate and subtropical environments. The BSi_{rs} concentration in the MS, 0-15 cm soil depth, (2.8 ± 1.3 g Si kg^{-1}) and BS, 24-51 cm soil thickness, (17.9 ± 2.3 g Si kg^{-1}) are generally higher compared to the 0.5 ± 15 g Si kg^{-1} measured by Desplanques (2006) from a 21-yr rice cultivated soil developed on fluvial deposits (0-25 cm soil depth) in Camargue, France. Our measurements in the MS and BS

are also higher compared to the 156-yr wheat BSi concentration (1.8 ± 1.7 g Si g^{-1}) which accumulated in a chromic luvisol (0-23 cm soil depth) in Harpenden, UK (Guntzer et al., 2012). Li et al. (2014) obtained 6.9 ± 1.1 g Si g^{-1} from the Gleysol (0-5 cm soil depth) in subtropical Southeast China grown with local rice cultivar for 50 yrs. The measurement of Li et al. (2014) is approximately twofold higher than the BSi_{rs} concentration we obtained in the MS horizon but is about threefold lower than that found in the BS horizon. The higher BSi contents in the MS and BS may be attributed to the higher amount of weatherable silicate minerals from the young developing ash soil. In addition, there is an increased rate of weathering as influenced by the relatively higher precipitation and temperature in our study site compared to those mentioned above.

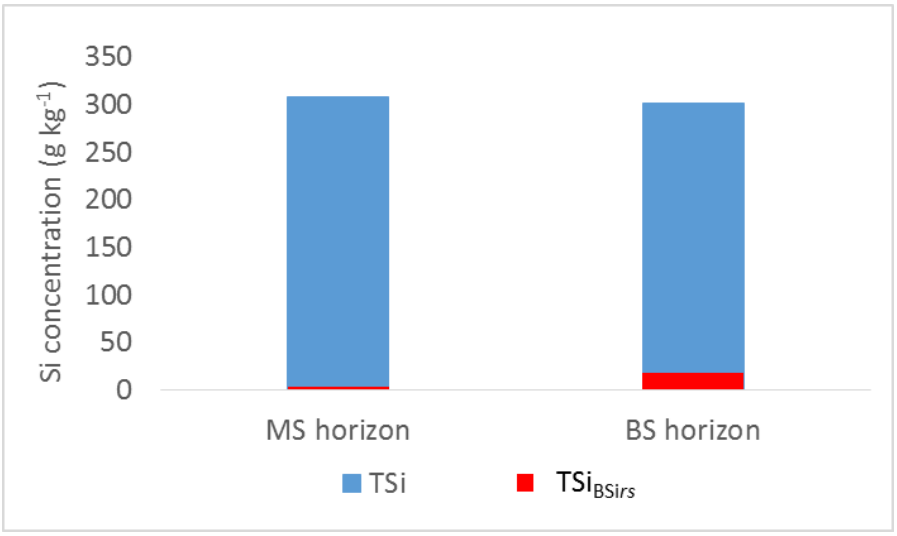

Figure 4.12. Proportion of silicon concentration of BSi_{rs} from the total Si concentration of the MS and BS silt-sized fraction at Bamban, Tarlac province. *'MS' (modern soil); 'BS' (buried soil); 'TSi' (total Si of MS and BS minus the TSi from BSirs), 'TSi$_{BSirs}$' (total Si of BSi_{rs} extracted from the soil horizons); n=4 (MS), n=3 (BS).*

It is also important to consider that the variation in the phytolith concentration of our samples compared to other studies conducted in the different climatic environment may also be affected by the type of plant species, air temperature and humidity, plant transpiration, and parent material (i.e. variation in Si content). For instance, the warm climatic condition in our study site may encourage a higher rate of plant transpiration and may, therefore, increase the rate of silica uptake.

4.4.4 Predicted and measured stocks and fluxes of extracted rice phytoliths in soil horizons

Stocks and estimated fluxes of measured BSi_{rs} in the soil horizons and ash layer

The stocks, estimated fluxes and dissolution rates of BSi_{rs} in the MS and BS are shown in Table 4.7. Knowing the BSi_{rs} stocks of MS and BS, we estimated the rate of Si accumulation (flux) from BSi_{rs} restitution to the MS and BS that received sheath biomass for 13 and 39 years, respectively. We also calculated the predicted BSi stocks and fluxes of the MS and BS using the simple mass balance equations (Eq. 4.8[a-f]) below:

$$PBSi_{rs(MS)} = \frac{\left[Y_{MS} \times \left(\frac{B_{rs}}{100}\right)\right] \times \left[\frac{\overline{PSi_{rs(SiO2)}}}{100}\right] \times (t_{MS})}{2.1393} \qquad \textbf{Eq. 4.8a}$$

$$PBSi_{rs\ (BS)} = \frac{\left[Y_{BS} \times \left(\frac{B_{rs}}{100}\right)\right] \times \left[\frac{\overline{PSi_{rs(SiO2)}}}{100}\right] \times (t_{BS})}{2.1393} \qquad \textbf{Eq. 4.8b}$$

$$fBSi_{rs(MS)} = \frac{\left[\frac{\overline{BSi_{rs}(MS)}}{t_{MS}}\right] \times \left[\frac{\overline{PSi_{rs(SiO2)}}}{100}\right] \times 1000}{2.1393} \qquad \textbf{Eq. 4.8c}$$

$$fBSi_{rs(BS)} = \frac{\left[\frac{\overline{BSi_{rs}(BS)}}{t_{BS}}\right] \times \left[\frac{\overline{PSi_{rs(SiO2)}}}{100}\right] \times 1000}{2.1393} \qquad \textbf{Eq. 4.8d}$$

$$fPBSi_{rs(MS)} = \frac{\left[\frac{PBSi_{rs}(MS)}{t_{MS}}\right] \times 1000}{2.1393} \qquad \textbf{Eq. 4.8e}$$

$$f\mathrm{PBSi}_{rs\,(\mathrm{BS})} = \frac{\left[\frac{\mathrm{PBSi}_{rs\,(\mathrm{BS})}}{t_{\mathrm{BS}}}\right] \times 1000}{2.1393} \qquad \textit{Eq. 4.8f}$$

where $\mathrm{PBSi}_{rs(\mathrm{MS})}$ and $\mathrm{PBSi}_{rs(\mathrm{BS})}$ are the predicted BSi_{rs} stocks in MS and BS accumulated during 13 and 39 years, respectively, expressed in kg Si m^{-2}, DW *(Eqs. 4.8a-b).* The $f\mathrm{BSi}_{rs(\mathrm{MS})}$ and $f\mathrm{BSi}_{rs\ (\mathrm{BS})}$ are the estimated/recalculated BSi_{rs} fluxes (g Si m^{-2} y^{-1}, DW) based on the stocks of MS and BS, respectively *(Eqs. 4.8c-d).* $f\mathrm{PBSi}_{rs(\mathrm{MS})}$ and $f\mathrm{PBSi}_{rs(\mathrm{BS})}$ are the predicted BSi_{rs} fluxes (g Si m^{-2} y^{-1}, DW) for MS and BS, respectively *(Eqs. 4.8e-f).* Y_{MS} and Y_{BS} are the estimated biomass stocks (g m^{-2} y^{-1}), incorporated into the MS and BS horizons, whereas B_{rs} is the fraction of the sheath from the estimated biomass stock (~70 %, Castillo et al, 2012). Here we assumed that only the phytolith from the sheath biomass (BSi_{rs}) is incorporated back into the soil, whereas the leaves are exported from the field based on farmers' practice. $\mathrm{PSi}_{rs(\mathrm{SiO2})}$ is the mean concentration of PSi [$SiO_2 \cdot H_2O$] in the rice sheath (16 wt.%; Fig. 4.7). Y_{MS} and Y_{BS} stocks are computed for both the 'low' (Scenario A and C, respectively) and 'high' (Scenario B and D, respectively) yield assumptions of the MS and BS, respectively (method section 4.2.9). The period during which biomass was incorporated back in the MS, t_{MS}, is 13 yrs while in the BS, t_{BS} is 39 yrs. $\overline{\mathrm{BSi}_{rs\,(\mathrm{MS})}}$ and $\overline{\mathrm{BSi}_{rs\,(\mathrm{BS})}}$ are the mean BSi_{rs} stocks in the MS and BS, respectively (Table 4.5) expressed in kg m^{-2}. The factor, 1000, is used to convert the $\overline{\mathrm{BSi}_{rs\,(\mathrm{MS})}}$, $\overline{\mathrm{BSi}_{rs\,(\mathrm{BS})}}$, $\mathrm{PBSi}_{rs(\mathrm{MS})}$ and $\mathrm{PBSi}_{rs(\mathrm{BS})}$ from kg m^{-2} to g m^{-2}.

On the average, a high BSi_{rs} stock is preserved in the silt-size fraction BS (24 to 51 cm thick) ranging from 6.8 ± 2.0 kg Si m^{-2} while that of the MS (14 to 15 cm thick) ranges from 0.3 ± 0.1 kg Si m^{-2} (Table 4.7). The large difference (~23x) is affected by two major factors. First, BS has a longer accumulation period of BSi_{rs} from rice sheath restitution than MS, 39 years in BS *vs.* 13 years in MS. Second, BS accumulated higher BSi_{rs} due to higher available Si released from glass and primary

minerals after the weathering period of ~500 years. This large pool of available Si may have stimulated higher uptake by plants resulting in higher BSi_{rs} accumulation in BS from biomass restitution even before it was buried by ash as previously discussed in section 4.4.2.

Table 4.7. Measured and predicted silicon stocks, estimated fluxes and dissolution rates of BSi_{rs} in the modern and buried soils of three soil profiles at Bamban, Tarlac province.

HORIZON	[1]MEASURED BSi_{rs}	[2]PREDICTED BSi_{rs} STOCK		[3]PREDICTED BSi_{rs} FLUX		[4]ESTIMATED BSi_{rs} FLUX	[5]TOTAL DISSOLUTION OF MEASURED BSi_{rs}	[6]ESTIMATED DISSOLUTION RATE OF BSi_{rs}
		Low yield	High yield	Low yield	High yield			
	---------- *kg m^{-2}* ----------			---------- *g m^{-2} yr^{-1}* ----------			*mg m^{-2}*	*mg m^{-2} y^{-1}*
MS	0.3 ± 0.1	0.3	0.6	18	46	23 ± 11	35 ± 15	2.7 ± 1.2
BS	6.8 ± 2.0	0.3	1.4	6	37	175 ± 51	808 ± 224	20.7 ± 5.8

All the values are expressed as Si equivalent of the BSi_{rs}. [1]Mean BSi_{rs} stock; [2]predicted BSi_{rs} stocks from 'low' (Scenario A and C in the MS and BS, respectively) and 'high' (Scenario B and D in the MS and BS, respectively) biomass yield assumptions (method section 4.2.9); [3]predicted BSi_{rs} fluxes from 'low' and 'high' biomass yield assumptions and years of accumulation; [4]recalculated flux based on the measured value and number of years of accumulation; [5]calculated by multiplying the estimated annual dissolution rate of BSi_{rs} by 13 and 39 years for MS and BS horizons (silt-sized fractions), respectively; [6]computed following Equations 4.9[a-f]; 'BSi_{rs}' (rice sheath phytoliths extracted in soil); 'MS' (modern soil, 0-15 cm soil depth); 'BS' (buried soil, ~38 to 72 cm soil depth); n = 3.

The measured BSi_{rs} stock (0.3 ± 0.1 kg Si m^{-2}) in MS is similar to its predicted stock in the 'low' yield assumption (0.3 kg Si m^{-2}) (Table 4.7). However, in the case of BS, the measured BSi_{rs} stock (7.2 ± 2.1 kg Si m^{-2}) is 24 and 5 times higher than its predicted stocks for 'low' (0.3 kg Si m^{-2}) and 'high' (1.4 kg Si m^{-2}) yield assumptions. Similarly, measured BSi_{rs} flux in MS (23 ± 11 g Si m^{-2} yr^{-1}) is close to the predicted 'low' BSi_{rs} flux (18 g Si m^{-2} yr^{-1}) while BSi_{rs} flux in BS (175

± 54 g Si m^{-2} yr^{-1}) is about ten times higher than its predicted 'high' BSi_{rs} flux (37 g Si m^{-2} yr^{-1}).

The BSi_{rs} stock and estimated flux in the MS are close to the 'low' predicted values due to the varying amount of biomass restitution every year during the 13 years of rice production. The local farmers were not able to get good yields from their rice crop and can only plant once a year during the initial re-establishment of rice production in 2005, especially during the first few years due to insufficient irrigation and fertilizer inputs (as per farm owners' interview).

In the case of BS, the large difference between the predicted and measured BSi_{rs} stocks of the BS horizon may be due to the actual number of years that the soil has been grown to rice. The duration of time that the BS horizon has been cultivated to rice may be longer than what the farmers reported to us. Tarlac province is known to be one of the largest rice producers in Central Luzon since 1929 on record (Gleeck, 1981; Santiago, 2015). Assuming that rice was grown in the BS from 1929-1991 and with the high yield assumption, the estimated BSi_{rs} flux can be lowered down to 30 %, from 175 ± 54 g Si m^{-2} yr^{-1} (39 years) to 116 ± 32 g Si m^{-2} yr^{-1} (62 years). However, it is still three times higher than the predicted BSi_{rs} flux to the BS for 'high' yield assumption (37 g Si m^{-2} yr^{-1}).

Other factors that can contribute to higher estimated BSi_{rs} flux in the BS are *(1)* higher biomass restitution than the predicted 'high' assumption which are greatly influenced by crop yield, fertilization, potential yield of rice variety used, rate of biomass export, and moisture content of the biomass, soil fertility, and/or *(2)* higher PSi_{rs} content in plant tissues that are returned to the soil as BSi_{rs}. The latter can be influenced by Si availability in the soil, type of parent material, plant transpiration, and degree of weathering (Henriet, 2008; Opfergelt et al., 2008; White et al., 2012; Cornelis et al., 2010).

The accumulation of BSi in soils is influenced by the duration of crop cultivation as shown in recent studies, i.e. higher BSi stocks are observed in soils grown with crops for a longer timescale and hence received higher biomass input. The BSi stock of 21-yr agricultural rice (1975 to 2003) in fluvisol/reductisol (25-cm thick) at Camargue, France accumulated 0.80 kg Si m^{-2} (Desplanques et al., 2006). It is approximately three times higher than the stock in MS horizon (0.3 kg Si m^{-2}; Table 4.7) but nine times lower than that of the BS horizon (7.2 kg Si m^{-2}; Table 4.7). The BSi stocks measured in 156-yr wheat cultivated chromic Luvisol (23 cm thick) at Harpenden, UK is 7.3 kg Si m^{-2} (Guntzer et al., 2012); it is ~24 times higher compared to the MS (0.3 kg Si m^{-2}; Table 4.7) but is comparable with the BS (7.2 kg Si m^{-2}; Table 4.7). Since MS has received rice biomass for only 13 years, it has accumulated lower BSi while that of BS horizon grown for 39 years (according to farmer's interview) has accumulated higher BSi contents that are comparable with that of 156-yr wheat cropping duration. The BS horizon as mentioned earlier may have been grown to rice for far longer time (~62 years) than the 39 years reported to us by the local farmers.

Different plant types and cultivar have different abilities to take up Si (e.g. Tuna et al. 2008) which can also explain the differences in BSi_{rs} contents we measured from the other land-uses. For instance, Indica rice varieties showed genotypic differences in the Si accumulation rate (Swain et al., 2016). It was reported that the active Si absorption by rice roots are mediated by a gene transporter (LSi1) which makes it more efficient in accumulating Si among other species such cucumber and tomato where Si absorption is mediated only by diffusion (Ma et al., 2006; Sangster and Hodson, 1986).

The MS and BS horizons accumulate BSi_{rs} at the estimated rates of 23 ± 11 g Si m^{-2} yr^{-1} and 175 ± 51 g Si m^{-2} yr^{-1}, respectively (Table 4.7). The estimated BSi from a trachytic ash soil (15-cm thick) grown with bamboos at the Reunion Island (Indian Ocean) between 3820 ± 85 and 335 ± 90 yr B.P is 55 ± 10 g Si m^{-2} yr^{-1} (Meunier, 1999), which is

approximately two times higher than MS but three times lower than what we obtained in the BS horizon. The reported estimate/measurement of Si cycling from BSi in the 25-cm thick 21-yr rice soil grown in fluvisol/reductisol at Camargue, France is 58 g Si m^{-2} yr^{-1} (Desplanques et al., 2006). In the alluvial paddy soils of Shounai Plain, Japan, the contribution of BSi is 107 g Si m^{-2} yr^{-1} (Makabe et al., 2009) are three to four times higher compared to our measurements in MS but are two to three times lower than that of the BS. Li et al. (2013) reported a BSi accumulation flux of 19 g Si m^2 yr^{-1} in rice Gleysol of Jiaxing, China collected from the surface soil (0—10 cm) after 50 years of cultivation which comparable to what we obtained in the MS but is nine times lower than that of the BS.

In general, BSi_{rs} in the BS have comparatively higher stocks and fluxes even after being buried with ash and have not received additional BSi_{rs} for 13 years since the 1991 ash deposition. As mentioned earlier, the impact of humid tropical climate characterized by high precipitation and high temperature plus the nature of ash parent material consisting of easily weatherable silicates could have facilitated the higher uptake of DSi and flux of BSi_{rs} to the BS horizon during the pre-eruption years. The stock of BSi_{rs} in the BS horizon may not have been significantly leached as well after this horizon has been buried with ashfall. There is no evidence of leaching of BSi_{rs} from the MS horizon to the ash layer as we did not observe the presence of BSi_{rs} in the BS horizon (Table 4.5).

Estimated dissolution rates of measured BSi_{rs} in the soil horizons

To determine the influence of dissolution on the current measured BSi_{rs} stocks of MS and BS horizons, we calculated the total dissolution and rates based on the established dissolution rate of bamboo BSi derived from the experiment of Fraysse, et al. (2006). Dissolution rates (g m^{-2} y^{-1}) of the BSi in the MS and BS horizons are estimated using Equations [4.9a-f] and results are presented in Table 4.7:

$$r\mathrm{BSi}_{rs(\mathrm{MS})} = \frac{\frac{d\mathrm{BSi}_{rs(\mathrm{MS})}}{t_{\mathrm{MS}}} \times \left[\mathrm{SA}_{\mathrm{BSi}_{rs(\mathrm{MS})}}\right]}{2.1393} \qquad \textbf{Eq. 4.9a}$$

$$r\mathrm{BSi}_{rs(\mathrm{BS})} = \frac{\frac{d\mathrm{BSi}_{rs(\mathrm{BS})}}{t_{\mathrm{BS}}} \times \left[\mathrm{SA}_{\mathrm{BSi}_{rs(\mathrm{BS})}}\right]}{2.1393} \qquad \textbf{Eq. 4.9b}$$

$$d\mathrm{BSi}_{rs(\mathrm{MS})} = \left[\frac{\left(\frac{\overline{\mathrm{BSi}_{rs(\mathrm{MS})}} \times \frac{\overline{\mathrm{PSi}_{rs(\mathrm{SiO_2})}}}{100}}{899}\right)}{\left(\mathrm{SA}_{\mathrm{BSi}_{rs(\mathrm{MS})}}\right)}\right] \times (r\mathrm{B} \times 899) \times 1000 \qquad \textbf{Eq. 4.9c}$$

$$d\mathrm{BSi}_{rs(\mathrm{BS})} = \left[\frac{\left(\frac{\overline{\mathrm{BSi}_{rs(\mathrm{BS})}} \times \frac{\overline{\mathrm{PSi}_{rs(\mathrm{SiO_2})}}}{100}}{899}\right)}{\left(\mathrm{SA}_{\mathrm{BSi}_{rs(\mathrm{BS})}}\right)}\right] \times (r\mathrm{B} \times 899) \times 1000 \qquad \textbf{Eq. 4.9d}$$

$$\mathrm{SA}_{\mathrm{BSi}_{rs(\mathrm{MS})}} = \left[\mathrm{SA}_{\mathrm{b}} \times \overline{\mathrm{BSi}_{rs(\mathrm{MS})}}\right] \qquad \textbf{Eq. 4.9e}$$

$$\mathrm{SA}_{\mathrm{BSi}_{rs(\mathrm{BS})}} = \left[\mathrm{SA}_{\mathrm{b}} \times \overline{\mathrm{BSi}_{rs(\mathrm{BS})}}\right] \qquad \textbf{Eq. 4.9f}$$

Where $r\mathrm{BSi}_{rs(\mathrm{MS})}$ and $r\mathrm{BSi}_{rs(\mathrm{BS})}$ are the mean estimated dissolution rates of $\overline{\mathrm{BSi}_{rs(\mathrm{MS})}}$ and $\overline{\mathrm{BSi}_{rs(\mathrm{BS})}}$ stocks in the MS and BS horizons, respectively, expressed in mg BSi_{rs} m^{-2} soil y^{-1} (Eqs. 4.9[a-b]). $d\mathrm{BSi}_{rs(\mathrm{MS})}$ and $d\mathrm{BSi}_{rs(\mathrm{BS})}$ are the total dissolution of BSi_{rs} per unit surface area of BSi_{rs} during 13 and 39 years in the MS and BS horizons, respectively, expressed as mg BSi_{rs} m^{-2} BSi_{rs} (Eqs. 4.9c-d). $\mathrm{SA}_{\mathrm{BSi}_{rs(\mathrm{MS})}}$ and $\mathrm{SA}_{\mathrm{BSi}_{rs(\mathrm{BS})}}$ are the total specific surface areas of mean $\overline{\mathrm{BSi}_{rs(\mathrm{MS})}}$ and $\overline{\mathrm{BSi}_{rs(\mathrm{BS})}}$ stocks in the MS and BS horizons per unit surface area, respectively, expressed as m^2 BSi_{rs} m^{-2} BSi_{rs} assuming that rice BSi has a similar specific surface area as bamboo BSi (Eqs. 4.9[a-b]). SA_b is the specific surface area of bamboo BSi per unit weight (159 m^2 BSi g^{-1} BSi; Fraysse et. al., 2006). rB is the dissolution rate of bamboo BSi at a pH 5.5 (1.12×10^{-4} mol BSi m^{-2} BSi y^{-1}; Fraysse et al., 2006) that was assumed to be similar to that of rice BSi. The constant '899' is the conversion factor of g $\mathrm{SiO_2}$ to mole $\mathrm{SiO_2}$ (1 mol $\mathrm{SiO_2}$ = 899 g $\mathrm{SiO_2}$).

$PSi_{rs(SiO_2)}$ is the mean concentration of PSi [$SiO_2 \cdot H_2O$] in the rice sheath (16 wt.%, Fig. 4.7). The factor '1000' is used to convert g to mg.

To date, there are very few studies that determined the dissolution rates of BSi and no reports to our knowledge were documented on BSi from rice. Bamboo, a monocotyledon belonging to the grass family *Poaceae*, is also a high Si-accumulator like rice (Ma & Takahashi, 2002). The dissolution rate of bamboo BSi (1.12×10^{-4} mol BSi m^{-2} BSi yr^{-1}) are comparable to that of other plants including horsetail (1.65×10^{-4} mol BSi m^{-2} BSi yr^{-1}), larch (9.58×10^{-5} mol BSi m^{-2} BSi yr^{-1}) and fern (1.21×10^{-4} mol BSi m^{-2} BSi yr^{-1}) from the dissolution experiments of Fraysse et al. (2006; 2009; 2010). They also exhibit comparable specific surface areas per unit weight, i.e. bamboo (159 m^2 BSi g^{-1} BSi), horsetail (228 m^2 BSi g^{-1} BSi), larch (179 m^2 BSi g^{-1} BSi), fern (210 m^2 BSi g^{-1} BSi). Bamboo bulliform BSi exhibit the same shape and size as that of rice bulliform BSi (Zuo et al., 2016), hence the dissolution rate of BSi_{rs} is assumed to be comparable with that of bamboo BSi.

The total Si loss from BSi_{rs} dissolution in the MS (35 ± 15 mg Si m^{-2}) and BS (808 ± 224 mg Si m^{-2}) after 26 and ~500 years, respectively, are very low (Table 4.7). The mean rate of BSi_{rs} dissolution per year in the MS and BS are 2.7 ± 1.2 mg Si m^{-2} y^{-1} and 20.7 ± 1.8 mg Si m^{-2} y^{-1}, respectively. Therefore, dissolution cannot explain the large difference between the measured and predicted BSi_{rs} in both MS and BS.

Based on the estimated dissolution rates of BSi_{rs} (Table 4.7), the stock of BSi_{rs} in the BS will be depleted in 365,666 years while that of MS is 121,899 years. The calculated half-lives of BSi (i.e. larch and horsetail) for a typical pH of soil solutions (4–5) range between 0.5 and 3 years (Fraysse et al., 2009). Fraysse et al. (2009) also calculated the maximal half-life time of BSi in soils based their measurement of the geometric size of BSi (50 μm; larch and horsetail) and molar volume measured by Lasaga (1984). The maximal half-life varies from 25,000 years for pH=7 to 250,000 years for pH=4 (Fraysse et al., 2009). In our soil profile, the calculated half-lives of the BSi in the MS (pH=4.82-5.12)

and BS (pH=4.82-5.87) horizons based on its dissolution rate are 60,950 and 182,833 years, respectively, which are within the calculated half-life of BSi by Fraysse et al. (2009) using the geometric size and molar volume of BSi.

Several studies reported the long shelf-life of BSi in soils. Meunier et al. (2014) reported long residence times of BSi ranging from 340 to 900 yrs in grasslands growing on Santa Cruz chronosequence in California and dominated by strong seasonal variabilities of the Mediterranean climate; only a small proportion of BSi is annually released to pore water and can be cycled back to plants. Under specific physicochemical conditions, BSi can remain in soils for thousands (Wilding, 1967; Parr & Sullivan, 2005) or even millions of years (Strömberg et al., 2007; Rovner, 1983; Twiss, 1987; Piperno, 1988; Carter, 1999). The BSi remains in volcanic soils and peatland sediments are reported to age 0 to 8000 years BP (Parr & Sullivan, 2005).

The weatherability of BSi similar to silicate minerals depends on environmental factors such as temperature and pH as well as the physicochemical characteristics of the minerals (White and Brantley 1995; Heaney et al. 1994). For instance, the dissolution of BSi is minimal at pH=3 and increases with increasing pH (Fraysse et al. 2006). The BSi solubility also varies depending on the Si/Al ratio, the surface area of the BSi, and the water content of the soil (Bartoli, 1985; Bartoli and Wilding, 1980), BSi morphology and association with organic matter (Watteau and Villemin, 2001). Phytoliths may also be associated with sesquioxides and organic matter within aggregates which increases their chemical resistance and slows their weathering rates (Piperno, 2006). Despite the long residence time and low concentration in soils of BSi, it is one of the most important soluble sources of Si due to their higher dissolution rate which is one order of magnitude faster than that of primary silicates and clays (Fraysse et al., 2006, 2009, 2010; Keller et al., 2012).

4.5 Conclusion

The contribution of BSi, to the Si pool of a young volcanic ash soil, is non-negligible. Specifically, the BSi_{rs} contributes 1 wt.% and 6 wt.% Si to the total Si contents of the MS and BS horizons of a young volcanic soil, respectively. The addition of ash and subsequent cultivation of rice promoted the formation of BSi_{rs} due to the active plant uptake of DSi that has been released from the weathering of silicate mineral and glass constituents of the ash. The estimated BSi_{rs} accumulation in the 26-yr developing MS was 23 ± 11 g Si m^{-2} y^{-1} during 13 years of rice cultivation as shown in Figure 4.13.

The predicted total Si flux (PSi) of rice phytoliths from whole plant biomass to the MS is 28 and 70 g Si m^{-2} y^{-1} for the 'low' and 'high' yield assumptions, respectively. Since 30 % of the total biomass (mainly leaves) are exported after harvesting (Castillo et al., 2012), only 19 g Si m^{-2} y^{-1} ('low') and 48 g Si m^{-2} y^{-1} ('high') Si flux from PSi_{rs} are potentially returned to the soil, whereas the 9 g Si m^{-2} y^{-1} ('low') and 22 g Si m^{-2} y^{-1} ('high') from PSi_{rl} are lost from the system.

The BSi_{rs} (Si) stocks in the MS and BS are 0.3 ± 0.1 and 6.8 ± 2. 0 kg Si m^{-2}, respectively. The estimated total dissolution rate of BSi_{rs} is very low amounting to 35 ± 15 mg Si m^{-2} in the MS horizon and 808 ± 15 mg Si m^{-2} in the BS horizon after 13 and ~500 years, respectively. With the dissolution rate of 20.7 ± 5.8 mg Si m^{-2} y^{-1} in the BS, it will take 365,666 years before all the BSi_{rs} are depleted in this horizon. The MS, however, will continue to receive BSi_{rs} from biomass restitution.

Ash deposition, ~38 cm thick, disrupted the BSi pool by burying a considerable stock BSi_{rs} in the BS horizon that is difficult to access for shallow-rooted crops like rice. Furthermore, the surface ash deposit has prevented the continuous deposition of BSi_{rs} from rice biomass recycling on this horizon. Since BSi_{rs} is not readily leached, a considerable stock was preserved. Mixing of the MS with the BS

horizon during plowing will aid in the transfer of the BSi_{rs} stored in the BS horizon on the surface soil. In turn, this rich source of BSi_{rs} can provide a slow-release source of Si for the rice plants.

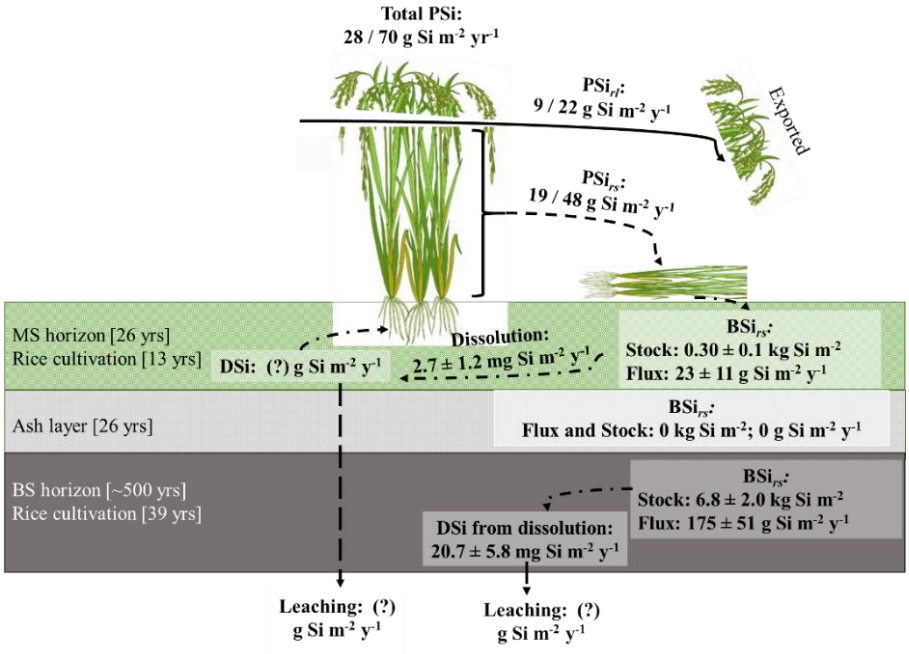

Figure 4.13. Phytolith (Si) stocks and estimated fluxes in a soil-paddy rice plant system affected by the 1991 Pinatubo ash deposit at Bamban, Tarlac province. *Total PSi is the predicted phytolith (Si) flux to the MS horizon from the total biomass-based on 'low' and 'high' yield assumptions (Table 4.6). The phytoliths from rice leaves, PSi_{rl} (~30 % of rice biomass), are exported, hence, it is lost in the soil-plant system. The phytoliths from rice sheaths, PSi_{rs} (~70 % of rice biomass), are incorporated back to the MS horizon as BSi_{rs}. The estimated BSi_{rs} flux in MS and BS horizon is based on 'low' and 'high' biomass yield assumptions (Table 4.7). The estimated dissolution rate of the measured BSi_{rs} fluxes in MS and BS is based on the dissolution rate of bamboos (after Fraysse et al., 2006; Table 4.7). Leaching losses of DSi and BSi_{rs} are not measured in this study.*

4.6 References

Ball, T., Chandler-Ezell, K., Dickau, R., Duncan, N., Hart, T. C., Iriarte, J., Lentfer, C., Logan, A., Lu, H., Madella, M., Pearsall, D.M., Piperno, D. R., Rosen, A. M., Vrydaghs, L., Weisskopf, A., & Zhang, J. (2015). Phytoliths as a tool for investigations of agricultural origins and dispersals around the world. *Journal of Archaeological Science*, 1–14.

Bartoli, F., 1981. Le cycle biogéochimique du silicium sur roches acides. Application à deux systèmes forestiers tempérés. Thèse de Doctorat, Université de Nancy I, 187 p.

Bartoli, F., Wilding, L.P., 1980. Dissolution of biogenic opal as a function of its physical and chemical properties. Soil Sci. Soc. Amer. J. 44, 873–878.

Bartoli, F., Wilding, L. P. (1980). Dissolution of biogenic opal as a function of its physical and chemical properties. *Soil Sci. Soc. Amer. J. 44*, 873–878.

Bascomb, C. L. (1968). Distribution of pyrophosphate-extractable iron and organic carbon in soils of various groups. *Journal of Soil Science*, *19*, 251-268.

Blakemore, L. C., Searle, P. L. & Daly, B. K. (1987). Methods for chemical analysis of soils. *Bur. Sci. Rep. 80,* N. Z. Soil Bur. Lower Hutt, New Zealand. 43 p.

Buol, S. W., Hole, F. D., McCracken, R. J. & Southard, R. J. (1997). Soil genesis and classification, Fourth Edition. Iowa State University Press.

Carnelli, A. L, Madella, M., & Theurillat, J.P. (2001). Biogenic silica production in selected alpine plant species and plant communities. *Annals of Botany 87*:425-434.

Castillo, M. B., Mamaril, C. P., Paterno, E. S., Sanchez, P. B., Badayos, R. B., & Sta Cruz, P. C. (2012). Soil Chemical and Physical Properties with Rice Straw Management During Fallow Period. *Philippine Journal of Crop Science (PJCS)*, *37*(1), 15–26.

Chapman, H. D. (1965). Cation exchange capacity. In *Black CA (ed) Methods of soil analysis: Part 1, Physical and mineralogical methods.* American Society of Agronomy and Soil Science Society of America, Madison, pp 891–901.

Conley, D. J. (2002). Terrestrial ecosystems and the global biogeochemical silica cycle. *Global Biogeochem Cy 16*:1121–1128.

Cornelis, J. T., Dumon, M., Tolossa, A. R., Delvaux, B., Deckers, J., & Van

Ranst, E. (2014). The effect of pedological conditions on the sources and sinks of silicon in the vertic planosols in southwestern Ethiopia. *Catena*, *112*, 131–138.

Chao, T. T., & R. F. Sanzolone. (1992). Decomposition techniques. *Journal of Geochemical Exploration, 44,* 65-106.

Clarke, J. (2003). The occurrence and significance of biogenic opal in the regolith, *In Earth-Science Reviews, Volume 60,* Issues 3–4, 2003, Pages 175-194.

Cornelis, J. T., Ranger, J., Iserentant, A., & Delvaux, B. (2010). Tree species impact the terrestrial cycle of silicon through various uptakes. *Biogeochemistry*, *97*, 231–245.

Dahlgren, R. A., Saigusa, M., & Ugolini, F. C. (2004). The Nature, Properties, and Management of Volcanic Soils. *Advances in Agronomy, 82*, 113–182. https://doi.org/10.1016/S0065-2113(03)82003-5.

Delvaux, B., Herbillon, A. J., & Vielvoye, L. (1989). Characterization of a weathering sequence of soils derived from volcanic ash in Cameroon. Taxonomic, mineralogical and agronomic implications. *Geoderma, 45*, 375–388. https://doi.org/10.1016/0016-7061(89)90017-7.

Deshmukh, R. K., Ma, J. F., & Bélanger, R. R. (2017). Role of Silicon in Plants. *Frontiers in Plant Science.* https://doi.org/10.3389/978-2-88945-352-8

Desplanques, V., Cary, L., Mouret, J.-C., Trolard, F., Bourrié, G. & Grauby, O. (2006). Silicon transfers in a rice field in Camargue (France). *Journal of Geochemical Exploration*, 88, 190–193.

Dobermann, A., & Fairhurst, T. H. (2000) Rice: nutrient disorders and nutrient management. International Rice Research Institute, Los Banos.

Dove, P. M. (1995). Kinetic and thermodynamic controls on silica reactivity in weathering environments. *Rev. Mineral Geochem. 31*, 235–290.

Dove, P. M, Han, N., Wallace A. F., De Yoreo, J. J. (2008). Kinetics of amorphous silica dissolution and the paradox of the silica polymorphs. *Proceedings of the National Academy of Sciences 105*:9903-9908.

FAO. (1998). Report of the fifth external programme and management review of International Rice Research Institute (IRRI). Food and Agriculture Organization of the United Nations.

Fraysse, F., Pokrovsky, O. S., & Meunier, J. D. (2010). Experimental study of terrestrial plant litter interaction with aqueous solutions. *Geochimica et Cosmochimica Acta*, *74*(1), 70–84. https://doi.org/10.1016/j.gca.2009.09.002.

Fraysse, F., Pokrovsky, O. S., Schott, J., & Meunier, J. D. (2009). Surface chemistry and reactivity of plant phytoliths in aqueous solutions. *Chem. Geol. 258*, 197–206.

Fraysse, F., Pokrovsky, O. S., Schott J., & Meunier, J. D. (2006). Surface properties, solubility, and dissolution kinetics of bamboo phytoliths. *Geochim. Cosmochim. Acta 70*, 1939–1951.

Gallego, L., & Distel, R. A. (2004). Phytolith assemblages in grasses native to central Argentina. *Annals of Botany*, *94*, 865–874. https://doi.org/10.1093/aob/mch214.

Gérard F., Mayer, K. U., Hodson, M. J., & Ranger, J. (2008). Modeling the biogeochemical cycle of silicon in soils: Application to a temperate forest ecosystem. *Geochimica Et Cosmochimica Acta 72*:741-758.

Gleeck, L. E. (1981). Nueva ecija in american times: homesteaders, hacenderos & politicos. Manila: Historical Conservation Society.

Grotzinger, J. P., & Jordan, T. H. (2014). Understanding earth. Seventh Edition. Printed in the United States of America.

Guntzer, F., Keller, C., Poulton, P. R., Mcgrath, S. P., & Meunier, J. (2012). Long-term removal of wheat straw decreases soil amorphous silica at Broadbalk, Rothamsted. Plant Soil (2012), 352, 173–184. https://doi.org/10.1007/s11104-011-0987-4.

Hart, D. M. (1992). A field appraisal of the role of plant opal in the Australian environment. Ph.D. thesis, Department of Earth Sciences, Macquarie University, Australia (unpublished).

Heaney, P. J., Prewitt, C. T., Gibbs, G. V. (Eds). (1994). Silica: physical behavior, geochemistry, and materials applications. *Reviews in mineralogy 29*, Mineralogical Society of America.

Henriet, C. (2008). Silicon in banana (Musa spp.): a soil-plant system approach. PhD thesis. UCL. UCL - AGRO - Sciences agronomiques et ingénierie biologique.

Herbillon, A. J. (1989). Chemical estimation of weatherable minerals present in the diagnostic horizons of low activity clay soils. 8th. Int. Soil Classif. Workshop 1986 (Brazil), pp. 39-48.

Hodgson, J. M. (1976). Soil survey field handbook: describing and sampling soil profiles. Soil Survey of England, Harpenden.

Jones, L. H. P., & Handreck, K. A. (1967) Silica in soils, plants, and animals. Adv Agron 19:107–149.

Jones, R. L. & Beavers, A. H. (1964). Aspects of catenary and depth distribution of opal phytoliths in Illinois soils. *Soil Sci. Soc. Am. Proc. 28*: 413–416.

Keller, C., Guntzer, F., Barboni, D., & Meunier, J. (2012). Comptes Rendus Geoscience Impact of agriculture on the Si biogeochemical cycle : Input from phytolith studies ´ ochimique du silicium : apport des e les phytolithes, *344*, 739–746.

Kelly, E. F. (1990) Methods for extracting opal phytoliths from soil and plant material. In *Workshop on biotic indicators of global change*, Seattle, Washington.

Klotzbücher, T., Marxen, A., Vetterlein, D., Schneiker, J., Türke, M., van Sinh, N., Manh, N., van Chien, H., Marquez, L., Villareal, S., Bustamante, J.V., Jahn, R. (2015). Plant-available silicon in paddy soils as a key factor for sustainable rice production in Southeast Asia. *Basic and Applied Ecology, 16*, 665–673.

Kottek, M., Grieser, J., Beck, C., Rudolf, B., & Rubel, F. (2006). World Map of the Köppen-Geiger climate classification updated. *Meteorol. Z., 15,* 259-263. DOI: 10.1127/0941-2948/2006/0130.

Lanning, F. C. (1963). Silicon in rice. *Plant Constituents, 11(5)*, 435–437. https://doi.org/10.1021/jf60129a024.

Lasaga, A. (1984). Chemical kinetics of water-rock interactions. *J. Geophys. Res. 89*, 4009–4025.

Li, Z., Song, Z., & Cornelis, J. (2014). Impact of rice cultivar and organ on elemental composition of phytoliths and the release of bio-available silicon. *Frontiers in Plant Science, 5*(October), 1–8. https://doi.org/10.3389/fpls.2014.00529.

Li, Z., Song, Z., & Jiang, P. (2013). The production and accumulation of phytoliths in rice ecosystems: a case study to Jiaxing Paddy Field. *Acta Ecologica Sinica.* Vol. 33. No. 22.

Luo, W., Yang, Y., Yao, L., Chen, Z., Li, J., Yin, C., Zhang, J., Lin, L. & Gan, H. (2016). Phytolith records of rice agriculture during the Middle Neolithic in the middle reaches of Huai River region, China. *Quaternary International, Volume 426,* 2016, pp. 133-140.

Ma, J. F. & Takahashi, E. (1990). Effect of silicon on the growth and phosphorus uptake of rice. *Plant and Soil, 126*, 115–119.

Ma, J. F., Miyake, Y., & Takahashi, E. (2001). Silicon as a beneficial element for crop plants. In Datnoff, L. E., Snyder, G. H., & Korndörfer, G. H. (Eds.), *Silicon in agriculture*. pp. 17–39. Amsterdam: Elsevier.

Ma, J. F., Tamai, K., Yamaji, N., Mitani, N., Konishi, S., & Katsuhara, M. (2006). A silicon transporter in rice. *Nature, 440*, 688–691.

Makabe, S., Kakuda, K., Sasaki, Y., Ando, T., Fujii, H., & Ando, H. (2009). Relationship between mineral composition or soil texture and available silicon in alluvial paddy soils on the Shounai Plain, Japan. *Soil Sci. Plant Nutr. 55*, 300–308

Madella, M., & Zurro, D. (2009). Phytoliths – Recognition. Archaeobotany-Wiki. In *Phytoliths – Introduction. Archaeobotany-Wiki*. http://archaeobotany.dept.shef.ac.uk/wiki/index.php/ Phytoliths_-_Introduction.

Madella, M., Alexandre A., & Ball, T. (2005). International code for phytolith nomenclature 1.0. *Annals of Botany 96*, 253-260.

Madella, M., Powers-Jones, A. H., & Jones, M. K. (1998). A simple method of extraction of opal phytoliths from sediments using a non-toxic heavy liquid. *Journal of Archaeological Science, 25*(8):801-803.

Mehra, O. P., & Jackson, M. L. (1960). Iron oxides removal from soils and clays by dithionite-citrate system buffered with sodium bicarbonate. In *Proceeding of 7th National Conference Clay Minerals*, Washington, pp 317-327.

Meunier, J. D., Colin, F., & Alarcon, C. (1999). Biogenic silica storage in soils. *Geology 27*, 835–838.

Meunier, J. D., Keller, C., Guntzer, F., Riotte, J., Braun, J. J., & Anupama, K. (2014). Assessment of the 1% Na2CO3 technique to quantify the phytolith pool. *Geoderma, 216*, 30–35. https://doi.org/10.1016/j.geoderma.2013.10.014.

Munsterman, D., & Kerstholt, S. (1996). Sodium polytungstate, a new non-toxic alternative to bromoform in heavy liquid separation. *Review of Paleobotany and Palynology 91*:417-422.

Newhall, C. G., & Punongbayan, R. S. (1996). Fire and mud. Eruptions and Lahar of Mount Pinatubo, Philippines. Philippine Institute of Volcanology and Seismology, Quezon City. University of Washington Press, Seattle, and London. Printed in Hongkong.

Oehler, J. H. (1979). Deposition and diagenesis of biogenic silica. In *Biogeochemical cycling of mineral-forming elements (Trudinger, P.A., and Swaine, D.J., eds.)*, Elsevier, Amsterdam, pp. 467-483.

Opfergelt, S., Delvaux B., AndrÉ, L., & Cardinal, D. (2008). Plant silicon isotopic signature might reflect soil weathering degree. *Biogeochemistry 91*, 163–175.

Oyama, M. (1991). Revised standard soil color charts. Published by Utrecht Van Boekhoven-Bosch. United States Department of Agriculture, Soil Conservation Service (1971). Compiled and edited by Rebecca Burt. Soil survey field and laboratory methods manual. 2014. *Soil survey investigations Report No. 51*. Version 2.

Parr, J. F., and Sullivan, L. A. (2005). Soil carbon sequestration in phytoliths. *Soil Biol. Biochem. 37*, 117–124. doi: 10.1016/j.soilbio.2004.06.013.

Page, J. R., Miller, R. H., Keeney, D. H., Baker, D. E., & Roscoe, J. R. (Eds.) (1982). Methods of soil analysis: Part 2, chemical and microbiological properties, 2nd edn, Madison, WI.

Pansu, M., & Gautheyrou, J. (2006). Handbook of Soil Analysis: Mineralogical, Organic and Inorganic Methods. Springer, 993 p.

PhilRice. (2019). FAQs on Philippine Seedboard (PSB)/ NSIC Rice Varieties. Accessed online, Accessed online, February 22, 2019, 10:58 A.M. http://www.pinoyrice.com/rice-varieties/.

PhilRice. (2018). Rice yield summary results. Accessed online, November 18, 2018, 11:00 A.M. https://dbmp.philrice.gov.ph/palaystat/profile/.

Piperno, D. R. (1988). Phytolith Analysis: an Archaeological and Geological Perspective. Academic Press, San Diego, p. 280.

Piperno, D.R. (2006). Phytoliths: A Comprehensive Guide for Archaeologists and Paleoecologists. Oxford: Altamira Press.

Puppe, D., Höhn, A., Kaczorek, D., Wanner, M., Wehrhan, M., & Sommer, M. (2017). How big is the influence of biogenic silicon pools on short-term changes in water-soluble silicon in soils? Implications from a study of a 10-year-old soil-plant system. *Biogeosciences*, *14*, 5239–5252. https://doi.org/10.5194/bg-14-5239-2017

Rouiller, J., Burtin, G., & Souchier, B. (1972). La dispersion des sols dans l'analyse granulométrique. Méthode utilisant les résines échangeuses d'ions. *ENSAIA Nancy 14*: 194-205. Scaillet & Evans, 1997.

Saigusa, M. (2000). Growth of rice and its silicon nutrition. *Kagaku To Seibutsu. 38.* 514-519.

Santiago, F. A. (2015). A Historical Evaluation of The Emergence of Nueva Ecija as the Rice Granary of the Philippines. In *DLSU Research Congress* (Vol. 3, pp. 1–9).

Sauer, D., Saccone, L., Conley, D. J., Herrmann, L., & Sommer, M. (2006). Review of methodologies for extracting plant-available and amorphous Si from soils and aquatic sediments. *Biogeochemistry*, *80*(1), 89–108. https://doi.org/10.1007/s10533-005-5879-3.

Savant, N. K., Snyder, G. H., & Datnoff, L. E. (1997). Silicon management and sustainable rice production. *Adv. Agron. 58,* 151-199.

Scaillet, B., & Evans, B. W. (1999). The 15 June 1991 Eruption of Mount Pinatubo. Phase equilibria and Pre-eruption P–T–fO_2–fH_2O Conditions of the Dacite Magma. Journal of Petrology 40:3, pp. 381-411.

Sobecki, T. M. (1990). Field procedure for base saturation and cation-exchange capacity (CEC) by ammonium acetate, pH 7, Version 1.0. USDA–SCS, National Soil Survey Center, Lincoln, NE.

Soil Survey Staff. (2014). Soil Survey Field and Laboratory Methods Manual. *Soil Survey Investigations Report No. 51*, Version 2.0. R. Burt and Soil Survey Staff (Ed.). U.S. Department of Agriculture, Natural Resources Conservation Service.

Song, Z. L., Wang, H. L., Strong, P. J., Li, Z. M., & Jiang, P. K. (2012). Plant impact on the coupled terrestrial biogeochemical cycles of silicon and carbon: implications for biogeochemical carbon sequestration. *Earth-Sci. Rev. 155*, 319–331. doi: 10.1016/j.earscirev.2012.09.006.

Takahashi, T., & Sato, A. (2000). Silicon fertility of paddy fields in Hachirogata reclaimed land, Akita Prefecture. J. *Soil Sci. Plant Nutr. 71*, 881-883.

Tavakkoli, E., Lyons, G., English, P., & Guppy, C. N. (2011). Silicon nutrition of rice is affected by soil pH, weathering and silicon fertilization. Journal of Plant Nutrition and Soil Science, 174, 437–446.

Twiss, P. C., Suess, E., & Smith, R. M. (1969). Morphological Classification of Grass Phytoliths. *Soil Science Society of America Journal*, *33*(1), 109–115.

Twiss, P. C. (1987). Grass-opal phytoliths as climatic indicators of the Great Plains Pleistocene. In *Johnson WC, ed. Quaternary environments of Kansas. Lawrence: Kansas Geological Survey*, 179–188

Wada, K. (1989). Allophane and imogolite. In Dixon, J. B., & Weed, S.B. (Eds.), *Minerals in soil environments, 2nd edn*. Soil Sci. Soc. Am., Madison, WI. pp, 1051-1087.

Watteau, F., & Villemin (2001). Ultrastructural study of the biogeochemical cycle of silicon in the soil and litter of a temperate forest. *Eur. J. Soil Sci., 52*, 385–396.

White, A. F., Vivit, D. V., Schulz, M. S., Bullen, T. D., Evett, R. R., & Aagarwal, J. (2012). Biogenic and pedogenic controls on Si distributions and cycling in grasslands of the Santa Cruz soil

chronosequence, California. *Geochimica et Cosmochimica Acta, 94,*72–94.

White, A. F., Brantley, S. L. (Eds). (1995). Chemical weathering rates of silicate minerals. *Reviews in Mineralogy 31*, Mineralogical Society of America.

Wilding, L. P. (1967). Radiocarbon dating of biogenetic opal. *Science 156*, 66–67. doi: 10.1126/science.156.3771.66.

Wilding, L. P., & Drees, L. R. (1971). Biogenic opal in Ohio soils. *Soil Sci. Soc. Am. Proc. 35*, 1004–1010.

Wolff-Boenisch, D., Gislason, S. R., Oelkers, E. H., & Putnis, C. V. (2004). The dissolution rates of natural glasses as a function of their composition at pH 4 and 10.6, and temperatures from 25 to 74 °C. Geochimica et Cosmochimica Acta 68: 4843-4858.

Yoshida, S., Onishi, Y., & Kitagishi, K. (1959). The chemical nature of silicon in rice plants. *Soil Sci Plant Nutr 5:*127–133

Yoshida, S. (1981). Fundamentals of rice crop science. Los Baños, Laguna: International Rice Research Institute.

Yuan, G., Lavkulich, L. M., & Wang, C. (1993). A method for estimating organic-bound iron and aluminum contents in soils. *Commun. Soil Sci. Plant Anal. 24*(11&12):1333–1343.

Zhao, Z., & Pearsall, D. M. (1998). Experiments for improving phytolith extraction from soils. *Journal of Archaeological Science 25*:587-598.

Zuo, X., Lu, H., Li, Z., Song, B., Xu, D., Zou, Y., Wang, C., Huan, X., & He, K. (2016). Phytolith and diatom evidence for rice exploitation and environmental changes during the early mid-Holocene in the Yangtze Delta. *Quaternary Research, 86*, 304–315.

Chapter 5 Phosphorus status in soils forming in the pyroclast deposits from the 1991 Plinian eruption of Mt. Pinatubo, Philippines

5.1 Introduction

Phosphorus (P), next to nitrogen (N), is one of the most limiting essential nutrients in soils as it occurs in small quantities (Smith et al. 2015; Blaskó, 2011). It is involved in photosynthesis and other key physiological and biochemical processes in plants (Pansu & Gautheyrou, 2006; Blaskó, 2011). Plants takes up P from the soil solution primarily in the monovalent form, i.e. HPO_4^{2-}; the other ionic species $H_2PO_4^-$ and PO_4^{3-} usually occur in minor amounts at typical soil pH values between 5 and 6 (Roy et al., 2006).

The primary source of P in soils is P mineral weathering and organic matter mineralization (Blaskó, 2011; Uchida, 2000). Phosphate bioavailability decreases with increasing soil development due to the immobilization of P into organic matter, precipitation in secondary minerals (i.e. Ca-, Fe-, and Al-phosphates), and adsorption to secondary nanocrystalline allophanes and Al and Fe (hydr) oxides (Figure 2.6; Pierzynski et al., 2000, Smith et al., 2015). The adsorption through ligand exchange to allophanes, Fe- and Al-(hydr)oxides are favored in acidic conditions as these constituents develop a positive electrical charge. The adsorption is specific, making hydrogen phosphates nearly immobile and thereby reducing its availability to plants. With time, adsorbed phosphates may be occluded within the structure of Fe- and Al-(hydr)oxides, becoming completely inaccessible (Nanzyo et al., 1993; Parfitt, 1980).

Tropical soils usually contain low P reserves due to a higher degree of mineral weathering, faster P mineralization from organic matter, and greater P fixation to secondary Al/Fe-(hydr)oxides (Dabin, 1980). Most of the bioavailable P comes from organic matter recycling. Hence, crop

production in these regions requires supplemental fertilization to alleviate P deficiency and increase yields (National Research Council, 1993). Volcanic soils are also often limited in P due to the presence of poorly crystalline short-range-order minerals (SRO), such as allophanes, imogolite, ferrihydrite, and of Al/Fe-organic complexes. These compounds have high anion exchange capacities and often develop a positive surface charge, thereby enhancing strong P adsorption (Dahlgren et al., 2004; Shoji & Takahashi, 2002). Therefore, soil P fertility and plant use efficiency of P fertilizers in mature volcanic soils are usually very low (Shoji & Takahashi, 2002).

Most volcanic soils develop on extrusive fragmented magmatic rocks (pyroclasts) but they can also develop from lava flows (Dahlgren et al., 2004; Shoji et al., 1993). The P content of extrusive magmatic rocks (acidic to basic) varies roughly in the range of 0.1 to 1 vol.% (Deer et al. 1992). Phosphorus is typically encountered in primary magmatic minerals in the form of apatite [$Ca_5(PO_4)_3(F,Cl,OH]$ (Nanzyo & Yamasaki, 1998; Nanzyo et al., 1997). The solubility of apatite in aqueous solutions increases when the pH decreases (Nanzyo et al., 1999; Nakamaru et al., 2000). In volcanic soils, apatite weathering is the main source of plant-available P (Dahlgren et al., 2004; Nanzyo & Yamasaki, 1998) and has been shown to contribute to the rapid revegetation of volcanic ash soils when N is present (Shoji & Takahashi, 2002; Nanzyo, 2002).

A fresh deposit of tephra (< 2-64 mm-sized fragmented pyroclasts) on an existing volcanic soil can act as a new source of P and temporarily alleviate P limitation in the soil (Nanzyo et al., 1997; Engelstad et al., 1974). In 1991, the eruption of Mt. Pinatubo blanketed a surface area of 2000 km^2 with approximately 5 km^3 (DRE) of dacitic tephra (Melosantos et al.. 1996; Newhall & Punongbayan, 1996). The cumulative volume of lahar deposited from 1991 to 1993 is ~1.9 km^3, covering an area of ~770 km^2 (Punongbayan et al., 1993; Leone & Gaillard, 1999). Most of the soils that received pyroclast deposits (i.e. tephra and lahar) were agricultural soils grown to rice, sugarcane, corn,

vegetables, and root crops (Herrera, 1992; Rantucci, 1994). Prior to the eruption, the farmers used to apply fertilizers containing N, P, and potassium (K) to improve yield (Nelson, 2013; Mendoza & Cabangbang, 1992).

This study aims (1) to determine the total P and plant-available P contents in soils developed from the 26-yr Mt. Pinatubo pyroclast (i.e. ash, pumice, lahar) deposits; (2) to compare these values with those found in the former soils buried by the volcanic deposit from the 1991 eruption; and (3) to evaluate the influence of pedogenesis and varying land uses on total P content, plant-available P, and phosphate retention.

5.2 Materials and Methods

5.2.1 Site characterization and soil sampling

This research utilized the same set of samples as those described in Chapter 3. The five sampling sites (2 soil profile pits per site) are located in the provinces of Pampanga (Porac, Floridablanca), Tarlac (Bamban), and Zambales (San Marcelino) at Central Luzon, Philippines (Fig. 3.1). The procedure of sampling and the characterization of the individual soil profiles are described in Chapter 3 section 3.2.1. The selected sampling sites consisted of three non-cultivated soils affected by ashfall, [1] forest (Fo-Ash; i.e. P1-a, P-b), [2] grassland in high-altitude (Gr-HA-Ash; i.e. P4-a, P4-b), [3] grassland in low altitude (Gr-LA-Ash; i.e. P3-a, P3-b), and two cultivated soils grown to irrigated rice, one affected with ashfall [4] (IR-Ash; i.e. P2-a, P2-b) and another with lahar [5] (IR-Lahar, i.e. P5-a, P5-b). The soil profile photos and description are illustrated in Figure 3.2. A detailed morphological description of each soil profile is presented in Table A3.1.

5.2.2 Soil physical and chemical analysis

Sample preparation is described in Chapter 3 method section 3.2.2. All the chemical analyses on P were conducted on the fine-earth fraction < 2 mm (bulk) of the soil horizons (MS and BS) and pyroclast layers (i.e. ash, pumice, lahar) of each soil profile. The chemical analyses were done in duplicates for some samples randomly selected for every analysis.

Total P analysis

Total P (Pt_{total}) is the sum of all forms of P in the soil, i.e. organic, inorganic, occluded and plant-available P (Pansu and Gautheyrou, 2006). The P_{total} in the soil and pyroclasts was carried out through loss on ignition at 1000 °C followed by borate fusion and dissolution of fusion beads in 10 % nitric acid (HNO_3) (Chao & Sanzolone, 1992). The extract was subsequently measured using Inductively Coupled Plasma-Atomic Emission Spectrophotometer (ICP-AES) and expressed in mg kg^{-1}.

Plant-available P (Modified Bray P2 Method)

The plant-available P (P_{avail}) extraction method proposed by Bray and Kurtz (1945) was based on solubilization of P compound in acid followed by the action of fluoride anion to reduce the activity of the Al^{3+}, Fe^{3+}, and Ca^{2+} cations by forming complexes with the latter. It measures P_{avail} in adsorbed and acid-soluble phosphate forms. It provides an estimate of the relative bioavailability of inorganic ortho-phosphate (PO_4-P) in soils in acid to neutral pH (Dewis & Freitas, 1970). It cannot be used in calcareous soils due to the random neutralization of the reagent, dissolution of calcium carbonate and precipitation of calcium fluoride (Pansu & Gautheyrou, 2006).

Five grams of soil or pyroclast sample were treated with 35 ml Bray solution (0.03 M NH_4F + 0.1 M HCl; pH 1.5), agitated for 5 minutes

and then filtered. The hydrochloric acid (HCl) and ammonium fluoride (NH_4F) removes easily acid-soluble forms of P, largely Ca phosphates. The NH_4F dissolves Al and Fe phosphate precipitates by forcing complexation with the metal ions under acidic conditions. The P_{avail} in the extract is determined using ICP-AES and expressed in mg kg^{-1}. We also analyzed the P_{avail} of the 1991 Mt. Pinatubo ash deposit which was collected few months after the eruption (September 1991) at the western side of Mt. Pinatubo by Prof. Alain Bernard of Université Libre de Bruxelles, Belgium.

Since our samples originated from recently deposited volcanic materials, the P extracted from the soil using the Bray P2 method would represent the P_{avail} released from calcium apatite. The contribution of P from dacite glass dissolution, if there is any, may not be significant. The mean P content of dacite glass is 1100 mg kg^{-1} (n=3) but the dissolution rate is very slow, i.e. 1 x 10^{-9} mol m^{-2} s^{-1} at pH 4 (25°C) (Wolff-Boenisch et al., 2004) compared to that of natural apatite which immediately dissolves at pH 4 (25 °C), i.e. 1 x $10^{-0.003}$ mol m^{-2} s^{-1} (Harouiya et al., 2007).

The modified Bray P2 method was used in this study because it can extract a considerable proportion of the P bound to active Al in addition to the P bound to Ca compared to the Truog method where only a small proportion of the P bound to active Al is extracted (Nanzyo et al., 1997). The Truog method (Truog, 1930) for P_{avail} extraction has become a popular P extraction method in Japan as it effectively dissolves the P_{avail} from Ca phosphates, followed by Bray II, Mehlich No. 3, Olsen, and anion exchange resin methods (Uchida, 2000). However, the P extracted by the Bray and Kurtz method has been shown to be well-correlated with crop yield response on most acid and neutral soils in the United States (i.e. Midwest and North Central) and New Zealand regions (Pierzynski, 2000; Sherrell, 1970).

Phosphate retention (P-retention)

The P retention (P_{ret}) method proposed by Blakemore et al. (1981) uses the equilibration of a soil sample with a solution containing soluble P, and measurement of phosphate remaining in solution. It refers to the percent P retained by the soil after equilibration with 100 mg kg^{-1} P solution containing soluble P for 24 hours (Eq. 5.1). The lower the pH, the higher the concentration of polyvalent cations (i.e. Al, Fe) and the greater the rate of P retention (Pansu & Gautheyrou, 2006).

A 2-gram bulk sample was mixed with 10 ml P-retention solution for 24 h. The P-retention solution was prepared by mixing 4.40 g potassium dihydrogen phosphate (KH_2PO_4), 16.4 g anhydrous sodium acetate (CH_3COONa), and 11.5 ml glacial acetic acid in 1 L distilled water. The mixture was centrifuged at 2000 rpm for 15 minutes. An aliquot of the supernatant was analyzed using the ICP-AES.

P_{ret} = Initial P concentration – P remaining in sample solution ***Eq. 5.1***

Where 'P_{ret}' is the P retained in the sample after equilibration with the 'initial P concentration' of 100 mg kg^{-1} P solution expressed in percentage; 'P remaining in the sample solution' is the measured P in the extract after 24 hours of shaking.

5.3 Results

5.3.1 Phosphorus contents of the modern soil and pyroclast deposit

The mean contents of P_{total}, P_{avail}, P_{avail} to P_{total} ratio (P_{avail}/P_{total}), and P_{ret} of the soil horizons and pyroclast layers of the soil profiles varying in land use are shown in Figure 5.1 to 5.2 and Table A5.1.

Fo-Ash (P1-a, P1-b). In the two soil profiles, the MS horizon, ash, and pumice layers contain comparable quantities of P_{total}, ranging from 574 to 853 mg kg^{-1}. The P_{avail} content in the MS horizon of P1-a and P1-b soil profiles differ by ~one order of magnitude (92 and 212 mg kg^{-1}, respectively) (Fig. 5.1). The ash and pumice layers contain 104 to 199 mg kg^{-1} P_{avail}. The P_{avail}/P_{total} ratio of the MS horizon, ash, and pumice layers range from 0.16 to 0.26 for the two soil profiles. The MS horizon has a P_{ret} value of 4.23 and 8.62 % in the P1-a and P1-b soil profiles, respectively. The ash and pumice layers from both soil profiles did not retain any P (Fig. 5.2).

IR-Ash (P2-a, P2-b). The P_{total} content in the MS horizon of the P2-a and P2-b is (528 and 547 mg kg^{-1}), respectively. The P_{total} content measured for the remobilized ash, ash and pumice layers varies between 454 and 796 mg kg^{-1}. The P_{avail} content of the MS horizon (78 and 87 mg kg^{-1} in P2-a and P2-b, respectively) is two to three times lower compared to that measured for the remobilized ash and ash layers (202-258 mg kg^{-1}). The pumice layer has 55 and 88 mg kg^{-1} P_{avail} in the P2-a and P2-b soil profiles, respectively. The P_{avail}/P_{total} of the MS horizon and pumice layer for both soil profiles range from 0.12 to 0.18, i.e. significantly lower than the ratio values inferred for the remobilized ash and ash layers (P_{avail}/P_{total} = 0.28-0.43). The MS horizon retained 11.79 and 15.79 % P in the P2-a and P2-b soil profiles, respectively which is two times higher than the P_{ret} in the remobilized ash layer (7.26 % in P2-a and 5.56 % in P2-b). The ash and pumice layers have P_{ret} values ranging from 0.73 to 4.89 %.

Gr-LA-Ash (P3-a, P3-b). The P_{total} contents in the MS horizon and pyroclast layers of the two soil profiles, P3-a and P3-b, are comparable and range from 500 to 717 mg kg^{-1}. The P_{avail} contents of the MS horizon and pumice layer in the two soil profiles also fall in the same range of values (55-72 mg kg^{-1}). In contrast, P_{avail} in the ash layer is threefold higher, i.e. 163 and 180 mg kg^{-1} in P3-a and P3-b soil profiles, respectively. Accordingly, the P_{avail}/P_{total} ratio in the MS horizon and pumice layers (0.09-0.12) is lower than in the ash layer (0.23-0.27). The MS horizons and pumice layers do not retain P, whereas P_{ret} in the ash layer amounts to ~4.3 and 1.9 % in the P3-a and P3-b soil profiles, respectively.

Gr-HA-Ash (P4-a, P4-b). The P_{total} content of the MS horizon and pyroclast layers range from 490 to 751 mg kg^{-1}. The P_{avail} content of the MS horizon in the P4-a and P4-b soil profiles (131 and 166 mg kg^{-1}, respectively) is significantly higher than that of the pumice layer (71 mg kg^{-1} in P4-a and 55 mg kg^{-1} in P4-b), but lower compared to that of the ash layer (232 in P4-a and 228 in P4-b mg kg^{-1}). The P_{avail}/P_{total} ratio in the P4-a and P4-b soil profiles is higher in the MS horizon (0.21 and 0.22, respectively) and ash layer (0.31 and 0.32, respectively) in comparison to the pumice layer (0.14 and 0.11, respectively). The MS horizon of P4-a soil profile does not retain P, but the P4-b soil profile retains a small quantity of P, i.e. 4.5 %. Phosphorus retention is not observed in the pumice and ash layers.

IR-Lahar (P5-a, P5-b). The P_{total} content in the MS horizon of P5-a and P5-b soil profiles varies by ~twofold (233 and. 470 mg kg^{-1}, respectively). Compared to the lahar layers (494 mg kg^{-1}, P5-b, and 631 mg kg^{-1}, P5-b), the MS horizon has a lower P_{total}. Similarly, the P_{avail} content between the MS horizon in P5-a (22 mg kg^{-1}) and P5-b (90 mg kg^{-1}) soil profiles varies by as much as three times. The lahar 1 layer has ~two times lower P_{avail} content, i.e. 62 and 68 mg kg^{-1} in P5-a and P5-b soil profiles, respectively, compared to the lahar 2 layer, i.e. 115 and 116 mg kg^{-1}, respectively. Consequently, the P_{avail}/P_{total} ratio of the lahar 1 layer (i.e. 0.12 and 0.11 in P5-a and P-b profiles, respectively)

is ~two times lower than that of lahar 2 layer (i.e. 0.21 for both soil profiles), whereas the MS horizon has a more variable P_{avail}/P_{total} ratio (i.e. 0.09 and 0.19 in P5-a and P-b profiles, respectively). Phosphorus retention in the MS horizon of P5-a and P5-b soil profiles is 7.2 and 10.2 %, respectively. The lahar 1 and lahar 2 layers have lower P_{ret} values ranging from 0 to 2.5 % for the two soil profiles.

5.3.2 Phosphorus contents of the buried soils

Fo-Ash (P1-a, P1-b). The P_{total} content of the BS horizon is 330 in the P1-a and 376 mg kg^{-1} in the P1-b soil profile. The P_{avail} content is 4 and 5 mg kg^{-1}, respectively. The P_{avail}/P_{total} ratio is very low (~0.01) for this horizon. The P_{ret} values for P1-a and P1-b soil profiles are 26.1 and 21.6 %, respectively.

IR-Ash (P2-a, P2-b). The BS horizon in the IR-Ash soil contains 241-250 mg kg^{-1} P_{total}. The P_{avail} content in is 26 mg kg^{-1} in P2-a and 22 mg kg^{-1} in P2-b. The P_{avail}/P_{total} ratio in the P2-a and P2-b soil profile is 0.11 and 0.09, respectively, and the P_{ret} is 12.2 and 3.3 %, respectively.

Gr-LA-Ash (P3-a, P3-b). The BS horizon of the P3-a and P3-b soil profiles has a P_{total} content of 414 and 444 mg kg^{-1}, respectively, and P_{avail} content of 37 and 18 mg kg^{-1}, respectively. The P_{avail}/P_{total} is 0.08 in the P3-a and 0.04 in the P3-b soil profile. The P_{ret} values are low, i.e. 3.5 % (P3-a) and 2.2 % (P3-b).

Gr-HA-Ash (P4-a, P4-b). The P_{total} content in the P4-a and P4-b soil profiles is 620 and 742 mg kg^{-1}, respectively. The BS horizon has only 1 mg kg^{-1} P_{avail} content in the P4-a and 2 mg kg^{-1} in the P4-b soil profile. The P_{avail}/P_{total} is also very low, only ~0.01 in both soil profiles. The P_{ret} in the P4-a and P4-b soil profiles is 10.1 and 13.6 %, respectively.

IR-Lahar (P5-a, P5-b). The BS horizon has 683 and 741 mg kg^{-1} P_{total} in the P5-a and P5-b soil profiles, respectively. Comparable P_{avail}

contents are measured in the P5-a and P5-b (139 and 132 mg kg^{-1}), respectively. The P_{avail}/P_{total} is 0.20 (P5-a) and 0.18 (P5-b). The P_{ret} in the P5-a and P5-b soil profiles are 16.2 and 11.0 %, respectively.

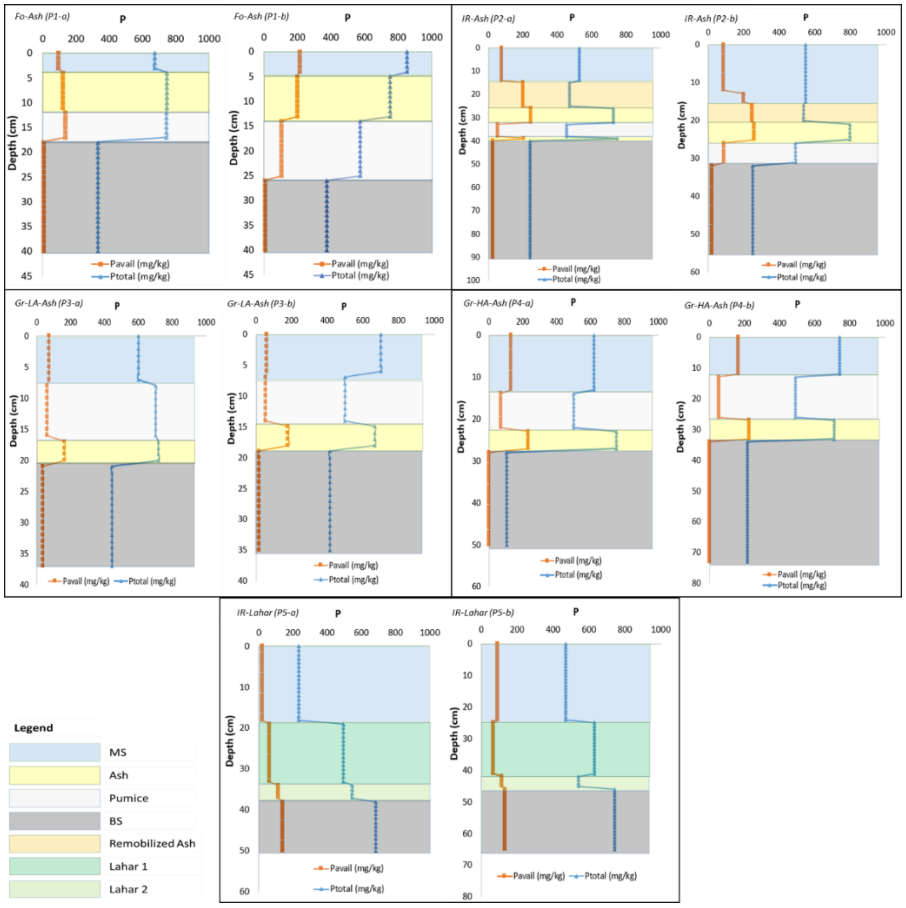

Figure 5.1. Variations with depth of the total P (P_{total}) and plant-available P (P_{avail}) contents in the Fo-Ash (P1-a, P1-b; Tarlac province), IR-Ash (P2-a, P2-b; Tarlac province), Gr-LA-Ash (P3-a, P3-b; Pampanga province), Gr-HA-Ash (P4-a, P4-b; Pampanga province) and IR-Lahar (P5-a, P5-b; Zambales province) soil profiles. *Total P (P_{total}), Plant-available P (P_{avail}).*

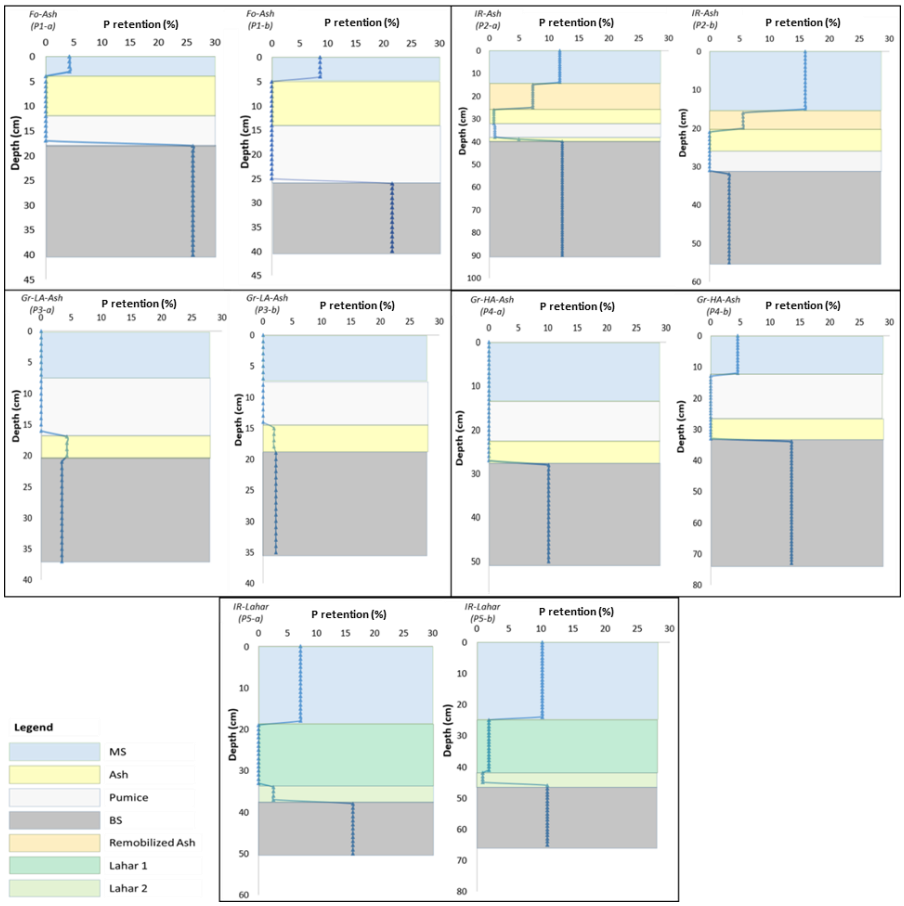

Figure 5.2. Variations with depth of the P retention (P_{ret}) in the Fo-Ash (P1-a, P1-b; Tarlac province), IR-Ash (P2-a, P2-b; Tarlac province), Gr-LA-Ash (P3-a, P3-b; Pampanga province), Gr-HA-Ash (P4-a, P4-b; Pampanga province) and IR-Lahar (P5-a, P5-b; Zambales province) soil profiles.

5.4 Discussion

For each land-use type, the P_{total} and P_{avail} contents and P_{ret} values vary between the two soil horizons that were sampled. For example, the MS of the two IR-Lahar soils differs markedly in terms of their P_{total} and P_{avail} contents (Fig. 5.1; Table A5.1). We attributed this to heterogeneities in the composition of the pyroclast parent material, weathering degree, horizon thickness, the volume of crop cover and biomass restitution, etc. Reyes & Neue (1991) reported that the physical and chemical characteristics of the 1991 lahar materials from Mt. Pinatubo vary due to mixing and sedimentation processes involving various proportions of fresh pyroclasts, lithics and former sediments (including soils). Nevertheless, in most cases, differences between the soil profile types emerge despite the intra-site heterogeneities.

5.4.1 Total phosphorus content

Phosphorous in soils occurs in both inorganic and organic forms. The proportions of inorganic and organic P vary depending on soil type and weathering degree but in general, inorganic P amounts to 35-70 % of P_{total}, with the rest corresponding to organic P (Sharpley, 1995; Mishra et al., 2017; Crews et al., 1995). Due to the large accumulation of organic matter in most volcanic soils, organically bound P constitutes often an important pool. The lowest and highest P_{total} contents measured in the MS correspond to the IR-lahar (233-470 mg kg^{-1}) and Fo-Ash (673-853 mg kg^{-1}) soils, respectively (Fig. 5.1; Table A5.1). The P_{total} content in the young soils developed on the ash from the 1883 eruption of Krakatoa volcano in Indonesia varies between 413 and 710 mg kg^{-1} (Schlesinger et al., 1998). Gudmundsson et al. (2014) report a higher total P (1671-1902 mg kg^{-1}) in the first 20 cm of non-cultivated Silandic Andisols in Iceland. The total P content of ash-derived Andisols from Chile varies between 993 and 3469 mg kg^{-1} (Escudey et al., 2001). Shoji et al. (1993) indicate that the total P content in 25 Andisol pedons from various districts of Japan ranges from ~1000 to 3900 mg kg^{-1}.

The most important factors influencing the status of P in Andisols are chemical weathering, biocycling, and fertilization (Shoji et al. 1993; Dahlgren et al. 2004). Unweathered tephra contains a significant amount of P and this tends to increase with the tephra Si content (Nanzyo et al., 1997; Nanzyo & Yamasaki, 1998; Nanzyo et al., 2003). Phosphorous in tephra reflects largely the presence of apatite of magmatic origin (Nanzyo et al., 1997; Schlesinger et al., 1998; Nanzyo & Yamasaki, 1998; Nanzyo et al., 2003). The general chemical formula of apatite is $Ca_5(PO_4)_3X$ ($X = F^-, Cl^-, OH^-$). Although it has a moderate solubility, chemical weathering of apatite in tephra is an important source of P for plants and microbes (Nanzyo et al., 2010; Nanzyo & Kanno, 2018). Several studies highlight the occurrence of apatite as a minor mineral phase in the 1991 Mt. Pinatubo tephra deposit (Bernard et al., 1996; Nanzyo et al., 1997; Nakamaru et al., 2000; Castillo & Punongbayan, 1996). The P_{total} content reported for the 1991 Pinatubo fresh tephra 'tephra$_{(1991)}$' varies to some extent, i.e. 916 mg kg^{-1} (ash; Castillo & Punongbayan, 1996), 829 mg kg^{-1} (pumice; Castillo & Punongbayan, 1996), 742 mg kg^{-1} (ash; Bernard et al., 1996), and 715 mg kg^{-1} (tephra; Nanzyo et al., 1997). With these values, it is apparent that the P_{total} is generally lower by 2 to 67 % (Table A5.1) in the MS than in the tephra$_{(1991)}$ except for Fo-Ash/a (853 mg kg^{-1}) and Gr-HA-Ash/a (742 mg kg^{-1}) soils where the values are a little above when compared to that of Nanzyo et al. (1997).

Except in some soils (IR-Lahar/a,b, Gr-LA-Ash/a, Fo-Ash/a), the P_{total} content of the MS horizon is similar or higher than that of its parent material (C horizon; i.e. ash, pumice or lahar deposit immediately underlying the MS horizon) (Fig. 5.3; Table A5.1). The net gain or loss of P in a non-cultivated soil during pedogenesis will depend on the relative importance of various processes, such as weathering, mineralization, immobilization, and adsorption, as summarized by the following equation:

leachable P + available P = mineralization + weathering – immobilization – adsorption ***Eq. 5.2***

where *leachable P* is the P in organic, inorganic (i.e. primary and secondary minerals), and occluded forms (i.e. Fe/Al-(hydr)oxides); *available P* is the solution P that is available for plant uptake; *mineralization* is the P released from organic matter mediated by microorganisms; *weathering* is the P released from the dissolution of primary and secondary minerals; *immobilization* is the intake of P by microorganisms; *adsorption* is the fixation of P in the surfaces of Al/Fe (hydr)oxides and secondary minerals.

In the absence of other processes, the dissolution of apatite (and possibly P occurring in the tephra's glassy component) during chemical weathering of the tephra should reduce P_{total} in the soil (Nanzyo et al, 2010). Since weathering is normally more pronounced in the surface horizons, one would have expected lower P_{total} values in the MS samples than in the C horizon. This suggests that the latter is also subjected to weathering or that the MS receives additional inputs of P, for example in the form of fertilizers, or both. Partial dissolution of apatite occurring in a lahar deposit from Mt. Pinatubo was highlighted in a previous study (Nakamaru et al., 2000). Further, the ratio of P_{total} in the C horizon to that of $tephra_{(1991)}$ is systematically less than one except for Fo-Ash soil (Fig. 5.3). This supports the idea that chemical weathering has removed some of the P from the soil's parent material. Although weathering also affects the MS, the uptake of P by plants and its incorporation into organic forms reduce the net removal of P from modern soils. The latter process could be responsible for the maintenance of the P_{total} levels in the MS horizon of Fo-Ash soil. However, significant immobilization of P in the C horizon at depth does not occur as the input of fresh organic matter is probably limited.

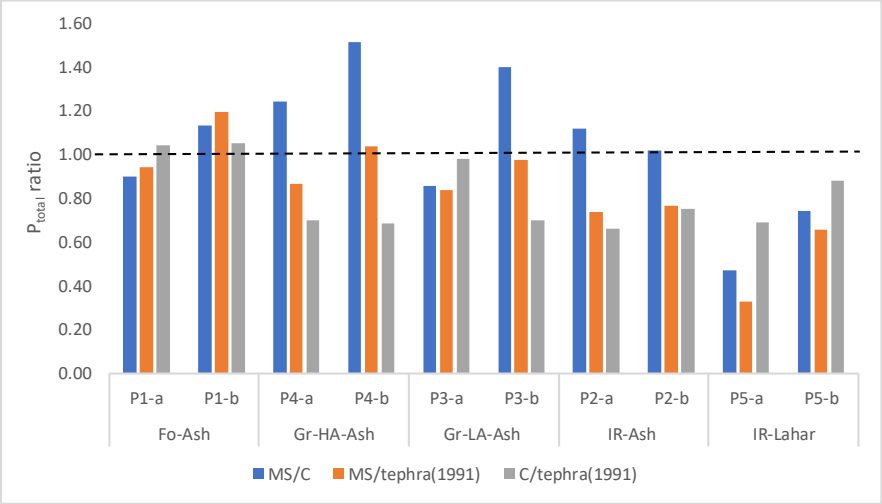

Figure 5.3. Total P content ratio of the modern soils to its tephra parent material; the C horizon [MS/C]; modern soil to the fresh tephra [MS/tephra$_{(1991)}$]; and C horizon to the fresh 1991 tephra [C/tephra$_{(1991)}$] of Fo-Ash (P1-a, P1-b; Tarlac province), IR-Ash (P2-a, P2-b; Tarlac province), Gr-LA-Ash (P3-a, P3-b; Pampanga province), Gr-HA-Ash (P4-a, P4-b; Pampanga province) and IR-Lahar (P5-a, P5-b; Zambales province) soil profiles. *'tephra$_{(1991)}$' P_{total} value adapted from Nanzyo et al. (1997).*

The lowest P_{total} contents in the MS are measured for the IR-Ash (528-547 mg kg^{-1}) and IR-Lahar (233-470 mg kg^{-1}) profiles, which both support rice cultivation. According to our survey (see chapter 6, i.e. R1 and L3 sites, respectively), rice has been cultivated on these soils for 13 years (2005-2017) and 12 years (2006-2017), respectively. The removal, after harvesting, of threshed rice straws and grains containing appreciable amounts of P has the effect of eliminating P from the soil and thus, of decreasing its P_{total} content. While the application of inorganic P fertilizer (~26 kg ha^{-1} cropping season^{-1}) to the IR-Ash soil limits the decline in total P, the IR-Lahar soil does not receive any P additions (except in 2006). This probably explains its low P_{total} content. We also note that flooding and drainage of paddy soils during the

growing season increases P losses compared to other soils (Sharpley, 1995; Duxbury & Perverly, 1978).

In all but the IR-Lahar soil, the P_{total} content of the BS is systematically lower (1.4 to 6.0 times) than that of the MS. It is also lower than the values measured in the pyroclast materials that overlay it (Fig. 5.1; Table A5.1). The BS derives from pyroclasts deposited by the previous Plinian eruption of Mt. Pinatubo, about ~500 years ago (Newhall & Punongbayan, 1996). This material could not be sampled but according to Pallister et al. (1996), it is also dacitic in composition and its mineral assemblage resembles that of the 1991 eruption products. Thus, one can reasonably assume that the P_{total} content was more or less in the same range as that of the 1991 eruption products. This implies that the comparatively depleted P_{total} values in the BS samples reflect the gradual loss of P due to apatite dissolution during chemical weathering. Although the BS always exhibits a significantly stronger capacity to retain P than the MS (Fig. 5.2; Table A5.1 except in IR-Ash/b profile), P adsorption on secondary mineral constituents (and possibly alumino-organic complexes) was probably not very efficient over the course of ~500 years of soil development. In addition, organic matter accumulation is limited in the BS, preventing the build-up of a significant organic P pool. As a result, the BS experienced a net loss of P and a reduction in P_{total}.

The BS with the highest P_{total} content corresponds to the IR-Lahar (P_{total} = 683-741 mg kg^{-1}). In contrast to the other BS samples, total P in this soil is on par with the values found in the MS (P_{total} = 528-853 mg kg^{-1}), suggesting weak weathering and/or retention of P in organic compounds and adsorbed forms. The organic carbon content of the IR-Lahar's BS is low (0.89-1.18 wt.%; Table A3.3) and compares with the other buried soils. Therefore, the accumulation of organic P is probably not responsible for the elevated P_{total} value. The Si_o content of the BS (0.10-0.11 wt.%; Table A3.4) from the IR-Lahar profile is ~2 to 5 times higher than in the other BS. Moreover, the Al_o content associated with SRO compounds is 2 to 3-fold higher than the other BS (0.26-0.30

wt.%; Table A3.4) except for Fo-Ash soil. These suggest the presence of reactive surfaces onto which P could be sorbed. The low pH values measured for the IR-Lahar's BS would favor weathering reactions. Nevertheless, the Si_o and Al_o contents are typical of weakly weathered and poorly developed soils (Shoji et al., 1993). Unfortunately, we cannot explain fully the high P_{total} content of the BS soil from the IR-Lahar profile.

5.4.2 Available phosphorus content

In soils developed on volcanic pyroclasts, bioavailable P originates from the chemical weathering of primary phosphorus-bearing minerals such as apatite (Dahlgren et al. 2004; Nanzyo & Yamasaki, 1998; Kawasaki, et al., 1992). Thus, appreciable amounts of P may be available in young volcanic soils due to rapid weathering of apatite, and low P retention due to low concentrations of active Al and Fe. Different types of acid solutions and methods have been used to evaluate plant-available P in fresh tephra and volcanic soils, i.e. Bray P2, Truog, Mehlich No. 3, Olsen, anion exchange resins (Pansu & Gautheyrou, 2006; Uchida, 2000). While the absolute values may slightly differ between methods, acid-extractable P in the Pinatubo tephra (72 mg kg^{-1}, Table A5.1) is within the range of values (~18–350 mg kg^{-1}) reported by Nanzyo et al. (1997) for tephra varying in composition from basalt to rhyolite. However, these authors report a much higher content of P_{avail} (i.e. ~350 mg kg^{-1}) for Mt. Pinatubo's ash, although their P_{total} value compares well with our result. Available P for our ash specimen is also 2.8 to 3.6 times lower than in the C horizon of the Fo-ash, IR-Ash, Gr-LA-Ash and Gr-HA-Ash soil profiles. These observations suggest that the P_{avail} measurement for the fresh ash sample is not representative and therefore, we will not use this value for the rest of the discussion. By referring to Nanzyo et al. (1997)'s analyses, the P_{avail}/P_{total} ratio in the $tephra_{(1991)}$ is ~0.5.

In the cases of the Fo-Ash, IR-Ash, and IR-Lahar/a soil profiles, there is less P_{avail} in the MS than in the ashy C horizon (Fig. 5.1; Table A5.1).

Recalling that the availability of P is dictated mainly by apatite in the primary mineral assemblage of the soil parent material, a reduced P_{avail} content in the soil points to the consumption of apatite through weathering. In support of this, Figure 5.4 indicates that the P_{avail}/P_{total} ratio in the MS and pyroclast deposits is lower than that of tephra$_{(1991)}$.

The evolution of the P_{avail}/P_{total} ratio with depth differs between the five soil profiles (Fig. 5.4; Table A5.1). For the Fo-Ash, Gr-LA-Ash and IR-Lahar soils, the MS horizon and C horizon display roughly similar P_{avail}/P_{ratio} ratio values, suggesting commonalities of weathering conditions. In contrast, in the IR-Ash, the P_{avail}/P_{ratio} ratio is lower (more than two times) in the MS than in the ash (C horizon) situated immediately beneath it. This may reflect a more intense dissolution of apatite in the surface soil. An opposite situation is found for the Gr-HA-Ash soil profile.

A plausible explanation for this behavior is that the pumice layer beneath the MS does not represent the parent material. As mentioned earlier (Chapter 3), the final phase of the 1991 eruption of Mt. Pinatubo produced fine-grained ash and according to Fig. 3.3d, this material fell over the area where the Gr-HA-Ash soil was sampled. The original P_{avail} and P_{total} contents of the pumice deposit are not known but could depart from that of the fresh ash from which the present-day MS has developed. The weathering may proceed at different rates in the pumice and ash materials due to differences in the hydrology of the deposits. For example, the dissolution of apatite may be enhanced in a fine-textured compared to a coarse-textured material due to greater specific surface area values and higher microporosity allowing water retention in the former. Nanzyo et al. (1997) showed that the fine size fraction of ash produced higher P_{avail} values than the coarse one. In IR-Ash soil, the difference in P_{avail}/P_{total} ratios in the MS and the underlying ash layer could have arisen due to the heterogeneous nature of the latter. As described in Chapter 3, this ash layer consists of remobilized ash materials (which may also contain eroded soil) carried by flood, hence

additional P_{avail} could come from this eroded soil materials and runoff water.

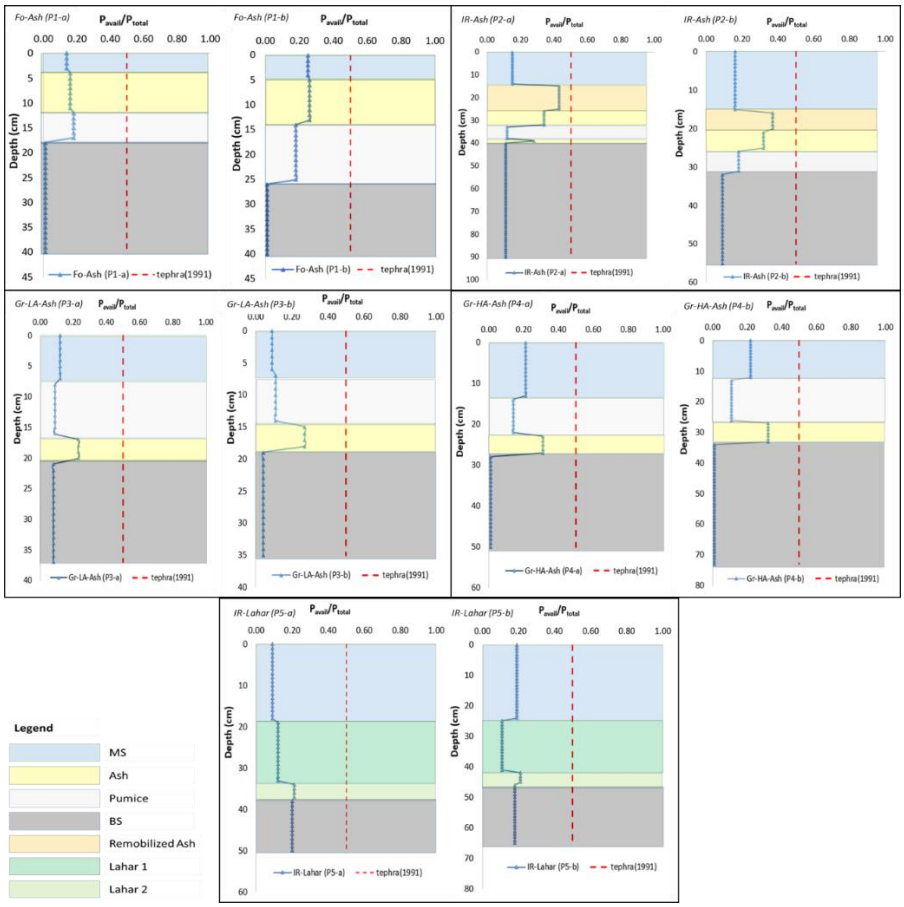

Figure 5.4. Variations with depth of the plant-available P to total P ratio (P_{avail}/P_{total}) in the Fo-Ash (P1-a, P1-b; Tarlac province), IR-Ash (P2-a, P2-b; Tarlac province), Gr-LA-Ash (P3-a, P3-b; Pampanga province), Gr-HA-Ash (P4-a, P4-b; Pampanga province) and IR-Lahar (P5-a, P5-b; Zambales province) soil profiles. **tephra$_{(1991)}$ is the 1991 Mt. Pinatubo fresh tephra, P_{avail}/P_{total} value adapted from Nanzyo et al. (1997).*

The P_{avail}/P_{total} ratio of the BS in the five soil profiles is always lower (by a factor of 2.5 to 50) than that of the tephra$_{(1991)}$ (Table A5.1), mirroring the significantly reduced P_{avail} contents measured in the BS samples, a likely consequence of chemical weathering and apatite dissolution. For the Fo-Ash and Gr-HA-Ash soils, P_{avail}/P_{total} ratio is at least an order of magnitude lower in the BS than in the MS. Again, this result points to more advanced weathering in the ~500 years old BS. A similar pattern is observed in the Gr-LA-Ash and IR-Ash profiles, but the differences in the P_{avail}/P_{total} ratios between the buried and surface modern soil are less pronounced. In contrast, the P_{avail}/P_{total} ratio of the BS in the IR-Lahar/a (IR-Lahar/b) profile is higher than (similar to) that of the corresponding MS. It is also higher than the ratio values found for the BS from the four other profiles. High P_{avail} may be linked to elevated apatite content in the parent material and/or weak weathering. The second possibility would be compatible with the high P_{total} value measured for the BS (see above).

Generally, the P_{avail} content of the MS in each soil profile (22-212 mg kg^{-1}; Fig. 5.1; Table A5.1) is above the critical limit for P deficiency, i.e. P_{avail} < 10 mg kg^{-1} (USDA-NRCS, 1994). Our P_{avail} values are also above those reported by Collado et al. (2013) for different soils from the Zambales province (P_{avail} < 10-15 mg kg^{-1}) measured prior to the 1991 eruption. Thus, the addition of tephra material can provide a significant amount of plant-available P during the early stage of weathering. The pyroclast layers in all the soil profiles also have sufficient contents of P_{avail} (55-258; Fig. 5.1; Table A5.1).

5.4.3 Phosphorus retention

Phosphorus retention is less than 20 % in all samples (Fig. 5.2; Table A5.1). Except in the IR-Ash soil, the BS always exhibits a higher P_{ret} than the MS. The ash, pumice and lahar materials have low P_{ret} varying between ~0 and 4.3 %. Phosphorus retention measures the quantity of P that can be held in the soil due to precipitation and/or adsorption on mineral and organic matter surfaces (Mishra et al, 2017; Satti et al.,

2007). Since weathering is responsible for the formation of SRO minerals such as allophanes, imogolite, and ferrihydrite in volcanic soils, P_{ret} has been shown to increase with the degree of weathering (Shoji et al., 1993). Allophanes, imogolite, and Al/Fe-(hydr)oxides have the ability to strongly adsorb P (as phosphate) through ligand-exchange and/or precipitation mechanisms (Parfitt, 1980; Nanzyo, 1988).

Young volcanic soils have low P_{ret} due to low contents of active Al and Fe, i.e. Al and Fe present in allophanes, hydr(oxides), and Al-Fe-organo complexes (Nanzyo et al., 1997). Volcanic soil formation is typically driven by the rapid dissolution of the glassy component of tephra and the release of large quantities of Si, Al, and Fe. As a result, the soil solution becomes supersaturated and poorly crystalline phases such as allophanes and ferrihydrite precipitate (Dahlgren et al., 1993; Ugolini & Dahglren, 2002). Aluminum and Fe can also form complexes with organic matter. The secondary constituents, in particular allophane and alumino-organic complexes, interact strongly with the P that gradually dissolves from apatite, eventually retaining it almost irreversibly (Takahashi & Dahlgren, 2016; Dalgren et al., 1997; Cross & Schlesinger, 1995; Sanchez, 1976). As a consequence, P availability decreases with increasing soil development.

According to Shoji et al. (1993), Andisols show a larger P_{ret} when the sum Al_o + ½ Fe_o increases (Al_o and Fe_o are the oxalate-extractable concentrations of Al and Fe, respectively; see chapter 3). This relationship is tested for our soil samples as shown in Fig. 5.5. The graph reveals the existence of a weak positive trend ($r = 0.50$, $p<0.001$) between P_{ret} and Al_o + ½ Fe_o for the soil horizons (MS and BS) and different parent material types (ash, pumice, lahar).

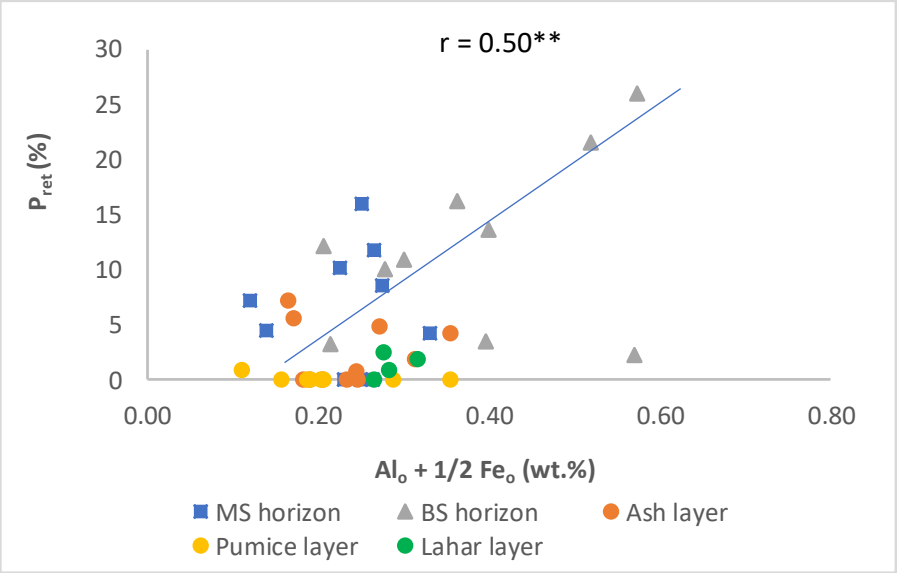

Figure 5.5. Plot graph of P retention vs. Al_o + ½ Fe_o in the soil horizons and pyroclast layers of Fo-Ash (P1-a, P1-b; Tarlac province), IR-Ash (P2-a, P2-b; Tarlac province), Gr-LA-Ash (P3-a, P3-b; Pampanga province), Gr-HA-Ash (P4-a, P4-b; Pampanga province) and IR-Lahar (P5-a, P5-b; Zambales province) soil profiles.

In Figure 5.6[a-b], the P_{ret} values obtained for the MS and BS of each soil are plotted against the corresponding total reserve in bases (TRB) and Fe_d/Fe_t, i.e. weathering indices (see chapter 3). Assuming a homogeneous composition of the parent material, a low TRB indicates higher weathering and vice-versa with Fe_d/Fe_t. For P_{ret} values at least a few percent, Figure 5.6a suggests an inverse relationship between P_{ret} and TRB ($r = 0.77$, $p<0.001$). Furthermore, the P_{ret} of MS and BS showed a positive relationship with Fe_d/Fe_t ($r = 0.78$, $p<0.001$) (Fig. 5.6b). These results are in agreement with the view that the capacity of volcanic soil to retain P increases with weathering (Shoji et al., 1993; Dahlgren et al., 2004).

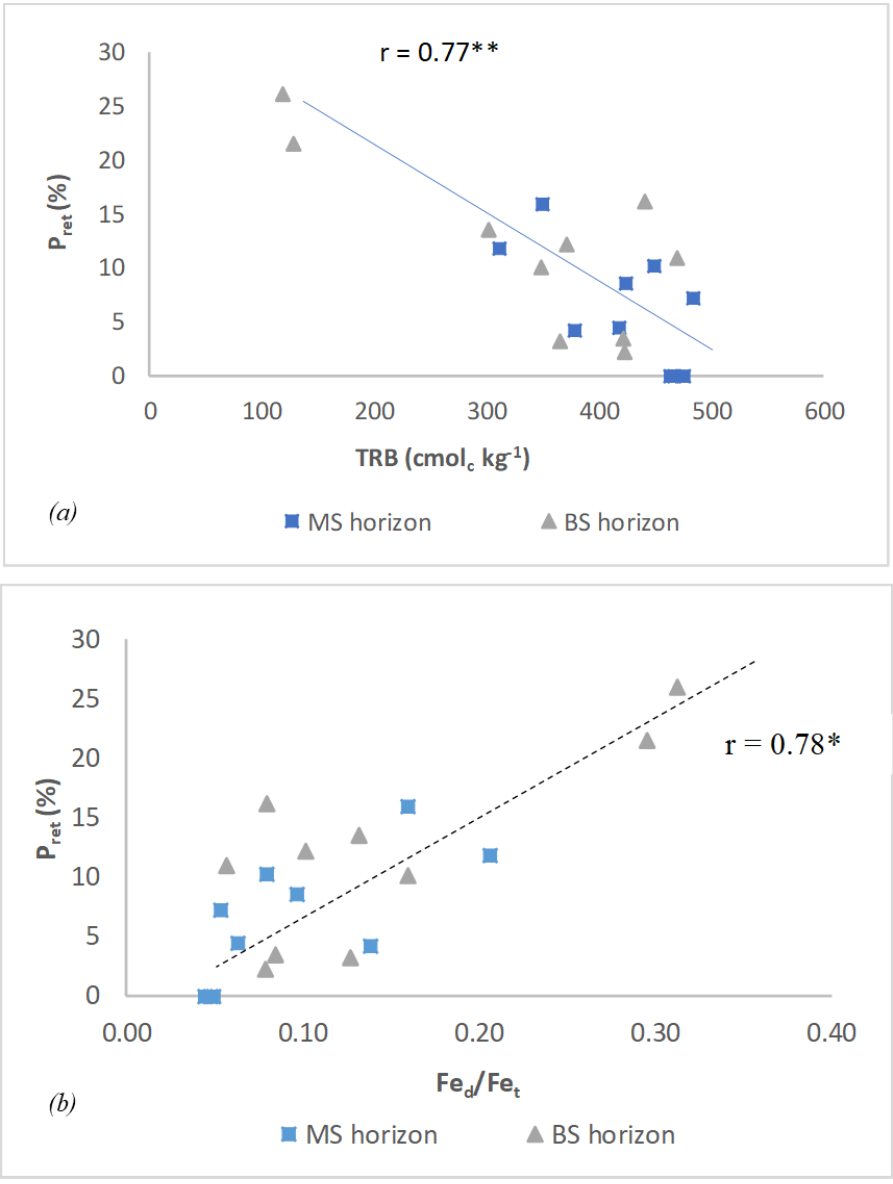

Figure 5.6. Plot graphs of P retention vs. *(a)* TRB and *(b)* Fe_d/Fe_t in the soil horizons of Fo-Ash (P1-a, P1-b; Tarlac province), IR-Ash (P2-a, P2-b; Tarlac province), Gr-LA-Ash (P3-a, P3-b; Pampanga province), Gr-HA-Ash (P4-a, P4-b; Pampanga province) and IR-Lahar (P5-a, P5-b; Zambales province) soil profiles.

There is no relationship between P_{ret} and Fe_o-Fe_p (data not shown). The Fe_o-Fe_p gives a measure of Fe in poorly crystalline phases such as ferrihydrite (Schaetzl & Anderson, 2005). This might be due to the low formation of Fe (hydr)oxide in both the MS and BS horizons. Furthermore, ferrihydrite interacts preferentially with dissolved silica and humic substances (Dahlgren et al., 2004; Schwertmann, 1988).

The positive relationship between P_{ret} and $Al_p + Fe_p$ ($r = 0.88$, $p<0.001$; Fig. 5.7) in the soil horizons and pyroclast layers shows the influence of Al/Fe-organic complexes on its capacity to retain P. The Al and Fe fractions extracted by Na-pyrophosphate are those adsorbed in organic complexes (Wada, 1989). As soil organic matter, Al, and Fe build up with the progression of weathering, the formation of Al/Fe-organo complexes also increases especially in the soil horizons. The P ions bind to the Fe/Al-(hydr)oxide surfaces by interacting with OH^- and/or OH^{2+} groups, thus, they have the ability to fix P and temporarily reduce its availability for plant uptake (Mishra et al., 2017).

Overall, the above results indicate that, even if small, the accumulation of SRO minerals, particularly allophanes and imogolite, and soil organic matter in response to weathering in the poorly developed MS and BS enhances the capacity of the young soils to retain P significantly. Based on an in-situ weathering experiment involving the tephra from the 1980 eruption of Mt. St. Helens, USA, Dahlgren et al. (1997) reached a similar conclusion. These authors noticed that 10 years of tephra weathering in a subalpine forest led to a sevenfold increase in P retention. Our data highlight a similar effect.

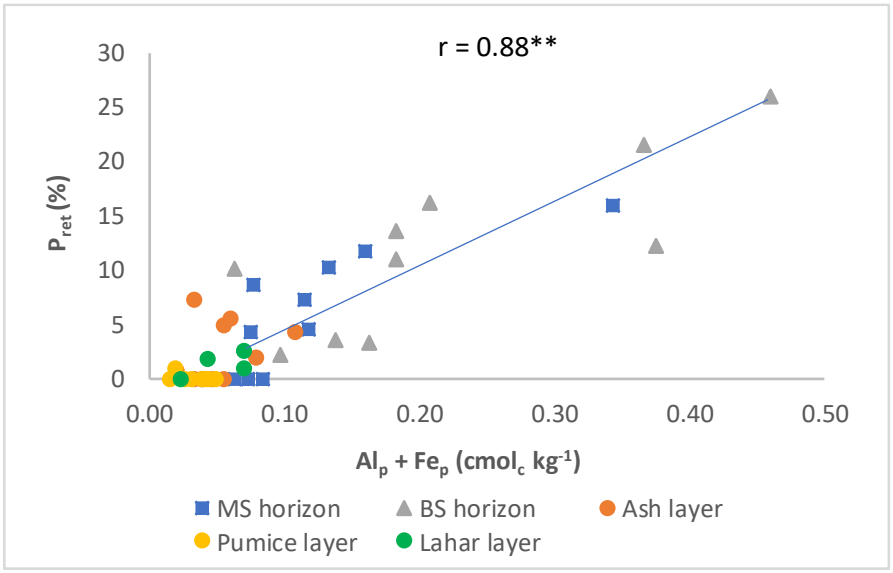

Figure 5.7. Plot graph of P retention vs. [Al_p + Fe_p] in the soil horizons and pyroclast layers of Fo-Ash (P1-a, P1-b; Tarlac province), IR-Ash (P2-a, P2-b; Tarlac province), Gr-LA-Ash (P3-a, P3-b; Pampanga province), Gr-HA-Ash (P4-a, P4-b; Pampanga province) and IR-Lahar (P5-a, P5-b; Zambales province) soil profiles.

5.5 Conclusion

Our assessment of the P status in the pyroclast-affected cultivated and non-cultivated soils 26-yr after deposition revealed that the P_{total} (233-853 mg kg^{-1}) and P_{avail} (22-212 mg kg^{-1}) contents in the developing modern soils are high enough to support the plants' P requirement especially for high-value crops such as rice. The emplacement of the 1991 Mt. Pinatubo pyroclasts provided a significant amount of plant-available P during the early stages of weathering due to the dissolution of P-bearing minerals, particularly apatite. The P retention (< 20 %) in the modern soils is low due to the small quantities of active Al and Fe from Al/Fe-(hydr)oxides, SRO minerals, and Al/Fe-organic complexes.

This indicates further that modern soils (including the partially weathered pyroclast deposits) across the different land uses have a low degree of weathering and are weakly developed. As such they can contain an ample reserve of plant-available P.

Some of the factors that influence the chemical weathering of pyroclasts and the P status in cultivated and non-cultivated young volcanic soils are the composition and heterogeneity of pyroclast deposit (i.e. type, thickness, grain size, presence of eroded sediments), and the kind of land use and management (i.e. volume of crop cover, biomass restitution, and removal, fertilization, drainage, runoff). In cultivated soils grown to rice, P availability and contents can be controlled by various mechanisms such as the intensity of crop production, biomass recycling (i.e. P removal from harvested grains and biomass, restitution), fertilization, and water drainage in addition to chemical weathering. The continuous crop cultivation and partial crop removal in the rice soils affected by ash and lahar are possible causal factors for its lower P_{total} and P_{avail} contents compared to the forest and grassland soils affected with ash.

The generally lower P_{total} and P_{avail} values in the buried compared to the modern soils, except for IR-Lahar, reflect the gradual loss of P with time due to apatite dissolution during chemical weathering. Higher P retention is observed in the ~500-yr buried soils compared to the modern soils due to the small build-up of active Al and Fe in SRO minerals (i.e. allophanes and imogolite) and Al/Fe-organic matter complexes in the course of pedogenesis. Moreover, the buried soils have a significantly higher net loss of P, i.e P_{total} and P_{avail} (except for IR-Lahar), due to lower rate of P fixation as the secondary materials (i.e. allophane, imogolite, Al/Fe-organic matter complexes) occurred in low quantities. The organic P pool is also low since the deposition of pyroclast deposit has impeded the addition of organic matter from biomass restitution in the buried soils.

5.6 References

Bernard, A., Knittel, U., Weber, B., Weis, D., Albrecht, A., Hattori, K., … Oles, D. (1996). Petrology and Geochemistry of the 1991 Eruption Products of Mount Pinatubo. In C.. Newhall & R. S. Punongbayan (Eds.), *Fire and mud, eruptions and lahars of Mount Pinatubo, Philippines* (pp. 767–797). Univ. Washington Press, Seattle.

Blakemore, L. C., Searle, P. L., & Daly, B. K. (1981). Methods for chemical analysis of soils, *New Zealand Soil Bureau Scientific Report*, lOA.

Blaskó, L. (2011). *Soil science*. Debreceni Egyetem. Agrár- és Gazdálkodástudományok Centruma. 162 p.

Bray, R. H., & Kurtz, L. T. (1945). Determination of total organic and available forms of P in soils. *Soil Sci. 59*:39.

Castillo, P. R., Punongbayan, R. S. (1996). Petrology and Sr, Nd, and Pb Isotopic Geochemistry. In R. S. Newhall, Christopher G., Punongbayan (Ed.), *Fire and Mud* (pp. 799–805). Philippine Institute of Volcanology and Seismology, Quezon City; University of Washington Press, Seattle, and London.

Chao, T. T., & Sanzolone, R. F. (1992). Decomposition techniques. *Journal of Geochemical Exploration, 44,* 65-106.

Collado, W. B., Monteza, R. M., Dollentas, R. T., De Dios, J. L., D., & Torre, J. P., Bibar, J. E., Badayos, R. B., Soliman, A. E. (2013). *Simplified Keys to Soil Series - Zambales. Soil Series Guidebook* (ISBN 978-9). Philippine Rice Research Institute Maligaya, Science City of Muñoz, Nueva Ecija.

Cross, A. F., & Schlesinger, W. H. (1995). A literature review and evaluation of the Hedley fractionation: applications to the biogeochemical cycle of soil phosphorus in natural ecosystems. *Geoderma. 1995; 64*: 197-214.

Dabin, B. (1980). Phosphorus deficiency in tropical soils as a constraint on agricultural output. In *soil-related constraints to food production in the tropics.* (pp. 217–232). Los Baños, Laguna.

Dahlgren, R. A., Dragoo, J. P., & Ugolini, F. C. (1997). Weathering of Mt. St. Helens tephra under a cryic-udic climatic regime. *Soil Science Society of America Journal*, *61*, 1519–1525.

Dahlgren, R. A., Saigusa, M., & Ugolini, F. C. (2004). Nature, properties, and management of volcanic soils. *Advances in Agronomy*, *82*, 113–182. https://doi.org/10.1016/S0065-2113(03)82003-5.

Deer, W. A., Howie, R. A., & Zussman, J. (1992). An introduction to the rock-forming minerals. 2nd ed. Longman Scientific and Technical, Essex, England.

Duxbury, J. M., and J. H. Peverly. (1978). Nitrogen and phosphorus losses from organic soils. Journal of Environmental Quality 7:566-570.

Engelstad, O. P. Jugsujinda, A., De Datta, S. K. (1974). Response by flooded rice to phosphate rocks varying in citrate solubility. *Soil Science Society of America Proceedings 38*: 524-529.

Escudey, M., Galindo, G., Foerster, J. E., Briceño, M. A., Díaz, P. & Chang, A. C. (2001). Chemical forms of phosphorus of volcanic ash derived soils in Chile. *Communications in Soil Science and Plant Analysis 32*: 601-616.

Gudmundsson, T., Gudmundsson, S. T., & Thorvaldsson, G. (2014). Soil phosphorus fractionation in Icelandic long-term grassland field experiments. *Icelandic Agricultural Sciences, 27*(1), 81–94

Harouiya, N., Chaïrat, C., Köhler, S. J., Gout, R., & Oelkers, E. H. (2007). The dissolution kinetics and apparent solubility of natural apatite in closed reactors at temperatures from 5 to 50 °C and pH from 1 to 6. *Chemical Geology Including Isotope Geoscience*, *244*(2007), 554–568. https://doi.org/10.1016/j.chemgeo.2007.07.011.

Herrera, I. O. (1992). Mt. Pinatubo R & D program of the department of agriculture-Region III. In *Proceedings of the symposium on sustainable agricultural development of Mt. Pinatubo-affected areas*. November 5-6, 1992. Farming Systems and Soil Resources Institute, College of Agriculture, University of the Philippines, Los Banos, College, Laguna.

Kawasaki, H., Hayashi, K., & Kitazaki, Y. (1992). Characteristics of the Handa pyroclastics flow abundant in available phosphorus. *Kyushu Nogyo Kenkyu, 53*: 57 p.

Leone, F., & Gaillard, J. C. (1999). Analysis of the institutional and social responses to the eruption and the lahars of Mount Pinatubo volcano from 1991 to 1998 (Central Luzon, Philippines). *GeoJournal, Vol. 49*, pp. 223–238.

Mishra, G., Debnath, S., & Rawat, D. (2017). Managing phosphorus in terrestrial ecosystem: a review. *European Journal of Biological Research*, *7*(3), 255–270. https://doi.org/10.5281/zenodo.854681.

Mendoza, T. C., & Cabangbang, R. P. (1992). Effects of Mt. Pinatubo eruption in crop production systems. *The Philippine Agriculturist*, *75*(1 & 2), 1–8.

Nakamaru, Y., Nanzyo, M., & Yamasaki, S. (2000). Utilization of apatite in fresh volcanic ash by pigeon pea and chickpea. *Soil Sci. Plant Nutri., 46*:591-600.

Nanzyo, M. (2002). Unique properties of volcanic ash soils. *Glob. Environ. Res. 6.*

Nanzyo, M., & Yamasaki, S. (1998). Phosphorus-bearing mineral in fresh, andesite and rhyolite tephras in the northern part of Japan. *Phosphorus Research Bulletin, 8*, 95–100.

Nanzyo, M., & Kanno, H. (2018). Role of inorganic soil constituents in selected topics. In *Inorganic constituents in soil*. https://doi.org/10.1007/978-981-13-1214-4_6.

Nanzyo, M., Dahlgren, R., & Shoji, S. (1993). Chemical characteristics of volcanic ash soils. In: Shoji, S., Nanzyo, M., Dahlgren, R. *Volcanic ash soils. Genesis, properties and utilization. Developments in Soil Science 21*. Elsevier. Amsterdam-London-New York-Tokyo.

Nanzyo, M., Nakamaru, Y., & Yamasaki, S. (1999). Inhibition of apatite dissolution due to formation of calcium oxalate coating. *Phosphorus Res. Bull. 9*, 17-22.

Nanzyo, M., Takahashi, T., Sato, A., Shoji, S., & Yamada, I. (1997). Dilute acid-soluble phosphorus in fresh air-borne tephras and fixation with an increase in active aluminum and iron. *Soil Science and Plant Nutrition, 43* (4), 839–848. https://doi.org/10.1080/00380768.1997.10414650.

Nanzyo, M., Yamasaki, S. & Honma, T. (2003). Changes in content of trace and ultratrace elements with an increase in noncrystalline minerals in volcanic ash soils of Japan. *Clay Science 12.*

Nanzyo, M., Kanno, H., & Takahashi, T. (2010). Organic carbon accumulation in Andosols:(3) Occurrence of apatite and biotite in young and matured volcanic ash soils, and discussions on nutrient supply for ecosystems. *Soil Science, 164*(3), 2007–2007. Retrieved from ttp://ir.library.tohoku.ac.jp/re/handle/10097/48840

National Research Council. (1993). Soil and Water Quality: An Agenda for Agriculture. Washington, DC: The National Academies Press. https://doi.org/10.17226/2132

Nelson, G. L. (2013). Land Rehabilitation Techniques of Rice Farmers in Pampanga (Philippines) after the Mt. Pinatubo Eruption. *Asia Life Sciences, 22*(1), 155–181.

Newhall, C. G., Punongbayan, R. S. (Ed.). (1996). Fire and Mud: Eruptions and lahars of Mount Pinatubo, Philippines. Philippine Institute of

Volcanology and Seismology, Quezon City; University of Washington Press, Seattle, and London.

Pallister, J. S., Hoblitt, R. P., Meeker, G. P., Knight, R. J., & Siems, D. F. (1996). Magma mixing at Mount Pinatubo: Petrographic and chemical evidence from the 1991 deposits. In *Fire and mud. Eruptions and Lahar of Mount Pinatubo, Philippines*. (Eds: Newhall, C.G. and Punongbayan, R.S.) Philippine Institute of Volcanology and Seismology, Quezon City. University of Washington Press, Seattle, and London. Printed in Hongkong.

Pansu, M., & Gautheyrou, J. (2006). *Handbook of soil analysis: mineralogical, organic and inorganic methods*. Springer.

Parfitt, R. L. (1980). Chemical properties of variable charge soils. *Soils With Variable Charge.*, (January), 167–193.

Pierzynski, M., Sims, J. T., Vance, G. F. (2000). Soil phosphorus and environmental quality. In *Soils and Environmental Quality*, CRC Press, Boca Raton, USA,155-207.

Punongbayan, R. S., Tungol, N. M., Arboleda, R. A., DelosReyes, P. J., Isada, M., Martinez, M. L., Melosantos, M. L. P., Puertollano, J., Regalado, T. M., Solidum, R. U., Tubianosa, B. S., Umbal, J. V., Alfonso, R.A., Remotique, C. T. (1993). Impacts of the 1993 lahars and long-term lahar hazards and risks around Pinatubo volcano. *PHIVOLCS Internal Report*, Quezon City, 72 pp.

Rantucci, G. (1994). Geological Disaster's in the Philippines: The July 1990 earthquake and the June 1991 eruption of Mount Pinatubo - Description. Effects and Lessons Learned. Report in cooperation with PHILVOLCS, Rome: Italian Ministry of Foreign Affairs, Directorate-General for Development Cooperation.

Reyes, R. Y., & Neue, H. U. (1991). Characterization of the volcanic ejecta from Mount Pinatubo and its impact on rice production. *Philippine Journal of Crop Science*, *16*(2), 69–73.

Roy, R. N., Finck, A., Blair, G., & Tandon, H. (2006). Plant nutrition for food security: A guide for integrated nutrient management. *FAO Fertilizer and Plant Nutrition Bulletin*, (16), 21.

Satti, P., Mazzarino, M. J., Roselli, L., Crego, P. (2007). Factors affecting soil P dynamics in temperate volcanic soils of southern Argentina. *Geoderma. 2007*; 139: 229- 240.

Sanchez, P. A. (1976). Properties and management of soils in the tropics. Wiley, New York, NY, 1976: 259-260.

Schaetzl, R., Anderson, S. (2005). Soils: Genesis and Geomorphology. In *Cambridge University Press*. https://doi.org/10.2136/vzj2007.0030br.

Schwertmann, U. (1988). Occurrence and formation of iron oxides in various paleoenvironments. In *Iron in Soils and Clay Minerals* (Eds: Stucki, J.W.), Reidel, Norwell, MA, pp. 267-308.

Schlesinger, W. H., Bruijnzeel, L. A., Bush, M. B., Klein, E. M., Mace, K. A., Raikes, J. A., & Whittaker, R. J. (1998). The biogeochemistry of phosphorus after the first century of soil development on Rakata Island, Krakatau, Indonesia. *Biogeochemistry*, *40(1)*, 37–55. https://doi.org/10.1023/A:1005838929706.

Sharpley, A. N. (1995). Soil phosphorus dynamics: agronomic and environmental impacts. *Ecological Engineering*, *5*, 261–279. https://doi.org/10.1016/0925-8574(95)00027-5.

Sherrell, C. G. (1970). Comparison of chemical extraction methods for the determination of "available" phosphate in soils: I. Correlation between methods and yield and phosphorus uptake by white clover grown on 16 North Island soils in the glasshouse. *New Zealand Journal of Agricultural Research*, *13*(3), 481–493. https://doi.org/10.1080/00288233.1970.10421597.

Shoji, S., & Takahashi, T. (2002). Environmental and agricultural significance of volcanic ash soils. *Global Environmental Research-English Edition*, *6*(2), 113–135.

Shoji, S., Nanzyo, M., & Dahlgren, R. (1993). Volcanic ash soils. Genesis, properties and utilization. *Developments in Soil Science 21*. Elsevier. Amsterdam-London-New York-Tokyo.

Smith, P., Cotrufo, M. F., Rumpel, C., Paustian, K., Kuikman, P. J., Elliott, J. A., … Scholes, M. C. (2015). Biogeochemical cycles and biodiversity as key drivers of ecosystem services provided by soils. *Soil*, *1*, 665–685. https://doi.org/10.5194/soil-1-665-2015.

Uchida, R. (2000). Essential nutrients for plant growth: Nutrient functions and deficiency symptoms. In R. Silva, J,.A., Uchida (Ed.), *Plant Nutrient Management in Hawaii's Soils, Approaches for Tropical and Subtropical Agriculture* (pp. 31–55). College of Tropical Agriculture and Human Resources, University of Hawaii at Manoa.

USDA-NRCS. (1994). Soil Phosphorus: Soil Quality Kit- Guides for Educators. *United States Department of Agriculture: Natural Resources Conservation Service*, 1–6. Retrieved from

http://www.nrcs.usda.gov/Internet/FSE_DOCUMENTS/nrcs142p2_053254.pdf.

Wolff-Boenisch, D., Gislason, S. ., Oelkers, E. ., & Putnis, C. (2004). The dissolution rates of natural glasses as a function of their composition at pH 4 and 10. 6, and temperatures from 25 to 74 ° C. *Geochimica et Cosmochimica Acta*, *68*(23), 4843–4858. https://doi.org/10.1016/j.gca.2004.05.027.

Chapter 6 Rebuilding agriculture after the 1991 Plinian eruption of Mt. Pinatubo, Philippines: soil constraints and adaptation strategies

6.1 Introduction

Volcanic eruptions are feared not only for the fatalities that they may cause but also for the socio-economic impacts of their associated hazards. Tephra, gases, lava flows, pyroclastic flows, debris flows (or lahars) are volcanic products that can result in severe losses in the industry and agricultural economy of a volcanic region. Reducing volcanic risk becomes more difficult especially for overpopulated developing countries that host a large number of active volcanoes, for example, Indonesia, Philippines and Vanuatu (Brown et al., 2015). The hazards of explosive eruptions are felt immediately by the agriculture sector as most cultivated lands lie on the flanks of active volcanoes. Depending on the strength of volcanic eruption and the severity of its hazards, croplands may suffer losses from plant damage, death of existing crops, abrupt changes on soil properties leading to yield decline, and decreased arable land area.

Volcanic soils are renown for their outstanding fertility, hence, they support intensive farming and attract a dense population (Shoji et al., 1993). The soils are often heavily cultivated in order to benefit from the natural fertilizing effects of volcanic products (Ugolini & Dahlgren 2002; Shoji and Takahashi, 2002). Around 0.84 % or 1.1 to 1.2 million km^2 of the world's land area is covered by Andisols, with ~60 % occurring in the tropics and the remaining half split between boreal and temperate regions (Dahlgren et al., 2004; Kimble et al., 2000; Soil Survey Staff, 1999). Andisols represent the majority of volcanic soils. They typically develop from the fragmented and unconsolidated tephra (pyroclasts) produced during explosive eruptions (Tan, 1984; Schaetzl & Anderson, 2005). Active volcanic regions are repeatedly affected by

widespread depositions of tephra. In high rainfall regions, these deposits can be remobilized quickly to form lahars.

Tephra falls, and to a lesser extent lahars, may partially or completely bury the surface soil and isolate it from the atmosphere. When the deposit is too thick, the buried soil can no longer be used. A new soil will develop as weathering in the tephra/lahar material progresses. However, the newly deposited pyroclastic materials can strongly impact the capability of agricultural land for crop production.

Agricultural recovery after a volcanic catastrophe is highly dependent on the intensity of volcanic eruption, the severity of volcanic hazards, government assistance and rehabilitation programs, and farmers' coping mechanisms/adaptation practices to manage the constraints. The catastrophic eruption of Mt. Pinatubo, Philippines from June 12-15, 1991 ejected ~5.3 km^3 (DRE) of dacitic magma in the form of tephra (~10.4 km^3) which covered more than 2000 km^2. This eruption is a classic example of how a single volcanic eruption could weaken the flourishing agricultural economy of the Central Luzon region (Scott et al., 1996; Melosantos et al., 1996; Mercado, 1996; Benson, 1997). It has been coined as the second largest in the 20th century, after the Novarupta (Katmai), Alaska eruption in 1912 but regarded as the most explosive eruption to affect a dense population (Newhall & Punongbayan, 1996). About 2.1 million persons were affected, 320 people were directly killed, and economic losses reached more than one billion US dollars (Leone & Gaillard, 1999; Gaillard, 2008).

The 1991 Mt. Pinatubo eruption ejected huge amounts of volcanic ash followed by lahar flows triggered by heavy monsoonal rains and tropical cyclones during and after the eruption (Janda et al., 1996). About 962 km^2 of agricultural land, where 800 km^2 are devoted to rice lands, were seriously affected by the ashfall (< 2 mm tephra). The cost to agriculture was estimated at Php1.5 billion (~25 million USD) and the cost of repairs to damaged infrastructure was Php3.8 billion (~ 62 million USD) (Global Volcanism Program, 2011). Lahar, on the other

hand, affected about 897 km^2 of agricultural land (Herrera, 1992). Moreover, lahars and floods affected 5 national and 176 communal irrigation systems that serviced 483 km^2 of farmlands in Central Luzon which lead to the decline in farming activities especially rice production (Gonzaga & Orejas, 2011; Presidential Task Force on Mt. Pinatubo, 1992). Sediment-clogged channels still overflow reaching some agricultural areas during heavy rains even after 24 years (Orejas, 2015).

Rice is one of the chief staple crops worldwide and about 91% of the world's rice is produced and consumed in Asia (IRRI, 1997). In the Philippines, rice production is the main staple food for 90 % of the population. It also an important source of income for the majority of farmers as Central Luzon plays the biggest rice-producing area of the country (Benson, 1997). Despite the negative consequences on soil and crop productivity imparted by volcanic hazards, farmers continue to cultivate the soil after the 1991 eruption. Around 500,000 people continue to live in cities and villages on broad, gently sloping alluvial fans surrounding the volcano (Newhall & Punongbayan, 1996). Given the Philippines' exposure to volcanic hazard risks and the importance of agriculture to the economy, it is crucial to understand the short-term impacts of the pyroclast deposition on crop production, and how the farmers adapted and recovered to the current conditions of the developing young volcanic soils. The short-term impacts and perennial constraints can lead to long-term difficulties if not addressed during the process of agricultural recovery.

Documenting the positive and negative consequences of the pyroclastic deposition at the early stage of soil development, which may also be affected by other farming and socio-economic conditions, will provide useful information in drafting recommendations for mitigation. Previous local studies have documented the early impacts of the pyroclast deposition on crop production, farmers' adaptation practices, and have recommended some rehabilitation strategies (Mendoza & Cabangbang, 1992; Nelson, 2013; Aganon & Undan, 1992; Aganon, et. al., 1996; Icamina, 1992; Samonte et al. 1992; Mateo, 1993).

Chapter 6: Soil constraints and adaptation strategies

The objectives of the study are to (1) determine the major constraints associated with the cultivation of the Mt. Pinatubo's pyroclast deposits, 26 years after the eruption, (2) identify the adaptation practices of farmers to cope with the land quality constraints, and (3) assess the current crop productivity and to compare it with previous figures. To achieve the research objectives, we interviewed farmers who were directly affected by the products of the 1991 Mt. Pinatubo eruption.

6.2 Materials and Methods

6.2.1 Reconnaissance survey and farmers' interview

The reconnaissance survey of the pyroclast (ashfall, remobilized ash, lahar) affected-areas and the semi-structured interview of farm owners and agricultural technicians were conducted in the provinces of Tarlac, Pampanga, and Zambales of Central Luzon Region between March and June 2017. The three provinces are within the boundaries of Mt. Pinatubo volcano and were identified as the most heavily affected by the 1991 eruption (Mercado, et al., 1996; Bautista, 1996).

Figure 6.1 illustrates the spatial distribution of the surveyed sites showing their relative distance to the Mt. Pinatubo crater, lahar, ash, and pyroclastic flows. It also shows the position of the sites in relation to the thickness of tephra-fall deposits from the June 12-15 eruption episode. Thirty-four sites were randomly selected but were limited to those accessible and by the availability of farm owners/agricultural technicians. The altitude of the sites ranged from 9 to 473 m.a.s.l. The ground distance of the sites from the Mt. Pinatubo crater varied from 19 to 40 km. The total number of sites surveyed in Tarlac, Zambales, and Pampanga provinces were 10, 11, and 13, respectively. Out of the 13 sites surveyed sites in Tarlac, five were affected by ash, two were affected with remobilized ash, and six were affected by lahar. In Pampanga, the sites affected by ash, remobilized ash, and lahar was four, three and, four, respectively. In Zambales, six of the sites were affected by ash, one is affected by remobilized ash, and three were affected by lahar.

The climate type of the three provinces is similar, having a tropical monsoon climate characterized by two pronounced seasons, dry from November-December to April-May, and wet during the rest of the year. The annual rainfall of the three provinces ranges from ~2300 to 3400 mm while the temperature average is 27 °C (PAGASA, 2007).

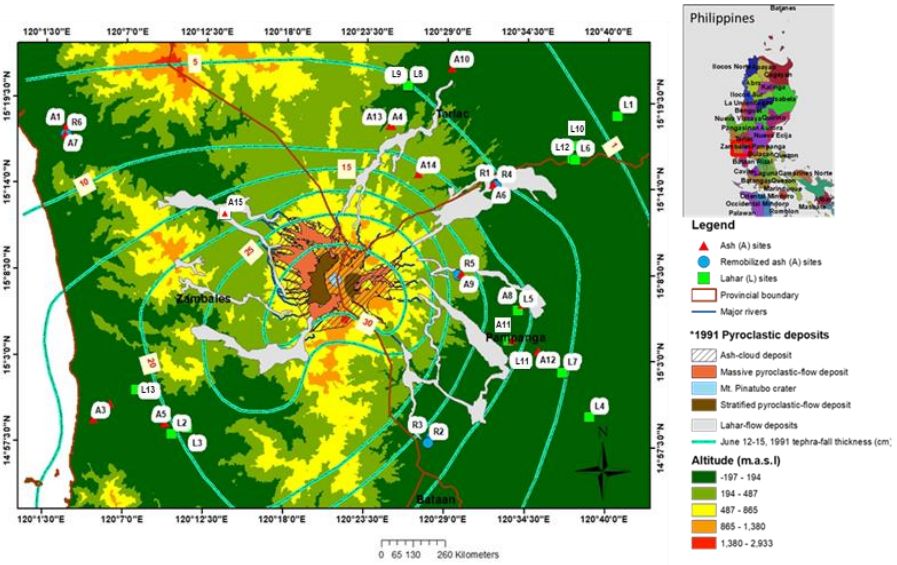

Figure 6.1. Geographical location and elevation maps of the surveyed sites in Tarlac, Pampanga, and Zambales provinces in relation to the distribution of 1991 lahar and pyroclastic flows, and thickness of tephra-fall deposits. *Major rivers include O'Donnell, Marella, Maloma, Balin Baquero, Maraunot, Bucao, Bangat, Malago, Sacobia, Abacan, Porac, Gumain, and Pasig; 1991 pyroclastic flow map adapted from Scott et al., (1996) as cited in Newhall and Punongbayan, (1996); Isopach map showing the extent and thickness of June 12-15, 1991 tephra-fall adapted from Melosantos et al., (1996); 1991 lahar map distribution adapted from short-term Pinatubo volcano hazard map produced by NEDA (National Economic and Development Authority) Region III and PHILVOCS (Philippine Institute of Volcanology and Seismology), Philippines, in 1991. 'A' ash affected, 'R' remobilized-ash affected, 'L' lahar-affected.*

An interview questionnaire guide (Table A6.1, see section 6.4.2), which included 45 items, was used to collect baseline information on the characteristics of the sites (i.e. type and thickness of pyroclast deposit, irrigation source, etc.), farmers' pre- and post-eruption crop management practices (i.e. cropping system, fertilization, etc.), crop yields, farming constraints, adaptation practices, and farmers'

perception on the land quality(ies) based on some indicators or land characteristics. A soil profile was excavated from each site to record the presence and depth of the 1991 pyroclastic deposit. A total of 15 ash-, 6 remobilized ash-, and 13-lahar affected areas was surveyed (Figure 6.1). A site affected by remobilized ash is distinguished from a site affected by lahar based on the granulometry of the volcanic deposit. In the former case, it is primarily comprised of fine ash and soil material remobilized locally during a flooding episode of the nearby land. A lahar deposit also originates from pyroclasts remobilized by water but the material is transported and deposited by a flow. The deposit is much more heterogeneous in size as it incorporates ash, tephra, pumices, fresh and old lithic rocks and soil (Vallance & Iverson, 2015; Newhall et al., 1997).

6.2.2 Structure of interview process and organization of data from the farmers' responses

Figure 6.2 shows the framework used to design the semi-structured interviews that were carried out to collect the information necessary for evaluating the impacts of different types of pyroclastic deposition on land qualities and crop productivity 26 years after the 1991 eruption of Mt. Pinatubo. The farmers and/or agricultural technicians were also asked to comment on how they adapted to the specified farming constraints.

In order to assess the performance of the land for crop production and to categorize the farming constraints specified by the farmers and/or agricultural technicians, we adapted the concept of land quality assessment proposed by Sys et al. (1991). The land/soil quality (LQ) pertains to the complex attribute of the land that can influence its suitability for specific kinds of land use such as crop production (FAO, 1976; 2007). Examples of land/soil qualities include topography, oxygen availability/rooting conditions, moisture availability, soil temperature regime, nutrient availability, workability, and resistance against erosion.

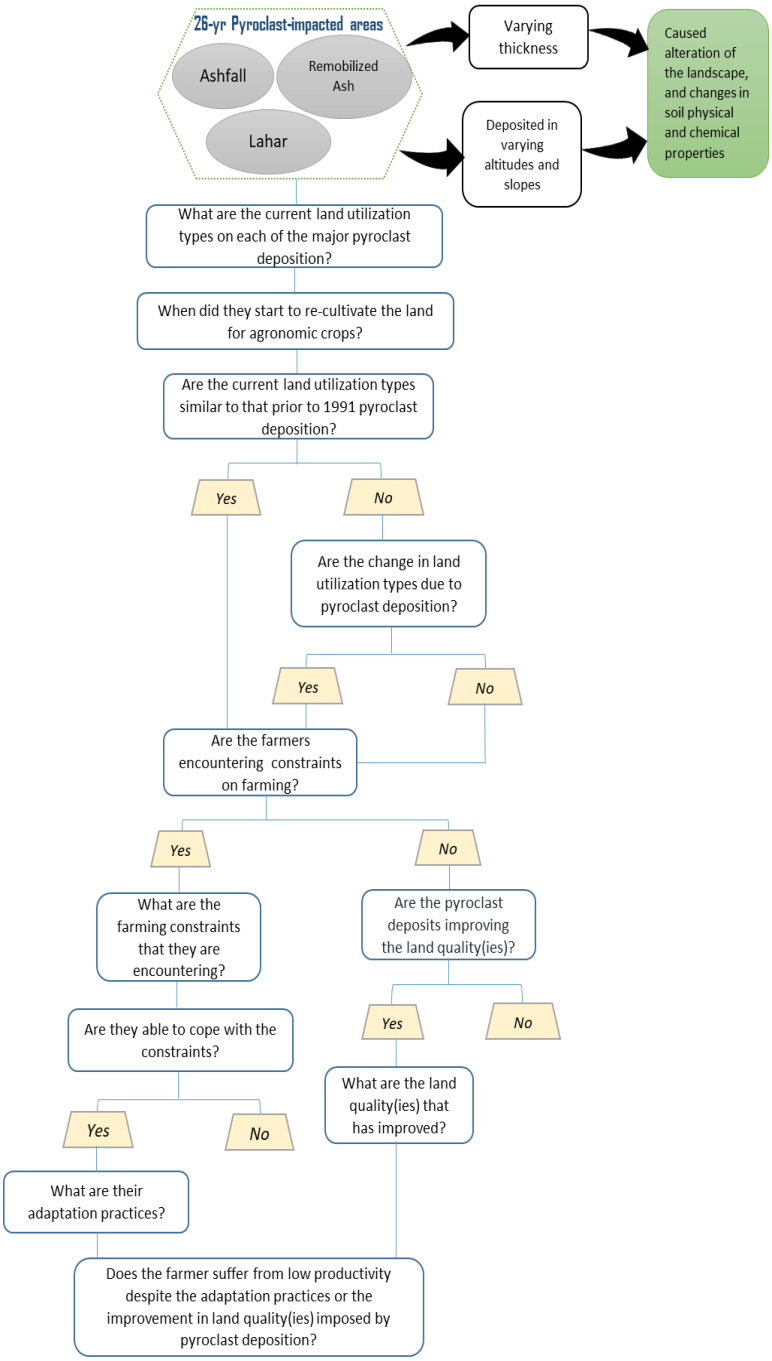

Figure 6.2. Flow diagram showing the structure of the questionnaire and the key topics that were discussed with the farmers and/or agricultural technicians.

The LQs can be measured, calculated, or estimated in terms of land/soil characteristics (LC). Land characteristics are attributes of the land that can be measured or estimated which singly or in aggregate influence the quality of the land. For instance, limitations on nutrient availability can be assessed by measuring the soil's CEC, pH, organic matter, macro- and micro-element contents. In our post-eruption survey, we rely on the personal experiences and observations as shared by the farmers and/or agricultural technicians for evaluating qualitatively the current situation, i.e. 26 years after the 1991 eruption of Mt. Pinatubo. Thus, we do not analyze the LCs to give a precise evaluation of the impact of pyroclasts in the land qualities.

Based on Figure 6.2, each of the sites affected by ash remobilized ash, and lahar is classified as land utilization type (LUT), which pertains to the specific cropping system and management of the farm. The LUT is the specific way of using the land with consideration of key attributes (FAO, 1976). Some of the key attributes include: produce, size of land holdings, land tenure, availability and source of irrigation, cultivation practices, mechanization and implements, crop yields, and farmers' technical knowledge. The key attributes used to describe the LUTs are the following:

Cropping system. This is described as a commodity-based LUT (e.g. rice-based cropping, rotation of different crops, multiple cropping, etc).

Size of landholdings. This refers to the total land size in hectare used for farming activities.

Land Tenure. This is the legal ownership or rights to the use of the land. This could be classified as private ownership or tenancy. Tenancy could still be classified as cash tenancy, labor tenancy or sharecropping with the landowner.

Availability and source of irrigation water. This refers to the presence and source of irrigation. The sources of irrigation are the *1)* national

irrigation system (NIS) – large and medium schemes (> 1000 ha area covered) operated and maintained by the government's national irrigation administration, *2)* communal irrigation system (CIS) – small-scale schemes (< 1000 ha area covered) and constructed by the government with the participation of farmer-beneficiaries through their irrigators associations, *3)* small farm reservoir (SFR) – a small water impounding earth dam structure to collect rainfall and run-off, typically has a reservoir area of about 300-2000 m^2 and designed for use in a single farm; embankment height above ground level is less than 4 meters and irrigation is done with PVC siphon pipes or pumps, *4)* shallow tube well (STW) – consist of tube or pipe vertically set into the ground at a depth of 20 to 60 feet for the purpose of suction lifting of water from shallow aquifers; can also be powered by electric motor equipped with pumping units, and *5)* spring – sourced from groundwater (NIA, 2018; BSWM, 2016). Other sources of water are derived from the diversion of free-flowing water aquifers, seepage from rivers, and diversion of water from dams and rivers.

Cultivation practices. These include the fertilizer application (type and rate), weed management, and crop protection practices.

Mechanization and implements. The classification range from *1)* fully mechanized production (farming entirely mechanized from transplanting to harvesting), *2)* partly mechanized (i.e. use of tractors, combine harvester, thresher but still involves human labor), and *3)* non-mechanized (use of animal-drawn implements and human labor).

Crop yield. The yield refers to the estimated amount of produce per unit area.

Technical knowledge. Levels of literacy, training and skills and receptiveness to innovation can be important differentiating features of LUTs.

6.3 Results

6.3.1 General description of the land utilization types

Current land utilization types of the pyroclast-affected sites

Table 6.1 describes the current LUTs in Tarlac, Pampanga, and Zambales provinces affected by ashfall, remobilized ash, and lahar based on the 34 respondents (i.e. 27 farmers, 4 agricultural technicians, 3 agricultural technicians who also manages a farm) and from existing information. The farmer respondents also included a group of Aetas in A9, A14, and R3 LUTs. The "Aeta" is a group of indigenous people who lives in the northern flanks of the volcano and depend their livelihood on cultivating root crops and other vegetables, hunting and fishing, and also on gathering plants and wild fruits in their surroundings (Barrato & Benaning, 1978; Reed, 1904).

The following characteristics are summarized: cropping system, altitude, slope, land cover, distance from Mt. Pinatubo, thickness of the 1991 pyroclast deposit as (i) reported by the farmers and (ii) measured in the field in 2017, distribution of the tephra fall from the paroxysmal 1991 eruption of Mt. Pinatubo, number of years after the eruption without cultivation, and pre- and post-eruption harvest yields. A general description of the current and pre-1991 eruption LUTs based cropping systems and management, i.e. specific crops grown, size of landholding, land tenure, irrigation source, fertilizer usage (types and rates), weed management, crop protection, crop yields, and technical know-how of the respondent farmer or agricultural technician is shown in Table A6.2. The land cover types identified through the reconnaissance surveys and farmer interviews conform to those inferred from the satellite image as shown in Figure 6.3 (PhilGIS, 2004a). The land cover types identified were cultivated areas mixed with brushland/grassland (CG), arable land, crops mainly cereals and sugar (Ar), cropland mixed with coconut plantation (Cr), eroded area (Er); grassland, grass covering >70 percent (Gr); and riverbed (Ri).

Table 6.1. General description of the land utilization types (LUT) associated with different types of pyroclastic deposits in Tarlac, Pampanga, and Zambales provinces.

LUT CODE	[1]LAND UTILIZATION TYPE (LUT) (Cropping pattern per year)		PROVINCE	MUNICIPALITY	BARANGAY	[2]ALTITUDE (m.a.s.l)	[3]SLOPE (%)	[4]DISTANCE FROM CRATER (km)	[5]LAND COVER	THICKNESS (cm) OF PYROCLAST DEPOSIT			YEARS BEFORE CROP RE-ESTABLISHMENT AFTER 1991 ERUPTION	[9]CROP YIELD (t ha^{-1} cropping^{-1})	
	CURRENT (2017)	PRE-1991 (1990)								[6]Farmer's interview	[7]Actual observation	[8]Tephra-fall thickness, June 12-15, 1991 tephra deposit		CURRENT (2017)	PRE-1991 (1990)
A. Ash															
A1	Rice (Rc)-Rc rotation	Rc-Rc rotation	Zambales	Botolan	Paudpod	22	0-4	37	CG	15	Ash layer not visible	5-10	3	5.0 (rice)	4.0 (rice)
A2	Rc-Rc rotation	Rc-Rc rotation	Zambales	San Narciso	Siminublan	26	0-4	31	Ar	20	Ash layer not visible	15-20	6	5.0 (rice)	6.0-7.5 (rice)
A3	Rc-Vegetable (Veg) rotation	Rc-Rc rotation	Zambales	San Narciso	Beddeng	16	0-4	31	Ar	31	25	15-20	0	3.6 (rice)	2.0-4.0 (rice)
A4	Rc-Corn (Co)-Co rotation	Rc-Rc rotation	Tarlac	Bamban	San Vicente	100	5-9	19	Cr	31	37	5-10	5	3.5 (rice); 7.0 (corn)	-
A5	Rc-Co rotation	Rc-Rc rotation	Zambales	San Marcelino	Lucero	45	0-4	26	Ar	31	25	15-20	1	2.0 (rice)	3.5-4.0 (rice)
A6	Rc-Rootcrop (Ro) rotation	Rc and Ro intercrop	Tarlac	Capas	Sta. Juliana	208	0-4	23	CG	< 31	Ash layer not visible	5-10	2	2.4-4.0 (rice)	4.0 (rice)
A7	Rc-[Ro or Veg] rotation	Rc-Rc rotation	Zambales	Botolan	Paudpod	29	0-4	37	CG	25	20	5-10	9	5.0 (rice)	-
A8	Veg monocropping	Ro and Veg intercropping	Pampanga	Porac	Paralaya	99	0-4	23	Er	-	32	10-15	4	-	-
A9	Veg-Ro rotation, intercropped with fruit trees (Fr)	Fr	Pampanga	Porac	Sapang uwak	273	0-4	16	CG	-	30	15-20	6	-	-
A10	Sugarcane (Su) monocrop	Su and Ro intercropping	Tarlac	Capas	Sta. Lucia	125	0-4	28	Ar	31	Ash layer not visible	1-5	0	50 (sugarcane)	50 (sugarcane)
A11	Ro-Su rotation	Su monocropping	Pampanga	Porac	Mitla	110	0-4	23	Ar	15	Ash layer not visible	10-15	1	50-300 (sugarcane)	> 100 (sugarcane)

Table 6.1 (cont'd). General description of the land utilization types (LUT) associated with different types of pyroclastic deposits in Tarlac, Pampanga, and Zambales provinces.

LUT CODE	[1]LAND UTILIZATION TYPE (LUT) (Cropping pattern per year)		PROVINCE	MUNICIPALITY	BARANGAY	[2]ALTITUDE (m.a.s.l)	[3]SLOPE (%)	[4]DISTANCE FROM CRATER (km)	[5]LAND COVER	THICKNESS (cm) OF PYROCLAST DEPOSIT			YEARS BEFORE CROP RE-ESTABLISHMENT AFTER 1991 ERUPTION	[9]CROP YIELD (t ha^{-1} cropping^{-1})	
	CURRENT (2017)	PRE-1991 (1990)								[6]Farmer's interview	[7]Actual observation	[8]Tephra-fall thickness, June 12-15, 1991 tephra deposit		CURRENT (2017)	PRE-1991 (1990)
A. Ash															
A12	Gr	Rc-Rc rotation	Pampanga	Porac	Mitla Proper	59	0-4	27	CG	-	Ash layer not visible	5-10	-	-	5.0 (rice)
A13	Forest (Fo) with some banana trees (Ban)	Rc and Ro intercropping	Tarlac	Capas	Maruglo	231	5-9	19	CG	< 31	Ash layer not visible	5-10	-	-	-
A14	Fo with Ban	-	Tarlac	Bamban	Sto. Niño	473	5-9	16	CG	-	15	10-15	-	-	-
A15	Veg and Ro intercropping	Su	Zambales	Botolan	Burgos	220	0-4	16	CG	31	Ash layer not visible	15-20	2	-	-
B. Remobilized ash															
R1	Rc-Rc rotation	Su and Rc intecropping	Tarlac	Bamban	San Vicente	90	0-4	23	Cr	31	30	5-10	14	3.6 (rice)	-
R2	Rc-Rc-[Rc and Veg] rotation	Rc-Co-Veg rotation	Pampanga	Floridablanca	Pabanlag	27	0-4	23	Ar	31	45	10-15	8	5.0-6.0 (rice)	-
R3	Rc-[Rc and Co]-Rc and Co] rotation	Rc-Co-Co rotation	Pampanga	Floridablanca	Pabanlag	36	0-4	22	Ar	-	25	15-20	3	5.0 (rice)	5.0 (rice)
R4	Rc-Veg rotation	Fishpond	Tarlac	Bamban	San Vicente	99	0-4	23	Cr	-	40.00	5-10	14	-	-
R5	Ro and Veg intercrop	-	Pampanga	Porac	Sapang uwak	252	0-4	15	CG	-	Ash layer not visible	15-20	-	-	-
R6	Mango trees (Ma)	Gr	Zambales	Botolan	Paudpod	22	0-4	37	CG	-	>80	5-10	-	-	-
C. Lahar															
L1	Rc-Rc-Rc rotation	Rc-Rc-Rc rotation	Tarlac	Concepcion	San Martin	47	0-4	40	Ar	3050	> 1000	<1	5	5.0 (rice)	5.0 (rice)
L2	Rc-[Rc or Ro] rotation	Rc-Rc-[Rc and Veg] rotation	Zambales	San Marcelino	Laoag	52	0-4	27	Ar	-	> 1450	15-20	2	4.0-4.5 (rice); 10.0 (sweet potato)	-

Table 6.1 (cont'd). General description of the land utilization types (LUT) associated with different types of pyroclastic deposits in Tarlac, Pampanga, and Zambales provinces.

LUT CODE	[1]LAND UTILIZATION TYPE (LUT) (Cropping pattern per year)		PROVINCE	MUNICIPALITY	BARANGAY	[2]ALTITUDE (m.a.s.l)	[3]SLOPE (%)	[4]DISTANCE FROM CRATER (km)	[5]LAND COVER	THICKNESS (cm) OF PYROCLAST DEPOSIT			YEARS BEFORE CROP RE-ESTABLISHMENT AFTER 1991 ERUPTION	[9]CROP YIELD (t ha^{-1} cropping^{-1})	
	CURRENT (2017)	PRE-1991 (1990)								[6]Farmer's interview	[7]Actual observation	[8]Tephra-fall thickness, June 12-15, 1991 tephra deposit		CURRENT (2017)	PRE-1991 (1990)
C. Lahar															
L3	[Rc and Veg]-[Co and Veg] rotation	[Rc and Veg]-[Rc and Veg] rotation	Zambales	San Marcelino	Rabanes	68	0-4	25	Ar	150	30	20-25	15	2.0 (rice)	5.4 (rice)
L4	Rc-[Co or Veg] rotation	Rc-Co rotation	Pampanga	Bacolor	Cabetican	9	0-4	36	Er	8240	> 1250	1-5	7	3.0 (rice)	5.0 (rice)
L5	Rc-[Co or Veg] rotation	Rc-Rc plus Co, Veg and Ro in other land parcels	Pampanga	Porac	Libutad	100	0-4	23	Er	50	>1250	10-15	4	4.5 (rice)	4.0-4.5 (rice)
L6	Rc-Su rotation	Rc-Rc-Rc rotation	Tarlac	Concepcion	Telabanca	45	0-4	33	Ar	6100	> 7500	1-5	5	1.4-5.0 (rice)	1.7-3.3 (rice)
L7	Veg monocropping	Rc-Rc rotation	Pampanga	Bacolor	Duhat	39	0-4	31	Ar	2500	> 1100	5-10	22	-	-
L8	Su monocropping	Rc-Rc-Rc rotation	Tarlac	Concepcion	Telabanca	56	0-4	24	Ar	6100	3500	5	8	40-42 [sugarcane]	2.5-4.0 (rice)
L9	Rc-Veg and Ro intercropping	Rc-Veg and Ro intercropping	Tarlac	Capas	Sta. Juliana	90	0-4	24	Ri	6100	-	5	4	0.5-1.0 [taro, <1 ha]	3-3.5 [taro, <1 ha]
L10	Gr	Rc and Co intercropping	Tarlac	Concepcion	Telabanca	47	0-4	24	Ar	-	> 1750	1-5	-	-	-
L11	Gr	Su	Pampanga	Porac	Mitla	85	0-4	33	Ri	-	> 1500	10-15	-	-	-
L12	Gr	Fr	Tarlac	Capas	Sta. Juliana	147	0-4	22	Ri	6100	-	1-5	-	-	-
L13	Fo	Rc-Ro rotation	Zambales	San Narciso	Namatacan	43	0-4	33	Ri	-	8000	15-20	-	-	4.0 (rice)

[1]The LUT shows the cropping system which can be a (1) rotation of two to three short-season crops per year grown in sequence during the wet and dry seasons, (2) monocropping, wherein only one type of crop is grown per year, and (3) intercropping consisting of several crops grown in one parcel of land; 'Rc' rice; 'Veg' vegetables; 'Co' corn; 'Ro' root crop; 'Su' sugarcane; 'Fr' fruit trees; 'Gr'

grassland; ‘Fo’ forest; ‘Ban’ banana, ‘Ma’ mango; crops inside a ‘[ ]’ are grown at the same time during a particular cropping period; [2]In the digital elevation map (Figure 6.2; PhilGIS, 2004b); [3]In the slope map (Figure A6.1; PhilGIS, 2004b); [4]Distance from the Mt. Pinatubo crater; [5]In the land cover map (Figure 6.3; PhilGIS, 2004a), i.e. cultivated area mixed with brushland/grassland (CG), arable land, crops mainly cereals and sugar (Ar), cropland mixed with coconut plantation (Cr), eroded area (Er); grassland, grass covering >70 percent (Gr); riverbed (Ri); [6]Depth of pyroclast layer after the 1991 eruption based on farmers interview; [7]Depth of pyroclast layer after 26 years (year 2017) determined from actual soil profile pit observation; ‘>’ sign indicates that the depth of pyroclastic deposit is deeper than that observed in the soil excavated in 2017; [8]In isopach map (Figure 6.1; Melosantos et al., 1996); [9]Current crop yield refers to the yield average during the previous cropping season prior to the time of interview in 2017 (current) while the pre-1991 crop yield shows the yield average prior to the 1991 eruption (on or before 1990) in no particular season of the year; ‘-‘ no response from the farmer.

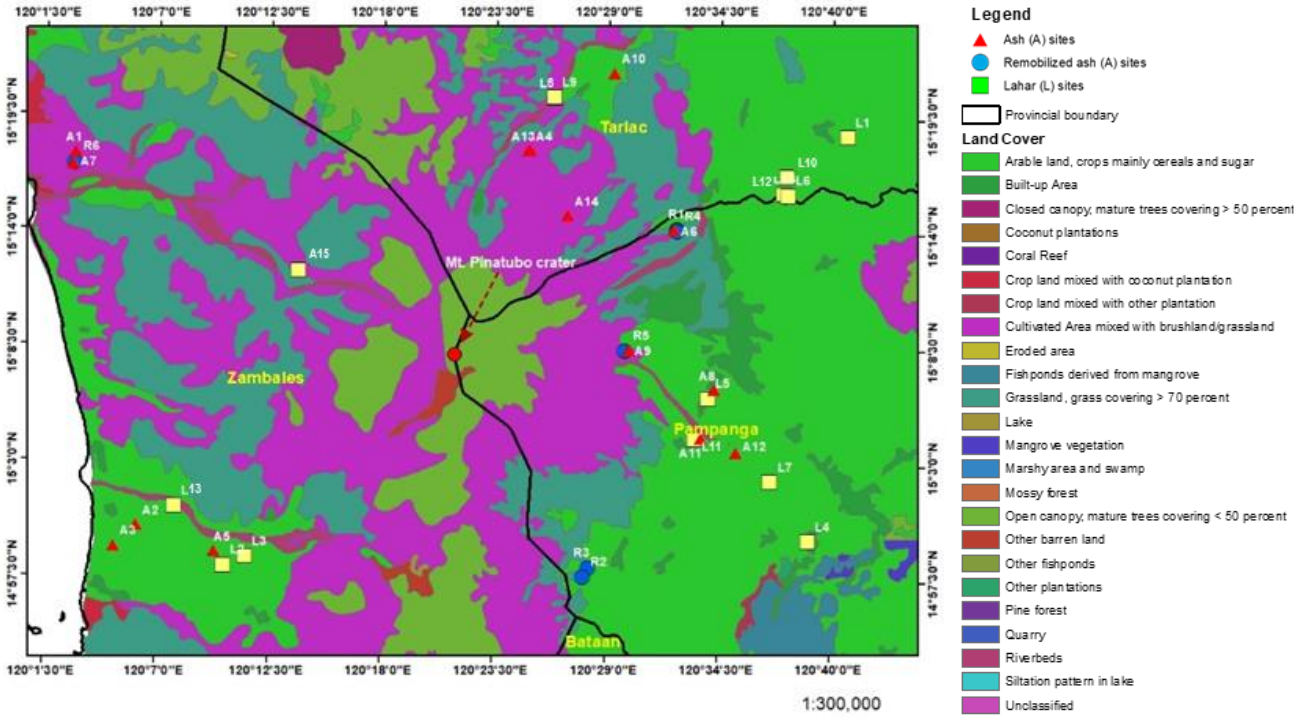

Figure 6.3. Land cover map of the pyroclast-affected sites in Tarlac, Pampanga, and Zambales provinces. *Basemap adapted from PhilGIS (2004a).*

The major crops grown in ash, remobilized ash, and lahar at present include cereals (mostly rice and corn), vegetables (i.e. leafy vegetables, legumes, cucurbits, onion), root crops (i.e. sweet potato, cassava, taro, turnip), and sugarcane. These crops are grown annually either as monocrop (i.e. only one crop grown annually) or mixed cropping, either in cropping rotation (i.e. 2-3 short season crops grown in sequence) or intercropping (i.e. the second crop grown in sequence in a year is mixed with other crops). The cultivated fields are found in areas of varying altitudes (9-252 m.a.s.l) and in gentle to slightly undulating slopes (0-9 %; Fig. A6.2). Fruit trees such as banana are grown in forested ash areas of higher altitudes, as observed at the A13 (231 m a.s.l.) and A14 (473 m.a.s.l.) sites. Mango is cultivated in a remobilized ash site at a lower altitude (22 m.a.s.l). Grassland vegetation is observed in one out of the 15 ash-affected sites, and in three out of the 13 lahar-affected sites.

According to Figure 6.1, all LUTs were exposed to tephra falls in 1991; the deposit thickness varied from <1 to 20 cm. The farmers reported that the ash- and remobilized ash-affected LUTs were covered by a thinner deposit (up to ~30 cm) compared to the lahar-affected LUTs, which sometimes were buried under more than 8.2 m of materials. Our observations on excavated soil profiles indicate that the 1991 pyroclast deposit is no longer visible in eight out of the 15 ash-affected LUTs and in one out of the six remobilized-ash LUTs.

Most of the farmers interviewed abandoned their farms temporarily after the 1991 eruption of Mt. Pinatubo. Farming resumed after 1 to 9 years in ash-, 3 to 14 years in remobilized ash-, and 2 to 22 years in lahar-affected LUTs. Farmers from seven ash LUTs declared a current average yield for rice in the range 2-5 t ha^{-1}. Comparable values are claimed in the cases of the remobilized ash LUTs (3.6 to 6.0 t ha^{-1} rice $cropping^{-1}$) and lahar LUTs (2 to 5 t ha^{-1} rice $cropping^{-1)}$. Sugarcane yields 50 to 300 t ha^{-1} in ash LUTs (i.e. A10 and A11) and 40 to 42 t ha^{-1} in a lahar LUT (i.e. L8). The yield of corn in A4 is reported to be 6.9 t ha^{-1}. Sweet potato production in L2 is 10 t ha^{-1}. The yield from taro in L9 is 0.5 to 1 t for less than 1 ha farm. Some of the farmers interviewed

provided information on their average yields they obtained from their recent production in comparison to what they usually harvest prior to the 1991 eruption. The present average yield of rice in A2, A5, and L3 LUTs are noted to decrease significantly by 1 to 3 t ha^{-1} compared to their pre-1991 production. In A1 LUT, however, the yield of rice has increased by 1 t ha^{-1} compared to the pre-1991 production. The rice yields obtained from A3, R3, L1, L5, and L6 at present are comparable to their production prior to the 1991 pyroclast deposition. Sugarcane yields at present are comparable with that of the pre-1991 eruption in both A10 and A11 with yields ranging from 50 to 300 t ha^{-1}.

Current and pre-1991 cropping system and management of the land utilization types

The age of the farmers/agricultural technicians interviewed, mainly men, range between 35 to 85 years old with 5 to ~50 years of farming experience (Table A6.2). Twenty-four percent of the surveyed farms are owned by the farmers while the rest are under cash or sharecropping tenancy. In a cash or sharecropping tenancy, the farmer cultivates the land and shoulders the expenses for crop production. Afterward, the farmer pays the landowner for the use of the land either by annual rental fee or in the percentage of the harvested crop in monetary or goods.

The farm areas of all the LUTs range from < 1 to 8.8 ha where thirty-eight percent are considered small-hold farms having less than two hectares of land (Sys et al., 1991). Sixteen out of the 34 farmers interviewed were able to attend seminars or training about farming led by the local government or non-government agencies. One farmer (A15) mentioned that his farm has been used as an experimental area by a research institution on the application of organic (chicken dung) and inorganic fertilizers, and the methods of planting in lahar.

Rice is the major crop grown across the LUTs at present and during pre-1991 crop production system, respectively, i.e. ash LUTs (50 and 64 %, respectively) remobilized ash LUTs (67 and 50 %, respectively), and

lahar LUTs (50 and 79 %, respectively) followed by root crops, vegetables, and sugarcane. Rice is often grown as a monocrop (2-3 seasons per year) or as the main crop in a cropping rotation, typically grown during the wet season from June to December. Corn, vegetables, and/or root crops are commonly grown during the dry season (i.e. January to May). The majority of the rice farmers are utilizing inbred rice varieties during the pre-1991 eruption and at present, some of the LUTs have tried to grow the higher yielding-hybrid varieties (i.e. A5, R2, R3, L2, L3, L5). The sources of irrigation are the national irrigation system, communal irrigation system, shallow tube well, small farm reservoir, seepage from rivers, spring, deep well, diversion of water from dams/dikes, free-flowing water, and rainfall. Fertilizers are applied in the majority of the LUTs, i.e. 74 and 50 % of the 34 LUTs (including ash, remobilized ash, and lahar sites) at current and pre-1991 cropping systems, respectively. The types of fertilizers applied are inorganic fertilizers (i.e. urea [46-0-0 % Nitrogen (N)-Phosphorus (P)-Potassium (K)], complete [14-14-14 % N-P-K], muriate of potash [0-0-60 % N-P-K], ammonium sulfate [21-0-0-24 % N-P-K-Sulfur (S)]), and organic fertilizers (i.e. chicken manure, commercial organic fertilizers, molasses [for sugarcane]) applied singly or in combination. The fertilizer rates supplied vary with the type of crops grown, the period of cultivation (i.e. current and pre-1991), and the financial capability of the farmers.

Weed management is done by manual weeding, sometimes in conjunction with herbicides. Pesticides are applied as necessary to control insect pests and diseases. Many of the LUTs at present are already partly mechanized; the farmers use a hand tractor for land preparation (8 out of 15 in ash-, 4 out of 6 in remobilized ash, and 9 out of 13 in lahar-LUTs) but in some cases, it is still coupled with animal-drawn implements. Prior to the eruption, there were only four ash-, two remobilized ash-, and four lahar-LUTs out of the 15, 6, and 13 LUTs, respectively, which used tractors while the rest relied on draft animal powers and hand tools or was untilled.

The types of crops grown prior to and after the Mt. Pinatubo eruption did not change significantly although the cropping patterns/rotation in most of the LUTs have changed. This is the case for 3 out of the 14 ash LUTs, 2 out of the 5 remobilized ash LUTs, and 6 out of the 13 lahar LUTs. Only slight alterations in cultivation practices were reported for 8 out of the 14 ash LUTs, 2 out of the 5 remobilized ash LUTs, and 5 out of the 13 lahar LUTs. These concerns mostly the cropping pattern (i.e. the crops grown after the main crop) but the main crops such as rice (in the case of rice-based cropping system) are still grown. For example, the A3, A4, and A5 LUTs were grown with two cropping seasons of rice per year before 1991, but are now cultivated with rice during the wet season only and corn or vegetable during the dry season. For some LUTs however such as A12, L10, L11, and L12 which used to be cultivated for rice, sugarcane, and corn are now turned into grasslands. R4, which was utilized as a fishpond before 1991, is now cultivated with rice and vegetable. Only six out of the 34 sites (i.e. 3 from ash LUTs - A1, A2, A6, 1 from remobilized ash LUT – R3, and 2 from lahar LUT area – L9, L23) have returned to the same cropping system (rice-based) but it took the farmers 3 to 7 years before being able to recultivate the land after the eruption.

The change in land use or cropping system was not solely due to pyroclast deposition. In A11, sugarcane monocropping was converted to a cropping rotation of sugarcane with root crops (i.e. sweet potato), because there were no more available molasses (which commonly applied to the sugarcane crop as a fertilizer) in the market due to exportation. In A15, sugarcane was converted to vegetable and root crop intercropping because the sugarcane mill where the farmer brings his produce for sugar extraction closed in the mid-80s.

In some LUTs, the impacts of pyroclast deposition on soil properties are reasons for the shift in land use, crop type, or cropping pattern. For instance, in A12, a previously rice-grown area has shifted to grassland because the squash crop that the farmer tried to grow in the pyroclast died after one week of no rain; the plants didn’t survive because of the

hot temperature of the soil, and the root dried up, turned white, and died. He further added that "before the eruption, the water stays in the soil even after five days but after the deposition of sand, it already dries up in one day". The farmer also reports that it was "very difficult to cultivate the land due to its stoniness". The same case is observed in L6, rice monocropping was changed to rice and sugarcane cropping rotation due to insufficient water for the sustenance of rice production during the dry season. The farmer noted that sugarcane requires less water and he can always harvest something as long as he uses fertilizers. The farmer at L8 also switched to sugarcane monocropping as the rice wilted when grown in the lahar deposit. In L11, the cropland was turned into grassland as the sugarcane grew poorly due to the sandy texture and high temperature of the lahar deposit resulting in drought, and ineffectiveness of applied fertilizers according to the agricultural technician. In L13, previously grown with rice and root crops is now under forest vegetation due to the increased topography of the land after lahar deposition resulting in difficulty of accessing water for irrigation.

Some LUTs that were not used for agriculture prior to the 1991 eruption of Mt. Pinatubo are now grown with crops. For example, LUT R6 used to be a grassland but is now grown with mango. LUT R4 had a very shallow water table prior to the eruption and was being utilized as a fishpond. After the deposition of remobilized ash materials, the farmer decided to plant rice and vegetables.

6.3.2 Land quality constraints on crop production as perceived by the farmers/agricultural technicians

Table A6.3 to A6.4 summarises the land quality constraints and positive effects, respectively, imposed by pyroclastic deposition and from other factors that are not directly caused by the pyroclasts that affect their crop productivity. It also shows the adaptation practices of the farmers in response to their identified constraints.

Land quality constraints in relation to the presence of a pyroclast deposit

A large proportion of the farmers conveyed that after the pyroclast deposition, the soil became sandy, the water drained fast, and the soil easily dries up (i.e. 9 out of the 15 ash-, 4 out of the 6 remobilized ash-, and 11 out of the 13 lahar-LUTs). Stoniness was also causing the fast drainage of water according to farmers in A12, L1, L4, L7. However, two farmers reported that the soils, although sandy, had become sticky or muddy upon wetting (i.e. A1, A6). Poor crop and root growths resulting in low yields or death of the plants were reported in 8 ash-, 4 remobilized ash-, and 9 lahar-LUTs. Some of the rice farmers encountered similar symptoms on their transplanted seedlings wherein the plant leaves turn reddish, growth is stunted which eventually wilts and die (Fig. 6.4). They observed this to occur during the wet season (i.e. A1, A4, R1, L2, L3, L4). Flooding causes the chlorosis (i.e. reddish coloration) and death of rice seedlings a few days after transplanting as referred to by the farmers in LUTs mentioned previously. A farmer in L4 LUT who also serves as the municipal agriculturist identified this problem as zinc deficiency.



Figure 6.4. Young rice plants grown in lahar soil at San Marcelino, Zambales showing stunted growth and chlorosis.

A sugarcane farmer said that after the ash deposition, the extracted sugar in his harvest had decreased which he believes to be due to the low potassium content of the ash (i.e. A11). Weed infestation is also noted as a direct consequence of the pyroclast deposition (i.e. L4). The hardness of the pyroclast deposit disrupted the normal growth of plants due to difficulty for root expansion according to the farmers in A3, A5, L2, L6, L7 LUTs. The soil workability is also compromised due to the sandy texture, hardness, and stoniness of pyroclast deposits, especially in lahar LUTs, where farmers mentioned that the material hardens like a "cement" (i.e. 7 ash-, 3 remobilized ash-, 8 lahar-LUTs). The temperature of the pyroclast deposit also tended to increase during the cropping season and this was detrimental and sometimes lethal to plant root growth (i.e. 3 ash-, 1 remobilized ash-, 4 lahar-LUTs).

Another constraint that has become persistent after the eruption is flooding, which temporarily causes waterlogging (i.e. 4 ash-, 1 remobilized ash-, 6 lahar-LUTs) depending on the intensity of the rain (Fig. 6.5). This is suspected to induce zinc deficiency as mentioned earlier. Proneness to surface erosion due to flooding during heavy rains is a constraint in LUTs A4, A5, A10, A11, L2, L3. The deposition of eroded materials from nearby mountain slopes is experienced in R4. The L9 located at low altitudes is still flooded with lahar at present during the rainy season.



Figure 6.5. Waterlogging during the rainy season in a lahar soil (LUT L9) cultivated with taro at Capas, Tarlac.

Few farmers also complained about the whitish, sometimes rusty, acidic water that rises up from the groundwater during the wet season which causes the death and sterility of the rice plants (i.e. A5, L1, L4). There is also the presence of foul-smelling dark mud which the farmers suspect to cause the poor plant growth (L1, L4, L9). According to the farmer of L9 LUT, when the black mud is buried with yearly lahar deposition up to the present, the growth of rice improves. Water scarcity is a serious problem, especially during the summer months due to less rainfall and a deeper groundwater level. The areas relying on STW and which source out water from spring waters and SFR (i.e. 4 ash-, 4 remobilized ash-, 4 lahar-LUTs) are more vulnerable to drought due to the difficulty of tapping water supply (i.e. 4 ash-, 2 remobilized ash-LUTs). This problem is even more acute in areas located at higher altitudes (i.e. A13, A14, L13).

The scarcity in water supply had been aggravated after the 1991 eruption as most of the irrigation facilities buried or damaged by pyroclast deposits (but lahar in particular) have not yet been rehabilitated (i.e. A3, A5, A12, L3, L8). Figure 6.6 shows a vast area of land in San Narciso, Zambales unutilized during the dry season due to lack of water supply. Ironically, these areas are also subject to flooding during the wet season because the riverbed had become shallow after the lahar deposition. According to the agricultural technician interviewed, during the rainy season, the seepage from the riverbed causes runoff which affects the fertilization and growth of the rice plants grown in this area.

Land quality constraints in relation to other factors

Other external factors that cause poor crop growth are weed, (i.e. A2, L4) pest, and disease infestation (6 ash-, 5 lahar-LUTs), and climatic hazards, i.e. typhoons and heavy rains (7 ash-, 1 remobilized ash-, 1 lahar-LUTs). Crop production is less during the dry season especially in areas where there is a limited supply of irrigation.

(a)  *(b)* 

Figure 6.6. Lahar-affected soils in San Narciso, Zambales left barren during the dry season due to lack of irrigation but is flooded during the wet season *(a)*, rice plants grown in a portion of the land during the dry season but has wilted due to severe moisture stress *(b)*.

6.3.3 Adaptation of farming practices

Adaptation to constraints in relation to the presence of a pyroclast deposit

Deep plowing using a disc hoe to a depth of 50 cm was the initial rehabilitation approach of six ash-, two remobilized ash, and two lahar-affected LUTs to mix the pyroclastic deposits with the original soil (A1, A2, A4, A5, A11, A15, R1, R2, L3, L5). This was done through the initiative of the local government in 1992. Only a few of the sites where the irrigation facility was buried with the pyroclastic deposition were repaired with the aid of the local government (i.e. A1, L1, L2). Farmer organizations financed and managed the installation and maintenance of a communal irrigation facility that would support many adjacent farms (i.e. A2, A4, R1). Other farmers installed their own irrigation facilities such as water pumps (STW, electric pump, deep well), and constructed small farm reservoirs (i.e. 6 ash-, 1 remobilized ash-, and 3 lahar-LUTs) (i.e. Fig. 6.7a-c). Some connected from water sources such as rivers, dams, spring, and free-flowing water through leveling and canal construction (i.e. 4 ash-, 1 remobilized ash-, and 4 lahar-LUTs)

(i.e. Fig. 6.7d). One farmer installed a drip irrigation system on his farm (i.e. L7). The farmers in LUTs A9, A12, L6, L8 only relied on rainfall as their source of moisture due to a lack of finances to install new irrigation facilities. Some of the farmers adapted to the fast drying of their soils by increasing the frequency and volume of irrigation (i.e. A3, A4, A10, L5).

(a)  *(b)* 

(c)  *(d)* 

Figure 6.7. Some types of irrigation systems installed/constructed by farmers in pyroclast-affected farms, *(a)* deepwell, *(b)* small farm reservoirs, *(c)* engine-powered water pump, *(d)* diversion of free-flowing water.

A farmer in LUT A3 tried to conserve moisture by spreading the crop residues over his field (i.e. A3; Fig. 6.8). To overcome the difficulty in planting rice in the hard and dry soil, the soil was saturated first before transplanting (i.e. R2, L3). Planting of rice was also done by direct seeding wherein the seeds are scattered in the field (i.e. A5, L6). Rocks

in the pyroclast were removed by manual and mechanical removal with the aid of a tractor (i.e. L7) or collection of the rocks and burying them deep under the soil (i.e. L1).



Figure 6.8. Mulching of rice straw residues to conserve moisture in a vegetable farm affected by ash at San Narciso, Zambales (LUT A3).

To address the poor crop growth and low yields, the farmers resort to the application of higher doses of inorganic fertilizers (i.e. A4, A5, A6, R2, L1) while others have supplied organic fertilizers such as chicken manure and commercial organic fertilizers (compost) in addition to inorganic fertilizers (i.e. 7 ash LUTs, 3 remobilized ash LUTs, 4 lahar LUTs). Some of the farmers mixed the pyroclast with the original through plowing and/or rotavation during land preparation (A1, A15, R1, L1, L5, L9).

A farmer in L4 LUT applies fertilizers in between the rice plants and then covers it by furrowing (i.e. L4). In L6 and L8, the farmers scraped off the surface lahar and then plowed the remaining lahar material. The Aeta farmer in A9 LUT removed the ash in the sloping areas and planted the original soil with banana but in the flat areas where he planted cassava and taro, the ash was not removed. The farmer in A6 and L2 LUTs chose good/high yielding crop varieties to get better yields while the farmer in A11 decided to rotate the cropping of cassava and sugarcane depending on the vigor of the crops and market demand.

Planting at the original soil through digging and removal of the pyroclast is done by the farmer in A15 LUT. The reddening of the rice leaves and death of rice seedling was ameliorated by draining the soil (i.e. L4) and applying zinc sulfate (i.e. A1, A4, R1, L2, L3, L4). The zinc sulfate applied was a subsidy from the local government which is part of the rehabilitation program for Pinatubo-affected farms. The agricultural technicians advised the use of zinc sulfate to ameliorate the soils with problems on zinc deficiency.

The weed problem which a farmer attributed to the deposition of pyroclast deposit was eradicated by plowing under the pyroclast material and continuous cultivation (i.e. L4). The increase in temperature of pyroclast affected LUTs is amended by the frequent and higher rates of irrigation (i.e. A4).

Constraints on hard structure and stoniness during land preparation are attenuated through the use of mechanical hand tractors (i.e. A5, R2, R3, L1, L2, L3, L4, L6, L7), frequent irrigation (i.e. L5), watering the soil before plowing (i.e. A4, R1, L3) and additional hired laborers to cultivate the land (i.e. A2, R3, L2). Rice is planted by dry direct seeding instead of wetbed and transplanting methods (i.e. A5, L6). The earlier adaptation practice by a farmer in A5 LUT to the poor root growth due to the hard structure of the ash is by digging a hole and seeding at the buried soil.

The LUTs which are prone to waterlogging and poor drainage due to flooding are drained by destroying the bunds/dikes (in the case of paddy soils) to drain excess water (i.e. A2), planting of rice is done by either transplanting of rice at shallow depths or direct seeding to avoid the submergence of the seedlings with the water table (i.e. A1) and growing of rice in the submerged area because no other crop can grow on it (i.e. L3). Erosion constraints are prevented by not removing the weeds and by adjusting the planting calendar to avoid the heavy rain and flooding periods especially during the rice-growing season (i.e. R4).

Government aid in the agricultural rehabilitation, aside from deep plowing, was in the form of seed (i.e. A2, A4, A5, R2, R3, L2, L7) and fertilizer subsidies (i.e. A2, A3, L3), such as distribution of zinc sulfate (i.e. A2, A3, L3), and the rehabilitation of national irrigation system (NIS) (i.e. A1, L1, L2). Some farmers indicate that they did not receive any form of assistance from the government (i.e. A7, A8, A10, A12, R1, R4, L9).

Adaptation to constraints in relation to other constraints

Other constraints on farming which are not directly influenced by a pyroclast deposit but which have exacerbated the land quality constraints of the current growing conditions of the crops such as climatic hazards (i.e. occurrence of typhoons that induces flooding and erosion) are avoided by adjusting the planting calendar (i.e. R4), destroying dikes to drain floodwater (i.e. A8), not cultivating the field during the rainy season to avoid crop yield loss from flooding (i.e. A15, L9), and in extreme cases, leaving the field idle permanently due to very shallow water table (i.e. L12).

Water scarcity during the dry season are ameliorated by installing supplemental irrigation systems such as STW and SFR, leveling the area and constructed diversion canals to divert water from rivers or dams (i.e. A7, A8, L1), adjusting the planting calendar for rice to maximize water availability during the rainy season and escape too much heat during summer season (i.e. L3), utilizing the moisture left after the harvest of the first crop by plowing the soil immediately and planting the subsequent crop (i.e R5), dividing the farm among different crops of different water requirement during the dry season (for instance, rice and sweet potato, are intercropped instead of growing rice only (i.e. L2), shifting in crop type being grown: i.e. rice was replaced by root crops, vegetables, corn, or sugarcane (i.e. A7, A8, L6) which require less water during the dry season, turning the dry season into a fallow period when there is no water available (i.e. A7), leveling the soil for easier and even distribution of water (i.e. R3), and continuing to

cultivate crops even if the water is insufficient and survival of plant is uncertain (i.e. A7). The areas that have difficulty to tap water, especially those located in high altitudes, turned into a forest (i.e. A13, A14). However, the Aetas in A14 still benefited from the forest products, for instance, timber is converted to charcoal. Some banana trees are also grown in these forest areas as sources of food and sold to lowlanders as their source of income.

Pest problems are managed by applying insecticides and pesticides (i.e. A4, A8, L3, L4, L5, L9), adjusting the planting calendar to escape the months with heavy pest infestation (i.e. A4), and employing traditional management practices such as covering the sown rice seeds with mud to protect from bird infestation (i.e. L4).

6.4.4 Positive effects of pyroclast materials on crop production as perceived by the farmers

The positive effects of pyroclastic deposits on land qualities were seldom testified and tended to occur mainly in ash-affected soils and rarely in lahar affected areas. The sandy nature of the pyroclast deposition was beneficial in improving the drainage and aeration of the subsoil and favored the growth of vegetables (i.e. A6, A8, A3), respectively. Furthermore, the addition of pyroclast in 5 ash LUTs, 3 remobilized ash LUTs, and 1 lahar LUT has improved the workability as the soil structure became more friable and easy to cultivate. In A10, the farmer claimed that his sugarcane yield has improved after ash deposition because the buried soil, which is a hardpan, had deepened, but eventually, the yield declined in some portions of his farm where the ash has been washed away by the rain (Fig. 6.9). The farmers noted that soil nutrition has improved (for 7 ash LUTs and 1 remobilized ash LUT) as reflected by the improved germination and crop growth (i.e. A8; Fig. 6.10). The growth of sugarcane and extracted sugar has been claimed to increase in a lahar affected soil (i.e. L8; Fig. 6.11). According to the farmer in A6, the ash mixed with the original soil has improved the resistance of the soil to erosion.

(a)  *(b)* 

Figure 6.9. Sugarcane farm affected by ash in Capas, Tarlac (LUT A10) *(a)*, soil profile showing the hardpan below the 20 cm surface ash layer *(b)*.

(a)  *(b)* 

Figure 6.10. Spring onion *(a)* and camote tops *(b)* grown in an ash-affected soil (LUT A8) in Porac, Pampanga .



Figure 6.11. Sugarcane grown in a lahar soil (LUT L8) at Concepcion, Tarlac.

6.4 Discussion

6.4.1 Land/soil quality constraints in relation to the type of pyroclastic deposit

Except for a few sites in the ash-affected LUTs (A3, A10), the deposition of pyroclastic materials during the 1991 eruption of Mt. Pinatubo resulted in the temporary abandonment of agricultural fields regardless of location, type, and thickness of the volcanic deposit. Some of the agricultural sites visited never recovered from ash and lahar deposition, and are no longer cultivated (A12, A13, L10, L11, L12, L14). Our survey reveals that this is a consequence of the destruction of major irrigation systems, unfavorable soil properties, poor crop performance, and lack of capital to purchase crop inputs and install new or repair the damaged irrigation system. In other places where the cultivation of the eruption-impacted fields resumed, the farmers have been facing a variety of land quality constraints regardless of the nature of the volcanic deposit (i.e. ash, remobilized ash, lahar) covering the formerly cultivated soil. The main constraints identified and which are common to the three types of pyroclastic material relate to poor water retention in the soil, high drainage, nutrient limitations, and low soil workability.

Water-related constraints

Poor water holding capacity in soil reflects high hydraulic conductivity values, usually resulting in low water content (Hillel, 1998). The soil-water characteristics (soil water potential and hydraulic conductivity) are primarily determined by soil texture (sand, silt and clay contents) (Hillel, 1998). It is well known that water infiltration and hydraulic conductivity increase from clayey to sandy soils. For example, the large dataset compiled by Rawls et al. (1982) for ten soil texture classes indicates that the saturated hydraulic conductivity of soil with a sand texture (K_s = 21 cm h^{-1}) is ~350 times greater than that of clay soil (K_s = 0.06 cm h^{-1}). Structure (the grouping of soil particles into porous

compounds) also plays a role as it influences soil porosity. Increased organic matter content generally produces soil with increased water holding capacity and hydraulic conductivity, largely as a result of its influence on soil aggregation and associated pore space distribution (Hudson, 1994).

According to the grain size analysis of the soil profiles described in chapter 3 (Fig. 3.5; Table A3.2), the texture of the cultivated soils in the lahar- (IR-Lahar) and ash- (IR-Ash) impacted area will vary between loamy sand and silt loam, respectively. Referring again to Rawls et al. (1982), one may expect K_s values on the orders of 6.0 cm h^{-1} and ~0.7 cm h^{-1}, respectively, for these two soil texture classes. We also note large diameter (> 2 mm) gravel particles and small rocks present in the lahar material will decrease the amount of soil matrix in which water can be stored or conducted (Saxton et al., 1986). Clearly, cultivation on lahar materials will likely be rendered difficult due to rapid drainage, in accordance with the issue pointed out repeatedly by farmers growing rice, corn, vegetables, root crop, and sugarcane in the lahar-affected soils. Further, these areas may develop drought conditions at the slightest water desaturation of the surface soil.

Rawls et al. (1982) proposed a linear regression equation to estimate the soil-water content at different soil-water potential values:

$$\theta_p = a + b\,(\%\ \text{sand}) + c\,(\%\ \text{silt}) + d\,(\%\ \text{clay}) + e\,(\%\ \text{SOM}) + f\,(\text{BD},\ \text{g cm}^{-3}) \quad \textit{Eq. 6.1}$$

where θ_p is the volumetric soil water content (%), SOM is the organic matter content, BD is the bulk density, and $a, b, c, d, e\ and\ f$ are regression coefficients. Using the values for $a, b, c, d, e\ and\ f$ provided in Table 3 of Rawls et al. (1982), it can be seen that the clay content is the most important texture factor in the soil-water potential-content relationship and that the equation has a small sensitivity to organic matter and BD. Given the low SOM content estimated in our soils (~1-

3.5 %, Table A3.3), organic matter probably has a minor influence on soil moisture. Based on Eq. 6.1 and the grain size data from Table A3.2, we estimated θ_p for the loamy sand texture representative of the 26-year old lahar material. At field capacity (i.e. soil-water potential of 10 kPa), θ_p will not exceed ~15 %, decreasing to ~11 % at the point of wilting (i.e. soil-water potential of 1500 kPa). As already emphasized by Icamina (1992), growing rice on lahar implies high percolation rates and poor water economy. Water is also difficult to impound as the bunds easily slake and destabilize when watered.

The farmers also report poor water retention in the ashy soils grown to rice, although these soils may have K_s values (~0.7 cm h^{-1}) roughly one order of magnitude higher than those typifying a soil developing in a lahar deposit. However, it is desirable for the K_s of a paddy field to be lower than ~0.04 cm h^{-1} in order to maintain flooding water levels (Singh, 2011). Thus, the ash soils probably do not meet this criterion either. For the silt loam texture that represents the cultivated surface ash soil, we calculated from Eq. 6.1, a θ_p of 45 and 17 % at field capacity and wilting point, respectively. Although the soil water characteristics are better in the case of the young soils developing from ash materials than in those forming from lahars, there is a similar issue of poor water retention and insufficient soil moisture.

The texture of the buried soils in the two cultivated soils examined in chapter 3 does not differ massively from that of their corresponding modern soils (Table A3.2). This would imply a more or less similar water holding capacity and drainage conditions of the agricultural soils prior to the 1991 eruption of Mt. Pinatubo. Most farmers acknowledged that the pre-1991 soil water characteristics are more ideal compared to the new volcanic deposits and as a result, they have to tap significantly more water in order to meet the water requirement of plants. The buried soil is more weathered than the surface soil and prior to burial, it probably contained more organic matter than what we measured. This might have sufficed to enhance the structure and hence, water retention.

Some farmers at five ash-impacted sites (A1, A2, A4, A5, and A7) and one lahar-affected site (L13) reported that poor soil drainage and waterlogging was a recurrent issue, especially after a heavy rain event. This is contradictory to the previous finding that emphasizes the poor water holding capacity of the newly formed soils. As suggested earlier, the buried soil underlying the 1991 ash/lahar deposit should not impede the downward water flow. We note that all the sites where waterlogging constitutes a problem are located near a riverbank (Fig. 6.1). One conceivable explanation to reconcile the two apparently antagonistic observations relates to the impact on the riverbeds from recurrent events of lahar deposition since 1991. Several investigations indicate that the river channels have been clogged by lahars and as a result, the height of the riverbed has raised (Gonzaga & Orejas, 2011; Mizuta, 2009). During heavy rainfall, the rise in the water level may lead to rapid infiltration into the adjoining lowlands covered by the ash and lahar materials and thus, to temporary waterlogging. Nelson (2013) interrogated rice farmers affected by lahars in Pampanga Province and reported occurrences of such phenomenon. Ironically, it appears that farmers had to move closer to rivers so that they can tap enough water to irrigate their crops, in particular during the dry summer months.

Nutrient-related constraints

Several farmers (A5, A7, A10, R1, L2, L3, L8, L9) evoked soil/groundwater acidity as a factor explaining poor plant and root growth. It has been shown that Mt. Pinatubo's lahars have acidic pH values ranging from 4.2 to 5.1 (Reyes & Neue, 1991). Twenty-six years after the eruption, we also measured a low pH_{H2O} = 3.35-3.53 for the lahar material (IR-Lahar) from a rice field in San Marcelino, Zambales (Fig. 3.8a and Table A3.3 in the results section of Chapter 3). In addition, the other cultivated soil profile analyzed earlier (IR-Ash) also display relatively low pH_{H2O} values = 4.62-4.91. At pH ~4.5, Al becomes soluble and its presence in the soil solution can harm plant growth and notably root development (Pansu & Gautheyrou, 2006). This might account for the "acidity" issue evoked by the rice farmers.

Although the origin of the acidic pH values in the MS is not entirely clear, they seem to be associated with paddy fields. Paddy field soils are soils under submergence with varying redox conditions caused by the alternation of wetting and drying. Major elements affected by redox conditions in soil are C, N, Mn, Fe, and S. Changes in water saturation also leads to pH fluctuations. For example, the reductive dissolution of iron oxides consumes protons (Nanzyo & Kanno, 2018). Some farmers reported a foul smell when the paddy soils (A1 and A2) are waterlogged. This suggests the emission of hydrogen sulfide, which may be a product of the microbial reduction of dissolved sulfate in the presence of organic matter. The source of this sulfate is probably anhydrite contained in Mt. Pinatubo's ejecta.

Under reducing conditions, the soil solution may become saturated with respect to pyrite (FeS_2), leading to its precipitation. Upon drainage and oxygenation of the soil pores, pyrite may be oxidized, releasing acidity in the form of sulfuric acid. Such conditions can affect rice production due to enhanced solubility, and hence Al toxicity at low pH values. In addition, acidic conditions can enhance the loss of nutrients such as Ca, Mg, Zn, and Cu. The availability of P may equally be depressed due to adsorption on the positively charged soil secondary mineral (Neild et al., 1998; Nanzyo & Kanno, 2018). Examples of non-volcanic soils dominated by pyrite are alluvial soils intermittently inundated by seawater during low and high tides. These areas become highly acidic ($pH < 3.5$) due to sulfide oxidation when these coastal plains are opened up for crop production (Shamshuddin, 2006; Shamshuddin et al., 2004). The acidity of this so-called "acid sulfate soils" ($pH < 3.5$) is derived from the subsequent dissolution and release of large amounts of Al^{3+} from Al containing materials in the soil solution and exchange complex which is reported to affect crop and root growths such as in oil palm (Auxtero & Shamshuddin, 1991), cocoa (Shamshuddin et al., 2004), and rice (Elisa et al., 2016) production. Hydrogen sulphide gas (H_2S) formation is also reported to occur in non-volcanic lowland rice acid sulfate soils. The presence of H_2S prevents the roots from absorbing

nutrients, causing black crown and root rot in rice, symptoms known as bruzone “akiochi” disease (Shamshuddin et al., 2014).

Zinc deficiency appears to affect rice cultivation in both the ash- and lahar-impacted areas. Zinc limitation produces several symptoms in rice, usually appearing two to three weeks after transplanting of seedlings. The leaves develop brown blotches and streaks that may fuse to cover the older leaves entirely, plants remain stunted, and in severe cases, cause the plants to die. If the plants recover, it will show a substantial delay in maturity and reduction in yield (Yoshida & Tanaka, 1969; Van Breemen & Castro, 1980; Neue & Lantin, 1994). These symptoms appear to coincide with the description of the farmers. Fresh pyroclastic materials are inherently low in available Zn (Brehler & Wedepohl, 1978). Besides, precipitation of zinc sulfide may occur under waterlogged conditions in paddy soils and makes zinc temporarily unavailable (Carbonell-Barrachina, et al., 2000). Zinc can also form complexes with phosphate, reducing its availability (Alloway, 2008; Imtiaz, 1999). As the plant-available P in irrigated rice ash and lahar-affected soils showed a high concentration (Chapter 5; Table A5.1; i.e. R1), we hypothesize that the zinc deficiency may also relate to the pool of the bioavailable P associated the with the ash and lahar’s pyroclast material.

Soil workability

Workability is a desirable soil condition during tillage. Workability refers to the condition of the soil when tillage operations can be executed without causing structural damage. In lahar deposits, the presence of stones and boulders decreases soil workability. Sometimes, this material is buried deep into the soil. The soil may also become hard upon cycles of wetting and drying, possibly a result of the cementing of particles via salt precipitation. Additionally, rearrangement of soil particles with different sizes may also lead to soil hardening (Hillel, 1998), where the layering of ash and pumice materials during the

different phases of the eruption of Mt. Pinatubo may promote compaction.

6.4.2 Adaptation and rehabilitation strategies

The time elapsed before cultivation after the 1991 eruption varied among the farmers. The principal factor was the operator's financial capacity to install new or rehabilitate the damaged irrigation facilities. It was necessary to rent tractors to plow the abandoned fields filled with grasses, drain those submerged, and level the land where the original landscape was altered at different scales by the volcanic deposits. Although the local government provided financial assistance for rehabilitating crop cultivation, some farms (7 out of the 34 sites surveyed) did not receive such aids and in this case, agricultural restoration merely relied on farmers' financial capability and adaptive skills.

Although rice remains to be the major crop grown in most LUTs affected by the pyroclast deposits due in part by the necessity to produce this crop for the farmers' own consumption, most of them diversified their cropping system mainly to cope with the constraint on limited water availability. Notably, farmers shifted from rice monocropping to growing rotation crops as these can survive under low moisture conditions. For instance, instead of growing rice for two to three consecutive seasons per year, rice is only grown during the wet season when rain and/or supplementary irrigation is sufficient to meet its water requirement. The second crop is replaced either by vegetables, root crops, and even sugarcane which are more tolerant of arid soil conditions. Farmers in some lahar-affected areas were forced to abandon rice cultivation and to grow sugarcane or root crop (i.e. L7, L8) due to very limited water supply.

Several interviewees told us that they adapted their practices based on trials and errors, but they also weighed the choice of crops based on their financial capability to support the material inputs (i.e. seeds,

fertilizers) and labor requirements for the production of a particular crop. However, the agricultural recovery process was not only shaped by the financial capacity of the farmers to provide the necessary inputs but also by their indigenous knowledge, acquired skills from years of experience, advice from the seminars which they have attended and from agricultural technicians, and determination to revive their stricken lands despite the failures and losses from the initial crops they cultivated during the re-establishment of their farms. Most farmers were innovative enough to install irrigation facilities such as shallow tube wells, construct small farm reservoirs, formed farmer groups to construct communal irrigation systems, access water from deep well, dams, free-flowing water, and springs to support the water needs of their crops. The difficulty in land preparation due to hard structure was resolved with the use of hand tractors singly or in combination with animal-drawn implements. The farm operators also learned adaptive methods to rice under the hard structure and shallow riverbed soils by direct seeding and shallow transplanting, respectively. According to one farmer, scraping off the surface lahar (2-2.5 ft.) from the thick deposition improved the sugarcane yield.

The farmers also certified that plowing and mixing of ash with original soil improve the productivity of their soil and the addition of a higher rate of fertilizers containing N, P, K, and S are necessary to improve the growth and increase the crop yields. Further, they figured that high yields can be obtained from crops that are sufficiently irrigated for their whole crop duration. Farmers learned to diversify their cropping based on what they experienced to be more suitable to the type of soil they have now and from what crop they will earn more profit. They also choose good quality and high yielding varieties such as hybrid rice varieties to increase their yields. Hybrid rice typically displays heterosis or hybrid vigor such that when it is grown under the same conditions as comparable high-yielding inbred rice varieties it can produce up to 30 % more rice (IRRI, 2019). For some, they adjusted the planting calendar that would maximize the availability of water, reduce pest incidence, and avoid heavy monsoonal rains and typhoon season.

Most of the farmers who are experiencing Zn deficiency in their soils have applied zinc sulfate. The addition of Zn fertilizers by soil or foliar application has been shown to increase Zn concentration in cereal grains but the extent of the increase differs among crop species (Hafeez et al., 2013). Aside from the application of Zn fertilizers, the recycling of crop residues, organic manures, and cultivation of Zn efficient genotypes have been recommended to combat zinc deficiency (Singh, 2008).

In former agricultural areas that have become forests, the rural communities find the timber for house construction, bamboo, and woods sold as charcoal. They also grow banana and other edible weeds which are more useful, income-generating and only require less to no recurrent inputs.

6.4.3 Crop productivity in relation to soil constraints and farmers adaptation practices

The 1991 eruption of Mt. Pinatubo had caused major impacts on the booming rice production of Tarlac, Pampanga, and Zambales. The Central Luzon region where these provinces lie is considered as the rice granary of the Philippines as it accounted for 17.5% of the national production from 1988 to 1992, and 14.7% of the gross hectarage (Benson, 1997). Among the three provinces, Tarlac had the largest area devoted to rice production with 105,100 ha followed by Pampanga with 51,590 ha, and Zambales with 28,060 ha in the year 1990. After the 1991 pyroclast deposition, the arable rice area was reduced by 25 % in Pampanga, 12 % in Tarlac, and 48 % in Zambales. Furthermore, the volume of production in Pampanga and Zambales markedly decreased by 23 and 53 %, respectively while that of Tarlac was not affected (PSA, 2016). According to Gonzaga & Orejas (2011), Zambales sustained the highest impact as about 80 percent of the pyroclastic materials flowed on its side while the other 20 percent in Pampanga and

Tarlac. Agricultural lands remain to be at risk of lahar deposition as flooding during typhoons and monsoonal rains, from June to November, continue to remobilize the pyroclasts in the middle slopes of Mt. Pinatubo and the eight rivers draining to Pampanga, Zambales and Tarlac provinces even after 24 years (Orejas, 2015).

The recovery in crop productivity of the 9 ash LUTs, 3 remobilized ash LUTs, and 8 lahar LUTs after 26 years was assessed in terms of harvested crop yield. The farmers in these LUTs declared the average yields they obtained from their main crop during the period of the survey in 2017 and within the period prior to the eruption (1990). Table 6.2 shows the current and pre-1991 management of the LUTs in terms of cropping system, the thickness of pyroclast deposit, fertilization type and rate, and type of seed variety used. It also shows the comparison of their current (2017) and pre-1991 yield production with that of the regional yield average in 2017 and 1990, respectively. Table 6.3 shows the comparison of the LUTs in terms of the type of irrigation and cultivation method, the major constraints due to pyroclast and non-pyroclast factors, the farmers' adaptation to these constraints, and the present condition of their farms and soils.

Table 6.2. Comparison of the current and pre-1991 management of land utilization types, thickness of pyroclast deposits, fertilization rate, type of variety used, farmers crop yields, and comparative regional crop yield averages at present (2017) and during pre-1991 production (1990).

No.	LUT CODE	LAND UTILIZATION TYPE (LUT) (CROPPING PATTERN PER YEAR)		[1]THICKNESS (cm) OF PYROCLAST DEPOSIT		[2]FERTILIZATION TYPE AND RATE (N-P-K-S kg ha^{-1} cropping^{-1})		[3]TYPE OF SEED VARIETY USED		[4]FARMER'S CROP YIELD (t ha^{-1} cropping^{-1})		[5]YIELD AVERAGE RANGE IN THE REGION (t ha^{-1} cropping^{-1})	
		Current (2017)	Pre-1991 (1990)	Farmer's interview	Actual observation	Current	Pre-1991 eruption	Current	Pre-1991 eruption	Current	Pre-1991	Year 2017	Year 1990
	A. Ash												
1	A1	Rice (Rc)-Rc rotation	Rc-Rc rotation	15	Ash layer not visible	IF: 180-42-42 + $ZnSO_4$	IF	Rc [inbred varieties]	Rc [inbred and traditional varieties]	5.0 [rice]	3.5-4.0 [rice]	4.2-5.1 [rice]	3.5-3.7 [rice]
2	A2	Rc-Rc rotation	Rc-Rc rotation	20	Ash layer not visible	IF: 89-18-18-36	IF	Rc [inbred varieties]	Rc [inbred and traditional varieties]	3.9-5.0 [rice]	6.0-7.5 [rice]	4.2-5.1 [rice]	3.5-3.7 [rice]
3	A3	Rc-Vegetable (Veg) rotation	Rc-Rc rotation	31	25	OF (i.e. 250 kg ha^{-1} chicken manure)	IF	Rc [inbred varities]		2.5 [rice]	2.0-4.0 [rice]	4.2-5.1 [rice]	3.5-3.7 [rice]
4	A4	Rc-Corn (Co)-Co rotation	Rc-Rc rotation	31	37	IF: 60-14-14 [rice]; 240-56-116 [corn] + OF [compost; 1.3 t ha^{-1} yr^{-1}] + ZnSO4	60-14-14	Rc and Co [hybrid varieties]	-	3.5 [rice]; 6.9 (corn)	-	4.2-5.1 [rice]; 5.6 (corn)	-
5	A5	Rc-Co rotation	Rc-Rc rotation	31	25	IF	IF	Rc [inbred variety]; Corn [hybrid variety]	Rc [inbred variety]	2.0 [rice]	3.5-4.0 [rice]	4.2-5.1 [rice]	3.5-3.7 [rice]
6	A6	Rc-Rootcrop (Ro) rotation	Rc and Ro intercrop	< 31	Ash layer not visible	IF: 92-14-14-36 [rice]	IF	Rc [inbred and traditional varieties]	Rc [inbred and hyrid varieties]	2.4-4.0 [rice, <1 ha]	4.0 [rice]	4.2-5.1 [rice]	3.5-3.7 [rice]
7	A7	Rc-[Ro or Veg] rotation	Rc, Fr, and woods intercropping	25	20	IF: 53-0-0-60 [rice]	-	Rc [inbred variety]	-	5.0 [rice]	-	4.2-5.1 [rice]	-
8	A10	Sugarcane (Su) monocrop	Su and Ro intercropping	31	Ash layer not visible	IF + OF (i.e. 6 t ha^{-1} molasses) [sugarcane]		-	-	50 [sugarcane]	50 [sugarcane]	50.2 [sugarcane]	81.8 [sugarcane]
9	A11	Ro-Su rotation	Su	15	Ash layer not visible	IF: 53-0-0 [rice]; 276-0-0 [sugarcane]	IF + OF (i.e. molasses)	-	-	50-300 [sugarcane]	> 100 [sugarcane]	50.2 [sugarcane]	81.8 [sugarcane]
	B. Remobilized ash												
10	R1	Rc-Rc rotation	Su and Rc intecropping	31	30	IF: 64-7-7 + $ZnSO_4$	IF: 14-4-0	Rc [inbred varieties]	-	3.6 [rice]	-	4.2-5.1 [rice]	-
11	R2	Rc-Rc-[Rc and Veg] rotation	Rc-Co-Veg rotation	31	45	IF: 86-17-17 + OF (i.e. 1 t ha^{-1} chicken manure, 1.5 t ha^{-1} commercial organic) [rice]	-	-	Rc [hyrid varieties]	3.9-6.3 [rice]	-	4.2-5.1 [rice]	-
12	R3	Rc-[Rc and Co]-Rc and Co] rotation	Rc-Co-Co rotation	-	25	IF: 120-28-28 (rice); 162-28-28-48 (corn)		Rc [inbred and hybrid varieties]; Co [hydrid variety]	Co [inbred variety]; Rc [traditional variety]	4.0-5.0 [rice]	5.0 [rice]	4.2-5.1 [rice]	3.5-3.7 [rice]

Table 6.2 (cont'd). Comparison of the current and pre-1991 management of land utilization types, thickness of pyroclast deposits, fertilization rate, type of variety used, farmers crop yields and comparative regional crop yield averages at present (2017) and during pre-1991 production (1990).

No.	LUT CODE	LAND UTILIZATION TYPE (LUT) (CROPPING PATTERN PER YEAR)		[1]THICKNESS (cm) OF PYROCLAST DEPOSIT		[2]FERTILIZATION TYPE AND RATE (N-P-K-S kg ha^{-1} $cropping^{-1}$)		[3]TYPE OF SEED VARIETY USED		[4]FARMER'S CROP YIELD (t ha^{-1} $cropping^{-1}$)		[5]YIELD AVERAGE RANGE IN THE REGION (t ha^{-1} $cropping^{-1}$)	
		Current (2017)	Pre-1991 (1990)	Farmer's interview	Actual observation	Current	Pre-1991 eruption	Current	Pre-1991 eruption	Current	Pre-1991	Year 2017	Year 1990
	C. Lahar												
13	L1	Rc-Rc-Rc rotation	Rc-Rc-Rc rotation	3050	> 1000	IF: 152-68-28	IF	Rc [inbred varieties]	Rc [inbred varieties]	5.0 [rice]	5.0 [rice]	4.2-5.1 [rice]	3.5-3.7 [rice]
14	L2	Rc-[Rc or Ro] rotation	Rc-Rc-[Rc and Veg] rotation	-	> 1450	IF: 119-14-14-120 [rice] + $ZnSO_4$	IF	Rc [inbred and hybrid varieties]	-	5.0 [rice]; 10.0 (sweet potato)	-	4.2-5.1 [rice]; 8.6 [sweet potato]	-
15	L3	[Rc and Veg]-[Co and Veg] rotation	[Rc and Veg]-[Rc and Veg] rotation	150	~30	IF: 92-0-0-24 [rice] + ZnSO4	IF + $ZnSO_4$	Rc [inbred and hybrid varities]	Rc [inbred varieties]	3.9 [rice, >1 ha]	5.4 [rice]	4.2-5.1 [rice]	3.5-3.7 [rice]
16	L4	Rc-[Co or Veg] rotation	Rc-Co rotation	8240	> 1250	IF + $ZnSO_4$		-	-	3.0 [rice]	5.0 [rice]	4.2-5.1 [rice]	3.5-3.7 [rice]
17	L5	Rc-[Co or Veg] rotation	Rc, Co, Veg and Ro intercropping	50	>1250	IF: 48-25-55 [rice]	IF: 117-25-55 [rice]	Rc [hybrid variety; Co [hybrid variety]	Co [local variety]	4.5 [rice]	4.0-4.5 [rice]	4.2-5.1 [rice]	3.5-3.7 [rice]
18	L6	Rc-Su rotation	Rc-Rc-Rc rotation	6100	> 7500	IF: 69-0-0 + OF (chicken manure) [rice]	IF: 92-0-0	-	-	1.4-5.0 [rice]	1.7-3.3 [rice]	4.2-5.1 [rice]	3.5-3.7 [rice]
19	L8	Su monocropping	Rc-Rc-Rc rotation	6100	3500	IF: 200-0-0-53 [sugarcane]	IF: 78-0-0-36 [rice]	-	Rc [traditional varieties]	40-42 [sugarcane]	-	50.2 [sugarcane]	-
20	L9	Rc-Veg and Ro intercropping	Rc-Veg and Ro intercropping	6100	-	IF: [taro]	IF: 57-0-0-12 [rice] IF [taro]	Rc [inbred varieties]	-	0.5-1.0 [taro, <1 ha]	3-3.5 [taro, <1 ha]	8.3 [taro]	7.0 [taro]

[1]Thickness of pyroclast deposit from 1991 Mt. Pinatubo eruption based on farmers' interview, thickness of the pyroclast based on actual observation in 2017 (26 years after the eruption); [2]Fertilization type and rate (kg ha^{-1}) applied for each LUT for IF fertilizers which stand for inorganic or chemical fertilizers, OF for organic fertilizers (i.e. chicken manure or commercial organic fertilizer;

nutrient supplied not accounted due to unavailability of data on the nutrient content), NPKS stands for nitrogen-phosphorus-potassium-sulfur, '$ZnSO_4$' zinc sulfate (farmer did not specify the amount applied); [3]Rice varieties is differentiated as traditional or local, inbred, and hybrid; [4]Average yield obtained by the farmer at current (2017) and pre-1991 (1990) production, [5]Average yield of crops in Region III (Central Luzon) during the periods of 2017 and 1990 (PSA, 2019, BAS, 2015), the range of grain yields for rice encompasses both irrigated and rainfed rice. Rc' rice; 'Veg' vegetables; 'Co' corn; 'Ro' root crop; 'Su' sugarcane; 'Fr' fruit trees; 'Gr' grassland; 'Fo' forest; 'Ban' banana, 'Ma' mango; crops inside a '[ ]' are grown at the same time during a particular cropping period, (-) no data.

Table 6.3. Comparison of the current and pre-1991 management of land utilization types, cultivation method, major constraints, adaptation practices, and present condition as perceived by the farmers.

No.	LUT CODE	LAND UTILIZATION TYPE (LUT)		[1]TYPE OF IRRIGATION		[2]CULTIVATION METHOD		MAJOR CONSTRAINTS		MAJOR ADAPTATION PRACTICE		PRESENT CONDITION OF THE FARM AND SOIL ACCORDING TO THE FARMER
		Current	Pre-1991	Current	Pre-1991	Current	Pre-1991	Pyroclast impact	Non-pyroclast impact	Pyroclast impact	Non-pyroclast impact	
	A. Ash											
1	A1	Rc-Rc rotation	Rc-Rc rotation	NIS		mechanized using tractor and animal-drawn implements		sandy but gets muddy upon wetting, poor growth, flooding	typhoons, pest and disease	deep plowing once, fertilizer application, zinc sulfate to control reddening of rice leaves and death of seedlings, transplanting at shallow depth, rehabilitation of NIS, planting at shallow depth, and direct dry seeding	-	NIS was rehabilitated so they were able to grow rice again
2	A2	Rc-Rc rotation	Rc-Rc rotation	CIS		tractor and animal-drawn implements		sandy, easily dries up, hard structure, flooding	limited water, typhoons, pest and disease, weeds	deep plowing once, hired more laborers for land prep, fertilizer application, destroying bunds to drain excess water	frequent plowing to eradicate weeds	improved growth since 2 years ago, insufficient water supply
3	A3	Rc-Veg rotation	Rc-Rc rotation	Deepwell	CIS	tractor and animal-drawn implements		poor root growth due to hard structure, sandy, easily dries up,	typhoons that cause flooding, pest and disease	installation of water source, frequent watering, fertilization (including organic) application, mulching of crop residues	-	loose structure good for vegetables
4	A4	Rc-Co-Co rotation	Rc-Rc rotation	CIS, spring, electric water pump	Electric water pump	tractor	animal-drawn	sandy, easily dries up, acidity, high soil temp, hard structure, uneven soil depth, poor growth (reddening of leaves and death of rice seedlings), low yield, erosion-prone, flooding	erosion prone, pest and disease	deep plowing once, high irrigation rate, fertilizer application including organic fertilizer and zinc sulfate	pesticide application, seeds covered with to protect from bird infestation	easier to till at present, mixing of pyroclast with the soil has improved the plant growth

Table 6.3 (cont'd). Comparison of the current and pre-1991 management of land utilization types, cultivation method, major constraints, adaptation practices, and present condition as perceived by the farmers.

No.	LUT CODE	LAND UTILIZATION TYPE (LUT)		[1]TYPE OF IRRIGATION		[2]CULTIVATION METHOD		MAJOR CONSTRAINTS		MAJOR ADAPTATION PRACTICE		PRESENT CONDITION OF THE FARM AND SOIL ACCORDING TO THE FARMER
		Current	Pre-1991	Current	Pre-1991	Current	Pre-1991	Pyroclast impact	Non-pyroclast impact	Pyroclast impact	Non-pyroclast impact	
	A. Ash											
5	A5	Rc-Co rotation	Rc-Rc rotation	Water pump	NIS	tractor	animal-drawn	more sandy than pre-1991, easily dries up, soil acidity, hard structure, poor plant and root growths, erosion prone, flooding, poor drainage	erosion prone, typhoons	deep plowing once, increased rate of fertilizer application , mechanized land preparation using tractor, direct rice seeding	-	Yields they obtain at present is lower than during pre-1991, steady source of water is needed, spring water that is acidic kills the plant
6	A6	Rc-Ro rotation	Rc and Ro intercrop	STW	Spring and SFR	tractor	animal-drawn	sandy but gets muddy upon wetting, soil acidity	insufficient water supply especially during dry months, pest and disease during the rainy season	increased rate of fertilizer application, choice of good quality and high yielding seed varieties	-	improved workability, drainage, and seed germination, not easily eroded after the ash was mixed with the soil
7	A7	Rc-[Ro or Veg] rotation	Rc-Rc rotation	Electric pump (during dry season); rainfall (wet season)	diversion of water from the river	tractor and animal-drawn implements	animal-drawn	difficult to till due to hard structurem poor drainage/waterlogging	insufficient water supply especially during dry months, flood-prone, typhoon incidence; sticky consistence and hard structure, presence of hardpan, very difficult to till	fertilizer application	installation of irrigation facilities, levelled the area and constructed canals to divert water from the lake, shift in crop type grown, rice is grown only when there is water	easier to cultivate after the pyroclast addition than prior to eruption, the soil is already recovering, insufficient water is the main problem, does not cultivate during dry season when there is no water
8	A10	Su monocrop	Su and Ro intercropping	SFR collected from river, STW	STW	tractor		sandy, easily dries up, soil acidity	erosion-prone especially during rainfall events, presence of hardpan	fertilizer application (inorganic and organic fertilizers)	frequent and higher rate of irrigation	ash improved the structure and workability of the soil, and plant growth but declined after 10 years of deposition when the ash was washed away by rain, yield is lower compared to pre-1991

Table 6.3 (cont'd). Comparison of the current and pre-1991 management of land utilization types, cultivation method, major constraints, adaptation practices, and present condition as perceived by the farmers.

No.	LUT CODE	LAND UTILIZATION TYPE (LUT)		[1]TYPE OF IRRIGATION		[2]CULTIVATION METHOD		MAJOR CONSTRAINTS		MAJOR ADAPTATION PRACTICE		PRESENT CONDITION OF THE FARM AND SOIL ACCORDING TO THE FARMER
		Current	Pre-1991	Current	Pre-1991	Current	Pre-1991	Pyroclast impact	Non-pyroclast impact	Pyroclast impact	Non-pyroclast impact	
	A. Ash											
9	A11	Ro-Su rotation	Su	Rainfall		tractor and animal-drawn		sandy, easily dries up, hard structure, low in K	erosion-prone, insufficient water supply	deep plowing once, fertilizer application, cropping rotation depending on the vigor of plants and market demand	-	rainfall is the only source of irrigation during pre- and post-1991 crop production, molasses is not available anymore in the market
	B. Remobilized ash											
10	R1	Rc-Rc rotation	Su and Rc intecropping	CIS, spring	SFR	tractor and animal-drawn implements		sandy, easily dries up, soil acidity, high soil temperature, waterlogging due to lahar	sticky consistence and hard structure, difficult to cultivate	deep plowing once, higher fertilizer rate applied, addition of zinc sulfate, watering before plowing, mixing of ash with buried soil	-	ash improved the structure and workability; soil is easy to cultivate at present; the plant growth improved after mixing the ash with soil
11	R2	Rc-Rc-[Rc and Veg] rotation	Rc-Co-Veg rotation	STW		tractor	animal-drawn	sandy, easily dries up; hard structure, poor plant growth	insufficient water supply especially during dry months, weed infestation	deep plowing once, increased rate of fertilizer application, watering before transplanting, mechanized plowing, use of hybrid rice varieties	herbicide application to eradicate weeds	The soil has already recovered, plant growth is already good so they started to lessen the fertilizer rate, the yields are similar to that of the pre-1991 produce
12	R3	Rc-[Rc and Co]-Rc and Co] rotation	Rc-Co-Co rotation	STW		tractor	tractor and animal-drawn implements	sandy, easily dries up; hard structure; poor crop growth	insufficient water supply especially during dry months, sticky soil consistence and hard structure	increased rate of fertilizer application, mechanized plowing, area is leveled for even distribution of water, hired more laborers during land cultivation	-	-

Table 6.3 (cont'd). Comparison of the current and pre-1991 management of land utilization types, cultivation method, major constraints, adaptation practices, and present condition as perceived by the farmers.

No.	LUT CODE	LAND UTILIZATION TYPE (LUT)		[1]TYPE OF IRRIGATION		[2]CULTIVATION METHOD		MAJOR CONSTRAINTS		MAJOR ADAPTATION PRACTICE		PRESENT CONDITION OF THE FARM AND SOIL ACCORDING TO THE FARMER
		Current	Pre-1991	Current	Pre-1991	Current	Pre-1991	Pyroclast impact	Non-pyroclast impact	Pyroclast impact	Non-pyroclast impact	
	C. Lahar											
13	L1	Rc-Rc-Rc rotation	Rc-Rc-Rc rotation	NIS	STW	tractor		sandy, easily dries up, hard structure, stoniness, difficult to cultivate, poor crop growth	pest and disease infestation especially during rainy season	mixing of lahar materials during plowing, increased fertilization rate, mechanized plowing, stone removal, rehabilitated the irrigation facility	pesticide application	NIS was rehabilitated so they were able to grow rice again, soil emits a foul odor, lahar behaves like a "cement", waterlogging incidence which makes it possible to grow rice
14	L2	Rc-[Rc or Ro] rotation	Rc-Rc-[Rc and Veg] rotation	NIS		tractor	animal-drawn	sandy, easily dries up, acidity, high soil temp, hard structure, poor growth (reddening of leaves and death or rice seedings), low yield, waterlogging	insufficient water supply during dry months, flood-prone, shallow water table, erosion prone	increased fertilization rate, application of zinc sulfate to control death of seedlings, mechanized plowing, choice of good and high yielding varieties (i.e. hybrid rice), hired more laborers during land cultivation	farm is divided between rice and sweet potato during the second cropping due to insufficient irrigation	Irrigation from NIS is not available all year round; at present, the soil is not as hard as before but still needs to be cultivated; it takes a long time for root expansion
15	L3	[Rc and Veg]-[Co and Veg] rotation	[Rc and Veg]-[Rc and Veg] rotation	Diversion of water from dike	NIS	tractor	animal-drawn	sandy, easily dries up, hard structure, soil acidity, stoniness, poor plant growth, whitish water rises up from groundwater during second cropping that affects yield, reddening of leaves and death of seedlings, waterlogging	insufficient water supply during dry months, flood-prone, erosion prone, pest and disease	deep plowing once, adjust planting calendar to maximixe rain water and escape heat during summer months, soil is saturated before plowing and transplanting, fertilizer application, application of zinc sulfate in patches, mechanized plowing	pesticide application	Yields they obtain at present is lower than during pre-1991 production
16	L4	Rc-[Co or Veg] rotation	Rc-Co rotation	STW, diversion of free flowing water during rainy season	Free flowing water	tractor	animal-drawn	stoniness (big and small sizes), weed infestation due to pyroclast, poor plant growth and low yield, reddening of rice leaves and death of seedlings, waterlogging	flood-prone	fertilizer application, draining of water and zinc sulfate application, direct seeding of rice, continous cultivation to improve soil fertility, mechanized plowing, fertilizer applied between rice plants then covered	herbicide application and plowing under to eradicate weeds, adjusting of planting calendar to escape heavy weed infestation	Yields they obtain at present is lower than during pre-1991 production, presence of mud with foul odor which the farmer attributes to zinc deficiency

Table 6.3 (cont'd). Comparison of the current and pre-1991 management of land utilization types, cultivation method, major constraints, adaptation practices, and present condition as perceived by the farmers.

No.	LUT CODE	LAND UTILIZATION TYPE (LUT)		[1]TYPE OF IRRIGATION		[2]CULTIVATION METHOD		MAJOR CONSTRAINTS		MAJOR ADAPTATION PRACTICE		PRESENT CONDITION OF THE FARM AND SOIL ACCORDING TO THE FARMER
		Current	Pre-1991	Current	Pre-1991	Current	Pre-1991	Pyroclast impact	Non-pyroclast impact	Pyroclast impact	Non-pyroclast impact	
17	L5	Rc-[Co or Veg] rotation	Rc, Co, Veg and Ro intercropping	STW	Spring, SFR	tractor	animal-drawn	sandy, easily dries up, hard structure	insufficient water supply during dry months; pest and disease during rainy season	deep plowing once, continuous plowing to mix ash with buried soil, fertilizer application (inorganic and organic), frequent and higher rate of irrigation	pesticide application	-
18	L6	Rc-Su rotation	Rc-Rc-Rc rotation	rainfall	SFR	tractor	-	sandy, easily dries up, hard structure	insufficient water supply during dry months; pest and disease during rainy season	fertilizer application, mechanized plowing, growing rice in the lower areas of the field where water is available, scraping of lahar while the remaining lahar is plowed	shift in crop type, i.e. rice to sugarcane which require less water during the dry season cropping	Yields they obtain at present is lower than during pre-1991 production
19	L8	Su monocropping	Rc-Rc-Rc rotation	rainfall	SFR	tractor	animal-drawn	sandy, easily dries up, soil acidity, poor plant growth, flooding	shallow water table	scraping of lahar (7-8 ft.) while the remaining lahar is plowed improved yield, fertilizer application	-	Yields they obtain at present is lower than during pre-1991 production; very friable consistence which is not favored by the farmer; high sugar content of the stalks; improved yield after partial scraping of lahar
20	L9	Rc-Veg and Ro intercropping	Rc-Veg and Ro intercropping	Spring water	SFR	tractor and animal-drawn implements		soil acidity, poor crop growth and low yield, flooding, prone to deposition of eroded materials	pest and disease	mixing of lahar with buried soil	does not cultivate during the rainy season due flooding	lahar deposition up to present, presence of dark mud with foul smell, whitish water which rises from groundwater cause sterility and yellowing of rice

[1]Irrigation type: National irrigation system (NIS), communal irrigation system (CIS), small farm reservoir (SFR), shallow tube well (STW); [2]Cultivation method: mechanized land preparation ('tractor'), non-mechanized land preparation using draft animals with attached plow tool ('animal-drawn'); rice (Rc); vegetables (Veg); corn (Co); root crop (Ro); sugarcane (Su); fruit trees (Fr); grassland (Gr); forest (Fo); banana (Ban), mango (Ma).

The 20 LUTs presented in Table 6.3 are generally rice-based except for two ash and one lahar-LUT that grow sugarcane (i.e. LUT A10, A11, L9) and 1 lahar LUT that cultivates taro root crop (i.e. L9). Corn is grown as a rotation crop with rice in A3. Sweet potato is also grown as a rotation crop with rice in L2. Generally, the rice yields from the LUTs across the different types of pyroclast deposits ranging from 4.0 to 7.5 t ha^{-1} in pre-1991 are even higher than that of the 1990 regional rice yield average of 3.5 to 3.7 t ha^{-1}, except for L6 which had lower average yield ranging from 1.7 to 3.3 t ha^{-1} and A3 with a lower yield range of 2.0 to 4.0 t ha^{-1}. Similarly, the yield of taro in L9 obtained by the farmer in pre-1991 eruption ranging from 3.0 to 3.5 t <1 ha^{-1} is approximately two times lower than the regional yield average of 7 t ha^{-1}. The sugarcane yield in A10 is also lower by 30 t ha^{-1} compared to the 1990 yield average of 80 t ha^{-1}.

These suggest that rice, in general, has been productive during pre-1991 eruption despite the occasional non-pyroclastic factors (i.e. pest and disease, typhoons) which affected their yields. At present, the rice yields of the ash-, remobilized ash-, and lahar-LUTs ranging from 4 to 6 t ha^{-1} are already at par with the regional rice yield in 2017 ranging from 4.2 to 5.1 t ha^{-1} (i.e. A1, A2, A7, A10, A11, R2, R3, L1, L2, L5). However, there are still some LUTs whose yields are below the 2017 average yield in the region (i.e. rice-based - A3, A4, A5, A6, R1, L3, L4, L6, sugarcane –L8, taro – L9). The rice-based LUTs had a low yield average ranging from 1.4 to 4.0 t ha^{-1}.

For sugarcane, the yields obtained in ash LUTs have already recovered yielding an average of 50 t ha^{-1} (i.e. A10) and 50 to 300 t ha^{-1} (i.e. A11) and even exceeded the regional yield average of 50 t ha^{-1} while that of the lahar LUT (i.e. L8) had slightly lower yield average that ranged from 40 to 42 t ha^{-1} even though the farmer declared an improved growth and sugar content of their produce with the addition of lahar (Fig. 4.11). The average yield of taro in the lahar LUT (i.e. L9) that ranged from 0.5 to 1.0 t ha^{-1} is very low compared to the regional average of 8.3 t ha^{-1} and is also three times lower compared to the yield obtained prior to the eruption (i.e. 3.0-3.5 t ha^{-1}). On the other hand, the

corn average yield of 7 t ha^{-1} in the ash LUT (i.e. A4) had increased from the regional yield of 5.6 t ha^{-1}. Sweet potato grown on lahar (i.e. L2) has also increased compared to the regional average (10.0 vs. 8.6 t ha^{-1}).

The crop productivity after 26 years is not be completely dictated by the type or thickness of the pyroclastic deposit. Some of the lahar-affected LUTs with thick deposition of pyroclastic material was able to obtain favorable yields that are comparable with the regional average and some of those ash-affected LUTs with thinner deposition of pyroclastic material still obtained low rice yields. The yields of other crops such as sugarcane imply a more favorable response in ash-affected LUTs than in lahar although, this may not be conclusive as only a few sites were compared.

Low yields are still produced in the ash- and remobilized ash LUTs (i.e. A3, A4, A5, A6, and R1), despite the reported enhanced soil workability due to the loose structure and friable consistency of pyroclast (except for A5), inorganic and/or organic fertilizer application, use of good quality inbred and/or hybrid varieties, and mechanized land preparation. One of the common problems that these LUTs encountered are intensified flooding due to the shallow water table leading to temporary waterlogging and poor drainage accompanied by a foul smell, and soil acidity. The intrusion of spring water during the rainy season which is acidic kills the plant according to the farmer in A5. In the same manner, the lahar LUTs which exhibited low crop productivity at present (i.e. L3, L4, L6, L8, L9), have similar constraints concerning acidity, flooding due to the shallow water table, and poor drainage which typically occurs during the wet season. In rice-based LUTs of both ash and lahar (i.e. A4, R1, L3, L4), the farmers complained about the reddish coloration of rice leaves, poor growth, and death of rice seedlings which they associate to Zn deficiency.

6.5 Conclusion

The 1991 Plinian eruption of Mt. Pinatubo deposited varying types (i.e. ash, remobilized ash, lahar) and thicknesses (~15 cm-8 m) of pyroclastic materials on cultivated fields mainly grown to rice and other crops such as corn, sugarcane, root crops, and vegetables. The lands were rendered idle for periods varying between a few months to 22 years after the eruption. Since cultivation resumed, the farmers have been facing several issues as the deposits affected negatively the land/soil quality and productivity of croplands. Poor plant growth and low yields are the major impacts of the pyroclastic deposits, especially during the initial crop re-establishment period.

We categorized the constraints identified by the farmers into primary (direct) and secondary (indirect) impacts of pyroclast deposition as presented in Figure 6.12. The inherent nature of ash and lahar materials, typically having low water retention and nutrient-holding capacities due to the coarse grain size and low degree of weathering, are addressed by the farmers through various adaptation practices such as increased rates of water and fertilizer (organic and/organic) application, change in crop or cropping pattern which requires less water utilization, mechanized land preparation, change in seeding method, mixing the surface soil with the buried soil, choice of good quality seeds, etc.

Flooding is a major and persistent constraint that was exacerbated by pyroclast deposition and which limits crop productivity even up to the present. The rise of riverbeds due to the thick deposition of lahar (and ash) has made the groundwater shallow, especially during the rainy season. Periodical waterlogging and poor drainage are inferred to induce other soil constraints such as Zn deficiency and possibly Al toxicity. In addition, P-induced zinc deficiency is also hypothesized to arise under the intermittent moisture condition of paddy rice ash and lahar soils.

At present, most of the farmers have already recovered and are able to increase their yield comparable with the regional yield average. The improvement in structure, consistency, tillage conditions and soil fertility are noted to occur in some of the ash-affected areas based on the farmers' perception. The farms which have difficulty in achieving high yields are those which experience acidity problems especially during periods of flooding. Some of the areas that have compounded constraints that are beyond the financial capability of farmers for restoration have become grasslands or forests. Some of the identified soil limitations such as Zn are amended by Zn fertilizer application and draining of excess water as recommended by the agricultural technicians. However, the problem of acidity has been very difficult to address for the farmers, notably because they never encountered this problem before the eruption.

Unless appropriate mitigation strategies to resolve floods are implemented, secondary constraints (i.e. Zn deficiency and acidity) will continue. Irrigation facilities that would ensure sufficient water supply in croplands especially during the dry season must also be provided as a limitation in the water supply is a common complaint of the farmers. Moisture availability is very important as it drives weathering processes to increase the nutrient supplying capacity of the pyroclast deposits.

Organic matter addition (i.e. biomass recycling, animal manure, compost, etc.) is recommended to improve the structure, permeability, water- and nutrient holding capacity of soils affected by ash and lahar. Mixing of the pyroclast materials with the buried soil may help increase the available nutrients and expedite weathering. Lime such as dolomite can be applied to ameliorate the soil pH conditions to precipitate aluminum as inert Al hydroxides to reduce its availability (Ismail et al, 1993), although it could lead to precipitation of calcium sulfate. It is also not recommended that farmers utilize fertilizers containing ammonium and sulfur as it may intensify the soil acidity levels.

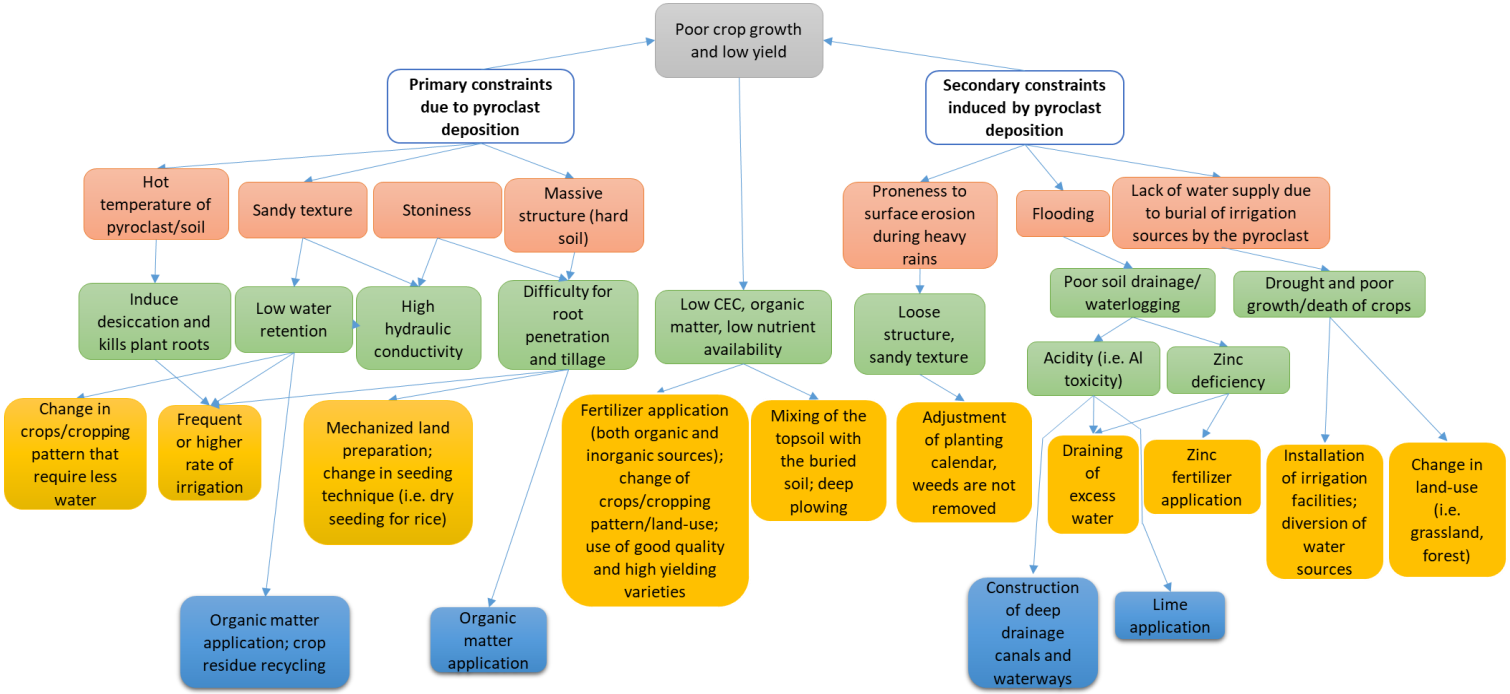

Figure 6.12. Primary and secondary constraints on land/soil qualities imposed by pyroclast deposition, the impacts on crop and soil productivity, and the recommended adaptation strategies based on farmers' practices and from published sources. *Information on red and orange boxes are responses from farmers, green boxes are the interpretation of the constraints, blue boxes are recommendations based on the interpretation of the constraints.*

6.6 References

Aganon, C. P., & Undan, R. C. (1992). CLSU's research and development activities in Mt. Pinatubo-affected areas. *In: Proceedings of symposium on sustainable agricultural development of Mt. Pinatubo-affected areas.* November 5-6, 1992. Farming Systems and Soil Resources Institute, College of Agriculture, University of the Philippines, Los Banos, College, Laguna.

Aganon, C. P., De La Cruz, N., Patricio, M. G. & Galindez, J. L. (1996). Fertilizer management for promising crops in ash and lahar laden areas in Central Luzon, Philippines; A Research and Development Effort. *Philippine Journal of Crop Science*, May. Volume no. 21 Supplement no. 1. page 18.

Alloway, B. J. (2008). *Zinc in Soils and crop nutrition.* (Second edition). IZA and IFA Brussels, Belgium and Paris, France.

Auxtero, E. A., & Shamshuddin, J. (1991). Growth of oil palm (Elaeis guineensis) seedlings on acid sulfate soils as affected by water regime and aluminum. *Plant Soil, 137*, 243–257, 1991.

Barrato Jr., C.L., & Benaning, M. N. (1978). Pinatubo Negritos (Revisited*). Field Report Series No 5*. Quezon City: Philippine Center for Advanced Studies Museum.

Bautista, C. B. (1996). The Mount Pinatubo disaster and the people of Central Luzon. In *Newhall CG, Punongbayan RS (eds) Fire and Mud: Eruptions and Lahars of Mount Pinatubo, Philippines.* Philippine Institute of Volcanology and Seismology, Quezon City. University of Washington Press, Seattle, and London. Printed in Hongkong.

Benson, C. (1997). The economic impact of natural disasters in the Philippines. *Overseas Development Institute Working Papers*, (99). https://doi.org/0 85003 248 2.

Brehler, B., & Wedepohl K. H. (1978). In *Wedepohl, K. H. (Ed). Handbook of Geochemistry (p.125). Vol. II/3*. Springer-Verlag, Berlin; 1978.

Brown, S. K., Auker, M. R., & Sparks, R. S. J. (2015). Populations around Holocene volcanoes and development of a population exposure index. In *Loughlin, S. C., Sparks, S., Brown, S. K., Jenkins, S. F., V.-B., C. (Eds.). Global Volcanic Hazards and Risk*. Cambridge University Press. https://doi.org/10.1017/CBO9781107415324.004.

BAS. (2005). Crop statistics of the Philippines 1990-2004. Department of Agriculture. Bureau of Agricultural Statistics.

Carbonell-Barrachina, A. A., Jugsujinda, A., Burlo, F., Delaune, R. D., Patrick, W. H. (2000). Arsenic chemistry in municipal sewage sludge as affected by redox potential and pH. *Water Res 34*:216–224.

Dahlgren, R. A., Saigusa, M., & Ugolini, F. C. (2004). The nature, properties, and management of volcanic soils. *Advances in Agronomy, 82*, 113–182. https://doi.org/10.1016/S0065- 2113(03)82003-5.

Elisa, A. A., Ninomiya, S., Shamshuddin, J., & Roslan, I. (2016). Alleviating aluminum toxicity in an acid sulfate soil from Peninsular Malaysia by calcium silicate application. *Solid Earth, 7*(2), 367–374. https://doi.org/10.5194/se-7-367-2016.

FAO. (1976). A framework for land evaluation. Food and Agriculture Organization, Soils bulletin 32.

Gaillard, J. (2008). Alternative paradigms of volcanic risk perception: The case of Mt. Pinatubo in the Philippines. *Journal of Volcanology and Geothermal Research 172* (2008), 315-328.

Global Volcanism Program. (2011). Report on Pinatubo (Philippines). In *Wunderman, R (Ed.), Bulletin of the Global Volcanism Network, 36*:11. Smithsonian Institution. Accessed June 21, 2016.

Gonzaga, R. & Orejas, T. (2011). Zambales bore burnt of Mt. Pinatubo's fury. *Inquirer Central Luzon, Philippine Daily Inquirer.* June 16, 2011. Accessed June 23, 2017, 6:37 AM.

Hafeez, B., Khanif, Y. M., & Saleem, M. (2013). Role of Zinc in Plant Nutrition- A Review. *American Journal of Experimental Agriculture*, *3*(2), 374–391.

Herrera, I. O. (1992). Mt. Pinatubo R & D program of the department of agriculture-Region III. In *Proceedings of symposium on sustainable agricultural development of Mt. Pinatubo- affected areas*. November 5-6, 1992. Farming Systems and Soil Resources Institute, College of Agriculture, University of the Philippines, Los Banos, College, Laguna.

Hillel, D. (1998). Environmental soil physics. *Fundamentals, Applications, and Environmental Considerations.* Academic Press, pp771.

Hudson, B. (1994). Soil organic matter and available water capacity. *J. Soil Water Conserv. 49*:189–193.

Icamina, P. (1992). Life after Pinatubo: Conjuring crops from fire, mud, and ash. *Press Foundation of Asia, Phil. The FAO review (FAO) 24*:2 pp.23-28.

Imtiaz, M. (1999). Zn deficiency in cereals. *Ph.D. Thesis Reading University*, U.K.

Ismail, H., Shamshuddin, J., & Syed Omar, S. R. (1993). Alleviation of soil acidity in a Malaysian Ultisol and Oxisol for corn growth. *Plant Soil 151*, 55–65.

IRRI. (1997). Rice Almanac, International Rice Research Institute, Makati City, Philippines.

IRRI. (2019). Hybrid rice. https://www.irri.org/hybrid-rice. IRRI. Accessed Nov 12, 2019 6:47 AM.

Janda, R. J., Daag, A. S., Delos Reyes, P. J., Newhall, C. G., Pierson, T. C., Punongbayan, R. S., Rodolfo, K. S., Solidum, R. U., Umbal, J. V. (1996). Assessment and response to lahar hazard around Mount Pinatubo, 1991 to 1993. In *Newhall CG, Punongbayan RS (eds) Fire and Mud: Eruptions and Lahars of Mount Pinatubo, Philippines.* Philippine Institute of Volcanology and Seismology, Quezon City, and University of Washington Press, Seattle, pp 107–139.

Kimble, J. M., Ping, C. L., Sumner, M. E., & Wilding, L. P. (2000). Andisols. In *Sumner, M. E. (Ed) Handbook of Soil Science*, pp. E209-224, CRC Press, Boca Raton, FL.

Mateo, L. (1992). Characterization and amelioration of lowland rice soils affected by volcanic ejecta from Mt. Pinatubo. *Doctor of Philosophy. Dissertation manuscript.* 127 p. Philippines.

Melosantos, M. O. P, Solidum, R. U., Scott, W. E., Quiambao, R. B., Umbal, J. V., Rodolfo, K. S., Tubianosa, B. S., Delos Reyes, P. J., Alonso, R. A., & Ruelo, H. (1996). Tephra falls of the 1991 eruptions of Mount Pinatubo. In *Newhall, C.G. and Punongbayan, R.S. Fire and mud (Eds). Eruptions and Lahar of Mount Pinatubo, Philippines.* Philippine Institute of Volcanology and Seismology, Quezon City. University of Washington Press, Seattle, and London. Printed in Hongkong.

Mendoza, T. C., & Cabangbang, R. P. (1992). Effects of Mt. Pinatubo eruption in crop production systems. *The Philippine Agriculturist*, *75*(1 & 2), 1–8.

Mercado, R., Bertram J., Lacsamana T., & Pineda, G. (1996). Socioeconomic impacts of the Mount Pinatubo eruption. In Newhall, C., & Punongbayan R (Eds.). Fire and Mud. Eruptions and lahars of Mount Pinatubo, Philippines, University of Washington Press, Seattle, pp. 1063- 1070.

Mizuta, S. (2009). Pinatubo Hazard Urgent Mitigation Project-Phase II. Mitsubishi Research Institute, Inc.

Nanzyo, M., & Kanno, H. (2018). Role of inorganic soil constituents in selected topics. In *Inorganic Constituents in Soil*. https://doi.org/10.1007/978-981-13-1214-4_6.

Neild, J., O'Flaherty, P., Hedley, P., Underwood, R., Johnston, D., Christenson, B., & Brown, P. (1998). Impact of a volcanic eruption on agriculture and forestry in New Zealand. MAF Policy Paper 99/2. July 1998.

Nelson, G. L. (2013). Land rehabilitation techniques of rice farmers in Pampanga (Philippines) after the Mt. Pinatubo Eruption. *Asia Life Sciences, 22(1)*, 155–181.

Neue, H. U., & Lantin, R. S. (1994). Micronutrient toxicities and deficiencies in rice in soil mineral stresses. In *Yeo, A. R., & Flowers, T. J. (Eds.). Approaches to Crop Improvement* (pp. 175- 200). Berlin: Springer-Verlag;

Newhall, C. G., & Punongbayan, R. S. (1996). Fire and mud. Eruptions and Lahar of Mount Pinatubo, Philippines. *Philippine Institute of Volcanology and Seismology,* Quezon City. University of Washington Press, Seattle, and London. Printed in Hongkong.

Newhall, C., Hendley, J. W., & Stauffer, P. H. (1997) The cataclysmic 1991 eruption of Mount Pinatubo, Philippines, U.S. Geological Survey Fact Sheet 113–97.

Orejas, T. (2015). Philvocs: Pinatubo lahar threats not over. *Inquirer Central Luzon, Philippine Daily Inquirer*. June 16, 2015. Accessed June 24, 2017, 7:05 AM.

PAGASA, 2007. Climate Map of the Philippines based on the Modified Corona Classification. Prepared by CDS/CAB/PAGASA/DOST. March 2007. Philippine Atmospheric, Geophysical, and Astronomical Services Administration.

PhilGIS, 2004a. Land Cover. Philippine GIS Data Clearinghouse. Data Link: https://drive.google.com/file/d/0B8qrCcaQIB4zRzNnMFFCaXJMcUU/view?usp=sh...

PhilGIS, 2004b. Digital elevation data. Philippine GIS Data Clearinghouse. Data Link: http://philgis.org/desired-gis-data/elevation.

Presidential Task Force on Mt. Pinatubo. (1992). Rehabilitation and Reconstruction Program for Mt. Pinatubo-Affected Areas, Task Force Mt. Pinatubo.

PSA. 2016. Palay production and land area. Philippine Statistics Authority, PSA Complex, East Avenue, Diliman Quezon City, Philippines 1101.

PSA. 2019. Crop statistics of the Philippines 2014-2018. Department of Agriculture. Philippine Statistics Authority, PSA Complex, East Avenue, Diliman Quezon City, Philippines 1101.

Rawls, W. J., Brakensiek, D. L., & Saxton, K. E. (1982). Estimation of soil water properties. *Trans. ASAE 25*:1316–1320.

Reed, W. A. (1904). Negritos of Zambales. Ethnological Survey Pub. Manila: Department of Interior.

Reyes, R. Y., & Neue, H. U. (1991). Characterization of the volcanic ejecta from Mount Pinatubo and its impact on rice production. *Philippine Journal of Crop Science, 16*(2), 69–73.

Samonte, H. P., Nanzyo, M., Ocampo, A. M., Kimura, K., Kanno, H., Ito, T., … Chino, M. (1992). Improving the production of corn and rice with controlled availability fertilizers (CAF) in Pinatubo Lahar. *NRCP Research Journal, 3*(2).

Saxton, K. E., Rawls, W. J., Romberger, J. S., Papendick, R. I. (1986). Estimating generalized soil-water characteristics from textures. *Soil Science Society of America Journal 50(4)*:1031-1036.

Schaetzl, R., Anderson, S. (2005). Soils: Genesis and Geomorphology. Cambridge University Press. Cambridge university press Cambridge, New York, Melbourne, Madrid, Cape Town, Singapore, São Paulo Cambridge. https://doi.org/10.2136/vzj2007.0030br.

Scott, K. M., Janda, R. J., de la Cruz, E., Gabinete, E., Eto, I., Isada, M., Sexon, M., and Hadley, K. C. (1996). Channel and sedimentation responses to large volumes of 1991 volcanic deposits on the east flank of Mount Pinatubo. In Newhall, C. G. & Punongbayan, R. S. (Eds.) *Fire and Mud: Eruptions and Lahar of Mount Pinatubo, Philippines.* Philippine Institute of Volcanology and Seismology, Quezon City. University of Washington Press, Seattle, and London. Printed in Hongkong.

Shamshuddin, J. (2006). Acid sulfate soil in Malaysia. *UPM Press,* Serdang.

Shamshuddin, J., Muhrizal, S., Fauziah, C. I., & Van Ranst, E. (2004). A laboratory study of pyrite oxidation in acid sulfate soils. *Commun. Soil Sci. Plant, 35*, 117–129, 2004.

Shamshuddin, J., Azman, E. A., Shazana, R. S., Ishak, C., Panhwar, Q., & Naher, U. (2014). Properties and Management of Acid Sulfate Soils in Southeast Asia for Sustainable Cultivation of Rice, Oil Palm, and Cocoa. *Advances in Agronomy. 124*. 91-142. 10.1016/B978-0-12-800138-7.00003-6.

Shoji, S., Nanzyo, M., & Dahlgren, R. A. (1993). Genesis of volcanic ash soils. In *Volcanic Ash Soils: Genesis, properties, and utilization. Developments in Soil Science 21*, Elsevier, Amsterdam-London- New York-Tokyo.

Shoji, S., & Takahashi, T. (2002). Environmental and agricultural significance of volcanic ash soils. *Global Environmental Research-English Edition, 6*(2), 113–135.

Singh, M. V. (2008). Micronutrient Deficiencies in Crops and Soils in India. In *Alloway, B.J. (Ed). Micronutrient Deficiencies in Global Crop Production (p.93-125).* Springer Science+Business Media BV.

Singh, K. B. (2011). Dynamics of Hydraulic Properties of Puddled Soils. In *Elango, L. (Ed.). Hydraulic Conductivity - Issues, Determination, and Applications.* ISBN: 978-953-307-288-3.

Soil Survey Staff. (1999). Soil taxonomy - a basic system of soil classification for mapping and interpreting soil surveys. US Department of Agriculture-Natural Resources Conservation Service, Washington, D.C.

Sys, I. C., Van Ranst, E., & Debaveye, I. J. (1991). Land Evaluation Part II. Methods in land evaluation. *Agricultural Publication*, Brussels Belgium.

Tan, K. H. (1984). Andosols. Van Nostrand Reinhold Company Inc. Benchmark Papers in Soil Sciences, Volume 4.

Ugolini, F. C., & Dahlgren, R. A. (2002). Soil Development in Volcanic Ash, 69–81 pp.

Vallance, J. W., & Iverson, R. M. (2015). Lahars and their deposits. In *The Encyclopedia of Volcanoes, Second Edition* (pp. 649–664). Elsevier Inc. https://doi.org/10.1016/B978-0-12-385938-9.00037-7.

Van Breemen, N., & Castro, R. U. (1980). Variation in zinc deficiency in rice along a toposequence of soils in Tiaong, Quezon Province, Philippines. III Cropping experiment. *Plant and Soil. 57*: 215-221.

Yoshida, S, & Tanaka, A. (1969). Zinc deficiency of the rice plant in calcareous soils. *Soil Science and Plant Nutrition 15*:75–80.

Chapter 7 Conclusions and Perspectives

7.1 General Conclusions

This Ph.D. research described the early stages of weathering and soil formation processes of pyroclast (tephra and lahar) materials produced by the catastrophic 1991 Mt. Pinatubo eruption. The impact of weathering of these new deposits, under varying vegetation types, on the ~500-yr soil isolated from the surface by burial was also assessed. The new information was used subsequently to supplement a quantitative investigation of biogenic silica (phyolith) accumulation in the 26-yr ash soil-grown to rice and its persistence in the buried soil. Phosphorus is usually a limiting nutrient in mature volcanic Andisols. However, the addition of fresh volcanic pyroclasts can act as a source of plant-available P. We compared the total and plant-available P status in the new soil developing from the 1991 pyroclast deposits with that corresponding to the buried soils. Finally, based on farmer interviews, we documented the main soil-related constraints, adaptation strategies and current crop productivity of the agricultural lands that were heavily impacted by the tephra and lahars. This information was then analyzed in light of the soil properties as characterized in the previous chapters.

Chapter 3 shows that the 1991 tephra materials deposited in the forest, grassland, and rice land-use types and the lahar emplaced in a rice soil have been subjected to minor chemical weathering. Organic carbon accumulation, formation of secondary SRO minerals and/or phyllosilicates (1:1 and 2:1 clays), and CEC development in the modern soil (MS) remain very limited. The organic C is probably mostly stabilized as organometallic (Al and Fe) complexes. Although the tephra/lahar-buried soils (BS) showed a slightly higher degree of soil development compared to the MS, their degree of weathering is also weak. Apparently, ~500 years of pedogenesis were not sufficient to establish Andic properties in these soils. Both the MS and BS are classified as Entisols.

Chapter 4 demonstrates that the contribution of phytolith from rice sheath biomass (BSi_{rs}) to the Si pool of a young volcanic ash soil is significant as it accounts for 23 ± 11 g Si m^{-2} y^{-1} and 175 ± 51 g Si m^{-2} y^{-1} in the MS and BS, respectively. However, the bulk of Si is likely contained in the glass component, especially in the MS. The addition of ash and subsequent cultivation of rice promoted the formation of BSi_{rs} in the MS. This is facilitated by the active plant uptake of dissolved Si released from the silicate constituents of the ash through weathering. The deposition of a ~38 cm-thick ash deposit prevented further addition of BSi_{rs} from rice biomass restitution. As long as the concentration of dissolved Si in the soil solution remains close to saturation with respect to amorphous silica, this pool of BSi_{rs} in the BS will not be readily leached and the stock of BSi_{rs} will probably remain stable for long periods of time.

Chapter 5 highlights that weathering from the 1991 pyroclast deposits released a significant amount of plant-available P during the early stage of weathering. This is attributed to the presence of apatite in Pinatubo's tephra. Some of the factors that may influence the P status in cultivated and non-cultivated young volcanic soils are the composition and heterogeneity of the pyroclast deposits (i.e. type, thickness, grain size, presence of eroded sediments), and the kind of land use and management (i.e. volume of crop cover, biomass restitution, and removal, fertilization, drainage, runoff). At Pinatubo, the generally lower P_{total} and P_{avail} values in the BS compared to the MS reflect the gradual loss of apatite during chemical weathering. Accordingly, the higher P retention measured in the ~500-yr BS compared to the 26-yr MS may reflect the small buildup of active Al and Fe in SRO minerals (i.e. allophanes and imogolite) and Al/Fe-organic matter complexes, which can bind P.

Chapter 6 confirms that the 1991 pyroclast deposits of varying types (i.e. ash, remobilized ash, lahar) and thicknesses (~15 cm-8 m) have affected negatively the soil quality and productivity of croplands, especially during the agricultural rehabilitation period. Based on the farmers' survey, we were able to identify the primary constraints

imposed by the pyroclast deposition as well as the secondary impacts induced by the deposits. Main soil constraints are poor water retention, high drainage, nutrient limitations, and low workability. Flooding is a major and persistent constraint that was exacerbated by pyroclast deposition and which limits crop productivity even up to the present. Currently, most of the farmers have already recovered and are able to increase their yield comparable with the regional yield average. However, the problem of soil acidity encountered in both tephra and lahar soils has been very difficult to address for the farmers, notably because they had never encountered this problem before the eruption.

7.2 Limitations and Perspectives

The results obtained from this research call for further investigations. Some suggestions are proposed in the following sections.

Pedogenesis and nutrient release in soils developing from tephra and lahar deposits

In Chapter 3, our findings revealed that the formation of SRO minerals (allophane/imogolite, ferrihydrite) in the 26-yr MS and even the ~500-yr BS are very low. Other secondary clay minerals such as the 1:1 (i.e. kaolinite, halloysite) and 2:1 (i.e. vermiculite, smectite) phyllosilicates and to a lesser extent, Al/Fe-organo complexes, seems to occur in both the MS and BS, even if in low amounts. We attributed the formation of 1:1 and 2:1 phyllosilicate minerals to the weathering of primary minerals while the SRO minerals, particularly the allophane/imogolite and ferrihydrite, are formed primarily from the Si, Fe, Al byproducts of silicate glass weathering. The presence of 1:1 and 2:1 clay minerals in the MS and BS seems to depend on the type of vegetation cover and possibly drainage conditions. Additional studies should be conducted in order to provide a robust assessment of the physical and chemical conditions that favour clay precipitation during the early stage of silica-rich tephra weathering. For instance, slow drainage or waterlogging followed by dry and warm conditions may be responsible for the formation of 1:1 and 2:1 clay minerals, i.e. halloysite and smectite, respectively, due to limited Si and base cation leaching. Directly related to weathering

investigations, the hydrology of the soils that are being formed in the tephra and lahar deposits vary to a large extent depending on the grain size and thickness of the deposits. It affects the soil moisture status and water flows, thereby influencing the dissolution of minerals and leaching of dissolved elements. Moisture retention curves should be established for these soils and should be compared to the water properties of the BS.

It would also be useful to improve our understanding of the mechanisms by which the presence of soil organic matter, 2:1 phyllosilicates and drainage conditions averts the formation of short-range order minerals during the early stage of pyroclast weathering under a humid tropical condition. The low quantities of allophane/imogolite detected in the tephra soils from Pinatubo may also relate to (1) inherently high silica concentration of soil being developed from a dacite parent rock and which has not been excessively leached with the time span of weathering in the MS and BS, (2) dissolution of silicate glasses contribute to the neoformation phyllosilicates via resilication, (3) formation of more stabilized Al/Fe-organo complexes limiting the availability of Al and Fe for allophane/imogolite formation, (4) incorporation of Al into the hydroxyl-Al interlayers of the 2:1 phyllosilicates that serve as a sink for Al released by weathering. Further, leaching of Si and base cations from the 1991 pyroclast deposit likely influence pedogenesis in the underlying BS. This process, and the reactions that underpin it, are poorly documented in the scientific literature and could be investigated further in the Pinatubo region.

Potassium is an important essential element for plant growth, grain production, pest resistance, and tolerance to adverse climatic conditions and lodging especially in cash crops including rice, sugarcane, and banana (IRRI, 2002). In Chapter 6, a farmer claimed that the release of K from lahar is responsible for the increase in sugar content but the yield obtained from sugarcane is still lower than the pre-1991 production. The opposite is observed by the farmer in ash-affected soil also grown with sugarcane. Thus, it seems relevant to determine the availability of K, and potentially other key nutrient elements, in different types of dacitic pyroclast deposits during the early stage of weathering and how it can affect the production as well as the fruit/seed quality. Similarly, farmers indicate the occurrence of zinc deficiency

that limits their rice production. The validity of this claim should be verified and if confirmed the precise causes should be identified.

As the tephra and lahar soils are still young, the major source of plant-available P may have been derived from primary mineral weathering, particularly apatite. The organic P pool is inferred to be low in both the MS and BS developed from tephra and lahar deposits due to their generally low estimated SOM content (Chapter 5). Phosphorous availability is regulated by both geochemical and biochemical processes, the latter may also influence P distribution in the short-term as the soil starts to accumulate organic matter from biomass restitution. The release of P in organic matter is via bacterial and fungal decomposition and P mineralization (Jurinak et al., 1986; Walbridge, 1991). Quantification of the P mineralized and immobilized in organic matter/microbial biomass can be a good indicator of the capacity of SOM to hold and release P during the early stage of weathering in the MS and BS. The sequential fractionation proposed by Hedley et al. (1982) may be used to separate the forms of organically bound soil P from the geochemically bound fractions. Furthermore, this method allows the estimation of the labile and non-labile inorganic P pools. The labile P is assumed to be available to microbial and vegetation communities in the short-term because it rapidly desorbs from the surface of soil particles while the non-labile P fractions are tightly bound to soil particles (i.e. Al and Fe phosphates), hence unavailable to plants (Cross & Schlesinger, 1995).

Soil organic carbon and biological activity in soils developing from tephra and lahar deposits

We inferred that the low organic matter content in the BS is due to the halt of biomass restitution and continuous mineralization of the pre-existing organic carbon content (Chapter 3). Furthermore, the low organic C accumulation may reflect the low amounts of SRO minerals available for adsorption. Fractionation of the soil organic C into pools characterized by different stabilities could be carried out. Several laboratory methods exist but for young volcanic soils, the densimetric separation may be the most appropriate (Dabin, 1976; Monnier et al., 1962; Ladd et al., 1977). In doing so, the distribution of organic C in organomineral complex, associated with mineral surfaces and as free

compounds can be assessed. Incubation experiments could also be used to determine the respiration rate of the MS vs BS soils and for different vegetation covers.

Microorganisms play an important role in weathering, oxidation/reduction, and immobilization/mineralization of elements such as C, N, P, and S (Lal, 2016). Microbial activity depends on the availability of organic matter and moisture and their abundance and type are influenced by the kind of vegetation and soil temperature levels. Chemical and mineralogical analyses aimed to understand the mechanisms involved in weathering and the availability of nutrients should be supported by biological studies. For instance, the decomposition rate of stored organic carbon in buried soils may be dictated by the survival and persistence of microorganisms under such conditions. Phosphorus in the soil can be immobilized in the microbial biomass (i.e. bacteria, fungi) serving as important storage for P in soils. Silica can be absorbed by microorganisms such as diatoms and sponges in irrigation waters which can affect the silicon biogeochemical cycling of cultivated tephra and lahar soils. The redox chemistry of sulfur may be influenced by sulfate-reducing bacteria, primarily of the genus *Desulfovibro*. Below pH 4.0, the bacteria, *Thiobacillus ferroxidans* are the most active oxidizers which can oxidize the sulfide gas to sulfuric acid (Elisa et al., 2011) which may add up to the acidity of tephra and lahar-derived soils.

Acidity in agricultural soils developing from lahar and tephra deposits

Very few studies dealt with the characterization and soil development in lahar deposits (Bliss, 1980; Grifal, 1980; Vallance, 2015). Our study provides new information that contributes to the understanding of the problems faced by farmers during the rehabilitation of agriculture in the lahar-affected areas. The lahar soil grown with rice (IR-Lahar) exhibited very low pH values in its MS (pH_{H2O} and pH_{KCl}=3.4-3.5) and BS (pH_{H2O}=3.9-4.6, pH_{KCl}=3.8-4.2) (Table A3.3; Chapter 3). Similarly, low pH values are also encountered rice farms affected by tephra falls.

The low pH values are below the optimum pH (measured in the solution of submerged soil) for rice which is ~6.6 (Bhaskaran & Varghese, 2009), which could, therefore, affect the normal growth of rice. Toxic levels of Al^{3+} may develop in the soil solutions, potentially harming plant roots and growth crops (Pagani et al., 2020).

In our survey, the acidity of lahar-derived soils has been reported as a causal factor in the decline of rice productivity. The acidity of tephra and lahar soils are hypothesized to initiate from either of the following factors: (1) oxidation/reduction reactions due to alternate wetting and drying in paddy fields may result in increased concentrations of Al^{3+}, Mn^{2+} and/or Fe^{2+} from in-situ primary mineral dissolution/oxidation or charged in irrigation water that passed through lahar sediments, and (2) oxidative dissolution of pyrite, which precipitates during weathering or originates from former sediments carried by lahar deposits, releasing Fe^{2+} and sulfuric acid (H_2SO_4). A clear distinction of the source of acidity and its concentration in both the tephra and lahar derived soils should be obtained. Chemical analysis of the irrigation water, the water source, and groundwater should be done to verify the concentration of dissolved Al^{3+}, Mn^{2+}, Fe^{2+} and their contribution to decreased pH values. The presence, formation, origin, content, and dissolution of pyrite in the ash and lahar soils subjected to waterlogging should also be studied. Overall, further investigations are needed in order to determine the factors and processes responsible for the development of acidic conditions in the young soils forming from the lahar and tephra materials.

In terms of soil acidity remediation, the most common method to increase soil pH is the application of limestones such as $CaCO_3$, and $MgCO_3$. Efficacy trials on the proper type, timing, and method of lime application, and drainage of excess water should be done to increase the pH levels of acidic soils. The use of ammonium sulfate by rice farmers may accentuate soil acidity levels. Its contribution to decreasing the pH values in both ash and lahar soils needs to be assessed.

Recommendations to improve the fertility and workability of pyroclast especially in lahar soils

In Chapter 6, we identified that 14 out of 20 farmers cultivating either rice, sugarcane, corn or sweet potato seem to have already recovered from the negative impacts of pyroclast deposition as their current crop yields are comparable with the regional yields. This may be attributed to their coping strategies (i.e. irrigation and fertilization at higher rates, mechanized cultivation, mixing of the pyroclast deposit with the buried soil) which addressed the main constraints on low water and nutrient holding capacity, and low workability as a consequence of limited weathering (Chapter 3 and 6). Among the recommendations to improve the quality of the soils developing from tephra and lahar is organic matter addition, mixing of the pyroclast materials with the buried soil, lime application to ameliorate acidity, and avoidance of fertilizer inputs containing ammonium and sulfur which may induce an increased level of soil acidification. Additional research and field trials should be conducted to verify the efficacy of organic matter, lime, and fertilizer application, and to establish the appropriate type, method, timing, and rates of application under varying conditions (i.e. type and thickness of pyroclast deposit, crop type, moisture conditions, pH levels, etc.).

7.3 References

Bhaskaran, U. P., & Varghese, T. (2009). Effect of submergence on alleviation of soil acidity and availability of nutrients in a rice-rice ecosystem. *The Proceedings of the International Plant Nutrition Colloquium XVI*. California Digital Library, University of California.

Dabin, B. (1976). Méthode d'extraction et de fractionnement des matières humiques du sol. Application à quelques études pédologiques et agronomiques dans les sols tropicaux. Cah. Orstom, *Sér. Pédol., XIV*, 287–297.

Elisa, A. A., Shamshuddin, J., & Fauziah, C. I. (2011). Root elongation, root surface area and organic acid exudation by rice seedling under Al^{3+} and/or H^{+} stress. *Amer J Agric Bio Sci. 6*: 324-331.

Hedley, M. J., Stewart, J. W. B., & Chauhan, B. S. (1982). Changes in inorganic and organic soil phosphorus fractions by cultivation practices and by laboratory incubations. *Soil Sci. Soc. Am. J.*, 46: 970-976.

Ladd, J. N., Parsons, J. W. & Amato, M. (1977). Studies of nitrogen immobilization and mineralization in calcareous soils – I, Distribution of immobilized nitrogen amongst soil fractions of different particle size and density. *Soil Biol. Biochem., 9*, 309–318.

IRRI. (2002). Nutrient deficiency symptoms in rice. Better crops international, 16. Special Supplement. International Rice Research Institute.

Jurinak, J. J., Dudley, L. M., Allen, M. F., & Knight, W. G. (1986). The role of calcium oxalate in the availability of phosphorus in soils of semiarid regions: A thermodynamic study. *Soil Sci., 142*: 255-262.

Lal, R. (2016). Encyclopedia of Soil Science. *Boca Raton: CRC Press*, https://doi.org/10.4324/9781315161860.

Monnier, G., Turc, L., & Jeanson–Luusinang, C. (1962). Une méthode de fractionnement densimétrique par centrifugation des matières organiques du sol. *Ann. Agron, 13*, 55–63.

Walbridge, M. R. (1991). Phosphorus availability in acid organic soils of the lower North Carolina coastal plain. *Ecology, 72*: 2083-2100.

Chapter 7: Conclusions and Perspectives

Chapter 8 Appendices

8.1 Appendices for Chapter 3

Table A3.1. Detailed morphological description of the soil profiles collected from selected sites in Tarlac, Pampanga, and Zambales.

Sampling site (soil profile) codes: Fo-Ash **(**P1-a and P1-b)
GPS Coordinates: 15°14'44.0" N, 120°26' 47.8" E (P1-a); 5°14'44.0" N, 120°26'46.5" E (P1-b)
Land use: Forest
Vegetation: *Tectona grandis, Imperata cylindrica*
Location: Sitio Sto. Niño, Brgy. San Vicente, Bamban, Tarlac
Altitude (m.a.s.l): 503 (P1-a); 512 (P1-b)
Slope (%): 23-40
Ground distance from Mt. Pinatubo (km): ~ 15
Annual precipitation (mm): 2,002 (PAGASA, 2019)
Air temperature / Soil temperature regime: 27 °C (PAGASA, 2007) / Hyperthermic
Drainage / Soil moisture regime: Well-drained / Udic
Parent material: Dacitic ash
Date of sampling: April 13, 2018

PROFILE CODE	HORIZON/ LAYER	DEPTH (cm)	DESCRIPTION	PROFILE PHOTO
Fo-Ash (P1-a)	Modern soil	0-3	Dull yellowish brown (10YR 5/3), dry; brownish black (10YR 3/2), moist; sandy clay loam; not sticky; slightly plastic, many medium and fine roots, granular, friable; 0.75 g cm^{-3} BD; clear smooth boundary	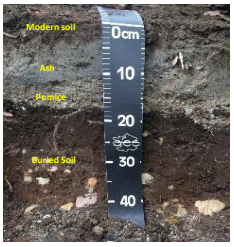
	Ash	3-11	Light gray (10YR 7/1), dry; brownish gray (10YR 4/1), moist; sandy loam; not sticky; slightly plastic, common medium and coarse roots, clear smooth boundary	
	Pumice	11-17	Light gray (5Y 7/1), dry; grayish yellow brown (10YR 6/2), moist; sandy; not sticky; not plastic, structureless; clear smooth boundary	
	Buried soil	17-40	Dull yellowish brown (10YR 5/3), dry; brownish black (7.5YR 3/2), moist; clay loam; slightly sticky; very plastic, subangular blocky, common distinct red mottles	
Fo-Ash (P1-b)	Modern soil	0-4	Grayish yellow brown (10YR 6/2), dry; brownish black (10YR 2/2), moist; sandy clay loam; not sticky; slightly plastic; many medium and fine roots, granular, friable; 0.85 g cm^{-3} BD; clear wavy boundary	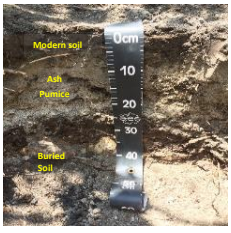
	Ash	4-13	Light gray (5Y 8/1), dry; grayish olive (5Y 5/2), moist; sandy loam; not sticky; slightly plastic; common medium and coarse roots, clear wavy boundary	
	Pumice	13-25	Light gray (5Y 8/1), dry; grayish olive (5Y 4/2), moist; sandy; not sticky; not plastic; structureless, abrupt smooth boundary	
	Buried soil	25-40	Dull yellowish brown (10YR 5/3), dry; brownish black (10YR 2/2), moist; clay loam; slightly sticky; very plastic; subangular blocky, common distinct red mottles	

Chapter 8: Appendices for Chapter 3

Sampling site (soil profile) codes: IR-Ash **(**P2-a and P2-b)
GPS Coordinates: 15°14'14.4" N 120°32'21.5" E (P2-a); 15°14'16.4" N 120°32'18.1" E (P2-b)
Land use: Irrigated rice
Vegetation: NSIC Rc160 (modern rice variety)
Location: Brgy. San Vicente, Bamban, Tarlac
Altitude (m.a.s.l): 87 (P2-a); 105 (P2-b)
Slope (%): 0-9
Ground distance from Mt. Pinatubo (km): ~23
Annual precipitation (mm): 2,002 (PAGASA, 2019)
Air temperature / Soil temperature regime: 27 °C (PAGASA, 2007) / Hyperthermic
Drainage / Soil moisture regime: Moderately to poorly drained / Udic
Parent material: Remobilized ash (dacitic)
Date of sampling: September 19, 2017

PROFILE CODE	HORIZON/ LAYER	DEPTH (cm)	DESCRIPTION	PROFILE PHOTO
IR-Ash (P2-a)	Modern soil	0-14	Dull yellowish brown (10YR 4/3), dry; brown (10YR 4/4), moist; silt loam; plowed; not sticky; very plastic; many distinct yellow mottles; subangular blocky; many fine and coarse roots; 0.79 g cm^{-3} BD; clear smooth boundary	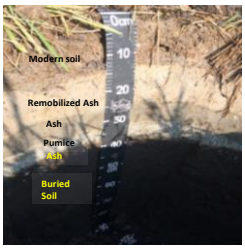
	Remobilized Ash	14-25	Light gray (5Y 7/2), dry; grayish yellow (2.5Y 6/2), moist; silt loam; moderately sticky; moderately plastic; subangular blocky to granular; very few fine roots; clear smooth boundary	
	Ash	25-32	Light gray (2.5Y 7/1), dry; grayish yellow (2.5Y 5/2), moist; sandy loam; not sticky; slightly plastic; subangular blocky to granular; very few fine roots; clear smooth boundary	
	Pumice	32-38	Light gray (2.5Y 7/1), dry; light gray (2.5Y 7/1), moist; sandy; not sticky; not plastic; structureless; small rock fragments present; clear smooth boundary	
	Ash	38-39	Yellowish brown (2.5Y 5/4), dry; olive brown (2.5Y 4/4), moist; loam; not sticky; slightly plastic; granular; clear smooth boundary	
	Buried soil	39-90	Dark brown (10YR 3/4), dry; brownish black (10YR 2/3), moist; loam; moderately sticky; very plastic; subangular blocky; many distinct red mottles	
IR-Ash (P2-b)	Modern soil	0-12	Dull yellowish brown (10YR 5/4), dry; dark brown, (10YR 3/4) moist; silt loam; plowed; not sticky; very plastic; many distinct yellow mottles; subangular blocky; many fine and coarse roots; 0.81 g cm^{-3} BD; abrupt wavy boundary	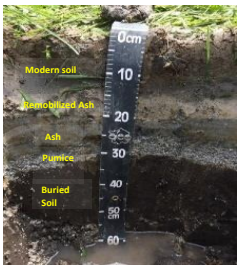
	Modern soil	12-15	Dull yellow orange (10YR 6/3), dry; brown (10YR 4/4), moist; silt loam; plowed; not sticky; very plastic; many distinct yellow mottles; subangular blocky; many fine and coarse roots; clear smooth boundary	
	Remobilized Ash	15-20	Grayish yellow (2.5Y 7/2), dry; yellowish brown (2.5Y 5/3), moist; silt loam; moderately sticky; moderately plastic; granular to subangular blocky; very few fine roots; abrupt wavy boundary	
	Ash	20-25	Light gray (2.5Y 7/1), dry; grayish yellow (2.5Y 6/2), moist; sandy loam; not sticky; slightly plastic; subangular blocky to granular; very few fine roots; abrupt smooth boundary	
	Pumice	25-31	Grayish yellow (2.5Y 6/2), dry; dark grayish yellow (2.5Y 5/2), moist; sandy; not sticky; not plastic; structureless; small rock fragments present; clear smooth boundary	
	Buried soil	31-55	Dark brown (10YR 3/4), dry; brownish black (10YR 2/2), moist; loam; moderately sticky; very plastic; subangular blocky; many distinct red mottles	

Chapter 8: Appendices for Chapter 3

Sampling site (soil profile) codes: Gr-LA-Ash **(**P3-a and P3-b)
GPS Coordinates: 14°58'24.1" N, 120°27'37.5" E (P3-a); 14°58'23.4" N 120°27'37.2" E (P3-b)
Land use: Grassland
Vegetation: *Paspalum conjugatum*
Location: Brgy. Pabanlag, Floridablanca, Pampanga
Altitude (m.a.s.l): 40 (P3-a); 46 (P3-b)
Slope (%): 0-9
Ground distance from Mt. Pinatubo (km): ~22
Annual precipitation (mm): 2,002 (PAGASA, 2019)
Air temperature / Soil temperature regime: 27 °C (PAGASA, 2007) / Hyperthermic
Drainage / Soil moisture regime: Well drained / Udic
Parent material: Dacitic pumice
Date of sampling: September 20, 2017

PROFILE CODE	HORIZON/ LAYER	DEPTH (cm)	DESCRIPTION	PROFILE PHOTO
Gr-LA-Ash (P3-a)	Modern soil	0-7	Grayish yellow brown (10YR 5/2), dry; brownish black (10YR 2/3), moist; loamy sand; granular; not sticky; not plastic, many fine to medium roots; 0.98 g cm^{-3} BD; abrupt wavy boundary	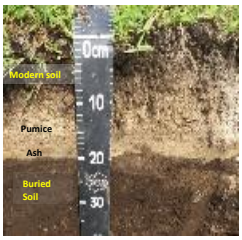
	Pumice	7-16	Light gray (10YR 8/1), dry; dull yellow orange (10YR 7/2), moist; sand; not sticky; not plastic; structureless; very few small rock fragments; abrupt wavy boundary	
	Ash	16-20	Grayish yellow (2.5Y 7/2), dry; olive brown (2.5Y 4/4), moist; sandy clay; not sticky; slightly plastic; common fine to medium roots, very friable, granular; clear wavy boundary	
	Buried soil	20-37	Dull yellowish brown (10YR 5/3), dry; brownish black (10YR 2/3), moist; sandy loam; not sticky; not plastic; subangular blocky, few very fine roots	
Gr-LA-Ash (P3-b)	Modern soil	0-6	Grayish brown (7.5YR 4/2), dry; black (7.5YR 2/1), moist; loamy sand; not sticky; not plastic; granular; many fine to medium roots; 1.02 g cm^{-3} BD; clear wavy boundary	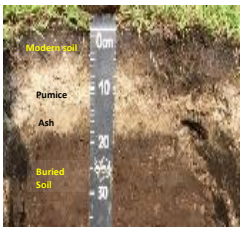
	Pumice	6-14	Dull yellow orange (10YR 7/2), dry; grayish yellow brown (10YR 6/2), moist; sandy; not sticky; not plastic; structureless; very few small rock fragments; abrupt wavy boundary	
	Ash	14-18	Grayish yellow (2.5Y 7/2), dry; yellowish brown (2.5Y 5/3), moist; sandy clay; not sticky; slightly plastic; very friable; granular clear wavy boundary	
	Buried soil	18-35	Dull yellowish brown (10YR 5/3), dry; brownish black (10YR 2/3), moist; sandy loam; not plastic; not sticky; subangular blocky, few very fine roots	

Chapter 8: Appendices for Chapter 3

Sampling site (soil profile) codes: Gr-HA-Ash **(**P4-a and P4-b)
GPS Coordinates: 15°08'22.4" N; 120°29'56.8" E (P4-a); 15°08'21.6" N; 120°29'50.2" E (P4-b)
Land use: Grassland
Vegetation: *Lantana camara, Corchorus olitorious, Ipomoea alba*
Location: Brgy. Sapang uwak, Porac, Pampanga
Altitude (m.a.s.l): 283 (P4-a); 286 (P4-b)
Slope (%): 23-40
Ground distance from Mt. Pinatubo (km): ~16
Annual precipitation (mm): 2,002 (PAGASA, 2019)
Air temperature / Soil temperature regime: 27 °C (PAGASA, 2007) / Hyperthermic
Drainage / Soil moisture regime: Well-drained / Udic
Parent material: Dacitic pumice
Date of sampling: September 21, 2017

PROFILE CODE	HORIZON/ LAYER	DEPTH (cm)	DESCRIPTION	PROFILE PHOTO
Gr-HA-Ash (P4-a)	Modern soil	0-13	Grayish yellow (2.5Y 6/2), dry; brownish black (2.5Y 3/2), moist; sandy clay loam; not sticky; slightly plastic; many coarse and fine roots; granular; friable; 0.79 g cm^{-3} BD; clear smooth boundary	
	Pumice	13-22	Grayish yellow (2.5Y 7/2), dry; grayish yellow (2.5Y 6/2), moist; sandy; not sticky; not plastic; structureless; clear wavy boundary	
	Ash	22-27	Grayish yellow (2.5Y 7/2), dry; yellowish brown (2.5Y 5/3), moist; clay; not sticky; moderately plastic; subangular blocky to granular; clear smooth boundary	
	Buried soil	27-50	Brown (7.5YR 4/3), dry; dark brown (7.5YR 3/3), moist; sandy loam; slightly sticky; very plastic; subangular blocky; many distinct red mottles	
Gr-HA-Ash (P4-b)	Modern soil	0-12	Grayish yellow brown (10YR 4/2), dry; dark grayish yellow (2.5Y 4/2), moist; sandy clay loam; not sticky; slightly plastic; many coarse and fine roots; granular; friable; 0.93 g cm^{-3} BD; clear wavy boundary	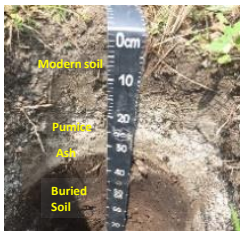
	Pumice	12-26	Light gray (5Y 7/2), dry; grayish olive (5Y 6/2), moist; sandy; not sticky; not plastic; structureless; clear wavy boundary	
	Ash	26-33	Light gray (5Y 7/2), dry; grayish olive (5Y 5/2), moist; clay; not sticky; moderately plastic; subangular blocky to granular; clear smooth boundary	
	Buried soil	33-73	Dark brown (7.5YR 3/4), dry; brownish black (7.5YR 2/2), moist; sandy loam; slightly sticky; very plastic; subangular blocky; many distinct red mottles	

Chapter 8: Appendices for Chapter 3

Sampling site (soil profile) codes: IR-Lahar **(**P5-a and P5-b)
GPS Coordinates: 14°58'28.9" N, 120°11'25.1" E (P5-a); 14°58'28.5" N, 120°11'24.2" E (P5-b)
Land use: Irrigated ash
Vegetation: NSIC Rc222 (modern variety; dry season); Pioneer 77 (hybrid variety; wet season)
Location: Brgy. Rabanes, San Marcelino, Zambales
Altitude (m.a.s.l): 48 (P5-a); 45 (P5-b)
Slope (%): 0-9
Ground distance from Mt. Pinatubo (km): ~25
Annual precipitation (mm): 3,502 (PAGASA, 2019)
Air temperature / Soil temperature regime: 27 °C (PAGASA, 2007) / Hyperthermic
Drainage / Soil moisture regime: Moderately drained / Udic
Parent material: Lahar
Date of sampling: April 13, 2018

PROFILE CODE	HORIZON/ LAYER	DEPTH (cm)	DESCRIPTION	PROFILE PHOTO
IR-Lahar (P5-a)	Modern soil	0-18	Brownish gray (10YR 5/1), dry; black (10YR 2/1), moist; loamy sand; plowed; not sticky; not plastic; structureless, big and small rock fragments, many fine and medium roots, gravelly; 0.79 g cm^{-3} BD; clear wavy boundary	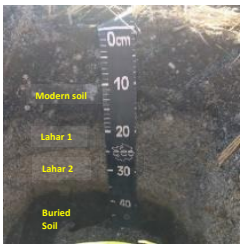
	Lahar	18-34	Light gray (2.5Y 8/1), dry; grayish yellow (2.5Y 7/2), moist; sandy; not sticky; not plastic; structureless, few fine roots, big and medium rock fragments, abrupt smooth boundary	
	Lahar	34-37	Light gray (2.5Y 8/2), dry; dull yellow (2.5Y 6/3), moist; sandy; not sticky; slightly plastic; small rock fragments, common fine distinct reddish to yellowish mottles, structureless; clear smooth boundary	
	Buried soil	37-50	Yellowish gray (2.5Y 6/1), dry; brownish black (10YR 2/2), moist; sandy clay loam; not sticky; moderately plastic; subangular blocky, common fine roots	
IR-Lahar (P5-b)	Modern soil	0-24	Yellowish gray (2.5Y 6/1), dry; dark grayish yellow (2.5Y 4/2), moist; loamy sand; plowed; not sticky; not plastic; structureless, big and small rock fragments, many fine and medium roots, gravelly; 0.91 g cm^{-3}; clear smooth boundary	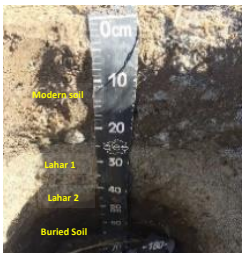
	Lahar	24-42	Light gray (2.5Y 8/1), dry; grayish yellow (2.5Y 7/2), moist; sandy; not sticky; not plastic; structureless, few fine roots, big and medium rock fragments; clear smooth boundary	
	Lahar	42-45	Pale yellow (2.5Y 8/3), dry; dull yellow (2.5Y 6/4), moist; sandy; not sticky; slightly plastic; small rock fragments, common fine distinct reddish to yellowish mottles, structureless; clear smooth boundary	
	Buried soil	45-65	Yellowish gray (2.5Y 5/1), dry; brownish black (2.5Y 3/1), moist; sandy clay loam; not sticky; moderately plastic; subangular blocky, common fine roots	

Table A3.2. Particle-size distribution in the Fo-Ash (P1-a and P1-b, Tarlac province), IR-Ash (P2-a and P2-b, Tarlac province), Gr-LA-Ash (P3-a and P3-b, Pampanga province), Gr-HA-Ash (P4-a and P4-b, Pampanga province) and IR-Lahar (P5-a and P5-b, Zambales province) soil profiles.

DEPTH		HORIZON/ LAYER	PARTICLE-SIZE DISTRIBUTION					
			SAND (50 µm – 2 mm)		SILT (2–50 µm)		CLAY (< 2 µm)	
[1]a	[1]b		a	b	a	b	a	b
cm			---------- *wt.%* ----------					
0-3	0-4	Modern soil	58.5	n.a.	8.0	n.a.	30.1	n.a.
3-11	4-13	Ash	80.2	n.a.	2.4	n.a.	15.3	n.a.
11-17	13-25	Pumice	69.7	n.a.	3.7	n.a.	24.9	n.a.
17-40	25-40	Buried soil	29.6	n.a.	32.2	n.a.	36.4	n.a.
0-14	0-15	Modern soil	12.4	26.5	67.3	53.8	17.7	16.5
14-25	15-20	Remobilized Ash	3.3	7.3	79.9	74.2	14.4	16.2
25-32	20-25	Ash	56.3	52.8	36.5	39.8	4.1	4.4
32-38	25-31	Pumice	94.3	n.a.	1.9	n.a.	4.3	n.a.
38-39	-	Ash	47.6	n.a.	43.6	n.a.	6.2	n.a.
39-90	31-55	Buried soil	47.6	44.1	30.9	36.5	18.1	17.0
0-7	0-6	Modern soil	83.9	n.a.	3.9	n.a.	11.1	n.a.
7-16	6-14	Pumice	94.8	n.a.	1.2	n.a.	3.1	n.a.
16-20	14-18	Ash	51.7	n.a.	5.2	n.a.	40.4	n.a.
20-37	18-35	Buried soil	75.3	n.a.	8.5	n.a.	14.6	n.a.
0-13	0-12	Modern soil	67.3	n.a.	3.1	n.a.	27.9	n.a.
13-22	12-26	Pumice	91.3	n.a.	1.3	n.a.	6.9	n.a.
22-27	26-33	Ash	41.3	n.a.	3.8	n.a.	51.8	n.a.
27-50	33-73	Buried soil	56.9	n.a.	24.2	n.a.	18.0	n.a.
0-18	0-24	Modern soil	82.7	n.a.	3.8	n.a.	11.9	n.a.
18-34	24-42	Lahar 1	95.2	n.a.	1.0	n.a.	3.1	n.a.
34-37	42-45	Lahar 2	49.7	n.a.	6.4	n.a.	41.7	n.a.
37-50	45-65	Buried soil	62.8	n.a.	9.3	n.a.	25.9	n.a.

[1,2] Two soil profile pits per sampling site; 'n.a.' not analyzed

Table A3.3. Major soil chemical properties in the Fo-Ash (P1-a and P1-b, Tarlac province), IR-Ash (P2-a and P2-b, Tarlac province), Gr-LA-Ash (P3-a and P3-b, Pampanga province), Gr-HA-Ash (P4-a and P4-b, Pampanga province) and IR-Lahar (P5-a and P5-b, Zambales province) soil profiles.

PROFILE CODE	DEPTH		HORIZON/ LAYER	pH				BD		CEC		BS		ORGANIC C		SOM		P RETENTION		TOTAL N	
				H_2O		KCl															
	cm							*g cm $^{-3}$*		*cmol $_c$ kg $^{-1}$*		*%*		*wt.%*		*wt.%*		*%*		*%*	
	a[1]	b[2]		a	b	a	b	a	b	a	b	a	b	a	b	a	b	a	b	a	b
Fo-Ash (P1)	0-3	0-4	Modern soil	6.68	7.60	5.97	7.16	0.75	0.85	3.85	4.17	162	192	1.34	1.23	2.30	2.12	4.23	8.62	0.14	0.13
	3-11	4-13	Ash	6.27	7.07	5.53	6.46	-	-	0.97	1.23	139	162	0.34	0.24	0.58	0.40	0.00	0.00	0.05	0.02
	11-17	13-25	Pumice	5.93	7.24	5.26	6.41	-	-	1.44	1.64	78	135	0.26	0.24	0.45	0.41	0.00	0.00	0.03	0.02
	17-40	25-40	Buried soil	5.63	6.85	4.16	5.45	-	-	9.66	7.11	56	136	1.83	1.28	3.15	2.20	26.06	21.55	0.18	0.11
IR-Ash (P2)	0-14	0-15	Modern soil	4.62	4.91	4.13	4.19	0.79	0.81	8.73	6.77	50	55	2.03	1.45	3.49	2.80	11.79	15.97	0.30	0.25
	14-25	15-20	Remobilized Ash	5.85	5.99	4.99	4.76	-	-	3.58	4.39	74	77	0.19	0.30	0.33	2.18	7.26	5.56	0.10	0.21
	25-32	20-25	Ash	5.78	6.1	5.28	5.02	-	-	1.17	0.90	101	151	0.07	0.10	0.12	0.52	0.73	0.00	0.06	0.09
	32-38	25-31	Pumice	5.45	6.03	5.04	5.23	-	-	3.38	1.35	14	52	0.17	0.08	0.29	0.17	0.92	0.00	0.80	0.07
	38-39	-	Ash	5.72	-	4.86	-	-	-	3.56	-	66	-	0.16	-	0.28	0.14	4.89	-	0.10	0.08
	39-90	31-55	Buried soil	4.76	5.81	4.18	5.03	-	-	7.80	7.59	49	73	0.96	0.61	1.65	1.05	12.21	3.26	0.17	0.11
Gr-LA-Ash (P3)	0-7	0-6	Modern soil	5.53	5.72	4.79	4.88	0.98	1.02	2.67	2.08	129	159	1.81	1.34	3.11	2.30	0.00	0.00	0.14	0.14
	7-16	6-14	Pumice	6.52	6.19	4.87	4.79	-	-	1.18	1.19	93	73	0.16	0.24	0.28	0.41	0.00	0.00	0.02	0.04
	16-20	14-18	Ash	6.22	6.02	4.67	4.66	-	-	2.43	2.21	108	94	0.20	0.30	0.34	0.52	4.31	1.88	0.02	0.04
	20-37	18-35	Buried soil	5.97	5.94	4.52	4.71	-	-	2.52	2.54	123	106	0.46	0.43	0.79	0.74	3.49	2.23	0.06	0.07

Table A3.3 (cont'd). Major soil chemical properties in the Fo-Ash (P1-a and P1-b, Tarlac province), IR-Ash (P2-a and P2-b, Tarlac province), Gr-LA-Ash (P3-a and P3-b, Pampanga province), Gr-HA-Ash (P4-a and P4-b, Pampanga province) and IR-Lahar (P5-a and P5-b, Zambales province) soil profiles.

PROFILE CODE	DEPTH		HORIZON/ LAYER	pH				BD		CEC		BS		ORGANIC C		SOM		P RETENTION		TOTAL N	
				H_2O		KCl															
	cm							*g cm^{-3}*		*cmol$_c$ kg^{-1}*		*%*		*wt.%*		*wt.%*		*%*		*%*	
	a[1]	b[2]		a	b	a	b	a	b	a	b	a	b	a	b	a	b	a	b	a	b
Gr-HA-Ash (P4)	0-13	0-12	Modern soil	5.60	5.62	4.87	4.40	0.79	0.93	1.47	1.53	109	90	0.61	1.01	1.05	1.74	0.00	4.51	0.08	0.10
	13-22	12-26	Pumice	6.11	6.09	4.88	4.78	-	-	1.06	1.21	57	45	0.08	0.08	0.14	0.14	0.00	0.00	0.02	0.01
	22-27	26-33	Ash	6.18	6.56	4.64	4.54	-	-	1.90	1.54	91	116	0.11	0.09	0.19	0.15	0.00	0.00	0.03	0.02
	27-50	33-73	Buried soil	6.01	6.33	4.55	4.46	-	-	3.96	5.63	120	106	0.38	0.94	0.65	1.62	10.10	13.59	0.05	0.10
IR-Lahar (P5)	0-18	0-24	Modern soil	3.35	3.53	3.44	3.49	0.79	0.91	2.08	2.33	130	192	0.90	0.79	1.55	1.36	7.23	10.21	0.10	0.09
	18-34	24-42	Lahar 1	5.09	5.75	4.38	4.94	-	-	0.99	1.14	75	54	0.08	0.09	0.14	0.15	0.00	1.86	0.01	0.02
	34-37	42-45	Lahar 2	5.95	5.89	4.61	4.53	-	-	2.53	2.07	131	174	0.11	0.13	0.19	0.22	2.53	0.91	0.02	0.02
	37-50	45-65	Buried soil	3.88	4.64	3.84	4.22	-	-	3.44	2.90	167	130	1.19	0.89	2.05	1.53	16.22	10.95	0.13	0.09

[1,2] Two soil profile pits per sampling site; '-' no ash layer; 'CEC' cation exchange capacity by ammonium acetate pH 7; 'BD' bulk density; 'BS' base saturation; 'SOM' soil organic matter; 'total N' total nitrogen.

Table A3.4. Oxalate-extractable Si, Al, and Fe, DCB-extractable Fe, and pyrophosphate extractable Al and Fe in the Fo-Ash (P1-a and P1-b, Tarlac province), IR-Ash (P2-a and P2-b, Tarlac province), Gr-LA-Ash (P3-a and P3-b, Pampanga province), Gr-HA-Ash (P4-a and P4-b, Pampanga province) and IR-Lahar (P5-a and P5-b, Zambales province) soil profiles.

PROFILE CODE	DEPTH *cm*		HORIZON/ LAYER	Si_o		Al_o		Fe_o		Fe_d		Al_p		Fe_p		Allophane/ Imogolite		Ferrihydrite		Al_p/Al_o		Fe_p/Fe_o		Fe_o/Fe_d		$Al_o + 1/2Fe_o$	
				wt.%																						*wt.%*	
	a[1]	b[2]		a	b	a	b	a	b	a	b	a	b	a	b	a	b	a	b	a	b	a	b	a	b	a	b
Fo-Ash (P1)	0-3	0-4	Modern soil	0.034	0.033	0.11	0.10	0.43	0.36	0.46	0.30	0.04	0.04	0.03	0.04	0.24	0.24	0.74	0.61	0.39	0.40	0.07	0.11	0.95	1.17	0.33	0.27
	3-11	4-13	Ash	0.016	0.025	0.04	0.07	0.40	0.34	0.15	0.14	0.02	0.03	0.01	0.01	0.12	0.18	0.69	0.57	0.57	0.44	0.03	0.03	n.i.	n.i.	0.25	0.23
	11-17	13-25	Pumice	0.029	0.023	0.07	0.06	0.56	0.26	0.17	0.17	0.03	0.03	0.02	0.01	0.20	0.16	0.95	0.43	0.42	0.52	0.03	0.05	n.i.	n.i.	0.35	0.19
	17-40	25-40	Buried soil	0.041	0.050	0.32	0.30	0.51	0.44	1.84	1.52	0.24	0.19	0.22	0.18	0.29	0.35	0.86	0.75	0.75	0.64	0.44	0.40	0.28	0.29	0.57	0.52
IR-Ash (P2)	0-14	0-15	Modern soil	0.040	0.034	0.09	0.08	0.35	0.34	0.43	0.38	0.04	0.12	0.12	0.22	0.28	0.24	0.59	0.58	0.46	1.57	0.34	0.65	0.81	0.90	0.26	0.25
	14-25	15-20	Remobilized Ash	0.045	0.040	0.07	0.06	0.18	0.22	0.32	0.36	0.01	0.01	0.03	0.05	0.32	0.29	0.31	0.37	0.10	0.21	0.14	0.22	0.57	0.61	0.16	0.17
	25-32	20-25	Ash	0.024	0.018	0.04	0.03	0.42	0.35	0.19	0.20	0.00	0.01	0.02	0.02	0.17	0.13	0.71	0.60	0.12	0.19	0.04	0.05	n.i.	n.i.	0.24	0.20
	32-38	25-31	Pumice	0.019	0.016	0.02	0.02	0.17	0.37	0.12	0.09	0.01	0.01	0.01	0.01	0.13	0.11	0.29	0.62	0.32	0.28	0.07	0.02	n.i.	n.i.	0.11	0.21
	38-39	-	Ash	0.043	-	0.05	-	0.45	-	0.39	-	0.01	-	0.05	-	0.30	-	0.76	-	0.14	-	0.11	-	n.i.	-	0.27	-
	39-90	31-55	Buried soil	0.032	0.030	0.09	0.06	0.24	0.31	0.33	0.38	0.25	0.09	0.13	0.07	0.22	0.21	0.41	0.53	2.85	1.55	0.54	0.23	0.72	0.82	0.21	0.21
Gr-LA-Ash (P3)	0-7	0-6	Modern soil	0.009	0.009	0.07	0.07	0.38	0.32	0.14	0.16	0.06	0.05	0.03	0.02	0.06	0.07	0.65	0.55	0.78	0.74	0.07	0.07	2.64	1.98	0.26	0.23
	7-16	6-14	Pumice	0.019	0.014	0.06	0.05	0.29	0.28	0.08	0.08	0.03	0.03	0.01	0.01	0.13	0.10	0.49	0.48	0.59	0.66	0.03	0.03	n.i.	n.i.	0.20	0.19
	16-20	14-18	Ash	0.030	0.026	0.12	0.10	0.46	0.43	0.28	0.25	0.06	0.05	0.05	0.03	0.21	0.18	0.79	0.73	0.51	0.51	0.10	0.07	n.i.	n.i.	0.35	0.31
	20-37	18-35	Buried soil	0.022	0.020	0.14	0.13	0.51	0.88	0.36	0.38	0.09	0.06	0.05	0.03	0.15	0.14	0.87	1.50	0.66	0.49	0.09	0.04	1.40	2.33	0.40	0.57

Table A3.4 (cont'd). Oxalate-extractable Si, Al, and Fe, DCB-extractable Fe, and pyrophosphate extractable Al and Fe in the Fo-Ash (P1-a and P1-b, Tarlac province), IR-Ash (P2-a and P2-b, Tarlac province), Gr-LA-Ash (P3-a and P3-b, Pampanga province), Gr-HA-Ash (P4-a and P4-b, Pampanga province) and IR-Lahar (P5-a and P5-b, Zambales province) soil profiles.

PROFILE CODE	DEPTH *cm*		HORIZON/ LAYER	Si_o		Al_o		Fe_o		Fe_d		Al_p		Fe_p		Allophane/ Imogolite		Ferrihydrite		Al_p/Al_o		Fe_p/Fe_o		Fe_o/Fe_d		$Al_o + 1/2Fe_o$	
				---------- *wt.%* ----------																						*wt.%*	
	a[1]	b[2]		a	b	a	b	a	b	a	b	a	b	a	b	a	b	a	b	a	b	a	b	a	b	a	b
Gr-HA-Ash (P4)	0-13	0-12	Modern soil	0.014	0.015	0.07	0.08	0.36	0.12	0.16	0.18	0.04	0.07	0.02	0.05	0.10	0.11	0.62	0.20	0.67	0.86	0.05	0.41	2.34	0.66	0.25	0.14
	13-22	12-26	Pumice	0.019	0.016	0.05	0.04	0.48	0.24	0.22	0.06	0.02	0.02	0.01	0.00	0.14	0.12	0.81	0.40	0.51	0.59	0.01	0.01	n.i.	n.i.	0.29	0.16
	22-27	26-33	Ash	0.020	0.020	0.06	0.05	0.25	0.28	0.22	0.21	0.03	0.02	0.03	0.02	0.14	0.14	0.43	0.47	0.48	0.47	0.11	0.08	n.i.	n.i.	0.18	0.19
	27-50	33-73	Buried soil	0.047	0.031	0.14	0.21	0.27	0.38	0.59	0.60	0.05	0.10	0.02	0.08	0.33	0.22	0.45	0.65	0.33	0.48	0.06	0.22	0.45	0.64	0.28	0.40
IR-Lahar (P5)	0-18	0-24	Modern soil	0.005	0.014	0.02	0.06	0.20	0.34	0.16	0.22	0.04	0.04	0.08	0.10	0.04	0.10	0.34	0.57	1.78	0.66	0.39	0.28	1.25	1.50	0.12	0.22
	18-34	24-42	Lahar 1	0.007	0.023	0.02	0.05	0.48	0.53	0.07	0.07	0.02	0.03	0.01	0.01	0.05	0.16	0.82	0.90	0.65	0.59	0.01	0.03	n.i.	n.i.	0.27	0.32
	34-37	42-45	Lahar 2	0.031	0.032	0.09	0.07	0.37	0.43	0.26	0.34	0.03	0.02	0.04	0.05	0.22	0.23	0.63	0.73	0.33	0.36	0.11	0.13	n.i.	n.i.	0.28	0.28
	37-50	45-65	Buried soil	0.110	0.101	0.30	0.26	0.13	0.07	0.22	0.17	0.12	0.12	0.08	0.06	0.78	0.72	0.23	0.13	0.41	0.46	0.63	0.84	0.61	0.43	0.36	0.30

[1,2] Two soil profile pits per sampling site; estimated allophane/imogolite and ferrihydrite contents based on Eq. 3.5 and 3.6, respectively; oxalate-extracted Al and Fe (Al_o. Fe_o); DCB extracted Fe (Fe_d); pyrophosphate extractable Fe and Al (Fe_p, Al_p); 'n.i.' not included; '-' no ash layer.

Table A3.5. Indices to assess the degree of weathering of the Fo-Ash (P1-a and P1-b, Tarlac province), IR-Ash (P2-a and P2-b, Tarlac province), Gr-LA-Ash (P3-a and P3-b, Pampanga province), Gr-HA-Ash (P4-a and P4-b, Pampanga province) and IR-Lahar (P5-a and P5-b, Zambales province) soil profiles.

PROFILE CODE	DEPTH		HORIZON/ LAYER	TRB		Fe_d/Fe_t		Al:Si	
	cm			*cmol$_c$ kg^{-1}*					
	a[1]	b[2]		a	b	a	b	a	b
Fo-Ash (P1)	0-3	0-4	Modern soil	378	423	0.14	0.10	0.28	0.26
	3-11	4-13	Ash	505	463	0.05	0.04	0.29	0.25
	11-17	13-25	Pumice	423	414	0.06	0.06	0.26	0.27
	17-40	25-40	Buried soil	118	128	0.31	0.30	0.46	0.45
IR-Ash (P2)	0-14	0-15	Modern soil Remobilized	311	349	0.21	0.16	0.22	0.24
	14-25	15-20	Ash	330	338	0.21	0.20	0.19	0.20
	25-32	20-25	Ash	486	484	0.07	0.06	0.26	0.26
	32-38	25-31	Pumice	483	460	0.03	0.03	0.31	0.29
	38-39	-	Ash	428	-	0.13	-	0.24	-
	39-90	31-55	Buried soil	370	365	0.10	0.13	0.28	0.25
Gr-LA-Ash (P3)	0-7	0-6	Modern soil	463	475	0.05	0.04	0.30	0.31
	7-16	6-14	Pumice	434	443	0.03	0.04	0.24	0.30
	16-20	14-18	Ash	437	431	0.09	0.09	0.26	0.25
	20-37	18-35	Buried soil	422	422	0.08	0.08	0.33	0.30
Gr-HA-Ash (P4)	0-13	0-12	Modern soil	467	418	0.05	0.06	0.28	0.23
	13-22	12-26	Pumice	437	432	0.08	0.03	0.27	0.27
	22-27	26-33	Ash	434	419	0.08	0.08	0.25	0.23
	27-50	33-73	Buried soil	348	301	0.16	0.13	0.35	0.32
IR-Lahar (P5)	0-18	0-24	Modern soil	483	449	0.05	0.08	0.26	0.24
	18-34	24-42	Lahar 1	493	473	0.02	0.02	0.30	0.28
	34-37	42-45	Lahar 2	434	422	0.09	0.12	0.25	0.24
	37-50	45-65	Buried soil	440	469	0.08	0.06	0.27	0.27
*$ash_{(1991)}$				547				0.28	
*$pumice_{(1991)}$				517				0.27	

[1,2] Two soil profile pits per sampling site; *Data on the 1991 fresh ash '$ash_{(1991)}$' and pumice '$pumice_{(1991)}$' samples adapted from Castillo and Punongbayan (1996); *$ash_{(1991)}$ sample was collected at the northeast flank of the volcano; *$pumice_{(1991)}$ was collected near the Clark Airbase; the $pumice_{(1991)}$ value is the average composition of two phenocryst-rich pumice samples; 'TRB' total reserve in bases; 'Fe_d/Fe_t' DCB extracted Fe to total Fe; 'Al:Si' aluminum to silicon ratio.

Table A3.6. Mean contents of total and exchangeable bases in the Fo-Ash (P1-a and P1-b, Tarlac province), IR-Ash (P2-a and P2-b, Tarlac province), Gr-LA-Ash (P3-a and P3-b, Pampanga province), Gr-HA-Ash (P4-a and P4-b, Pampanga province) and IR-Lahar (P5-a and P5-b, Zambales province) soil profiles.

PROFILE CODE	DEPTH		HORIZON/ LAYER	TOTAL BASES								EXCHANGEABLE BASES									
				TOTAL Ca		TOTAL K		TOTAL Mg		TOTAL Na		Ca^{2+}		K^{+}		Mg^{2+}		Na^{+}		SUM OF BASE CATIONS	
	cm			---------- *cmol$_c$ kg^{-1}* ----------																	
	a[1]	b[2]		a	b	a	b	a	b	a	b	a	b	a	b	a	b	a	b	a	b
Fo-Ash (P1)	0-3	0-4	Modern soil	148	165	24	28	90	108	115	122	4.34	7.05	0.44	0.25	1.10	0.41	0.38	0.29	6.26	8.00
	3-11	4-13	Ash	208	178	24	28	124	121	149	136	0.65	1.55	0.09	0.12	0.17	0.16	0.44	0.17	1.35	1.99
	11-17	13-25	Pumice	160	162	32	29	94	83	137	140	0.67	1.61	0.11	0.13	0.17	0.31	0.17	0.16	1.13	2.21
	17-40	25-40	Buried soil	44	47	7	10	36	36	31	35	3.98	6.64	0.44	0.25	0.75	2.53	0.22	0.23	5.39	9.66
IR-Ash (P2)	0-14	0-15	Modern soil Remobilized	93	117	40	34	67	80	110	118	3.06	2.51	0.15	0.14	0.90	0.79	0.28	0.23	4.40	3.67
	14-25	15-20	Ash	86	93	54	50	65	70	125	124	1.78	2.12	0.12	0.16	0.52	0.75	0.21	0.35	2.63	3.37
	25-32	20-25	Ash	187	182	27	29	120	125	152	148	0.82	0.85	0.05	0.06	0.24	0.28	0.08	0.17	1.18	1.36
	32-38	25-31	Pumice	208	195	17	20	82	77	175	168	0.33	0.43	0.03	0.03	0.08	0.14	0.04	0.11	0.49	0.70
	38-39	-	Ash	152	-	32	-	104	-	140	-	1.48	-	0.14	-	0.43	-	0.31	-	2.35	-
	39-90	31-55	Buried soil	152	151	10	10	98	98	112	106	2.86	3.86	0.09	0.05	0.80	0.93	0.10	0.19	3.84	5.56
Gr-LA-Ash (P3)	0-7	0-6	Modern soil	193	198	22	20	104	114	144	142	2.58	2.56	0.15	0.13	0.57	0.44	0.13	0.17	3.44	3.30
	7-16	6-14	Pumice	166	192	33	21	87	77	148	153	0.48	0.57	0.13	0.05	0.11	0.13	0.38	0.11	1.11	0.86
	16-20	14-18	Ash	163	156	32	35	108	102	135	138	1.66	1.38	0.21	0.21	0.39	0.33	0.37	0.16	2.63	2.08
	20-37	18-35	Buried soil	182	181	13	13	96	86	131	142	2.44	2.04	0.20	0.14	0.41	0.45	0.06	0.07	3.12	2.69

[1,2] Two soil profile pits per sampling site; '-' no ash layer

Table A3.6 (cont'd). Mean contents of total and exchangeable bases in the Fo-Ash (P1-a and P1-b, Tarlac province), IR-Ash (P2-a and P2-b, Tarlac province), Gr-LA-Ash (P3-a and P3-b, Pampanga province), Gr-HA-Ash (P4-a and P4-b, Pampanga province) and IR-Lahar (P5-a and P5-b, Zambales province) soil profiles.

PROFILE CODE	DEPTH		HORIZON/ LAYER	TOTAL BASES								EXCHANGEABLE BASES									
				TOTAL Ca		TOTAL K		TOTAL Mg		TOTAL Na		Ca^{2+}		K^{+}		Mg^{2+}		Na^{+}		SUM OF BASE CATIONS	
	cm			---------- *cmol$_c$ kg^{-1}* ----------																	
	a[1]	b[2]		a	b	a	b	a	b	a	b	a	b	a	b	a	b	a	b	a	b
Gr-HA-Ash (P4)	0-13	0-12	Modern soil	180	149	29	35	115	107	143	126	1.10	0.94	0.20	0.16	0.20	0.15	0.10	0.13	1.60	1.38
	13-22	12-26	Pumice	183	181	23	24	71	72	159	156	0.36	0.34	0.07	0.03	0.11	0.10	0.06	0.07	0.60	0.54
	22-27	26-33	Ash	157	148	36	35	111	104	130	132	1.05	1.16	0.28	0.20	0.25	0.24	0.16	0.17	1.73	1.78
	27-50	33-73	Buried soil	143	121	13	13	92	86	101	82	3.67	5.09	0.50	0.31	0.48	0.41	0.10	0.18	4.76	5.99
IR-Lahar (P5)	0-18	0-24	Modern soil	189	167	23	30	136	120	135	132	1.78	3.07	0.04	0.05	0.56	0.79	0.32	0.58	2.71	4.49
	18-34	24-42	Lahar 1	211	196	19	22	97	106	167	149	0.48	0.36	0.04	0.04	0.14	0.11	0.08	0.11	0.74	0.62
	34-37	42-45	Lahar 2	158	154	29	29	108	106	137	134	2.35	2.53	0.14	0.20	0.60	0.62	0.21	0.24	3.31	3.59
	37-50	45-65	Buried soil	172	188	27	24	119	129	123	127	4.58	2.93	0.13	0.08	0.87	0.59	0.16	0.18	5.74	3.79

[1,2] Two soil profile pits per sampling site; '-' no ash layer

Table A3.7. Major and trace element composition in the Fo-Ash (P1-a and P1-b, Tarlac province), IR-Ash (P2-a and P2-b, Tarlac province), Gr-LA-Ash (P3-a and P3-b, Pampanga province), Gr-HA-Ash (P4-a and P4-b, Pampanga province) and IR-Lahar (P5-a and P5-b, Zambales province) soil profiles.

PROFILE CODE	DEPTH *cm*		HORIZON/ LAYER	SiO_2		Al_2O_3		Fe_2O_3		CaO		MgO		Na_2O		K_2O		TiO_2		MnO		P_2O_5	
				wt.%																			
	a[1]	b[2]		a	b	a	b	a	b	a	b	a	b	a	b	a	b	a	b	a	b	a	b
Fo-Ash (P1)	0-3	0-4	Modern soil	61.60	62.81	17.49	16.60	4.69	4.50	4.13	4.63	1.82	2.17	3.58	3.79	1.15	1.31	0.53	0.52	0.15	0.11	0.15	0.20
	3-11	4-13	Ash	62.43	64.10	18.07	16.21	4.15	4.52	5.82	4.97	2.51	2.43	4.61	4.22	1.11	1.32	0.44	0.53	0.14	0.11	0.17	0.17
	11-17	13-25	Pumice	64.87	64.37	16.89	17.28	4.00	3.92	4.49	4.54	1.89	1.68	4.25	4.32	1.53	1.37	0.48	0.47	0.09	0.09	0.17	0.13
	17-40	25-40	Buried soil	51.31	52.16	23.44	23.67	8.40	7.32	1.25	1.31	0.72	0.73	0.96	1.08	0.32	0.45	0.92	0.79	0.15	0.17	0.08	0.09
IR-Ash (P2)	0-14	0-15	Modern soil	66.59	65.28	14.55	15.49	2.94	3.37	2.62	3.28	1.35	1.62	3.42	3.64	1.91	1.58	0.32	0.39	0.10	0.09	0.12	0.13
	14-25	15-20	Remobilized Ash	70.83	69.41	13.69	14.07	2.16	2.52	2.39	2.62	1.30	1.40	3.88	3.85	2.55	2.36	0.24	0.28	0.10	0.08	0.11	0.12
	25-32	20-25	Ash	62.77	63.17	16.59	16.14	4.00	4.55	5.25	5.09	2.42	2.52	4.70	4.60	1.26	1.35	0.47	0.50	0.10	0.11	0.17	0.18
	32-38	25-31	Pumice	60.40	63.20	19.00	18.17	5.21	3.73	5.82	5.45	1.66	1.56	5.44	5.21	0.82	0.93	0.57	0.46	0.08	0.07	0.10	0.11
	38-39	-	Ash	65.16	-	15.46	-	4.30	-	4.25	-	2.09	-	4.33	-	1.53	-	0.50	-	0.12	-	0.17	-
	39-90	31-55	Buried soil	62.21	64.76	17.54	15.96	4.67	4.23	4.24	4.22	1.97	1.98	3.46	3.29	0.46	0.48	0.57	0.59	0.16	0.11	0.06	0.06
Gr-LA-Ash (P3)	0-7	0-6	Modern soil	60.53	59.05	18.23	18.12	4.28	5.22	5.41	5.55	2.09	2.29	4.47	4.41	1.05	0.96	0.53	0.74	0.10	0.11	0.14	0.16
	7-16	6-14	Pumice	66.66	63.12	16.12	18.74	3.58	3.28	4.65	5.38	1.76	1.56	4.58	4.73	1.53	0.98	0.46	0.41	0.08	0.07	0.16	0.11
	16-20	14-18	Ash	63.83	65.10	16.84	16.20	4.62	3.75	4.55	4.37	2.18	2.06	4.17	4.27	1.49	1.65	0.60	0.45	0.10	0.09	0.16	0.15
	20-37	18-35	Buried soil	59.18	60.40	19.51	17.93	6.14	6.84	5.09	5.06	1.94	1.74	4.05	4.40	0.62	0.60	0.87	0.88	0.13	0.12	0.10	0.09

[1,2] Two soil profile pits per sampling site; Data on the 1991 fresh ash 'ash$_{(1991)}$' and pumice 'pumice$_{(1991)}$' samples adapted from Castillo and Punongbayan (1996); the ash$_{(1991)}$ sample was collected at the northeast flank of the volcano while the pumice$_{(1991)}$ were collected near the Clark Airbase; '-' no ash layer

Table A3.7 (cont'd). Major and trace element composition in the Fo-Ash (P1-a and P1-b, Tarlac province), IR-Ash (P2-a and P2-b, Tarlac province), Gr-LA-Ash (P3-a and P3-b, Pampanga province), Gr-HA-Ash (P4-a and P4-b, Pampanga province) and IR-Lahar (P5-a and P5-b, Zambales province) soil profiles.

PROFILE CODE	DEPTH *cm*		HORIZON/ LAYER	SiO_2		Al_2O_3		Fe_2O_3		CaO		MgO		Na_2O		K_2O		TiO_2		MnO		P_2O_5	
				---------- *wt.%* ----------																			
	a[1]	b[2]		a	b	a	b	a	b	a	b	a	b	a	b	a	b	a	b	a	b	a	b
Gr-HA-Ash (P4)	0-13	0-12	Modern soil	61.97	65.28	17.24	15.03	4.48	3.97	5.04	4.18	2.32	2.16	4.42	3.92	1.36	1.65	0.56	0.44	0.10	0.11	0.14	0.17
	13-22	12-26	Pumice	64.81	65.56	17.42	17.90	3.74	2.93	5.13	5.06	1.44	1.46	4.93	4.84	1.08	1.11	0.46	0.35	0.07	0.07	0.11	0.11
	22-27	26-33	Ash	65.35	66.61	16.11	15.44	3.80	3.61	4.41	4.14	2.24	2.10	4.03	4.08	1.69	1.66	0.46	0.42	0.10	0.09	0.17	0.16
	27-50	33-73	Buried soil	58.63	59.20	20.56	18.85	5.27	6.50	4.00	3.38	1.86	1.72	3.12	2.55	0.59	0.60	0.64	0.78	0.17	0.15	0.02	0.05
IR-Lahar (P5)	0-18	0-24	Modern soil	62.84	64.12	16.26	15.63	4.28	4.00	5.28	4.68	2.75	2.42	4.19	4.09	1.09	1.40	0.44	0.43	0.11	0.10	0.05	0.11
	18-34	24-42	Lahar 1	61.68	63.27	18.41	17.40	4.58	4.66	5.90	5.49	1.95	2.13	5.17	4.63	0.87	1.02	0.53	0.58	0.09	0.09	0.11	0.14
	34-37	42-45	Lahar 2	65.44	65.81	16.08	15.56	3.89	3.94	4.44	4.30	2.19	2.13	4.25	4.15	1.38	1.36	0.43	0.41	0.09	0.09	0.13	0.12
	37-50	45-65	Buried soil	61.66	61.78	16.91	16.77	3.89	4.31	4.81	5.26	2.39	2.61	3.80	3.95	1.26	1.14	0.48	0.55	0.09	0.10	0.16	0.17
*$ash_{(1991)}$				62.66		17.25		4.37		5.57		2.79		5.15		1.40		0.50		0.10		0.21	
*$pumice_{(1991)}$				64.05		17.01		4.19		5.36		2.45		4.70		1.47		0.52		0.09		0.19	

[1,2] Two soil profile pits per sampling site; Data on the 1991 fresh ash 'ash$_{(1991)}$' and pumice 'pumice$_{(1991)}$' samples adapted from Castillo and Punongbayan (1996); the ash$_{(1991)}$ sample was collected at the northeast flank of the volcano while the pumice$_{(1991)}$ were collected near the Clark Airbase; '-' no ash layer

8.2 Appendices for Chapter 4

Table A4.1. Morphological characteristics of the lowland rice soil profiles from Bamban, Tarlac province.

PROFILE	CODE	GPS COORDINATES	ELEVATION	DEPTH	HORIZON/ LAYER	DESCRIPTION
#			*m a.s.l*	*cm*		
P1	P1 - 1	15°14'14.4" N 120°32'21.5" E	87	0-14	Modern soil	Dull yellowish brown (10YR 4/3), dry; brown (10YR 4/4), moist; silt loam; plowed; not sticky; very plastic; many distinct yellow mottles; granular to subangular blocky; many fine and coarse roots
	P1 - 2			14-25	Remobilized Ash	Light gray (5Y 7/2), dry; grayish yellow (2.5Y 6/2), moist; silt loam; moderately sticky; moderately plastic; subangular blocky to granular; very few fine roots
	P1 - 3			25-32	Ash	Light gray (2.5Y 7/1), dry; grayish yellow (2.5Y 5/2), moist; sandy loam; not sticky; slightly plastic; granular to subangular blocky; very few fine roots
	P1 - 4			32-38	Pumice	Light gray (2.5Y 7/1), dry; Light gray (2.5Y 7/1), moist; sand; not sticky; not plastic; porous; structureless, rock fragments
	P1 - 5			38-39	Ash	Yellowish brown (2.5Y 5/4), dry; olive brown (2.5Y 4/4), moist; loam; not sticky; slightly plastic; granular
	P1 - 6			39-90	Buried soil	Dark brown (10YR 3/4), dry; brownish black (10YR 2/3), moist; loam; moderately sticky; very plastic; subangular blocky; many distinct red mottles
P2	P2 - 1	15°14'16.4" N 120°32'18.1" E	105	0-12	Modern soil	Dull yellowish brown (10YR 5/4), dry; dark brown, (10YR 3/4) moist; silt loam; plowed; not sticky; very plastic; many distinct yellow mottles; granular to subangular blocky; many fine and coarse roots
	P2 - 2			12-15	Modern soil	Dull yellow orange (10YR 6/3), dry; brown (10YR 4/4), moist; silt loam; plowed; not sticky; very plastic; many distinct yellow mottles; granular to subangular blocky; many fine and coarse roots
	P2 - 3			15-20	Remobilized Ash	Grayish yellow (2.5Y 7/2), dry; yellowish brown (2.5Y 5/3), moist; silt loam; moderately sticky; moderately plastic; subangular blocky to granular; very few fine roots
	P2 - 4			20-25	Ash	Light gray (2.5Y 7/1), dry; grayish yellow (2.5Y 6/2), moist; sandy loam; not sticky; slightly plastic; subangular blocky to granular; very few fine roots
	P2 - 5			25-31	Pumice	Grayish yellow (2.5Y 6/2), dry; dark grayish yellow (2.5Y 5/2), moist; sand; not sticky; not plastic; porous; structureless, rock fragments
	P2 - 6			31-55	Buried soil	Dark brown (10YR 3/4), dry; brownish black (10YR 2/2), moist; loam; moderately sticky; very plastic; subangular blocky; many distinct red mottles

Table A4.1 (cont'd). Morphological characteristics of the lowland rice soil profiles from Bamban, Tarlac province.

PROFILE	CODE	GPS COORDINATES	ELEVATION	DEPTH	HORIZON/ LAYER	DESCRIPTION
#			*m a.s.l*	*cm*		
P3	P3 - 1	15°14'14.9" N 120°32'20.7" E	100	0-15	Modern soil	Dark yellow orange (10YR 6/3), dry; brown (10YR 4/4), moist; silt loam; plowed; not sticky; very plastic; many distinct yellow mottles; granular to subangular blocky; many fine and coarse roots
	P3 - 2			15-34	Remobilized Ash	Light gray (5Y 7/1), dry; grayish yellow (2.5Y 6/2), moist; silt loam; moderately sticky; moderately plastic; granular to subangular blocky; very few fine roots
	P3 - 3			34-41	Ash	Grayish yellow (2.5Y 6/2), dry; grayish yellow (2.5Y 5/2), moist; sandy loam; not sticky; granular to subangular blocky; very few fine roots
	P3 - 4			41-44	Pumice	Dull yellow (2.5Y 6/4), dry; yellowish brown (2.5Y 5/3), moist; sand; not sticky; not plastic; porous; structureless, rock fragments
	P3 - 5			44-45	Ash	Dull yellow (2.5Y 6/4), dry; olive brown (2.5Y 4/6), moist; sandy loam; not sticky; slightly plastic; granular; very few fine roots
	P3 - 6			45-73	Buried soil	Dark brown (2.5Y 3/4), dry; black (10YR 2/1), moist; loam; not sticky; slightly plastic; subangular blocky; many distinct red mottles

Table A4.2. Total element concentration (< 2 µm) in the soil horizons, ash, and pumice layers from lowland rice soil profiles at Bamban, Tarlac province.

PROFILE	DEPTH	HORIZON/ LAYER	MAJOR OXIDES								TOTAL BASES				
			SiO_2	Al_2O_3	Fe_2O_3	CaO	MgO	Na_2O	K_2O	TiO_2	Ca	K	Mg	Na	TRB
#	*cm*		*wt.%*								*$cmol_c\ kg^{-1}$*				
	1991 Ash deposit[1]		62.66	17.25	4.37	5.57	2.79	5.15	1.40	0.50	199	30	138	180	547
P1 - 1	0-14	Modern soil	66.59	14.55	2.94	2.62	1.35	3.42	1.91	0.32	93	40	67	110	311
P1 - 2	14-25	Remobilized ash	70.83	13.69	2.16	2.39	1.30	3.88	2.55	0.24	86	54	65	125	330
P1 - 3	25-32	Ash	62.77	16.59	4.00	5.25	2.42	4.70	1.26	0.47	187	27	120	152	486
P1 - 4	32-38	Pumice	60.40	19.00	5.21	5.82	1.66	5.44	0.82	0.57	208	17	82	175	483
P1 - 5	38-39	Ash	65.16	15.46	4.30	4.25	2.09	4.33	1.53	0.50	152	32	104	140	428
P1 - 6	39-90	Buried soil	62.21	17.54	4.67	4.24	1.97	3.46	0.46	0.57	152	10	98	112	370
P2 - 1	0-12	Modern soil	64.55	15.72	3.45	3.36	1.66	3.69	1.54	0.39	120	33	82	119	354
P2 - 2	12-15	Modern soil	66.00	15.25	3.28	3.20	1.59	3.60	1.62	0.38	114	34	79	116	344
P2 - 3	15-20	Remobilized ash	69.41	14.07	2.52	2.62	1.40	3.85	2.36	0.28	93	50	70	124	338
P2 - 4	20-25	Ash	63.17	16.14	4.55	5.09	2.52	4.60	1.35	0.50	182	29	125	148	484
P2 - 5	25-31	Pumice	63.20	18.17	3.73	5.45	1.56	5.21	0.93	0.46	195	20	77	168	460
P2 - 6	31-55	Buried soil	64.76	15.96	4.23	4.22	1.98	3.29	0.48	0.59	151	10	98	106	365
P3 - 1	0-15	Modern soil	66.14	15.06	3.16	3.20	1.51	3.79	1.78	0.35	114	38	75	122	349
P3 - 2	15-34	Remobilized ash	70.79	13.41	2.09	2.30	1.27	3.89	2.53	0.23	82	54	63	125	324
P3 - 3	34-41	Ash	63.49	16.59	4.37	5.11	2.25	4.64	1.13	0.52	182	24	112	150	468
P3 - 4	41-44	Pumice	60.96	19.05	4.60	5.79	1.43	5.39	0.73	0.55	207	16	71	174	467
P3 - 5	44-45	Ash	63.58	16.30	4.90	4.71	2.00	4.61	1.26	0.45	168	27	99	149	443
P3 - 6	45-73	Buried soil	66.73	14.84	4.01	3.66	1.78	2.95	0.47	0.52	131	10	88	95	324

[1]Adapted from Castillo & Punongbayan, 1996; 'TRB' (total reserve in bases)

Table A4.3. Photomicrographs of individual BSi (BSi_{rs}, BSi_g), and non-BSi (GSi) observed from the lowland rice soil profile horizons (MS, BS, and ash layer) at Bamban, Tarlac province.

TYPES AND MORPHOLOGIES OF BSI AND GSI	RELATIVE SHAPES AND SIZES OF BSI AND GSI (250x magnification)
I. BSi (Rice)	
1. Bulliform (cuneiform, fan-shaped)	
2. Bilobate (dumbbell with scooped ends)	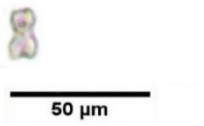
II. BSi (Other Grasses)	
A. Elongate class	
1. Elongate, smooth, non-spinose rod	
2. Elongate, concave ends	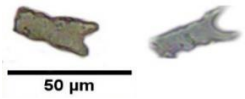
3. Elongate, spiny with pavement	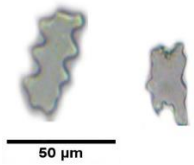

4. Elongate, sinuous



B. Festucoid class (wet, cool habitat)

1. Rectangular-shaped common bulliform



2. Square-shaped common bulliform

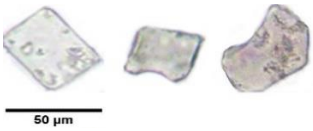

3. Circular crenate

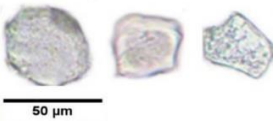

4. Round-shaped

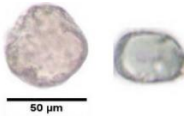

5. Elliptical



Panicoid class (wet, warm habitat)

1. Cross, thick shank

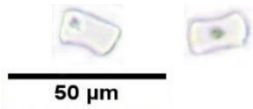

2. Irregular complex dumbbell

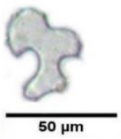

C. Chloridoid class (dry, warm habitat)

1. Chloridoid, Long saddle shape

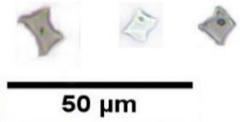

E. Polyhedrons with conical projection (scutiform-bulliform shape from reed or other Cyperaceae)	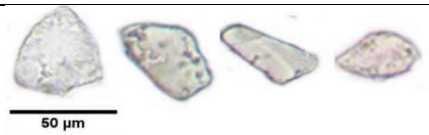
III. Non-BSi (GSi, silicate/volcanic glass)	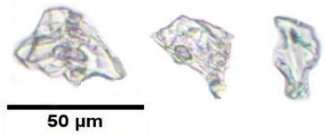

Morphologies of BSi_{rs} adapted from Zuo et al. (2016), Luo et al. (2016), Ball et al. (2015); BSi_{g} are adapted from Twiss et al., (1969); and GSi (Madella & Zurro, 2009).

8.3 Appendices for Chapter 5

Table A5.1. Phosphorus contents along with soil profile depth of the different land-use types in selected sites of Tarlac, Pampanga, and Zambales provinces.

PROFILE CODE	[a]DEPTH		HORIZON/ LAYER	P_{total}		P_{avail}		P_{avail}/P_{total}		P RETENTION	
	a	b		a	b	a	b	a	b	a	b
	cm			---------- *mg kg* $^{-1}$ ----------						----- *%* ----	
[b]tephra$_{(1991)}$				715		354		0.50			
[c]Sep 1991 Ash				-		72 ± 11		-			
Fo-Ash (P1)	0-3	0-4	Modern soil	673	853	92	212	0.14	0.25	4.23	8.62
	3-11	4-13	Ash	746	752	121	199	0.16	0.26	0.00	0.00
	11-17	13-25	Pumice	745	574	134	104	0.18	0.18	0.00	0.00
	17-40	25-40	Buried soil	330	376	4	5	0.01	0.01	26.06	21.55
IR-Ash (P2)	0-14	0-15	Modern soil	528	547	78	87	0.15	0.15	11.79	15.97
	14-25	15-20	Remobilized Ash	472	537	202	201	0.43	0.37	7.26	5.56
	25-32	20-25	Ash	727	796	248	258	0.34	0.32	0.73	0.00
	32-38	25-31	Pumice	454	492	55	88	0.12	0.18	0.92	0.00
	38-39	-	Ash	749	-	206	-	0.28	-	4.89	-
	39-90	31-55	Buried soil	241	250	26	22	0.11	0.09	12.21	3.26
Gr-LA-Ash (P3)	0-7	0-6	Modern soil	600	700	72	62	0.12	0.09	0.00	0.00
	7-16	6-14	Pumice	701	500	62	55	0.09	0.11	0.00	0.00
	16-20	14-18	Ash	717	666	163	180	0.23	0.27	4.31	1.88
	20-37	18-35	Buried soil	444	414	37	18	0.08	0.04	3.49	2.23
Gr-HA-Ash (P4)	0-13	0-12	Modern soil	620	742	131	166	0.21	0.22	0.00	4.51
	13-22	12-26	Pumice	500	490	71	55	0.14	0.11	0.00	0.00
	22-27	26-33	Ash	751	710	232	228	0.31	0.32	0.00	0.00
	27-50	33-73	Buried soil	104	217	1	2	0.01	0.01	10.10	13.59
IR-Lahar (P5)	0-18	0-24	Modern soil	233	470	22	90	0.09	0.19	7.23	10.21
	18-34	24-42	Lahar 1	494	631	62	68	0.12	0.11	0.00	1.86
	34-37	42-45	Lahar 2	546	542	115	116	0.21	0.21	2.53	0.91
	37-50	45-65	Buried soil	683	741	139	132	0.20	0.18	16.22	10.95

[a] Two pseudo-replicate soil profiles for each sampling site; [b] P contents of 1991 Mt. Pinatubo fresh tephra (Nanzyo et al., 1997); [c] P_{avail} content of September 1991 Mt. Pinatubo ash (sample donated by Prof. Alain Bernard, ULB, Belgium), n=2.

8.4 Appendices for Chapter 6

Table A6.1. Guide questionnaire used in the characterization of pyroclast-affected sites and assessment of farmers' adaptation practices on land quality constraints.

Questionnaire Number: _____
Date of Interview: _____
Location of Farm: _____
GPS Waypoint Number: _____

A. Farmer's Profile
Name: _____ Age: ___ Gender: ____
Farming experience (duration and no. of years): _____
Land tenure: ☐ private ownership ☐ tenancy ☐ communal ownership ☐ state ownership
Tenancy: ☐ Cash tenancy ☐ Labor tenancy ☐ Sharecropping

B. Description of the Farm
Total area of farm (ha): _____
Crop(s) grown and area (ha):_____
Average depth of water table (ft): Dry season: _____, Wet season: _____
Irrigation source: ☐ NIA ☐ CIA ☐ Spring ☐ SWIP ☐ STW ☐ SFR ☐ Rainfed
Position in the landscape: ☐ Top slope ☐ Middle slope ☐ Bottom
Depth of ashfall deposit (cm): _____, ☐ Deposited ☐ Remobilized
Depth of Lahar deposit (cm): _____

C. Crop management practices before and after the volcanic eruption

1. Inputs and Yields

CROP(S)	VARIETY (ies)	CROPPING PERIOD	AVERAGE YIELD	INPUTS (kind, rate, frequency of application)	COST OF PRODUCTION AND INCOME (Php)

2. Management Practices

CULTURAL MANAGEMENT	METHOD	FREQUENCY	LABOR REQUIREMENT	ESTIMATED COST (Php)
Land Preparation				
Planting				
Fertilization (kind, amount, timing)				
Weeding				
Pest management				
Irrigation				
Harvesting				

Year the farm was cultivated again after eruption? _____

Reason(s) for (not) choosing the same crop as before the eruption: _____

Constraints encountered on crop production:_____

Adaptation practices to cope with the constraints:_____

D. Farmer's observation on changes in some land quality indicators

LAND QUALITY INDICATORS/ CHARACTERISTICS	FARMER'S OBSERVATION IN DESCRIPTIVE TERMS:			
	Current	**After Eruption**	**Constraints**	**Management/ Adaptation**
Crop growth				
Soil color				
Soil depth				
Soil pH				
Drainage				
Erosion hazard				
Soil texture				
Soil workability				
Conditions affecting seed germination				
Flood hazard				
Rooting Conditions				
Potential for mechanization				

Other Information :

Government support/year (if any): _____

Non-government support/year (if any): _____

Trainings and seminars attended after eruption: _____

Affiliation to farming organizations: _____

Other Sources of Income : _____

Table A6.2. Description of the land utilization types affected by pyroclast deposits based on farmer/agricultural technician interview in Tarlac, Pampanga, and Zambales provinces based on key attributes.

KEY ATTRIBUTES	ASH-AFFECTED LAND UTILIZATION TYPES											
	LUT-A1		LUT-A2		LUT-A3		LUT-A4		LUT-A5		LUT-A6	
	CURRENT	PRE-1991	CURRENT	PRE-1991	CURRENT	PRE-1991	CURRENT	PRE-1991	CURRENT	PRE-1991	CURRENT	PRE-1991
Cropping System	Rc-Rc rotation		Rc-Rc rotation		Rc-Veg rotation	Rc-Rc rotation	Rc-Co-Co rotation	Rc-Rc rotation	Rc-[Co or Veg] rotation	Rc-Rc plus Co, Veg and Ro in other land parcels	Rc-Ro rotation	Rc and Ro intercrop
Specific types of crops grown	Rc [inbred varieties]	Rc [inbred and traditional varieties]	Rc [inbred varieties]	Rc [inbred and traditional varieties]	Veg [tomato, eggplant, lady's finger spring onion, hot pepper]; Rc [inbred variety]	Rc [inbred varities]	Rc and Co [hybrid varieties]	-	Rc [inbred variety]; Corn [hybrid variety]	Rc [inbred variety]; Veg [chili pepper, tomato, squash, sponge gourd]; Ro [cassava, sweet potato]	Rc [inbred and traditional varieties]	Rc [inbred and hyrid varieties]
Size of land holding (ha)	8.8		2		1		0.8		2.2		3	
Irrigation	NIS		CIS		Deepwell	CIS	CIS, spring, electric water pump	Electric water pump	Water pump	NIS	STW	Spring and SFR
Fertilization (types and rates)	IF (180-42-42 kg NPK ha^{-1})	IF	IF (85-18-18-36 kg NPKS ha^{-1})	IF	OF (i.e. chicken manure)	IF	IF (60-14-14 kg NPK ha^{-1} for rice; 240-56-116 kg NPK ha^{-1} for corn), OF	IF (60-14-14 kg NPK ha^{-1})	IF	IF	IF (92-14-14-36 kg NPKS ha^{-1})	IF
Weed management	manual weeding		herbicides	manual weeding	manual weeding	herbicides	herbicides	manual weeding	manual weeding	herbicides	manual weeding	
Crop protection	pesticides		pesticides		none	pesticides	pesticides		pesticides		none	pesticides
Mechanization	partly mechanized		partly mechanized		partly mechanized		partly mechanized	non-mechanized	partly mechanized	non-mechanized	partly mechanized	non-mechanized
Implements	tractor, animal (carabao)-drawn implements, thresher		tractor, animal- drawn, thresher		animal- drawn, tractor, combine harvester	animal-drawn, tractor	tractor	animal- drawn	tractor	animal- drawn	tractor	animal- drawn
Crop yield	5 t ha^{-1} $cropping^{-1}$	4 t ha^{-1} $cropping^{-1}$	5 t ha^{-1} $cropping^{-1}$	6.0-7.5 t ha^{-1} $cropping^{-1}$	3.6 t ha^{-1} $cropping^{-1}$ (rice)	2-4 t ha^{-1} $cropping^{-1}$	3.5 t ha^{-1} $cropping^{-1}$ (rice); 7.0 t ha^{-1} $cropping^{-1}$ (corn)	-	2 t ha^{-1} $cropping^{-1}$ (rice)	3.5-4.0 t ha^{-1} $cropping^{-1}$	2.4-4 t ha^{-1} $cropping^{-1}$ (rice)	4 t ha^{-1} $cropping^{-1}$ (rice)
Land Tenure	tenant		sharecropping		cash tenancy		owned		cash tenancy		owned	
Age/Gender	62 / Male		- / Male		50 / Male		44 / Male		58 / Male		49 / Male	
Farming experience (# of years)	> 50		-		38		30		45		35	
Respondent	Farmer		Farmer/Agricultural technician		Farmer		Farmer		Farmer		Farmer	
Technical knowledge	seminars attended about farming		seminars attended about farming; college/agriculture graduate		seminars attended about farming		seminars attended about farming		none		seminars attended about farming; elementary undergraduate	

Table A6.2 (cont'd). Description of the land utilization types affected by pyroclast deposits based on farmer/agricultural technician interview in Tarlac, Pampanga, and Zambales provinces based on key attributes.

KEY ATTRIBUTES	ASH-AFFECTED LAND UTILIZATION TYPES											
	LUT-A7		LUT-A8		LUT-A9		LUT-A10		LUT-A11		LUT-A12	
	CURRENT	PRE-1991	CURRENT	PRE-1991	CURRENT	PRE-1991	CURRENT	PRE-1991	CURRENT	PRE-1991	CURRENT	PRE-1991
Cropping System	Rc-[Ro or Veg] rotation	Rc-Rc rotation	Veg monocrop	Ro and Veg intercrop	Veg-Ro rotation with Fr	Fr	Su monocrop	Su, Ro intercrop	Ro-Su intercropping	Su	Gr	Rc-Rc rotation
Specific types of crops grown	Ro [sweet potato, cassava]; Veg [sitao, mungbean]; Rc [inbred variety]	Fr [mango]	Veg [spring onion, camote tops, pechay, mustard, spinach]		Veg [spring onion]; Fr [coconut, jackfruit, mango]	Fr [coconut, jackfruit, mango]	-	Ro [sweet potato]	Ro [cassava]	-	cogon grass	-
Size of land holding (ha)	3		1.7		-	-	3.5		1		3	
Irrigation	Electric pump (during dry season); rainfall (wet season)	diversion of water from the river	Electric Pump, SFR	Rainfall	Rainfall	-	SFR collected from river, STW	STW	Rainfall		Rainfall	STW
Fertilization (types and rates)	IF (53-0-0-60 kg NPKS ha^{-1})	not fertilized	IF and OF	IF	none	none	IF and OF (i.e. molasses)		IF (53-0-0 kg NPK ha^{-1} for rice; 276-0-0 kg NPK ha^{-1} for sugarcane)	IF and OF (i.e. molasses)	none	urea
Weed management	manual weeding	manual weeding	manual weeding		manual weeding	none	manual weeding		manual weeding		none	manual weeding
Crop protection	pesticides	none	none	none	none	-	none		none		none	pesticides
Mechanization	partly mechanized	non-mechanized	non-mechanized		non-mechanized	-	partly mechanized		non-mechanized		not mechanized	
Implements	hand tractor, animal-drawn	animal- drawn	hand tools	animal- drawn	animal- drawn	none	hand tractor		animal-drawn		none	animal-drawn
Crop yield	5 t ha^{-1} $cropping^{-1}$ (rice)	-	-	-	-	-	50 t ha^{-1} $cropping^{-1}$ (sugarcane)		50-300 t ha^{-1} $cropping^{-1}$ (sugarcane)	>100 t ha^{-1} $cropping^{-1}$ (sugarcane)	none	5 t ha^{-1} $cropping^{-1}$
Land Tenure	sharecropping		cash tenancy		-		owned		owned		-	
Age/Gender	59 / Male		45 / Male		-		56 / Male		44 / Male	-	67 / Male	
Farming experience (# of years)	-		14	-	-		31		25	-	50	
Person interviewed	Farmer/Agricultural technician		Farmer		Farmer		Farmer		Farmer		Farmer	
Technical knowledge	seminars attended about farming		seminars attended about farming		-	-	seminars attended about farming		-		-	

Table A6.2 (cont'd). Description of the land utilization types affected by pyroclast deposits based on farmer/agricultural technician interview in Tarlac, Pampanga, and Zambales provinces based on key attributes.

KEY ATTRIBUTES	ASH-AFFECTED LAND UTILIZATION TYPES						REMOBILIZED ASH-AFFECTED LAND UTILIZATION TYPES					
	LUT-A13		LUT-A14		LUT-A15		LUT-R1		LUT-R2		LUT-R3	
	CURRENT	PRE-1991	CURRENT	PRE-1991	CURRENT	PRE-1991	CURRENT	PRE-1991	CURRENT	PRE-1991	CURRENT	PRE-1991
Cropping System	Fo with Ban	RR and Ro intercropping	Fo with Ban	-	Veg and Ro intercropping	Sugarcane	Rc-Rc rotation	Su and Rc intecropping	Rc-Rc-[Rc and Veg] rotation	Rc-Co-Veg rotation	Rc-[Rc and Co]-Rc and Co] rotation	Rc-Co-Co rotation
Specific types of crops grown	Fo [i.e. acacia, bamboo]	Ro [taro, sweet potato]	-	-	-		-	-	hybrid varities	Veg [bitter gourd]	Rc [inbred and hybrid varieties]; Co [hydrid variety]; Veg [sitao, turnip]	Co [inbred variety]; Rc [traditional variety]
Size of land holding (ha)	>1		>1		-		2		2.1	-	1.3	
Irrigation	Rainfall		Rainfall	-	Diversion of free flowing water	-	CIS, spring	SFR	STW		STW	
Fertilization (types and rates)	none		none	-	IF and OF	-	IF (64-7-7 kg NPK ha^{-1})	IF (14-4-0 kg ha^{-1} NPK)	IF and OF (86-17-17 kg NPK ha^{-1})	-	IF (120-28-28 kg NPK ha-1 for rice; 162-28-28-48 kg NPKS ha-1 corn)	
Weed management	none	manual weeding	none	-	manual weeding	-	herbicides		herbicides	-	herbicides	manual weeding, herbicides
Crop protection	none	-	none	-	-	-	pesticides		pesticides	-	pesticides	
Mechanization	not mechanized		non- mechanized	-	non-mechanized	-	partly mechanized		partly mechanized	non-mechanized	partly mechanized	
Implements	-	animal-drawn	none	-	animal-drawn	-	animal- drawn, tractor, combine harvester	animal- drawn, tractor, thresher	tractor	animal-drawn	hand tractor, combine harvester	animal-drawn, tractor
Crop yield	-		none	-	-	-	3.6 t ha^{-1} $cropping^{-1}$	-	5-6 t ha^{-1} $cropping^{-1}$ (rice)	-	5 t ha^{-1} $cropping^{-1}$ (rice)	
Land Tenure	-		-		-		tenant		owned		owned	
Age/Gender	-		49 / Male		-		69 and 45 / Males		63 / Male		62 / Male	
Farming experience (# of	-		35		-		38		44		40	
Person interviewed	Farmer		Farmer		Farmer		Farmer		Farmer		Farmer	
Technical knowledge	-		-		learned from a research institution on crop and fertilizer management after pyroclast deposition when his area was used as an experimental field		seminars attended about farming	-	seminars attended about farming	-	seminars attended about farming	

Table A6.2 (cont'd). Description of the land utilization types affected by pyroclast deposits based on farmer/agricultural technician interview in Tarlac, Pampanga, and Zambales provinces based on key attributes.

KEY ATTRIBUTES	REMOBILIZED ASH-AFFECTED LAND UTILIZATION TYPES						LAHAR-AFFECTED LAND UTILIZATION TYPES					
	LUT-R4		LUT-R5		LUT-R6		LUT-L1		LUT-L2		LUT-L3	
	CURRENT	PRE-1991	CURRENT	PRE-1991	CURRENT	PRE-1991	CURRENT	PRE-1991	CURRENT	PRE-1991	CURRENT	PRE-1991
Cropping System	Rc-Veg rotation	Fishpond	Ro and Ve intercropping	-	Ma	Gr	Rc-Rc-Rc rotation		Rc-[Rc or Ro] rotation	Rc-Rc-[Rc and Veg] rotation	[Rc and Veg]-[Co and Veg] rotation	[Rc and Veg]-[Rc and Veg] rotation
Specific types of crops grown	Veg [tomato, eggplant, bitter gourd, sitao, sweet potato tops, squash]	-	Ro [cassava], Veg [sweet potato tops, eggplant]	-	-	-	Rc [inbred varieties]	Rc [inbred varieties]	Rc [inbred and hybrid varieties]; Ro [sweet potato]	Veg [sitao, mungbean]	Rc [inbred and hybrid varities]; Veg [sitao, turnip]	Rc [inbred varities]; Veg [sitao, mungbean]
Size of land holding (ha)	0.7		-				4.5		0.5		1.5	
Irrigation	STW	-	Rainfall	-	Rainfall		NIS	STW	NIS		Diversion of water from dike	NIS
Fertilization (types and rates)	IF (2-0-0-2 kg NPKS ha^{-1} for tomato) and foliar fertilizer	-	IF	-	-	-	IF (152-68-28 kg NPK ha^{-1})	IF	IF (119-14-14-120 kg NPKS ha^{-1})	IF	IF (92-0-0-24 kg NPKS ha^{-1})	IF
Weed management	manual weeding	-	manual weeding	-	none		herbicides	manual weeding	manual weeding		herbicides	manual weeding
Crop protection	pesticides	-	none	-	none		Pesticides		pesticides when needed		pesticides	none
Mechanization	partly mechanized	-	non-mechanized	-	non-mechanized		partly mechanized		partly mechanized	non-mechanized	partly mechanized	non-mechanized
Implements	animal-drawn, tractor	-	animal-drawn	-	-	-	tractor, combine harvester	tractor	hand tractor	animal-drawn	tractor, rotavator, animal drawn	animal-drawn
Crop yield	-	-	-	-	-	-	5 t ha^{-1} $cropping^{-1}$		4-4.5 t ha^{-1} $cropping^{-1}$ (rice); 10 t ha^{-1} $cropping^{-1}$ (sweet potato)	-	2 t ha^{-1} $cropping^{-1}$ (rice)	5.4 t ha^{-1} $cropping^{-1}$ (rice)
Land Tenure	owned		-		-		owned		sharecropping		sharecropping	
Age/Gender	67 / Male		-		-		-		35 / Male		58 / Male	
Farming experience (# of years)	-		-		-		-		25		35	
Person interviewed	Farmer		Agricultural technician		Agricultural technician		Farmer		Farmer		Farmer	
Technical knowledge	none		-		-	-	seminars attended about farming		seminars attended about farming		-	

Table A6.2 (cont'd). Description of the land utilization types affected by pyroclast deposits based on farmer/agricultural technician interview in Tarlac, Pampanga, and Zambales provinces based on key attributes.

KEY ATTRIBUTES	LAHAR-AFFECTED LAND UTILIZATION TYPES									
	LUT-L4		LUT-L5		LUT-L6		LUT-L7		LUT-L8	
	CURRENT	PRE-1991	CURRENT	PRE-1991	CURRENT	PRE-1991	CURRENT	PRE-1991	CURRENT	PRE-1991
Cropping System	Rc-Co or Veg rotation	Rc-Co rotation	Rc-[Co or Veg] rotation	Rc-Rc plus Co, Veg and Ro in other land parcels	Rc-Su rotation	Rc-Rc-Rc rotation	Veg monocrop	Rc-Rc rotation	Su monocrop	Rc-Rc-Rc rotation
Specific types of crops grown	Corn [hybrid varities]	-	Rc [hybrid variety; Co [hybrid variety]	Co [local variety; Veg [chili pepper, tomato, squash, sponge gourd], Ro [cassava, sweet potato]	-	-	tomato, eggplant, peanut, lady's finger, bottlegourd, watermelon	-	-	Rc [inbred variety]
Size of land holding (ha)	3.5		2		3		2		4.5	
Irrigation	STW, diversion of free flowing water during rainy season	Free flowing water	STW	Spring, SFR	rainfall	SFR	STW, drip irrigation (spray)	-	rainfall	SFR
Fertilization (types and rates)	IF	IF	IF (48-25-55 kg NPK ha^{-1}) and OF (chicken manure) for rice	IF (117-25-55 kg NPK ha^{-1} for rice)	IF (69-0-0 kg NPK ha^{-1}) for rice and OF (chicken manure, molasses)	IF (92-0-0 kg NPK ha^{-1})	IF, OF, and foliar fertilizer	IF (76-34-14 kg NPK ha^{-1})	IF (200-0-0-53 kg NPKS ha^{-1})	IF (78-0-0-36 kg NPKS ha^{-1})
Weed management	herbicides	-	herbicides	manual weeding, herbicides	-	herbicides	manual weeding, weeder		manual weeding	
Crop protection	pesticides	-	pesticides		-		-	pesticides as needed	none	pesticides
Mechanization	partly mechanized		partly mechanized	non-mechanized	partly mechanized	-	partly mechanized	non-mechanized	partly mechanized	non-mechanized
Implements	tractor	animal-drawn	hand tractor	animal-drawn	tractor	-	tractor, weeder	animal-drawn	tractor	animal-drawn
Crop yield	3 t ha^{-1} cropping^{-1} (rice)	5 t ha^{-1} cropping^{-1} (rice)	4.5 t ha^{-1} cropping^{-1} (rice)	4.0-4.5 t ha^{-1} cropping^{-1} (rice)	1.4-5.0 t ha^{-1} cropping^{-1} (rice)	2-4 t ha^{-1} cropping^{-1} (rice)	-	-	40-42 t ha^{-1} cropping^{-1} (sugarcane)	2.5-4 t ha^{-1} cropping^{-1} (rice)
Land Tenure	owned		-		-		owned		owned	
Age/Gender	62 / Male		- / Male		- / Female		85 / Male		42 / Male	
Farming experience (# of years)	40-50		12		51		35		5	
Person interviewed	Farmer/Agricultural technician		Farmer		Farmer		Farmer		Farmer	
Technical knowledge	-		attended seminars/trainings		-		-		-	

Table A6.2 (cont'd). Description of the land utilization types affected by pyroclast deposits based on farmer/agricultural technician interview in Tarlac, Pampanga, and Zambales provinces based on key attributes.

KEY ATTRIBUTES	LAHAR-AFFECTED LAND UTILIZATION TYPES									
	LUT-L9		LUT-L10		LUT-L11		LUT-L12		LUT-L13	
	CURRENT	PRE-1991	CURRENT	PRE-1991	CURRENT	PRE-1991	CURRENT	PRE-1991	CURRENT	PRE-1991
Cropping System	Rc-Veg and Ro intercropping	Rc-Veg and Ro intercropping	Gr	Rc and Co intercropping	Gr	Su monocrop	Gr	Fr	Fo	Rc-Ro rotation
Specific types of crops grown	Ro [taro]	Ro [taro, sweet potato], Veg [peanut, sitao]	-		-		-	Guava	agoho, *Chromolaena* sp. weed species	Rc [inbred variety]; Ro [cassava]
Size of land holding (ha)	2		>1		>1		>1		10	
Irrigation	Spring water	SFR	-		-		-		-	CIS
Fertilization (types and rates)	IF (57-0-0-12 kg NPKS ha^{-1} for rice; IF for taro)	IF (57-0-0-12 kg NPKS ha^{-1} for rice, IF for taro)	-		-		-		-	IF (138-28-28-76 kg NPKS ha^{-1} for rice)
Weed management	herbicides		-		-		-		-	manual weeding, herbicides
Crop protection	pesticides		-		-		-		-	pesticides
Mechanization	partly mechanized		-		-		-		-	partly mechanized
Implements	animal-drawn, tractor		-		-		-		-	animal-drawn
Crop yield	0.5-1 t <1 ha^{-1} $cropping^{-1}$ (rice)	1.5-2.5 t <1 ha^{-1} $cropping^{-1}$ (rice); 3-3.5 t <1 ha^{-1} $cropping^{-1}$ (taro)	-		-		-		-	4 t ha^{-1} $cropping^{-1}$ (rice)
Land Tenure	owned		-		-		-		cash tenancy	
Age/Gender	60 / Male		-		-		49 / Male		60 / Male	
Farming experience (# of years)	40		-		-		35		42	
Person interviewed	Farmer		Agricultural technician		Agricultural technician		Farmer		Farmer	
Technical knowledge	elementary undergraduate; attended seminars about herbicides		-		-		-		attended seminars/trainings	

Irrigation: National irrigation system (NIS), communal irrigation system (CIS), small farm reservoir (SFR), shallow tube well (STW); **Fertilization:** inorganic fertilizers (IF), organic fertilizers (OF); **Mechanization and implements**: *1)* fully mechanized (farming entirely mechanized from transplanting to harvesting), *2)* partly mechanized (i.e. use of tractors, combine harvester, thresher but still involves human labor), and *3)* non-mechanized (use of animal-drawn implements and human labor); rice (Rc); vegetables (Veg); corn (Co); root crop (Ro); sugarcane (Su); fruit trees (Fr); grassland (Gr); forest (Fo); banana (Ban), mango (Ma); Person interviewed: either the farmer, agricultural technician, or agricultural technican who also manages a farm (farmer/agricultural technician).

Table A6.3. Perception of the farmers/agricultural technicians on the constraints related to pyroclastic deposition and also by other factors (classified as pyroclast or non-pyroclast impact) on land qualities and associated land characteristics indicating the specific land utilization types where it is observed, and the specific adaptation practices employed to cope with the specified constraints.

LAND QUALITY	FARMERS' CONSTRAINTS BASED ON LAND CHARACTERISTICS (LUT CODE)	FARMERS' ADAPTATION PRACTICES (LUT CODE)
Moisture availability	***Pyroclast impact*** <u>Soil texture</u> • Water drains and dries easily due to sandy texture **(A2, A3, A4, A5, A8, A10, A11, A12, R1, R2, R3, R6, L1, L2, L3, L5, L6, L7, A15, L8, L10, L11, L12, L13)** • Sandy but gets sticky/muddy upon wetting **(A1, A6)**	• Installation of irrigation systems (i.e. water pumps, STW, diversion canals, SFR) to utilize groundwater and river water **(A3, A8)** • Frequent water application for crop use **(A3, A10)** • Frequent and higher rate of irrigation **(A4, A10, L5)** • Scraping of lahar materials through quarrying **(L6)** • Spreading of crop residues from vegetable cropping as mulch to conserve moisture **(A3)** • Soil is saturated with water before transplanting **(R2, L3)** • Direct dry seeding of rice due to limited moisture **(A5, L6)**

Pyroclast impact	
<u>Poor drainage and waterlogging</u> • Always submerged with water and difficult to drain especially after a rain event **(A4, A5, A7, L31)** and accompanied with a foul smell **(A1, A2)**	
Pyroclast impact	
<u>Stoniness</u> • Presence of big and/or small-sized stones hasten drainage **(A12, L1, L4, L7)**	• Removal of stones manually and mechanically using a tractor **(L7)** • Rocks were collected and buried deep under the soil **(L1)**
Pyroclast impact	
<u>Flooding incidence</u> • Flooding incidence especially during the rainy season **(A1, A2, A4, A5, R4, L2, L3, L4, L7, L8, L9)** • Flooding due to shallow riverbed/water table **(A1, L12)**	• Planting calendar is adjusted to avoid rainy months that induce flooding **(R4)** • Soil is being drained when flooded **(L4)** • Flood prone area with shallow water table are not cultivated/grown to crops, hence, became a grassland **(L12)**

	Non-pyroclast impact	
	<u>Water scarcity during summer months</u> • Drought due to insufficient water supply especially during the dry season, i.e. less rainfall, low supply of irrigation, deeper groundwater level **(A2, A6, A7, A11, R1, R2, R3, R5, L2, L3, L5, L6)**	• Installation of irrigation systems (i.e. water pumps, STW, diversion canals to connect water from rivers or dams, SFR) to utilize groundwater and river water **(A7, A8, L1)** • Planting calendar is adjusted especially for the rice to maximize water availability during the rainy season and escape too much heat during summer season **(L3)** • After the harvest of the first crop, the farmer plows the area once again to make use of the water underneath for the utilization of the subsequent crop **(R5).** • The farm is divided among crops due to insufficient water during the dry season (i.e. mixed cropping of rice and sweet potato instead of rice crop only) **(L2)** • Shift in crop type being grown, i.e. rice was replaced by sweet potato and vegetables **(A7)** or sugarcane **(L6)** which require less water during the dry season • The dry season cropping becomes a fallow period when there is no water available **(A7)** • The area is leveled for easier and even distribution of water **(R3)** • Continue to grow crops even if the water is insufficient and survival of plant is uncertain **(A7)**

		• Leveled the area and constructed canals to divert water from the lake **(A7)**
	Non-pyroclast impact <u>Water limitation due to the inaccessible water source</u> • Drought due to lack of water supply (difficult to access) **(A9, A12, A13, A14, R6, L13)**	• Did not cultivate for crop production and just made use of forest products **(L13)**. • Depends on rainfall for moisture **(A9)**
	Non-pyroclast impact <u>Topography</u> • Areas located in high altitudes have difficulty in accessing water **(A13, A14)** • Difficult to tap water due to increased elevation after lahar deposition **(L13)**	• Did not cultivate with high-value crops due to poor crop growth, hence, the land turned into the forest (**A13, A14)**. • With time, banana trees were planted as food and income source **(A13, A14)** • Benefited from forest products, i.e. timber is converted to charcoal **(A13)**
Nutrient Availability	***Pyroclast impact*** • Poor plant and root growth attributed to groundwater acidity **(A5, A7, A10, R1, L2, L3, L8, L9)**	• Mixing of the pyroclasts with the original through plowing and/or rotavation during land preparation **(A1, A15, R1, L1, L5, L9)**

	• Poor plant and root growths, and low yield due to poor soil nutrition **(A1, A4, A5, A6, A9, A12, A13, A14, R1, R2, R3, R5, L1, L2, L3, L4, L8, L9, L10, L11, L12)** • Weed infestation induced by pyroclast **(L4)** • Low in K required by sugarcane **(A11)**	• Application of both inorganic (i.e. urea, complete, ammosul, muriate of potash) and organic fertilizers (i.e. chicken manure, crop residues, foliar) **(A1, A3, A4, A5, A8, A11, A15, R1, R2, R3, L4, L5, L7)** • Applies double rate of inorganic fertilizers compared to the rates prior to eruption **(A4, A5, A6, R2, L1)** • Application of higher rate of fertilizers compared to their practice prior to eruption **(A1, R1, L2)** • Fertilizer is applied in between the rice plants then covered **(L4)** • Scraping of some lahar materials and the remaining lahar is plowed **(L6, L8)** • Choice of good/high yielding crop varieties (i.e. sweet potato, rice) **(A6, L2)** • Planting at the original soil by digging and removal of the pyroclast **(A15)** • Cropping rotation (for instance sugarcane to cassava and vice versa) depending on the vigor of crops and market demand **(A11)** • Removal of ash in sloping areas and plant fruit trees such as banana **(A9)**

		• Continuous cultivation to improve soil fertility **(L4)** • Soil is turned over to kill weeds **(L4)**
	Pyroclast impact	
	• Chlorosis (reddish coloration) and death of rice seedlings attributed to zinc deficiency **(A1, A4, R1, L2, L3, L4)** • Zinc deficiency, induced by waterlogging, causes stunted growth and early death of rice plants **(L4)** • Nutrient deficiencies due to waterlogging **(L4)**	• Zinc sulfate is applied to control the reddening of rice leaves and death of rice seedlings **(A1, A4, R1, L2, L3, L4)** • Frequent plowing/cultivation to eradicate weeds **(A2**) • Draining the soil to amend nutrient deficiencies **(L4)** • Application of herbicides to eradicate weeds **(R2)**
	Non-pyroclast impact	
	• Weed infestation **(A2, R2)**	• Application of herbicides to eradicate weeds **(R2, L4)**
Oxygen availability/ availability of foothold for roots	***Pyroclast impact*** <u>Soil structure</u> • Poor root growth due to hard structure **(A3, A5, L2, L6, L7)**	• Direct seeding and digging a hole using a bamboo where the farmer sows the seeds **(A5)**

	Non-pyroclast impact	
	<u>Topography/position in the landscape</u> • Poor drainage/waterlogging due to shallow water table especially during the rainy season which affects plant and root growths **(A1, A2, A4, A5, A7, L2, L3, L8, L9, L12)**	• During the wet season, transplanting at shallow depth or direct seeding of rice is done to avoid submergence of seedlings with the water table **(A1)** • Rice is grown on submerged areas because no other crop can grow on it **(L3)** • Destroying some bunds/dikes to drain excess water **(A2)**
Correct soil temperature regime	***Pyroclast impact*** • Soil temperature gets high affecting plant growth **(A4, A12, A13, R1, L2, L7, L10, L11)**	• Frequent and higher rate of irrigation **(A4)**
Workability (ease of cultivation)	***Pyroclast impact*** • Hard structure or becomes hard upon draining of water **(A2, A3, A5, A6, A10, R1, R2, R3, L1, L2, L3, L5, L6, L7)**	• Mechanized land preparation using tractor **(A5, R2, R3, L1, L2, L3, L4, L6, L7)** • Frequent water application to avoid hardening of the soil **(L5)** • Direct dry seeding of rice due to hard soil **(A5, L6)** • Soil is watered before plowing to ease cultivation (**A4, R1, L3**)

	• Difficult to till due to hard structure **(A4, A7, L1, L2, L3)** • Presence of stones **(A12, L4)** • Became more sandy than prior to eruption inducing hard structure **(A1, A3, A5, A15, A12, R2, L3)**	• Hired more laborers to work on land preparation because the soil is hard and difficult to cultivate (**A2, R3, L2)**
Resistance against erosion	***Pyroclast impact*** • Prone to erosion during rainfall events which induce flooding **(A4, A5, A10, R4, L2, L3)** • The area is prone to deposition of eroded materials from the upper mountain slopes **(R4)** • Flooded by lahar materials up to the present during the rainy season due to its low altitude and landscape position **(A15, L9)**	• Weeds are not removed to prevent erosion **(R4)** • Planting calendar is adjusted to avoid heavy rain and flooding periods especially for rice **(R4)**

Climatic hazards affecting plant growth	***Non-pyroclast impact*** • Typhoons and heavy rains which causes flooding and poor crop growth **(A1, A2, A3, A5, A7, A8, A15, R4, L9)**	• Destroying some bunds/dikes to drain excess water **(A2)** • Adjusting of planting calendar for the rice to escape months with high occurrence of heavy rain and floods **(R4)** • Does not cultivate during the rainy season **(A15, L9)**
Pest and disease infestation	***Non-pyroclast impact*** • Pest and/or disease infestation especially during the rainy season **(A1, A2, A3, A4, A6, A8, L1, L3, L5, L6, L9)**	• Application of pesticides/insecticides **(A4, A8, L3, L4, L5, L9)** • Seeds covered with mud to protect from bird infestation **(A4)** • Adjusting the planting calendar to escape heavy pest infestation **(L4)**

Table A6.4. Perception of the farmers/agricultural technicians on the positive effects on land qualities and associated land characteristics of pyroclastic deposits indicating the specific land utilization types where it is observed.

LAND QUALITY	LAND CHARACTERISTICS ([1]LUT CODE)
Oxygen availability/ availability of foothold for roots	• Improved drainage due to sandy texture **(A6)** • Presence of sand helped in the aeration of the subsoil **(A8)** • Loose structure is favorable for vegetables **(A3)** • Sandy texture is favorable for rooting of vegetables (**A8, R4**)
Nutrient Availability	• Yield improved after ash deposition because the hardpan had deepened but declined after 10 years when the ash was washed away by rain **(A10)** • Crop growth improved **(A8, A10, A11, R6)** • Improved root growth due to the addition of ash (**A2, A8, A10, R4)** • Seedling growth is good **(R4)** • Seed germination improved **(A6)** • High sugar content of sugarcane **(L8)**

Workability (ease of cultivation)	• Ash made the soil friable and easier to cultivate **(A11, R1, R4)** • Soil is hard upon drying but easy to cultivate **(A6)** • Sandy texture of ash improved the structure and workability **(A6, A8, A10, R4)** • More friable **(A8, A11, R3, L8)** • Easier to till **(A4, A6, A8, A10, A11, R3, R4)**
Resistance against erosion	• Not easily eroded when the ash was mixed with the soil **(A6)**

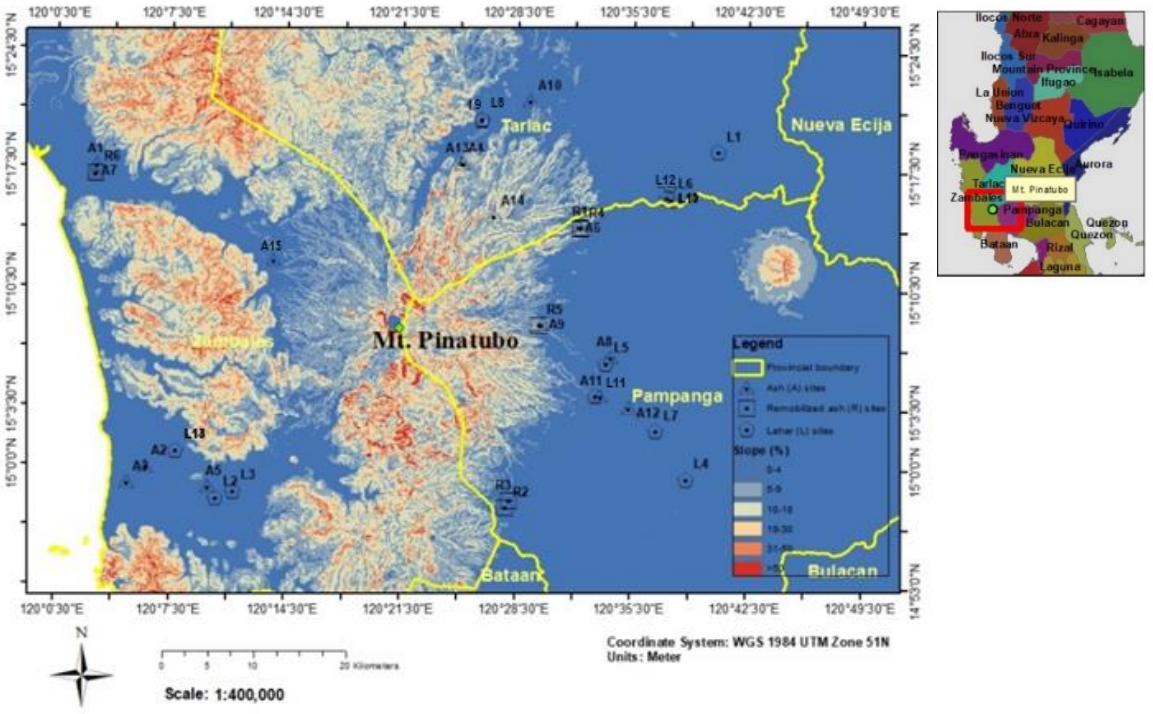

Figure A6.1. Slope map of the pyroclast-affected sites in Tarlac, Pampanga, and Zambales provinces. Relatively flat (0-4 %), gently undulating (5-9 %), slightly undulating (10-18 %), strongly undulating (19-30 %), rolling (> 30 %). *Basemap adapted from PhilGIS (2004b).*

Publications

Poster presentations

Quimbo, M. C., Delmelle, P., & Sanchez, P. B. (2018). Plant-available phosphorus in young volcanic soils developed on pyroclasts from the 1991 eruption of Mt. Pinatubo, Philippines. *Midi de rencontre des étudiants-chercheurs 2018*. Louvain-la-Neuve, Belgium, 26/10/2018).

Quimbo, M. C., Delmelle, P., Opfergelt, S., & Sanchez, P. B. (2018). Phytolith stock of a 26-yr volcanic ash soil in Tarlac, Philippines. *Young Researches Overseas Day*. Brussels, Belgium, 07/12/2018.

Peer-reviewed journal papers

Quimbo, M. C., & Mamaril, C. P. (2015). Growth and yield responses of NSIC Rc11 and Inipot-Ibon to different nitrogen rates under upland condition. *IAMURE International Journal of Ecology and Conservation. Vol. 15.* July 2015. pp. 214-231.

Quimbo, M. C., & Mamaril, C. P. (2015). Organic fertilizer efficacy and financial viability of upland rice (Oryza sativa L.) production, in Los Baños, Philippines. *Philippine Agricultural Scientist. Vol. 98* No. 2. pp. 174-189. June 2015.

Quimbo, M. C., Mamaril, C. P., & Tafere, K. S. (2014). Organic versus inorganic management on the yield and soil fertility of irrigated lowland rice. *Annals of Tropical Research. January – June 2014, Vol. 36* (1) Pages: 32-49.

Quimbo, M. C., Mamaril, C. P., Paterno, E. S., Sta. Cruz, P. C., Sanchez, P. B., & Badayos, R. B. (2012). Managing rice residues

and fertilization to improve nutrient use and productivity of irrigated lowland rice. *Annals of Tropical Research. July – December 2012, Vol. 34* (2) Pages: 1-25.

Castillo, M. B., & Mamaril, C. P. (2012). Comparative performance of biofertilizers on irrigated lowland rice (Oryza sativa L.). *Annals of Tropical Research. January – June 2012, Vol. 34* (1) pp. 29-51.

Castillo, M. B., Mamaril, C. P., Paterno, E. S., Sanchez, P. B., Badayos, R. B., & Sta. Cruz, P. C. (2012). Soil chemical and physical properties with rice straw management during fallow period. *Philippine Journal of Crop Science (PJCS). April 2012, 37* (1):15-26. Crop Science Society of the Philippines.

Tuaño, A. P., Xu, Z., **Castillo, M. B.,** Mamaril, C. P., Manois, R. V., Romero, M. V., & Juliano, B. O. (2011). Content of tocols, γ-oryzanol and total phenolics and grain quality of brown rice and milled rice applied with pesticides and organic and inorganic nitrogen fertilizer. *Philipp Agric Scientist, Vol. 94 No. 2*, 211-216. June 2011.

Book

Mamaril, C. P., **Castillo, M. B.,** & Sebastian, L. S. (2009). Facts and myths about organic fertilizers. *PhilRice.* Maligaya, Science City of Muñoz, Nueva Ecija. November 2009.